# Palaeoecology and systematics of Ordovician biotas from Welsh volcaniclastic deposits

by

Joseph Peter Botting

Thesis submitted to
The University of Birmingham
for the degree of
DOCTOR OF PHILOSOPHY

School of Earth Sciences,
The University of Birmingham,
September 2000.

## Abstract

The effects of explosive volcanism on local ecosystems are investigated in Middle Ordovician siliciclastics from the Welsh Basin. Bulk sampling analysis has provided quantitative data, regarding population proportions and abundance, following ash deposition in nearshore, shallow dysaerobic basin, and deeper basinal facies. Consistent ecological effects include the destruction of small sessile benthos by rapid burial, followed by re-establishment of mobile and opportunistic taxa, and a bimodal, planktic-benthic bloom in dysaerobic facies. The results are explained through vertical circulation initiated by turbid surface waters following ash deposition. Upwelling of subsurface, nutrient-rich waters of stratified basins is accompanied by downwelling of oxygenated surface waters, entrained into broadly spaced columns. The duration and nature of the events are investigated by ecological, sedimentological, and mechanical approaches, and high sedimentation rate invoked, resulting from seismicity associated with local volcanism.

Systematic studies are included on Porifera, Echinodermata and Palaeoscolecida, the unusual preservation of each resulting from volcanism-related processes. The poriferan fauna provides significant information on non-lithistid demosponges and hexactinellids, including the earliest representatives of several groups. Rapid silicification of the proteinaceous skeleton of two species indicates a new source of soft-tissue preservation. Echinoderms comprise the most diverse pre-Caradoc fauna known from Britain, including six crinoids, three asteroids, and a cystoid.

Acknowledgements

Firstly and multiply, I offer generous homage to the editorial prowess, intellectual catalysis, and eternal availability of my supervisor, Alan Thomas. Of particular note was his ability to shepherd my mind away from strange and fruitless avenues, when stalking that slight surrealism that is the Ordovician. His input, though hopefully not overt in the finished work, should not be underestimated – and that is the mark of a true teacher. He also provided great, but non-invasive support when the days became dark; this was perhaps more important than he realises. Complementing Alan was the "formal" input of a transient advisory panel comprising Paul Smith, Hugh Sinclair and Andy Chambers – the contribution of each has been thought-provoking, and very useful. Paul Smith, in particular, has provided substantial input in many aspects, and read part of the manuscript.

Many others have helped with specialist knowledge, of whom the most significant are Rosie Widdison (the endless wonder of crinoids), Phil Donoghue (numerous small black things, and how to analyse them cladistically), Andy Chambers (making some sense of mangled volcanics) Pete Turner (sedimentology) and Rob Mullen (geochemical analysis). Additional (and often essential) information was freely given by Nigel Woodcock (Cambridge University), Peter Sheldon (Open University), Petr Kraft (Charles University, Prague), Pat Bergstrom and Roger Cooper (New Zealand), Olle Hints (Estonia), Barry Webby (Australia), Dorte Mehl (Berlin) and Marcelo Carrera (Argentina); prodigious appreciation to all.

Technical support was amply provided by Aruna Mistry (photography), Sue Dipple (SEM, Materials and Metallurgy), John Coundon and Paul Hands (thin sectioning), Alan Dean (computing), Phil Broom (rock transportation) and Jon

Clatworthy (curation). My thanks also to Mike Dorling (Sedgwick Museum, Cambridge), Bob Owens (National Museum of Wales, Cardiff), Steve Tunnicliff (B.G.S., Keyworth), and Paul Taylor, Dave Lewis and Sarah Long (Natural History Museum, London) for access to specimens. John Davies (Countryside Commision for Wales) was instrumental in arranging fieldwork at protected sites, and showed great zeal with a pick-axe at Bach-y-Graig (as did Bill Wimbledon, also of CCW). Jenny Lloyd and my very own Clan Shaw provided welcoming accommodation in deepest Wales, along with a variety of youth hostel and B&B owners. My thanks to these, and to all landowners who graciously allowed access, often with refreshing enthusiasm – or was it amusement? Oh, and thanks also to fellow inmates Rich "Penguin" Hodgkinson and Ben Furlong, for maintaining constant fluctuations in the reality:insanity ratio, in the room where it is Always Christmas. And the rest of you, too: you know who you are. I would also have liked to thank Lao Tzu, Loreena McKennitt, Franz Liszt and Thargor the Barbarian, but perhaps that's pushing it a bit.

My family has been ever supportive of this peculiar choice of career, and without them, the result would have been very different. One day I hope to persuade them that it really is interesting...

The financial support of the University of Birmingham, including the Scanlon Fund, and of a grant from the Geologists' Association are warmly acknowledged.

Dedicated to the memory of my grandmother, Elsa Shaw, and all that she stood for. The wisdom of the Traveller was hers.

CONTENTS

# List of Figures

# List of Tables

## List of Plates

(explanations opposite plates)

### Plates 1-13: Porifera



### Plates 14-15: Palaeoscolecida

Plates 16-19: Echinodermata

Plate 16. *Cefnocrinus nodosus* gen. et sp. nov.

Plate 17. *Iocrinus llandegleyi* sp. nov.; *C. nodosus* gen. et sp. nov.

Plate 18. *I.* cf. whitteryi

Plate 19. *Caleidocrinus* cf. turgidulus; indeterminate crinoids; asteroids.

# 1. INTRODUCTION

## 1.1 OBJECTIVES

Extensive pyroclastic volcanism has been cited as a plausible catalyst for both mass extinction (Courtillot 1990; Javoy and Courtillot 1989) and biodiversification (Miller 1997). However, few palaeoecological data exist on the local effects of volcaniclastic or pyroclastic deposition in marine biotas. Any hypotheses of the large-scale ecosystemic effects of volcanism must consider local effects, in addition to inferred regional geochemical or climatic variations.

The primary aim of this thesis is to investigate, through detailed logging, the effects of volcaniclastic deposition on *in situ* communities through a range of siliciclastic facies in the Ordovician of the Welsh Basin. These include both shallow, near-shore communities, and deeper-water facies containing semi-independent planktic and benthic ecosystems. Processes operating within the different regions will be correlated, and integrated into a generalised scheme. It is hoped that these generalisations will have implications both for interpretation of the fossil record, and for modern conservation practices.

The majority of the study is concentrated in the Builth-Llandrindod Inlier of Powys. An investigation of this nature provides new information on local palaeoenvironmental interpretations, and elucidates aspects of the stratigraphy and palaeoecology. While some taxonomic groups have been intensively studied, most rare groups are almost unknown. In particular, millimetre-scale fossils will be examined intensively for the first time. Fine-scale faunal assemblage variations will be qualitatively related to levels of dysoxia, particularly from Llanvirn siltstones of the Llandrindod area.

The lack of previous research into this broad field precludes a definite conclusion; such a study can only be an introduction, allowing specific aspects to be investigated in future. The aim is to produce a broad framework of fundamental results, including possible generalisations. Interpretations, and estimates of their general applicability, will allow the development of testable palaeoecological hypotheses. Variation on these findings should be anticipated under other environmental conditions, but potential implications of the generalised data will be considered.

Systematic studies of rare or undescribed taxa are attempted where practicable, with particular emphasis on sponges and echinoderms.

## 1.2 LITERATURE: PALAEOECOLOGY OF MARINE VOLCANISM

Much of the impetus for this project derives from the lack of previous research. The only explicit analysis of benthic ecosystems subjected to ancient volcaniclastic burial is that of Heikoop *et al.* (1997), who compared a Pleistocene reef community to a Cretaceous offshore, soft-bottom community. They confirmed that sessile, filter-feeding ecosystems are much more strongly affected than mobile taxa. Their study also noted enhanced preservation potential, relating to rapid burial without increased hydraulic energy, and early diagenetic effects.

Tipper (1976), Clarkson and Howells (1981), and Batchelor and Clarkson (1993) provide brief notes on brachiopod faunas associated with a Llandovery bentonite of the North Esk Inlier, southern Scotland. In this example, a diverse brachiopod fauna of *Clorinda* Community-type below the bentonite was replaced by a non-diverse, oportunistic brachiopod fauna following it. Quantitative data were not provided.

S. Rigby and S. Davies have publicly discussed their results from black shales of the Scottish Silurian, where bimodal graptolite blooms immediately followed some bentonites; this work is presently unpublished. The blooms follow a consistent pattern, with a lower bioturbated part dominated by siculae and immature specimens, and an upper laminated part by adults. Chemical analyses of the bentonites indicate two distinct suites, differentiated by uranium levels. Only the high-uranium beds produced graptolite blooms, leading to their hypothesis of inorganic nutrient addition. Uranium is concentrated in derived magmas due to its incompatibility, where the levels of iron are also enriched among most andesites. Iron is known as a biologically limiting nutrient, being essential for the seven known species of oceanic nitrogen-fixing bacteria (Falkowski *et al.* 1998; Butler 1998). The addition of iron and phosphate to the surface waters is presently undergoing intensive research from commercial sources, for the purposes of unconstrained fish farming (e.g. Carpenter *et al.* 1995). The initial response to Fe enrichment is generally an extremely rapid plankton bloom, with photosynthetic efficiency tripling over three days; the decline is equally rapid. It is not presently clear whether the cause of Rigby and Davies' blooms was direct addition of this nature, or circulation of the upper water column, since iron concentration increases rapidly to a depth of several hundred metres (Butler 1998). Benthic oxygenation was not discussed, although clearly indicated by the bioturbation.

Swain (1996) investigated ostracod diversity through a series of bentonite-rich, shallow (estimated up to 50 m) carbonates and siliciclastics in the Caradoc and Ashgill of north-central USA. The Diecke metabentonite, in particular, is associated with elevated extinction rates among several invertebrate groups. He found that ostracod diversity is more notable for diversification than for extinction, and that the

extinctions appear not to have been directly related to the bentonites. He interprets this pattern as showing enhanced speciation through nutrient enrichment, over 1.5 million-year intervals following the volcanic pulses. However, the duration of this interval is incompatible with the experimental plankton studies described above (Carpenter *et al.* 1995), and the process is not explained further.

There are several related, but less explicit references. Lockley (1984) described the taphonomic and mixing processes associated with volcanogenic deposition, exemplified by the Llanvirnian Howey Brook Main Feeder section of the Builth Inlier. He did not discuss the ecological effects of the deposition. Peralta and Beresi (1999) describe a sequence from the Lower-Middle Ordovician San Juan Formation of Argentina, but only general faunal assemblage data was provided, and a variety of possible causes for such variation were noted. The most significant effect was a decline in faunal abundance over the upper interval, which contains numerous bentonites in an argillaceous background. Vavrdová (1999) describes microplankton blooms from the Arenig-Llanvirn of Bohemia, correlated with the formation of oolitic ironstones, which are laterally continuous with black shales. The formation of these beds was probably due to periodic upwelling and overturning of nutrient-rich bottom waters through a number of processes, particularly storms. It was noted that the ironstones typically form above either conglomerate or tuff horizons, although the tuffs were not directly implicated in their formation.

The local effects of contemporary volcanism have also been sparsely studied. Benthic surveys of shallow Antarctic bays were fortuitously interrupted by eruptions on Deception Island in 1967, 1969 and 1970. The first eruption occurred just prior to sampling, so that the initial communities are not known. The faunal response was described in detail by Gallardo *et al.* (1977), providing an important indication of the

effects on soft-bodied organisms. Their results show complex patterns that were inconsistent between eruptions. The third event had the greatest effect, producing an extraordinary proliferation of echiurids and polychaetes, recorded 18 months after eruption and declining rapidly. Infauna was subsequently restricted, without obvious cause, while molluscs and echinoderms were largely unaffected, and crustacean abundance reduced to near zero. The authors did not attempt to explain these results, but highlight the need for further research. Their results are discussed in detail in sections 3.7 and 7.2.

The eruptions of Mt Redoubt, Alaska, severely affected salmon fisheries in Cook Inlet (Dorava and Milner 1999). The primary influence on faunas in adjacent fluvial systems was massively increased sediment discharge and deposition, including a period of months during which sediment redistribution occurred. Benthic ecological samples were taken five years after eruption; comparison with a nearby, unaffected river allowed estimates of residual effects. The results were ambiguous, but apparently recorded elevated benthic abundance in the affected region; faunal composition had returned to normal. Elevated turbidity attested to continued redistribution of the original massive deposits over at least five years.

Although there must be many references that briefly mention this subject, few have been emphasised, and there is no concensus on the processes causing the observed faunal changes.

## 1.3 Regional Geology

The areas investigated are the Builth-Llandrindod Inlier ("Builth Inlier" hereafter), the Llanwrtyd Wells district, and the Capel Curig region of Snowdonia (Fig. 1.3.1). Study was restricted to these areas in order to characterise a range of

environmental settings in sufficient detail for generalisation. Other areas considered for investigation were the Shelve Inlier, Pembrokeshire and the Barrandian of Bohemia. The Builth Inlier was preferred to the similar Shelve succession because of the known existence of a diverse, *in situ* shallow-water assemblage at the Llandegley Rocks site (section 2.2), while bentonites are rarely exposed in fossiliferous Middle Ordovician successions of Bohemia (P. Kraft, *pers. comm.*, and pers. obs.). Facies preserved in Pembrokeshire largely duplicate the deeper facies discussed below, and could form the basis of independent studies.

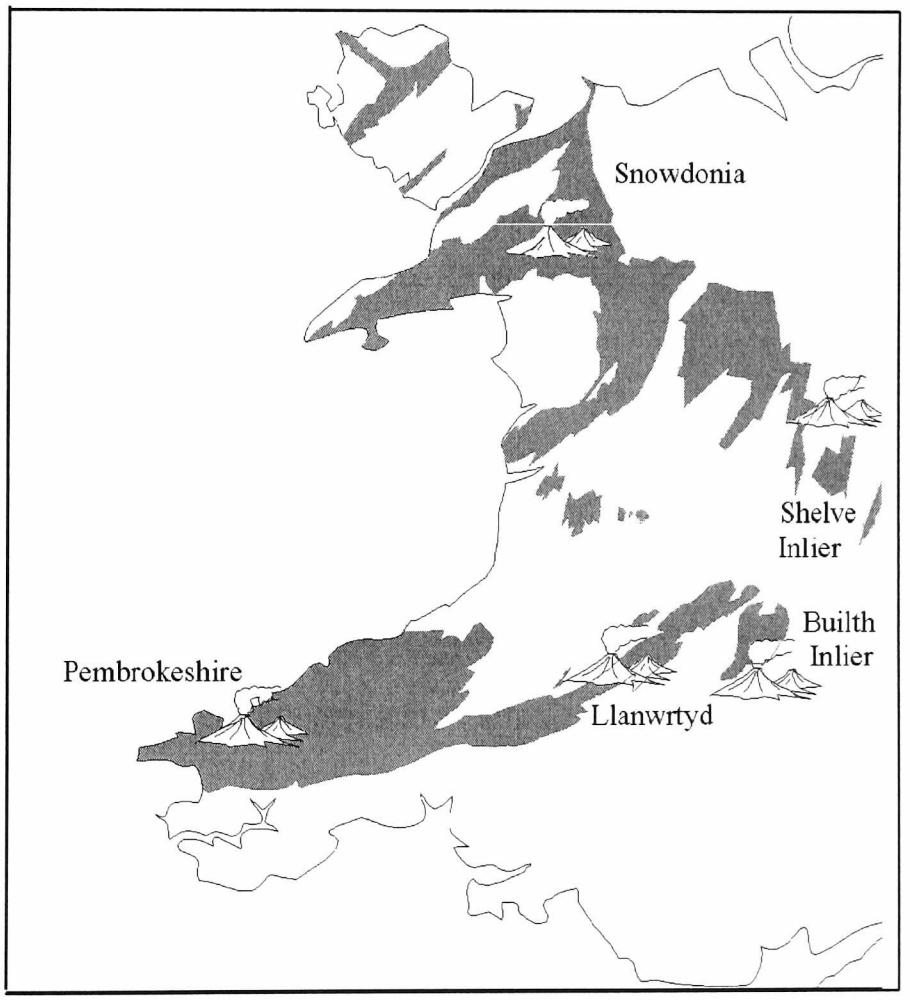


Figure 1.3.1: *Outline map of Wales, showing Ordovician outcrop and primary volcanic centres. Ordovician outcrop based on Harper and Owen (1996) and British Geological Survey (1994).*

| | | | | | | | |
|---|---|---|---|---|---|---|---|
| ASHGILL | Hirnantian | | *persculptus* | | Builth - Llandrindod | Llanwrtyd Wells | Capel Curig |
| | | | *extraordinarius* | | | | |
| | Rawtheyan | | *pacificus* | *anceps* | | | |
| | | | *complexus* | | | | |
| | Cautleyan | | | | | | |
| | Pusgillian | | *complanatus* | | | | |
| CARADOC | | | *linearis* | | | | |
| | | Onnian | *morrisi* | *clingani* | | | |
| | Steffordian | Actonian | | | | | |
| | | Marshbrookian | *caudatus* | | | | |
| | Cheneyan | Woolstonian | | | | LW 1-2 | LS 1 |
| | | Longvillian | | | | | PLW 1 |
| | Burrellian | Soudleyan | *foliaceus (=multidens)* | | | | Crafnant/Snowdon Volcanic Fm. |
| | | Harnagian | | | | | |
| | | Costonian | *gracilis* | | | Llanwrtyd Volcanics | |
| | Aurelucian | Velfreyan | | | | | |
| LLANVIRN | Llandeilian | | *teretiusculus* | | | BG 1-3 | |
| | Abereiddian | | *murchisoni* | | | HB 1-3 | |
| | | | | | Builth Volcanic Fm. | LR 1 | |
| | | | *artus* | | | Llandegley Tuffs | |
| ARENIG | Fennian | | *hirundo* | | | | |
| | | | *gibberulus* | | | | |
| | Whitlandian | | *simulans* | | | | |
| | | | *varicosus* | | | | |
| | Moridunian | | ? ? | | | | |
| | | | *phyllograptoides* | | | | |
| TREMADOC | Migneintian | | *murrayi* | | | | |
| | | | *sedgwickii* | | | | |
| | | | *salopiensis* | | | | |
| | Cressagian | | *tenellus* | | | | |
| | | | *flabelliformis* | | | | |

Figure 1.3.2: *Ordovician stratigraphy, based on Fortey* et al. *(1995) and Fortey* et al. *(2000), including positions of the ecological logs presented in chapters 2 and 3.*

## 1.3.1 Builth Inlier, Powys

### 1.3.1.1 Regional Setting

The Middle Ordovician sediments of the Welsh Basin were deposited in a fault-bounded back-arc basin related to the Iapetus subduction zone (Cope *et al.* 1992;

Woodcock 1984). The palaeogeographical location of Avalonia was discussed by Harper *et al.* (1996) and Torsvik and Trench (1991), but is generally considered southern subtropical. The primary arc development occurred from Northern England westward to Leinster, eastern Ireland, during the Llanvirn (*sensu* Fortey *et al.* 1995) to lower-middle Caradoc. The basin was bounded to the southeast by the Midland Platform (Fig. 1.3.3), probably continuous with Pretannia to the south. A probably emergent region, the Irish Sea Horst Complex, consistently restricted access to the west. Open routes to the ocean basins were probably developed to the southwest from Pembrokeshire, westward from Anglesey, and eastward through the north Midlands. The emergent extent and variability of the northern arc region is uncertain. Access to the Welsh Basin appears to have been most restricted during the Upper Llanvirn to Lower Caradoc (Cope *et al*. 1992).

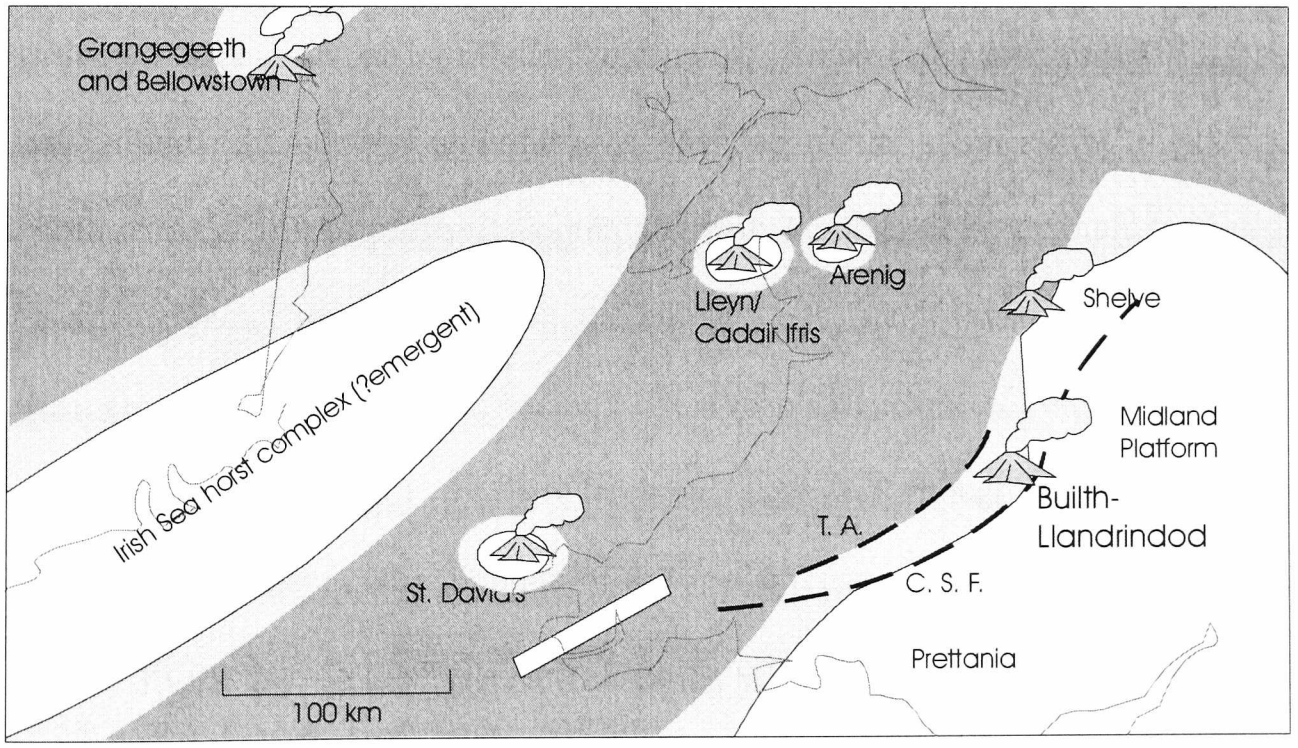


Figure 1.3.3: *Palaeogeography of the Welsh Basin region during late Llanvirn (*D. murchisoni *Biozone); adapted from Cope* et al. *(1992). T. A., Tywi Anticline; C. S. F. Church Stretton Fault.*

The Builth Inlier bordered the southeast margin of the Welsh Basin, although its position may have shifted slightly, relative to other Ordovician inliers, along the Pontesford Lineament or associated strike-slip splays (Trench *et al.* 1991; Woodcock 1987). Precise proximity to emergent regions is uncertain, although there is little doubt that topography included local volcanic islands during the *Didymograptus murchisoni* and possibly *Didymograptus artus* biozones (Jones and Pugh 1949). Although this interpretation has been debated, the upper Llandegley Rocks succession, described in section 2.2, is strongly indicative of the evolution of a local volcanic island. The same development is represented by the Gelli Hill succession. Most of the volcanism occurred during the uppermost *artus* Biozone and/or lower to middle *murchisoni* Biozone (discussed in section 1.3.1.2). This may have been related to the penecontemporaneous Stapeley Ashes of Shropshire (Lynas 1983), although Trench *et al.* (1991) suggested a significant time difference, based on palaeomagnetic evidence. The surrounding siliciclastics are dominantly black siltstones, commonly dysaerobic to anoxic, and widely interpreted as having been deposited in deep water; Sheldon (1987a) estimated several hundred metres for the *teretiusculus* Biozone. However, Cope (1999, p. 469) attributed the taphonomic characteristics of lower *murchisoni* bivalve faunas to "current and/or tidal winnowing," around the local volcanic islands, in what would typically be interpreted as deeper-water sediments. Davies *et al.* (1997, p. 15) suggested a shelf setting, generally below storm wave base.

There are several lines of evidence pertaining to water depth during the *murchisoni* and *teretiusculus* biozones:

1. The palaeogeographic reconstructions of Anderton *et al.* (1979) and Cope *et al.* (1992) imply a position within at most 20 km of the modern position of the Midland Platform during the Llanvirn. Allowing for 50% crustal shortening (Phillips

*et al.* 1976), the maximum probable distance from the continental palaeoshoreline is around 30 km. Comparison with modern basin margin gradients yields plausible limits for water depth.

The Sea of Japan is a modern back-arc basin, in which the 200 m bathymetric contour is reached at around 30 to 40 km offshore from Japan, but less (five to ten kilometres) off the Korean coast, steepening thereafter. The Sea of Okhotsk, behind the Kuril subduction zone, shows shallower gradients, with the 200 m contour reached at up to 200 km offshore. Similar basin margins in Indonesia (e.g. Celebes Sea, Sulu Sea, Banda Sea) show gradients similar to the Japanese coast of the Sea of Japan, although with substantial variation. Nowhere does the gradient approach that off Korea, which is very unusual.

A first probable estimate of water depth, 30 km off the southeast margin of the Welsh Basin, may therefore be taken as between 50 and 200 m. However, there is a slight probability of reaching dramatically greater depths.

2. Excluding continental slopes and subduction trenches, the steepest inorganic bathymetry is related to oceanic islands, where slopes can exceed 20 metres per kilometre. Numerous bentonites and other tuffs around the *murchisoni – teretiusculus* transition may be investigated regarding proximity to their source, to provide a secondary bathymetric estimate. Isopach data from modern eruptions allow distances to be extrapolated from tuff thickness. Modern terrestrial examples are reported by Bursik *et al.* (1993), Glaze and Self (1991), and Hildreth and Drake (1992), with marine isopach maps described by Carey and Sigurdsson (1980).

Tuff thicknesses from the Builth Inlier are frequently in excess of 10 cm, with occasional beds exceeding 50 cm. The source of these beds has not been positively identified, but is generally assumed distant. Most isopach maps emphasize the distal

deposits, since these are the most homogeneous. A comparison of the maximum ejecta thickness with distance, of several large modern eruptions, was provided by Fisher and Schminke (1984). However, isopach data are highly dependent on wind direction. Since neither the position of the vents nor the prevailing wind direction can be deduced with certainty, a range of possible distances for each isopach must be produced, with estimated probability distributions.

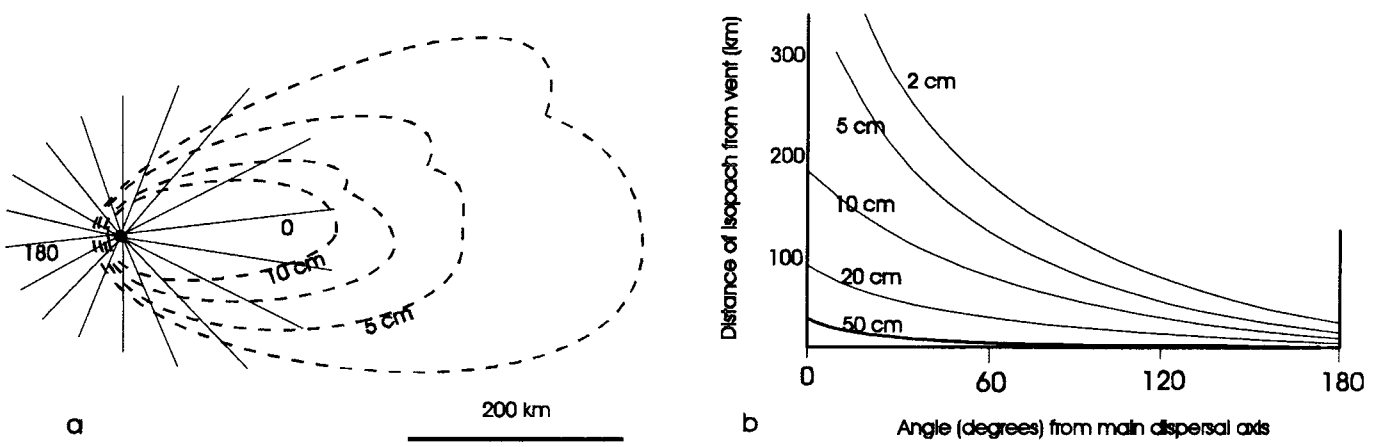


Figure 1.3.4: (a) *Schematic ejecta distribution for a 2 km$^3$ eruption, illustrating dependence on wind direction (based on Carey and Sigurdsson 1980; Bogaard 1983; Watkins* et al. *1978; Fisher and Schminke 1984); (b) variation in isopach ranges with displacement from dispersal axis of the same eruption; may be read as an approximate probability distribution.*

over hundreds of kilometres, there is often a rapid thickness increase close to the vent (e.g. Porter 1973; Williams and Goles 1968, cited in Fischer and Schminke 1984). Figure 1.3.4 portrays schematic thickness variation away from the dispersal axis, based on an eruption of approximately 2 km$^3$ (Vesuvius; Bogaard 1983, cited in Fisher and Schminke 1984, p. 172). This plot overestimates distances from source, because of diagenetic compaction of bentonites, which may have been reduced by up to 70%. Tuffs in excess of 1 m thickness occur throughout the Bach-y-Graig stream section, and include the 50-cm bentonite BG 1 (section 3.3). It is assumed that typical eruption size during the Ordovician of Avalonia was similar to recent eruptions, although Huff *et al.* (1993) described a volumetrically enormous ash bed

distributed through Baltica and Laurentia. Several Llandrindod bentonites, even if on the dispersal axis, would almost certainly have been within 100 km of the source. Given the approximate probability distribution of dispersal orientation (Fig. 1.3.4 b), there is a 75% chance that the source was within 20-30 km. Although a full-scale investigation would be required for confirmation, the most probable distance to the bentonite source for the Llandrindod region was less than 30 km.

Comparison of tuff compositions with dolerite intrusions and associated lavas provides limited data due to magma fractionation and alteration, but the results are fully consistent with dolerites/lavas and bentonites being comagmatic (section 1.3.1.3). Immobile element signatures of the only other known local volcanic source at this time (Shelve) are only partially overlapping. The Newmead unconformity during the upper part of the *murchisoni* Biozone at the Builth volcanic edifice suggests that this area may have been the source. A distance of approximately 8-10 km is fully consistent with tuff thicknesses, and would be appropriate for eruptions on the scale of 1-2 $km^3$, with variable wind direction. Assuming a maximum gradient of 20m/km, this implies a maximum depth of 200 m, and probably less.

3. Faunal assemblages show several indicators of water depth. The trilobite fauna is dominated by benthic taxa, notably asaphids, raphiophorids, trinucleids and calymenids. Pelagic forms are rare. Although trilobites are rare in the *murchisoni* Biozone, this appears to be due to anoxia; where present, the same taxa are dominant. The visual systems of the benthic taxa vary greatly, from the large, well-developed eyes of *Ogyginus* and *Ogygiocarella* to the small holochroal eyes of *Platycalymene*; *Cnemidopyge* and trinucleids were blind. (Increasing abundance of trinculeids and calymenids through the *H. teretiusculus* and *N. gracilis* biozones may indicate increasing light limitation, correlated with eustatic deepening.) The assemblage

closely resembles the Raphiophorid Community of Fortey and Owens (1978), and is distinct from the inshore *Neseuretus* Community, the shelf-edge Olenid Community, and the deep-water atheloptic assemblage. Trilobites thus indicate a middle shelf environment, estimated at approximately 50-150 m water depth.

4. Recent sponges occur in almost all normal marine settings, and are often considered among the most tolerant of benthic taxa. However, Rhoades and Morse (1971), in analysing the comunities of the Black Sea, report that sponges are limited to the upper 130 m, a shallower depth than molluscs, coelenterates, crustacea and polychaetes. Although this reflects oxygenation more than depth, there may be strong similarities with fault-bounded, stratified shallow basins like that postulated for the Llandrindod region. An undescribed sponge fauna from the Llanfawr Quarries, Llandrindod, contains at least ten species, including protospongioids, dictyosponges, advanced reticulosids and monaxonid demosponges. Diverse asssemblages containing both hexactinellids and demosponges are very rare in fine-grained facies, even in the Lower Palaeozoic, but become common in shallow, particularly carbonate-dominated shelves.

5. The fauna exposed in the River Ithon east of Castle Bank is dominated (~80%) by orthoconic nautiloids, but in all other aspects is typical of the middle *teretiusculus* Biozone. Orthocone-dominated, non-condensed assemblages are very unusual, although discussed by Soja *et al.* (1996) and Tasch (1955), among others. In general, cephalopod concentrations are believed to represent shallow deposits (often wave and tide-influenced), with abundance probably related to co-ordinated reproduction. Estimates of water depth may be obtained from implosion of body chambers in well-preserved specimens (Westermann 1973) but all specimens from fine-grained sediments of the Builth Inlier are flattened and decalcified.

6. The scarcity of ichnofauna has raised comment from other workers, with no examples previously known from fine sediments of the Builth Inlier (P. Sheldon, *pers. comm.*). This study has revealed three occurrences (Llandegley Rocks, Bach-y-Graig, and Gilwern Hill), all associated with ash deposition. While this may be partly due to benthic oxygenation allowing colonisation to occur, benthic faunas are otherwise numerous. Trilobites are often preserved in articulated condition, but no *Cruziana*-like traces have been recorded. If traces were destroyed by physical reworking, the degree of articulation must be attributed to high sedimentation rates, for which there is substantial evidence (see 3.7). Persistent benthic currents should have produced aerobic conditions, but a position near mean wave base (50-100 m) may have allowed constant, but limited fluid motion, erasing ichnofauna without enhancing oxygenation.

7. The morphology and thickness variation of ash beds, resulting from depositional processes, is dependent to some extent on water depth. This is fully investigated in Appendix C and section 3.7, but has yielded a tentative upper limit of 170 m, more probably 100-150 m.

Overall, the environmental setting appears to have been a temporary volcanic island complex surrounded (geographically and temporally) by nearshore (5-30 km), dysaerobic shelf basin facies, of water depth 50-150 m, with at least episodically high sedimentation rates.

### 1.3.1.2 Stratigraphy

The biostratigraphic succession of the Builth Inlier (Fig. 1.3.5) is based on graptolite zonation (Elles 1939; Hughes 1989). Trilobites were incorporated into the stratigraphy of Elles (1939), and were reviewed taxonomically by Hughes (1969, 1971, 1979). Sheldon (1987a, b) provided detailed analyses of variation within several

trilobite lineages. Other groups have been poorly studied, with published descriptions restricted to brachiopods (Lockley 1983; Lockley and Williams 1981; Williams *et al.* 1981; Sutton *et al.* 1999, in press), bivalves (Cope 1999) and crinoids (Donovan and Gale 1989). Brief notes regarding associated faunas were presented by Elles (1939), Jones and Pugh (1941, 1949), Lockley and Williams (1981) and Hughes (1969). Microfossils have been almost entirely neglected.

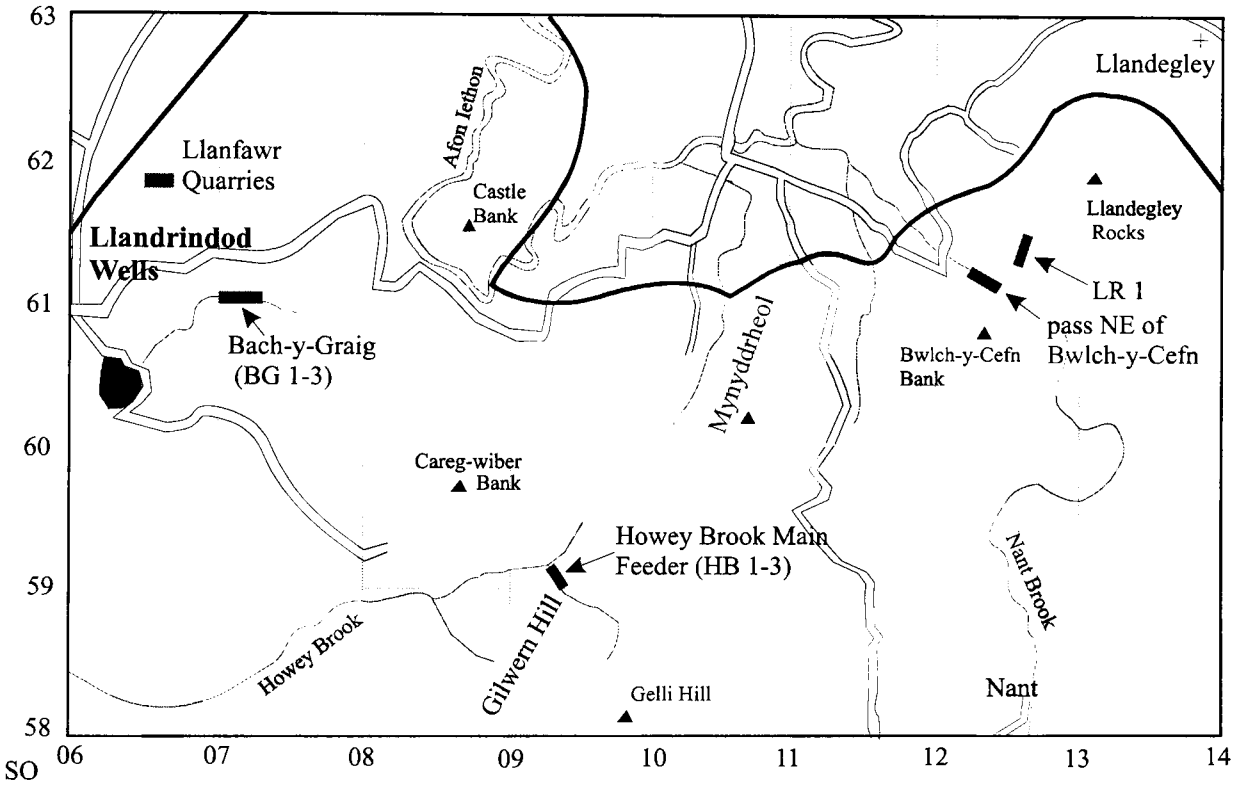


Figure 1.3.5: *Locality map for the northern part of the Builth Inlier, Powys. Sections mentioned in the text are marked by shaded rectangles. (1 km grid.).*

Lithostratigraphy is laterally inconsistent and diachronous, with structural complexity between limited shale outcrops. The shale succession ranges from the *D. artus* Biozone (base not seen) to the lower *N. gracilis* Biozone, within the Llanvirn Stage of the global Darriwillian Series, and the lowermost Caradoc. Thick volcanics and associated coarse clastics occur within the uppermost *artus* (?) and *murchisoni* biozones. The stratigraphy has been summarised by Elles (1939), Jones and Pugh (1941, 1949), Hughes (1969), George (1970), Williams *et al.* (1976). and Institute of Geological Sciences (1977). among others (Fig. 1.3.5). Although many of these are

broad summaries, there is substantial contradiction over the timing of onset of the main volcanic episodes.

Much of the confusion relates to the biostratigraphic position of the Llandegley Rocks succession, whose upper part is continuous with the Gelli Hill beds and the lower Builth Volcanics. According to Elles (1939), all significant volcanism

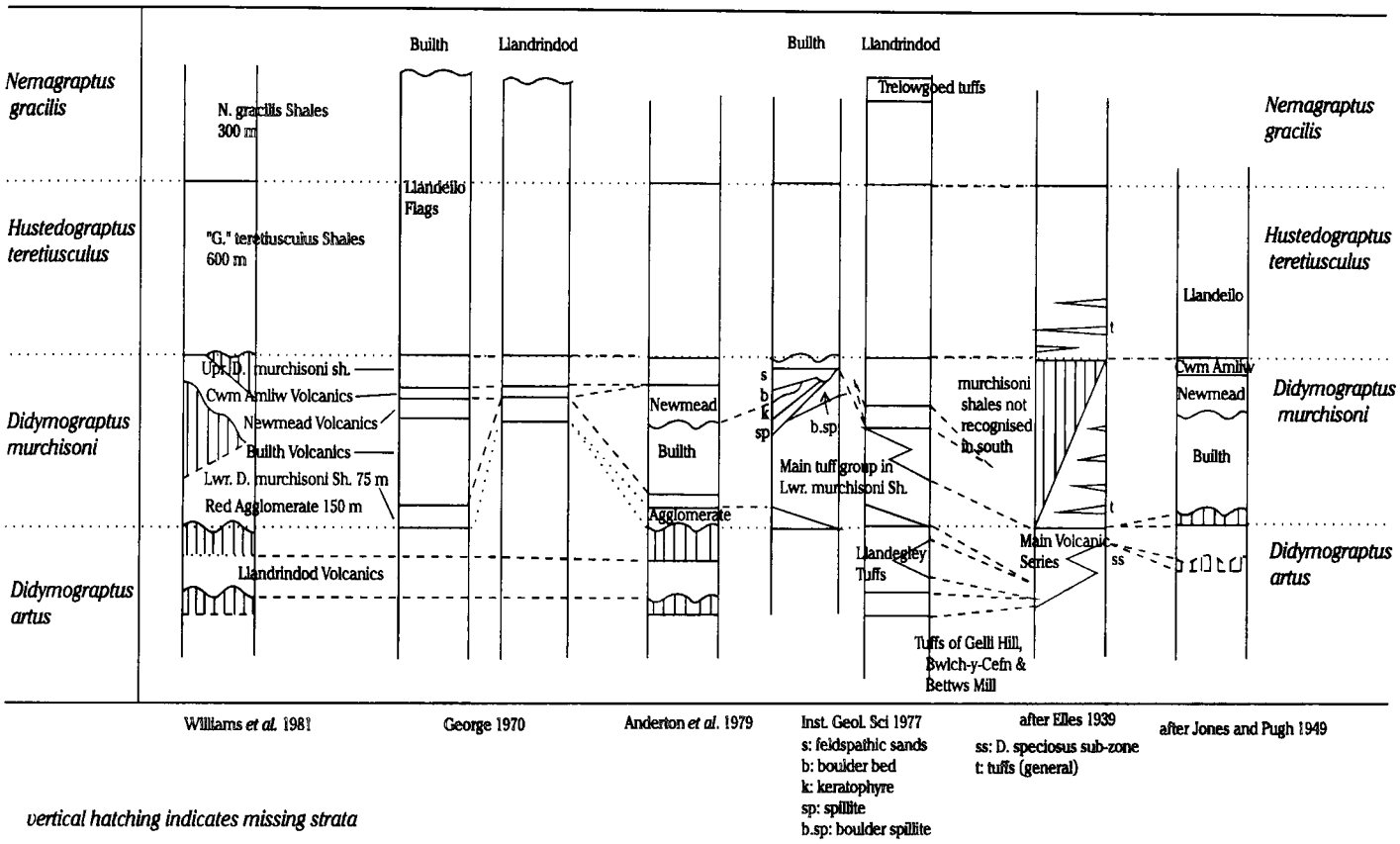


Figure 1.3.6: *Representative selection of stratigraphic interpretations of the Builth – Llandrindod Inlier. Almost all modern stratigraphies are based on Jones and Pugh (1949), although Elles (1939) contradicted this on several points. Most of the complication arises through biostratigraphical ambiguity of didymograptid-dominated assemblages.*

in the inlier occurred during the upper part of the *artus* Biozone, part of which she attributed to the *Didymograptus speciosus* Subzone. However, that subzone is indistinguishable from the lower part of the *D. murchisoni* Biozone (Kennedy 1989). In contrast, Jones and Pugh (1941, 1949) recorded *murchisoni* Shales below the Builth Volcanic Formation in the south, attributing the entire volcanic sequence to the *murchisoni* Biozone. However, Jones and Pugh (1941) only explicitly stated a record of the *murchisoni* Shales in the Howey Brook section, and from a continuation of

these beds around Dol-Fawr, to the south. In the Howey Brook itself, (Jones and Pugh 1941, p. 188), they were said to "pass downwards by alternations of shales and ashes into the lateral equivalent of the Red Agglomerate group." They did not describe further collections from this sequence, therefore giving no evidence that the beds are entirely within the *D. murchisoni* Biozone. Although stating that the shales underlying the Builth Volcanic Formation are referable to the *D. murchisoni* Biozone, they did not give examples of localities or collections. Since graptolites are uncommon within the Builth Volcanic Formation and its lateral equivalents, its stratigraphic position is presently unclear; however, Cope (1999) recorded fragmentary graptolites characteristic of the *D. murchisoni* Biozone some distance below the volcanics.

The Howey Brook Main Feeder (Gelli Hill) section records the upper *murchisoni* Shales passing eastwards into the lateral equivalent of the Builth Volcanics, across a northeast-southwest trending fault (Institute of Geological Sciences 1977). The exposed thickness of the volcanics is much less than at Builth, and the proportion of pyroclastics compared with siliciclastics decreases markedly to the north. The basal volcanic unit is the rhyolitic tuff of Llandegley Rocks (Llandrindod Ash of some authors), which also marks the base of the Builth Volcanic Formation to the south. This is overlain by distinctive laminated ashes, also known from more fully developed beds at Llandegley Rocks, which contain spinose diplograptids. Preservation is poor, in a granular matrix, but the species is similar to "*Orthograptus whitfieldi*" of Elles and Wood (1918), a poorly recognised taxon of unknown stratigraphic value. At Gelli Hill, a series of volcaniclastic and pyroclastic deposits follows, interspersed with an increasing proportion of shale and ashy shale units. The lowest datable fine sediment horizon is a 1 m exposure of pale ashy shales, equivalent to those exposed in the pass northeast of Bwlch-y-Cefn (GR SO 123 612),

described by Elles (1939). At Bwlch-y-Cefn they contain abundant *D. murchisoni* and a sparse, but moderately diverse shelly fauna (Appendix D), while the Gelli Hill site contains a monospecific association of *Diplograptus foliaceus*, which appears at the base of the *murchisoni* Biozone. Although this refers the upper part of the Builth Volcanics to the lower *murchisoni* Biozone with certainty, the position of the boundary remains unclear.

Discoveries of *D. artus* overlying the laminated ashes (basal Builth Volcanic Formation) at Llandegley Rocks may indicate the eponymous biozone. However, the species also occurs throughout the Gelli Hill succession in the *D. murchisoni* Biozone, sometimes in great abundance (e.g. log HB 3). *D. artus* and *D. murchisoni* are mutually exclusive at most horizons, but dominance fluctuated rapidly and repeatedly

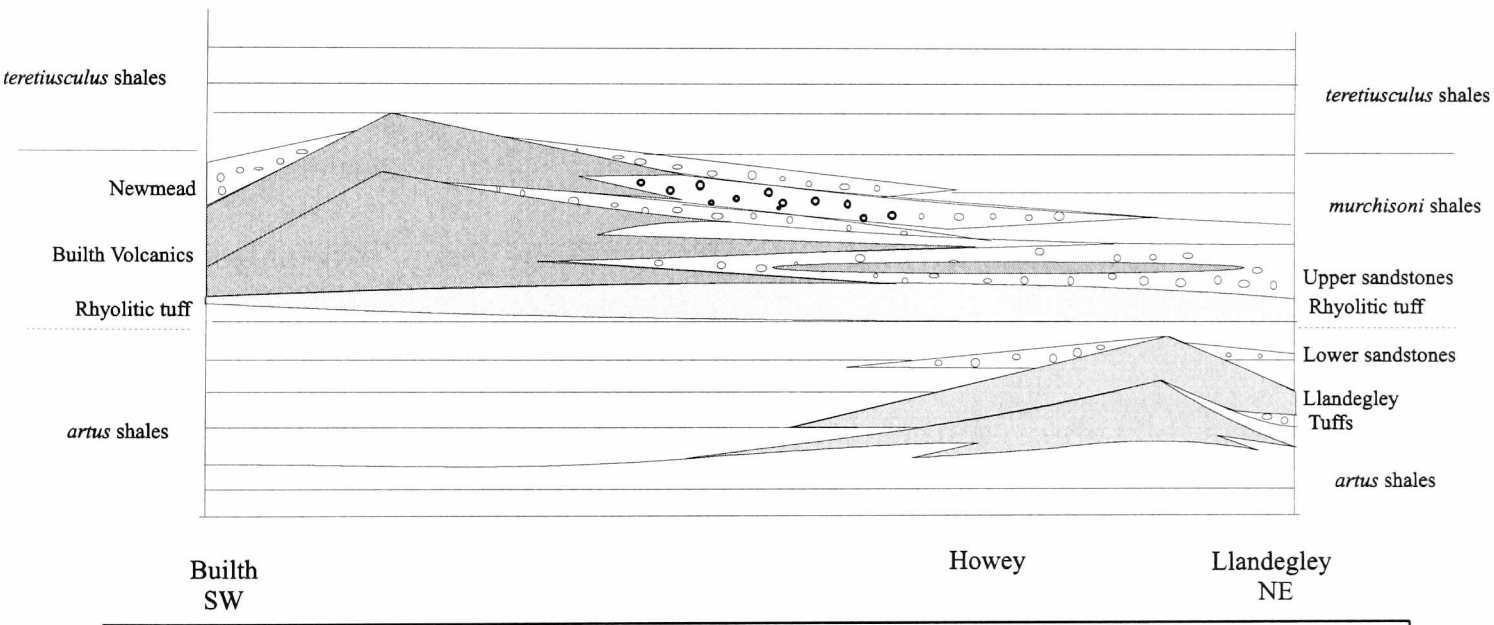


Figure 1.3.7: *Schematic volcanic evolution of the Builth – Llandrindod Inlier, showing correlation with biozonal boundaries, and identifying the Llandegley Tuffs as representing a distinct volcanic development.*

throughout the succession. This may reflect environmental factors that are not obvious in sedimentology, or result from chaotic population dynamics. Hence, the presence of *D. artus*, and absence of *D. murchisoni* indicates neither the biozone of the former, nor even the basal part of the latter. The use of diplograptids is essential in dating the boundary within the Builth Inlier.

Underlying the rhyolitic tuff are ashy siltstones of the Camnant Mudstone Formation (Davies *et al.* 1997), which in the north include a lesser volcanic episode, generally referred to as the "Tuffs of Llandegley," or of Gelli Hill (Institute of Geological Sciences 1977). Although usually regarded as separate units, exposures on Llandegley Rocks and Gelli Hill are very similar, but lack of exposure and ubiquitous faulting prevent accurate tracing. The volcanics occupy similar or identical stratigraphic positions. Given the considerable thickness (estimated 150-200 m) of extrusive material at Llandegley Rocks and Mynyddrheol (previously considered a

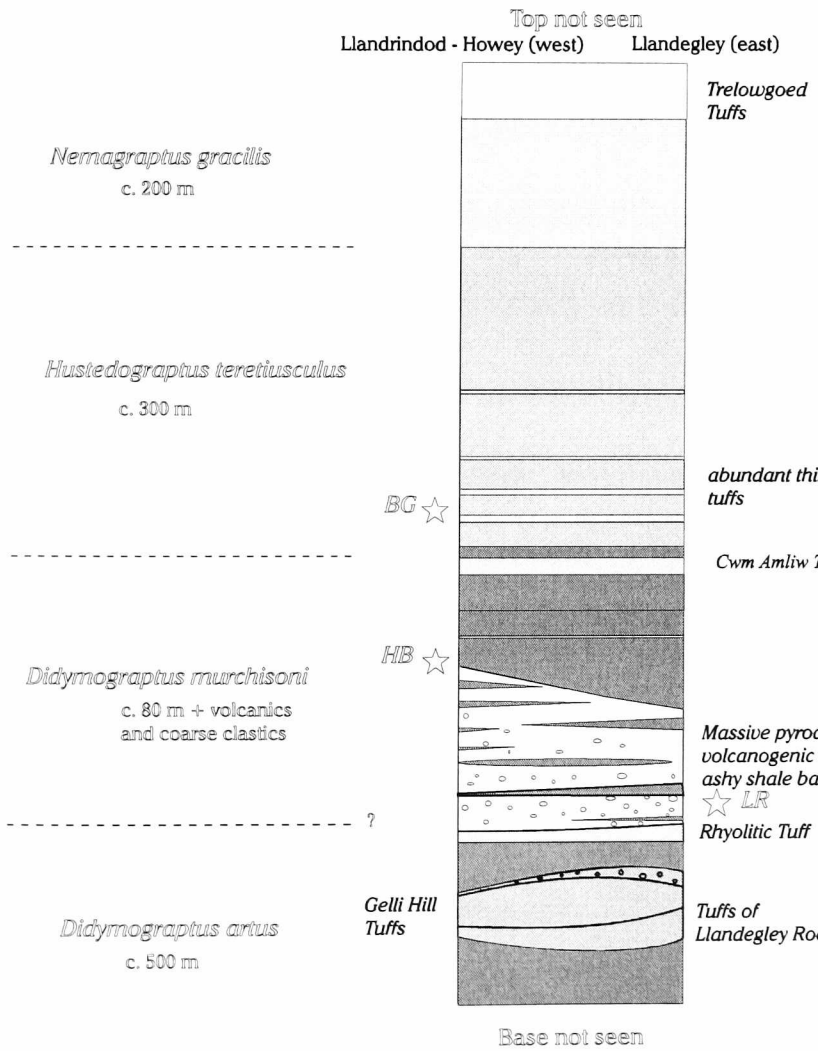


Figure 1.3.8: *Generalised stratigraphy of the northern part of the Builth Inlier, showing lateral variation; adapted from several sources, with additional data. Sections marked by stars: LR: Llandegley Rocks HB: Howey Brook Main Feeder (Gelli Hill) BG: Bach-y-Graig.*

keratophyric intrusion), it is more parsimonious to assume a single volcanic episode, with erosion represented by coarse sandstone deposits on Llandegley Rocks (see 2.2.1). The Llandegley Rocks succession is discussed further in section 2.2; the

volcanic history and correlation of the inlier is schematically summarised in Fig. 1.3.7.

The duration of the Builth Volcanic Formation in the southern part of the area remains uncertain, although the base is everywhere marked by the isochronous rhyolitic tuff. Most of the *murchisoni* Biozone is absent, or represented by coarser deposits, since overlying shales appear to be entirely within the *H. teretiusculus* Biozone (Sheldon 1987a). The stratigraphy of the northern part of the inlier, which has provided all sections used in this study, is summarised in fig. 1.3.8. The upper surface of the Builth Volcanic Formation is diachronous, but conformable in the north, where the transition is seen at Bwlch-y-Cefn and Gelli Hill. The upper *murchisoni* Biozone Newmead sandstones of the Builth district, and the controversial shoreline unconformity (Jones and Pugh 1949) appear to be absent there. However, the Llandegley Rocks succession and fauna are indicative of shore-face conditions (section 2.2), suggesting nearby emergence. In general, water depth increased northwards while the Builth Volcanic Formation was deposited, but deepened southward during deposition of the underlying Llandegley volcanic episode.

The sections analysed in this study are from the uppermost *artus* (?) Biozone (LR 1), lower *murchisoni* Shales (HB 1-3) and lower *teretiusculus* Shales (BG 1-3). Detailed descriptions of the relevant parts of the succession are provided during discussion of individual sections.

#### 1.3.1.3 Faunas

Faunal associations within the Builth Inlier have been investigated only at a rudimentary level. Elles (1939) recorded occurrence data for several sites, but did not

attempt to generalise the assemblage patterns, except to denote graptolite-trilobite biozones. Llanvirn brachiopod communities of the Welsh basin were described by Williams *et al.* (1981), Lockley and Williams (1981), and Lockley (1983). Caradoc associations and communities of the eastern Welsh Basin were discussed by Pickerill (1977), Pickerill and Brenchley (1979), Hurst (1979), and Lockley (1980, 1983), Watkins and Berry (1979) analysed benthic and planktic Ludlow faunas of Shropshire. Faunas investigated in this study are separable into coarse sandstone and siltstone lithologies, although intermediate facies occur elsewhere in the area.

Coarse sandstone assemblages of the Builth Inlier are dominated by the nearshore *Hesperorthis* community (Williams *et al.* 1981; Lockley 1983, 1984), and a range of slightly deeper, *Dalmanella*-based assemblages (Williams *et al.* 1981; Lockley and Williams 1981). Mixing of these communities was described from a volcaniclastic debris flow at Gelli Hill (Lockley 1984; Suthren and Furnes 1980), at a horizon almost identical to that of the Llandegley Rocks fauna (section 2.2). A *Glyptorthis*–based assemblage above Graig Farm, Llandegley Rocks (SO 1275 6187; Appendix D) represents a variation on the *Dalmanella – Gelidorthis* Community of Williams *et al.* (1981). Trilobites are dominated by *Ogyginus* and calymenids, closely resembling the nearshore *Neseuretus* Community of Fortey and Owens (1978).

Associations dominated by inarticulate brachiopods are poorly defined, with a gradational transition between assemblage compositions (Lockley 1983). The epibiotic, cementing *Schizocrania* characterises a consistent anoxic/dysaerobic association (Williams *et al.* 1981), where there is some evidence of a pseudoplanktic habit (Lockley and Antia 1980). The recognition of a distinct *Schizocrania* palaeocommunity was questioned by Lockley (1983), although the wide occurrence of a broadly defined inarticulate community was confirmed. Rare specimens of

*Monobolina, Pseudolingula, Schizocrania* and *Apatobolus* occur in variable proportions. However, the micromorphic *Apatobolus micula* is much more widespread than previously thought, and although partly pseudoplanktic (Botting and

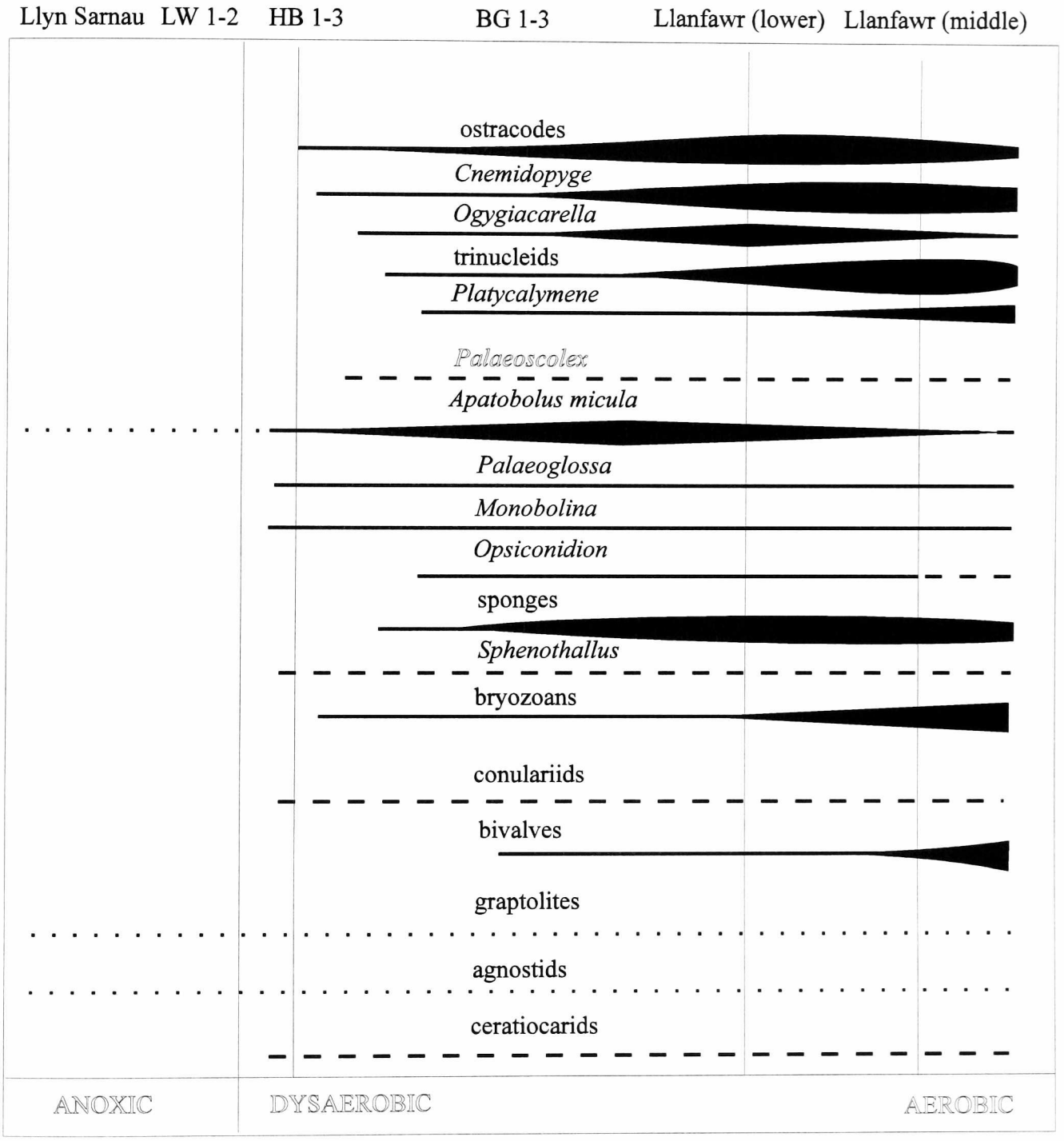


Figure 1.3.9: *Variation in faunal composition with oxygenation (other factors presumed constant) in the Builth Inlier, Powys, based on data presented herein, and illustrating levels of the described sections. Thickness of bars indicates schematic relative abundance. Dashed: rare taxa; dotted: planktic/ pseudoplankic. Division into formal sub-communities is inappropriate at this stage, but there is clear potential for future work.*

Thomas 1999), benthic populations may provide the basis of a sub-community. The locally abundant *Opsiconidion nuda* (Sutton *et al.*, in press) shows a sporadic distribution suggesting oxygen dependence, which may be regionally consistent.

Ordovician lingulids of Wales and the Welsh borderland have been taxonomically reviewed by Sutton *et. al.* (1999, in press).

Trilobites from fine-grained sediments of the Builth Inlier are dominated by *Ogyginus*, *Ogygiacarella*, *Cnemidopyge*, trinucleids, *Platycalymene* and *Barrandia*. The mixed visual systems of these taxa are characteristic of the Raphiophorid Community of Fortey and Owens (1978), although variations in the abundance of trinucleids, and the ratio of raphiophorids to asaphids, suggest potentially finer subdivision. The rarity of pelagic taxa and absence of olenids clearly distinguish the Builth assemblages from deep-water Olenid (Fortey and Owens 1978) and Atheloptic (Fortey and Owens 1987) Communities. Implications for water depth were discussed in section 1.3.1.1.

Although faunal associations among particular taxonomic groups are known in detail, there have been no attempts to resolve fine-scale, total faunal assemblage variations within black shales and siltstones of the Builth district, or elsewhere. Oxygenation, water depth and grainsize are probably the most important parameters constraining benthos distribution, depending on environment (Brenchley and Pickerill 1993). However, it is not known whether these factors had varying significance for different groups, or how palaeocommunities based on different groups were interrelated. The detailed logs used in this study have enabled patterns of faunal composition under varying oxygenation to be derived (Fig. 1.3.9). In addition to environmental correlation, whole-ecosystem biofacies provide a guide for the occurrence of inconspicuous taxa. For example, sponges appear to be absent from beds lacking trinucleids, despite the presence of other benthic trilobites, while palaeoscolecids can occur among any benthic faunas. The relative significance of oxygenation events or background fluctuations can be estimated by detailed

comparison of assemblages. It is unclear whether the patterns derived here will have significance outside the Builth region, or at other times.

Possible pseudoplanktic organisms cannot easily be accommodated, but are incorporated as far as possible. The rare presence of articulate brachiopods is particularly problematical, and is probably controlled largely by substrate. Most inarticulate brachiopods are presumed to have been dominantly benthic, in some cases showing clear facies dependence (e.g. *Opsiconidion*). *Sphenothallus* and related organisms were almost certainly benthic (van Iten *et al.* 1996; Neal and Hannibal 2000). Local fluctuations relating to grainsize or water chemistry may contradict these patterns, which should be treated as generalisations only.

#### 1.3.1.4 Volcanism

Volcanism in the Middle Ordovician of Wales was related to subduction of the Iapetus Ocean, and possibly the Tornquist Sea, between Avalonia and Baltica (McKerrow *et al.* 1991). The overall setting of British Ordovician volcanism was summarised by Stillman (1984) and discussed above. The Builth volcanics are now widely agreed to be almost entirely calc-alkaline in nature, confirming a subduction-related origin, in contrast to Jones' (1941) opinion that most were tholeiitic.

The Builth Inlier is a celebrated example of a volcanic island complex (Jones and Pugh 1949), similar to that at Shelve (Lynas 1983), but better preserved. It is therefore surprising that few precise data are available on the nature and composition of the numerous tuffs, though the penecontemporaneous dolerite intrusions and lavas have been subject to detailed morphological (Jones and Pugh 1946, 1948a, 1948b) and geochemical (Furnes 1978; Smith and Huang 1995) analysis. A single bentonite from the *gracilis* Biozone of Llanfawr Quarry, Llandrindod, has been analysed, along

with eleven from the *artus* Biozone of Shelve (Huff *et al.* 1993). Further examples from the Caradoc and Ashgill of Mid- and North Wales were also included. Furnes (1978) restudied the entire Builth volcanic suite; these results were briefly summarised by Bevins *et al.* (1984). Overall, the Builth volcanism contained elements of both arc and oceanic origin, with a range of fractionation and eruption products. Five bentonites from the *murchisoni* and *teretiusculus* biozones of the Llandrindod area have been analysed in this study, and compared with the published data of Huff *et al.* (1993) (Table 1.1).

Extensive alteration of volcanics precludes the use of major element compositions for comparison. This is due to both modern weathering and low-level metamorphism, estimated from conodont colour indices to have reached 190 - 210°C (Epstein *et al.* 1977). The new samples show clear enrichment in Na, with loss of Ca and probably Fe; other mobile elements are therefore unreliable. The use of "immobile" element ratios theoretically allows realistic comparison of altered samples, although even these must be treated cautiously.

Standard ratios of Nb/Y, Zr/TiO2 and Ce/Y are compared between two sample sets from the Builth inlier, a third from Shelve, and a fourth from the Caradoc of Carmel, Powys (Table 1.1). Niobium, zirconium and yttrium were considered essentially immobile in Builth Inlier samples by Smith and Huang (1995). Huff *et al* (1993) interpreted those with low niobium levels (including two from Shelve) as containing some degree of ocean ridge influence. Those with low Y and Nb, including the Llanfawr sample, are attributed to syn-collisional or arc volcanism. The great majority are typical of intra-plate granitic magmas (Pearce *et al.* 1984). The new Llandrindod samples fall into the intra-plate – arc range, and are entirely consistent with a local source, as suggested by Huff *et al.* (1993).

| | Ce/Y | Nb/Y | Zr/TiO2 | n |
|---|---|---|---|---|
| Llanfawr (*gracilis*) | 6.9 | 0.467 | 0.029 | 1 |
| Shelve (*artus*) | 1.70 ± 0.59 | 0.35 ± 0.13 | 0.037 ± 0.023 | 11 |
| **Llandrindod (*murchisoni* & *teretiusculus*)** | **1.17 ± 0.28** | **0.30 ± 0.091** | **0.030 ± 0.023** | **5** |
| Carmel (lower Caradoc) | 1.88 ± 0.81 | 0.51 ± 0.12 | 0.063 ± 0.043 | 8 |

TABLE 1.1: *comparison of mean and standard deviation of standard ratios, among Llanvirn and Caradoc bentonites from Powys. All data except Llandrindod samples are from Huff et al. (1993).*

The *N. gracilis* Biozone bentonite from Llanfawr, although only represented by a single sample, is clearly separable from the other three sets based on Ce/Y and Nb/Y values. This might be expected, given that the upper *teretiusculus* Biozone in the Builth Inlier is essentially devoid of ash. Differences between the Shelve and

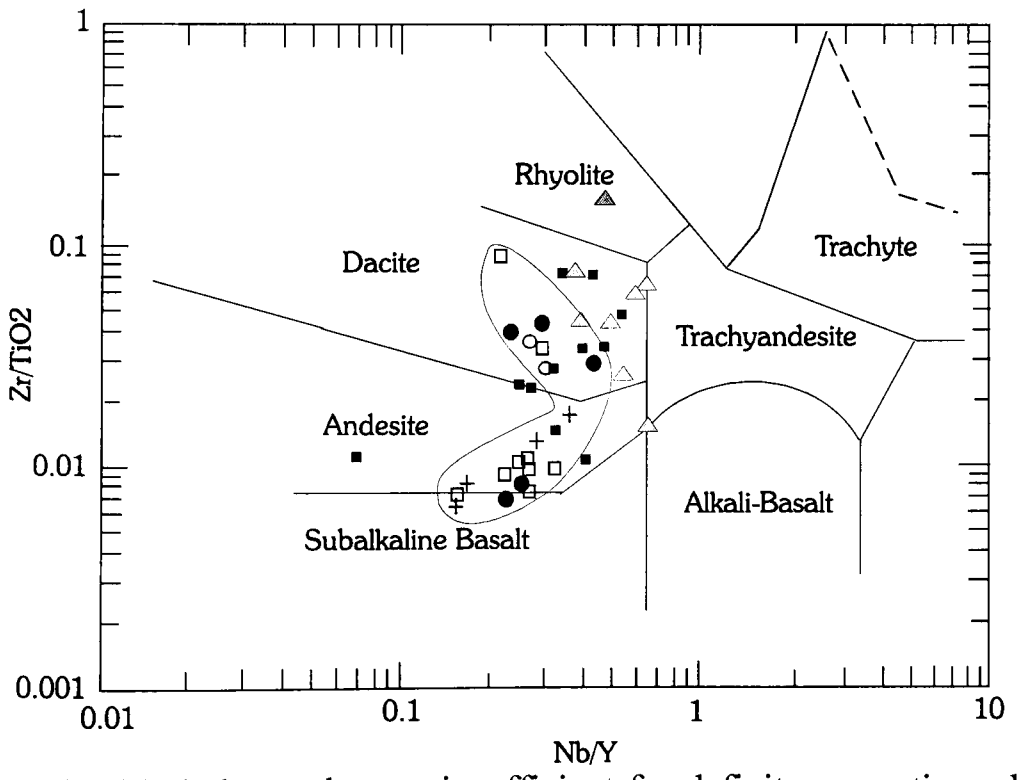


Figure 1.3.10: *Zr/TiO2 – Nb/Y classification of rocks of the Builth-Llandrindod Inlier, after Winchester and Floyd (1978). Crosses: dolerites; open circles: Llandrindod Volcanic Formation (=rhyolitic tuff); open squares: Builth Volcanic Formation (all from Smith and Huang 1995). Black circles: tuffs (present analyses).*

*Shaded triangles: Carmel, Caradoc; dark squares: Shelve, Llanvirn (Huff* et al. *1993).*

Llandrindod samples are insufficient for definite separation, although the correlation is not perfect. A common deep source, slightly modified by fractionation pathways and crustal contamination, explains these differences plausibly, but without certainty.

Corresponding ratios for lower Caradoc bentonites of Carmel, Mid-Wales (Huff *et al.* 1993), are extremely variable. There is uncertain evidence of multiple sources, since different pairs of samples show similarity with respect to different ratios. The significance of the Carmel bentonite compositions must remain uncertain, and the possibility of severe alteration considered.

A comparison of bentonite composition with that of the Builth Inlier dolerites and lavas (Smith and Huang 1995) allows further refinement of possible source recognition (Fig. 1.3.10). The bentonite analyses fall clearly within the trace element compositional range of local eruption products. While not proving conclusively that the same source was responsible for their emplacement, the clear distinction of the Carmel bentonites (Huff *et al.* 1993) illustrates the significance of this correlation. The Shelve data, while possessing a mean similar to that of Builth, show a different range and overall trend. Overall, geochemical composition is consistent with the source of the *murchisoni* and *teretiusculus* Biozone bentonites being that of the associated intrusions and lavas. Eruption of the Builth volcanic cone at this time would also be consistent with the Newmead unconformity (Jones and Pugh 1949), which is overlain by *teretiusculus* Shales.

## 1.3.2 Llanwrtyd Wells, Powys

### 1.3.2.1 Regional Setting

Eustatic sea level rise during the Caradoc progressively flooded parts of the emergent Midland Platform (Fig. 1.3.11, Cope *et al.* 1992). Volcanic activity on the southwestern side of the Welsh Basin declined during the *teretiusculus* Biozone, and was restricted to Snowdonia and Ireland by the *D. multidens* Biozone, and to a small centre at Portrane by the *D. clingani* Biozone (Cope *et al.* 1992; Anderton *et al.*

1979). An exception to this pattern is the activity associated with the Llanwrtyd area of Powys, predominantly during the early *gracilis* Biozone (Stamp and Wooldridge 1923; Cave and Rushton 1996). Basaltic breccias of the Trelowgoed Volcanics near Llandrindod may also be of *gracilis* age, but their position is uncertain.

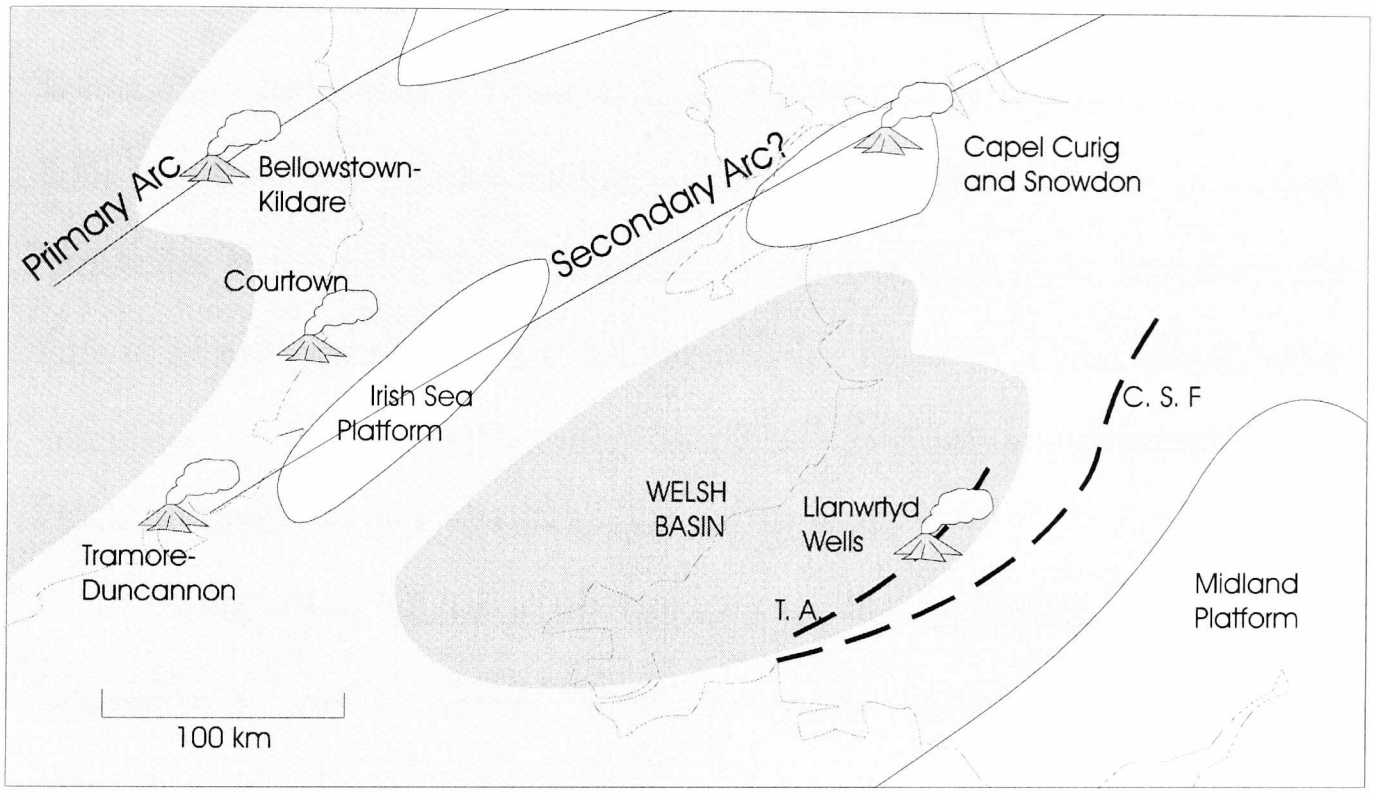


Figure 1.3.11: *Palaeogeographic setting of Llanwrtyd Wells during middle Caradoc (*D. multidens *Biozone); C. S. F., Church Stretton Fault; T. A., Tywi Anticline. Based on Cope* et al. *(1992).*

The Llanwrtyd sequence, exposed in the centre of the Tywi Anticline, comprises alternating black/grey mudstones and turbiditic sandstones, with ashes, lavas and volcaniclastic breccias. Mudstones are typically unbioturbated, with variable pyrite development, representing consistent benthic anoxia. The faunas are generally restricted, with rare graptolite-dominated units in mudstones, and occasional shelly debris in calcareous sandstones. Extensive slumping, and the lack of hemipelagic lamination, is suggestive of high depositional rates and steep local topography (Cave and Rushton 1996).

The igneous rocks of Llanwrtyd have not been analysed. In general character, they range from basaltic (as flows and shallow intrusions) to fine siliceous tuffs. Many beds show evidence of violent transport, represented by mass flow deposits, ash-flow tuffs or tuffaceous debris flows. Most are characteristic of submarine eruption, although locally shallow water depths are suggested by certain shelly faunas. Pyroclastics usually comprise highly angular, shardic pumice grains, angular lithic fragments and euhedral feldspar crystals. Fine air-fall tuffs are not certainly attributable to the local volcanic complex, but may represent slight emergence; thin tuffs of *gracilis* age also occur at Llandrindod, but appear to be unrelated to earlier volcanism (1.3.1.3). There is presently insufficient geochemical data to compare the Llanwrtyd tuffs with those of the Caradoc of Llandrindod.

The standard environmental interpretation is a deep-water, basinal setting adjacent to a slope in the east, with sedimentation strongly affected by a local volcanic cone.

### 1.3.3.2 Stratigraphy

The stratigraphy of the Llanwrtyd district has been reviewed recently by Cave and Rushton (1996), based on the Gilfach Farm borehole. This followed the original description of Stamp and Wooldridge (1923), who recognised black mudstones of the *Diplograptus multidens* Biozone, confirmed by basal Caradoc shelly faunas in local rottenstones. Additional information was provided by Davies (1933) and Jones (1949), who studied the entire region between Llandovery and Rhayader, although little emphasis was placed on the Caradoc succession. The Llanwrtyd area was also mapped by J. Davies (*pers. comm.*), emphasising the regional structure.

The most complete Ordovician section occurs in Nant Cerdin, 2 km north of Llanwrtyd Wells. The stream valley cuts through the centre of the Tywi Anticline, resulting in concentric exposure of the volcanic sequence, summarised in fig. 1.3.12. Limited graptolitic faunas in units 2 and 4 have been interpreted (Stamp and Wooldridge 1923) as equivalent to the Scottish *Climacograptus wilsoni* Biozone ("*Dicranograptus* Shales"), equivalent to the upper part of the *D. multidens* Biozone of the Anglo-Welsh region. The latter biozone is in need of revision (Rushton 1990), but appears to be recognisable near Rhayader (Davies *et al.* 1997). The *multidens* Biozone is approximately equivalent to the *foliaceus* Biozone, preferred for British stratigraphy by Fortey *et al.* (2000).

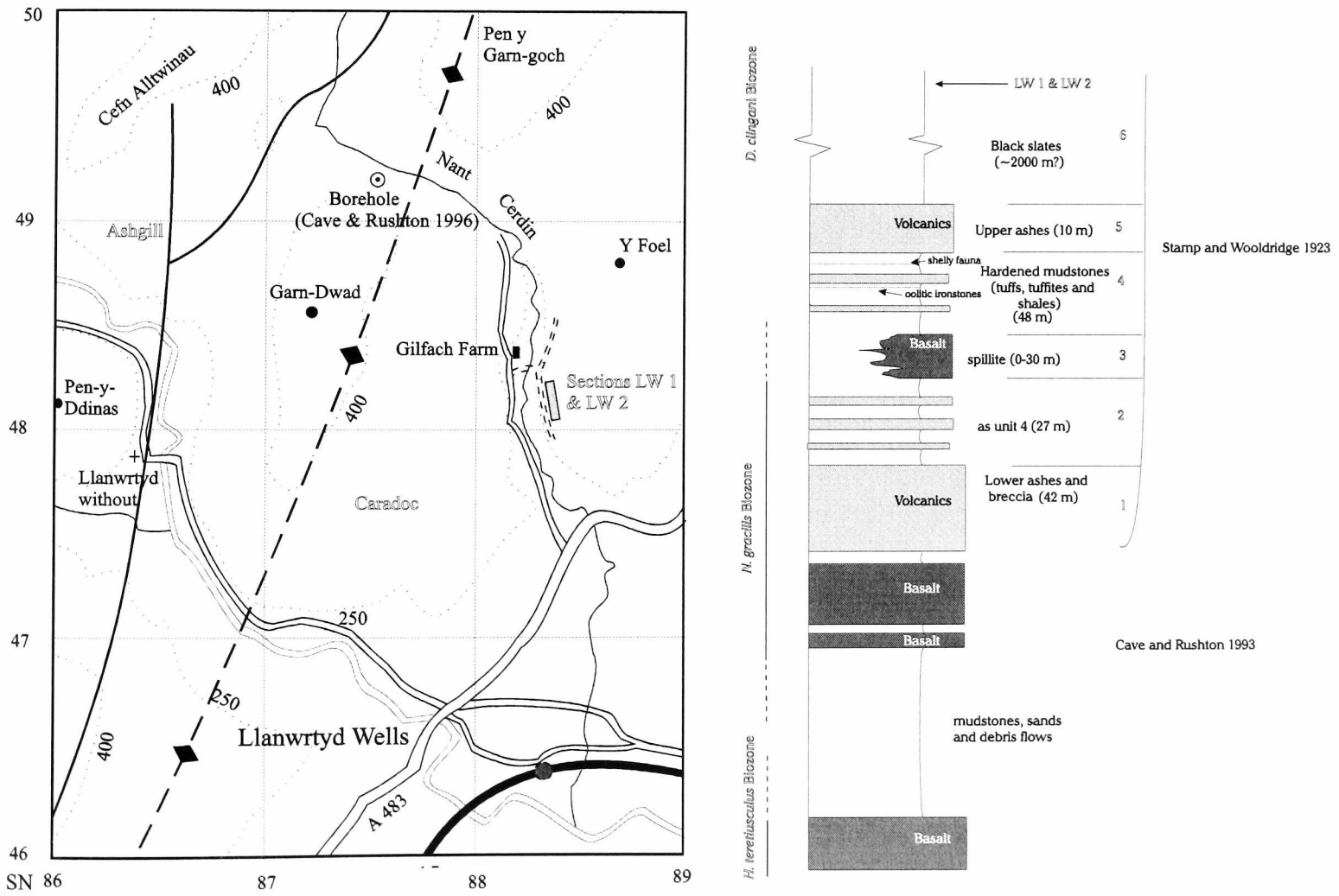


Figure 1.3.12: a, *Local map of Llanwrtyd Wells region, Powys, showing location of sections LW1 and LW 2.* B, *Generalised stratigraphy of Llanwrtyd Wells succession, based on Stamp and Wooldridge (1923), Cave and Rushton (1996), and new data.*

The Gilfach Farm Borehole was located in the centre of Nant Cerdin, and revealed the lower part of the sequence, terminating in basalts of the *teretiusculus* Biozone. The highest beds seen were those of *N. gracilis*, correlated with the lower part of unit 1 of Stamp and Wooldridge (1923). Exposures of units 2 and 4 allowed further graptolite faunas to be collected, indicating that these are referable to the top *gracilis* to lower *multidens* biozones, significantly lower than previously reported.

Overlying the upper ash beds are the "black slates," unit 6 of Stamp and Wooldridge (1923). These slates reach great thickness (circa 2100 m; Davies 1933), but have generally been dismissed as monotonous, undatable and extensively deformed. Previous authors have reported that the succession is almost unfossiliferous; a limited shelly fauna was recovered from thin grits (Davies 1933), and the slates have yielded some indeterminable graptolite fragments (Stamp and Wooldridge 1923). Cave and Rushton (1996) ignored the sequence above the upper ashes, apparently identifying these with the "*Dicranograptus* Shales." If this was an intended attribution of the black slates to the *D. multidens* Biozone, it was not explicit.

Sections LW1 and LW2 occur within these "unfossiliferous" black slates, exposed in a previous forestry cutting on Y Foel, 1 km southeast of the Gilfach Farm borehole. The beds are monotonous, pale grey and black shales interbedded on a centimetre-scale, and containing rare, thin bentonite horizons and occasional fine sand laminae. The beds are pervasively cleaved, generally at around 10° to bedding planes, but sometimes approaching parallel. A locally abundant, graptolite-dominated macrofauna has been recovered:

*Dendrograptus* sp.

*Glyptograptus*? sp.

*Amplexograptus* sp.

*Lasiograptus* sp. cf. *harknessi*

*Pseudoclimacograptus* sp. (fragment)

*Dicranograptus clingani*

*Apatobolus*? *micula*

Indet. lingulid

Indet. ceratiocarids(?)

The presence of *D. clingani* is diagnostic of the *Climacograptus caudatus* sub-zone of the *D. clingani* Biozone; *L. harknessi* and the other identifiable genera also occur in this interval. This assemblage is also known from the St. Cynllo's Slate Formation of the Rhayader district (Davies *et al.* 1997), which is likely to be a lateral equivalent.

Chitinozoans also occur, including an extremely large *Rhabdotheca*? sp., (over 2 mm) apparently undescribed but similar to *R*? *minnesotensis* (Stauffer) and *Conochitina elegans* Eisenack (Jenkins 1967, 1969). Both of these are referred to the Caradoc, of Oklahoma and Ludlow respectively. Smaller *Conochitina* species are also present.

### 1.3.3 Capel Curig, Gwynedd

#### 1.3.3.1 Regional Geology

Following the Llanvirn volcanic episode of the southern Welsh Basin, the Lower-Middle Caradoc was marked by abundant explosive and effusive volcanism in North Wales, in a broad corridor from Lleyn to Capel Curig (Fig. 1.3.11). The source composition varied from basaltic to rhyolitic, with products emplaced through submarine, and probably subaerial eruptions (Rast *et al.* 1958). The origin of the major volcanic deposits is disguised by alteration, recrystallisation and tectonic deformation, in most cases preventing definitive establishment of the mode of

emplacement. However, most of the volcanics appear to be thick ash-flow deposits, including the Capel Curig Formation (Howells and Leveridge 1980), the Crafnant Volcanic Formation (Howells *et al.* 1973), and the Snowdon Volcanic Formation. Basaltic eruptions were restricted to the basinal regions between volcanic cones.

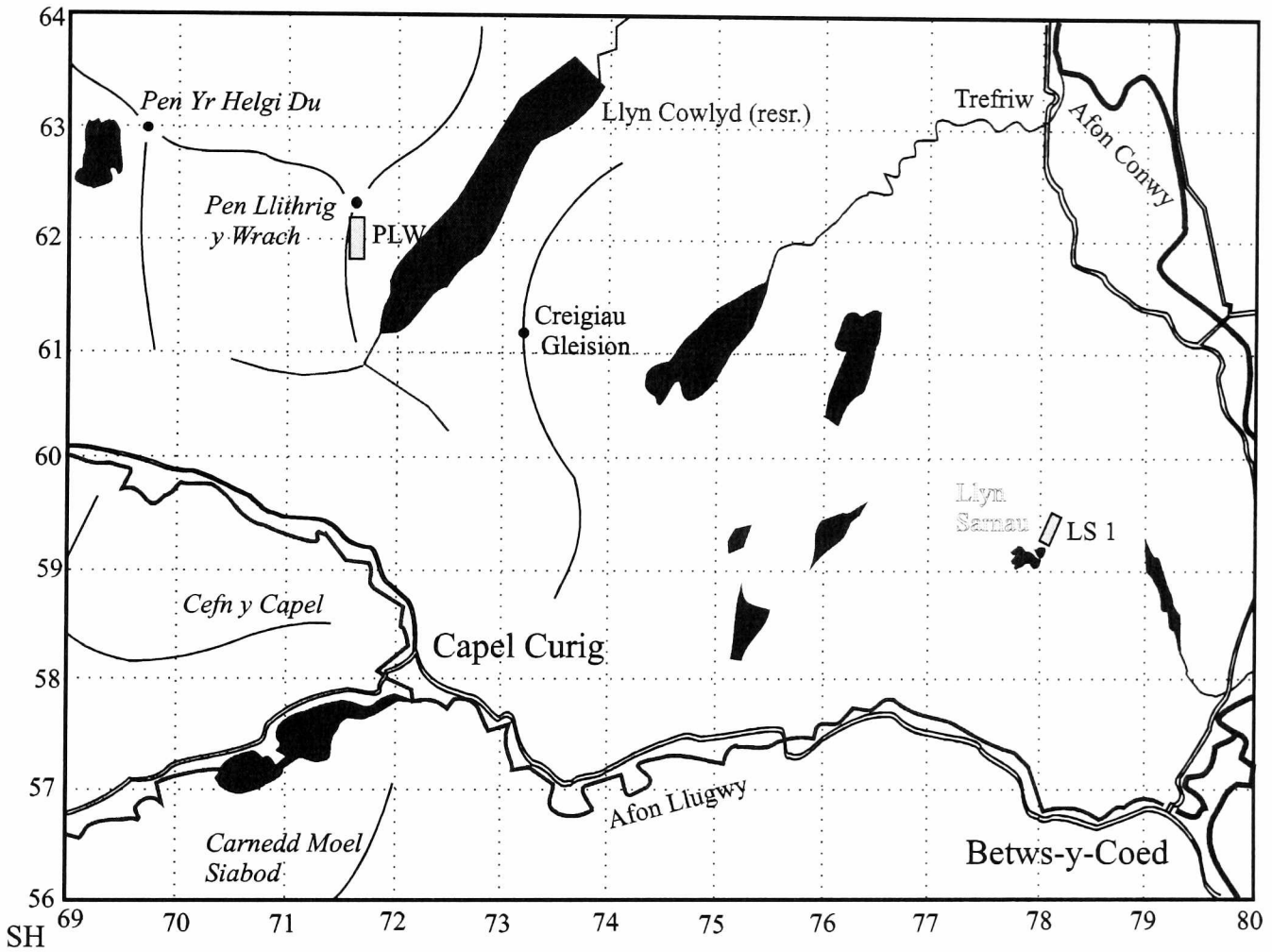


Fig. 1.3.13: *Location map for sites PLW 1 and LS 1, in the Capel Curig region of North Wales. Scale: 1 km grid.*

Substantial intrusive rocks are associated with the volcanics; these were dominated by dolerites, including numerous quartz- and albite-dolerite dykes (Smith and George 1961). Intercalated with the igneous rocks are variable thicknesses of graptolitic slates and subordinate sandstones containing shelly faunas. In some places, such as the lower Rhyolitic Tuffs of Moel Siabod, pebble beds indicate nearby emergence.

The volcanics are interpreted as having dominantly arc characteristics (Bevins *et al.* 1984), despite being approximately 100 km southeast of the primary Lake District – Leinster arc development. It is possible that this reflects a change in the angle of subduction, allowing a secondary arc complex to develop. The rarity of arenaceous deposits implies steep submarine gradients, compatible with an immature arc setting. The associated faunas are dominantly graptolitic, suggesting anoxic deep waters. In rarer shelly faunas, brachiopods and trilobite fragments dominate; crinoids, ostracodes and molluscs are rare. The shelly deposits are almost entirely transported, restricted to dense fragmental bands, well exposed at various sites between Capel Curig and Betws-y-Coed. The only demonstrably *in situ* shelly community is that exposed in fine sandstones on the east face of Pen Llithrig-y-Wrach, northwest of Capel Curig, where at least two pavements of *Plaesiomys multifida*? are preserved with articulated valves in vertical orientation. Further shelly faunas occur on the Ricks and Racks (Capel Curig) and on the north ridge of Tryfan, while others have been reported by Romano and Diggens (1970) from Dolwyddelan.

Throughout the Llanvirn and lower Caradoc of Snowdonia occur thin, laterally restricted pisolitic ironstones (Pulfrey 1933; Smith and George 1973). Most are fossiliferous, including abundant sponge spicules within phosphatic nodules. At Aber and Lleyn, Trythall *et al.* (1987) reported the presence of stromatolitic crustal growths (implying shallow water, within the photic zone) and phosphatised sponges. Vavrdova (1999) reported similar iron ores from the Ordovician of Bohemia, invoking overturning of a stratified water column for their formation, with the upwelling of iron-rich deep waters. Possible sources of such overturning include severe storms, and deposition of ash-fall tuffs (see chapter 3).

1.3.3.2 Stratigraphy

The North Wales geology comprises a semi-complete succession of Cambrian to Silurian sediments with extensive, episodic volcanism. The Capel Curig region is dominated by the largely conformable (Howells *et al.* 1973, p. 30) lower Caradoc Crafnant Volcanic Series and associated siliciclastics (Fig. 1.3.14). Contemporaneous limestones occur 5 km to the south. The Lower Crafnant Tuff is underlain by the Lower Rhyolitic Tuff Formation, which includes large rounded pebbles at Moel Siabod. The Lower Crafnant Tuff comprises three main volcanic units, described in detail by Howells *et al.* (1973), interspersed with slates, siltstones and sandstones. Diggens and Romano (1968) described the sequence around Llyn Cowlyd, the location of section PLW 1. The volcanic units are primarily distinguished on petrological observations, and by their relative positions in the field. The Crafnant Tuffs appear to be a lateral continuation of the Snowdon Volcanic Group.

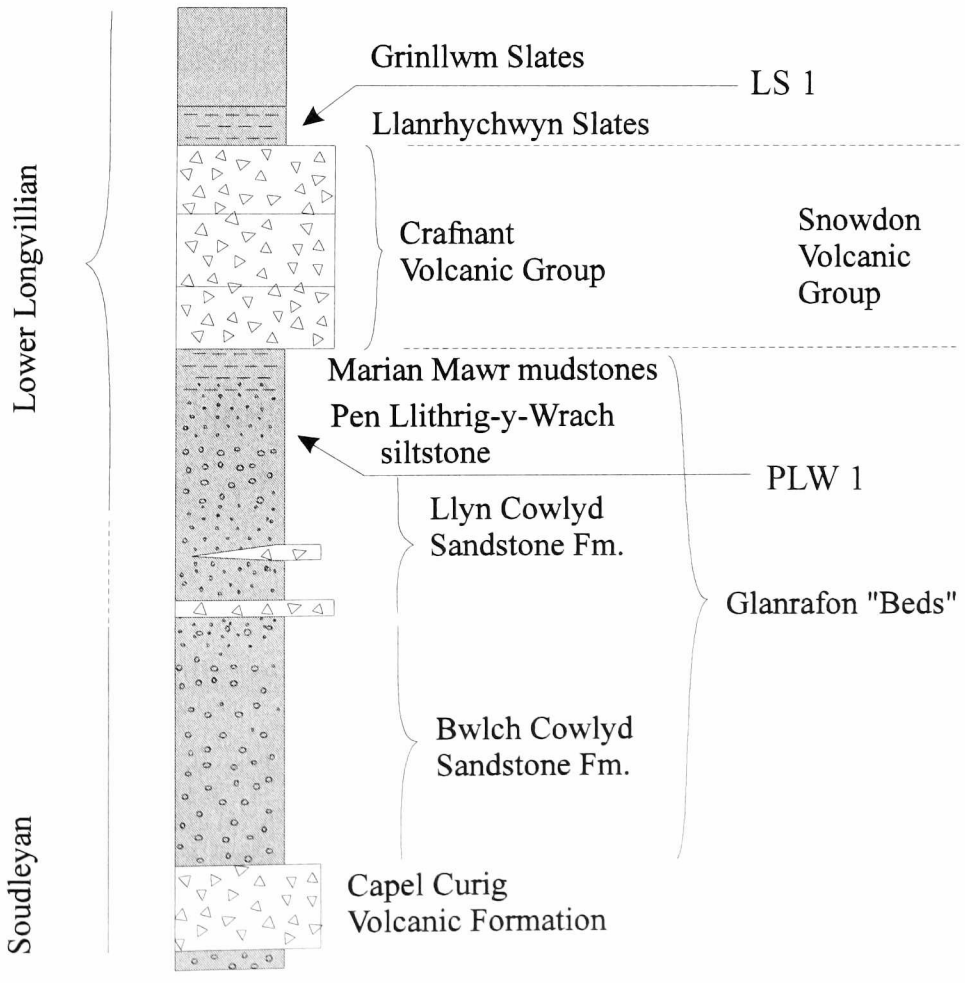


Figure 1.3.14: *Schematic stratigraphy of the Capel Curig district of North Wales, based on Howells* et al. *(1978) and Diggens and Romano (1968).*

Overlying the Crafnant volcanics is a succession of cleaved mudstones, the Black Slates of Llanrwchwyn and Dolwyddelan. Biostratigraphic data are available from graptolites, and to a lesser extent from shelly faunas. The graptolites indicate a position in the *D. multidens* Biozone (Williams and Bulman 1931), but more specific diagnosis has not been possible. Graptolites collected during this research were too poorly preserved for species-level identification. Brachiopods from the Snowdon Volcanic Formation and the underlying Glanrafon Beds confirm a Longvillian (possibly Soudleyan), Lower-Middle Caradoc age (Romano and Diggens 1970). The Pen Llithrig-y-Wrach Siltstone Formation, which contains section PLW 1, was attributed to the Lower Longvillian (Diggens and Romano 1968), based on trilobites.

## 1.4 References


Anderton, R., Bridges, P. H., Leeder, M. R. and Sellwood, B. W. 1979. *A dynamic stratigraphy of the British Isles*. Unwin Hyman, London; 301 pp.

Batchelor, R. A. and Clarkson, E. N. K. 1993. Geochemistry of a Silurian metabentonite and associated apatite from the North Esk Inlier, Pentland Hills. *Scottish Journal of Geology* **29**, 123-130.

Bevins, R. E., Kokelaar, B. P., and Dunkley, P. N. 1984. Petrology and geochemistry of lower to middle Ordovician rocks in Wales: a volcanic arc to marginal basin transition. *Proceedings of the Geologists' Association* **95**, 333-437.

Bogaard, P. v. d. 1983. Die eruption des Laacher See Vulcans. *Ruhr University Bochum Ph. D. dissertation*, 348 pp.

Botting, J. P. and Thomas, A. T. 1999. A pseudoplanktonic inarticulate brachiopod attached to graptolites and algae. *Acta Universitatis Carolinae: Geologica* **43**, 333-335.

BRENCHLEY, P. J., AND PICKERILL, R. K. 1993. Animal-sediment relationships in the Ordovician and Silurian of the Welsh Basin. *Proceedings of the Geologists' Association* **104**, 81-93.

BRITISH GEOLOGICAL SURVEY 1994. *The rocks of Wales; geological map of Wales,* Her Majesty's Stationery Office, London.

BURSIK, M. I., MELEKESTSEV, I. V. AND BRAITSEVA, O. A. 1993. Most recent fall-deposits of Ksudach Volcano, Kamchatka, Russia. *Geophysical Research Letters* **20**, 1815-1818.

BUTLER, A. 1998. Acquisition and utilization of transition metal ions by marine organisms. *Science* **281**, 207-210.

CAREY, S. N. AND SIGURDSSON, H. 1980. The Ruseau Ash: deep-sea tephra deposits deposits from a major eruption on Dominica, Lesser Antilles. *Journal of Volcanology and Geothermal Research* **7**, 67-86.

CARPENTER, S. R., CHISHOLM, S. W., KREBS, C. J., SCHINDLER, D. W. AND WRIGHT, F. W. 1995. Ecosystem experiments. *Science* **260**, 324-327.

CAVE, R. AND RUSHTON, A. W. A. 1996. The Llandeilo (Ordovician ) Series in the core of the Tywi Anticline, Llanwrtyd, Powys, UK. *Geological Journal*, **31**, 47-60.

CLARKSON, E. N. K. AND HOWELLS, Y. 1981. Upper Llandovery trilobites from the Pentland Hills, near Edinburgh. *Palaeontology* **24**, 507-536.

COPE, J. C. W. 1999. Middle Ordovician bivalves from Mid-Wales and the Welsh borderland. *Palaeontology* **42**, 467-499.

COPE, J. C. W., INGHAM, J. K. AND RAWSON, P. F. 1992. Atlas of palaeogeography and lithofacies. *The Geological Society of London Memoir* **13**, 153 pp.

COURTILLOT, V. 1990. Deccan volcanism at the Cretaceous-Tertiary boundary: past climatic crises as a key to the future. *Palaeogeography, palaeoclimatology, palaeoecology* **189**, 291-299.

DAVIES, J. R., FLETCHER, C. J. N., WATERS, R. N., WILSON, D., WOODHALL, D. G. AND ZALASIEWICZ, J. A. 1997. *Geology of the country around Llanilar and Rhayader*, British Geological Survey, The Stationery Office, London.

DAVIES, K. A. 1933. The geology of the country between Abergwesyn (Breconshire) and Pumpsaint (Carmarthenshire). *Quarterly Journal of the Geological Society* **89**, 172-201, 2 pl.

DIGGENS, J. N. AND ROMANO, M. 1968. The Caradoc rocks around Llyn Cowlyd, North Wales. *Geological Journal* **6**, 31-48.

DONOVAN, S. K. AND GALE, A. S. 1989. *Iocrinus* in the Ordovician of England and Wales. *Palaeontology* **32**, 313-323.

DORAVA, J. M. AND MILNER, A. M. 1999. Effects of recent volcanic eruptions on aquatic habitat in the Drift River, Alaska, USA: implications at other Cook Inlet region volcanoes. *Environmental Management* **23**, 217-230.

ELLES, G. L. 1939. The stratigraphy and faunal succession in the Ordovician rocks of the Builth-Llandrindod Inlier, Radnorshire. *Quarterly Journal of the Geological Society* **95**, 338-445.

ELLES, G. L. AND WOOD, E. M. R. 1901-1918. A Monograph of British Graptolites. *Monograph of the Palaeontolographical Society, London.*

EPSTEIN, A. G., EPSTEIN, J. B., AND HARRIS, L. D. 1977. Conodont colour alteration – an index to organic metamorphism. *United States geological Survey Professional Paper* **995.**

FALKOWSKI, P. G., BARBER, R. T. AND SMETACEK, V. 1998. Biogeochemical controls and feedbacks on Ocean Primary Productivity. *Science* **281**, 200-206.

FISHER, R.V. AND SCHMINCKE, H.-U. 1984. *Pyroclastic Rocks*. Springer-Verlag, Berlin, 472 pp.

FORTEY, R. A., HARPER, D. A. T., INGHAM, J. K., OWEN, A. W. AND RUSHTON, A. W. A. 1995. A revision series and stages from the historical type area. *Geological Magazine* **132**, 15-30.

FORTEY, R. A., HARPER, D. A. T., INGHAM, J. K., OWEN, A. W. AND RUSHTON, A. W. A. 2000. A revised correlation of Ordovician rocks in the British Isles. *Geological Society Special Report* **5**, 83 pp.

FORTEY, R. A. AND OWENS, R. M. 1978. Early Ordovician (Arenig) stratigraphy and faunas of the Carmarthen district, south-west Wales. *Bulletin of the British Museum of Natural History (Geology)* **30**, 225-294.

FORTEY, R. A. AND OWENS, R. M. 1987. The Arenig Series in South Wales. *Bulletin of the British Museum of Natural History (Geology)* **41**, 69-307.

FURNES, H. 1978.*Unpublished Ph. D. thesis.* University of Oxford.

GALLARDO, V. A., CASTILLO, J. G., RETAMAL, M. A., YANEZ, A., MOYANO, H. I. AND HERMOSILLA, J. G. 1977. Quantitative studies on the soft-bottom macrobenthic animal communities of shallow Antarctic bays. *In* LLANO, G.A. (ed.): *Adaptations within Antarctic ecosystems (Proceedings of the 3rd SCAR Symposium on Antarctic Biology),* Smithsonian Institution, Washington D.C., pp. 361-387.

GEORGE, T. N. 1970. *British Regional Geology: South Wales*. Institute of Geological Sciences, London. 152 pp.

GLAZE, L. S. AND SELF, S. 1991. Ashfall dispersal for the 16th September 1986, eruption of Lascar, Chile, calculated by a turbulent diffusion model. *Geophysical Research Letters* **18**, 1237-1240.

HARPER, D. A. T. AND OWEN, A. W. 1996. Stratigraphy. *In:* Harper, D.A.T. and Owens, A.W. (eds.): *Fossils of the Upper Ordovician.* The Palaeontological Association, London, 1st ed., p. 25.

HARPER, D. A. T., MAC NIOCAILL, C. AND WILLIAMS, S. H. 1996. The palaeogeography of early Iapetus terranes: an integration of faunal and palaeomagnetic constraints. *Palaeogeography, palaeoclimatology, palaeoecology*, **121**, 297-312.

HEIKOOP, J. M., TSUJITA, C. J., HEIKOOP, C. E., RISK, M. J. AND DICKIN, A. P. 1997. Effects of volcanic ashfall recorded in ancient marine benthic communities: comparison of a nearshore and an offshore community. *Lethaia* **29**, 125-139.

HILDRETH, W. AND DRAKE, R. E. 1992. Volcán Quizapu, Chilean Andes. *Bulletin of Volcanology* **54**, 93-125.

HOWELLS, M. F., AND LEVERIDGE, B. E. 1980. The Capel Curig Volcanic Formation. *Institute of Geological Sciences Report*, **80/6**, 16 pp., 7 pl.

HOWELLS, M. F., LEVERIDGE, B. E. AND EVANS, C. D. R. 1973. Ordovician ash-flow tuffs in eastern Snowdonia. *Institute of Geological Sciences Report*, **73/3**, 33 pp., 8 pl.

HOWELLS, M. F., LEVERIDGE, B. E., EVANS, C. D. R. AND NUTT, M. J. C. 1981. *Dolgarrog: Description of 1:25000 Geological Sheet SH 76.* Classical areas of British geology, Institute of Geological Sciences, London: Her Majesty's Stationery Office.

HUFF, W. D., MERRIMAN, R. J., MORGAN, D. J. AND ROBERTS, B. 1993. Distribution and tectonic setting of Ordovician K-bentonites in the United Kingdom. *Geological Magazine***130**, 93-100.

HUGHES, C. P. 1969. Ordovician trilobite faunas from central Wales (Part I). *Bulletin of the British Museum of Natural History (Geology)* **18**, 39-103.

HUGHES, C. P. 1971. Ordovician trilobite faunas from central Wales (Part II). *Bulletin of the British Museum of Natural History (Geology)* **20**, 115-182.

HUGHES, C. P. 1979. Ordovician trilobite faunas from central Wales (Part III). *Bulletin of the British Museum of Natural History (Geology)* **32**, 109-181.

HUGHES, R. A. 1989. Llandeilo and Caradoc graptolites of the Builth and Shelve inliers. *Palaeontographical Society of London Monograph* **141**, 89 pp., 5 pl.

HURST, J. M. 1979. Evolution, succession and replacement in the type upper Caradoc (Ordovician) benthic faunas of England. *Palaeogeography, Palaeoclimatology, Palaeoecology* **27**, 189-246.

JAVOY, M. AND COURTILLOT, V. 1989. Intense acidic volcanism at the Cretaceous-Tertiary boundary. *Earth and Planetary Science Letters* **94**, 409-416.

JENKINS, W. A. M. 1967. Ordovician Chitinozoa from Shropshire. *Palaeontology* **10**, 436-488.

JENKINS, W. A. M. 1969. Chitinozoa from the Ordovician Viola and Ferndale Limestones of the Arbuckle Mountains, Oklahoma. *Special Papers in Palaeontology* **5**, 44 pp., 9 pl.

JONES, O. T. 1949. The geology of the Llandovery district II: the northern area. *Quarterly Journal of the Geological Society* **105**, 43-64, 1 pl.

JONES, O. T., AND PUGH, W. J. 1941. The Ordovician rocks of the Builth district. *Geological Magazine* **78**, 185-191.

JONES, O. T. AND PUGH, W. J. 1946. The complex intrusion of Welfield, near Builth Wells, Radnorshire. *Quarterly Journal of the Geological Society* **102**, 157-188.

JONES, O. T. AND PUGH, W. J. 1948a. The form and distribution of dolerite masses in the Builth-Llandrindod inlier, Radnorshire. *Quarterly Journal of the Geological Society* **95**, 71-98.

JONES, O. T. AND PUGH, W. J.1948b. A multi-layered dolerite complex of laccolithic form, near Llandrindod Wells, Radnorshire. *Quarterly Journal of the Geological Society* **95**, 43-70.

JONES, O. T. AND PUGH, W.J. 1949. An Early Ordovician shoreline in Radnorshire, near Builth Wells. *Quarterly Journal of the Geological Society* **104**, 43-70.

KENNEDY, R. J. 1989. Ordovician (Llanvirn) trilobites from SW Wales. *Monograph of the Palaeontographical Society, London*, 55 pp, 14 pl.

LOCKLEY, M. G. 1980. The Caradoc faunal associations of the area between Bala and Dinas Mawddy, North Wales. *Bulletin of the British Museum of Natural History* (Geology) **33**, 165-235.

LOCKLEY, M. G. 1983. A review of brachiopod-dominated palaeocommunities from the type Ordovician. *Palaeontology* **26**, 111-145.

LOCKLEY, M. G. 1984. Faunas in a volcaniclastic debris flow from the Welsh Basin: a synthesis of palaeoecological and volcanological observations. *In* BRUTON, D.L. (ed.), 1984. *Aspects of the Ordovician System*, 195-201. Palaeontological Contributions from the University of Oslo, No. **295**, Universitetsforleget.

LOCKLEY, M. G. AND ANTIA, D. D. J. 1980. Anomalous occurrence of the Lower Palaeozoic brachiopod *Schizocrania*. *Palaeontology* **23**, 707-713.

LOCKLEY, M. G., AND WILLIAMS, A. 1981. Lower Ordovician Brachiopoda from mid and southwest Wales. *Bulletin of the British Museum of Natural History (Geology)* **34**, 1-78.

LYNAS, B. D. T. 1983. Two new Ordovician volcanic centres in the Shelve Inlier, Powys, Wales. *Geological Magazine* **120**, 535-542.

MCKERROW, W. S., DEWEY, J. F., AND SCOTESE, C. R. 1991. The Ordovoician and Silurian development of the Iapetus Ocean. *Special Papers in Palaeontology* **44**, 165-78.

MILLER, A. I. 1997. Dissecting global diversity patterns: examples from the Ordovician Radiation. *Annual Review of Ecology and Systematics* **28**, 85-104.

NEAL, M. L. AND HANNIBAL, J. T. 2000. Paleoecologic and taxonomic implications of *Sphenothallus* and *Sphenothallus*-like specimens from Ohio and areas adjacent to Ohio. *Journal of Paleontology* **74**, 369-380.

PEARCE, J. A., HARRIS, N. B. W. AND TINDLE, A. G. 1984. Trace element discrimination diagrams for the tectonic interpretation of granitic rocks. *Journal of Petrology* **25**, 956-83.

PERALTA, S. AND BERESI, M. 1999. Fossil assemblages and K-bentonite beds from the Upper Member of the San Juan Formation (Early Ordovician) Villicum Range, Precordillera, Argentina. *Acta Universitatis Carolinae: Geologica* **43**, 495-497.

PHILLIPS, W. E. A., STILLMAN, C. J., AND MURPHY, T. 1976. A Caledonian plate tectonic model. *J. Geol. Soc. London* **132**, 579-609.

PICKERILL, R. K. 1977. Trace fossils from the Upper Ordovician (Caradoc) of the Berwyn Hills, Central Wales. *Geological Journal* **12**, 1-16.

PICKERILL, R. K. AND BRENCHLEY, P. J. 1979. Caradoc marine benthic communities of the south Berwyn Hills, North Wales. *Palaeontology* **22**, 229-264.

PORTER, S. C. 1973. Stratigraphy and chronology of the late Quaternary tephra along the South Rift Zone of Mauna Kea volcano, Hawaii. *Geological Society of America Bulletin* **84**, 1923-1940.

PULFREY, W. 1933. Note on the occurrence of sponge spicules associated with the iron-ores of North Wales. *Annals and Magazine of Natural History* series 10, **11**, 67-76, 1 pl.

RAST, N., BEAVON, R. V. AND FITCH, F. J. 1958. Sub-aerial volcanicity in Snowdonia. *Nature* **181**, p. 508.

RHOADES, D. C. AND MORSE, J. W. 1971. Evolutionary and ecologic significance of oxygen-depleted marine basins. *Lethaia*, **4**, 413-428.

ROMANO, M. AND DIGGENS, J. N. 1970. Longvillian shelly faunas from the Dolwyddelan area, North Wales. *Geological Magazine* **106**, 603-606.

RUSHTON, A. W. A. 1990. Ordovician graptolite biostratigraphy in the Welsh Basin - a review. *Journal of the Geological Society of London* **147**, 611-614.

SHELDON, P. R. 1987a. Trilobite evolution and faunal distribution in some Ordovician rocks of the Builth Inlier, Central Wales. *Ph. D. Thesis, University of Cambridge*.

SHELDON, P. R. 1987b. Parallel gradualistic evolution of Ordovician trilobites. *Nature* **330**, 561-563.

SMITH, B. AND GEORGE, T. N. 1961. *British regional geology: North Wales*. Her Majesty's Stationery Office, London, 98 pp, 12 pl.

SMITH, T. E., AND HUANG, C. H. 1995. Geochemistry and petrogenesis of the igneous rocks of the Builth-Llandrindod Ordovician Inlier, Wales. *In* R. K.

SRIVASTARA AND R. CHANDRA (eds.), *Magmatism in relation to diverse tectonic settings*. A. A. Bolkema, Rotterdam.

SOJA, C. M., GOBETZ, K. E., THIBEAU, J., ZAVALA, E. AND WHITE, B. 1996. Taphonomy and palaeobiological implications of Middle Devonian (Eifelian) nautiloid concentrates, Alaska. *Palaios* **11**, 422-436.

STAMP, L. D. AND WOOLDRIDGE, S. W. 1923. The igneous and associated rocks of Llanwrtyd (Brecon). *Quarterly Journal of the geological Society* **74**, 16-46, 2 pl.

STILLMAN, C. J. 1984. Ordovician volcanicity. *In* BRUTON, D.L. (ed.) *Aspects of the Ordovician System*, Palaeontological contributions from the University of Oslo No. 295, Universitetsforlaget, pp. 183-194.

SUTHREN, R. J. AND FURNES, H. 1980. Origin of some bedded welded tuffs. *Bulletin of Volcanology* **43,** 61-71.

SUTTON, M. D., BASSETT, M. G. AND CHERNS, L. 1999. Lingulate brachiopods from the Lower Ordovician of the Anglo-Welsh Basin, Part 1. *Monograph of the Palaeontographical Society*, London.

SUTTON, M. D., BASSETT, M. G. AND CHERNS, L. *in press*. Lingulate brachiopods from the Lower Ordovician of the Anglo-Welsh Basin, Part 2. *Monograph of the Palaeontographical Society*, London.

SWAIN, F. M. 1996. Ostracode speciation following Middle Ordovician extinction events, north central United States. *In* Hart, M.B. (ed.) *Biotic Recovery from Mass Extinction Events,* Geological Society Special Publication **102**, pp. 97-104.

TASCH, P. 1955. Palaeoecologic observations on the orthoceratid coquina beds of the Maquoketa at Graf, Iowa. *Journal of Paleontology* **29**, 510-518.

TIPPER, J. C. 1976. The stratigraphy of the North Esk Inlier, Midlothian. *Scottish Journal of Geology* **12**, 15-22.

TORSVIK, T. H., AND TRENCH, A. 1991. The Ordovician history of the Iapetus Ocean in Britain: new palaeomagnetic constraints. *Journal of the Geological Society, London*, **148**, 423-425.

TRENCH, A., TORSVIK, T. H., SMETHURST., M. A., WOODCOCK, N. H. AND METCALF., R. 1991. A palaeomagnetic study of the Builth Wells—Llandrindod Wells Ordovician inlier, Wales: palaeogeographic and structural implications. *Geophysical Journal International*, **105**, 477-489.

TRYTHALL, R. J. B., ECCLES, C., MOLYNEUX, S. G. AND TAYLOR, W. E. G. 1987. Age and controls of ironstone deposition (Ordovician) North Wales. *Geological Journal* **22**, 31-43.

VAN ITEN, H., FITZKE, J. A. AND COX, R. S. 1996. Problematical fossil cnidarians from the Upper Ordovician of the north-central USA. *Palaeontology* **39**, 1037-1062.

VAVRDOVÁ, M. 1999. The acritarch succession in the Klabava and Sarka formations (Arenig – Llanvirn): evidence for an ancient upwelling zone. *Acta Universitatis Carolinae: Geologica* **43**, 263-265.

WATKINS, R. AND BERRY, W. B. N. 1977. Ecology of a Late Silurian fauna of graptolites and associated organisms. *Lethaia* **10**, 267-286.

WATKINS, N. D., SPARKS, R. S. J., SIGURDSSON, H., HUANG, T. C., FEDERMAN, A., CAREY, S. AND NINKOVICH, D. 1978. Volume and extent of the Minoan tephra from Santorini: new evidence from deep-sea sediment cores. *Nature* **271**, 122-126.

WESTERMANN, G. 1973. Strength of concave septa and depth limits of fossil cephalopods. *Lethaia* **6**, 383-403.

WILLIAMS, A., LOCKLEY, M. G. AND HURST, J. M. 1981. Benthic palaeocommunities represented in the Ffairfach group and coeval Ordovician successions of Wales. *Palaeontology* **24**, 661-694.

WILLIAMS, A., STRAHAN, I., BASSETT, D. A., DEAN, W. T., INGHAM, J. K., WRIGHT, A. D. AND WHITTINGTON, H. B., 1976. *A correlation of Ordovician rocks in the British Isles.* Geological Society, London, 74 pp.

WILLIAMS, H. AND BULMAN, O. M. B. 1931. The geology of the Dolwyddelan Syncline. *Quarterly Journal of the Geological Society of London* **87**, 425-458.

WILLIAMS, H. AND GOLES, G. 1968. Volume of the Mazama ash-fall and the origin of Crater Lake Caldera. *In* Dole, H. M. (ed.), *Andesite Conference Guidebook*, Oregon State Department of Geological and Mineral Industry Bulletin **62**, 37-41.

WINCHESTER, J. A. AND FLOYD, P. A. 1977. Geochemical discrimination of different magma series and their differentiation products using immobile elements. *Chemical Geology* **20**, 325-343.

WOODCOCK, N. H. 1984. Early Palaeozoic sedimentation and tectonics in Wales. *Proceedings of the Geologists' Association of London* **95**, 323-335.

WOODCOCK, N. H. 1987. Kinematics of strike-slip faulting, Builth Inlier, Mid-Wales. *Journal of Structural Geology* **9**, 353-363.

# 2. PALAEOECOLOGY OF ASH DEPOSITION IN SANDSTONE FACIES

## 2.1 METHODOLOGY

### 2.1.1 Basic methods

The ecological successions within volcanogenic sandstones facies of Llandegley Rocks and Pen Lithrig y Wrach have been investigated through bulk sampling. All fossils visible to the naked eye were recorded, and identified as far as possible, in order to reconstruct life assemblages; data related to relative proportions and, where possible, absolute abundance. Material was collected in samples of typically 1-5 kg, larger for the better-exposed Llandegley Rocks material. Several factors dictated the selection of suitable sites:

1. Exposure of a clastic or epiclastic sequence, which must include a discrete volcaniclastic or pyroclastic deposit. Exposure must extend both above and below the tuff. Limited deformation of the beds is acceptable, although undesirable.
2. The tuff bed must have clear upper and lower boundaries, although some reworking of the upper surface is expected.
3. Separation of the clastic sequence into distinct beds is preferred, allowing confident correlation over small distances.
4. A benthic fauna must be developed, ideally diverse. The fauna must show evidence of *in situ* or very local provenance. Fragmentary, shell bed or strongly winnowed material is unsuitable for this analysis.
5. Intervals of consistent sedimentary character may allow abundance data to be employed in addition to relative proportions. In this case, the tuff upper boundary must be abrupt.

Initial inspection of the site was followed by designation of interval boundaries and vertical limits of the section. A lithological log was drawn, and a comprehensive search of talus for fossil specimens provided estimates of species diversity and taxonomic composition. This allowed fragmentary specimens from the logs to be more easily identified.

The precise thickness of each interval was not critical to the analysis, but was recorded for accurate reconstruction of the ecological log. Interval boundaries were chosen to coincide with lithological transitions where possible, and with bed boundaries in more homogeneous parts of the succession. Where based on cross-laminated bedding surfaces, the precise thickness of these intervals varied laterally.

Samples were extracted in sequence, initially with similar mass at each level; additional samples were subsequently taken from poorly fossiliferous horizons, in order to provide comparable abundance between horizons. Extraction was performed by inserting chisels between natural bedding planes or fractures, and striking laterally with a one-pound hammer to loosen large blocks. In some cases, a small crowbar was employed. The removal of large blocks limited the amount of damage to fossils exposed on slab surfaces; any specimens noticed on exposed surfaces were wrapped separately.

### 2.1.2 Analytical Techniques

The samples were analysed by initially breaking slabs along natural bedding planes with a small hammer, removing those with specimens, and trimming to the smallest practical size. The remainder was then broken on an anvil into fragments whose maximum dimensions were 10 mm, cubed; fragments below this size were generally

not broken further. The only exceptions were those blocks retained due to included fossils, which could be several centimetres in diameter (see 2.1.3 for bias evaluation).

Reconstruction of abundance data, even from articulated material, is at best approximate, because of the uncertainties of sorting, winnowing, bioerosion, multiple exuviae and diagenetic loss. By no means all organisms in a community will fossilise, even among mineralised taxa. Any inferences of absolute abundance, or comparisons between disparate sections of similar sedimentology, must be treated with caution. The best that can be achieved in shallow-water coarse clastics, deposited under varying sedimentological conditions, is to establish changes in taxonomic proportions over a short section. This assumes that the sample size is sufficient for confidence in the data, and that the taphonomic conditions allowed preservation of a constant proportion of individuals among easily fossilisable taxa.

If sedimentological and other evidence suggests comparable sedimentation rate and taphonomic conditions through the section, relative abundance may be cautiously utilised. In these cases, consistency of patterns should be looked for between similar sections.

For organisms with multi-element skeletons, consistent estimates of the number or represented individuals must be derived. A distinction should be drawn between the number of individuals from which the fragments were derived, and the inferred abundance of the taxon. For example, an isolated crinoid ossicle indicates the presence of a single crinoid, as a single brachiopod valve represents an individual. However, such a sample suggests that brachiopods are more abundant than crinoids, since far larger samples would be required to produce sufficient ossicles to imply more than one crinoid individual. Consequently, although ten isolated ossicles only prove the existence of one individual, the implication is that a sample containing ten

ossicles represents a higher abundance of crinoids than a sample yielding one ossicle. This interpretation is dependent on the assumption of extensive scattering, since ossicle density will otherwise be dependent on proximity to the organism.

Standard palaeoecological analysis is based on establishing how many individuals can be shown to have definitely existed, in order to produce the observed fragments, with the emphasis on avoiding over-estimation. In taxa with multiple moult exuviae, this has led to the use of large divisors of fragment numbers. Trilobites are the most widely discussed example (e.g. Lockley 1980). Estimates involve taking the most abundant fragment (e.g. pygidium) and dividing this by any number between one (Hurst 1979; Watkins 1979) and ten (after Harrington 1959) to represent instars and adult moults. Williams *et al.* (1981) and Lockley (1980) employed an intermediate divisor of 4. This estimates the number of individuals that are proven to have been present in the sample. Thus, if the divisor is four, then three pygidia represent one individual. One pygidium is also usually assumed also to represent one individual (e.g. Lockley 1980), rather than employing fractions. A significant amount of information can potentially be lost through this procedure, where relative abundance changes are ignored if represented by a small number of specimens. In some cases, quantitative methods were not fully described.

In the interpretation of abundance, allowance must be made for the thickness of the sample. Nine pygidia, separated vertically by several centimetres each, carry greater significance than a cluster of nine on one bedding plane. The former almost certainly represents nine individuals, whereas one or two may explain the latter. This principle relates to all multi-element skeletons, irrespective of moulting. Reworking is normally invoked to negate this aspect, effectively making the sampled beds into a single homogenised layer. The likelihood of this can only be estimated from

sedimentological information, such as lamination, bedding planes, evidence of hardground or stromatolitic colonisation, or changes in grain characteristics. In many published examples, sample thickness averaged five metres (Lockley 1983), which could not have been deposited in the lifetime of an individual organism. This difficulty was reduced by using an average sample thickness of 15 cm in the initial log.

In the case of crinoids, sponges and other extreme multi-element skeletons, the situation is more problematic. Crinoid ossicles and sponge spicules (where mentioned at all), in any abundance, are typically counted as either one individual, or as presence/absence data. Given the potential significance of these groups in palaeoecololgical interpretations, a method that dismisses evidence of substantial abundance is badly flawed.

For the reasons explained, the methods of calculating abundance of each taxon are summarised below:

*Brachiopods*. For each species, add greater of pedicle/brachial counts to half the indeterminate valve counts. Sum species for total brachiopods. If pedicle/brachial bias is due to winnowing, indeterminate valves should be divided according to the observed ratio. However, since taphonomic factors could make either valve more difficult to identify, the observed ratio may differ from that of the true preserved population.

*Bivalves*. For each species, add highest of left/right valve counts to half of indeterminate valve counts. Sum species for total bivalves.

*Nautiloids, gastropods*. For each species, sum numbers of complete individuals and apertural fragments.

*Trilobites*. For each species, sum articulated specimens plus the most abundant of identical fragments of subequal size. Although there may be several adult moults of identical size, trilobites are insuffiently abundant for serious overestimates to occur.

*Crinoids*. Sum articulated specimens, and add one individual for each additional species represented by isolated material. Since the fauna is non-diverse, overestimates should be slight.

*Other echinoderms*. Sum articulated or semi-articulated specimens of each species.

*Sponges*. Sum articulated specimens for each species, or count one for obvious dissociated spicules; where individual spicules are clearly derived from a separate species, an additional individual is inferred. Thin sections allow a quantitative treatment of the isolated spicule abundance.

*Graptolites*. Sum individual specimens.

*Encrusting bryozoans*. Sum individual specimens.

*Ramose bryozoans*. Sum articulated specimens, plus one for each species represented in fragmentary form; branch diameter variation may be established through articulated specimens collected from talus.

*Conodonts*. Note presence, and number of specimens. Since these are rare, and likely to be missed due to small size, a qualified presence-absence criterion is sufficient.

*All other taxa*. Sum individuals specimens of each species.

### 2.1.3 Bias Evaluation

Despite careful quantitative analysis, and consistent processing techniques, systematic and random errors will inevitably exist. Although numerical estimates for most of

these are very difficult or impossible to prescribe, qualitative or semi-quantitative recognition of the deviation from calculated results can be achieved. The following sections attempt to develop methods of minimising or recognising the known biases.

*Small size bias.* The use of 10 mm cubes as the practical upper size limit for sample fragmentation incorporates a bias against specimens with dimensions below this threshold. Taxa such as ostracodes, as well as small brachiopods and fragments, have an increasing probability of remaining unexposed with decreasing size. The probability may be easily calculated for a small spherical fossil of a given radius:

For $r<R$, $P=(R-r)^3/R^3$

P: Probability of not exposing a given fossil within a sample fragment

R: Radius of sample fragment (approximated to cube)

r: radius of fossil, approximated as a sphere or cube.

Hence, to reconstruct estimates of the genuine abundance, A, from observed abundance, O:

$P=(A-O)/A$

Therefore, $A=O/(1-P)$

based on uniform fragment size. The estimate may be enhanced by assuming a log-normal distribution of sample fragment radius, with a maximum of 10 mm, although this has not been adopted here. While this allows more accurate estimates of recognised taxa, the process will also increase the bias against small, rare taxa, which may remain unnoticed.

*Large size bias.* As a result of the retention of fossils, rather than complete destructive analysis, blocks containing large fossils may also contain smaller fossils

within the matrix, thus acting as a secondary bias against small taxa. In this case, however, there is no definable size limit to those that might be overlooked, although in reality the block size is restrictive. This is only normally significant with articulated crinoids or large sponges, but also occurs with blocks which cannot safely be trimmed due to numerous specimens. This effect is only likely to affect seriously samples LR (10-12), which are dominated by large demosponges.

*Multi-element biases*. Any dual- or multi-element skeleton is more likely to be recorded than a homogeneous whole of equal individual frequency. Although easily controlled among large sample sizes, in small data sets, the bias can become serious. The probabilities involved are dependent on associated faunas, and are not subject to *a priori* generalisation. However, they can be approached through exhaustive Monte Carlo techniques. The proportion of a given taxon within a faunal sample asymptotically approaches the true value with increasing sample size. Therefore, through plotting the sample proportion as collection proceeds, equilibrium will be progressively approached. Although the small sample sizes involved are insufficient for a single sequence to reveal reliable trends, the process can be repeated following randomisation of the order of collection. The repeated plotting of several randomised sequences reveals an asymptotic trend, which may be extrapolated to estimate accurate proportions. This allows consistency between samples of greatly differing sizes.

There are problems with this approach. Firstly, the accuracy of the final result is restricted by the accuracy of the observed total; however, since the random variations involved in the initial inaccuracy are in large part due to the effects that are here minimised, the result must be an improvement on original estimates. If

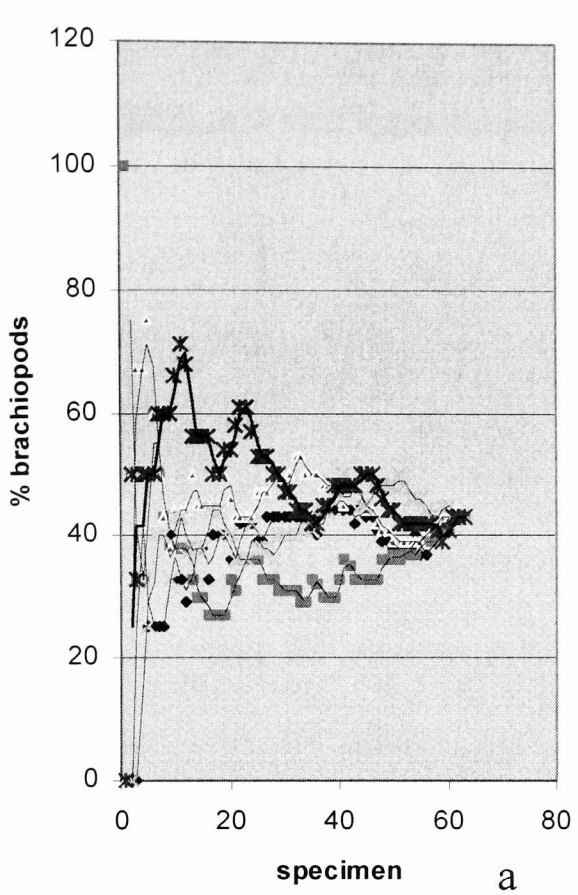


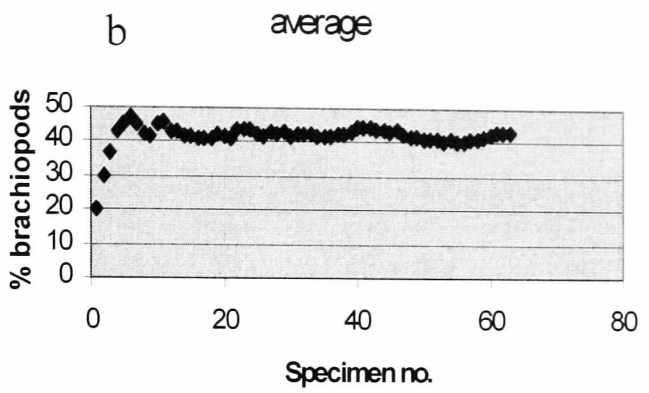


Figure 2.2.1: *Illustration of Monte Carlo techniques in estimating bias deriving from multi-element versus monopart skeletons: a, combined moving average plot of progressive brachiopod proportion over 5 randomised collection sequences; b, mean of the randomised data sets, showing rapidity of convergence to the observed value.*

equilibrium is reached quickly, this drawback is negated, since the influence of the total is minimal at early stages. Secondly, care must be taken where the number of small fragments of multi-part elements indicates more than one individual.

If any number of crinoid ossicles were taken as only one individual, then extrapolation of crinoid proportion to infinite sample sizes will result in zero abundance. The process is best applied in estimation of the relative proportions of brachiopods, trilobites, and monopart skeletons.

Equilibrium is approached much more rapidly, and with lower errors, where the taxon comprises a substantial proportion of both the total number of specimens and the reconstructed abundance data. The proportions of major groups may then be established accurately, and with reasonable confidence, while those of minor groups must be considered only approximate, even assuming a representative sample. Experimental use of this technique for brachiopods in the diverse fauna of sample LR 18 suggests that sample sizes in excess of thirty specimens, or twenty reconstructed individuals, provide proportional ratios correct to within approximately 5% (Fig.

2.1.1. A single moving average plot provides a moderately useful indication of true abundance, to within approximately 20%.

## 2.2 Llandegley Rocks, Builth Inlier

### 2.2.1 Local stratigraphy and lateral variation

Situated in the northeast corner of the Llandrindod Inlier, the Llandegley Rocks massif (Fig. 2.2.2) has been largely ignored. Elles (1939) described faunas from this area, including the stream section between Llandegley Rocks and Bwlch-y-Cefn; however, only the shales were studied in detail. Furnes (1978) interpreted the lithological succession, separating the lower and upper igneous developments (as below), although his interpretations of the upper volcanogenic sandstones as welded tuffs is not supported. Institute of Geological Sciences (1977) drew on work by O. T.

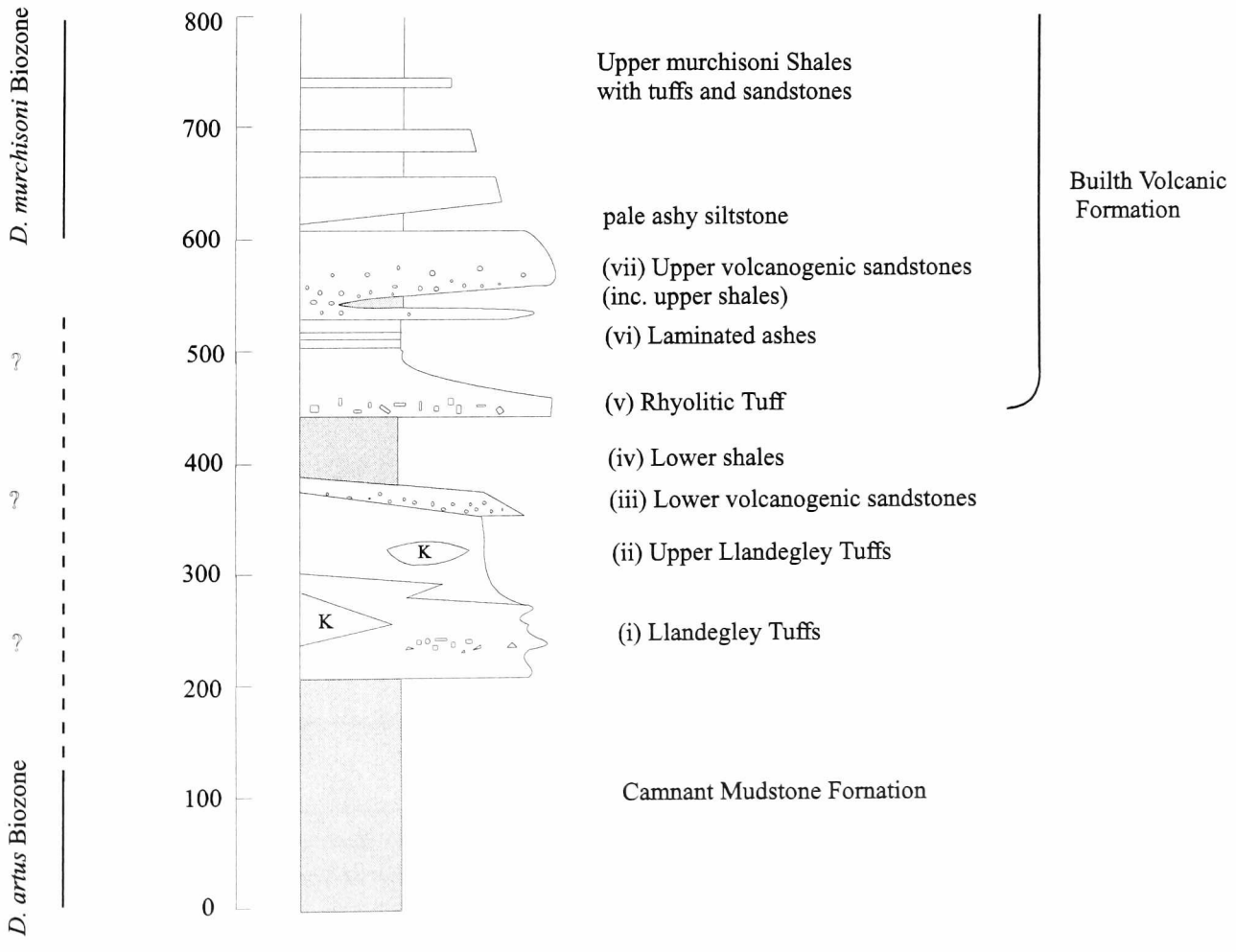


Figure 2.2.2: *Stratigraphic succession of the Llandegley Rocks area, using the definitions of Davies* et al. *1997. Terminology used here is not proposed formally, due to local variation and lack of data on traceable beds, but allows easier reference to the text. The geographical extent of the Llandegley Tuffs and overlying deposits is not clear, but their significance is usually underestimated. K: keratophyre intrusions.*

Jones and W. J. Pugh, but the Llandegley Rocks area appears to be otherwise unpublished.

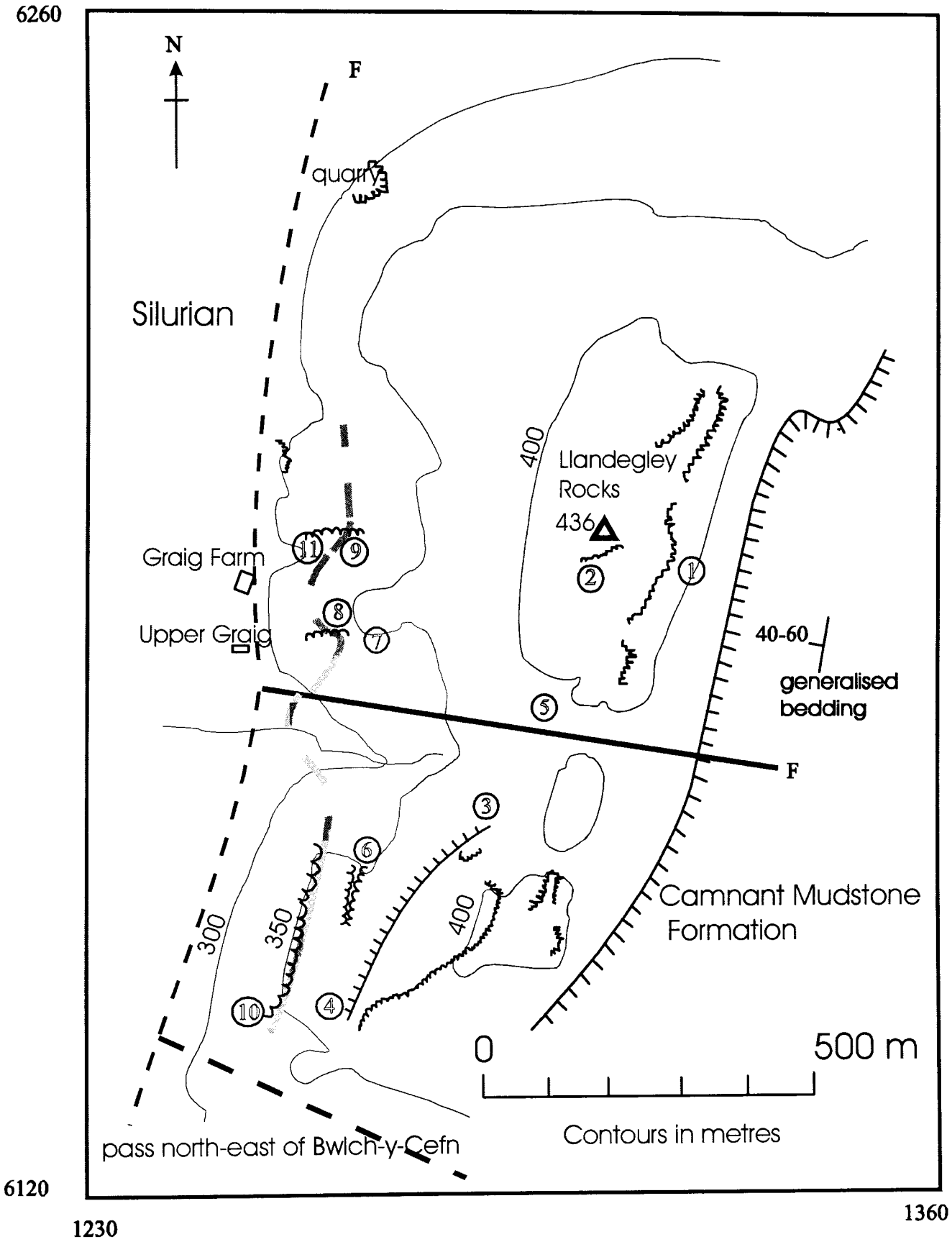


Figure 2.2.3: *Locality map of Llandegley Rocks, Builth Inlier, Powys; numbered localities are referred to in the text. Intermittent grey band indicates upper shale unit, in upper volcanogenic sandstones.*

The local succession is marked by extremely rapid lateral variation in lithology and fauna. Strike is consistent, structure simple, and good exposure allows much of the sequence to be studied in several locations. Numbers in brackets refer to localities in Fig. 2.2.3; unit numbers refer to those in Fig. 2.2.2.

i) "Llandegley Tuffs" of Institute of Geological Sciences (1977) (1), exposed as the eástern scarp overlying unexposed Camnant Mudstone Formation of Llandegley Rhos. Medium- to coarse-grained, blue-green granular volcanics with abundant plagioclase and some lithic clasts, lacking significant quartz or ferromagnesians. Grain size locally exceeding 10 mm, but typically less than 2 mm. The mode of emplacement is unclear, and the majority of beds may have been lavas (Furnes 1978). Occasional keratophyre intrusions, post-dating folding, some with columnar jointing.

ii) Upper part of "Llandegley Tuffs" (Institute of Geological Sciences 1977) (2), clearly differentiated by fine grain size. Generally pale green, flinty, homogeneous; includes relict hornblende and plagioclase, extensively albitised. Often shows complex distortion consistent with soft-sediment deformation. Consistent over observed range, reaching maximum exposed thickness at Mynyddrheol, previously considered an intrusion.

iii) Lower volcanogenic sandstones and ashes (3, 4, 5): crystal-rich medium sandstones, dominantly quartzofeldspathic, but including amphiboles and biotite. Locally fossiliferous, containing shallow-water articulate brachiopod and bivalve communities (4). At one location, the fauna, including trilobites, sponges and bryozoans, appears to be transported (3). Occasional thin shale bands (5), and keratophyic intrusions.

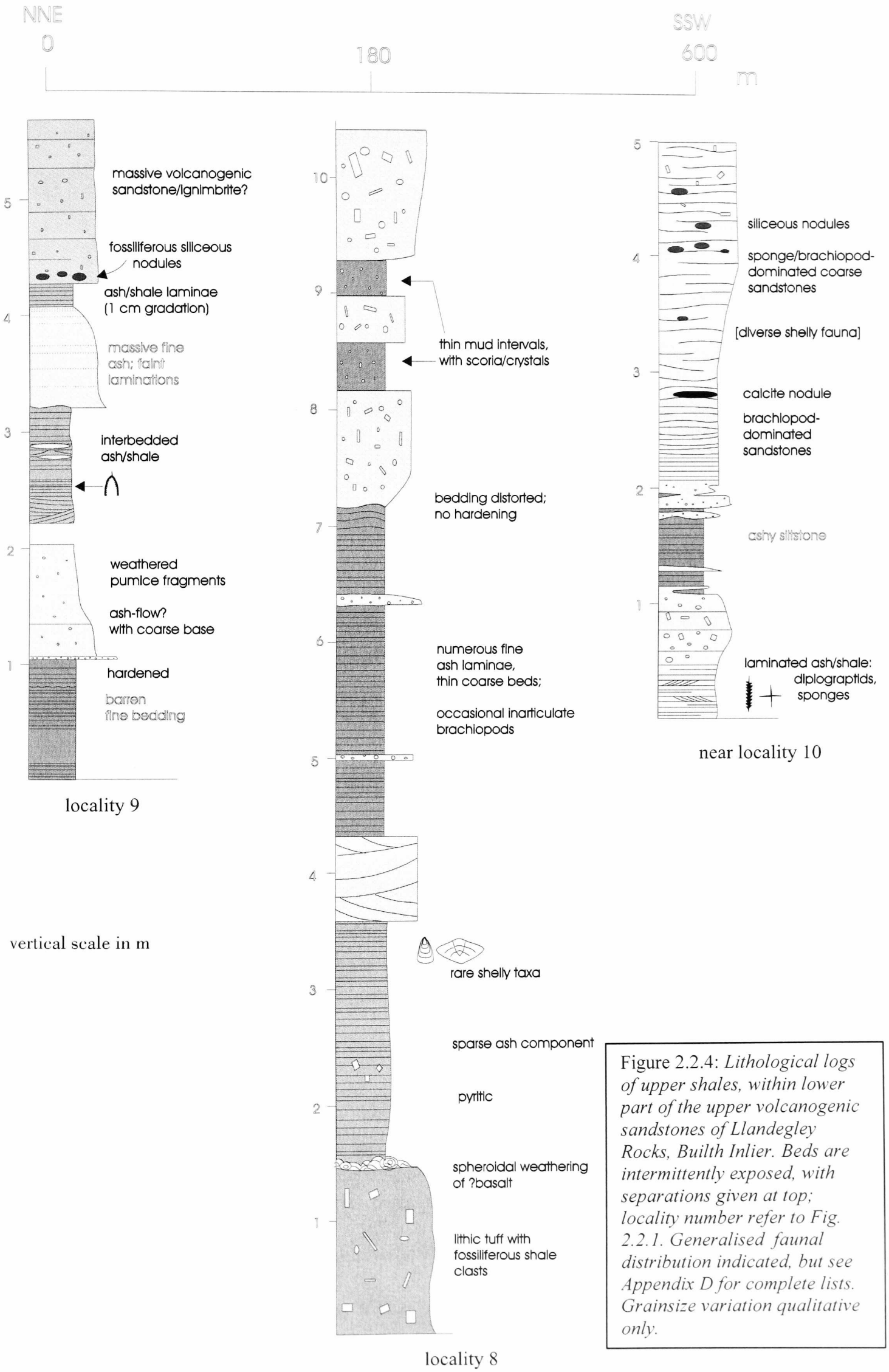


Figure 2.2.4: *Lithological logs of upper shales, within lower part of the upper volcanogenic sandstones of Llandegley Rocks, Builth Inlier. Beds are intermittently exposed, with separations given at top; locality number refer to Fig. 2.2.1. Generalised faunal distribution indicated, but see Appendix D for complete lists. Grainsize variation qualitative only.*

iv) Lower shales: largely unexposed siltstones and shales containing a sparse inarticulate brachiopod – trilobite fauna.

v) Rhyolitic tuff: "rhyolitic tuffs" of Institute of Geological Sciences (1977) (6), the "Llandegley Formation" of Suthren and Furnes (1980) and "rhyolitic ashes" of Jones and Pugh (1941, p. 16). Coarse crystalline tuff, fining upwards, frequently cross-bedded on small scale. Suthren and Furnes (1980) consider this unit to be a welded ash-flow tuff with a non-local source; the bed is recognisable throughout the Builth Inlier, with minor variation in thickness. However, exposures at Gelli Hill are strongly bedded, probably through reworking. This heterogeneity may reflect depositional conditions or source proximity.

vi) Laminated áshes (7): rhyolitic tuff at base grades into pale ashy siltstones, laminated with shales on 1 to 10 mm-scale. Primarily flat-laminated, with local asymmetric rippling. Commonly burrowed, and containing a sporadic graptolite fauna (spinose diplograptid reóåmbling *Orthograptus whitfieldi*), occasionally as concentrated beds. Hexactinellid sponge spicules abundant (*cf. Protospongia* Salter, *Triactinella* gen. nov.), very rare inarticulate brachiopods. Appear to comprise at least ten metres thickness, but exposure is extremely poor. Laminated beds are much reduced, but present at Gelli Hill.

vii) Upper shales (8, 9): thin silty shale within the basal fifteen metres of the upper volcanogenic sandstones (below); 0 to 12 m, with maximum thickness above Upper Graig (8). Contains frequent thin ash beds, including bentonites and

crystal tuffs. Limited fauna, comprising locally abundant *Apatobolus micula*, occasional trilobites (trinucleid, rhaphiophorid?, *Ogyginus corndensis*), and *Didymograptus artus* above Graig Farm (9). Micromorphic trace fossils occur on thin ash laminae, probably largely attributable to nematodes and small arthropods, but also including a micromorphic *Palaeodictyon*-like trace.

viii) Upper volcanogenic sandstones (10, 11): medium to very coarse quartzofeldspathic sandstone with abundant pumice shards; often pervasively silicified. Interpreted by Furnes (1978) as a welded tuff, the presence of brachiopods explained through their incorporation during deposition. While grain morphology is identical to modern ignimbrites, faunal distribution implies significant reworking, refuting pyroclastic deposition. Varies in character (Fig. 2.2.4) over short lateral distances, with possible lavas above Graig Farm. Diverse fauna near base, dominated by articulate brachiopods and sponges, but highly dependent on lateral position and local taphonomy. Above Graig Farm (11), fossils are primarily restricted to small siliceous nodules, containing a *Glyptorthis*-based assemblage that also includes *Pyritonema scopula*, crinoids, bryozoans and ostracodes. Rare mouldic brachiopods occur throughout the unit. Locality 10 contains section LR 1, and is the source of most of the material in chapters 4 and 6.

The upper part of the upper sandstones is poorly exposed, but contains massive tuffs and further, more substantial shale units in a disused quarry northeast of Graig Farm. This is comparable to the Howey Brook Main Feeder section, where shales gradually increase upwards, with sandstones eventually restricted to isolated beds. Pale ashy shales exposed in the pass south of

Llandegley Rocks appear in a similar context, but their position relative to the Llandegley Rocks exposures is uncertain. These are correlated with 1-4 m of similar lithology in the Gelli Hill section, and there comprise the lowest significant exposures of fine sediments above the laminated ashes.

The described sequence is best explained by the local development of two volcanic episodes. An initial coarse tuff/lava deposit (i), representing build-up of the cone, is overlain by a thick, calc-alkaline andesite (ii) from the primary eruptive episode, principally developed in the northern part of the inlier. This is followed by a succession of volcanogenic sandstones, grading upwards into siltstones. A second (and possibly distant) pyroclastic event, of rhyolitic magma, is followed by a quiescent episode of shallow-water deposition of shale/ash laminae, reflecting further rhyolitic eruptions or erosion of the underlying rhyolite. Massive, penecontemporaneous volcanism at Builth produced extensive erosional products, initially coarse volcanogenic sandstones, grading upwards into a silt-dominated environment (chapter 3). The northern sector displays relatively minor development of volcanics, but a thick sequence of erosional products.

The lateral thickness changes and rapid faunal transitions indicate high environmental gradients, typical of shoreface conditions (section 2.2.4). This is supported by grains exceeding 2 cm in diameter within the basal upper sandstones. The *Hesperorthis*-dominated brachiopod community is typical of shoreface conditions (Lockley 1983) while the Gl*yptorthis* community probably represents slightly deeper water. This is consistent with the erosion of an emergent region to the south.

In summary, the Llandegley Rocks succession records the successive evolution of two local volcanic cones, the first near Llandegley Rocks itself, and the

second at Builth, 8 km southwest. The cones were colonised by diverse shallow-water faunas during erosion, indicative of water depth; in the main (later) volcanic pulse, water depth increased northwards. The upper sequence resulted from eruption of the Builth Volcanics in the south, while the Llandegley Tuffs appear to be present only in the north. This suggests a southerly movement of the main volcanic centre following eruption of the Llandegley Tuffs.

### 2.2.2 Locality information

The primary fossiliferous site on Llandegley Rocks is the termination of the southwest ridge (GR SO 1252 6126). Fossils occur in the upper volcanogenic sandstones, immediately overlying the position of the upper shale unit, which is here reduced to negligable thickness. Outcrop is restricted to 1-2 m bedding slabs, parallel to the western scarp slope, and a small cutting through approximately 2 m of sandstones. Bedding orientation is 030/50 W. Extensive screes have developed below the outcrops, continuing for approximately 200 m northwards, although faunal diversity and preservation decline rapidly in this direction. Despite containing an abundant and obvious fauna, it has not previously been recorded as significantly fossiliferous, although Furnes (1978) mentioned the occurrence of brachiopods.

### 2.2.3 Sedimentology and taphonomy

The cutting through 2 m of fossiliferous sandstones has been extensively sampled in order to establish ecological, sedimentological and taphonomic patterns, summarised in Fig. 2.2.6. Sample thickness averaged 14.9 cm, with typically 6 to 15 kg sediment analysed, dependent on faunal abundance. The ecological sequence is summarised in Fig. 2.2.4. Although Furnes' (1978) interpretation as a welded pyroclastic flow is not

accepted, the immaturity of the volcanogenic sediment, and evidence for massive input are obvious.

Sedimentology is dominated by highly angular, often shardic or crystalline sandstones, with grainsize up to 20 mm, generally increasing upwards. Large clasts are dominantly scoriaceous, with occasional lithics; smaller grains domantly quartz and subeuhedral feldspar, with abundant scoriaceous bubble-wall shards, silicified. *Pyritonema* sponge spicules are volumetrically important in many beds, and typically distributed throughout the matrix; large aspicular demosponges comprise up to 20% volume of certain horizons.

Bedding planes are poorly preserved in coarse beds, and generally inconsistent throughout. Occasionally flat-bedded, but more usually showing low-angle cross-bedding, both symmetric and asymmetric, with amplitude up to 30 mm, and sometimes resembling interference rippling. Reworking by infauna was minimal, restricted to isolated sinuous burrows, 3-5 mm in diameter. Surface ichnofauna was largely destroyed by mechanical reworking, but is abundant at rare horizons. Thin (5-10 mm) tuffs occur through the succession, but are normally distorted by reworking; remnants occur in sample 16, with well-preserved tuffs in samples 2, and 8-10. No analyses are available, due to their extremely altered state, but the beds were contemporaneous with the nearby Builth Volcanics, which are assumed to represent the source region.

All horizons are pervasively silicified, with extremely rare, nodular calcite. Siliceous nodules, usually poikilitic, are very abundant in upper beds; lower beds generally lack nodules, but have fully silicified matrix. Originally calcitic organisms are almost entirely mouldic, with marginal silicification prior to dissolution of calcite, allowing unusual fidelity of surface detail. Breakage is rare, with an unusually high

proportion of articulated material, particuluarly sponges (chapter 4), echinoderms (chapter 6) and trilobites. Crinoids include preservation as mortality assemblages beneath bentonites, often flattened through both collapse and compaction. Limited winnowing is shown in bi-directional orientation of sponge spicules (Fig. 2.2.5), and in pedicle-dominated bias in the valve proportions of the strongly planoconvex *Hesperorthis*.

Replacement of proteinaceous sponge skeletons (*Pyritonema scopula* and *Palaeocallyoides improbablis* – see chapter 4) by silica represents a previously

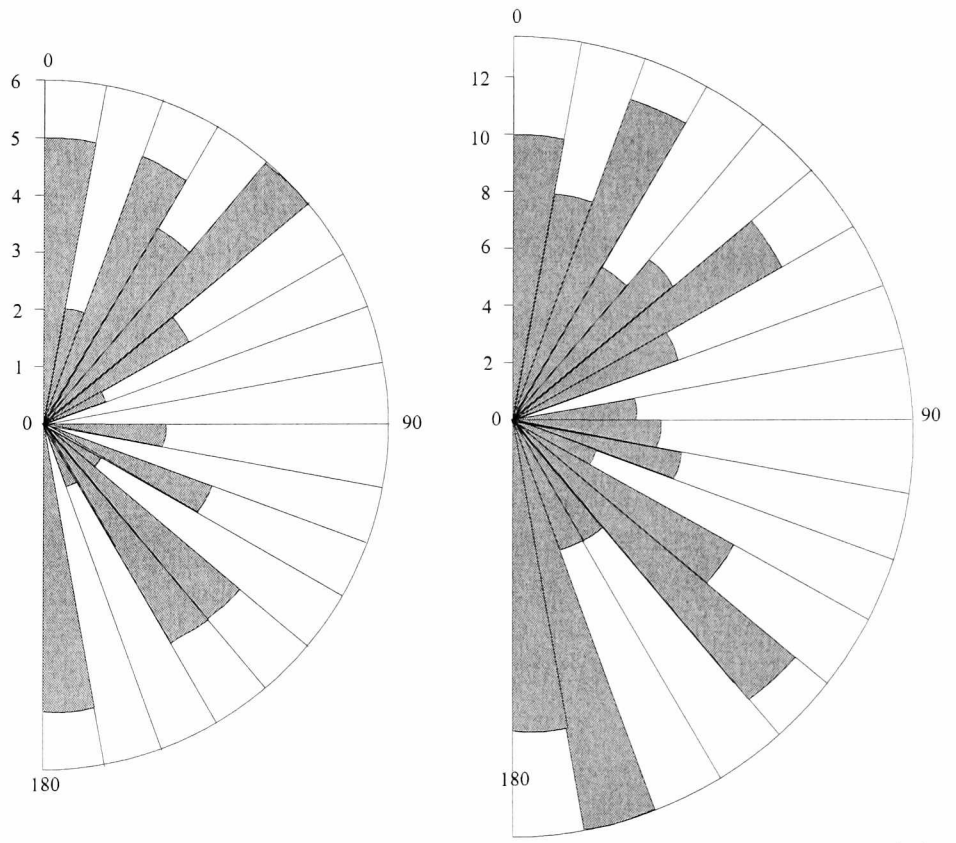


Figure 2.2.5: *Orientation data for monaxial sponge spicules on two calcareous slabs from locality 10, Llandegley Rocks. Bi-directional flow regime indicated, with regression suggesting similar flow conditions ($r_{max}$=0.89). Non-orthogonal flow directions suggest combined wave and current action.*

unknown mode of soft-tissue preservation. A similar process may have operated in the mouldic preservation of crinoids, through replacement of the organic surface layer (section 6.2). A single calcite nodule, nucleated on *Batostoma* sp. (Bryozoa), contains highly degraded remnants of pyritised bryozoan zooids, and possible remains of soft tissue in an associated microbrachiopod. Bioclasts within the nodule show filamentous overgrowth (presumed algal/cyanobacterial), again preserved in oxidised pyrite.

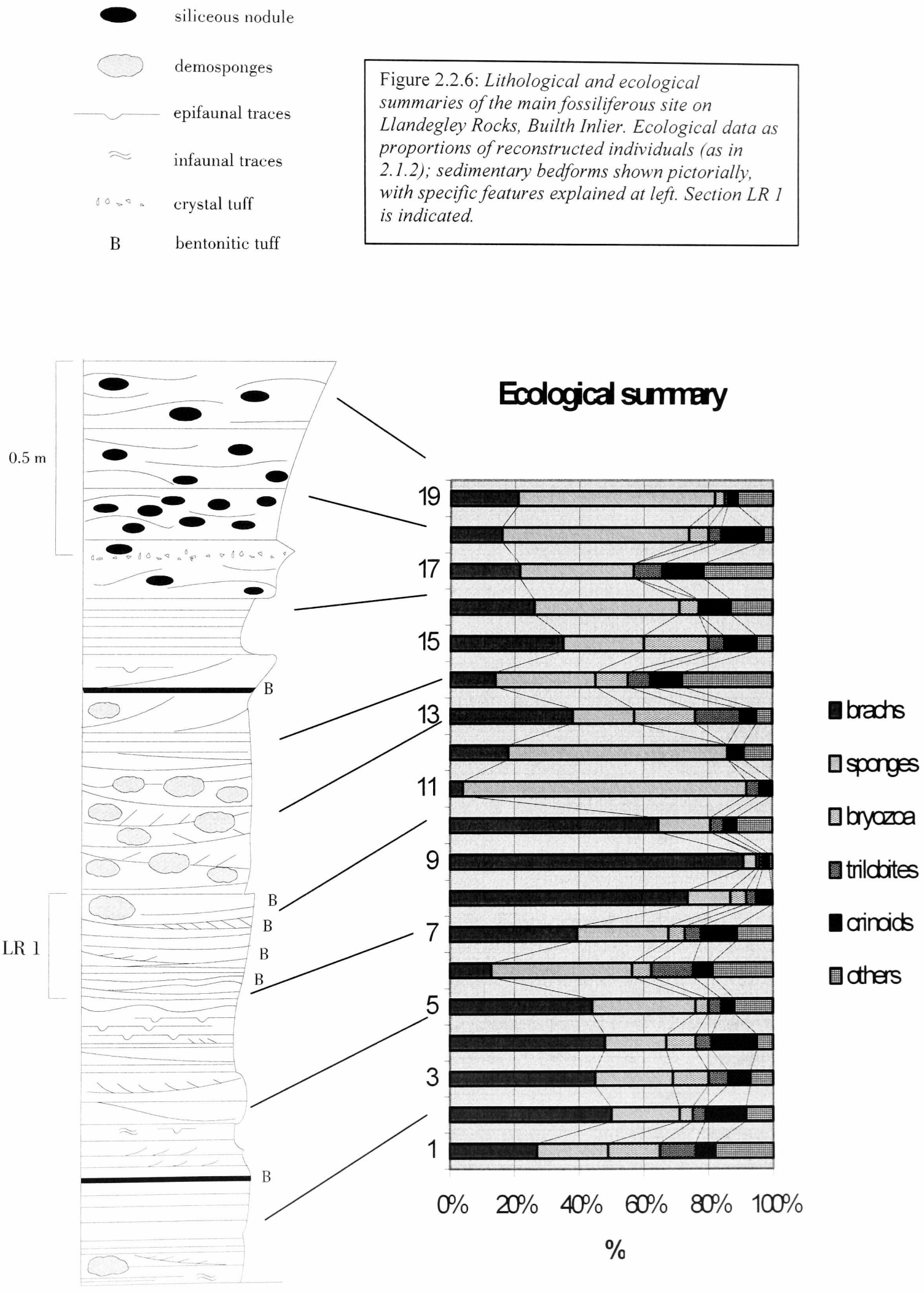


Figure 2.2.6: *Lithological and ecological summaries of the main fossiliferous site on Llandegley Rocks, Builth Inlier. Ecological data as proportions of reconstructed individuals (as in 2.1.2); sedimentary bedforms shown pictorially, with specific features explained at left. Section LR 1 is indicated.*

The ecological succession within the studied section comprises three main

phases. An initial, mixed brachiopod-bryozoan-trilobite fauna corresponds to the *Hesperorthis* Community of Williams *et al.* (1981), and remains stable until sample 4. Rather than representing the climax assemblage, however, brachiopod dominance gradually increases over the following 50 cm. Although changes in sedimentation rate cannot be assessed, most faunal components show little decline in abundance, suggesting that the change may be due to a genuine increase in brachiopod abundance. This progression is terminated by a series of four thin tuffs (samples 8-10; log LR 1). The second phase comprises a non-diverse, but extremely abundant demosponge community with only rare additional taxa. Demosponge abundance gradually declines from sample 10 to 12, grading into a diverse shelly community, similar to phase 1. This third phase differs from the original assemblage in that the monaxonid hexactinellid *Pyritonema scopula* (see chapter 4) dominates in the coarser sediments of samples 16-18.

Ichnofauna is limited to isolated burrows, usually less than 1 cm diameter, and rare beds with abundant surface traces (sample 5). Surface ichnofauna comprises simple sinuous tracks, although a *Cruziana*-like bilobed trail was recovered from scree. Comparison of epifaunal with infaunal trace fossil abundance yields only only partial correlation (Fig. 2.2.7), although sample 5 also correlates with the minimum in brachiopod abundance. The surface traces may have been preserved by a sudden increase in sedimentation rate (although there is no evidence of catastrophic burial), also reducing brachiopod abundance (compare LR I, below). The subsequent peak in infaunal trace fossils is likely to represent a genuine abundance increase, since preservation is less dependent on surface reworking. An increased level of mobile detritivores is also a ubiquitous characteristic of faunas immediately following ash-

fall (see 2.5, 3.6), but in this case appears to be due to the direct physical effects of sedimentation rate variations.

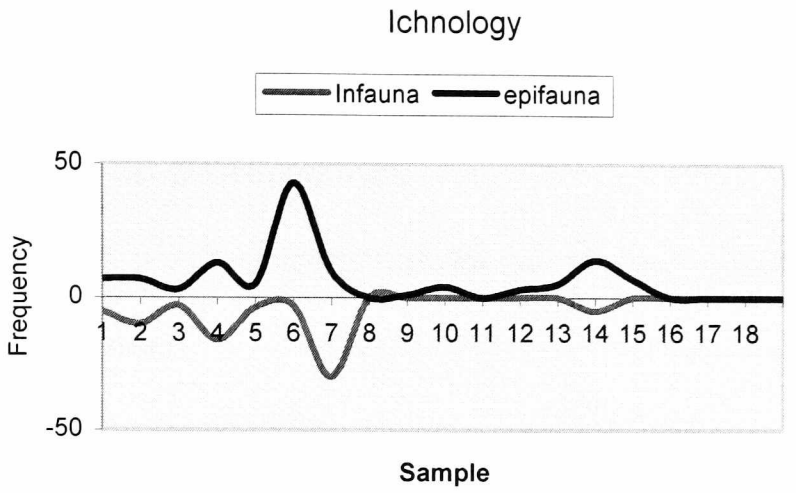


Figure 2.2.7: *Abundance of ichnofauna within the primary locality of Llandegley Rocks, Builth Inlier; infauna (below) and epifauna (above) are correlated at most horizons, but their maxima are displaced. Compare with fig 2.2.6*

### 2.2.4 Environmental interpretation

Although definitive evidence of water depth is lacking, several features of the Llandegley Rocks deposit allow a reasonably comprehensive palaeoenvironmental analysis:

(i) predominance of coarse sand and gravel among sediments;

(ii) local provenance of volcaniclastic particles shown by euhedral grains, extreme angularity, and scoriaceous shards;

(iii) poorly-preserved ripples, including symmetric, asymmetric and complex morphologies, and lack of surface ichnofauna, indicating consistently agitated conditions under wave and/or current influence;

(iv) ubiquitous presence of sponge spicules in all horizons;

(v) bi-directional allignment of sponge spicules on bedding surfaces, suggesting combined current and wave activity (Fig. 2.2.4);

(vi) benthic filamentous overgrowth, presumed algal or cyanobacterial, implying a position within the photic zone;

(vii) presence of diplograptid-dominated fauna in underlying laminated ashes, implying anomalously shallow conditions (Berry 1977);

(viii) several components of the fauna (articulated crinoids, bryozoans and sponges; pelmatozoan root structures; articulated trilobites inside nautiloid tests) imply an essentially *in situ* assemblage;

(ix) soft-tissue preservation in silica and silica/pyrite/calcite, indicating rapid mineralisation;

(x) dominance of the *Hesperorthis* brachiopod Community, representing shore-face facies (Williams *et al.* 1981).

These points indicate a diverse, shallow-water community, predominantly preserved *in situ*, above both storm wave base and photic limit, on the flanks of a volcanic cone. Mass input (or remobilisation) of locally-derived volcaniclastic material produced abrupt changes in pore-water chemistry, accompanied by rapid burial. Between mass deposition, the sediment was continuously agitated in an open shore-face setting, on a island landmass of unknown size (Jones and Pugh 1949). Sediment input may have resulted from storms or local seismicity. Grainsize generally increased through time, with ecological fluctuations between brachiopod- and sponge-dominated faunas. Occasional thin tuffs interrupted the succession, and are fully investigated below.

### 2.2.5 LR 1

Section LR 1 comprises a sequence of four preserved bentonites within homogeneous, coarse sandstones of samples 9-11 of the primary ecological log (2.2.6). The fauna is dominated by the articulate brachiopod *Hesperorthis* cf. *dynevorensis*, with a moderate majority of pedicle valves implying some local transport into the sampled

region. Articulated valves are uncommon, though present, and semi-articulated crinoid and bryozoan material indicates limited reworking. Sedimentary structures include asymmetric and symmetric ripples, varying in preserved amplitude and intensity through the log. Sediment is homogeneous, medium to coarse sand throughout, with very rare scoriaceous clasts; siliceous nodules are rare. Underlying beds include a more diverse, sparser fauna of brachiopods, sponges and other fragmentary shelly taxa; overlying beds are dominated by large, aspicular demosponges. Brachiopod abundance of LR 1 is shown in Fig. 2.2.8; complete data are provided in Appendix A.

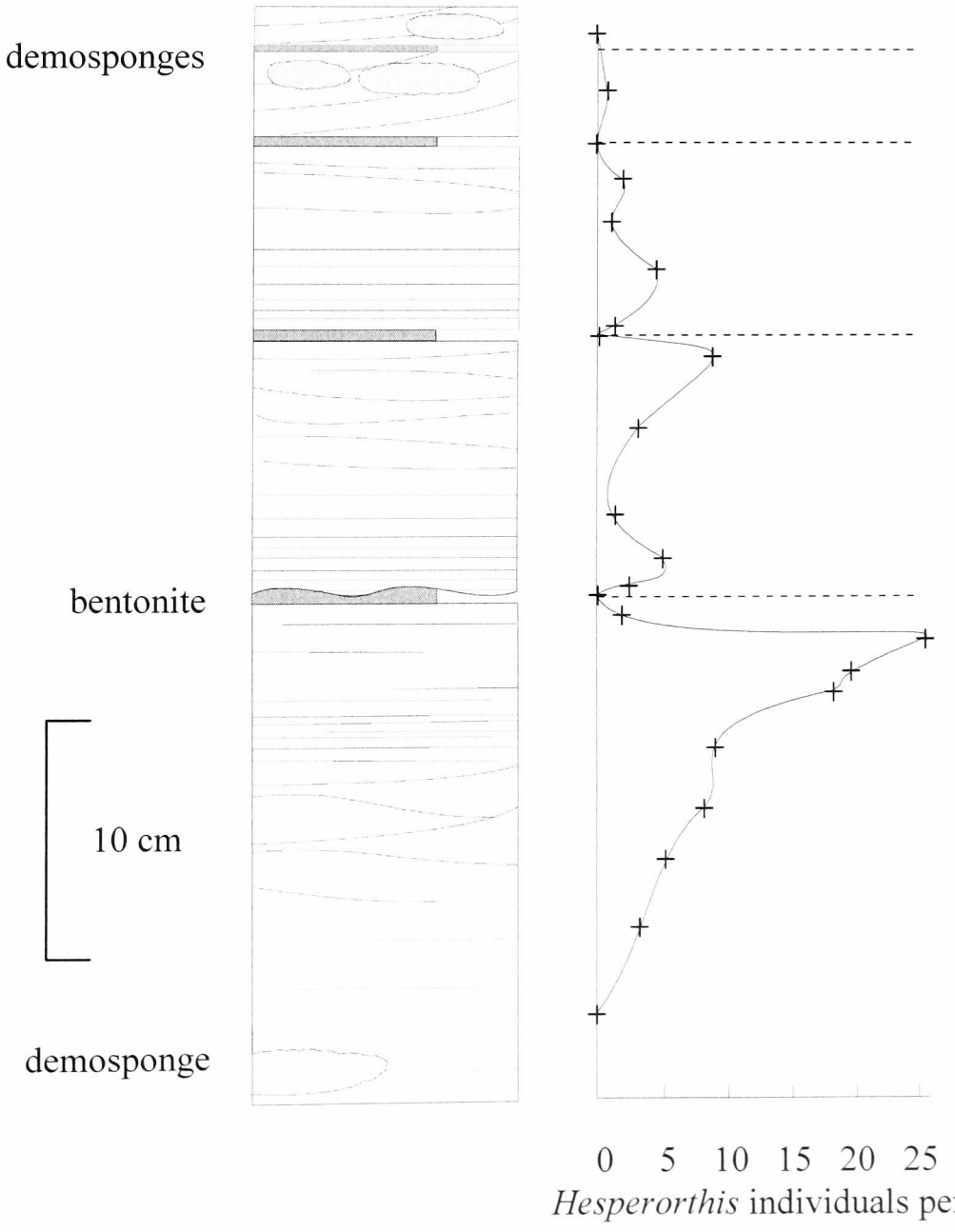


Figure 2.2.8: *Ecological log of section LR 1, comprising four tuffs within homogeneous sandstones; abundance of* Hesperorthis *individuals per kg.*

During the initial, sedimentologically stable phase, *Hesperorthis* abundance gradually increased towards total dominance; almost no other organisms are recorded until just below the first tuff. At this point, *Hesperorthis* abundance was reduced to almost zero, while crinoids, trilobites and bryozoa reappeared in small numbers. Following the tuff, *Hesperorthis* abundance gradually and eratically increased towards previous levels. This pattern is repeated for the three subsequent ash beds, with *Hesperorthis* abundance decreasing after each event. Eventually, the shelly community was replaced by abundant demosponges, approximately coinciding with a slight decrease in sediment grainsize.

The decreased abundance of *Hesperorthis* prior to deposition of tuff 1 may be due to briefly increased sedimentation rate, following local seismicity prior to eruption. This would be consistent with ash deposition causing ecological changes through a dominantly physical effect, as the pre-tuff and syn-tuff effects are very similar in character throughout LR 1.

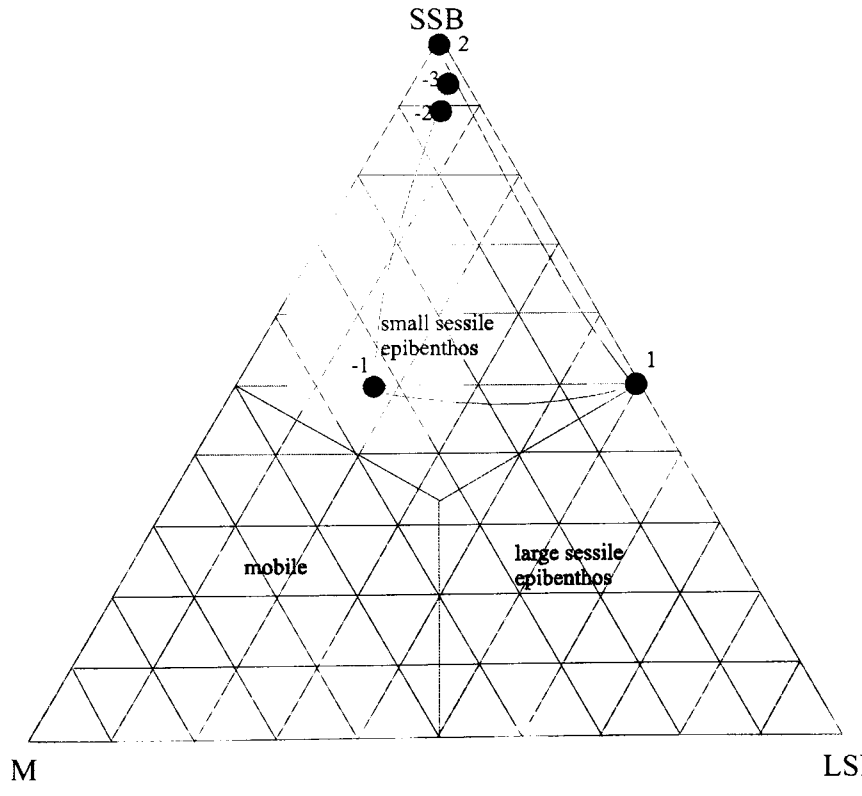


Figure 2.2.9: *Analsis of life-habits through LR 1(2), according to the benthic ternary system small sessile -large sessile –mobile. The stable community is dominated by small sessile taxa (articulate brachiopods) before and after ash-fall; during environmental stress, the other two categories were encouraged. Compare with Fig. 3.6.3.*

A second set of finely-spaced samples was analysed (LR 1(2)), immediately surrounding the lowest tuff, in order to provide larger data sets, although even in these

the abundance was statistically insignificant. However, the data are sufficient for approximate trophic/habit analysis, according to the ternary graph system of Scott (1978). Trophic group analysis yields limited results because of the scarcity of organisms in the critical interval. Although large sessile benthos and mobile epibenthos are apparently encouraged by ash-fall, there is no preserved increase in small mobile epibenthos, and no ichnological record.

Variation in habit through LR 1(2) is shown in Fig. 2.2.9. The limited data strongly support an increasing proportion of large sessile epibenthos and mobile benthos, and decreasing brachiopods (small sessile benthos). The data are insufficient for comprehensive trophic analysis, since almost all individuals are suspension-feeders. The only significant exceptions are trilobites, which are presumed scavengers/detritivores, after Pollard (1990). The reduction in brachiopods is reflected in temporary equilibration of suspension-feeders and detritivores, which appear to increase more significantly than large suspension feeders.

A combination of LR 1(2) and the equivalent samples from LR 1 yields sufficient data for a useful compound column chart in which all taxa are distinguished (Table 2.1, Fig. 2.2.6). Several of the observed trends appear to be significant:

1. *Iocrinus* was very rare in the initial brachiopod-dominated assemblage, became abundant during tuff deposition, and remained stable during the re-establishment of *Hesperorthis*.

2. Trilobites increased in abundance immediately before tuff deposition but appear to be absent thereafter, although they were a minor component of the stable *Hesperorthis* assemblage.

| | -3 | -2 | -1 | 1 | 2 | Total |
|---|---|---|---|---|---|---|
| **H. incognita** | 92 | 40 | 3 | 6 | 5 | 146 |
| **other brachs** | 1 | 2 | 1 | 0 | 0 | 4 |
| **Flexicalymene** | 1 | 1 | 1 | 0 | 0 | 3 |
| **other trilobites** | 0 | 1 | 2 | 0 | 0 | 3 |
| **Pinnatoporellid** | 1 | 1 | 0 | 0 | 0 | 2 |
| **Trepostome 1.6** | 1 | 0 | 0 | 0 | 0 | 1 |
| **Trepostome 3-4** | 1 | 1 | 0 | 0 | 0 | 2 |
| **Iocrinus** | 1 | 0 | 1 | 1 | 1 | 4 |
| **Alga** | 0 | 0 | 1 | 1 | 0 | 2 |
| **Total** | 98 | 46 | 9 | 8 | 6 | 167 |
| **mass/kg** | 3.40 | 1.75 | 1.45 | 2.55 | 1.45 | 10.60 |
| **D (individuals/kg)** | 28.8 | 26.3 | 6.2 | 3.1 | 4.1 | |
| **% brachiopods** | 95 | 91 | 44 | 75 | 83 | |

Table 2.1: *Combined data for logs LR 1(2) and the equivalent beds of LR 1, in abundance and abundance density. Sample numbers: -3 to 2, relative to tuff.*

Figure 2.2.10 (below): *Graphical view of proportional variation across the lowest tuff of LR 1.*

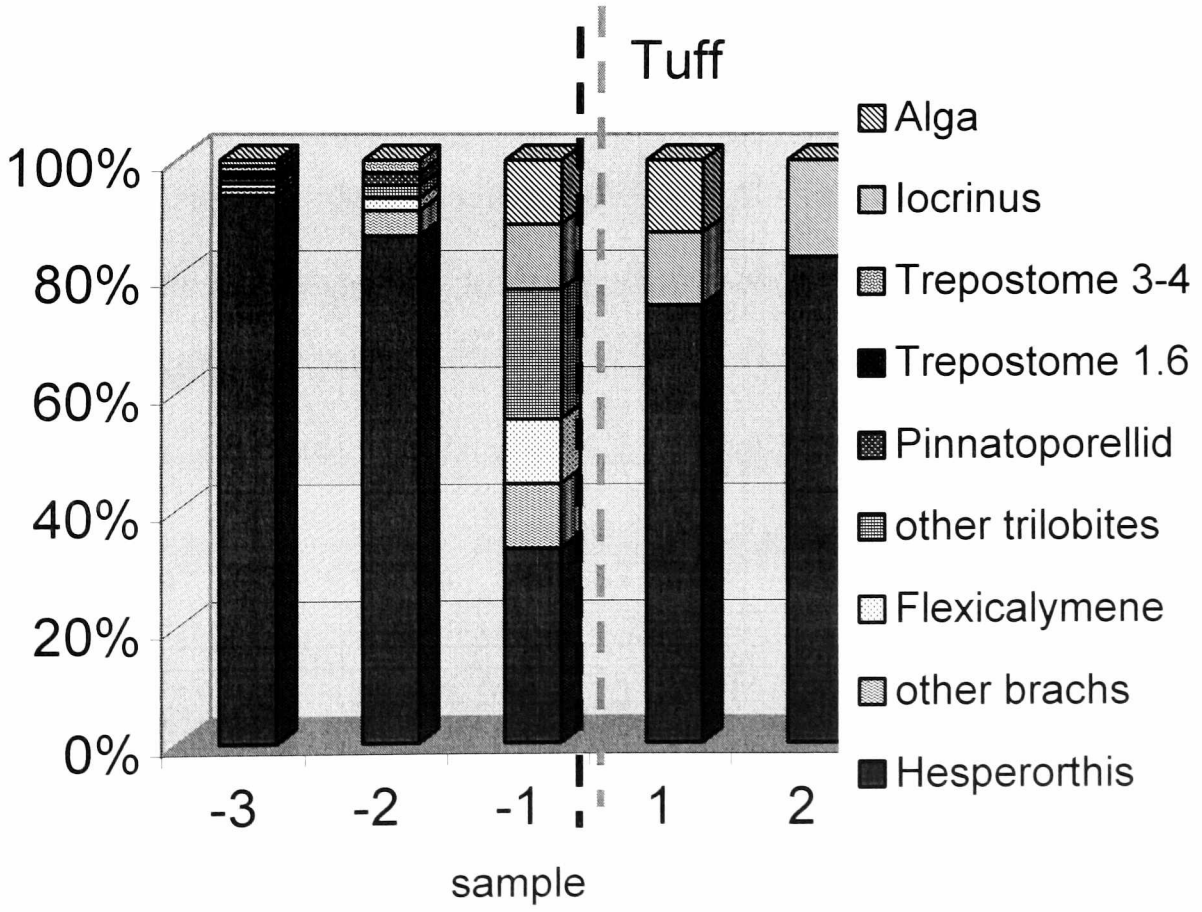

3. Algae are only preserved in the samples surrounding the tuff; this is almost certainly a taphonomic effect relating to rapid deposition.

4. In general, diversity remained stable prior to the tuff, although with minor groups increasing in proportion. Following the tuff, only crinoids remained unaffected, although brachiopods re-established rapidly.

5. Trepostome bryozoans appear very sensitive to environmental changes, and were excluded once the brachiopod decline had initiated.

The possible significance of the observed trends is discussed in section 2.5.

## 2.3 Pen Llithrig-y-Wrach, Capel Curig (SH 7165 6217)

### 2.3.1 Locality and sedimentology

Despite numerous transported shelly faunas in the Capel Curig – Betws-y-Coed district, very few localities contain *in situ* assemblages. The only demonstrably *in situ* shelly fauna recovered occurs in the upper Cwm Eigiau Group, on the east face of Pen Llithrig-y-Wrach, eastern Carneddau, 70 m south of the summit. The stratigraphy of the area around Llyn Cowlyd was detailed by Diggens and Romano (1968), who described the sampled lithology as the Pen Llithrig-y-Wrach Siltstone Formation, and attributed it to the Lower Longvillian. A limited shelly fauna contained *Howellites* cf. *antiquor*, dalmanellids, *Broeggerolithus* sp. and a calymenid. No tuffs were recorded from this unit, although occasional, probable accretionary lapilli suggest limited local volcanism.

The succession of cleaved siltstones and fine sandstones underlying unit 1 of the Lower Crafnant Tuff (Howells *et al.* 1981; Snowdon Volcanic Series of Diggens and Romano 1968) contains sporadic, dispersed shelly faunas dominated by an articulate brachiopod. Deformation of the beds prevents certain diagnosis, but it

appears to be *Plaesiomys multifida* (Salter), of which *Dinorthis multiplicata* Bancroft is a junior synonym (Cocks 1978); this species is an abundant component of local described faunas. Two horizons (one located in outcrop) comprise pavements of articulated *P. multifida*, oriented vertically with the pedicle embedded in the substrate, proving the fauna to be at least partly *in situ*. Such evidence is lacking in the intervening beds, although there are no shell accumulations, broken fragments are rare, and there is no sedimentological evidence of significant transport; however, sedimentary structures may have been destroyed by deformation or metamorphism, if originally present. Diggens and Romano (1968) report that this unit shows ubiquitous current-deposition, of variable orientation. Pyrite is locally abundant, often along specific horizons. The most reasonable interpretation is of a moderately shallow (c. 50 m) shelf setting with local transport only, almost certainly related to the nearby emergence of the western Carneddau volcanic source (Howells and Leveridge 1980). The overall setting is of a deepening-upwards sequence, underlain in most places by coarse sandstones.

The fauna is inferior to that of Llandegley Rocks in both diversity and preservation, although almost monospecific assemblages of *P. multifida* can reach high abundance. Fragmentary remains of trilobites and crinoids are associated with rare examples of other brachiopods, ostracodes?, graptolites?, large monaxial sponge spicules and bryozoans. The depauperacy of the recovered fauna may reflect the poor exposure of fossiliferous beds, and the limited accessibility of loose scree material, from which no additional taxa were recovered. In general character, however, the fauna is closely comparable to that of Llandegley Rocks, although significantly younger. The dominance of one species of articulate brachiopod, and the presence of large monaxial sponge spicules, is particularly significant. Sedimentation rate was

probably lower than at Llandegley Rocks, reflected in the finer grain size and greater abundance of brachiopods; somewhat deeper water is also likely.

Metamorphism has made bedding difficult to identify in most places, although it is revealed by the *Plaesiomys* pavements to locally parallel the east face. Bentonites are not obvious in the succession, possibly due to destruction by metamorphism; the only recognisable tuff horizon within fossiliferous beds comprised a thin band of vertically-oriented acicular phenocrysts, badly weathered, within a micaceous siltstone matrix. The proportion of fine particulate material in the original ash-fall is not known. The section cut acutely across bedding, allowing reasonable sample sizes of 3-5 cm thickness. Sub-orthogonal cleavage planes are approximately perpendicular to bedding, preferentially producing lath-shaped fragments on breakage.

Unfortunately, the locality has been lost to erosion during the winter of 1998-9, and only limited initial samples were initially collected. Relocation of outcrop fragments lower on the east face is not practicable, and extensive searches of the remaining exposures failed to yield further tuff horizons. The analysis of the initial samples, although certainly useful, is undeniably limited. Taxonomic proportions only have been utilised, since abundance is of unknown reliability; full data is provided in appendix B.

### 2.3.2 PLW 1

A series of nine initial samples were taken across horizontal exposures, at an acute angle to bedding, although precise orientation measurement was impossible due to the rarity of preserved sedimentary structures. The tuff comprised approximately 8 cm of pale brown-weathering, micaceous siltstone (weakly metamorphosed), with abundant relict acicular phenocrysts in vertical orientation. Cleavage occurs in two orientations

separated by 40-50°, each approximately orthogonal to bedding planes. Deformation of fossils was severe, preventing specific identification of most specimens, although recognition of distinct taxa was usually simple.

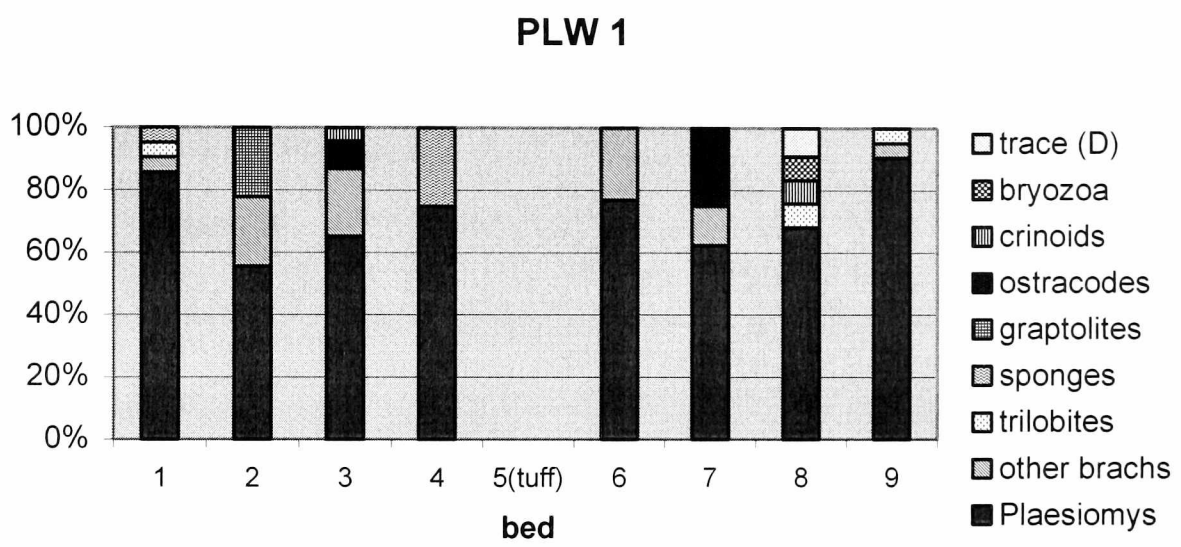


Figure 2.3.1: *Ecological log of section PLW 1, based on statistically limited data; only general features are reliable, although these are very similar to LR 1(2); compare with Fig. 2.2.6.*

Complete faunal data are provided in Appendix A, with variation of population proportions summarised in Fig. 2.3.1. Absolute abundance data are not appropriate due to uncertainty over original sedimentology. The following features are potentially reliable, due to their clarity:

1. The primary effect of ash-fall was to greatly reduce brachiopod dominance, from approximately 95% to around 60% of preserved organisms, although beds adjacent to the tuff contained almost no fossils. Recovery was equally rapid, with a return to original dominance in 5-8 cm.

2. Ostracodes became common during the early and late phases of environmental instability, but were excluded from both the stable *Plaesiomys* assemblage, and the low-abundance assemblages immediately before and after the tuff.

3. The initial effects were seen prior to the main ash deposition, although bentonitic material may have been present at this point in the log, but subsequently rendered unrecognisable by metamorphism.

4. Crinoids, bryozoa and trilobites occurred in low abundance at various points in the log; sponges were restricted to the pre-tuff deposits, although spicules occur immediately below the tuff.

Trophic/habit analyses are not appropriate, although there is an apparent trend towards larger suspension feeders (crinoids, sponges, bryozoans), and an approximate trend to increasing mobile epibenthos (ostracodes, trilobites). No certain predators were recorded.

## 2.5 Synthesis and interpretation

The data from LR 1 and PLW 1 share several features. Both involved a brachiopod-dominated assemblage (dominance over 90%) declining rapidly during or prior to tuff deposition, before re-establishing dominance thereafter. During their decline, mobile epibenthic detritivores (notably trilobites) and large sessile suspension-feeders (particularly crinoids) were encouraged, although bryozoans appear to have been as sensitive to fluctuating conditions as were brachiopods. A similar decline in brachiopods was observed in sample 5 of the main Llandegley Rocks succession (section 2.2.4), in which epifaunal (and subsequently infaunal) trace fossils are abundant.

The main ecological effects are consistent with increased sedimentation rate. A reduction in small sessile suspension feeders, while crinoids were unaffected or encouraged, suggests inhibited feeding due to increased suspended particles, perhaps

combined with direct burial. Large erect treopostomes, although raised above the level of brachiopods, may have suffered under increased turbidity due to the small size of the lophophore, compared with the feeding arms of crinoids. Trilobites would be expected to flourish under these conditions, as seen in the pre-tuff beds of LR 1 (2). Their rarity following the tuff in both LR 1 and PLW 1 suggests a restricted food supply, although sufficient suspended detritus was available to promote re-colonisation by brachiopods and crinoids.

Changes in ambient water chemistry are suggested by the rapid silicification of some fossils at Llandegley Rocks, although similar features are absent from Pen Llithrig-y-Wrach. Dissolution directly from the deposited ash particles is the most likely origin of silica oversaturation, since the inferred shallow water is volumetrically limited, and probably closed from wider circulation.

A comparison with published information shows that the observed patterns are widely consistent. Batchelor and Clarkson (1993) and Tipper (1976) describe the replacement of a diverse brachiopod assemblage by an opportunistic, non-diverse assemblage following a Llandovery bentonite in the North Esk Inlier. The lower grain-size and greater inferred water depth (offshore *Clorinda* Community) imply a facies intermediate between the present examples and those in chapter 3, but similarities between the ecological successions are significant. The destruction of a dominant brachiopod assemblage during ash deposition conforms to all data herein, as does the subsequent rapid re-colonisation by brachiopods. Opportunistic taxa dominate both communities in the volcanic island settings of LR 1 and PLW 1, while in the North Esk Inlier (Tipper 1976), diversified brachiopod palaeocommunities were more fully developed, but were again replaced by opportunists. This implies that

destruction of the original assemblages was almost total, and that re-colonisation occurred more by larval settling than through recovery of a remnant population.

## 2.6 References


Batchelor, R. A. and Clarkson, E. N. K. 1993. Geochemistry of a Silurian metabentonite and associated apatite from the North Esk Inlier, Pentland Hills. *Scottish Journal of Geology* **29**, 123-130.

Berry, W. B. N. 1977. Ecology and age of graptolites from graywackes in eastern New York. *Journal of Paleontology* **51**, 1102-1107.

Cocks, L. R. M. 1978. A review of the British Lower Palaeozoic brachiopods, including a synoptic revision of Davidson's monograph. *Monograph of the Palaeontographical Society, London* **131**, 1-256.

Davies, J. R., Fletcher, C. J. N., Waters, R. N., Wilson, D., Woodhall, D. G. and Zalasiewicz, J. A. 1997. *Geology of the country around Llanilar and Rhayader*, British Geological Survey, The Stationery Office, London.

Diggens, J. N. and Romano, M. 1968. The Caradoc Rocks around Llyn Cowlyd, North Wales. *Geological Journal* **6**, 31-48.

Elles, G. L. 1939. The stratigraphy and faunal succession in the Ordovician rocks of the Builth-Llandrindod Inlier, Radnorshire. *Quarterly Journal of the Geological Society* **95**, 338-445.

Furnes, H. 1978.*Unpublished Ph. D. thesis.* University of Oxford.

Harrington, H. J. 1959. General description of the Trilobita. *In* Moore, R. C. (ed.) *Treatise on invertebrate palaeontology*. New York and Lawrence, Part O, Arthropoda 1, 038-117.

HOWELLS, M. F. AND LEVERIDGE, B. E. 1980. The Capel Curig Volcanic Formation. *Institute of Geological Sciences Report*, **80/6**, 16 pp., 7 pl.

HOWELLS, M. F., LEVERIDGE, B. E., EVANS, C. D. R. AND NUTT, M. J. C. 1981. *Dolgarrog: Description of 1:25000 Geological Sheet SH 76*. Classical areas of British geology, Institute of Geological Sciences, London: Her Majesty's Stationery Office.

HURST, J. M. 1979. Evolution, succession and replacement in the type upper Caradoc (Ordovician) benthic faunas of England. *Palaeogeography, Palaeoclimatology, Palaeoecology* **27**, 189-246.

INSTITUTE OF GEOLOGICAL SCIENCES 1977. *Llandrindod Wells Ordovician Inlier; Geological Survey of Great Britain, 1: 25000*. Her Majesty's Stationery Office, London.

JONES, O. T. AND PUGH, W. J. 1949. An Early Ordovician shoreline in Radnorshire, near Builth Wells. *Quarterly Journal of the Geological Society* **104**, 43-70.

LOCKLEY, M. G. 1980. The Caradoc faunal associations of the area between Bala and Dinas Mawddy, North Wales. *Bulletin of the British Museum of Natural History* (Geology) **33**, 165-235.

LOCKLEY, M. G. 1983. A review of brachiopod-dominated palaeocommunities from the type Ordovician. *Palaeontology* **26**, 111-145.

PICKERILL, R. K. AND BRENCHLEY, P. J. 1979. Caradoc marine benthic communities of the south Berwyn Hills, North Wales. *Palaeontology* **22**, 229-264.

POLLARD, J. E. 1990. Evidence for diet. *In* Briggs, D. E. G. and Crowther. P. R. (ed.): *Palaeobiology: a synthesis*, Blackwell, Oxford, 362-367.

SCOTT, R. W. 1978. Approaches to trophic analysis of palaeocommunities. *Lethaia* **11**, 1-14.

SUTHREN, R. J. AND FURNES, H. 1980. Origin of some bedded welded tuffs. *Bulletin of Volcanology* **43,** 61-71.

TIPPER, J. C. 1976. The stratigraphy of the North Esk Inlier, Midlothian. *Scottish Journal of Geology* **12**, 15-22.

WATKINS, R. 1979. Benthic community organisation in the Ludlow Series of the Welsh Borderland. *Bulletin of the British Museum of Natural History* (Geology) **31**, 175-280.

WILLIAMS, A., LOCKLEY, M. G. AND HURST, J. M. 1981. Benthic palaeocommunities represented in the Ffairfach group and coeval Ordovician successions of Wales. *Palaeontology* **24**, 661-694.

# 3. PALAEOECOLOGY OF ASH DEPOSITION IN SILTSTONE AND SHALE FACIES

## 3.1 METHODOLOGY

### 3.1.1 Basic methods

Analysis of the ecological effects of tuffs in Middle Ordovician argillaceous sequences of the Welsh Basin relied on the analysis of bulk samples for abundance and faunal composition data. Sections were selected on the basis of the following principal characters:

1. the section must contain at least one discrete tuff horizon, within generally homogeneous sediments;
2. upper and lower boundaries should be abrupt; tuffs overlain by tuffites or tuffitic shales were not selected;
3. tectonic deformation is undesirable, although sometimes unavoidable; cleavage, where present, should be consistent, and approximately bedding-parallel where possible;
4. the section must contain an associated fauna, although even apparently barren strata often reveal fossils on detailed analysis. No bentonites observed from the Builth Inlier lacked an associated fauna, although the cuttings at Llanwrtyd contained at least one unsampled, thin bentonite which appeared, on inspection to have produced no response; a variety of tuffs in Snowdonia appeared within barren slates.

Three samples, 20 (± 2) mm thick, were taken below each tuff, and a continuous succession of between eight and twenty above, usually dictated by exposure. The samples (generally 100-400 g) were removed to the laboratory and weighed to 0.1g accuracy. A pin-hammer was employed to break the samples into

small flakes, a few millimetres square, and 0.5-1.0 mm thick. All specimens were retained, although some specimens were damaged, either accidentally or in order to further investigate the adjacent matrix. Larger fossiliferous blocks and unusable fragments were weighed at the end, and subtracted from the initial total.

The specimens were identified as far as possible, counted, and absolute abundance of major taxa calculated. Rare taxa were usually employed for presence-absence data only. In rare instances of super-abundance, complete destructive analysis was employed on 20-30 g samples.

Observation of fossils was enhanced by the use of a fibre-optic light source focused onto a small silicified sandstone "anvil." A standard binocular microscope was used to identify possible fossils visible to the naked eye, with a lower size limit of 0.3 to 0.5 mm. Water could only be used sparingly to increase contrast, since the shales are often friable and disintegrate on expansion/contraction.

### 3.1.2 Analytical techniques

Ordovician black shale faunas tend to be dominated by suspension-feeders and detritivores, particularly inarticulate brachiopods, graptolites and trilobites. However, soft-bodied taxa are relatively more abundant than in arenaceous faces (e.g. Conway Morris 1986), and so attempts to reconstruct trophic structure will be extremely incomplete. Although such an attempt could be made, based on comparisons with conservation lagerstätten, many exceptional deposits represent unusual environments, perhaps with atypical faunas; results here are therefore based entirely on the evidence available from preserved organisms. Ichnofaunas are extremely rare in the Builth Inlier, and rare burrowed horizons usually provide no indication of the trace-maker. Analysis has concentrated on the absolute abundance of preserved faunas. a process

subject to inherent errors (section 3.1.3). An initial assumption of homogeneous sedimentation rate (excluding the tuff) is incorporated into a simple plotting of the observed abundance of taxa, against position in the section; sedimentation rate is fully discussed in section 3.7.2.

The sample thickness of 20 mm was selected arbitrarily, but has certain *a posteriori* advantages for the Builth and Llanwrtyd samples. It is clear that some variation occurs within the thickness of each sample, and this is almost certainly non-linear. Averaging the abundance over reasonable sample thickness gives a better indication of trends in broad-scale environmental factors than much thinner intervals, in which minor, complex fluctuations in population dynamics may exert a strong influence. Although fine-scale data may be desirable in some cases to examine these effects, at this stage of research the overall patterns are of primary importance. There are also significant practical difficulties involved in taking thinner samples, which geometrically increase the time required for an already time-intensive process. Samples of greater thickness will begin to obscure the overall patterns, and in most cases will be of limited practical use.

Most taxa present comprise single or bipartite skeletons, which are easily translated into individual abundance values. Valves of inarticulate brachiopods tend to be hydrodynamically similar, with little chance of winnowing. Graptolite rhabdosomes are usually small and rarely fragmented, so that in most cases each occurrence can be treated as an individual, although care must be taken to ensure that one specimen is not counted in two separate sediment fragments. With high abundance of *Didymograptus,* however, the potential for confusion is removed through counting of proximal regions only. This is more time-consuming, since many proximal regions must be excavated, but is necessary to avoid serious bias.

Winnowing processes, as described by Williams and Rickards (1984) may alter the vertical distribution of graptolites. However, broken rhabdosomes are extremely rare in the studied samples, implying limited transport, and the potential problem is somewhat alleviated by the finite vertical sample thickness of 20 mm. Dendroids are sufficiently rare that any specimen is counted as an individual, although only their presence or absence is formally utilised.

Ostracodes, which occur in very variable abundance, are treated in a similar manner to brachiopods, although with caution. Multiple instars require consideration of multiple moults; however, only adults are reliably discernible to the naked eye, and juveniles may be disregarded. In general, ostracode population changes are so pronounced that detailed data are not required, beyond the position and approximate morphology of abundance peaks. Trilobites are uncommon in the sample sizes employed, and very rarely articulated; they are treated as presence-absence data for identifiable genera. Chitinozoans, distinguished as "*Rhabdotheca*" and "*Conotheca*" types, are counted as individuals, although this may be biased by occasional clusters. If the present interpretation as eggs (Gabbott *et al.* 1998; Paris and Nõlvak 1999) is correct, then it is unclear whether a cluster should be counted as a number of individuals (embryos), or as the remains of one individual (the mother). As with ostracodes, general abundance trends are the critical factor, although this potential bias must be recognised; both individuals and clusters are shown in Appendix B. Conodonts are sufficiently rare that elements were counted individually, except for a single bedding plane assemblage (BG1 (2): F).

Additional techniques, associated with the ecological analysis and used in specific situations, are described below.

i) Size distribution analysis of *Apatobolus micula*: length measurements of individual valves, used to estimate population characteristics. Bimodal and skewed distributions may reveal the presence of overlapping populations, or allow recognition of juvenile mortality as an indicator of stressed environmental conditions (cf. Williams and Rickards 1984).

ii) Pyrite framboid analysis (Wignall and Newton 1998) for recognition of anoxia. Pyrite framboids have been shown to form at the oxic-anoxic boundary; if this occurs in the water column, framboids sink rapidly and growth stops, leading to a consistently small diameter. If the boundary occurs within the sediment, framboids may grow to larger sizes, and a more varied distribution is observed (Wignall and Newton 1998). In dysaerobic conditions, the boundary may oscillate, or become indistinct, so that slight differences in the anoxic-dysaerobic conditions are observed in a gradational size distribution. Analysis was performed under high magnification petrological microscope, allowing resolution of c. 1 μm in transmitted light. In most cases, framboids were weathered to haematite and easily recognised. An arbitrary crack in the standard petrological slide was used as an area limit, and an adjacent region of the slide systematically scanned, with all framboids measured by comparison with a graticule or cross-hairs. Attribution of framboids within 2-μm divisions was sufficient for this process. Approximately 300 were counted per slide, although almost all were very small. No calibrated scales of quantitative oxygenation are presently available for this process, so the results allow recognition only of trends within sample series. Correlation of samples with benthic faunas in the ecological analysis

allows some recognition of relative levels of dysoxia, and their palaeoecological significance.

Apparent diameter may be affected by intersection of the framboids with the slide surface, but as very few have radius approaching the slide thickness, the bias is not severe. Since recognition of elevated oxygenation depends on the presence of larger framboids, this cannot produce the appearance of oxygenation where none exists, but serves to slightly reduce the apparent significance of the data.

### 3.1.3 Bias evaluation

The analytical process described in sections 3.1.1 and 3.1.2 contains certain unavoidable errors, the significance of which may be estimated.

*Background sedimentation rate*. Discussed in detail in section 3.7, sedimentation rate remains the most difficult variable to accurately quantify. While an approximate value may be estimated for a large, datable thickness, this incorporates variation on small scales, which may significantly affect the ecological results. Lamination thickness may be used as a guide, where present, but only if the causal process is assumed periodic, rather than episodic. On the scales involved (occasional laminae with 2-3 mm separation), lamination is unlikely to represent either annual or daily periodicity, although the possibility of tidal cycles cannot be ruled out. Since these cycles are difficult to distinguish from storms or terrestrial floods in marine sediments, speculation should be avoided. Overall, an approximately constant sedimentation rate must be assumed, unless there is reason for doubt. The most likely variation is a gradual decrease in post-tuff accumulation rate, resulting from enhanced

continental run-off and increased density of the nepheloid layer following eruption; this is equivalent to the following case.

*Dilution by ash reworking.* There is abundant evidence for biological reworking of ash beds into overlying sediments (Fisher and Schmincke 1984, p. 166). Ruddiman and Glover (1972) described significant ash incorporated into sediments up to 40 cm above the original bed. Secondary reworking on this scale will normally be evidenced as a diffuse upper boundary, and these beds were not analysed; however, some vertical mixing may be inevitable. The results of this on the ecological data will be an upwardly decreasing dilution of the background sedimentation rate, and correspondingly, a reduction in observed abundance near the base. There is little likelihood of the observed patterns being noticeably altered through this effect, although changes in abundance gradients might be expected.

*Small size bias.* The proportion of sub-millimetre fossils remaining undiscovered during analysis will be higher than for larger fossils, through the increased chance of remaining entirely enclosed within matrix. In the case of *A. micula* juveniles, where the lower size limit is around 0.3 mm, this may have important effects. Firstly, size distribution analyses must be assumed to contain a higher proportion of juveniles than are observed, the ratio increasing with decreasing size. This only significantly affects the smaller valves, and serves to decrease the distinctiveness of the most likely patterns. Any skew towards juveniles must be increased to give the true distribution, while an observed normal distribution should be considered slightly skewed towards juveniles. This effect is unlikely to require a lateral shifting of an observed mean, unless the peak is at small size, where this should be accentuated.

Chitinozoans are strongly subject to this effect, with, under normal circumstances, a maximum size of around 1.0 mm (2.1 mm at Y Foel, Llanwrtyd). However, only the absolute value is affected, since the size of an individual is constant for a given taxon. This implies that an observed abundance, while not accurate in an absolute sense, can be reliably compared with that in other samples, to indicate abundance changes. *Rhabdotheca*-like forms are obvious on bedding planes, whereas the smaller (0.3 mm) *Conotheca*-like varieties are more easily overlooked. Other small organisms (conodonts, scolecodonts, sponge spicules) are generally rare, and are typically useful only as presence/absence data.

Ostracodes are less strongly subject to size biases than their small diameter might suggest; this is due to their typically three-dimensional mouldic preservation increasing the likelihood of exposure in fragments of sub-millimetric thickness. However, they are subject to significant size variation, the smaller instars almost certainly below the level of resolution. Ostracod abundance must therefore be seen as reflecting sub-mature adult populations; a high abundance of juveniles will not necessarily be recorded.

*Preservational biases*. It is inconceivable that all fossilisable organisms were preserved. The composition and structure of organic remains dictate the relative proportion of different groups that will be preserved under given chemical, mechanical and biodegradatory conditions. In an extreme example, single specimens of palaeoscolecid worms are recorded from three sites, representing a probable infaunal component (similar-sized burrows are associated in BG1: D). This is the only infaunal organism recorded, but is probably extremely under-represented.

Calcareous organisms are almost invariably mouldic, with considerable relief. Dissolution of calcareous skeletons prior to lithification must have affected preserved

abundances, but to an unknown extent. No numerical allowance can be made for this factor, since the original environmental conditions are unobtainable; however, smaller organisms will undoubtedly be more strongly affected than larger, with the ostracod record particularly suspect. Oxygenation also increases the solubility of calcite, although relative oxygenation state can be obtained through pyrite framboid analysis (Wignall and Newton 1998). Hence, elevated ostracode abundance during oxygenated periods is strongly indicative of an expanded population.

Siliceous organisms are restricted to sponge spicules, an important indicator of benthic colonisation. These are often mouldic, suggesting that diagenetic dissolution was equally significant to that of calcareous organisms. Biostratinomic dissolution of sponge spicules (Land 1976) may prevent the recognition of benthos, but their widespread distribution in the samples studied suggests that the loss of all spicules from an entire sample is unlikely.

Organic and semi-organic remains of inarticulate brachiopods, graptolites, conodonts and scolecodonts are more likely to approximate their original abundance, but even here, there is no clear indication. For inarticulate brachiopods and graptolites, a constant proportion of each taxon was presumably preserved between samples, since the recorded patterns of abundance are extremely consistent (sections 3.2, 3.3).

## 3.2 Howey Brook Main Feeder SSSI, Builth Inlier

### 3.2.1 Locality

The large stream on Gelli Hill (SO 092 591) reveals an almost complete sequence through the lateral equivalents of the Builth Volcanics in the northern part of the Builth Inlier. The sequence include basal ignimbrites and/or lavas, overlain by coarse

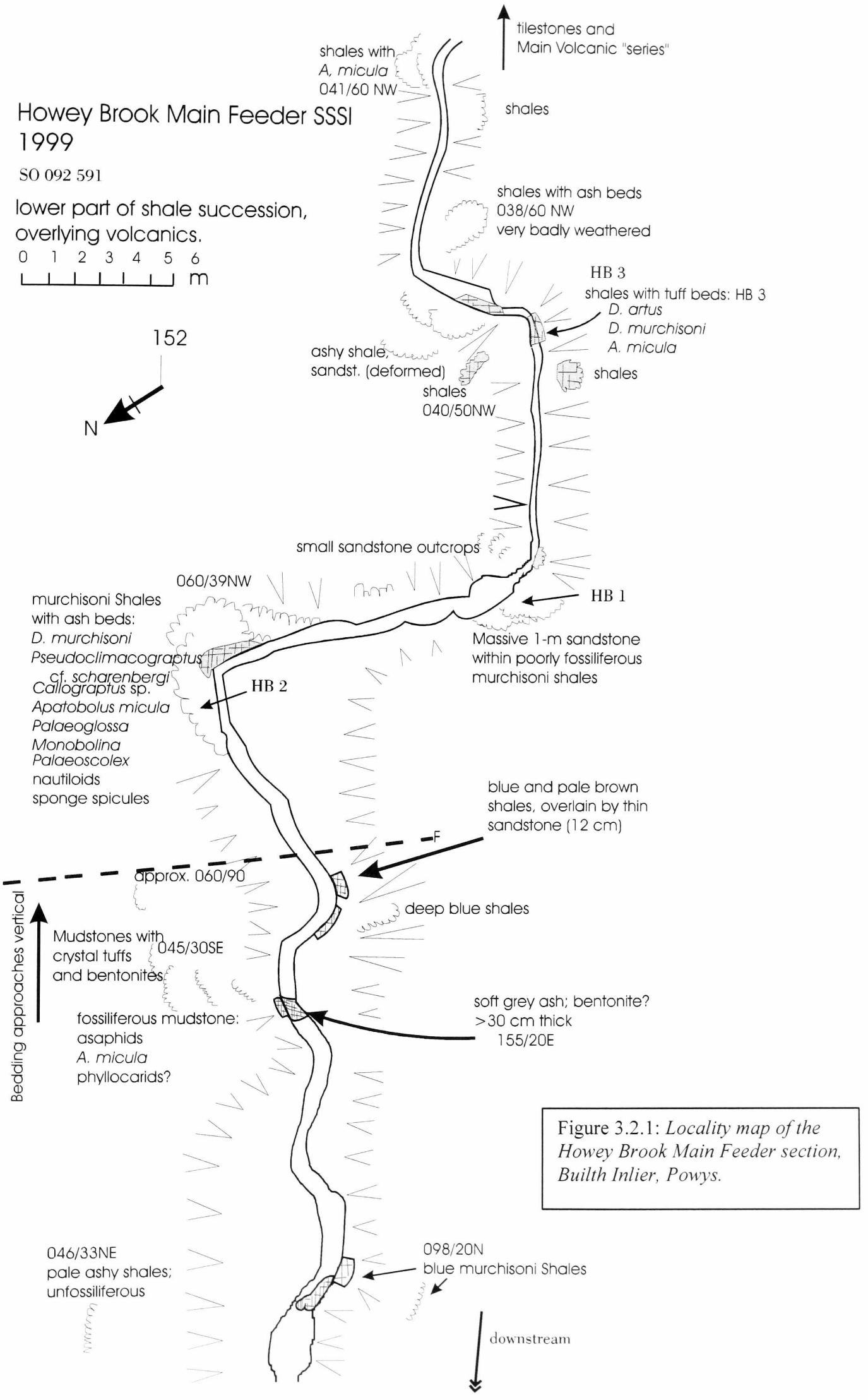


Figure 3.2.1: *Locality map of the Howey Brook Main Feeder section, Builth Inlier, Powys.*

volcaniclastic sandstones (some richly fossiliferous, see Lockley 1984), fine sandstones and shales, the proportion of shales increasing upwards. The highest (downstream) beds are graptolitic siltstones and shales normally attributed to the Upper *murchisoni* Shales (Fig. 3.2.1); these are faulted against undoubted Upper *murchisoni* Shales (Elles 1939) before the confluence with the Howey Brook. The lower part of the sequence is equated with the upper part of Llandegley Rocks, with sediments resulting from the erosion of the Builth volcanic cone.

The analysis of samples HB 1-3, from the lower part of the shale succession, has revealed beds of lower *murchisoni* Biozone, as discussed in 1.3.1.2. Although the sequence is locally faulted, there is no evidence of significant displacement. The succession contains several bentonites, and a locally abundant graptolite/inarticulate-dominated fauna lacking trilobites; the Upper *murchisoni* Shales, exposed downstream, contain *Ogygiacarella* and ceratiocarids.

### 3.2.2 Sedimentology and taphonomy

All analysed samples occur within dark grey, slightly micaceous siltstones. Maximum grain size is approximately 0.05 mm, excepting occasional pumice fragments and dispersed crystal tuff bands. Identifiable grains are dominated by rounded to angular quartz, muscovite flakes and subordinate angular plagioclase, usually degraded. Small (up to 30 μm, dominantly <5 μm) pyrite framboids are abundant, often marking organic fragments. Lamination is restricted to inconsistent, primarily sub-millimetre diameter organic layers, emphasised by linear framboid arrays, and plausibly representing disseminated algal fragments.

Sedimentary structures are obscure: indistinct and inconsistent 'rippled' beds are not certainly of primary origin, since small-scale compressional deformation

occurs locally. Deformation of organic laminae around buckled *A. micula* valves indicates limited soft-sediment deformation. Burrowing is usually not obvious, even in beds overlying ash horizons. Thin sections reveal sub-millimetre, simple infaunal traces that show reduced organic content, suggesting deposit-feeding through sediment ingestion.

Occasional sandstones and tuffites are interspersed with the shales; these are isolated influxes, possibly representing late-stage erosional events of the Builth volcanic cone.

Graptolites are usually preserved as graphitic films, rarely with significant organic material or partial pyritisation. Relief is limited, but fidelity of preservation is generally sufficient for specific identification. Fragmented rhabdosomes occur very rarely. Inarticulate brachiopods are preserved as black, presumed chitinophosphatic material, and invariably intact, although *A. micula* specimens are usually buckled. The proximal region of *A. micula* shells remains undeformed, but the remainder flattens, with characteristic radial creasing. The proximal region often shows a single axial crease, interpreted by Lockley and Williams (1981) as an original feature. There is no obvious dissolution in most cases, although some are preserved as thin brownish films, perhaps because of weathering. Rare trilobite fragments and other calcareous fossils are preserved as three-dimensional decalcified moulds, although nautiloids are strongly flattened. Sponge spicules are generally preserved as recrystallised silica.

A single articulated palaeoscolecid was recovered from HB 2, showing phosphatic preservation of dermal plates. Fragmentary algal remains are rare. Very rare ceratiocarids are preserved as thin graphitic films (small) or as moulds, with slight relief (large). Rapid descent and burial of planktic organisms is implied by the preservation of pseudoplanktic associations of *A. micula* with *Archiclimacograptus*

sp. (Botting and Thomas 1999), preserved in section HB 2. This may be the result of relatively shallow, quiet water with high sedimentation rates. Benthic anoxia (occasional dysoxia) would have reduced biodegradation.

### 3.2.3 HB 1

Section HB 1 (Fig. 3.2.2) comprises sparsely fossiliferous, homogeneous grey siltstones containing two closely-spaced tuffs (insufficient separation for sampling). *A. micula* is the dominant fossil, with rare graptolites. The generally low abundance prevented diverse faunal analyses, with data concentrated on *A. micula*.

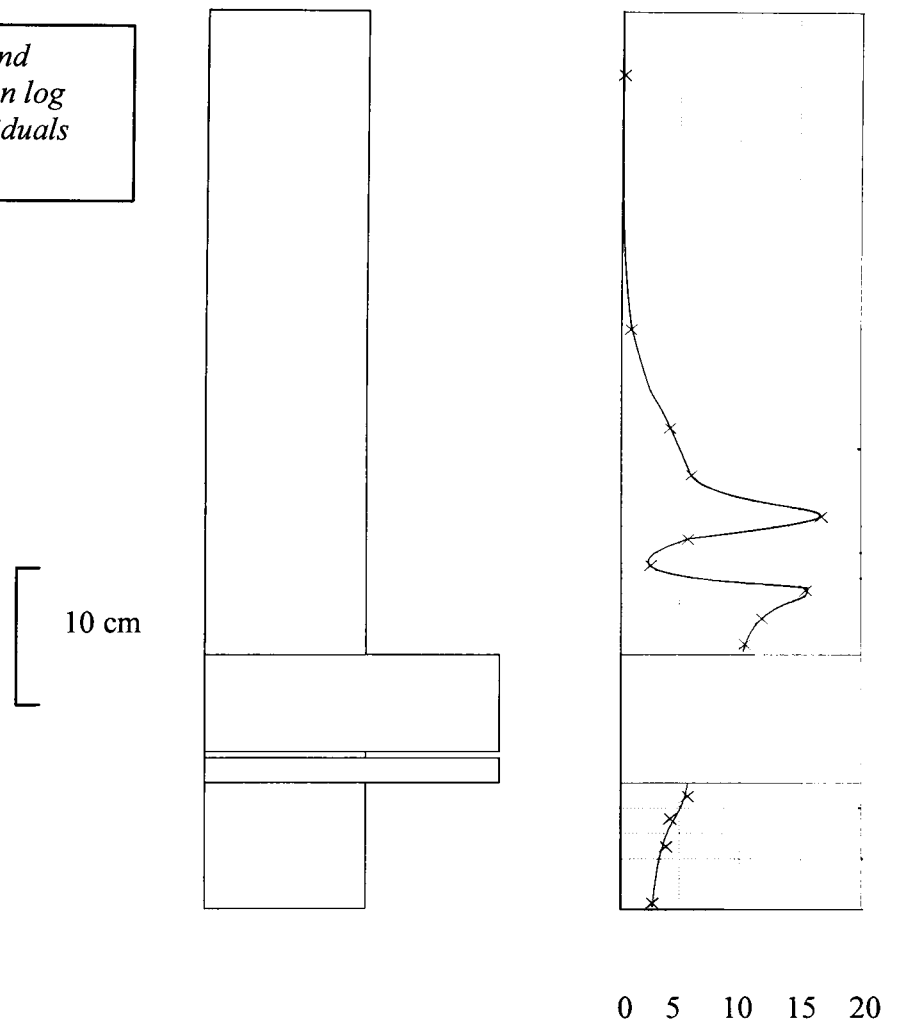


Fig. 3.2.2: *Distribution and abundance of* A. micula *in log HB 1, measured as individuals per 100 g.*

Initial levels of consistently 3 to 5 individuals per 100 g were replaced by elevated abundance following the tuff. A maximum of between 15 and 20 individuals per 100 g was reached on each of two abundance peaks, separated by a trough at close to pre-tuff levels. The second peak declined gradually to very low levels, maintained until at least 60 cm above the tuff.

The initial levels show a weak increase prior to eruption, a feature observed also in section HB 3 (although this may be due to an underlying tuff), and in the sandstones of Llandegley Rocks (LR 1). Possible causes of a consistent trend of this nature include weak blooms from low-level tuff addition of preliminary eruptions, or environmental destabilisation following seismic activity. However, there is presently little evidence of consistency, and this feature is not interpreted further at this stage.

A small preliminary sample at the level of the first peak recorded an abundance of close to 40 individuals per 100 g. The observed peaks are sufficiently sharp that this could represent a real phenomenon, with brief, higher abundance disguised by averaging over 2-cm intervals. Although didymograptids occur sporadically, with occasional indeterminate organic material (algal?), associated faunas are extremely restricted.

### 3.2.4 HB 2

Section HB 2 comprises a series of four thin tuffs within the Lower *murchisoni* Shales, exposed in a small cliff section (Fig. 3.2.3), and overlying thin sandstones and tuffites. The tuffs, in ascending order, comprise a thin pumiceous lamina, a coarse sandstone bed immediately overlain by a thin bentonite (6 cm), a coarse sandy tuff (5

cm) and a homogeneous fine tuff (3 cm). *Didymograptus murchisoni* and *Archiclimacograptus* sp. are common, occasionally forming apparent mortality beds. There are insufficient data to establish whether the size distributions are typical of winnowed or primary assemblages (Williams and Rickards 1984). The fauna is more diverse than that of HB 1, although this may reflect larger collections; excluding *A. micula* (see below), obvious benthos is limited to rare ostracodes and sponge spicules. The fauna includes associations of *A. micula* with *Archiclimacograptus* sp., described by Botting and Thomas (1999). Much of the evidence for the partly pseudoplanktic lifesytyle of *A. micula* (associations; size distributions – see below) derives from this locality.

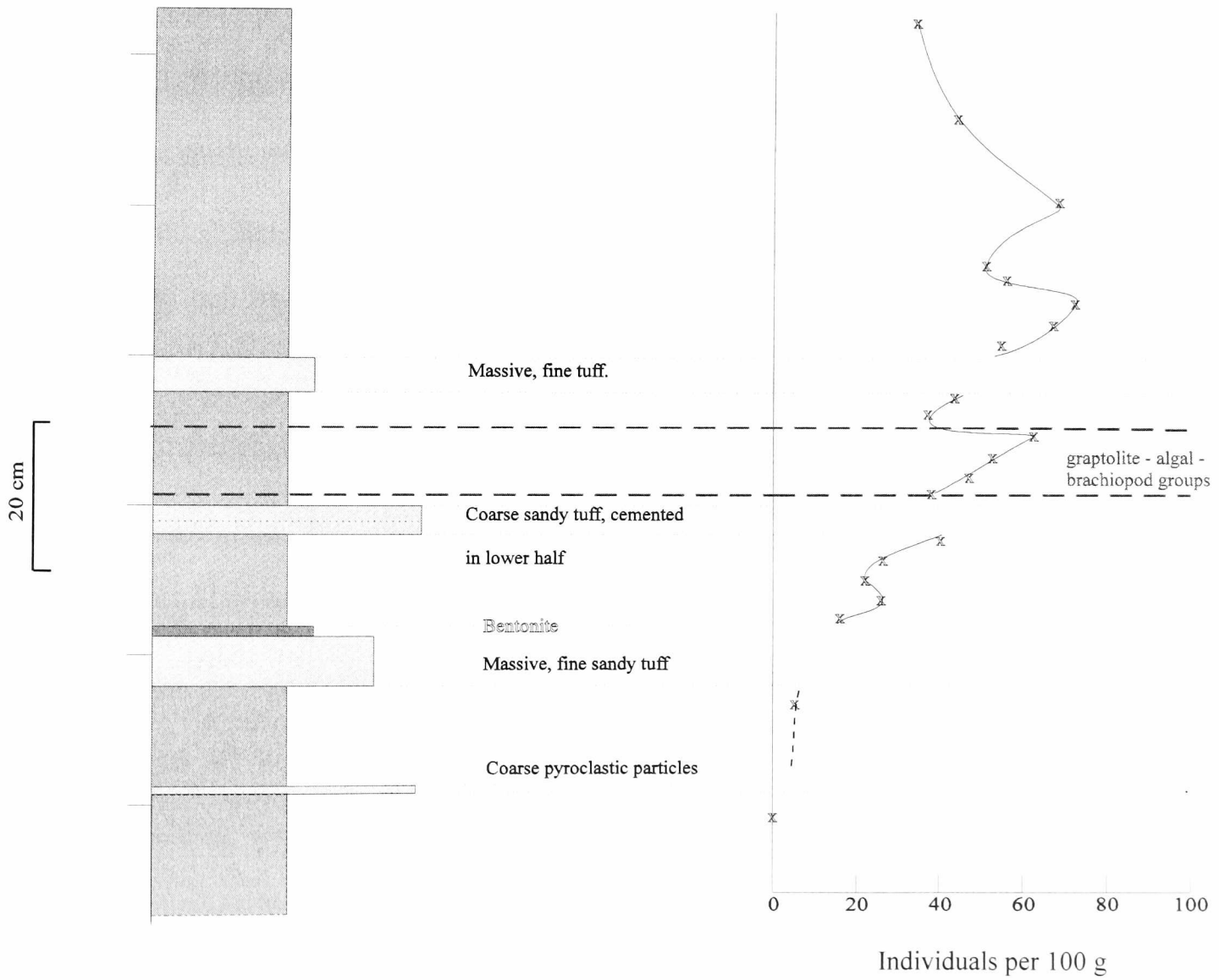


Figure 3.2.3: *Abundance of* A. micula *in section HB 2, showing graptolite mortality beds (dashed).*

Most data relate to *A. micula* abundance. Initial levels of 3-5 individuals per 100 g increase to a maximum of over 70 per 100 g following the fourth tuff. The first ash lamina has little or no effect on faunal abundance, while the following three are all followed by a bimodal increase in abundance, which is cumulative across each interval. Graptolite "mortality" beds follow the third tuff horizon. A gradual decline, the conclusion of which is not seen, follows the fourth tuff.

Analyses of *A. micula* size distributions have been performed on many of the samples, in order to establish population structures. The data reveal a consistent distinction between the two peaks in each bimodal bloom. The first peak shows an approximately normal distribution, while the second is strongly skewed towards juveniles. Between the two peaks, and during the decline from the second peak above the fourth tuff, the two populations appear to be superimposed. A bimodal population structure is difficult to achieve through winnowing, and is almost certainly indicative of two distinct populations.

The juvenile-dominated upper peak is the expected result of normal, high abundance conditions (Williams and Rickards 1984). A normally-distributed population is often the result of winnowing, but the presence of superimposed distributions implies the mixing of a winnowed sample with a primary one. This is problematic, since the current that deposits winnowed material would be expected to act also on the material at the depositional site. Slumping cannot explain the conservation of a smooth bimodal pattern, seen in all Builth Inlier samples; homogenisation would be expected, with abundance equalling the average of the two peaks. The consistent presence of the trough therefore indicates two independent populations of *A. micula*.

It may be argued that the two populations reflect different species, especially since available distinguishing features are few. The species has previously been split into subspecies, based on statistical analyses of length-width ratios (Lockley and Williams 1981). Further studies on more complete data sets refuted this separation (Sutton 1999); this accords with an analysis of over 500 valves from Llandegley Rocks. *A. micula* was an extremely variable species, but there is no evidence to support subdivision.

Evidence from clusters of *A. micula* with a monospecific graptolite host, or with no apparent nucleus (presumed algal) implies the presence of at least some pseudoplanktic *A. micula*. A pseudoplanktic interpretation of the species is plausible, given a distribution throughout Avalonia, and parts of Baltica (e.g. SM A51403, A40540, A40538), during the Middle Ordovician. A very similar specimen was also recovered from a borehole in Syria (SM A46581); *A. micula* is sufficiently inconspicuous that it may have been largely overlooked at other sites.

The presence of overlapping populations is therefore strong evidence of distinct communities, the initial peak interpreted as a pseudoplanktic population, and the second as benthic.

### 3.2.5 HB 3

Pale grey, micaceous siltstones containing an extremely abundant graptolite – inarticulate fauna. Although only one tuff (analysed in section 1.3.1.4) is included in the section, there is strong evidence that a second underlies this by some 10 cm, the section being cut by a small oblique fault. Exposure is very limited and underwater, with practical difficulties preventing field relationships from being established unequivocably.

The sampled section (figure 3.2.4) contains a non-diverse assemblage comprising pendent didymograptids, rare diplograptids, *A. micula*, *Monobolina crassa*, ceratiocarids? and a single conulariid. Benthic colonisation is shown by the *A. micula* distribution, and by small burrows in thin section. The didymograptid fauna changes dramatically in character in sample G, where *D. artus* is replaced by *D. murchisoni.* This does not represent the transition between the two biozones (section 1.3.1.2), but reflects a rapid transition in species dominance, the reason for which is uncertain. The two species oscillate in abundance throughout the Main Feeder succession.

*A. micula*: A fluctuating initial population (probably reflecting an underlying

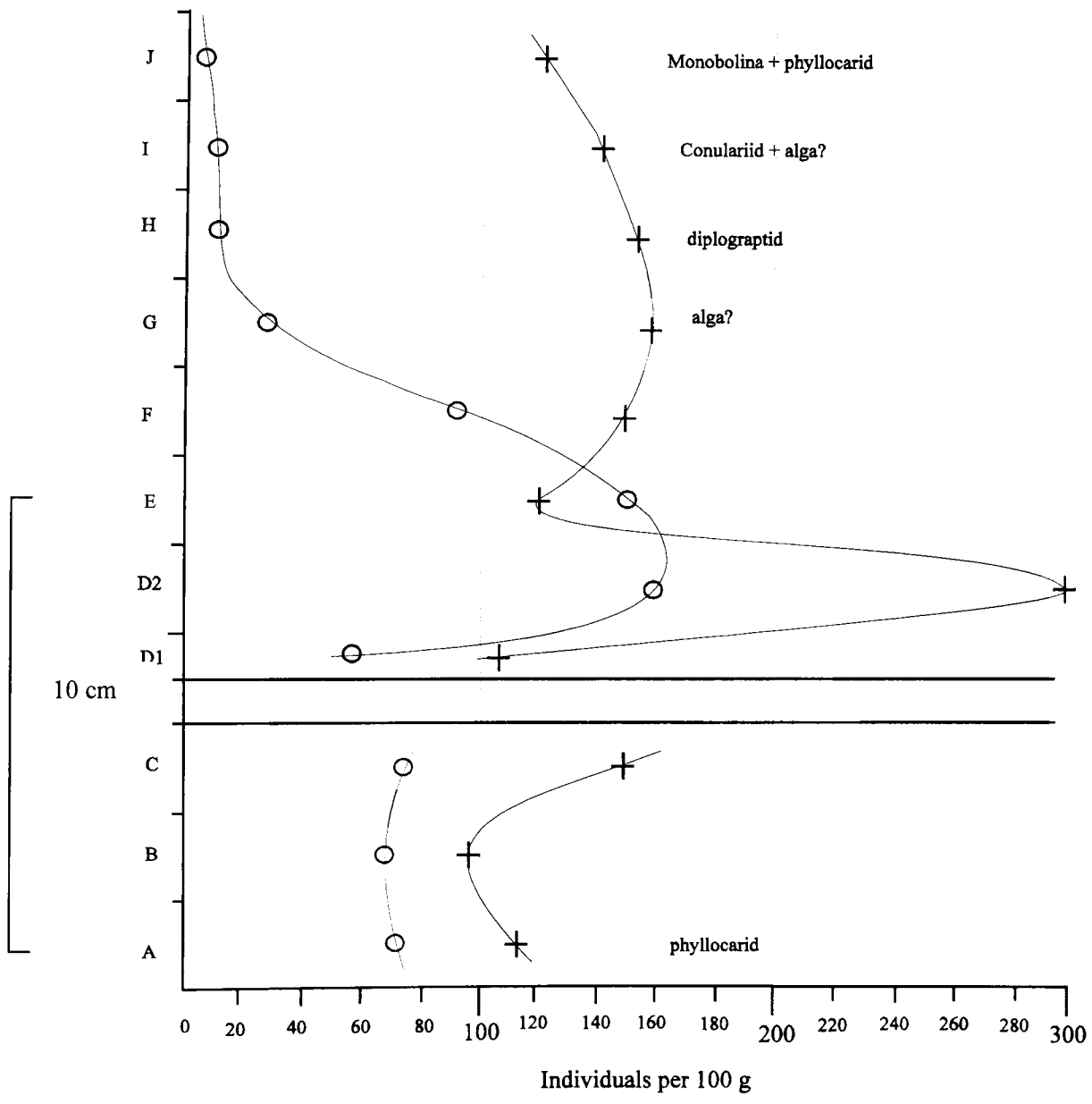


Figure 3.2.4: *Faunal abundance distribution for section HB 3. Circles: didymograptids; crosses:* A. micula*; all other organisms noted. Abundance is given in individuals per 100 g. Pre-tuff fluctuations may be due to a lower, unexposed tuff.*

tuff) is replaced by a dramatic bimodal bloom of very high abundance. The first peak maximum comprises up to 300 individuals per 100 g, followed by a dip to around 100. The second peak is strongly drawn out, reaching a maximum of around 160, and decreasing smoothly thereafter.

Didymograptids: A single initial peak, correlated with that of *A. micula*, is followed by a smooth exponential decline to low levels. There is no indication of the second *A. micula* peak. *Monobolina*, conulariids and ceratiocarids(?) occur within the second *A. micula* peak, although rare burrowing is concentrated in the lower samples.

It is possible to estimate changes in sedimentation rate across the tuff by comparing abundance between levels C and D1. If the tuff is assumed to represent a instantaneous time period, then the thin (10 mm) nature of sample D1 allows reasonable confidence that abundance recorded in this interval accurately approaches the immediately post-depositional level. For both didymograptids and *A. micula*, abundance decreased across the tuff by approximately 1.4, possibly suggesting a sedimentological, rather than ecological cause. This could be produced by increasing the non-volcanic sedimentation rate by at least 1.4, or through mixing of the upper layers of the tuff via bioturbation (Fisher and Schminke 1984, p. 170). Since bioturbation appears to have been limited to small isolated burrows, a change in

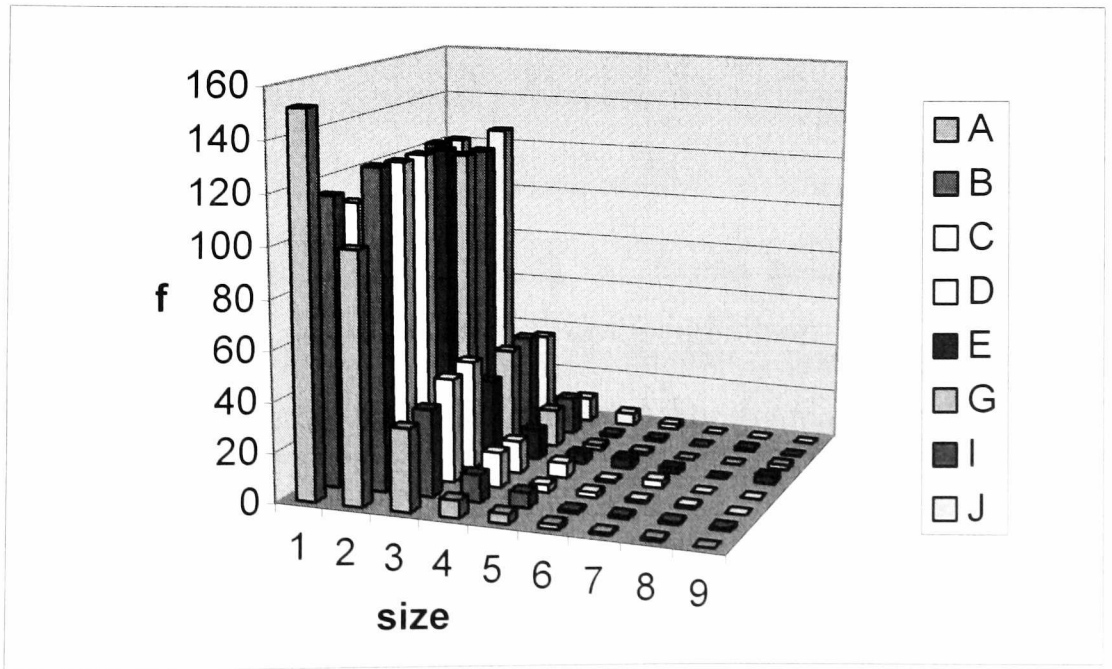


Figure 3.2.5: *Overall framboid size distribution (n/sample=300; N=2400). Size unit = approx.. 2 μm.*

ambient sedimentation rate may be more likely.

Analysis of pyrite framboid diameter (Wignall and Newton 1998) has been employed to estimate variation in benthic oxygenation, by the method described in section 3.1.2. The overall distribution is shown in Fig. 3.2.5, while skewness and larger framboid abundance are illustrated in Fig. 3.2.6. Thin sections of samples B, C and D show significant dispersed ash, although this is not obvious in hand-specimen. The data indicate increased oxygenation following ash-fall, although variation is irregular. Maximum abundance of larger fractions (>3; c. 5 μm) occurs immediately following ash deposition, after which an interrupted decrease approaches original proportions. This is also illustrated in skewness: since this concept refers to a normal distribution, rather than sub-logarithmic, lower positive skew indicates an increased

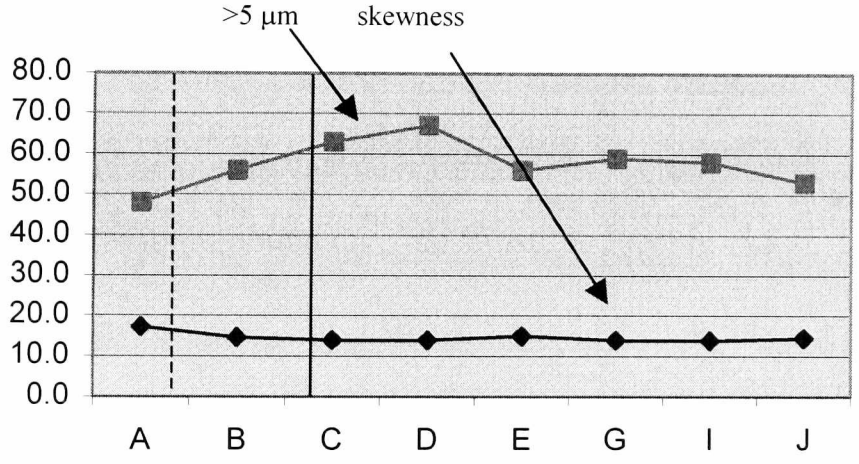


Figure 3.2.6: *variation of size fractions >5 μm (total) and skewness (x10) between samples; note that insufficient material from samples F and H was recovered for sectioning, following analysis. Significant ash input begins in B, with the main deposit between C and D.*

proportion of larger size divisions. This provides a measure of the entire data set, rather than individual size fractions. The skew shows a progressive decrease during ash deposition, with a generally slow increase until sample J. Data for sample E were anomalous, in that although the total number of larger framboids was relatively low, those present included several of the largest recorded. The presence of several framboids exceeding 20 μm diameter despite a relative paucity of slightly smaller sizes, may be indicative of heterogeneous oxygenation, with isolated pockets within otherwise anoxic sediment.

## 3.3 BACH-Y-GRAIG SSSI (SO 073 611)

### 3.3.1 Locality

The famous stream section northeast of Hillside (formerly Bach-y-Graig) was an important site in the work of Elles (1939), C. P. Hughes (1969, 1971, 1979), R. A. Hughes (1989) and Sheldon (1987 a, b). At the eastern end, it contains the *murchisoni-teretiusculus* transition, overlain by around 100 m of the lower *teretiusculus* Shales. The section is highly trilobitic in the lower and central parts, with abundant graptolites throughout; the upper part (Fig. 3.3.1), from which sections BG 1, 2 and 3 were obtained, is characterised by localised benthic anoxia and a reduction in the trilobite fauna. Outcrops higher in the biozone contain abundant benthic trilobites, but details of their distribution are unclear, as no complete transects are available.

The Bach-y-Graig section contains abundant bentonites, up to 55 cm thick, with calcareous ashes and crystal tuffs, derived from a reasonably local source (see section 1.3.1.1). The limestones reported by Elles (1939) appear to be absent, although calcareous nodules occur sporadically. Several small faults cut the section, the throws of which are unknown; however, there is no evidence for substantial displacement. The presence of *Protolloydolithus lloydi* in the upper exposures indicates that the entire sequence lies within the lower part of the *teretiusculus* Biozone.

### 3.3.2 Sedimentology and taphonomy

Background sediment comprises pale (BG 3) to dark grey, poorly sorted siltstones, with grain size typically less than 0.05 mm, and occasional grains up to 0.10 mm (very fine sand). The matrix is of fine silt/mud. Identifiable grains are dominantly

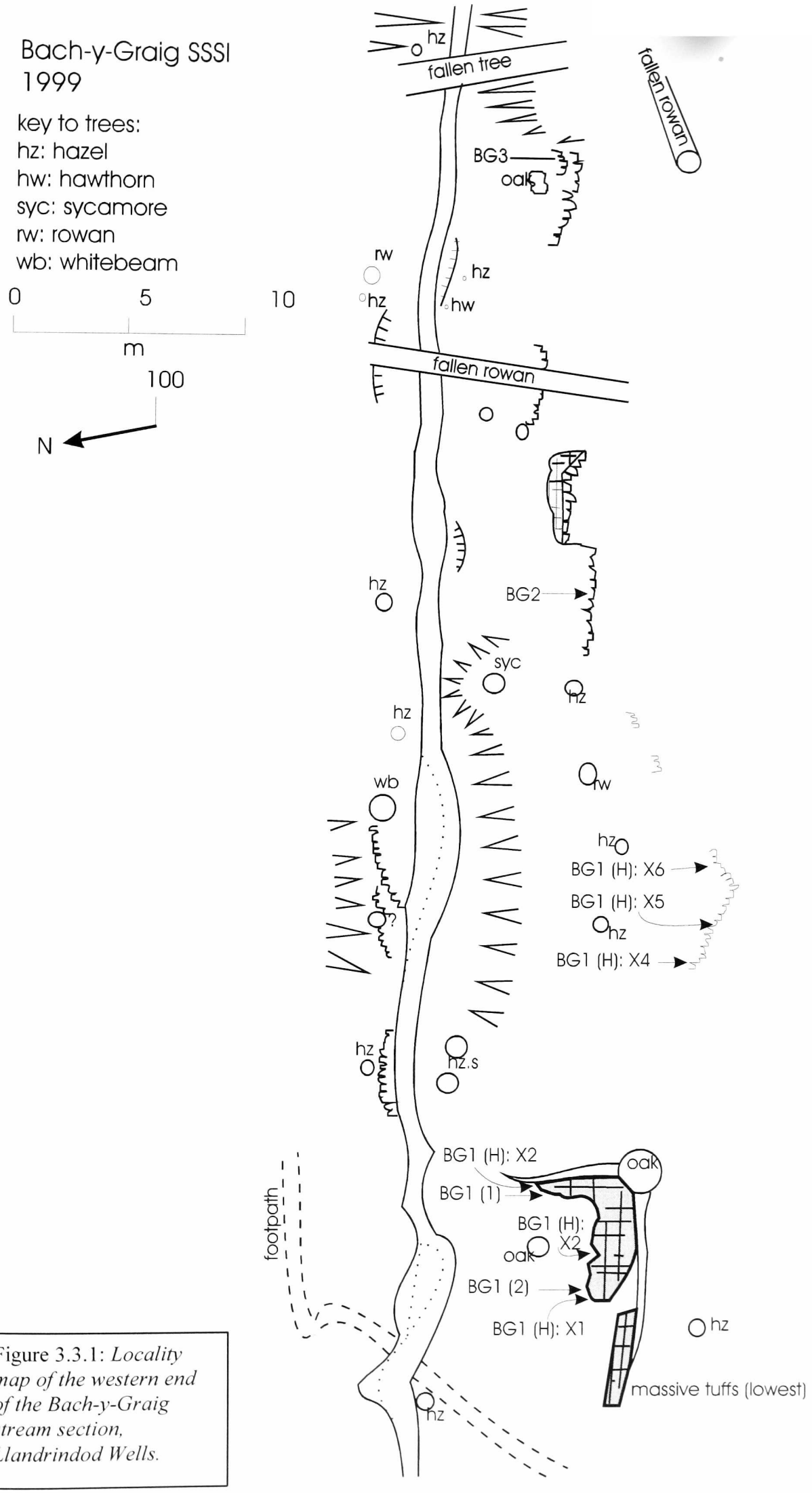


Figure 3.3.1: *Locality map of the western end of the Bach-y-Graig stream section, Llandrindod Wells.*

rounded to highly angular quartz, and mica flakes, with rare degraded feldspars; opaques are the most frequent accessory minerals. Pyrite occurs as abundant small framboids, and occasionally in cubic form. Organic material is ubiquitous at low to moderate levels, usually forming thin, inconsistent laminae emphasised by pyrite framboids. Occasional crystal (e.g. BG1: F) and clay tuff laminae occur, up to 2 mm in thickness; crystal tuffs are dominantly composed of quartz and plagioclase, often euhedral. Pumice clast remnants occur in siltstones throughout the section, but are generally less than 10 mm in diameter. Tuffs sometimes show weakly deformed bedding, probably due to soft-sediment deformation.

Current activity is seen in asymmetrical ripples at the upper boundaries of tuffs in BG 1 and BG 2. Slight rippling occurs locally up to 10 cm above the tuffs, but is indistinct and minor. There is no significant reworking of the main tuff deposits, although the secondary ash input of BG 1 is relatively diffuse. Millimetre-scale vertical and oblique burrowing is occasionally visible in hand specimen at the tuff upper surfaces, while frequent sub-millimetre, sediment-infilled burrows occur in thin sections.

Fossil preservation is almost identical to that in sections HB 1-3. Graptolites are common, preserved as graphitic films with slight relief; pyritisation affects a small proportion, but is rarely extensive. Inarticulate brachiopods vary between black chitinophosphate, thin brown, presumed organic veneers, and thin graphitic films. Conodonts are mouldic, often with a thin black external veneer; phosphatic plates on a single palaeoscolecid cuticle fragment are largely retained, as is the phosphatic test of *Sphenothallus*. Sponge spicules (siliceous) are recrystallised or mouldic. All calcareous organisms are mouldic, but small fossils are usually undeformed; this

includes ostracodes, trilobites, rare articulate brachiopods and heteractinid sponge spicules. Trilobites are rarely articulated, and usually occur as small fragments.

### 3.3.3 BG 1

The uppermost bentonite in the Bach-y-Graig stream exposures is the most intensely studied argillaceous section in this work. An initial data set (BG1 (1)) was followed by larger samples (BG1 (2)), two metres laterally from the original samples; finally, a horizontal sequence across 13 m of limited exposure was analysed, from immediately above the tuff (BG 1 (H)). Pyrite framboid size distributions were established for BG1 (2), in order to estimate benthic oxygenation (Wignall and Newton 1998). An initial interpretation of BG 1 and BG 2 was presented by Botting (1999).

The exposed succession comprises mudstones, siltstones and ashes, overlain by massive tuffs. Tuff BG 1 is a thick bentonite, varying in thickness between 41 and 55 cm, and containing weathered subspherical nodules, probably originally calcareous (cf. Briggs *et al.* 1996). Extensive excavation has failed to reveal any fresh nodules; original mineralogy may have been lost through Caledonian hydrothermal alteration. Secondary, minor ash input occurred after 8 to 10 cm, with additional, very slight input at 6 cm.

The pre-tuff fauna indicates anoxic conditions, although samples D to K contain rare benthic invertebrates. Burrowing occurs in the uppermost part of the main tuff, which is overlain by localised cross-bedding.

*BG 1 (1)* (Fig. 3.3.2). *A. micula* occurs at low levels (less than 5 per 100 g) prior to eruption, but rapidly proliferates into a distinct bimodal bloom, the second peak reaching 50% greater abundance than the first. An apparently rapid decline from

sample J to K is followed higher in the sequence by approximate equilibrium at 30 to 50 per 100 g (additional samples, not illustrated). Diplograptids show a complex bloom structure, following very low pre-tuff abundance. A low maximum corresponds to the first peak of *A. micula*, with a subsequent, corresponding low point. A more dramatic bloom occurs from H through J, at around twice the previous maximum. Ostracodes reach a maximum in samples D to F, continuing at low levels thereafter. The distributions of other taxa are shown in fig. 3.3.7.

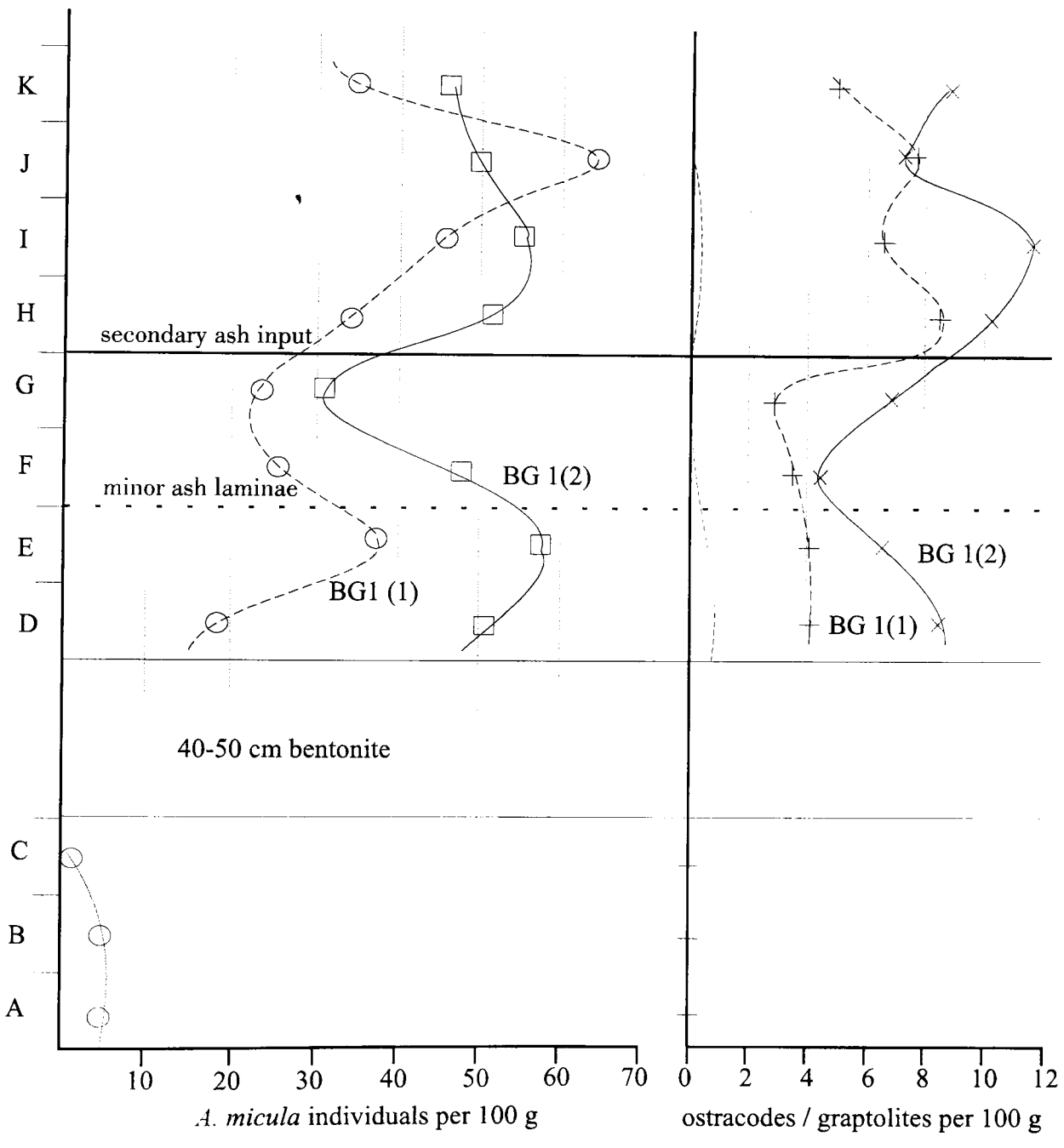


Figure 3.3.2: *Faunal abundance and distribution in logs BG 1(1) and BG 1(2):* o, A. micula *(BG 1(1)):* □, A. m. *(BG 1(2)):* +, *graptolites (BG 1 (1)):* x, *graptolites (BG 1(2)): unmarked line, ostracodes, approximated from low abundance in both logs. Vertical scale: 2 cm units.*

*BG1 (2).* (Fig. 3.3.2) *A. micula* shows a distribution very similar to that of BG1 (1), although with generally higher abundance. The increase is particularly obvious in the lower samples, while the upper peak is slightly flattened. Positions of maxima and minima correspond in all but the second maximum, which occurs one sample lower in BG 1(2).

Diplograptids begin at higher abundance in D, dropping to a minimum at F (one sample lower than in BG1 (1)), before rising to a single maximum in sample I. Ostracodes decline smoothly from a maximum in D, occurring at low levels thereafter. Sponge spicules occur in samples D to G. The full faunal distribution is shown in Fig. 3.3.7. The two chitinozoan morphotypes appear to have mutually exclusive distributions, and do not correspond in abundance to other groups.

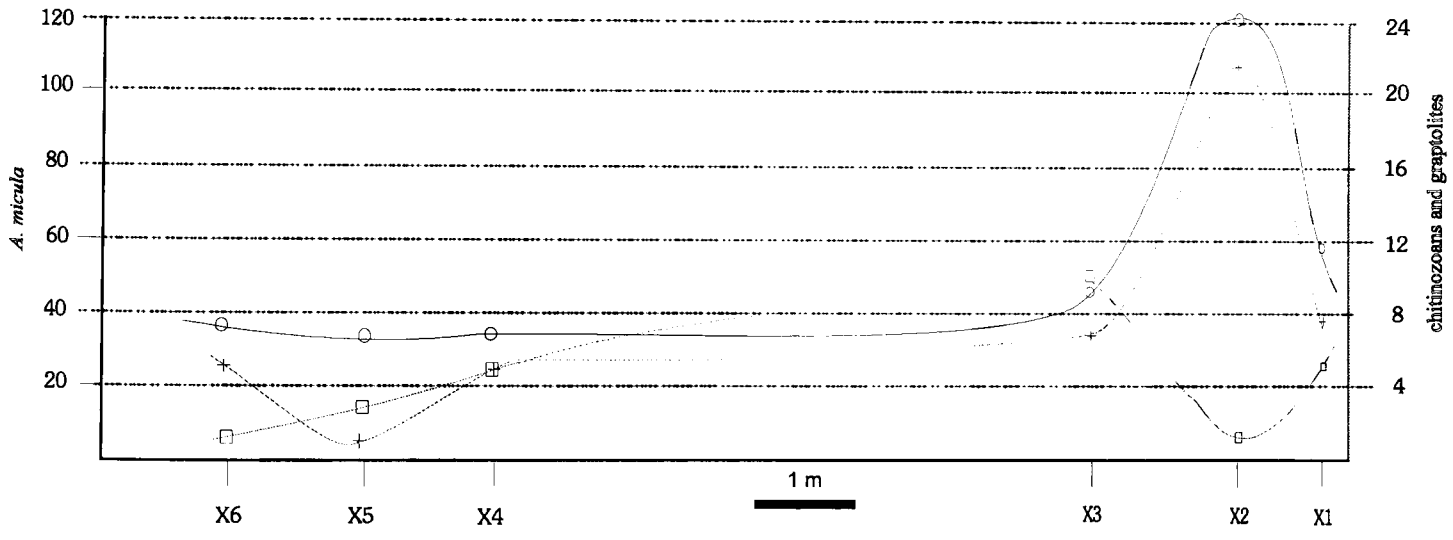


Figure 3.3.3: *Lateral variation within log BG 1 (H); samples correspond vertically to sample D of BG 1 (immediately above bentonite);* o, A. micula; □, *chitinozoans;* +, *graptolites; abundance in individuals per 100 g.*

*BG1 (H)* (Fig. 3.3.3). *A. micula* occurs at approximately constant levels above the thinner part of the tuff, but rises to a dramatic peak above the thickest area. The region of increased abundance reached a maximum width of 1.8 m. There is some indication of a slight trough adjacent to the peak, with a very gradual increase towards the lateral

deposits: sample BG1(1) D, taken between X2 and X3, yielded *A. micula* abundance of less than 20.

Diplograptids occur at low to moderate levels in lateral samples, with a distinct peak corresponding with that of *A. micula*. Chitinozoan maxima occur on either side of the *A. micula* peak, with a minimum abundance in the centre.

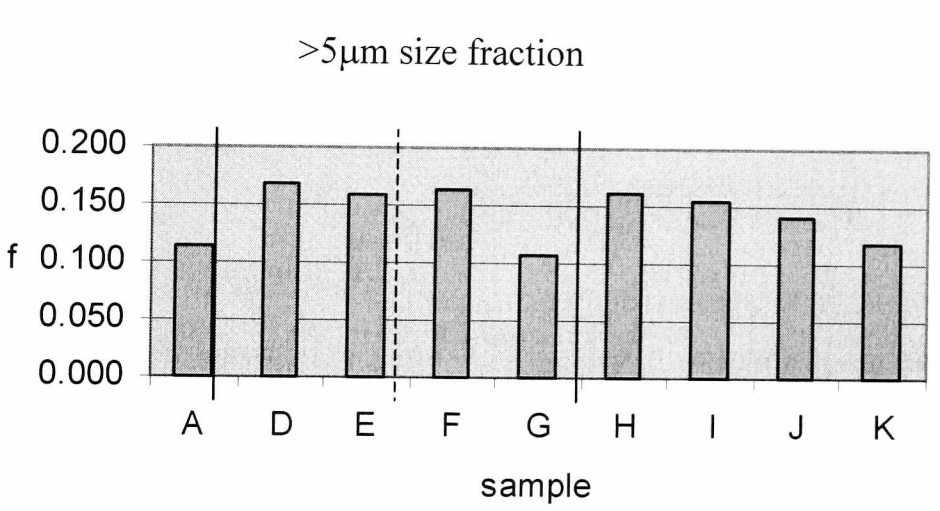


Figure 3.3.4: variation of pyrite framboid proportion greater than 5 μm in log BG 1. Vertical lines indicate main ash inputs, dashed where minor.

The size distribution of pyrite framboids shows clear evidence of limited benthic oxygenation (Wignall and Newton 1998). Although all samples are dominated by framboids of diameter less than 5 μm, larger framboids, indicating higher oxygenation levels, are most abundant immediately following ash input, then gradually decline to initial levels. This is most clearly seen among 5 to 7 μm framboids (Fig. 3.3.4), which are sufficiently common for statistical significance. Smaller framboids are insufficiently distinct from the anoxic population.

The results of the analysis clearly indicate increased oxygenation following the primary tuff and the ash influx of sample H, while also weakly recording the tuffitic element in sample F. Oxygenation appears to have been strongly dependent on

the extent of tuff deposition, the minor ash laminae producing only slight oxygenation.

### 3.3.4 BG 2

Section BG 2 (Fig. 3.3.5) contains a tripartite tuff bed of total thickness 27 cm, with additional dispersed ash laminae below, and in samples J and K. The main tuff deposit comprises a basal fine sandy tuff; a central, normally graded coarse to fine sand unit; overlain by a fine flinty ash. The upper surface shows ripple laminations, and slight

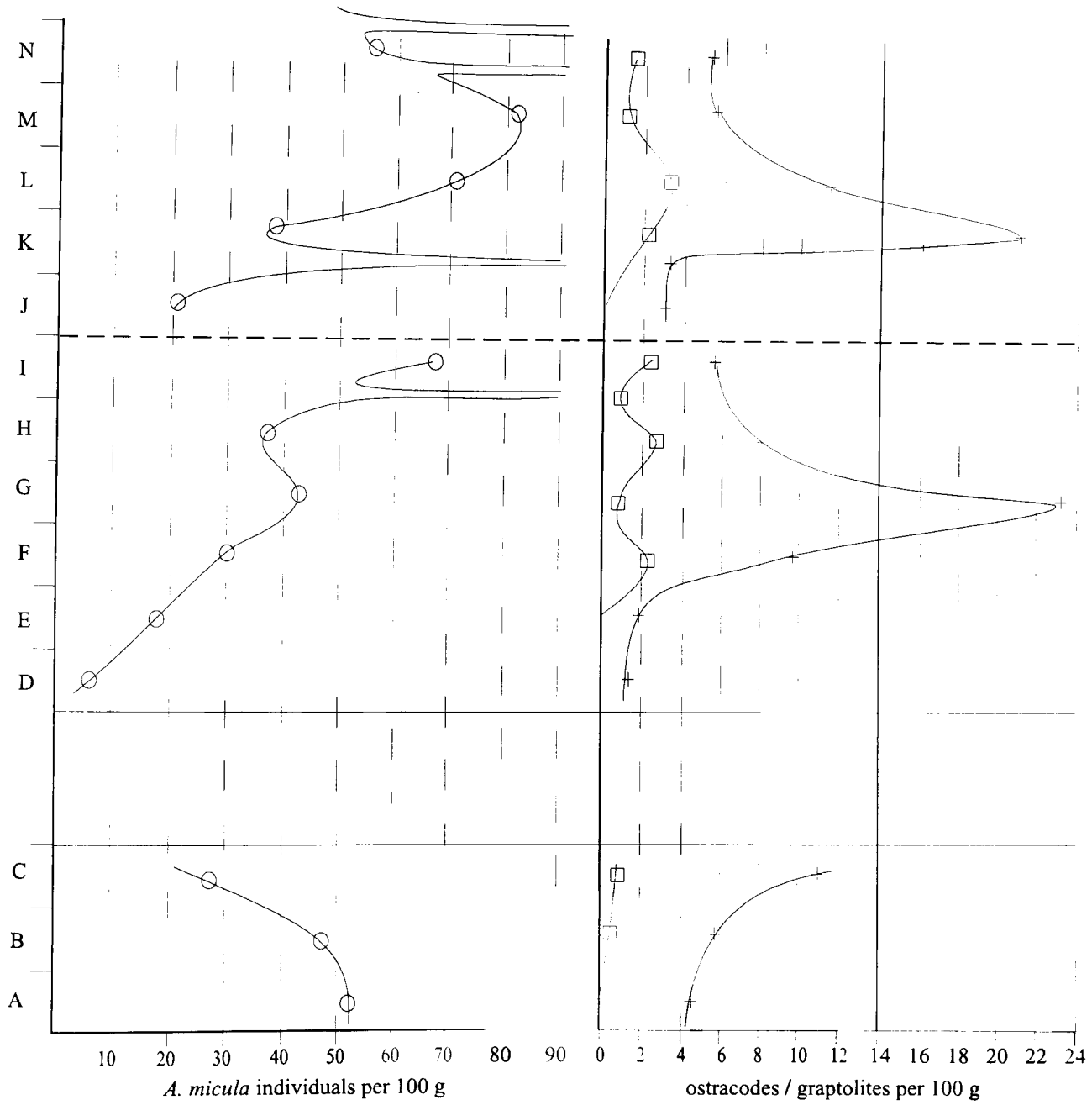


Figure 3.3.5: *Faunal abundance and distribution of log BG 2, in individuals per 100 g; o,* A. micula*; +, ostracodes; □, graptolites. Vertical scale: 2 cm units.*

ash reworking. Pale ash laminae in the surrounding shales are inconsistent, possibly slightly rippled, with occasional burrows. The pre-tuff fauna contains an abundant but non-diverse benthic population of *A. micula* and trilobites, indicating upper dysaerobic benthic conditions.

*A. micula* declined exponentially prior to eruption, probably due to the input of abundant ash particles. Abundance falls to near zero following the tuff, but then increases rapidly to a bimodal peak. The first peak is relatively minor, while the second is truncated by the ash laminae in J. The second peak then re-initiates from a level corresponding to the extrapolated abundance of the first population at this point. A rapid decline begins between M and N. The second peak, before and after the second ash input, contains occasional dense bands of *A. micula*, reaching abundance of up to 400 individuals per 100 g.

Diplograptids are rare throughout, oscillating at low levels, comparable with those of the benthic(?) lingulid *Palaeoglossa*. Ostracodes proliferated during the pre-tuff decline of *A. micula*, and were reduced to zero by the main deposit, but show a peak correlating to the first of *A. micula*. A second, sharp peak occurs following the ash input of J, but declines dramatically prior to the first *A. micula* peak.

### 3.3.5 BG 3

Two tuffs, separated by 2 cm, occur within pale grey siltstones. The upper tuff was subjected to XRF analysis (BG3 T2), which indicated andesitic composition. Graptolites are extremely rare, while an abundant but non-diverse benthos indicates dysaerobic conditions prior to eruption. There is no preserved evidence of current activity, and no obvious burrowing, although, by comparison with BG 1 and BG2,

both were probably present. The upper limit to the samples is dictated by restricted outcrop.

*A. micula* begins at nearly 20 per 100 g, rising in sample C to over 60 (Fig. 3.3.6). Following the first tuff, this falls to 22 per 100 g, rising to 45 following the second tuff. A dip to around 15 separates this from the second peak, which reaches over 50 per 100 g. The initial stages of decline are seen in sample J, prior to truncation of the outcrop.

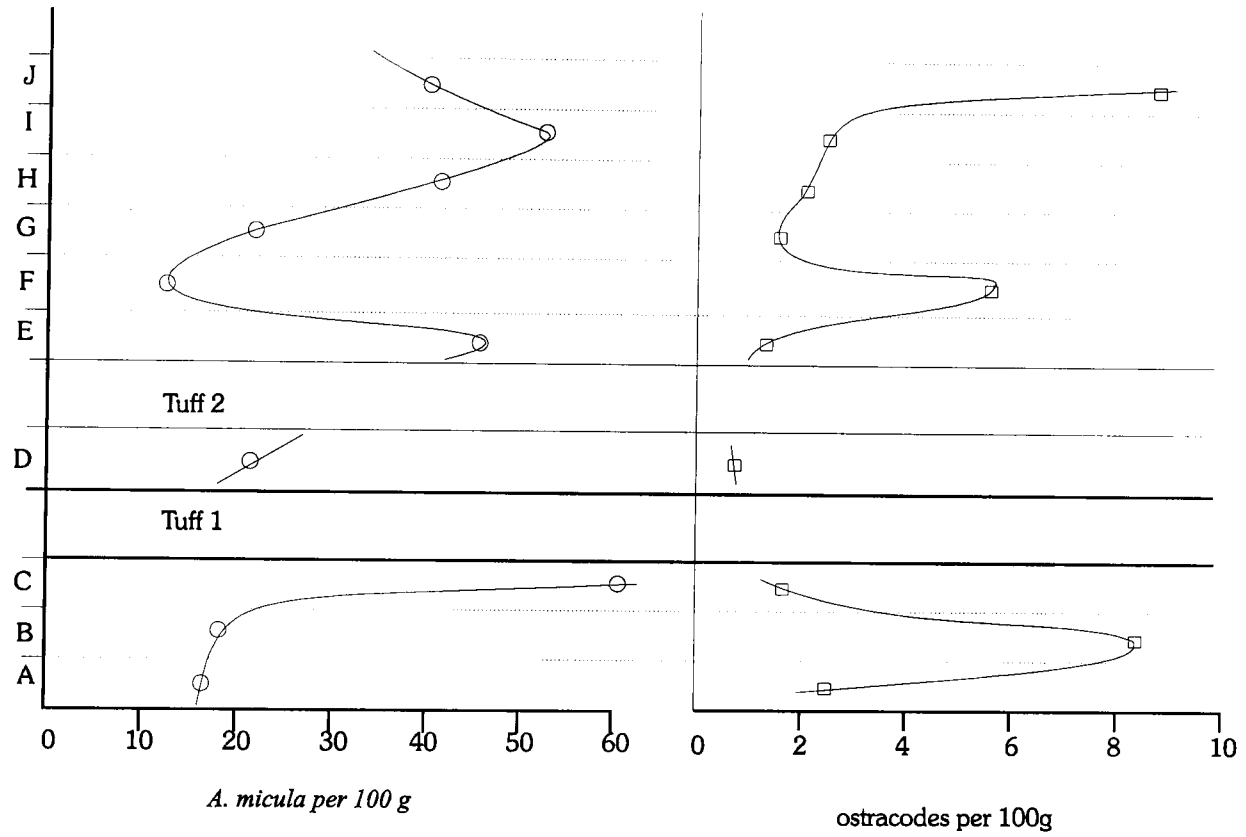


Figure 3.3.6: *distributions of* A. micula *and ostracodes in log BG 3; graptolites extremely rare. Vertical scale: 2 cm units.*

Graptolites are restricted to statistically insignificant siculae in the uppermost samples. Ostracode abundance fluctuated before the first tuff, after which it was reduced to very low levels. Following the second tuff, the population expanded to a peak post-dating that of *A. micula*. Subsequent constant levels continued until sample J, where a further proliferation occurred, in contrast to all other logs. Additional taxa are shown in Fig. 3.3.7.

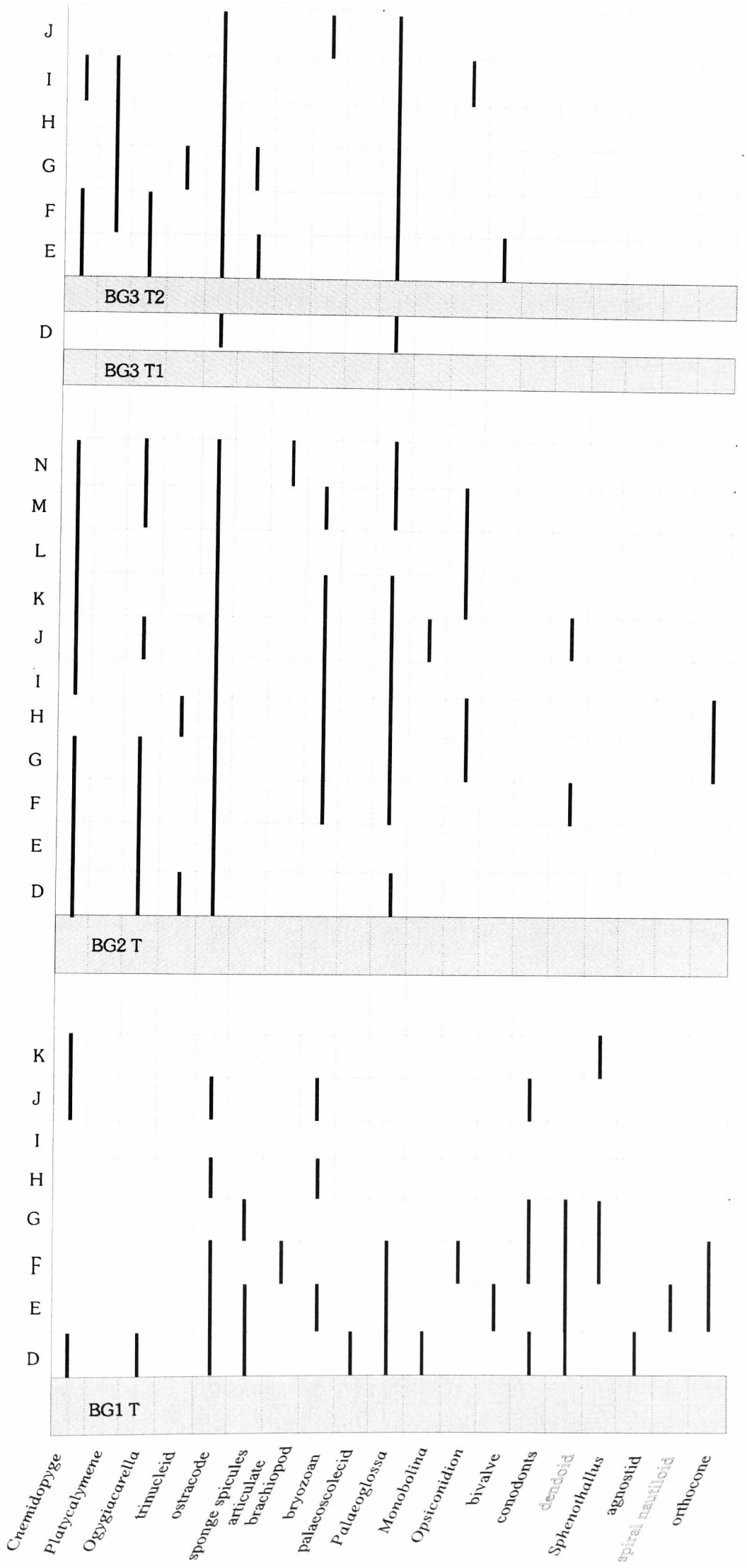


Figure 3.3.7: *occurrence data for identifiable rarer groups in post-tuff samples of sections BG 1, BG 2 and BG 3; ostracodes are included for comparison. Full numerical data are provided in Appendix B.*

## 3.4 Y FOEL, LLANWRTYD WELLS (SN 883 484)

### 3.4.1 Locality

The Gilfach Farm Borehole, described by Cave and Rushton (1996), was located in Nant Cerdin, 2 km north of Llanwrtyd Wells (Fig. 1.3.1). The Middle Ordovician volcanic sequence from the centre of the Tywi Anticline is surrounded by black slates of Caradoc/Ashgill age, previously regarded as unfossiliferous. However, disused forestry cuttings on the western slopes of Y Foel, which bounds the east side of Nant Cerdin, 1.5 km north of Llanwrtyd Wells, include fossiliferous exposures.

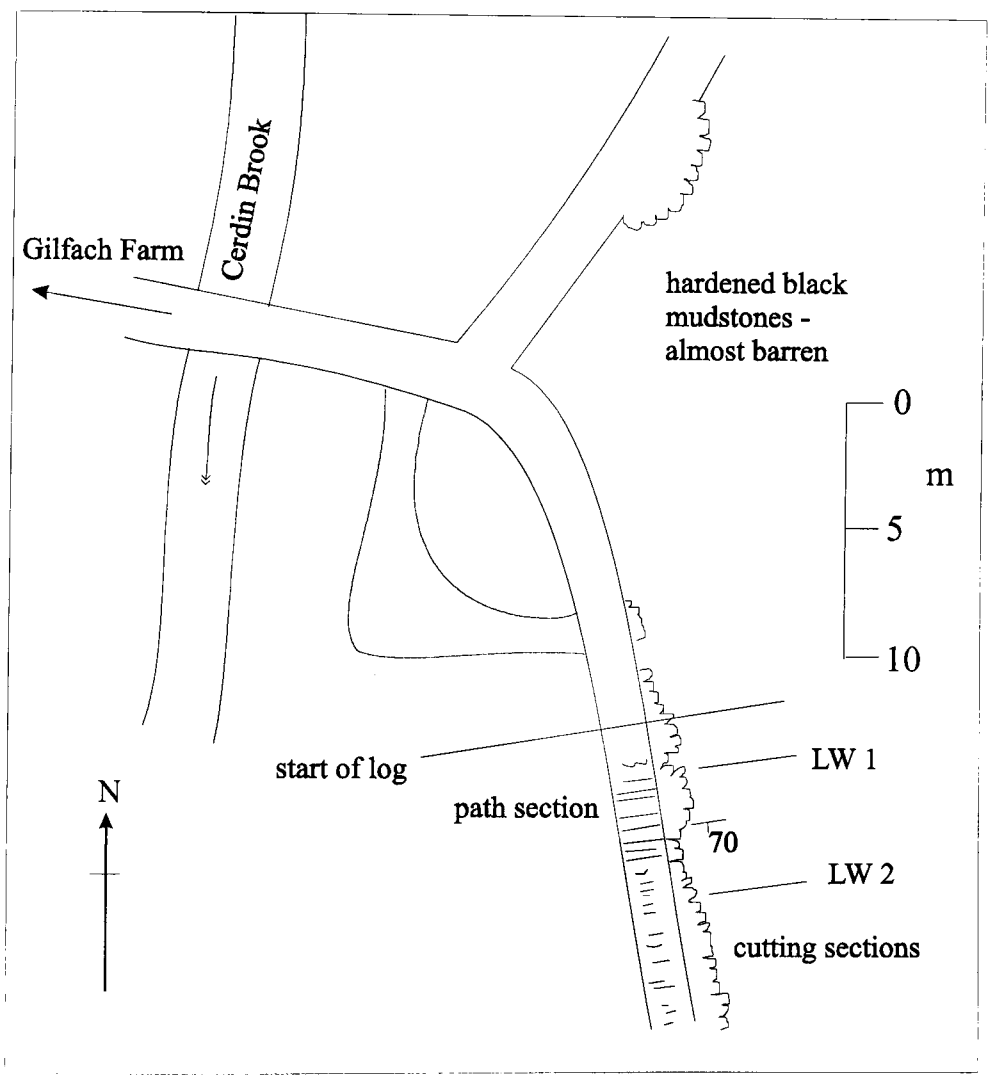


Figure 3.4.1: *Locality map of Y Foel track cutting, Llanwrtyd Wells.*

The cuttings are approached from Gilfach Farm, as shown in Fig. 3.4.1. The track branches after crossing the Allt Cerdin, with the northern branch leading to cuttings in hardened black slates from which a single, poorly-preserved bivalve(?) was recovered. The southern branch obliquely ascends the side of Y Foel, exposing

beds in lateral cuttings, and also in the base of the track. Bedding dips at 50-60° south, and is strongly cleaved in a sub-parallel orientation. Small-scale faulting approximately parallels bedding, with associated veining and silicification, locally severe. Veining is strongly associated with microfaulting around bentonites, across which cleavage may be refracted through up to 40°.

### 3.4.2 Sedimentology and Taphonomy

The exposed succession is shown in Fig. 3.4.2, and comprises black and grey slates, with occasional thin sand laminae and bentonites. Black slates dominate, and some or all of the paler beds may be secondarily bleached; weathering produces similar effects on the surface of some black horizons, possibly through the biological removal of carbon. Grain-size is consistently around 0.02 mm, except for rare fine sandstone laminae, none of which occur in the sampled beds. A single band of dispersed pyroclastic phenocrysts is incorporated into LW 1, containing euhedral plagioclase and quartz, with shardic fragments. These particles are volumetrically very minor, comprising less than 5% of the affected laminae, and an insignificant proportion of the whole.

Organic matter is abundant, and largely disseminated through the matrix. Innumerable microscopic organic flakes, deformed by adjacent sedimentary particles, were probably derived from algal detritus; the organic material is conspicuously absent from rare sub-millimetre burrows at some horizons. Pyrite framboids are extremely abundant, but almost exclusively smaller than 5 μm, suggesting anoxic, sulphidic benthic conditions (Wignall and Newton 1998).

Some parts of the sequence (not sampled) are prominently rippled, with wavelength up to 8 cm and preserved amplitude 1 cm. Although substantial bottom-

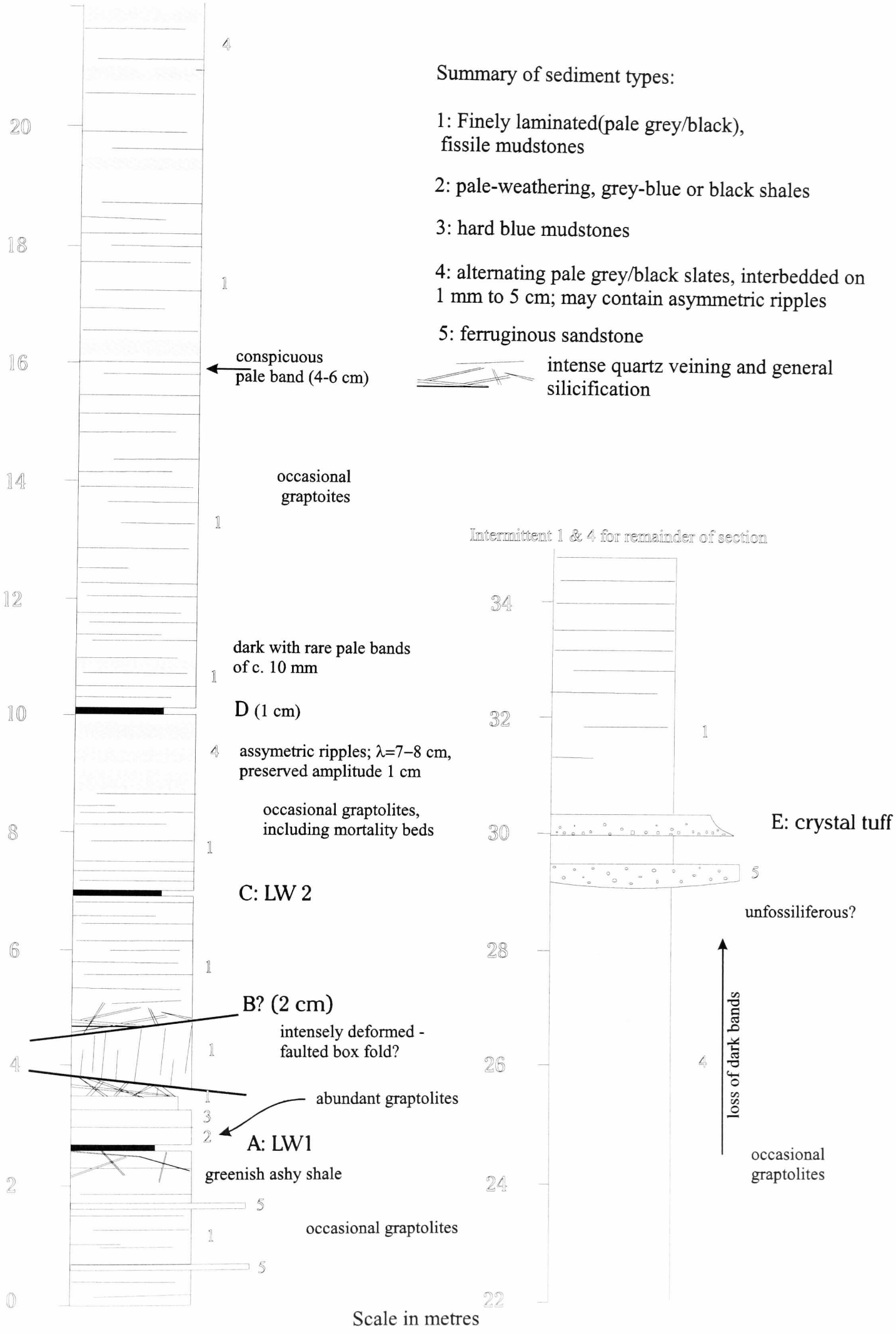


Figure 3.4.2: *Lithological succession exposed within the Caradoc black slates of the track cuttings on cuttings on Y Foel, Llanwrtyd Wells. A-E: tuff beds.*

water currents are implied, acting on silt-grade sediment, there is little obvious change in lithology. Pale and organic-rich laminae vary in relative proportions in both rippled and flat-laminated beds, and there is no obvious benthic fauna. Graptolites are rare in pale rippled beds, perhaps reflecting lower primary productivity. The possibility of the laminations representing sub-annual productivity cycles exists, given the suggestion by Cave and Rushton (1995) of unusually high sedimentation rates. Several centimetres in one year may be implausible for an offshore setting, however. Temporary sedimentation rates of up to 20 cm per year have been recorded following local earthquakes in New Zealand (Goff 1997), for the order of a decade; this issue is discussed fully in section 3.7.

Graptolites are preserved as a combination of organic material, after original collagen, and chlorite and/or muscovite films. Much of the organic material is lost, often leaving very thin deposits over most of the rhabdosome, with only the nema, thecal margins and spines preserved three-dimensionally. Surface films are invariably cracked and distorted. Most specimens are infilled by chlorite or mica, depending on their stratigraphical position, sometimes including partial replacement. Although strongly flattened, some relief is usually preserved in diplograptids. The thin rhabdosome of *Dicranograptus clingani*, however, invariably occurs as a micaceous film, with characteristically little preserved detail, while the only specimen of *Dendrograptus* comprises a graphitic film lacking obvious development of sheet silicates.

Inarticulate brachiopods are preserved as brownish or black deposits, often cracked and overgrown by acicular silica. Deformation has rendered diagnostic characters obscure, although growth lines are usually clear. No calcareous organisms occurred in the samples, so dissolution levels are uncertain; siliceous spicules in thin

section are obviously recrystallised, and may be secondary infills of mouldic preservation. Very thin, sub-ellipsoidal graphitic films may represent ceratiocarids or algal remains.

### 3.4.3 LW 1

Section LW 1 comprises a 4 cm bentonite within cleaved black mudstones, weathering pale grey, at the lower end of the Y Foel track cutting. Fine sand laminae occur below the bentonite. Up to approximately 7 cm above, refracted cleavage (intermediate between that in the bentonite and the slates) indicates a probable ashy component within the slates, although this is not obvious in thin section. Beds underlying the bentonite contain ubiquitous siliceous veining, which has destroyed bedding and prevents accurate sampling; a single sample was taken as close to the bentonite as possible. Less distorted beds some distance below were examined for fossils; although graptolites occur commonly, there are no dramatic abundance

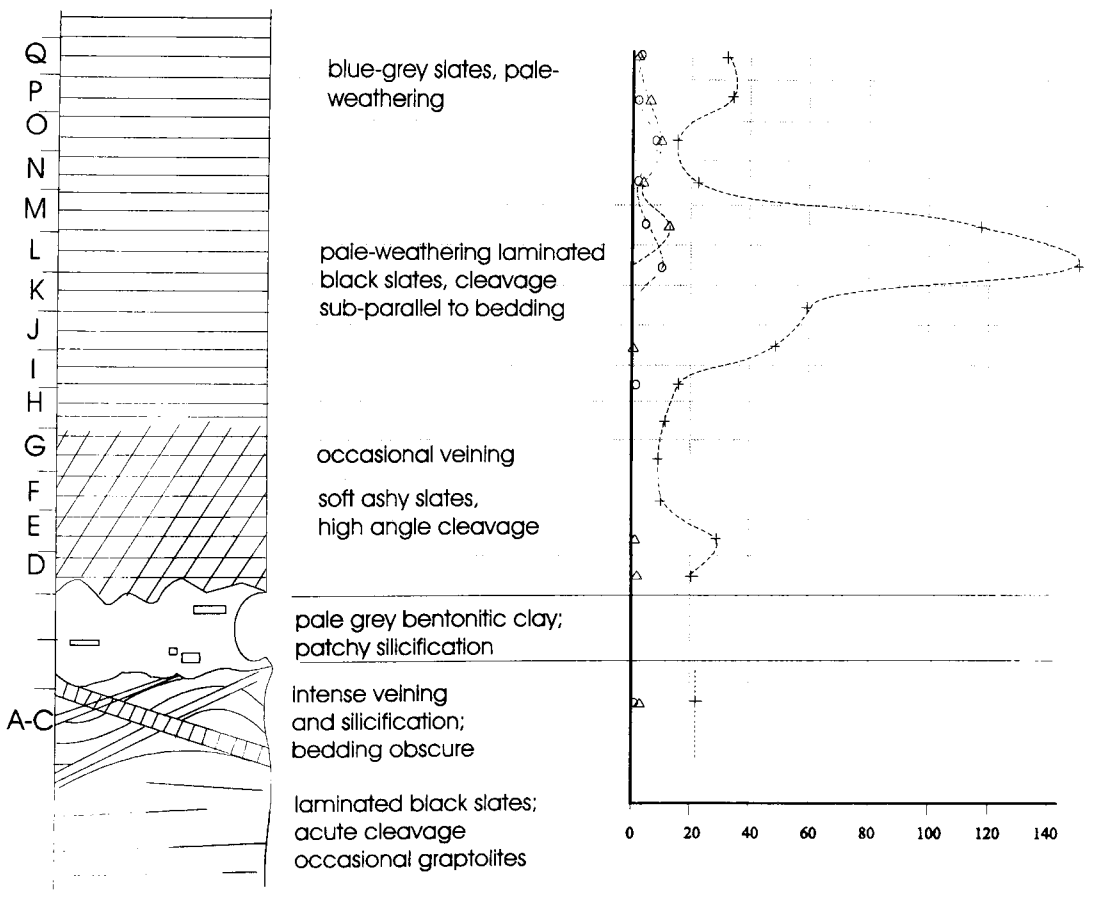


Figure 3.4.3: *Ecological log of section LW 1, with abundance recorded as individuals within 100 g of sediment.* +, *diplograptids;* o, Dicranograptus; Δ, *chitinozoans.*

changes.

The fauna of section LW 1 is dominated by diplograptids (Fig. 3.4.1), with lesser *Dicranograptus clingani*. Occasional inarticulate brachiopods and possible ceratiocarids are accompanied by large chitinozoans (resembling *Rhabdotheca*) in middle and upper beds, with very rare dendroids. A smaller chitinozoan, resembling *Conotheca*, also exists, but is elusive in hand specimen. A single bed (F) shows probable sponge spicules in thin section, associated with possible small burrows, but benthic macrofossils are absent.

Diplograptids immediately above the tuff occur at similar abundance (20 to 30 per 100 g) to those below, before declining by half until unit H. Thereafter, abundance increases sharply to 150 per 100 g, before a sudden decline to previous levels. After decreasing below 20 per 100 g, abundance appears to stabilize at levels around 30 per 100 g, similar to initial levels. *Dicranograptus* occurs sporadically, but rarely, until the main diplograptid peak, where a maximum abundance of 10 to 15 per 100 g was recorded. Abundance then oscillates, with decreasing maxima, for the remainder of the log.

Chitinozoans essentially mirror *Dicranograptus* in population abundance, appearing at similar levels during the diplograptid maximum, and decreasing through oscillations thereafter. In places, the oscillations coincide, although in the lowest samples in which they co-occur, their abundance appears inversely proportional. *Apatobolus micula* appears sporadically, at very low levels, throughout the sequence; these almost certainly represent a pseudoplanktic population. A single specimen of *Dendrograptus* sp. was recovered from the sample containing the diplograptid maximum.

### 3.4.4 LW 2

A section of lesser importance than LW 1, LW 2 comprises a 3 cm bentonite within a succession of grey and black slates, laminated on a millimetre-scale. Bedding is oblique to cleavage, which is pervasive and homogeneous. There is little or no variation in cleavage orientation, reflecting homogeneous sedimentology. Silicification is minor, restricted to occasional veining, although adjacent beds are locally distorted. For this reason, a single representative pre-tuff sample was taken. The preserved fauna is almost identical to that of LW 1; additional species are *Lasiograptus harknessi*? and an indeterminate lingulid.

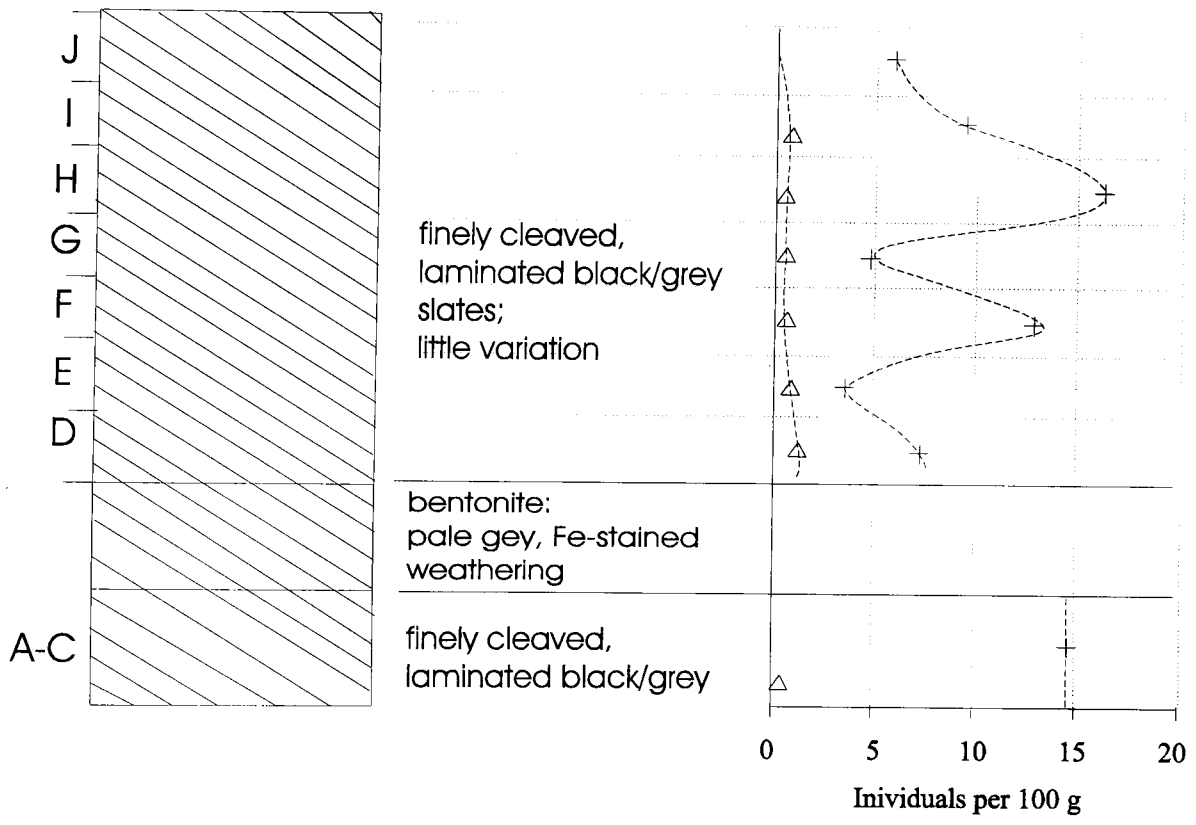


Figure 3.4.4: *Ecological log of section LW 2, with abundance recorded as individuals within 100 g of sediment. +, diplograptids; Δ, chitinozoans.*

Diplograptid abundance is initially around 15 per 100 g, but becomes extremely irregular following a 50% decline above the bentontite. Abundance oscillates within the range 4-17 per 100 g, before beginning to stabilise at 5-10. Although higher beds were not examined in detail, a field examination failed to reveal

significant variation above sample J; certainly, there was no peak comparable to that of LW 1.

*Dicranograptus* was apparently absent from this section, although chitinozoans occur in all samples except I. Chitinozoan abundance is low, decreasing upwards from a peak of 1.5 per 100 g in sample D; sample D also contains sponge spicules. *Apatobolus micula*, lingulids, conodonts and possible ceratiocarids occur rarely, in various samples (Appendix B).

## 3.5 Llyn Sarnau, Capel Curig (SH 7800 5924)

### 3.5.1 Locality

The forested hills north of Betws-y-Coed contain numerous disused mine workings in the Crafnant Tuffs, with associated siltstones and slates. The mines were worked for lead and zinc ores, which occur in fault-related mineralisation (Howells *et al.* 1978). Although dominantly unfossiliferous, exposures of slates are common, and contain locally abundant tuffs. Overlying the Upper Crafnant Tuffs, the black slates of Llanrhychwyn, correlated with those of Dolwyddelan (Williams and Bulman 1931), are referred to the *clingani* or *multidens* biozones (summarised by Howells *et al.* 1978).

Exposures of the Llanrhychwyn Slates at Llyn Sarnau contain sparsely graptolitic beds with rare, thin (0.5-3.0 cm) tuffs. Accessible exposures are limited to track cuttings at the northeastern margin, from which the data presented here were obtained. The site is 30 m southwest of a side-branch leading to a ruined building, on the east side of the track. Low, broken outcrops are partly covered by talus and overgrowth, and deformed by small-scale faulting. The slates are homogeneous, strongly cleaved at approximately 50° to bedding, and contain occasional

diplograptids, poorly-preserved in pyrite. A single, probably bentonitic tuff, 1 cm thick, can be traced intermittently through the outcrop, with additional fragments in the scree. For approximately two centimetres overlying the tuff, graptolites become abundant throughout the matrix.

### 3.5.2 Data

The poor preservation of fossils, tectonic deformation and condensed fossil distribution make standard analytical techniques inappropriate. Accurately splitting samples along finely-spaced bedding planes is impossible, while slicing by saw in this direction would remove too much material. The slabs were instead sliced vertically at intervals of 2-3 mm with a rotating diamond saw, and examined under water with a low-magnification binocular microscope. Mature graptolites in section appear as thin reflective lines, and an eyepiece graticule was used to measure the vertical distance

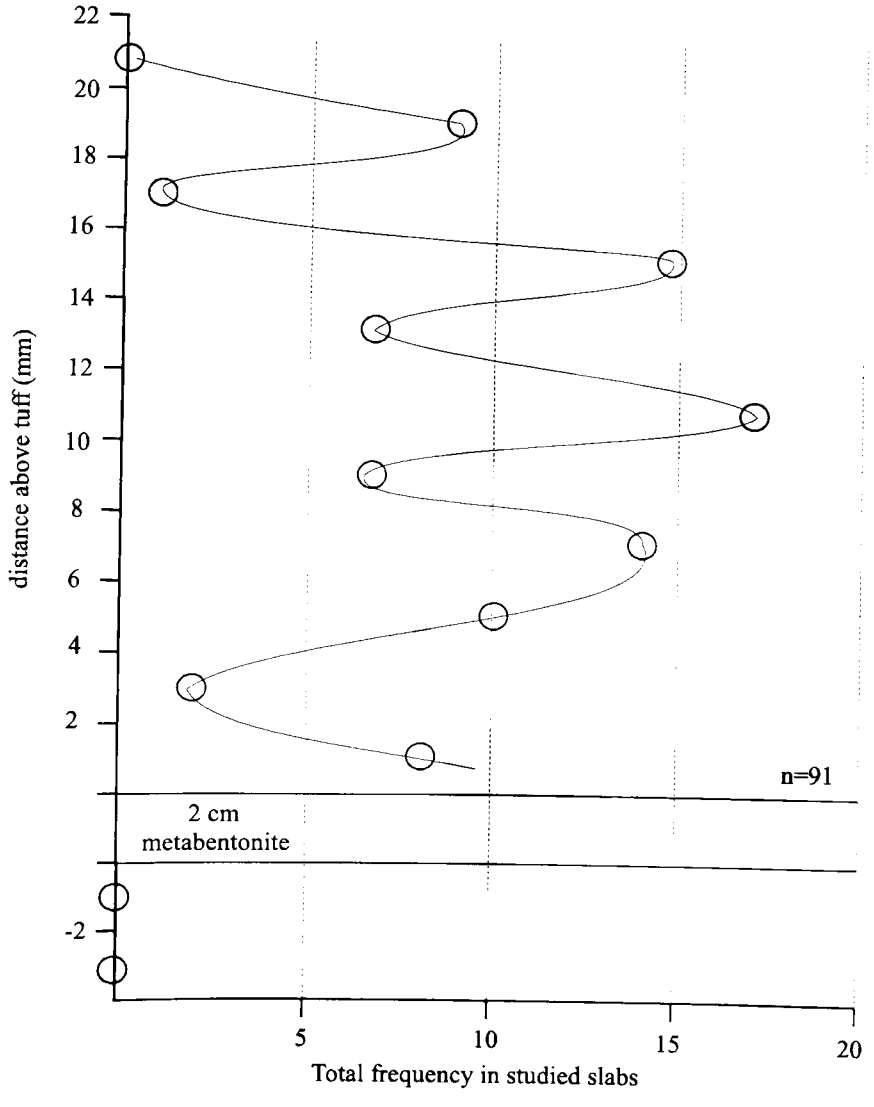


Figure 3.5.1: *Graptolite distribution on cut, slate slabs of LS 1. Abundance given is total counts for equal-area analysis; total 91 graptolites recognised in sectional view; siculae and juvenile specimens almost certainly overlooked. No other fossils.*

from the tuff. No other fossils are known from these beds, excepting possible chitinozoans, and all known graptolites are straight biserial forms.

Although several graptolites may cut through more than one section, there is little random bias; the overall effect is to slightly exaggerate abundance at all levels. Regularly spaced intermittent traces on one horizon were treated as a section through the thecae of one specimen, while irregularly spaced traces with slight vertical variation were assumed to represent multiple specimens. This method also reduces measurement errors incurred through specimens lying obliquely in the sediment. In order to reflect graptolite distribution accurately, slices must approximate to parallelograms, producing equal-area samples. This condition was almost invariably satisfied through natural cleavage.

The distribution of graptolites is shown in Fig. 3.5.1. An initial, almost barren succession (rare, isolated individuals) is overlain by a pseudo-symmetrical peak with strongly fluctuating abundance, the maximum around 12 mm above the tuff. Graptolites are absent above 20 mm. Abundance appears to have been subject to a secondary order of oscillation, with abundance at local minima weakly correlated with adjacent local maxima. There is no evidence of benthic colonisation, although rare organic fragments similar to chitinozoans occur in the most fossiliferous intervals. The palaeoecological significance of chitinozoans in unclear, and they must be presumed planktic in this case.

Since the observation technique only reliably recognises mature rhabdosomes, the distribution of siculae is not known. The observed distribution may reflect some combination of the following:

1. A real pattern reflecting primary productivity, with local maxima and minima corresponding to varying external factors (e.g. nutrient availability, temperature);

2. Variations in graptolite population states, between juvenile-dominated and mature communities. Graptolite reproduction is very poorly understood, and while strongly synchronised generation patterns are rare among modern organisms (e.g. cicadas), the possibility that graptolites followed a similar life cycle cannot be dismissed, particularly while the nature of synrhabdosomes remains enigmatic.

3. Biostratinomic mixing of an original smooth bloom that reflects underlying primary production; sedimentary structures have been lost through metamorphism.

Although these cases cannot be easily distinguished, there is some similarity between LS 1, and LW 1/LW 2, in erratically fluctuating populations, with a rapid decline from high levels immediately following ash-fall. The possible significance of these common features is discussed in section 3.7, where the pattern is interpreted as a real phenomenon, as in case 1 above.

## 3.6 SYNTHESIS

Faunal response to ash-fall in argillaceous settings was strongly dependent on the water depth and benthic oxygenation. The shallowest deposits were those of the Builth Inlier, where faunas were dominated by the partly pseudoplanktic inarticulate *Apatobolus micula*. In all cases, a bimodal bloom of *A. micula* occurred. This is interpreted, based on population structure, associated faunas, and benthic oxygenation levels, as representing a pseudoplankton bloom, followed by a benthic bloom. Graptolites showed a single bloom, corresponding to the first (pseudoplanktic) *A. micula* peak, most clearly shown in section HB 3. Ostracodes invariably achieved

maximum abundance immediately after ash-fall, sometimes prior to the inferred plankton bloom.

There is a consistent distinction between faunas from originally anoxic, compared with dysaerobic settings. In dysaerobic sections, the initial population was removed by extensive ash deposition, essentially equalising the faunal composition between sections. Following ash-fall, both anoxic and dysaerobic facies show a bimodal bloom of *A. micula*. In originally dysaerobic environments, however, the upper peak contains thin bands with very high abundance. Graptolites are replaced by ostracodes as the secondary taxonomic group in dysaerobic facies, with increased abundance of calcareous organisms. The abundance of the plankton peak is also reduced, relative to the benthic, in facies containing an established benthos before ash-fall.

Lateral variation in section BG 1 was extremely pronounced, and reflected thickness variations within the ash deposit. Laterally, highest *A. micula* abundance

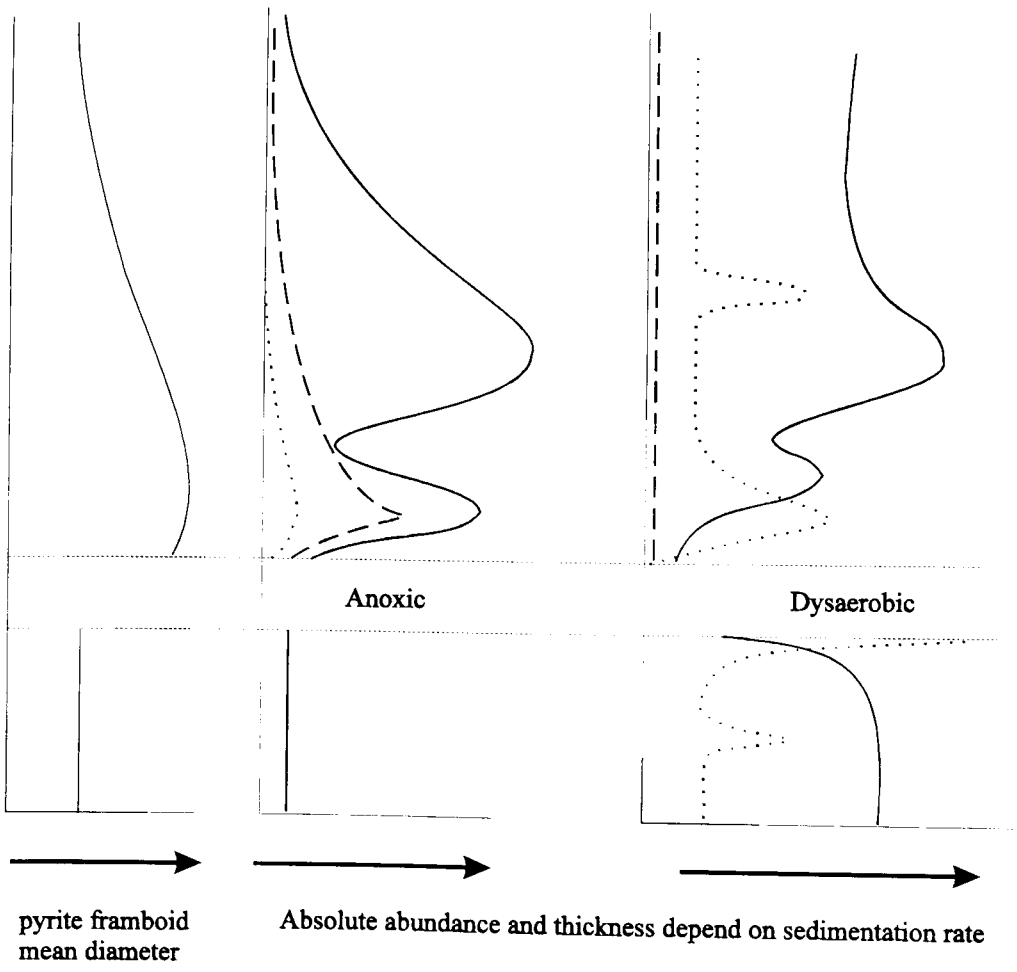


Figure 3.6.1: *Generalised pyrite framboid size distribution andfaunal abundance in dysaerobic and anoxic siltstones of the Builth Inlier; solid,* A. micula*; dashed, graptolites; dotted, ostracodes.*

occurred above the thickest part of the ash deposit, which was also associated with elevated graptolite levels. Chitinozoan abundance was also elevated, but reached maxima on either side of the *A. micula* / graptolite peak; the central region contained minimal chitinozoan abundance.

Analysis of pyrite framboid size distributions has revealed an increase in oxygenation, which peaked shortly after the ash-fall, decreasing to previous levels thereafter. Limited and laterally inconsistent evidence of current action occurs immediately above some tuffs. A generalisation of the observed patterns is shown in Fig. 3.6.1.

An examination of trophic groups and ecological niche occupation illustrates these trends in a different way. The standard ternary graphs of Scott (1978) may be utilised to some extent, although the threefold division of infaunal suspension, epifaunal suspension, and vagrant is inappropriate. Infaunal taxa were rare, and primarily or exclusively soft bodied, giving very low values; vagrant taxa should be subdivided into planktic and benthic groups. A replacement plot of sessile benthos, vagile benthos and plankton/nekton is employed, and suggested as a standard for black shale palaeoecological analysis. The suspension/detritus/predation ternary plot is more appropriate, although Lower Palaeozoic taxa rarely show direct evidence of trophic habits. Trilobites pose particular difficulty, and particular taxa have been variously inferred as predatory (Jensen 1990), detritivorous (Pollard 1990), or as chemautotrophic symbionts (Fortey 1999). Trilobites in this study contain examples of most of the possible habits, but the lack of trace fossils precludes an ichnological perspective. It is likely that many trilobites were scavengers/detritivores, but they are here separated from particulate detritivores in a combined predator/scavenger category. Ceratiocarids and ostracodes were probably detritivores, bivalves

suspension-feeders, and the putative cnidarian *Sphenothallus* was almost certainly benthic (van Iten *et al.* 1996; Neal and Hannibal 2000), and probably (like all cnidarians) predatory. Suspension-feeding organisms are easily recognised through morphological considerations.

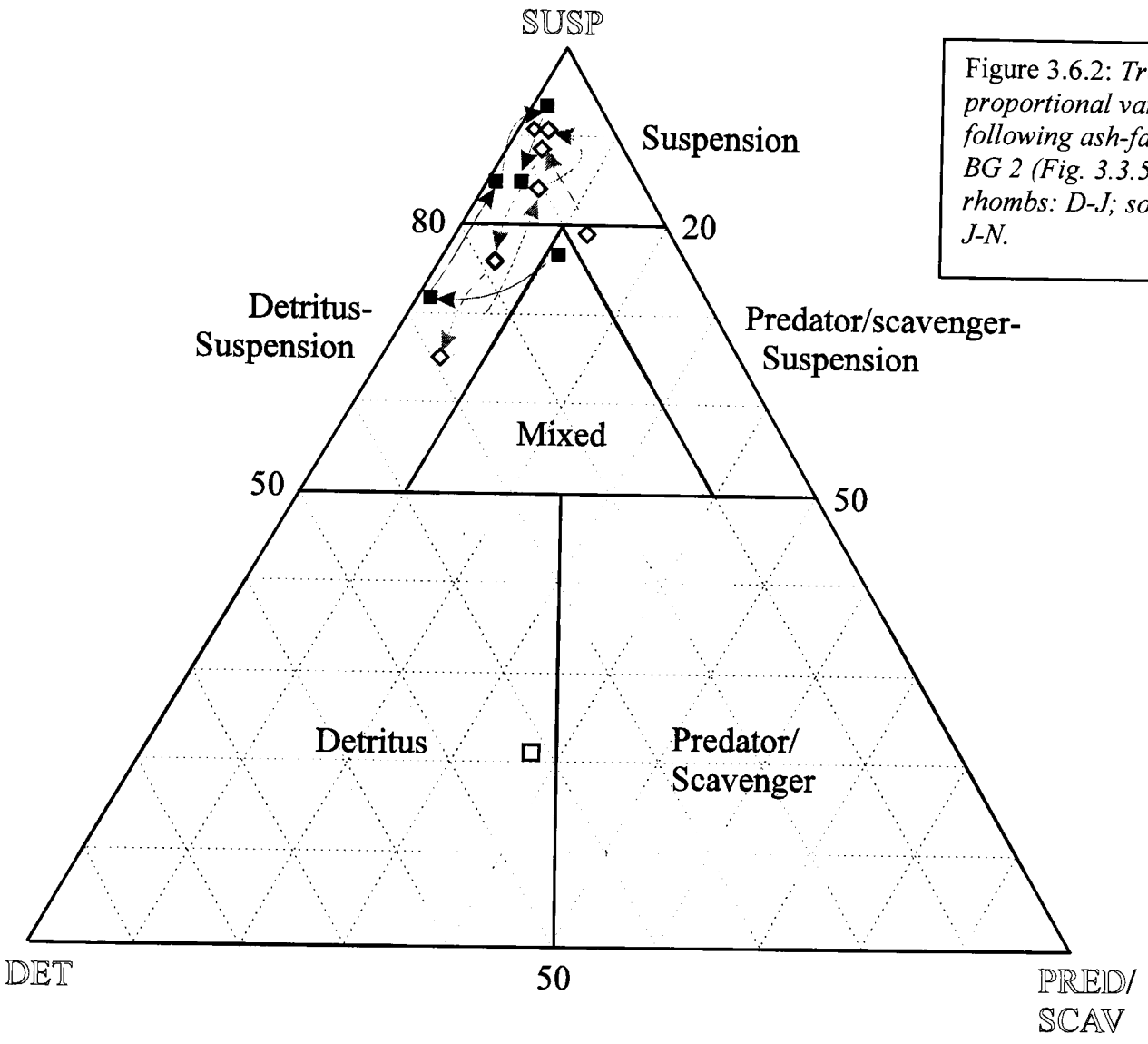


Figure 3.6.2: *Trophic group proportional variation following ash-fall, based on BG 2 (Fig. 3.3.5); open rhombs: D-J; solid squares: J-N.*

The immediate effect of ash fall is to shift the combined apparent community from suspension-feeding to detritus-suspension (Fig. 3.6.2), prior to and during the initial *A. micula* peak. Predators/scavengers only exceed preserved detritivores immediately following ash-fall, prior to the ostracod bloom. The second peak shows a return to a suspension-feeding community, with greater detritivore abundance than predator. Most or all of these trends result from the high dominance expressed during blooms of each major taxon.

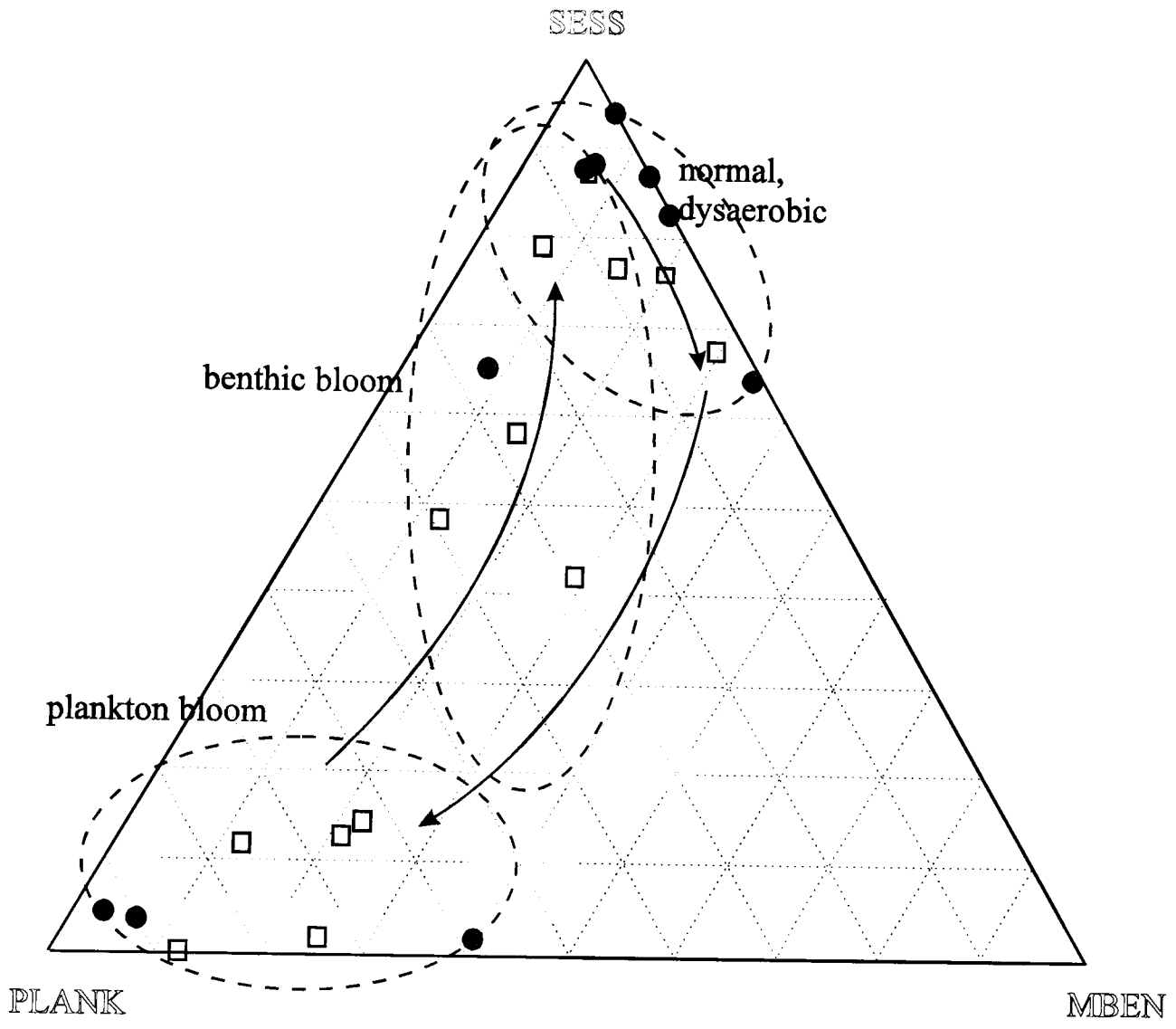


Figure 3.6.3: *Ecological niche variation following ash-fall, based on BG 2 (squares) and BG 3 (circles).*

Ternary diagrams of sessile benthos, mobile benthos and plankton/nekton show consistent results, summarised in Fig. 3.6.3. In order to utilise the data, separation of *A. micula* planktic and benthic populations has been attempted, by extrapolating the initial peak. Since the two populations were largely independent, plankton abundance should have been dependent only on internal population dynamics. However, there is no way to separate individuals of each habit, and the representation is an approximation only. The resultant graphs show a very rapid transition from normal conditions into the planktic bloom, while the reversal through benthic bloom to normal conditions is more gradational. This conforms with limited

recent data of Gallardo *et al.* (1977) and Carpenter *et al.* (1995), among others, in which plankton blooms both arise and decline more rapidly than benthic ones.

The deeper-water, dominantly anoxic deposits of Llanwrtyd revealed severe perturbation of planktic faunas, with very sparse evidence of minimal benthic colonisation. Diplograptid abundance was reduced following tuff deposition, although sometimes with fluctuating levels. In one case, this was followed by a major plankton bloom, comprising graptolites and chitinozoans. Evidence of benthic colonisation was limited to very rare, possible sponge spicules and rare burrows produced through sediment ingestion.

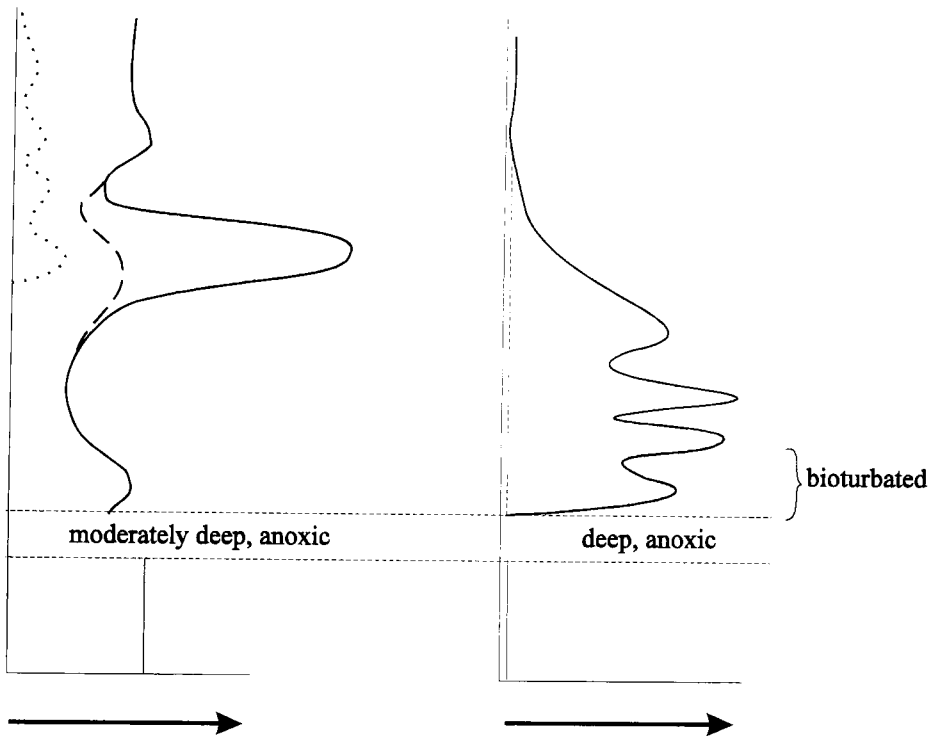


Fig. 3.6.4: *General observed trends in graptolite abundance from deeper-water facies; dashed lines indicate known alternative scenarios; dotted line indicates additional planktonic organiusms.*

The deep-water slates of North Wales appear to accord with both the patterns observed at Llanwrtyd, and unpublished data from the Southern Uplands of Scotland (S. Rigby and S. Davies, *pers. comm.*). In the latter, the tuff is followed by a major, bimodal plankton bloom. The lower unit comprises siculae and immature specimens, while the upper is dominated by adults. Detailed analyses are difficult in condensed sequences, but other taxa appear to be very rare or absent. The Scottish material

showed bioturbation during the lower interval, although this was absent from that of North Wales. Examination of the condensed Ordovician/Silurian boundary section of of Dobb's Linn, Scotland, also apparently showed extensive bloom patterns, although no formal treatment has been performed. The above observations are generalised in Fig. 3.6.4.

## 3.7 INTERPRETATION

### 3.7.1 Mechanisms

The plankton blooms described in section 3.6 have some similarity to those expected through inorganic nutrient addition. This process has also been suggested by S. Rigby and S. Davies (*pers. comm.*), to explain apparent dependence on tuff composition. The critical element in plankton blooms appears to be iron, documented by Falkowski *et al.* (1998) and others as essential for oceanic nitrogen fixation. However, the addition of iron to surface waters from direct dissolution fails to explain benthic oxygenation and colonisation. Although ash particles will trap microscopic air particles prior to descent, this is unlikely to be very significant. Crystal tuffs would trap far less air than pumiceous deposits, although there appears to be no dependence on composition (basaltic andesite to rhyodacite) among Welsh examples. In addition, the duration of experimental, fallout-induced surface blooms is of the order of one week (Carpenter *et al.* 1995), suggesting that additional processes must have operated in the examples studied here. Thickness variations in the tuff and rapid lateral variation in overlying faunal abundance are also unaccounted for by simple iron addition.

A fluid mechanical approach to ash-fall on water surfaces provides an alternative hypothesis (Fig. 3.7.1). Previously, ash sedimentation has been implicitly

assumed to occur through individual particle settling. Theoretical and experimental considerations imply that in many cases, settling will occur through turbidity flows, as particle admixture increases the density of the surface waters. The situation is similar to Rayleigh-Taylor instability (Houseman and Molnar 1997), but involving miscible fluids. Chaotic interface fluctuations between the upper turbid layer and the

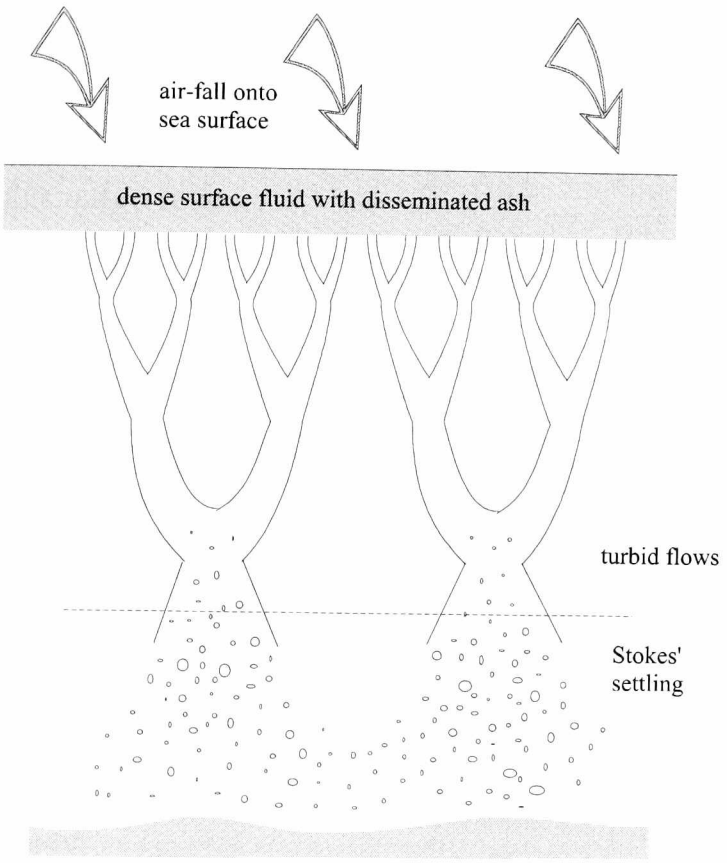


Figure 3.7.1: *generation of turbid downflow following ash deposition on sea surface, in 2 dimensions; concentration of finer particles in surface water, by surface tension and wave action, produces gravitational instability; discrete initiation points produce local circulation cells, which converge due to acquisition of surrounding fluid into flow tops; repeated convergence leads to broad, widely-dispersed columns, producing heterogeneous ash deposition. Beyond a critical depth (dependent on fluid and particle characteristics), flows break down through lateral fluid entrainment, resulting in individual particle settling in Stokes' regime. Not to scale.*

subsurface will result in vertical circulation even in a gravitationally stable configuration, known as double-diffusion finger convection (Green 1992; Green and Schettle 1986). From discrete initiation points, with mean separation dependent on fluid properties, the dense turbid fluid is siphoned into downwelling columns. Space considerations require the corresponding upwelling of lighter subsurface water, including circulation of deep waters.

During descent, entrainment of lateral ambient fluid causes adjacent flows to merge; repeated flow convergence results in very localised downwelling currents with large (c. 10 m) separation. This feature allows an attempt at quantitative modelling

(Appendix C). As downwelling proceeds, lateral entrainment progressively reduces the density of the turbid flow. This results in a decreasing descent rate, and eventually in flow breakdown. At this point, particles fall separately in the classical settling interpretation, at a rate prescribed by Stokes' Law. A fundamental prediction of any model based on this process is lateral thickness variation within the ash, over metres to tens of metres. Although similar effects could be produced by currents acting on uneven bottom topography, the distribution of faunas provides a discriminant, as discussed below.

The ecological results of fluid circulation are dependent on chemical gradients within the water column. Although some biologically important elements (particularly C, P and O) vary unpredictably across different regions, many elemental ions show consistent depth gradients in the oceans. Butler (1998) and Nozaki (1997) summarised elemental distribution, among which the biologically important, but limited, nutrients are clearly distinguishable through a common profile. All increase rapidly with depth, from close to zero, to a maximum at 500 to 2000 m; concentration then decreases gradually until the ocean floor. This profile, indicating severe limitation within surface waters, is common to N, Si, P, Fe, Ni and Zn, among others. The distribution of oxygen is typically a mirror image of this profile, with high surface concentration resulting from atmosphere-ocean equilibrium. An oxygen-minimum zone occurs at several hundred metres, followed in modern oceans by a slight increase at greater depth. The equivalent profile during black shale deposition is not known, although modern silled basins may provide analogues. The Black Sea is anoxic below approximately 200 m (Rhoades and Morse 1971), due to a complete lack of vertical circulation. A similar oxygen profile may have operated in the Builth Inlier, although the water depth was probably less than 200 m (section 1.3.1.1).

Any vertical circulation initiated by turbid downwelling will inevitably result in upwelling of water from the nutrient maximum zone. Plankton blooms resulting from this upwelling will utilise a far richer source than that derived from partial dissolution of the ash into surface waters. Loubere (2000) provided evidence that modern oceanic circulation changes are far more important than wind-blown dust in dictating primary productivity, while Nicol *et al.* (2000) described changes in faunal composition resulting from altered circulation patterns. The nutrients are also supplied gradually, continuing until circulation ends, and thereby allow blooms of much longer duration (see 3.7.2).

Under sufficiently shallow conditions, effects on benthos are equally dramatic. Deposition of large ash volumes was fatal for small sessile benthos and very small mobile epibenthos, probably through direct burial. Large mobile epibenthos and mobile infauna appear to be have been unaffected, as they were able to escape being buried. The bulk of ash deposition in deep water, following the 1992 eruption of Mt. Pinatubo, occurred within weeks (R. Cooper, *pers. comm.* 1999), sufficiently rapid to smother small benthos.

Downwelling columns contain oxygenated surface water, which partly replaces dysaerobic or anoxic bottom waters. However, restricted levels of organic carbon in normal surface (replacing deep) waters, prevent benthic proliferation. The initial response is seen in small, mobile epibenthos (ostracodes, rare trilobites) and shallow infauna (palaeoscolecids, other small worms?). Sessile suspension feeders are effectively excluded by limited food supplies. A secondary result of the plankton bloom is to enormously increase the downward flux of particulate organic matter. Although under normal circumstances less than 10% of organic particle flux reaches the ocean floor, this may be increased during a bloom event, since primary production

initially exceeds higher trophic levels. The proportion reaching the sea floor is strongly dependent on water depth in modern oceans, although the development of mesobathyal faunas during the Early Palaeozoic is obscure. A more strongly polarised surface-deep population distribution may have reduced organic recycling in the middle water column, allowing proportionately higher organic flux to reach the benthos. An apparent dependence of the magnitude of the plankton bloom on ambient benthic oxygenation is also explained by partial circulation. Where a significant benthos is developed, the mid-water nutrient reservoir is depleted, both through benthic utilisation, and gradual accessibility to plankton. For this reason, the plankton bloom in originally dysaerobic settings is less dramatic than an event with a fully anoxic sea floor, as consistently observed within the Builth Inlier.

The maximum of the plankton bloom would coincide with an increase in benthos, particularly sessile suspension feeders (brachiopods, bryozoans, sponges, crinoids), which were previously excluded by low benthic nutrient levels. The relationship between organic carbon accumulation rate and deposit feeder abundance was discussed by Sibuet *et al.* (1989), summarised in Tyson (1995). The utilisation of oxygen by benthos, and the aerobic decay of organic detritus, accelerate the reduction in oxygenation level and limit population size; this acceleration is weakly apparent in the pyrite framboid size distributions of BG 1 and HB 3. Eventually, the benthos was displaced if anoxic conditions were re-established, or stabilised under dysaerobic conditions. It is possible that the benthic phase was prolonged by the gradual release or utilisation of oxygen in metallic complexes within the ash, a factor which may further explain its duration, relative to the plankton bloom.

Lateral thickness variations within the tuff would inevitably result from localised descent of turbid water masses, as deposition would be concentrated at

downwelling centres. Circulation would continue for some time following deposition, through inertia and temperature effects. Once the ash is deposited, the descending surface waters would become lighter than the ambient water through their higher temperature, resulting partly from their original location, and exaggerated by heating from the ash. Although the ash may have cooled before reaching the sea surface, reduction in the albedo of the photic zone would allow abnormally high solar absorption. Such temperature effects were noted by Gallardo *et al.* (1977), although their extent is uncertain (quoted as both 0.3°C and 2-3°C).

Although the density inversion would probably result in post-depositional circulation, its duration would be limited by thermal diffusion and drag. Continued circulation beyond a few months should be detectable in post-tuff oxygenation levels and in lateral faunal distribution in immediately overlying beds. The pyrite analysis of BG 1 shows no evidence of increasing oxygenation; however, this may be indicated in HB 3 by an ambiguous oxygenation maximum (heterogeneous size distribution, including the greatest abundance of the largest observed sizes), around 2 cm above the tuff upper surface.

Lateral section BG 1(H) displays striking faunal variation, with a dramatic peak in planktic fossil (graptolite and *A. micula*) abundance near the thickest exposed part of the bentonite. The planktic maximum corresponds to a minimum of ostracodes (benthic) and chitinozoans (at least partly benthic), although the latter show maxima immediately on either side of their minimum. Ostracodes may have been inhibited by increased sedimentation at the downwelling centre. The chitinozoan distribution is also consistent with a downwelling centre, in which radial currents winnowed the extremely light vesicles, before redepositing them once the current becames too weak: in a radial flow, current strength is inversely proportional to the square of radius.

An alternative explanation for both tuff thickness variation and corresponding fossil abundance is a local topographical depression, under consistent benthic currents. Thickening of the tuff would result from a tendency to equilibrate topography, with small, light fossils concentrated in the centre of the depression. However, it is unlikely that biostratinomic concentration of organisms would be as effective as described, particularly given the absence of entanglement, clustering or imbrication. The ostracod minimum is also difficult to explain through taphonomic processes, although enhanced dissolution is conceivable amid a greater concentration of decaying organisms. However, chitinozoans are effectively insoluble, and are distributed in a way that seems difficult to explain without a radial current. The only conceivable alternative is of secondary redistribution by a very narrow turbidity current (or similar) flowing at right angles to the exposure, which could have redistributed chitinozoans in the observed way. However, there is no evidence of turbidity currents, laminations are sometimes visible, and small *A. micula* valves should have been affected in the same way by a concentrated current.

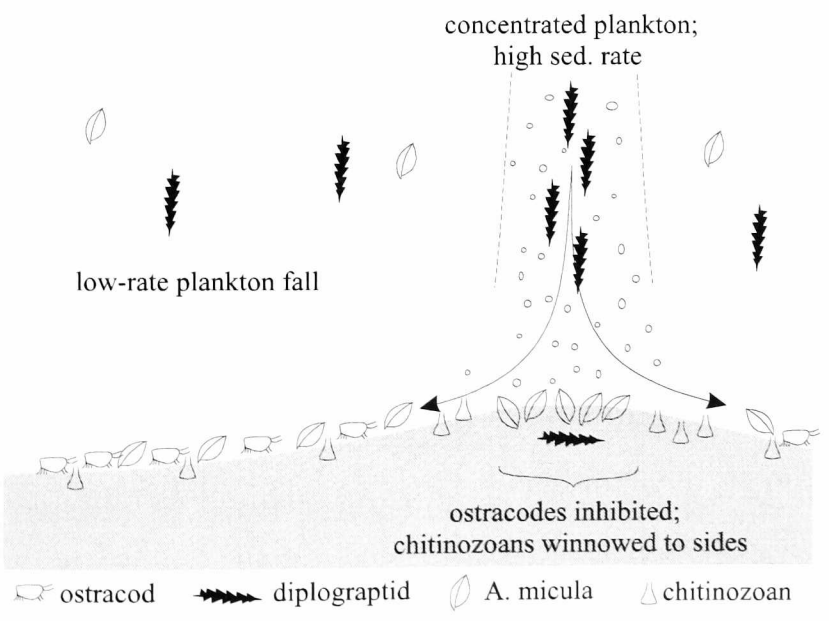


Figure 3.7.2: *schematic explanation of lateral faunal distribution in BG 1, and general depositional process; downwelling columns deposit concentrated plankton above thickest part of bentonite, with subequal abundance outside this region; ostracodes are inhibited by high sedimentation, and concentrated in lateral areas; chitinozoans largely deposited by columns, but winnowed away from downwelling centre by radial benthic flow.*

Although it may be possible to derive an alternative set of circumstances resulting in the observations from BG 1(H), these would have to be exceedingly

contrived. Overall, there is overwhelming evidence for localised points of downwelling fluid, immediately overlying the deposition of tuff BG 1, and subsequent faunal distribution patterns which are shared by all studied sections in the Builth Inlier.

Extrapolation of these processes into deeper settings, with more extensive benthic anoxia, allows explanation of the trends observed at Llanwrtyd Wells and Llyn Sarnau, Gwynedd. Plankton blooms, as mentioned above, were reliant only on circulation of the upper 200-500 m of the water column, producing large scale, protracted nutrient upwelling. Downwelling flows collapse at a depth dependent on particle size, sorting and abundance, but estimated at up to 500 m. The depth of flow breakdown defines the base of effective circulation, with water below this depth largely unaffected. In the deeper waters of North Wales (and the Silurian of southern Scotland), most of the circulation occurred within the upper, aerated part of the water column, producing an immediate plankton bloom. The erratic development observed at Llyn Sarnau may indicate some degree of anoxic upwelling, although unstable population dynamics might produce similar trends. Dependence on tuff composition reported by S. Rigby and S. Davies (*pers. comm.*) may be explained through structural or volumetric considerations. Flows will be initiated only above a critical particle abundance, which increases rapidly with particle size. Since chemically distinct bentonites were derived from different sources, scoriaceous particle size distribution (now unrecognisable due to divetrification) may have differed dramatically. The remains of larger pumice clasts are volumetrically unimportant, and would probably also have floated until long after the bulk of deposition. It is unlikely that they could be used to estimate the original grain-size distribution.

The Llanwrtyd Wells sections were deposited in an intermediate setting, with extensive benthic anoxia in a relatively confined basin, although water depth is uncertain. The fluctuating, but generally decreased, plankton response to ash-fall, in some cases culminating in a large-scale bloom, reflects the upwelling of anoxic water from depth. Graptolite abundance was decreased temporarily and erratically by eutrophic conditions, probably enhanced by phytoplankton blooms resulting from simultaneous nutrient upwelling. The presence of small-scale benthic colonisation at both Llanwrtyd and the Southern Uplands represents dysaerobic specialists, utilising small volumes of oxygen incorporated into the ash.

A brief maximum recorded immediately above LW 1, LW 2 and LS 1 may have resulted from immediate dissolution of iron from direct input of the ash, prior to significant anoxic upwelling.

### 3.7.2 Time-scales

The most problematic aspect of these data to reconcile with theory is that of

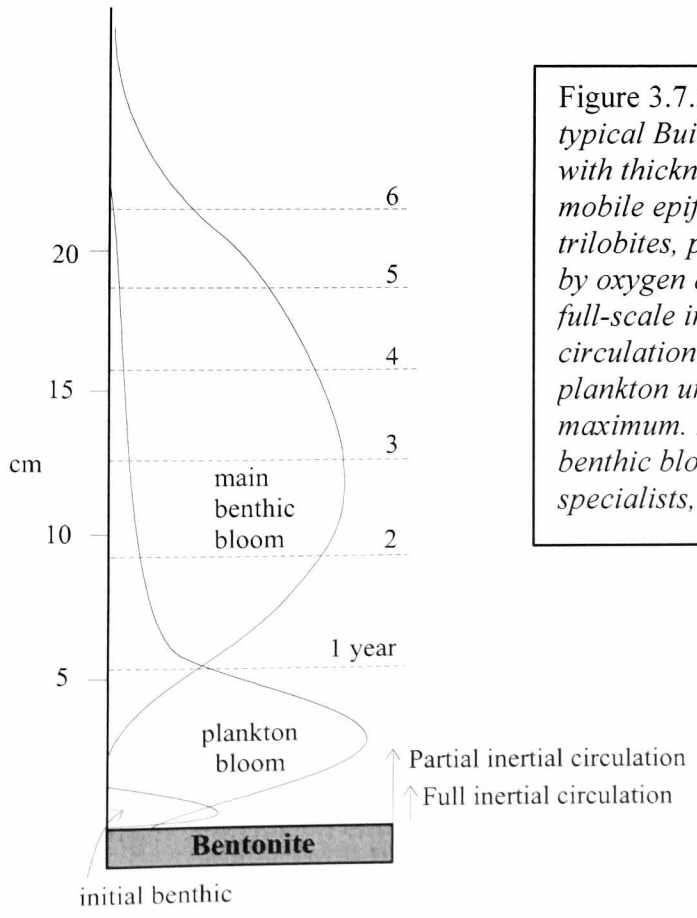


Figure 3.7.3: *Estimated duration of the phases of a typical Builth Inlier bloom structure, correlated with thickness. Initial benthic colonisation by mobile epifauna and shallow infauna (ostracodes, trilobites, palaeoscolecids and others), restricted by oxygen and/or food supplies after termination of full-scale inertial circulation. Shallow/partial circulation continues to supply nutrients to plankton until shortly before plankton bloom maximum. Decaying plankton at sea floor allows benthic bloom of suspension-feeding dysaerobic specialists, continuing until oxygen is removed.*

duration. Blooms within the Builth Inlier occurred over approximately 20 cm of sediment, slightly less at Llanwrtyd, and around 2 cm in the deeper-water settings of Snowdonia and Scotland. Modern deep marine (non-abyssal) sedimentation rates are typically in the range 10-50 mm/ky (e.g. Kuehl *et al.* 1993), while offshore shelf sediments rarely accumulate more than a few millimetres per year. On this basis, the observed blooms require hundreds to thousands of years for their deposition. A mean sedimentation rate calculated for the *teretiusculus* Biozone of the Builth Inlier from the age data of Harland *et al.* (1990) yields 0.2 to 0.3 mm/y, assuming no unconformities. Many of the highest recorded sedimentation rates in non-deltaic shelf settings are associated with seismic activity. Goff (1997) correlated historical earthquakes with sedimentation rate in a New Zealand bay, using several precise dating techniques. Although not all recorded earthquakes produced recognisable effects, some showed a subsequent increase in sediment input. The maximum observed rates exceeded 50 mm/y, averaged over 20 years; more typically, 20-30 mm/y, averaged over 20-30 years. The lowest accumulation rate recorded, during undisturbed periods, was 0.1 mm/y. Assuming a pseudo-exponential decline in sediment input, proximal accumulation rate during the earliest period following the earthquake must have been very rapid, probably exceeding 10 cm/y. Similarly, increased water turbidity was recorded in fluvial/inlet salmon fisheries of Alaska (Dorava and Milner 1999) following local eruption, continuing for at least 5 years, although sedimentation rates were not provided. Gallardo *et al.* (1977) suggested that extremely high sedimentation rates operated following the eruption, but appeared uncertain of their magnitude.

The effects of compaction must also be estimated. Goff (1997) appears to have assumed zero compaction in the Recent New Zealand cores, despite burial of up to 8.5

m. Given an exponential decline in sediment porosity with burial (Fisher and Scmincke 1984), there should be a significant compaction gradient within the cores. Compaction of fossils in Builth Inlier sections is generally minor. Trilobites are preserved in strong relief, and *A. micula* valves are buckled, but not flattened. Rare orthocones are also preserved with minimal distortion, despite decalcification. A quantitative estimate of compaction in siltstones of the Builth Inlier is around 1.2-1.3. Estimates for Llanwrtyd and North Wales are difficult to obtain because of the limited faunas, although the burial history of Llanwrtyd should be broadly similar to that at Llandrindod.

The source of the *murchisoni-teretiusculus* Builth Inlier bentonites was probably very local (1.3.1.4), and perhaps related to the Builth volcanism itself. Water depth, although uncertain, is unlikely to have exceeded 150 m, and was possibly as shallow as 50 m; the studied locations were within 10 km of the main volcanic pile. By comparison with the examples above, a sedimentation rate of at least 5 cm initially, decreasing thereafter, is conceivable. The rate of terrestrial run-off prior to the evolution of vascular plants is debatable, but was probably higher than in modern times, particularly following seismic disturbance. In the case of volcanism-related seismicity, redistribution of volcaniclastic debris would also increase sediment input to the shelf. While 20 cm of Builth Inlier siltstone may represent as little as 5 years, a total duration of weeks to months appears inconceivable.

Consideration of fluid (Appendix D), and faunal population mechanics provides an estimated maximum duration for the plankton bloom, by constructing limits on the length of circulation. Sedimentation of the ash would have occurred rapidly, mostly within a few weeks. Full-scale inertial circulation may have continued for several more weeks (see pyrite framboid analyses, 3.2.5 and 3.3.3), but longer-

term, partial circulation is more difficult to establish. However, mesoscale eddies from the North Atlantic Drift exist for several months to two years before resorption or disintegration (Brown *et al.* 1989). Although such isolated eddies are much larger than the proposed vertical circulation cells, the latter are more numerous, and total volume:interfacial area ratios may be comparable. Mesoscale eddy velocities are typically 0.1 m/s, similar to observed values for turbidity circulation (Appendix C). Overall momentum:drag ratios, and hence duration, are therefore of a similar order, although precise comparisons are not possible

While phytoplankton response is essentially instantaneous, suspension-feeding macrofauna will lag behind, with a full bloom community requiring several months to develop. There is no obvious mechanism for extending the bloom duration, since surface nutrient abundance would decrease rapidly (due to gravitational settling) once macrofauna became abundant. Inertial circulation could probably not have continued for longer than eight to ten months. The plankton bloom may therefore have occupied up to approximately one or two years, although the upper limit is poorly defined. On this basis, plankton blooms in the Builth Inlier would have been preserved in a maximum of 5-10 cm of sediment (discussed above). Since the characteristic position of the plankton peak is approximately 5 cm above the tuff, there is no contradiction in plausible bloom duration.

Benthic blooms are poorly understood, and evidence of population dynamics is restricted to only a few examples. Gallardo *et al.* (1977) reported that benthic community perturbation, dominated by a strong peak in polychaete and echiurid abundance, was declining two to four years after eruption. A similar order of magnitude is implied in the Builth Inlier samples, where benthic blooms generally comprise three to four times the sediment thickness of the plankton blooms.

Assuming a decreasing sedimentation rate, this may account for five to ten times the duration of the plankton bloom, i.e. 5-10 years.

Lower sedimentation rates between episodes of volcanic/seismic activity should be anticipated, indicated by sedimentological features or faunal abundance. Sheldon (1987a) provided detailed faunal logs of several Builth Inlier sections, in which trilobite abundance was generally much higher than in the sections presented here, although normalised abundance data were not provided. Unstudied outcrops higher in the succession are also highly trilobitic, as would be expected for relatively condensed sequences; graptolites and other organisms show similar variability.

The Llanwrtyd Wells samples are more problematic, in that their supposed basinal setting precludes the extreme accumulation rates attributed to nearshore Builth Inlier sediments. However, Cave and Rushton (1995) cited widespread slumping and soft-sediment deformation as evidence of unusually high accumulation rate; this was attributed to a position at the base of a submarine slope. Local shallow water (or emergence) is suggested by sandstones with localised shelly faunas, but the exact position of any volcanic islands is unclear. The large-scale graptolite bloom in LW 1 follows approximately 15 cm of low abundance, attributed to the effects of anoxic upwelling. Estimates of duration depend on both fluid mechanics, and subsequent diffusion of oxygen to the subsurface. A further complication may be the admixture, by mechanical or biological reworking, of the upper part of the bentonite with overlying sediment. If the entire region of refracted cleavage in LW 1 is presumed penecontemporaneous with the bentonite, the graptolite maximum occurs at around 6-8 cm. This is reasonable for a nearshore setting, but unlikely given the standard palaeoenvironmental interpretation of the Llanwrtyd district; unless additional factors were acting, the supposed open basinal setting is suspect. An alternative scenario may

be a steep-sided, fault-bounded and semi-isolated anoxic basin of shallow depth. The source of the bentonites is unknown, and proximity to emergent regions cannot be confidently quantified, although Mackie and Smallwood (1987) reported very shallow deposition during the Hirnantian, northwest of the Tywi Anticline. Although this coincided with glacioeustatic regression, a generally deep-water interpretation of the region is refuted. Available data regarding the Caradoc palaeoenvironment of Llanwrtyd is consistent with a semi-isolated, fault-bounded shallow anoxic basin (N. H. Woodcock, *pers. comm.*).

The bloom of log LS 1 (Snowdonia) extends through only 2 cm of sediment, but even this is unexpectedly long. A minimum period of several years is implied (in the standard, deep-water palaeoenvironmental interpretation) if seismic effects are discounted. The 2 cm thickness is also characteristic of the data of Rigby and Davies (*pers. comm.*), although they believe that sedimentation took place on a topographic high. Similar fossiliferous intervals follow some bentonites of the condensed Dob's Linn succession, although the banded graptolite distribution of this section (Williams and Ingham 1989) requires detailed study before their significance can be assessed. Unless sedimentation rate was extremely high in the sampled intervals, or most of the time taken to deposit each formation is not represented by rock, the effects of ash-fall must have lasted for many years in Snowdonia (centuries at Dobb's Linn). This would require a fundamental shift in oceanic circulation, resulting in semi-permanent upwelling in the affected region. Until the sensitivity of oceanic currents to external forcing is better understood, the possibility of metastable circulation systems cannot be discussed in detail. For comparison, regional thermohaline collapse and overturning (Heinrich events), triggered by meltwater influx and atmospheric circulation changes, last for up to 500 years (Seidov and Maslin 1999).

Since the proximity of LS 1 to palaeoshorelines is unclear (with extensive local volcanism and emergence in the underlying Crafnant Tuff Formation – log PLW 1), variations in sedimentation rate are favoured for this example. The source of bentonites is again unclear, but probably non-local, implying unusually high background sedimentation at this time. Insufficient data are presently available on the Scottish sections, although it appears that additional factors may have operated. Overall, the proposed model allows explanation of the studied fossiliferous intervals with little or no difficulty, although the possibility of additional unknown factors cannot be excluded.

## 3.8 References


Botting, J. P. 1999. The ecological effects of volcanic ash-fall in the marine Ordovician of Central Wales. *Acta Universitatis Carolinae: Geologica* **43**, 499-502.

Botting, J. P. and Thomas, A. T. 1999. A pseudoplanktonic inarticulate brachiopod attached to graptolites and algae. *Acta Universitatis Carolinae: Geologica* **43**, 333-335.

Briggs, D. E. G., Siveter, D. J. and Siveter, D. J. 1996. Soft-bodied fossils from a Silurian volcaniclastic deposit. *Nature* **382**, 248-250.

Brown, J., Colling, A., Park, D., Phillips, J., Rothery, D. and Wright, J. 1989. *Open University course: Ocean circulation.* Pergamon, Oxford.

Butler, A. 1998. Acquisition and utilization of transition metal ions by marine organisms. *Science* **281**, 207-210.

Carpenter, S. R., Chisholm, S. W., Krebs, C. J., Schindler, D. W. and Wright, F. W. 1995. Ecosystem experiments. *Science* **260**, 324-327.

CAVE, R. AND RUSHTON, A. W. A. 1996. The Llandeilo (Ordovician ) Series in the core of the Tywi Anticline, Llanwrtyd, Powys, UK. *Geological Journal*, **31**, 47-60.

CONWAY MORRIS, S. 1986. The community structure of the Middle Cambrian Phyllopod Bed (Burgess Shale). *Palaeontology* **29**, 423-467.

DORAVA, J. M. AND MILNER, A. M. 1999. Effects of recent volcanic eruptions on aquatic habitat in the Drift River, Alaska, USA: implications at other Cook Inlet region volcanoes. *Environmental Management* **23**, 217-230.

ELLES, G. L., 1939. The stratigraphy and faunal succession in the Ordovician rocks of the Builth-Llandrindod Inlier, Radnorshire. *Quarterly Journal of the Geological Society* **95**, 338-445.

FALKOWSKI, P. G., BARBER, R. T. AND SMETACEK, V. 1998. Biogeochemical controls and feedbacks on Ocean Primary Productivity. *Science* **281**, 200-206.

FISHER, R. V. AND SCHMINCKE, H. -U. 1984. *Pyroclastic Rocks*. Springer-Verlag, Berlin, 472 pp.

FORTEY, R. A. 1999. Olenid trilobites as chemautotrophic symbionts. *Acta Universitatis Carolinae: Geologica* **43**, 355-356.

GABBOTT, S. E., ALDRIDGE, R. J. AND THERON, J. N. 1998. Chitinozoan chains and coccoons from the Upper Ordovician Soom Shale Lagerstatte, South Africa: implications for affinity. *Journal of the Geological Society, London,* **155**, 447-452.

GALLARDO, V. A., CASTILLO, J. G., RETAMAL, M. A., YANEZ, A., MOYANO, H. I. AND HERMOSILLA, J. G. 1977. Quantitative studies on the soft-bottom macrobenthic animal communities of shallow Antarctic bays. *In* LLANO, G. A. (ed.):

*Adaptations within Antarctic ecosystems (Proceedings of the 3rd SCAR Symposium on Antarctic Biology),* Smithsonian Institution, Washington D.C., pp. 361-387.

GOFF, J. R. 1997. A chronology of natural and anthropogenic influences on coastal sedimentation, New Zealand. *Marine Geology* **138**, 105-117.

GREEN, T. 1992. The importance of double diffusion to the settling of suspended material. *Sedimentology* **34**, 319-331.

GREEN, T. AND SCHETTLE, J. W. 1986. Vortex rings associated with strong double-diffusive fingering. *Physics of Fluids* **29**, 2109-2112.

HARLAND, W. B., ARMSTRONG, R. L., COX, A. V., CRAIG, L. E., SMITH, A. G. AND SMITH, D. G. 1990. *A geologic timescale 1989.* Cambridge University Press, Cambridge, 263 pp.

HOUSEMAN, G. A. AND MOLNAR, P. 1997. Gravitational (Rayleigh-Taylor) instability of a layer with non-linear viscosity and the convective thinning of continental lithosphere. *Geophysical Journal International* **128**, 125-150.

HOWELLS, M. F., FRANCIS, E. H., LEVERIDGE, B. E. AND EVANS, C. D. R. 1978. *Capel Curig and Betws-y-Coed: Description of 1:25000 sheet SH 75.* Classical areas of British geology, Institute of Geological Sciences; London: Her Majesty's Stationery Office.

HUGHES, C.P. 1969. Ordovician trilobite faunas from central Wales (Part I). *Bulletin of the British Museum of Natural History* (Geology) **18**, 39-103.

HUGHES, C.P. 1971. Ordovician trilobite faunas from central Wales (Part II). *Bulletin of the British Museum of Natural History* (Geology) **20**, 115-182.

HUGHES, C.P. 1979. Ordovician trilobite faunas from central Wales (Part III). *Bulletin of the British Museum of Natural History* (Geology) **32**, 109-181.

HUGHES, R. A. 1989. Llandeilo and Caradoc graptolites of the Builth and Shelve inliers. *Monograph of the Palaeontographical Society, London* **141**, 89 pp., 5 pl.

JENSEN, S. 1990. Predation by Early Cambrian trilobites on infaunal worms - evidence from the Swedish Mickwitzia Sandstone. *Lethaia* **23**, 29-42.

KUEHL, S. A., FUGLSETH, T. J. AND THUNELL, R.C. 1993. Sediment mixing and accumulation rates in the Sulu and South China Seas: implications for organic carbon preservation in deep-sea sediments. *Marine Geology* **111**, 15-35.

LAND, L. S. 1976. Early dissolution of sponge spicules from reef sediments, north Jamaica. *Journal of Sedimentary Petrology* **46**, 967-969.

LOCKLEY, M. G. 1984. Faunas in a volcaniclastic debris flow from the welsh Basin: a synthesis of palaeoecological and volcanological observations. *In* Bruton, D.L. (ed.), 1984. *Aspects of the Ordovician System*, 195-201. Palaeontological Contributions from the University of Oslo, No. **295**, Universitetsforleget.

LOCKLEY, M. G. AND WILLIAMS, A. 1981. Lower Ordovician Brachiopoda from mid and southwest Wales. *Bulletin of the British Museum of Natural History (Geology)* **34**, 1-78.

LOUBERE, P. 2000. Marine control of biological production in the eastern equatorial Pacific Ocean. *Nature* **406**, 497-500.

MACKIE, A. H. AND SMALLWOOD, S. D. 1987. A revised stratigraphy of the Abergwesyn-Pumpsaint area, Mid-Wales. *Geological Journal* **22**, 45-60.

NEAL, M. L. AND HANNIBAL, J. T. 2000. Paleoecologic and taxonomic implications of *Sphenothallus* and *Sphenothallus*-like specimens from Ohio and areas adjacent to Ohio. *Journal of Paleontology* **74**, 369-380.

NICOL S., PAULY, T., BINDOFF, N. L., WRIGHT, S., THIELE, D., HOSIE, G. W., STRUTTON, P. G. AND WOEHLER, E. 2000. Ocean circulation off east Antarctica affects ecosystem structure and sea-ice extent. *Nature* **406**, 504-507.

NOZAKI, Y. 1997. A fresh look at element distribution in the North Pacific. *Eos* **78**, 221. *Also available at* www.agu.org/eos_elecas97025e.html.

PARIS, F. AND NÕLVAK, J. 1998. Biological interpretation and palaeobiodiversity of a cryptic fossil group: the "chitinozoan animal." *Geobios,* **32**, 315-324.

POLLARD, J. E. 1990. Evidence for diet. *In* BRIGGS, D. E. G. and CROWTHER, P. R. (ed.): *Palaeobiology: a synthesis*, Blackwell, Oxford, 362-367.

RHOADES, D. C. AND MORSE, J. W. 1971. Evolutionary and ecologic significance of oxygen-depleted marine basins. *Lethaia*, **4**, 413-428.

RUDDIMAN, W. F., AND GLOVER, L. K. 1972. Vertical mixing of ice-rafted volcanic ash in North Atlantic sediments. *Geological Society of America, Bulletin* **83**, 2817-2836.

SCOTT, R. W. 1978. Approaches to trophic analysis of palaeocommunities. *Lethaia* **11**, 1-14.

SEIDOV, D. AND MASLIN, M. 1999. North Atlantic deep water circulation collapse during Heinrich events. *Geology* **27**, 23-26.

SHELDON, P. R. 1987a. Trilobite evolution and faunal distribution in some Ordovician rocks of the Builth Inlier, Central Wales. *Ph.D. Thesis, University of Cambridge*.

SHELDON, P. R. 1987b. Parallel gradualistic evolution of Ordovician trilobites. *Nature* **330**, 561-563.

SIBUET, M., LAMBERT, C. E., CHESSELET, R. AND LAUBIER, L., 1989. Density of the major size groups of benthic fauna and trophic input in deep basins of the Atlantic Ocean. *Journal of Marine Research* **47**, 851-67.

SUTTON, M. D. 1999. Lingulate brachiopods from the Lower Ordovician of the Anglo-Welsh Basin, Part 1. *Monograph of the Palaeontographical Society*, London, 60 pp, pl. 1-8.

TYSON, R. V. 1995. *Sedimentary organic matter: organic facies and palynofacies.* Chapman and Hall, London, 615 pp.

VAN ITEN, H., FITZKE, J. A., AND COX, R. S. 1996. Problematical fossil cnidarians from the Upper Ordovician of the north-central USA. *Palaeontology* **39**, 1037-1062.

WIGNALL, P. B. AND NEWTON, R. 1998. Pyrite framboid diameter as a measure of oxygen deficiency in ancient mudrocks. *American Journal of Science* **298**, 537-552.

WILLIAMS, H. AND BULMAN, O. M. B. 1931. The geology of the Dolwyddelan Syncline. *Quarterly Journal of the Geological Society of London* **87**, 425-458.

WILLIAMS, S. H. AND INGHAM, J. K. 1989. The Ordovician – Silurian boundary stratotype at Dobb's Linn, southern Scotland. *In* HOLLAND, C. H. and BASSETT, M. G. (eds.) *A global standard for the Silurian System*; National Museum of Wales, Cardiff.

WILLIAMS , S. H. AND RICKARDS, R. B. 1984. Palaeoecology of graptolitic black shales. *In* BRUTON, D. L. (ed.): *Aspects of the Ordovician System*. 159-166. Palaeontological Contributions from the University of Oslo, No. 295, Universitetsforlaget.

# CHAPTER 4: SYSTEMATICS AND PALAEOBIOLOGY: PORIFERA

## 4.1 INTRODUCTION

Siliceous sponges have one of the poorest described fossil records among mineralised groups from the Welsh Lower Palaeozoic. This is due partly to the fragmental nature of the sponge skeleton, partly to the small size of the dissociated spicules, and partly due to genuine rarity. In addition, very few British palaeontologists have studied the group since M'Coy (1844, 1850), Salter (e.g. 1864), Hicks (1871), Hinde (1888) and Sollas (e.g. 1877). A few studies of small suites of isolated spicules (notably Pulfrey 1933; Lewis 1940) and some articulated material (Reid 1968) have been described this century. Reid (1958-1864) started, but did not complete, a monograph on Upper Cretaceous hexactinellids. Data on foreign sponges are increasing (see papers by Rigby, Mehl, and Carrera), but the endemism of many sponge faunas makes the information of limited value in the study of British faunas.

Although isolated spicules occur commonly in Cambrian to Silurian argillaceous sediments, they are usually overlooked or mentioned only in faunal lists. Isolated spicules tend to belong to three major groups. Stauracts and small monaxons (around 0.1-0.2 mm in ray diameter) from argillaceous sediments are generally referred to *Protospongia* Salter (1864), described in detail from North America (e.g. Dawson and Hinde 1889; Walcott 1920; Rigby 1966), but originally identified in the Middle Cambrian of South Wales. The diversity of Cambro-Ordovician *Protospongia*, and related forms, in North America is now known to be substantial. The generally poorly preserved specimens from the Welsh Basin are usually assigned to two species, *P. fenestrata* and *P. hicksi* Hinde (1888), which are differentiated by the ratio of ray length to diameter. A brief inspection of museum specimens indicates that the

diversity of British protospongiids is underestimated, and a revision of these forms is intended by the author.

The second abundant morphotype group comprises hexactine spicules and larger monaxons, assumed to originate in the corresponding root tufts, associated with many siliciclastic sediments in the Welsh Basin. In general, those from argillaceous sediments tend to be small, and difficult to recognise as hexactine for preservational reasons. Many spicules described as *Protospongia* are probably hexactine, with the third axis embedded in the matrix. Most are probably referable to the protospongioid reticulosids, which dominate fine sediment faunas in North America. Arenaceous sediments and shallow limestones, often associated with volcanic episodes, sometimes contain much larger morphotypes. These are almost invariably assigned to *Hyalostelia* and *Pyritonema*, thick-walled hexactinellids of the order Lyssakida. *Hyalostelia* was reviewed by Reid (1968), and shown to refer to a very specific morphological and spicular form, known only from the Carboniferous. *Pyritonema*, previously regarded as the root tuft of Ordovician *Hyalostelia*, is discussed below and shown to represent complete monaxonid sponges, derived from lyssakid ancestors.

The only other species occurring in any abundance are the lithistid demosponges. Genera such as *Astylospongia* Roemer and *Hindia* Duncan are elements of a Lower Palaeozoic pandemic fauna discussed by Carrera and Rigby (1999). Although not particularly common in Wales, their rigid structure greatly increased preservation potential, giving a strongly biased impression of the importance of this group relative to other sponges.

Uncommon spicule morphotypes include tylotes, ribbed monaxons, triaenes and uncinates (see section 4.2 for general spicule terminology). These are variously ascribed to hexactinellids, with other rare forms occasionally referred to a variety of

monaxonid demosponges (Lewis 1940). In general, specific attributions for these isolated spicules are considered invalid, due to similarities between members of unrelated species described below. Although individual spicules are unlikely to be diagnostic, assemblages may be compared to allow tentative interpretation of life associations; articulated specimens allow confirmation of these hypothetical relationships.

Most of the specimens described below are from the southwest ridge of Llandegley Rocks; refer to 2.2.1 and 2.2.2 for locality data.

## 4.2 Morphology and Classification

The morphological terminology of sponges has developed into a complex and diverse system, particularly regarding spicule morphotype nomenclature. The terms employed here are a reflection of the most commonly used variants in modern palaeontological literature, although there is no universal standardised format. Many features of modern sponge biology are difficult or impossible to apply in fossil material, due to the lack of soft tissue preservation. An example of this is the distinction between parietal gaps (holes through the sponge body) and incurrent canals (lined with filtration cells). In three-dimensionally preserved, thick-walled taxa, any large pore entering an enclosed cloaca is probably an inhalent canal; however, in thin-walled, sub-conical taxa with open cloacae, such gaps in the spicule structure cannot be accurately interpreted (e.g Rigby and Gutschick 1976).

In general form, sponges consist of a body wall, comprising soft tissue, spongin, spicules and/or incorporated clastic material (Fig. 4.2.1), through which inhalent canals converge into a central chamber, the cloaca. Fluid is then expelled through the exhalent canal, or osculum; several inhalent-exhalent systems may be

present in one individual, particularly among encrusting forms. The flow is maintained by the action of flagellate choanocyte cells (also employed in filtration) lining canal walls, although useful flow can also be achieved through the action of external currents of around 1 m/s. The internal canal structure may be divided broadly into ascon, sycon and leucon, based on increasing convolution, complexity and development of small flagellate chambers; however, this is generally difficult to apply to fossils, and is of limited phylogenetic significance.

There is widespread belief that the wall thickness of fossil sponges is directly comparable with the thickness that contained spicules. Although this is supported

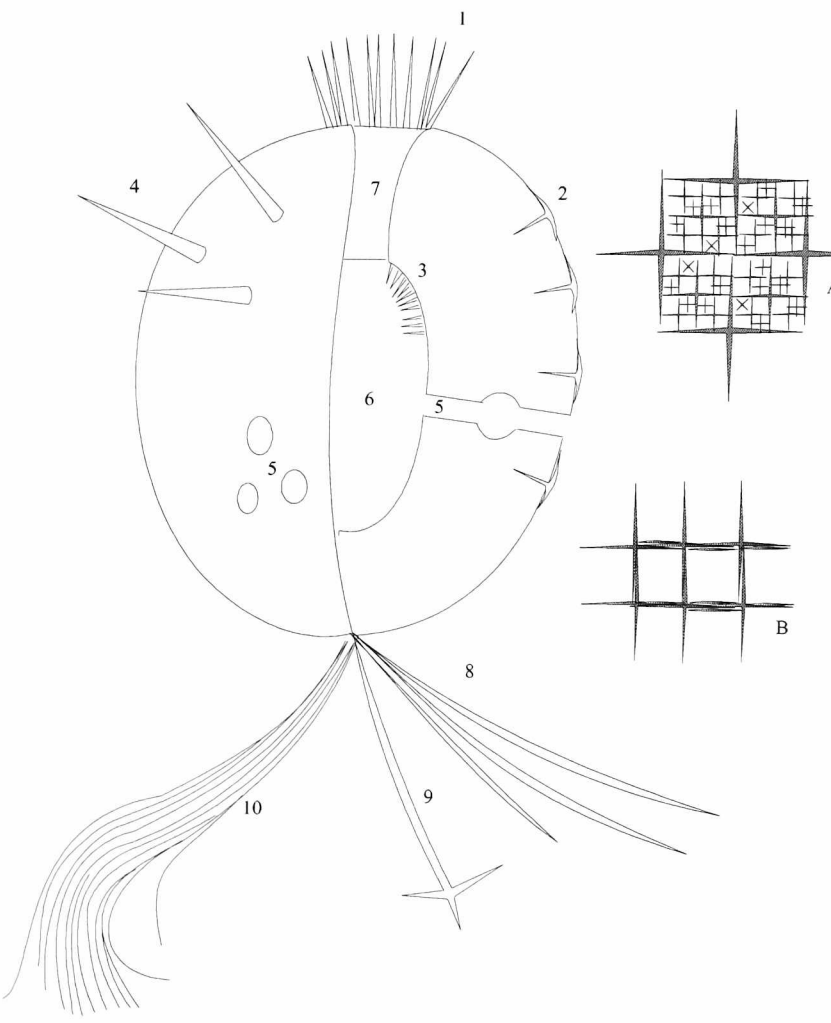


Figure 4.2.1: *Basic sponge morphology. 1: marginalia; 2: dermalia (usually clino-pentactine); 3: gastralia; 4: prostalia; 5: inhalent canals (simplified) with flagellate chamber; 6: cloaca; 7: exhalent canal (osculum); 8: enlarged monaxial root spicules; 9: anchorate rhabd (derived hexactine); 10: root tuft - ropy mass of elongate, fine monaxons.*

*A: quadruled stauractine arrangement (can also occur with hexactines); common to most protospongioids*

*B: tractose hexactinellid arrangement, typical of dictyospongioids, dictyids, and other advanced hexactinellids.*

by modern forms, which tend towards homogeneous spicule distribution within the wall thickness, this should not be assumed in all cases. The protospongioids (and others) often show a single spicular layer, which is presumed to represent the entire wall thickness, but since none have been preserved with soft tissue, this is uncertain.

The protosponge *Diagonella* occurs in the Burgess Shale (Rigby 1986), where entirely proteinaceous sponge taxa are known (e.g. *Vauxia gracilenta* Walcott, 1920), but with no indication of soft tissue. While this suggests a thin veneer of soft tissue overlying a spicular template, any arguments depending critically on wall thickness of Palaeozoic sponges should treat this issue with caution.

Spicules are described on the basis of morphology and location. While many body spicules are indistinguishable from each other, distinct morphotypes may occur at several locations (Fig. 4.2.1). The most important of these are marginalia (surrounding the osculum), gastralia (lining the cloaca), dermalia (plating of external wall), and prostalia (projecting beyond the wall). Root-tuft spicules may be isolated oxeas, rhabdose anchorate spicules, or intertwined, highly elongate oxeas forming a rope-like tuft; investigations of root tuft morphology are at an early stage. Terminology of spicule arrangement is moderately well developed, although only a few patterns are widely recognised. Most important is the quadruled arrangement (Fig. 4.2.1 A), in which regular hexactinellid spicules form a square array, with equal-sized spicules joined at tips. The intervening areas are infilled by several size orders (ray length halving at each order) in similar arrangement. Tractose patterns (Fig. 4.2.1. B) occur where spicule rays overlap to form a wide mesh of polyspicular fibres, although development may be limited to either vertical or horizonatal tracts. Variation within other array types is sufficient that accurate descriptions are invariably provided.

Description of spicule morphology is extremely complex for most morphotypes. A great diversity of nomenclature has evolved for geometrically consistent forms (e.g. De Laubenfels 1955), although only the unwieldy system of Butler (1961) has attempted standardisation in recent decades. Simple morphotypes

are classified semi-systematically by referring to the number of axes (-axon) and/or number of rays (-actine), giving, for example, triactine biaxon (T-shape). The most common morphotypes, ornamentations, and modes of fusion are shown in Fig. 4.2.2.

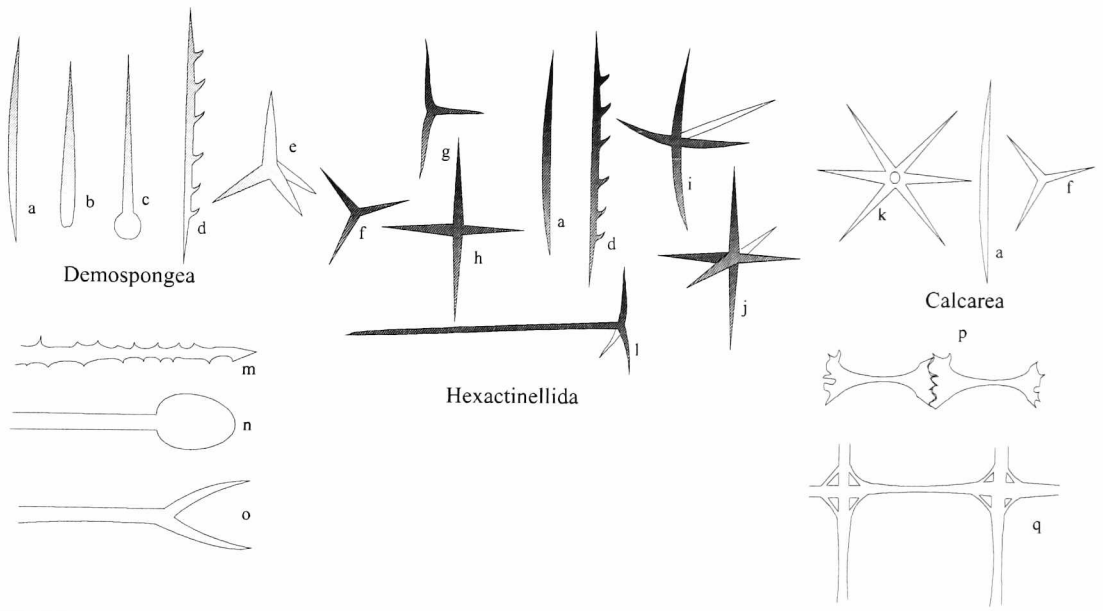


Figure 4.2.2: *Distribution of common spicule morphotypes and characteristics: a: oxea (diactine monaxon); b: style (monactine monaxon); c: tylostyle; d: uncinate; e: calthrops (tetractine tetraxon); f: regular triactine; g: tauactine (triactine biaxon); h: stauractine (stauract; tetractine biaxon); i: (clino-)pentactine (four rays recurved towards primary axis); j: regular hexactine (hexact; hexactine triaxon); k: polyactine; l: triaene (three rays recurved towards primary axis). Common ornamentation (refers to any number of rays): m: acantho-; n: tylo-; o: dicho-. Spicular fusion: p: lithistid (massive irregular overgrowth); q: Dictyida (Lyschniscida) (buttressing of tractose overgrowth).*

High-level classification of Palaeozoic sponges depends largely on the exclusivity of spicule morphotype occurrence, although evolutionary relationships are still poorly known. Widespread convergence of ray number and ornament complicates low-level phylogenetic hypotheses; among hexactinellids, it remains unclear whether hexactines or stauractines are primitive (Mehl *et al.* 1993). Recent molecular phylogenies by Zrzavy *et al.* (1998) and others suggest that the Calcarea evolved independently of the Demospongea and Hexactinellida, despite sharing two of their three basic morphotypes (oxeas and triactines) with both groups. Alternatively, Reiswig and Mackie (1983) isolated the Hexactinellida from all other groups, as a subphylum, based on cellular evidence. Uncinates, although dominantly found among

hexactinellids, also occur in certain demosponges. Some groups of Cambrian sponges (e.g. Leptomitidae) share characters of both demosponges and hexactinellids (De Laubenfels 1955; Rigby 1986). Several morphotypes may be present in any individual.

While some morphotypes are characteristic of a particular class (e.g. calthrops, tylotes?, hexactines, pentactines, and stauracts) the spicular components of many taxa (especially demosponges) are undiagnostic. Although monaxonid-only taxa are usually attributed to demosponges, spicule morphology alone is insufficient (c.f. *Pyritonema scopula* sp. nov.), and must be co-ordinated with other information. The erection of species based purely on isolated spicules is unacceptable (e.g. Zhang and Pratt 2000; section 4.5), except in the case of extremely distinctive morphotypes (e.g. Rigby and Webby 1988; Bengtson 1986), when only one morphotypical type should be defined.

In many aspicular species, selective incorporation of foreign spicules from the substrate may occur, particularly among the Dictyoceratida (Bergquist 1978, p. 88, 175). Some sponges were able to arrange spicule fragments within their tissue in order to mimic prostalia (e.g. *Miritubus erinaceus* sp. nov.). However, the fossil record of proteinaceous demosponges that lack authigenic spicules is extremely poor, and the taxonomic distribution of these traits cannot yet be established.

## 4.3 Taphonomy

Sponges from the southwest ridge of Llandegley Rocks have been preserved through a combination of abrupt burial and rapid silicification. The matrix contains abundant spicule fragments, implying that only a small proportion of specimens was preserved intact. A mobile substrate in an agitated flow regime is inferred, with high

velocities required to mobilise grain sizes greater than 1 cm. Generally low sedimentation rates (attested by the abundance of *Hesperorthis*, section 2.2.2) were interspersed with massive episodic influx, indicated by many articulated echinoderms and sponges. Some of these occurrences clearly represent mortality beds, with several specimens of articulated crinoids on one slab. Several thin tuffs are preserved in the more evenly bedded parts, with occasional articulated fossils on their lower surfaces. In addition, episodic sediment input may have resulted from seismicity, associated with eruption of the local volcanic cone.

The degree of silicification varies greatly, resulting in a range of articulated preservational styles. This variability is best seen in specimens of *Pyritonema scopula*, which is used primarily for the examples. This species contained very abundant, enlarged monaxonid spicules, and is the most common species at Llandegley Rocks. The three primary divisions may be classified as compacted, nodular, and marginally silicified.

1. Compacted (Fig. 1a)

Unsilicified, articulated material in which the body form is typically compacted by a factor of three to five. Spicules sometimes show axial dissolution, although extensive dissolution is uncommon. Spicules are preserved as chalcedonic silica, usually without further recrystallisation. Internal lamination is not preserved. The sponge interior is collapsed, without any trace of the spongin skeleton; spicules are broken into short lengths, but not greatly disturbed. Cementation of spicules is minimal, producing a cohesive yet highly porous mass, which shows little siliceous overgrowth. Clastic material is clearly visible between the spicules, concentrated by the reduced porosity. The external margin is distinct, and often silicified secondarily, post-

compaction. Compaction occurred early, due to decay of the protein skeleton, since the interior is unsilicified. The silicified margin typically extends outwards approximately 5 mm from the sponge surface. Dysideid sponges tend to be preserved as compactions, but it is less common among heavily spiculed groups. The only specimen of *Triactinella rigbyi*, and three paratypes of *P. scopula*, are of this type, however.

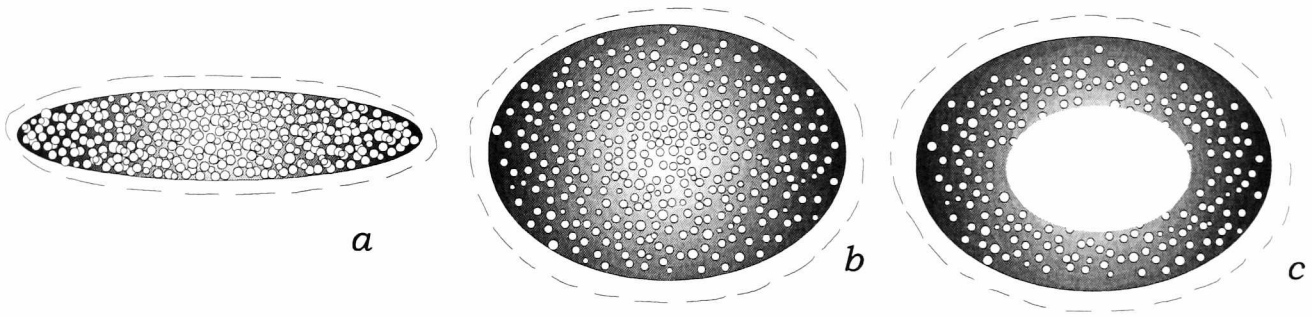


Figure 4.3.1: *primary taphonomic styles in the preservation of sponges at Llandegley Rocks, illustrated by* Pyritonema scopula*: a, compacted; b, nodular silicification, with external silica source; c, marginal silicification, with early migration of silica from central spicules to exterior.*

2. Nodular silicification (Fig. 1b)

In the very coarse upper beds, *P. scopula* becomes extremely abundant, and is typically preserved uncompacted, within siliceous nodules. The nodules are usually completely solid, although a gradation exists between this and the next category. Spicules are predominantly intact, but the axial canal is often enlarged; this may or may not be infilled with clear silica. There is no clear margin to the sponge, with the nodule grading into silicified sandstone matrix. Silicification is presumed to have initiated at the margin, since cavities only occur subcentrally.

In almost all examined specimens, carbonaceous material is present in isolated, sub-millimetric accumulations. No structure is visible in most examples, but others show consistent morphologies, and appear to represent the degraded remains of endoparasites. The carbonised fauna includes possible polychaetes and arthropods;

recent sponges often contain great numbers of endoparasitic annelids and arthropods (Bergquist 1978, p. 197). There is no evidence of the spongin skeleton in this preservational mode; all inter-spicular regions are homogeneously silicified. This preservation is known only in *P. scopula*, and then only in the uppermost, conglomeratic beds. The source of the silica was largely external to the sponge, presumably derived from oversaturated seawater following volcanogenic influx.

3. Marginal silicification (Fig. 1c)

This is the most frequent mode of preservation outside *P. scopula*, representing pre-compaction marginal silicification, which extends only a small distance internally. The outermost few millimetres of the sponge are incorporated into the silicified wall, which shows a distinct sponge margin, but continues on both sides. In some cases, the interspicular or parietal regions are silicified, and in others left largely clear. The interior of the sponge is entirely dissolved. The innermost spicules of the cemented wall usually have greatly expanded axial canals, often leaving only the external laminae intact.

This type of silicification occasionally preserved part of the spongin structure, at the interior wall margin. Silicification must have occurred extremely rapidly, with the primary source being dissolution of the interior spicules, and reprecipitation at the sponge margin. Spongin permineralisation occurred on a fine scale, in one case replacing the primary and secondary dermal mesh of *Palaeocallyoides improbabilis* gen. et sp. nov.; the other example is a partially nodular specimen of *P. scopula*, showing millimetre-scale tubes.

## 4.4 SYSTEMATIC PALAEONTOLOGY

Unless otherwise stated, the designated types are the only known specimens. Specimens are deposited in the Lapworth Museum, University of Birmingham.

### Class DEMOSPONGEA Sollas, 1875

### Order KERATOSIDA Grant, 1861

*Diagnosis* (after de Laubenfels 1955, p. E36). Skeleton of spongin only, except for foreign inclusions.

### Family ?SPONGIIDAE Gray, 1867

*Remarks*. The diagnosis of living representatives of this family depends on the identification of small (20-40 μm) flagellate chambers. Almost no fossil examples of this family are known with any certainty, although hollow, conical forms are often mistakenly referred to *Scyphia* Oken. De Laubenfels (1955, p. E36) states that over 200 occurrences of a diverse range of sponges have been assigned to the genus due to their hollow conical form. Identification of demosponge genera, and even species, based on overall morphology alone is highly subjective. Many recent species are strongly influenced by the ambient conditions, and vary markedly in form between localities. There are even cases of two species growing adjacently, and merging to form a genetic hybrid (R. Wood, pers. comm. 1996). Modern species and genera can be distinguished by incurrent canal structure, flagellate chamber size, form and distribution, and cellular characteristics, none of which are likely to be fossilised. Aspicular demosponge fossils are, however, rare enough to justify formal description, particularly given their numerical dominance in certain beds at the type locality.

Attribution of Early Palaeozoic forms to living genera, unless exceptionally preserved, cannot be justified because of the limited taxonomic significance of generally preservable features, and the poriferan tendency towards morphological convergence.

## Genus ONEROSICONCHA gen. nov.

*Etymology*. From the Latin *onerosus*, burdensome, and *concha*, shell, referring to the habit of encrusting large bioclasts. Gender *f.*

*Type species. O. gregalia* sp. nov.

*Diagnosis*. Large (20 cm) sponges with irregular outline based on oblate spheroid, lacking spicules and containing little or no incorporated clastic material. The surface is irregularly pitted and nodose, with multiple exhalent canals.

*Material.* Uncertain number of specimens preserved in fragmentary state. The uncertainty is due to the irregular outline, crowded growth distribution and large size.

### *Onerosiconchia gregalia* sp. nov.

Pl. 1, figs. 4, 6; Pl. 5, fig. 6; Pl. 8, fig. 5

*Etymology*. Latin, meaning gregarious.

*Holotype*. BU 2706: silicified external mould, probably compressed, from volcaniclastic sandstones in the uppermost *D. bifidus* Biozone of the south-west ridge of Llandegley Rocks, Llandrindod, Powys.

*Paratypes.* BU 2707, 2708, 2709; partial silicified external moulds.

*Diagnosis*. As for genus.

*Description*. Entirely proteinaceous sponges, reaching 6 cm (probably flattened) in depth. The surface is highly uneven, but with no discernible regularity; in places, a

millimetre-scale ridged texture is developed, and in others granular. No obvious ostia are seen, but these may be represented by numerous shallow pits and indentations on the upper surface. Many specimens have overgrown a bivalve, trilobite exuvium or other large bioclast, which is assumed to represent the nucleation site. The species tends to be highly gregarious where found, forming dense bands in coarse sandstones. The substrate is inferred to have been mobile, with massive episodic influx of volcanogenic sand. The gregarious "thicket" nature may be a mechanism by which burial is avoided or delayed, while attachment to large bioclasts probably also reflects agitated conditions.

*Remarks*. The erection of this species is encouraged by the lack of any similar known forms from the Lower Palaeozoic, and by the ecological significance of the species. Demosponges comprise the great majority of Recent sponge species, and appear also to dominate Ordovician assemblages, particularly those of the Lower to Middle Ordovician (Carrera and Rigby 1999). This apparent dominance is entirely due to the more preservable lithistids, and the existence of aspicular, proteinaceous demosponges as a dominant feature of a Middle Ordovician assemblage suggests that this understanding may be inaccurate. The diversity of proteinaceous demosponges, compared with hexactinellids, could have been much closer to that of the present than is generally supposed. Recent demosponges exist in almost all aquatic environments through a range of physiological adaptations (Bergquist 1978), but a predominantly near-shore early history would also have mitigated against their preservation.

Family DYSIDEIDAE Gray, 1867

*Remarks*. Living forms of the Dysideidae are recognised by eurypylous flagellate chambers, and by their fibres being cored with foreign debris (de Laubenfels 1955). The inclusion of abundant sand particles and foreign spicules enclosed in spongin fibres was used as the defining character by Gray (1867). Since the large (over 50 μm) flagellate chambers cannot easily be fossilised, attribution of fossils to this family is based on the occurrence of large volumes of foreign inclusions. It should be noted that other Recent families (e.g. Spongiidae) include debris in the cortical fibres. However, no other group contains the quantity involved with the Dysideidae, with the exception of those forms described by Gray (1867) as the order Arenosponia, family Xenospongiidae, but now attributed to hadromerid Tethyidae. (This group is discussed later, but appears to differ in that the substrate is cemented *in situ* to produce a solid base.) Other families contain relatively small quantities of foreign material, but it seems that no other modern families approach 20 to 30% volume of clastics.

## Genus ORDINISABULO gen. nov.

*Etymology*. From the Latin *ordino*, to sort, and *sabulo*, sand, reflecting the preferential use of certain grain sizes and foreign spicules. Gender *m*.

*Type species*. *Ordinisabulo quadragintaformis*, sp. nov., from volcaniclastic sandstones in the uppermost *D. bifidus* Biozone of the south-west ridge of Llandegley Rocks, Llandrindod, Powys.

*Diagnosis*. Globular to subconical dysideid sponges showing massive utilisation of well-sorted, generally fine sedimentary particles, and the preferential selection of spicule fragments. Large central cloaca of depth approximately one third sponge height.

*Ordinisabulo quadragintaforma* sp. nov.

Pl. 5, Figs. 4, 5, 7; text-fig. 4.4.1b.

*Etymology*. From the Latin *quadraginta*, forty, and *forma,* shape, in honour of the vast collection of second-hand spicules employed in its construction. Noun in apposition.

*Holotype*. BU 2710; complete three-dimensional specimen with intact infill, and limited preservation of internal structure, in two halves. Unconsolidated fragment has been used in spicule counts (see below). From volcaniclastic sandstones in the uppermost *D. bifidus* Biozone of the south-west ridge of Llandegley Rocks, Llandrindod, Powys.

*Paratype*. BU 2711; specimen from type locality, showing similar well-sorted infill, but unconsolidated. Spicule counts from this specimen are the most complete in the study.

*Diagnosis*. As for genus.

*Description*. Globular sponges, expanding slightly upwards to subconical form. Lumpy exterior, perhaps reflecting ostia or multiple osculae. Some indication of an axial, upwardly expanding cavity, assumed to represent the cloaca. Rim of sponge body raised above the sides of the primary osculum. No other canals preserved with certainty, although some indications of slightly smaller canals diverge from the cloaca at approximately 45°.

Sponge body infill is entirely clastic, well-sorted, and with preferential inclusion of foreign spicule fragments; spicule content appears substantially greater than in the surrounding matrix. Many spicule fragments sub-parallel with the sponge base, becoming strongly projecting higher up. The spicule morphotype range is discussed in the section on unassigned spicules, and is not taxonomically relevant;

there is no indication of selectivity among incorporated spicules. Inorganic particles dominantly sand grains and scoria shard fragments, typically 0.5 mm in diameter. Conodonts have also been recovered in small numbers, tentatively assigned to the genus *Baltoniodus*.

## Genus MIRITUBUS gen. nov.

*Etymology*. From the Latin *mirus*, infrequent, and *tubus*, tube, describing the consistent feature of rare internal mineralised canals. Gender *m*.

*Type species*. *Miritubus erinaceus* sp. nov., from volcaniclastic sandstones in the uppermost *D. bifidus* beds of the south-west ridge of Llandegley Rocks, Llandrindod, Powys.

*Diagnosis*. Elongate dysideid sponges with large axial canal and smaller divergent canals; limited incorporation of clastics, estimated at 30 percent of sponge body, by volume; monaxonid spicule fragments preferentially absorbed, and largely arrayed as dermal prostalia.

### *Miritubus erinaceus* sp. nov

Pl. 2, Figs. 1, 4, 5

*Etymology*. Latin, *erinaceus*, meaning hedgehog, refers to the radial array of dermal monaxon fragments.

*Holotype*. BU 2712; compacted but probably near-complete specimen, part and counterpart, from volcaniclastic sandstones, *D. murchisoni* - *D. artus* boundary of the south-west ridge of Llandegley Rocks, Llandrindod, Powys.

*Paratype*. BU 2713; partial specimen, laterally compressed, from the type locality.

*Diagnosis*. As for genus.

*Description.* Irregular, elongate outline with preserved length of 134 mm in holotype; width of 30 to 55 mm. Greatest expansion occurs 75 mm from distal end, tapering to 33 mm width at 30 mm, and expanding to 36 mm shortly after. Distal section tapers evenly thereafter to a rounded apex. Although the base is not seen, minimum width occurs at the broken proximal end. Total compressed thickness 18 mm at maximum width, giving estimated volume proportion (assuming radial symmetry) of one-third clastic material.

Clastic infill comprises all grainsizes up to 1.5 mm diameter, although dominated by smaller particles. Matrix contains abundant grains over 1.5 mm, implying preferential incorporation. Grainsize generally higher near base. Foreign spicules also greatly concentrated over background; numerous polydactyloid morphologies present, but no hexactinellid spicules recorded, reflecting availability or host selectivity. Most spicules randomly arranged in sponge interior, in random orientation. Outermost 10 mm contains elevated levels, most aligned at 45-60° to sponge margin. Adjacent spicules often almost exactly parallel. Many spicules extend beyond sponge margin as prostalia, although rarely more than 2 mm. Margin is abrupt and smooth.

Internal structure weakly preserved in holotype, but paratype is compressed further, and no canals remain. Axial canal extends most of length, comprising a series of chambers. Smaller voids diverge from axis at around 30°, although alignment is seen only in slight general elongation in this direction. The holotype shows pre-lithified breakage, the crack infilled by silica and clastics.

Rare tubular structures aligned vertically to bedding in both specimens. Diameter approximately 1 mm, with silicified wall of thickness 0.2 to 0.3 mm. Depth uncertain, but may extend through full compressed thickness. Origin of tubes

unknown. Although almost certainly preservational, they have not been observed in any other species. May represent marginal silicification of large canals.

*Remarks*. The overall form of the sponge and spicule utilisation are not known in other Llandegley rocks material. The internal canal structure shares characteristics with *Ordinisabulo quadragintaformis*, but morphologies are clearly distinct. Both appear to have had significant ability to select spicule fragments, although the mechanism is not understood. Chemical stimuli are almost certainly insufficient to distinguish monaxon from hexactinellid spicules, implying morphological discrimination.

## Genus FISTULA nov.

*Etymology*. Latin for pipe (musical), from the resemblance to an organ-pipe. Gender *f.*

*Type species*. *F. milvus* sp. nov.

*Diagnosis*. Erect tubular sponges expanding from narrow base until maximum width; thereafter width gradually decreasing. Body wall aspicular, composed of clastic particles. Deep axial cloaca.

### *Fistula milvus* sp. nov.

Pl. 3, Figs. 1–3; text-fig. 4.4.1a.

*Etymology*. Latin *milvus*, Kite; this region of Powys was among the last strongholds of the Red Kite, formerly close to extinction. They are now seen frequently at the type locality.

*Holotype*. BU 2714; single specimen showing most of lower region, central region including maximum width, and part of upper region; lacks terminations; from

volcaniclastic sandstones in the uppermost *D. bifidus* Biozone of the south-west ridge of Llandegley Rocks, Llandrindod, Powys.

*Paratype*. BU 2715; partial section through central region, showing maximum width, with part of both upper and lower regions; shows trace of cloaca. Locality as for holotype.

*Diagnosis*. Erect tubular sponge expanding from narrow base at expansion rate of one third until maximum width at 60 to 70 mm; thereafter width gradually decreasing at rate one seventh. Body wall aspicular, composed of clastic particles. Deep cloaca occupies central 50% of body, to at least 40 mm below maximum expansion.

*Description*. Elongate cylindrical sponge, expanding upwards to maximum width, decreasing slowly thereafter. Initial expansion rate one-third; maximum width in both specimens is 27 mm. Expansion rate decreases in approach to maximum over 5 mm, without abrupt angle. In holotype, maximum width occurs at height 60 mm, although basal termination not seen, and may extend for further 15 mm, by simple extrapolation. Width decreases above maximum, at rate one-seventh. Upper region extends at least 50 mm, possibly further.

Body wall thickness one quarter of sponge diameter, composed of moderately well sorted clastic particles, finer grade than matrix. In holotype, grain diameters are 1.5–3.0 mm; in paratype, 0.5–1.0 mm. Incorporated grain size appears to be constant over the entire height. Axial cloaca of width one half of sponge diameter in central and lower region; proportion is constant over observed width variation. Osculum and upper part of cloaca not seen.

Lower part of holotype preserves part of surface, silicified. Surface shows ornament of fine pits with typical diameter 0.5 mm, irregularly developed, and faint

transverse ridges, demarcated by pit concentration. Pits may represent ostia, and are of similar scale to pore spacing within clastic infill.

*Remarks.* The morphology described is typical of simple leucon or advanced sycon architecture. Inhalent canals were probably limited in dimension to little more than the pore space diameter, and the presence of large choanocyte chambers appears unlikely. However, the specimens are both laterally compressed by a factor of around two, with collapsed clastic structure, so the possibility of such features cannot be excluded.

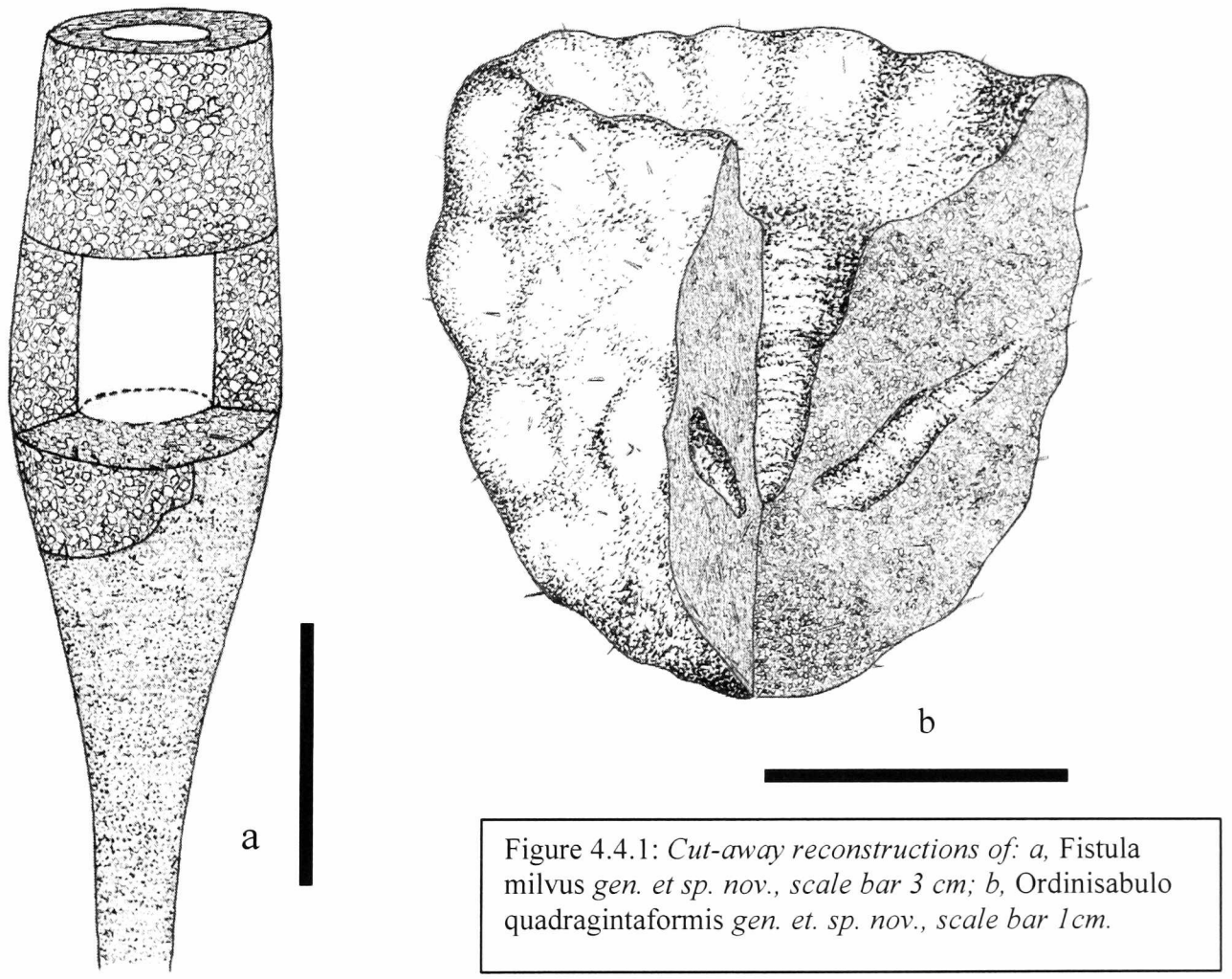


Figure 4.4.1: *Cut-away reconstructions of: a,* Fistula milvus *gen. et sp. nov., scale bar 3 cm; b,* Ordinisabulo quadragintaformis *gen. et. sp. nov., scale bar 1cm.*

Order HAPLOSCLERIDA Topsent, 1898

Family CALLYSPONGIIDAE? de Laubenfels, 1936

*Remarks*. Not previously known in fossil form, this family is defined largely on the basis of a complex proteinaceous skeleton, comprising primary, secondary, and sometimes teriary mesh orders in the specialised dermal layer (Bergquist 1978, p. 173-174, pl. 5b). Spicules, where present, are isolated oxeas or strongyles, enclosed within spongin fibres. Although highly unlikely to be preserved as fossils, the specimen described here shows that features of the spongin skeleton may be preserved even from the early Palaeozoic. Although other Haplosclerida, particularly the Adociidae, incorporate dermal specialisation, this is usually through the use of spicules.

Modern forms of this family have elaborately irregular dendritic growth form, in contrast to the simple conical morphology of the specimen described here. This suggests either superficial morphological divergence within the Callyspongiidae, retaining the fundamental structure, or convergence with a separate monaxonid demosponge family. Primitive fossil sponges of all types tend to have approximately conical form, so that divergence of morphology to the implied extent is reasonable.

## Genus PALAEOCALLYOIDES gen. nov.

*Etymology*. Latin, emphasizing the morphological similarity to the modern Callyspongiidae, and their relative age. Gender *f.*

*Type species*. *Palaeocallyoides improbabilis* sp. nov., from volcaniclastic sandstones in the uppermost *D. bifidus* beds of the south-west ridge of Llandegley Rocks, Llandrindod, Powys.

*Diagnosis*. Elongate subconical demosponges with large isolated monaxons arrayed parallel to the vertical axis of the sponge. Two orders of spongin fibre mesh in the dermal layer, with simple coarse reticulation of internal spongin skeleton.

*Palaeocallyoides improbabilis* sp. nov.

Pl. 2, Figs. 2, 3, 6; text-fig. 4.4.2.

*Etymology*. Latin, reflecting the improbable preservation of the diagnostic proteinaceous skeleton.

*Holotype*. BU 2716; articulated specimen with three-dimensional form preserved primarily as external mould; some internal structure, including spiculation and dermal spongin reticulation, is preserved; from volcaniclastic sandstones in the uppermost *D. bifidus* beds of the south-west ridge of Llandegley Rocks, Llandrindod, Powys. Only known specimen.

*Diagnosis.* As for genus.

*Description.* Steep-sided conical sponge, height exceeding 60 mm (distal region embedded in matrix), with rounded base. Maximum observed width 36 mm, possibly narrowing at distal margin. Sides diverge proximally at 10-20° from horizontal, approaching 80° after approximately 20 mm, vertically. Cloaca at least 23 mm deep, expanding upwards to lateral margins, walls thinning upwards. Upper margin asymmetrical, extending further into matrix than is visible on surface. Slight indication of curvature over entire sponge, through maximum of 15°.

Interior partially dissolved; up to 20 mm lateral wall thickness sporadically preserved. Proteinaceous skeleton supported large monaxial spicules, dominantly parallel to vertical axis. Alignment independent of lateral position, suggesting lateral spicules penetrated vertically through inclined body walls; however, no prostalia observed, and spicules may have terminated prior to margin. Spicules concentrated in central region, but occur throughout observed interior. Maximum observed diameter 0.4 mm, varying little; observed length up to 10 mm, incomplete. Entire spicules may

have been much longer. All observed spicules smooth, assumed oxeate. Although terminations not seen, no other termination types exist among isolated material of this size. Typical separation 1 mm, but occasional fragments apparently in contact; these may be displaced. Rare horizontal or oblique spicules appear to form part of original structure, although not necessarily characteristic.

Spicules supported by silicified proteinaceous material, forming reticulate mesh of incomplete radial tubes. Tube walls incomplete, perforated, but obvious through consistent radial orientation of primary canal spaces. Canals typically quadrangular to hexagonal in section, irregular; corners slightly rounded, sometimes approaching subcircular. Canals continuous over exposed lengths (up to 4 mm), but either branch, or expand greatly outwards. No indication of expansion in preserved areas, indicating continual origination of canals throughout thickness. Typical diameter of canals 0.3 to 0.6 mm, some smaller. There appears to be no specific transverse arrangement of canals, according to size or shape.

Dermal layer, approximately 5 mm in thickness, is preserved in upper right region of holotype. Dermal layer either thins dramatically proximally, or is not preserved in lower regions. Primary canal section become less regular distally, often irregularly rounded; transition into dermal layer not clearly seen. Orientation also variable, with radial structure visible. Canal walls highly perforate, with irregular openings up to 0.2 mm maximum dimension; many perforations smaller than 0.05 mm. Perforations comprise most of wall area, producing skeletal network of fine fibres which subdivide the primary fibre mesh outlined by irregular wall canal margins. Meniscal structures in angles of primary mesh sometimes imperforate, but generally less than 0.2 mm across.

No indication of attachment structure. Basal region poorly preserved, but shows primary characters of internal canal system. No apparent systematic variation in canal size, vertically, although regularity of canal morphology may increase slightly upwards. Some indication of small volume of clastic material incorporated into skeleton, particularly in lateral basal areas.

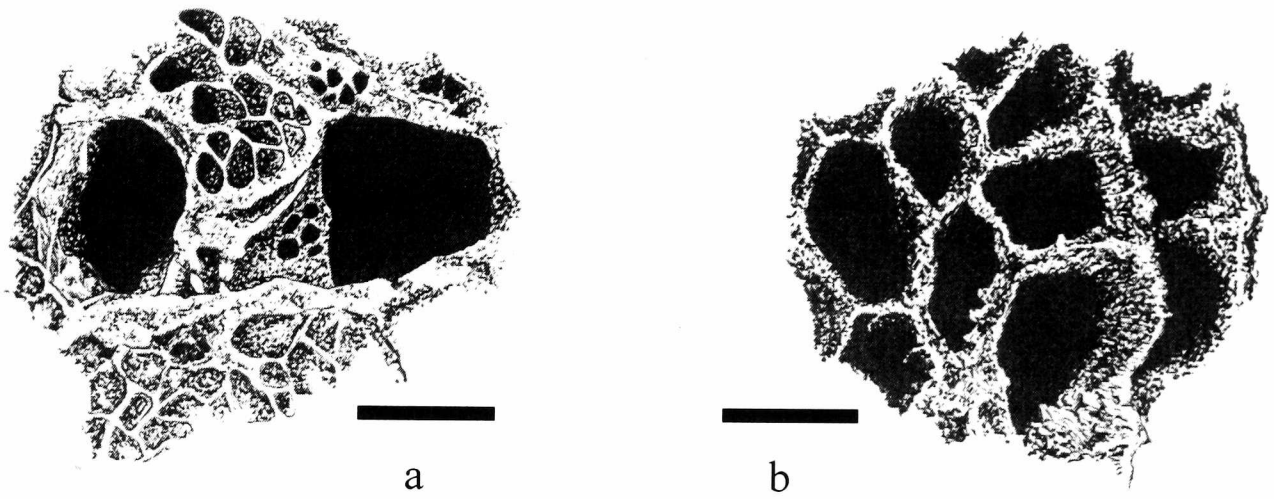


Figure 4.4.2: *Reconstruction of spongin skeleton of* Palaeocallyoides improbabilis *gen. et sp. nov: a, ectodermal, showing dual-order reticulation, scale bar 0.2 mm; b, endosomal, radial canals, scale bar 0.5 mm.*

*Remarks*. Without the preserved protein skeleton, recognition of this species would be very difficult. The comparative rarity of spicules and the presence of a cloaca distinguish *Palaeocallyoides* from *Pyritonema scopula*, but in flattened material, this may not be obvious. Few other taxa in Ordovician sediments comprise spicules that can be confused with the large monaxons described above. However, most accumulations of similar spicules are assumed to be hexactinellid root tufts. Under unusually quiet preservational conditions, the parallel arrangement of separate monaxons may be preserved. This cannot be assumed diagnostic, however, and it is apparent that certain identification with this species is dependent on preservation of the proteinaceous structure.

## "Order" LITHISTIDA Schmidt, 1870

*Remarks*. The Lithistida are known to be polyphyletic (de Laubenfels 1955). They are characterised by siliceous build-up on spicule surfaces, producing a massive architecture of irregular spicules termed desmas. Five suborders are recognised, based on the basic spicule morphotype and points of spicule conjunction. Some forms are clearly derived from the tetractinal demosponges (Tetracladina, some Anomocladina) while others seem to be derived from hexactinellid ancestors (some Eutaxicladina and Anomocladina). Some genera are apparently derived monaxonid demosponges (e.g. *Isoraphinia*, Megamorina). The distinctiveness of lithistid architecture and rarity of obvious intermediary forms have resulted in this artificial taxon being almost universally retained.

### Suborder EUTAXICLADINA Rauff, 1893

*Remarks*. Includes forms based on triactinal, tetractinal, and pentactinal or hexactinal morphotypes, in which spicules are linked by ray apices or centres, rather than junctions. The order is almost certainly polyphyletic, but distinguishing the number of rays is difficult in many cases, due to heavy siliceous overgrowth at junctions.

#### Family ASTYLOSPONGIIDAE Rauff, 1893

##### Genus MICROSPONGIA Miller and Dawson, 1878

*Type species. M. gregaria*, from the Cincinnatian (upper Caradoc-lower Ashgill) of the U.S.A.

*Diagnosis*. Globular, with radially arrayed canals formed by the regular arrangement of symmetric, often tuberculate dicranoclone desmas. Structure may be supported by large radial monaxons.

*Discussion*. This genus is better known as the widely accepted junior synonym *Hindia* Duncan (1879), originally described from the Middle Silurian of Tennessee. Confusion arises due to the uncertain description of the type specimens of *M. gregaria,* which may have included oxeate spicules in the supporting structure (Sinclair 1956). Such spicules are lacking in the type material of *Hindia sphaeroidalis*. If *M. gregaria* contains monaxons, synonymy with *Hindia* is refuted, and both names are retained. On this basis, the clear presence of monaxons in the present specimen implies a position outside *Hindia*, but possibly within *Microspongia*, if the type material does indeed contain monaxons. However, Rigby and Webby (1988) describe abundant *Hindia sphaeroidalis* as containing radial monaxons in almost every specimen, and include this feature in their diagnosis. If a variable feature, the absence of monaxons in the type material may be an acceptable variation within the genus, in which case the genera are synonymous.

*Hindia* is one of the few pandemic sponge genera, occurring in the Ordovician and Silurian of North America, Australia and Europe. Although the taxonomy is debatable, this distribution is certainly valid for the *Hindia-Microspongia* group as a whole.

*Microspongia*? sp.

Pl. 3, fig. 4

*Description*. Single specimen (BU 2717), diameter 5.5 mm, preserved three-dimensionally. Spicules with substantial siliceous overgrowth, and consequently difficult to diagnose. Skeletal architecture shows diagonal rhomboidal arrangement of rays in radial section, indicating tricranoclone, rather than hexactine-based, desmas. Tangential section shows polygonal canals, typically triangular to hexagonal. Spicule rays conjoin at apices, sometimes possibly junctions, with canals apparently retaining similar polygonal form over substantial length. Occasional radial monaxons support the structure, greatly exceeding other spicules in size; full length not seen, but largest fragments over 2 mm long, probably continuing through dermal region as prostalia. Smaller monaxons occur in central region, where main body spicules are too crowded and overgrown to distinguish canal structures.

Surface smooth, lacking features such as the ribs of *Astylospongia* Roemer. No obvious osculum, and no attachment structure. The specimen is adjacent to *Ordinisabulo quadragintaformis* gen. et sp. nov., in close contact with oscular region. This could indicate epifaunally attached life position, but evidence is very weak. A second, broken specimen is possibly referable to *Microspongia*?, showing unclear skeletal structure including rare monaxons. Again, close proximity to another sponge.

## Order POECILOSCLERIDA Topsent, 1898

### Family uncertain

### Genus POLYDACTYLOIDES gen. nov.

*Etymology*. Latin for "shaped like many fingers", referring to the characteristic uncinate spicules. Gender *m*.

*Type species. Polydactyloides trescelestus* sp. nov. from volcaniclastic sandstones of the uppermost *D. artus* or *D. murchisoni* Biozone, Lower Llanvirn; southwest ridge of Llandegley Rocks, Builth-Llandrindod Inlier, Powys.

*Other species. P. entropus* sp. nov., locality as above.

*Diagnosis.* Monaxonid demosponges characterised by a disordered, three-dimensional, primarily marginal lattice of diactine monaxons, also including uncinates in which individual spines are split into toothed frills; the number of points is variable within and between spicules and species.

*Remarks.* The lack of any indication of a hexactinellid affinity shows that complex spicule morphotypes should not be immediately attributed to the Hexactinellida. *Polydactyloides* is assigned to the demosponges because of the entirely monaxonid skeleton, without triaene anchorate spicules, and the lack of a regular spicule mesh.

High-level taxonomy of these demosponges is complicated by the lack of information regarding the taxonomic distribution of the uncinates. Although they occur widely within the Hexactinellida (Reid 1958b), their distribution within demosponges is less well known. Bergquist (1978) mentioned numerous examples of acanthose monaxons belonging to primarily the Poecilosclerida, Axinellida and Hadromerida. Fossil poecilosclerids are also frequently spiny (de Laubenfels 1955). However, spines within the demosponges tend to be simple, irregular protrusions with no obvious arrangement, in contrast with the lateral rows of recurved spines seen in many hexactinellids.

The character set of the Poecilosclerida, as defined by de Laubenfels (1955), includes the level of organisation found in these forms. However, family-level taxonomy of fossil poecilosclerids is based primarily on the spicular morphology and

architecture. The unique nature of the spicule morphotypes involved may justify the erection of a new family to accommodate them.

*Polydactyloides trescelestus* sp. nov.

Pl. 4, Figs. 1–4; Pl. 5, Fig. 1; Pl. 12, Figs. 1–5 ; text-figs. 4.4.3, 4.4.5.

*Etymology*. From the Latin *tres*, three and *scelestus*, criminal, referring to a hypothetically triple-hooked *uncus* (hence uncinate), used to drag away executed criminals.

*Holotype*. BU 2718; external mould of articulated specimen, approximately half complete, showing lower surface, including base and half of circumference; from volcaniclastic sandstones of the uppermost *D. artus* or *D. murchisoni* Biozone, Lower Llanvirn; southwest ridge of Llandegley Rocks, Builth-Llandrindod Inlier, Powys.

*Paratypes*. BU 2719, 2720, 2721; three specimens, each showing part of circumference, and including the diagnostic spicules. Locality as for holotype.

*Diagnosis*. *Polydactyloides* with frequent derived uncinates with dominantly three points per hook, very rarely more. Morphology mushroom-shaped, with lobate lateral margin, and short, upwardly expanding stem.

*Description*. *Polydactyloides* with stem rapidly expanding into discoid body with drooping margin. Height of stem in holotype 30 mm, width expanding from 10 to 25 mm. Stem may include a supporting bioclast; holotype contains erect *Balacrinus* pleuricolumnal at base, reflecting growth around live host. Lateral margin lobate on 10 – 30 mm scale; cap diameter approximately 80 mm, with apparent thickness 10 – 20 mm. Spiculation of loosely radiating monaxons embedded in base, increasing in density towards margin, where arrangement becomes irregular. Central monaxons

fragmentary, with maximum observed length 8 mm; all fragments straight, 0.1 to 0.3 mm thick.

Spicules mostly located near lobate margins and upper surface. Derived uncinates also located at margins, concentrated close to upper surface. Most penetrate sponge body to form interlocking framework between regular monaxons. Lateral smooth monaxons are generally subparallel to local surface.

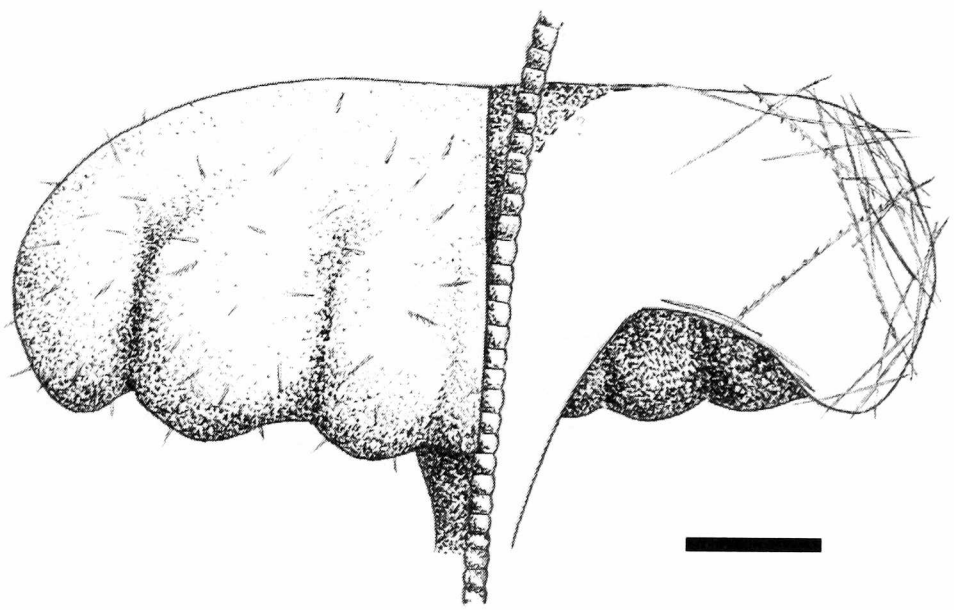

Figure 4.4.3: *Cut-away reconstruction of* Polydactyloides trescelestus *gen. et sp. nov., showing spicule distribution and erect crinoid pleuricolumnal at centre. Scale bar2 cm.*

Derived uncinates, although thinner than largest smooth monaxons (0.1 – 0.15 mm), exceed 5 mm in lengths. Toothed frills vary in number of prongs along-axis, with proximal region (away from which the teeth are directed) smooth, or with slight spinose projections. Flanges may be developed prior to establishment of teeth. Transition to fully toothed frills is gradational but rapid. Most uncinates reach maximum of three teeth per frill, either in single line, or two lines of frills, circumferentially displaced approximately 90° or 180°. Very rarely, spicules show higher number of teeth per frill, to maximum of five.

*Remarks.* The supposed function of all uncinates as root spicules, analogous to a triaene, is shown to be incomplete. In the holotype, the preservation appears to be undistorted, and shows original spicule relations, their terminations extending to, or through, the body walls. The uncinates are located at the margin of the sponge body,

near the growing tip, in variable orientations. The frills appear insufficiently large to function as anchoring structures against the smooth monaxons, and were probably attached to spongin fibres.

*Polydactyloides entropus* sp. nov.

Pl. 4, Figs. 5, 6; Pl. 5, Figs. 2, 3; Pl. 12, Figs. 6, 8, 10–13; text-figs. 4.4.4, 4.4.5.

*Etymology*. Reflecting the disorder of the spicular skeleton.

*Holotype.* BU 2722; articulated specimen, sectioned horizontally, showing range of spicules and part lateral outline; from volcaniclastic sandstones of the *D. artus* or *D. murchisoni* Biozone, Lower Llanvirn; southwest ridge of Llandegley Rocks, Builth-Llandrindod Inlier, Powys.

*Paratypes*. BU 2723, 2724, 2725; articulated specimen, sectioned vertically, showing range and utilisation of spicules; two partial specimens showing diagnostic spicules; locality as above.

*Diagnosis*. Flattened globose to ellipsoidal *Polydactyloides* in which the derived uncinates contain up to seven or eight well-defined prongs per frill, and comprise up to 15% of the total spicule content. Skeletal architecture disordered.

*Description.* Globose *Polydactyloides* with framework loosely consolidated by partially interlocking, multi-pronged uncinates and numerous smooth monaxons, although interlocking rarely preserved. Inter-spicule angles variable, but more commonly 90° than 60°. Uncinates with from five to eight points per spine, rarely fewer, and comprise 10-15 % of total spicule abundance. Frills usually occur in three lines, rotated through 90° and 180°. Distribution of uncinates apparently random; isolated individuals surrounded by smooth monaxons, but some clusters consisting

mainly of uncinates. Uncinates commonly sub-vertical, in contrast to generally horizontal smooth monaxons. A single stauract is seen in BU 2722, with a poorly developed secondary axis; no evidence of accidental incorporation, so possibly two overlain axial fibres at initiation of spicule secretion.

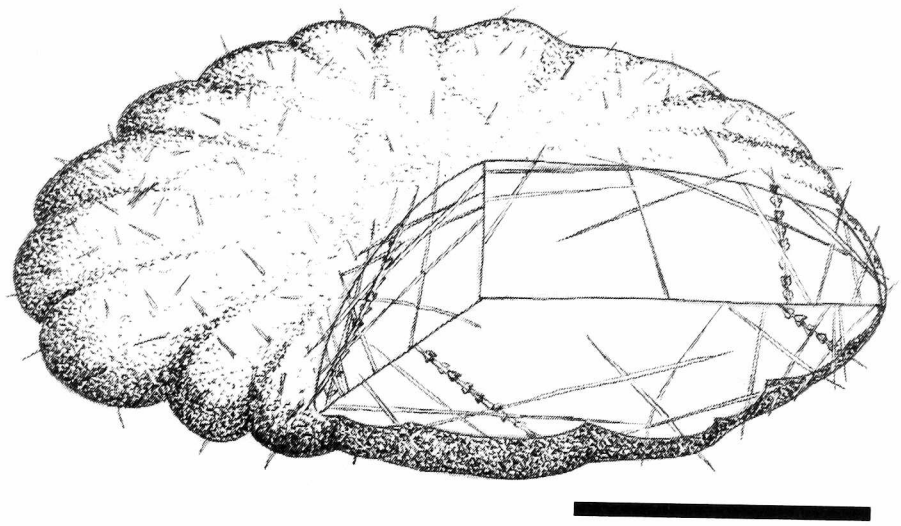

Figure 4.4.4: *Cut-away reconstruction of* Polydactyloides entropus *gen. et sp. nov., showing approximate morphology and spicule distribution. Scale bar 1 cm.*

Most specimens approximately 25 mm diameter, less than 10 mm high, although possibly slightly compressed; paratype BU 2725 is 40 mm in diameter. Paratype BU 2723 contains open regions surrounded by dense spicule masses, reaching 2 mm diameter. These may represent inhalant canal locations, although no indication of cloaca or osculum.

Remarks. The variation of spicule morphology among *Polydactyloides* is clearly shown by numerous isolated spicules, (summarised in Fig. 8), with the direction of evolution apparently clear. A comparison of *P. entropus* with *P. trescelestus* shows a reduction in size and complexity of the sponge body, while the overall architecture is retained. Uncinates tend to occur in vertical to oblique orientations, relative to smooth monaxons, and are concentrated near the lateral margins. This is less clear in *P. entropus* due to its smaller size. The lobate margin is retained, although the bulbous base of *P. trescelestus* appears to have been lost. Both

are important components of the spicule morphotype assemblages (discussed below) but their fluctuating proportions suggest that they were favoured by different conditions.

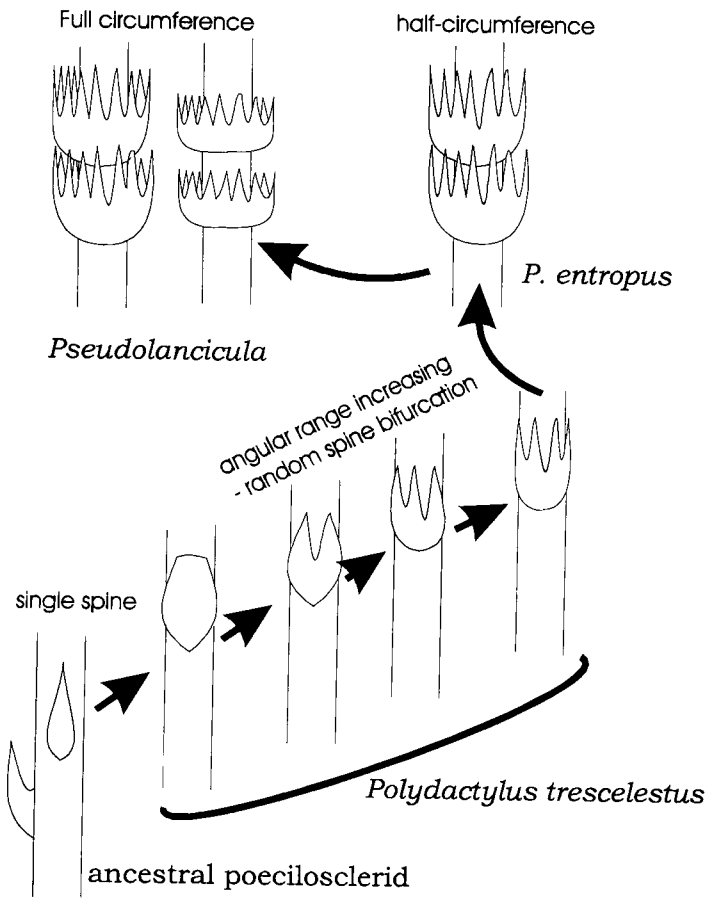


Fig. 4.4.5: *Proposed evolution of* Polydactyloides *and* Pseudolancicula *spicule morphology, derived from ancestral poecilosclerid.*

Genus PSEUDOLANCICULA Webby and Trotter, 1993

*Type species*. By monotypy *Pseudolancicula exigua* Webby and Trotter, 1993, from the Upper Ordovician of the Malongulli Formation, New South Wales.

*Diagnosis* (emended from Webby and Trotter, 1993). Polydactyloid demosponges in which the derived uncinates form goblet-shaped frills which completely encircle the primary axis.

*Distribution*. Known from the Upper Ordovician Malongulli Formation, New South Wales, the Lower Llanvirn (uppermost *artus* or *D. murchisoni* Biozone) volcanogenic sandstones of Llandegley Rocks, Powys, Wales, and possibly from Caradoc

phosphates at Pen-y-Garnedd, Montgomeryshire (Lewis 1940, Pl.1, figs 11, 12); isolated spicules only.

*Pseudolancicula* cf. *exigua* Webby and Trotter, 1993

Pl. 12, Figs. 7, 8; Text-fig. 4.4.5

*Material*. BU 2726, 2727; fragments of isolated spicules, recovered from *Ordinisabulo quadragintaformis*. No articulated material.

*Decription*. Monaxial fragments with goblet-shaped frills entirely encircling axis. Two morphotypes distinguished, as in Webby and Trotter (1993). In first, frills have parabolic lateral outline, terminating in circumferential array of up to 16 elongate spines, diverging according to parabolic form defined by goblet. Spines and intervening gaps irregular in size and distribution, reflecting repeated bifurcation of a single original spine, according to a random scheme (Fig. 4.4.5). Along-axis separation of parabolic cups typically two to three axial diameters.

Second morphotype flatter, with saucer-shaped cup initially diverging almost perpendicularly from stem. Abrupt change in angle produces series of short, almost axis-parallel spines, not overlapping overlying cup, in contrast with overlapping spines of primary morphotype. Along-axis separation of cups approximately one axial diameter.

*Remarks*. The specimens described here are less numerous and complete than the New South Wales material, and exact comparisons based purely on a slightly variable spicule morphotype are somewhat subjective. However, some consistent differences appear to exist: the frill is more regular in Webby and Trotter (1993), with relatively constant distances between points and little variation in the depth of gaps; the along-

axis distance between cups is greater in the Welsh material; and the spine length of the flat morphotype is also slightly increased. These characters, although significantly variable between spicules, may be sufficient to separate *P.* cf. *exigua* from the type species, although a formal treatment is considered inappropriate without articulated material.

Webby and Trotter (1993) discussed the possible relationships of *P. exigua* within the Porifera, but could reach no firm conclusion. Morphological similarities to Recent agelasid demosponges (Bergquist 1978) were rejected on compositional grounds, and no clear morphological analogues were found among the hexactinellids. Mostler (1990) described Lower Jurassic scopules, of which parts appeared similar to a miniature *P. exigua*, although the overall morphology of each spicule type is very different. The presence of the polydactyloid spicule morphologies provides an evolutionary basis for deriving *Pseudolancicula* among the demosponges.

Order uncertain

*Remarks.* The following specimens cannot be attributed with any certainty to known groups. The closest similarity appears with the original description of the modern *Xenospongia patelliformis* Gray, 1858, for which he erected the order Arenospongia Gray, 1867. This order is no longer used, and *Xenospongia* is confidently referred to the hadromerid Tethyidae (M. Sara, *pers. comm.*), based on the presence of radiating monaxons. The extensive use of inorganic detritrus was emphasised by Gray (1858), where he suggested the majority of the body to comprise sand and foreign spicules. In particular, concentric growth lines on the base suggest *in situ* cementation of the substrate. Given the lack of authigenic spicules in the present specimen, other similarity to *Xenospongia* probably has little significance, and these demosponges

must remain under open terminology. Although the Dysideidae and Spongiidae, among others, contain fibres cored with foreign debris, none show *in situ* cementation of the substrate by the growing organism. A close affinity with either of these groups is considered unlikely.

Indeterminate demosponges

Pl. 1, Figs. 1-3, 5

*Material*. BU 2718, 2729; two subcircular to ellipsoidal specimens, broken in the central horizontal plane, from volcaniclastic sandstones of the *D. artus or D. murchisoni* Biozone, Lower Llanvirn; southwest ridge of Llandegley Rocks, Builth-Llandrindod Inlier, Powys.

*Description*. Compressed sponges in medium-grained sandstones, one incomplete. Diameter of each approximately 6 cm, with slight asymmetry; the more complete specimen is elongated to 8 cm in one direction, the other less so. Body aspicular except for incorporated clastic material, which occurs as a shallow biconvex disc. Each specimen horizontally split along a bedding plane, so observed surface is an horizontal interior plane. Internal plane structure of irregular ridges, in other parts irregular or structureless. Clastic infill is well-sorted, fine sand with occasional monaxonid spicule fragments. No indication of organised spicule placement or incorporation. No evidence of internal canal structures, or of a cloaca.

*Remarks*. The rarity of specific identifying characteristics for this sponge prevents detailed discussion of affinities. That the sponge is somewhat compressed from a more erect form is weakly suggested by the ellipsoidal form of the impressions, implying compression oblique to bedding. The discoid form may be due to compression of an erect conical, globose, or cylindrical form. However, this would

require perfect vertical compression of one specimen, and equal epifaunal and infaunal extent for both in life position. A discoidal morphology is the more parsimonious. As discussed for the Dysideidae (p. 22), incorporation of clastic material is common to some degree among the aspicular demosponges. However, a discoid morphology is rare in this group, and the density of sand suggests *in situ* cementation of substrate, rather than entrapment of particles through inhalent canals .

## Class HEXACTINELLIDA Schmidt, 1870

### Order RETICULOSA Reid, 1958b

#### Superfamily PROTOSPONGIOIDEA? Finks, 1960

*Discussion.* Finks (1983) separated the Reticulosa into four superfamilies. The Protospongioidea comprise a dermal layer only (sometimes including prostalia, marginalia and basalia) of ranked, quadruled stauractines or lesser hexactines. This contrasts with Finks (1960), where the group was considered to include forms with multiple spicule layers, in some cases bundled, and including all hexactine and reduced spicule types.

The Dictyospongioidea (Hall and Clarke 1898) are characterised by a bilaminar wall with bundled stauracts in the outer wall, and an inner layer of monaxon tracts. The Hintzespongioidea (Finks 1983) comprise a protospongiid-like, reticulated outer layer over an inner layer of non-parallel hexactines and derivatives, marked by large parietal gaps (Rigby and Gutschick 1976). The related Dierespongioidea (Rigby and Gutschick 1976) contain a dermal layer of quadruled hexactinellid spicules (dominantly stauracts) and a gastral layer of irregularly oriented stauracts (sometimes including hexacts); canals are generally absent.

None of these superfamilies readily accommodates a fairly thick-walled, non-quadruled rectangular arrangement of triactine spicules only, with a dense gastral layer. The Protospongioidea is the only group in which hexactines are generally lacking, but their minimal wall thickness makes this affinity unlikely. Non-quadruled arrangements of parallel spicules are seen only in the Mattaspongiidae (Protospongioidea; Rigby 1970) and possibly in some species of *Cyathophycus* (Hintzespongioidea; Finks 1983; Rigby 1995). In each case, hexactines are dominant.

There is some evidence that the unusual spiculation of *Triactinella* may reflect a primitive condition (but see discussion below). The genus lacks the main features of the major derived clades (bilaminar wall (excluding gastralia), hexactines, spicule tracts), and appears fundamentally dissimilar to described forms, although the regular, uncemented mesh certainly indicates a reticulosid. On this basis, it is considered likely to represent a derived form of a primitive stock, and as such is best considered tentatively as close to the Protospongioidea, pending further discoveries.

## Family TRIACTINELLIDAE nov.

*Diagnosis*. Reticulosids with several layers of rectangularly arranged stauractine or triactine spicules, without ranked quadrules. Gastralia dense, primarily monaxonid.

*Remarks*. One species is presently known.

## Genus TRIACTINELLA gen. nov.

*Etymology*. From the unusual abundance of triactine spicules. Gender *f.*

*Type species. Triactinella rigbyi* sp. nov.

*Diagnosis*. Moderately thick-walled, vase-shaped sponges with reticulate dermal architecture of irregularly sized biaxon triacts and stauracts. Triacts are arranged in all orientations within single-order square to rectangular spicule mesh, often with superimposed rays. Marginalia comprise small, derived monaxons, including highly elongate biaxon triacts.

*Discussion.* Attribution of this genus to the Protospongioidea was discussed above. Few other families are currently placed within the Protospongioidea. The thick wall of *Triactinella* and lack of ranked quadrules clearly distinguish the genus from the Protospongiidae. The Mattaspongiidae (Rigby 1970) also have coarsely quadruled hexactines, with a dermal layer of felted monaxons.

Finks (1960) described the lyssakid genus *Carphites* (p. 125, pl. 43, 44, 46) from the Permian of the Guadaloupe Mountains, in which the body wall largely comprises triacts, with a dermal layer of enlarged hexacts. Although isolated triacts of *Triactinella* and *Carphites* are morphologically similar, there are few other similarities between the sponges. In *Carphites*, the triacts are randomly arranged in a dense mesh that comprises the thick wall. Hexacts are large and fully developed. Although direct derivation of *Carphites* from *Triactinella* is possible, the relationship would be remote. It should, however, be noted that some triacts in *Carphites* show similar incurvature of the primary axis, indicating either direct descent or convergence. Reduction of hexacts to triactines also occurs rarely among spicules of the dictyosponge *Stereodictyum orthoplactum* Finks 1960 (pl. 38, fig. 6); the example illustrated also displays the incurvature. This suggests convergence of fine morphology, perhaps related to structural constraints.

Ray reduction is known to occur from the hexactine condition, producing both pentactines and stauracts. However, Bergquist (1978) argued that stauractine spicules are more primitive than hexactines. The origins of hexactines and stauracts were also discussed by Mehl *et al.* (1993), with no definite conclusion possible.

At present it is not clear whether the biaxon triact state represents a primitive or derived variation on the stauract morphology. Generally, they are considered to be stauractines from which one ray has been lost, analogous to the hexactine origin of pentactines. Bengtson (1986) considered abundant biaxon triacts to be derived monaxons, but in this material the secondary ray was much shorter, and deformation of the primary axis lacking. An isolated biaxon triact attributed to *Triactinella rigbyi* sp. nov., from the type locality, shows a minute fourth ray in the incurvature opposite the ray of the secondary axis (paratype BU 2740), possibly showing the initiation of the stauract condition from a biaxon triact. If, instead, the triacts were derived from stauracts, it is difficult to understand the presence of the incurvature. Intuitively, the fourth ray would have been reduced without requiring deformation of the other rays, although the above discussion of *Carphites* suggests a general tendency towards this form. Secondary regrowth of the fourth ray following prior reduction must also be considered, and is perhaps more parsimonious than a complex morphology derived from a pre-protospongiid ancestor.

*Triactinella rigbyi* sp. nov.

Pl. 6, Figs. 5, 6; Pl . 7, Figs. 1, 2; Pl. 13, Fig. 11; text-fig. 4.4.6.

*Etymology*. For J. Keith Rigby and his profusion of poriferan papers.

*Holotype.* BU 2739; articulated specimen, flattened, from volcaniclastic sandstones of the uppermost *D. artus* or *D. murchisoni* Biozone, Lower Llanvirn; southwest ridge of Llandegley Rocks, Builth-Llandrindod Inlier, Powys.

*Paratype.* BU 2740; isolated biaxon triact showing a small proto-ray in the incurvature of the secondary axis. Recovered from the clastic infill of *Ordinisabulo quadragintaformis*, from the type locality.

*Diagnosis*. As for genus.

*Description.* Vase-shaped sponge of diameter 2 to 3 cm; initial expansion approximately parabolic, sides becoming nearly parallel after 20 mm. Overall height around 40 mm. Dense oscular lining of small derived monaxons, often single axis with small side projection, but most are unclear. More complex variations occur rarely. Exocoel thin, comprising square reticulate outer mesh of regular stauracts and biaxon triacts, grading into subsurface rectangular mesh of proximo-distally extended spicules of same types. Exterior triacts with all three rays of approximately equal length, with variable incurvature of primary axis at junction with secondary ray. Triacts often adjacent or overlapping; occasional regular stauracts in apparently random locations. In interior, spicules are elongated proximo-distally, some triactines approaching monaxon morphology, others forming narrow "T" shape. Several layers of triactinal and stauractine spicules visible in best-preserved part of body wall, although compression prevents accurate quantitative description. No clear evidence of consistent orders, although several spicule sizes present in any area.

Spicules show normal dissolution structures; axial canal often enlarged, sometimes leaving only external lamina. Axial canals occur in all rays. The attachment mechanism is not seen.

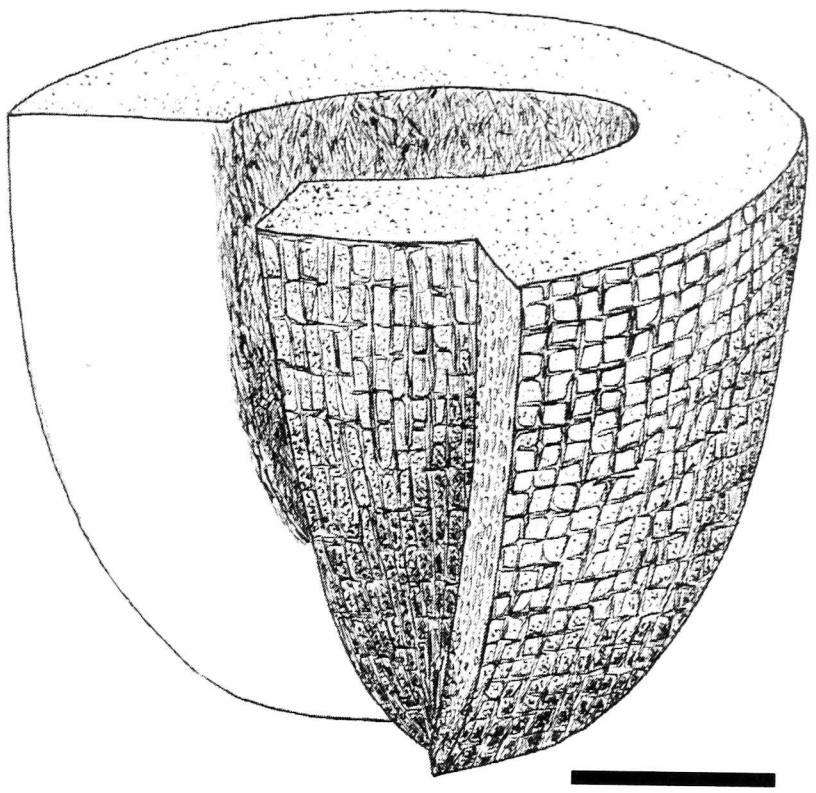

Figure 4.4.6: *Cut-away reconstruction of* Triactinella rigbyi *gen. et sp. nov., illustrating gradual variation in spicule morphology through wall thickness, and distinct gastralia. Scale bar1 cm.*

Superfamily DICTYOSPONGIOIDEA Hall and Clarke, 1898

(*nomen translatum*, Finks 1983)

Family DICTYOSPONGIIDAE Hall, 1884

*Remarks*. The Dictyospongiidae are an important Palaeozoic group of reticulate hexactinellids characterised by very thin (often single layer) walls containing tracts of stauractine and monaxonid spicules, often in bundles. They represent a derived protospongioid stock where the quadruled pattern is often visible, but with the quadrules filled by fine spicules. They reached greatest diversity in the Devonian, with very few Ordovician examples. Webby and Trotter (1993) record *Hydnodictya* from the Upper Ordovician of New South Wales, while *Acanthodictya* Hinde is present in the undifferentiated Ordovician of Little Metis, Quebec (Dawson and Hinde 1889). These beds may be partly Lower Ordovician in age, but the accepted date of the oldest known dictyospongiids is Upper Ordovician (Carrera and Rigby 1999), probably Caradoc. However, Finks (1983) gave the Upper Silurian as the first

occurrence of the superfamily Dictyospongioidea. The present specimen is therefore among the oldest known dictyospongiids.

## Subfamily DICTYOSPONGIINAE Hall, 1884

*Remarks*. Dictyospongiids in which the body is non-prismatic. Although assumed to be an artificial distinction (de Laubenfels 1955), it is worth noting that the ancestral protospongioids were subcircular. However, many species of *Cyathophycus* were approximately prismatic, and this genus was probably close to the ancestor of the Dictyospongioidea. Not previously known prior to the Silurian.

## Genus RETICULICYMBALUM gen. nov.

*Etymology*. Latin *reticulum*, net; *cymbalum*, cymbal, for the general appearance. Gender *m*.

*Type species*. *R. tres*, from volcaniclastic sandstones in the uppermost *D. bifidus* beds of the south-west ridge of Llandegley Rocks, Llandrindod, Powys.

*Diagnosis*. Conical dictyosponges with sides forming constant angle from vertical; spicules in three orders, forming quadruled mesh rigidified by abundant third order spicules; at least first and second order appear to be stauractine. Walls formed of one or few spicule layers, parietal gaps absent.

*Remarks*. It is widely believed that the dictyospongiids were derived from *Cyathophycus*-like protospongioids, probably during the Ordovician. The new genus shows several features which may be interpreted as derived, and which would not be expected in a Middle Ordovician representative. The simple conical form and unbundled spiculation is present in early protospongioids, but the probable ancestral group containing *Cyathophycus* was largely prismatic, with spicule tracts. Assuming

that the Dictyospongoidea were monopyhletic, *Acanthodictya* Hinde appears more primitive than *Reticulicymbalum*, showing irregular quadrules similar to some protospongiids, such as *Asthenospongia* (Rigby *et al.* 1981). The monaxon tracts and prismatic form of *Acanthodictya* are almost identical to some *Cyathophycus*, such as *C. quebecensis* (Dawson and Hinde 1889). The early occurrence of the apparently derived *Reticulicymbalum* increases debate regarding the environmental origin of the dictyospongiids. The presence of another derived form within this shallow marine setting suggests that the origins of the dictyospongiids, and perhaps other sponge groups, were in this type of environment. The paucity of sites recording these communities is explicable through the low preservation potential, relying on massive sediment input and rapid mineralisation. Offshore migration probably occurred later, although widespread dispersal of early forms implies unusually long-lived planktic larvae.

*Reticulicymbalum tres* sp. nov.

Pl. 6, Figs. 1–4

*Etymology*. Latin for three, after the number of spicule orders. Noun in apposition.

*Holotype*. BU 2741; silicified external mould retaining some spicules, with incomplete upper margin; slightly compressed vertically. Only known specimen.

*Diagnosis*. Shallow conical sponge (constant divergence from vertical, approximately 65°) with three orders of spicule mesh: first order stauracts 0.3 mm thick, spacing c. 5 mm; second order stauracts 0.18 to 0.20 mm thick, spacing 1.8 to 2.5 mm; third order spicules up to 0.1 mm thick, crowded inside second order quadrules. Vertical and horizontal arrangements similar.

*Description.* Circular dictyosponge at least 66 mm diameter, depth 24 mm, possibly slightly compressed. Base rounded, apparently unornamented over lowest 10 mm. Wall thickness maximum of 1 mm, with basal interior infilled with sediment (now prepared out). Sub-concentric and radial spicular mesh preserved in holotype, primarily as striations on silicified mould; most spicules are dissolved, with some incorporated into the silicified margin. Some spicules visible in the silica wall, with three sizes recognised.

One first order spicule visible, displaced 40° from horizontal, with two partial rays converging at 90°. Junction poorly seen, but orientation implies a stauractine nature. Prominent concentric ridges caused by slight compression occur at approximately 5 mm intervals, assumed to represent first order mesh. If rays join at apices, ray length is approximately 5 mm; more likely longer. Vertical ridges not highlighted by buckling, and difficult to separate from poorly-preserved secondary structure. Several second order spicules seen, one displaced and showing two convergent rays, as above, indicating stauractine. Maximum observed ray length 3.5 mm, thickness varying form 0.18-0.20 mm. Second order spicules form obvious reticulation, at vertical intervals of 1.2-1.8 mm; height-varying horizontal intervals 1.5-2.5 mm.

Third order spicules seen in several regions, primarily mouldic, densely packed in both vertical and horizontal tracts between second order spicules. Thickness approximately 0.10 mm, intervening gaps up to 0.1 mm. Ray lengths difficult to establish, but exceed 1 mm. Spicules may be monaxon or stauract; junctions impossible to identify due to the low preservational quality. If stauract, overlapping of up to ten rays required, creating 1 mm wall thickness; this is the estimated upper limit,

based on the extent of silicification. Third order monaxons would require thinner walls. Finer spicule orders appear to be absent.

## Order LYSSAKIDA Zittel, 1877

(*nomen correctum* de Laubenfels, 1955; ex. *Lyssakina*, Zittel 1877)

*Remarks*. Originally defined as hexactinellids without cementation of the spicules into a rigid mesh, the order was later placed by Finks (1983) into the subclass Hexasterophora (Schulze 1887). No diagnostic pre-Carboniferous microscleres are known, although all living hexactinellids contain either amphidiscs or asters. Attribution of Lower Palaeozoic taxa to either subclass is thus based on similarity to later forms believed to contain one of these morphotypes. The order Reticulosa Reid 1958, which appears to include ancestral hexactinellids (Rigby 1986), is included in the Amphidiscophora (Schulze 1877). This does not appear to be justified, since the characters involved in subdivision into these subclasses are specialisation of the dermal layer and form of parietal gaps and internal canals. These features are known to be plastic among various groups, including the heteractinids (Rigby 1975, 1977a, 1977b) and advanced reticulosid hexactinellids such as *Ratcliffespongia* Rigby and Church, 1990, *Cyathophycus* (e.g. Rigby 1995) and *Hintzespongia* Rigby and Gutschick, 1976. On this basis, the Stiodermatidae Finks (1960) is placed in a different subclass from the Lyssacina, when both appear to be derived from the amphidiscophoran order Reticulosa. Although it is difficult to argue against the distinction of amphidisc- versus aster-bearing sponges, the status of subclass is probably strongly overstated. Bergquist (1978, p. 222) also considered microsclere type to be of negligible phylogenetic significance. Not only is this taxonomic system

difficult to employ in the fossil record, to do so may be misleading. It is possible. however, that the Reticulosa and Lyssakida were distinct prior to the evolution of the protosponges, and the bilaminar development of the Hintespongiidae Rigby and Gutschick, 1976 is convergent with pre-existing thick-walled taxa. This scenario is weakly supported by preliminary cladistic analyses (section 4.5)

Superfamily MALUMISPONGIODEA Rigby, 1967

Family MALUMISPONGIIDAE? Rigby, 1967

*Remarks.* The superfamily was erected in order to contain a single Silurian species (*Malumnispongium hartnageli*) of thick-walled hexactinellid without specialised dermalia, layering, synapticulae or derived spicule morphotypes, and without fusion of the skeleton. These forms were not previously contained within either of the superfamilies used by Finks (1960) to subdivide the Lyssakida. They appear to be derived from the thick-walled *Hintzespongia* (Rigby and Gutschick 1976) lineage, through loss of the quadruled exterior lamina. Rigby (1967) considered the group more primitive than either the Brachiospongioidea or Euplectelloidea, a view supported by the extension of their range into the Ordovician.

The only significant differences separating the present species from the familial diagnosis are the small size of the parietal gaps and the relatively thicker walls. The small gap diameter may be due to the minute spicule size, although wall thickness may be significant. Until further examples of both groups are known, the erection of a new family appears unwarranted.

## Genus SPISSIPARIES

*Etymology*. From Latin *spissus*, thick and *paries*, wall; alluding to the nature of the body wall. Gender *m*.

*Type species*. *Hyalostelia minuta* Pulfrey, 1933.

*Other species*. *Hyalostelia delicata* Pulfrey, 1933.

*Diagnosis*. Thick-walled, elongate globular hexactinellids with small cloaca, comprising simple hexactines and monaxons only; internal structure of subglobose and irregular tubular canals. Monaxial root spicules may be uncinate.

*Discussion*. The only described genus sharing the lyssakid skeleton without specialised dermalia, layering or derived body spicules is *Malumispongia*. The most significant difference from this genus is the much greater wall thickness, since small spicule size may account for the relatively smaller canals in *Spissiparies*. This is considered sufficient to distinguish the genera. *Hyalostelia delicata* (Pulfrey) is also tentatively assigned to the new genus, since the original description showed little difference in spicule morphology. Articulated material is required for confirmation.

### *Spissiparies minuta* (Pulfrey)

Pl. 7, Figs. 3–5

1933 *Pyritonema minuta* Pulfrey, p. 259-261, pl. II.
1940 *Pyritonema minuta*; (Pulfrey) Lewis; p. 1-39, pls. I-IV.

*Material*. Single articulated specimen (BU 2738) preserved as external mould with adhering spicules; from Lower Llanvirn (uppermost *artus or D. murchisoni* Biozone) volcanogenic sandstones of the southwest ridge of Llandegley Rocks, Powys, Wales.

*Description*. Globose sponge, of diameter 35 mm and height 60 mm, with spheroidal cloaca, 18 mm diameter, off-centre on upper surface. Walls are covered with very small hexactines, of maximimum ray length 0.5 mm; maximum ray diameter is 0.1

mm. Most spicules are much smaller, approaching the limit of resolution for binocular microscopy. Rays usually taper constantly. No derived morphologies observed; all rays appear to be of equal length, straight, and unspined. The only other observed spicules are a single biaxon triact, and monaxons, rare outside of the root tuft region.

Although there is no regular skeleton, hexactines are occasionally joined at one point. Where pervasively silicified, rays often overlap to form walls of channels or spheroidal voids within the structure, of diameter less than 1 mm. There is no obvious distribution of spicule sizes within the sponge, and no indication of internal spicular density.

Root tuft spicules are visible in the lower lateral region, rather than opposite the cloaca, but are probably incomplete. Spicules comprise monoxons only, diameter 0.1 to 0.2 mm, and length at least 5 mm. Most are smooth, although at least one is uncinate; the projections may be flanged, but preservation is too poor for certainty. Monaxons are aligned, passing through the body wall, and separated by up to 1 mm within the body; separation outside of body is not known. The root tuft appears to be much less substantial than in *Hyalostelia.*

*Remarks. S. minuta* was described by Pulfrey (1933) based on isolated hexactine spicules, associated with more slender forms which he named *Pyritonema delicata.* The consistency of the hexactine morphology described here supports the morphological distinction of Pulfrey (1933), and provides additional information on the previously unknown overall morphology. However, Pulfrey noted that one ray was often extended, and occasionally knobbed or spined, none of which have been observed here. Since the type material comprises isolated spicules, seen in thin section, the attribution of these rarer forms to the species may be suspicious. This

problem serves to highlight the problems of species descriptions based purely on spicule assemblages.

Another Ordovician occurrence of *S. minuta* was described by Lewis (1940), in somewhat more detail. The spicule assemblage almost exactly matches that seen in the articulated specimen here, while the hexactine microscleres he described are shown to be part of a gradational size sequence. The attribution of a single isolated amphidisc fragment (now destroyed) to this species was speculative at best. Although Lewis (1940) did not record smooth monaxons as belonging to *H. minuta*, a large number of such associated spicules were indiscriminately assigned to an array of demosponge genera.

Superfamily UNCERTAIN

Family PYRITONEMIDAE nov.

*Diagnosis*. Monaxonid hexactinellids with hexactine spicules and their derivatives very rare or absent. Monaxons highly elongate, up to many cm in length, and up to 1 mm, rarely 1.5 mm in width. Spicules slightly divergent, becoming more so distally; spatial density of spicules generally increasing towards centre. No regularity or specialisation of spicules. May or may not incorporate clastic and bioclastic material.

*Included genera*. *Pyritonema* M'Coy (1850).

*Discussion*. The consistent absence or rarity of hexactinellid spicules associated with forms similar to *Pyritonema* has raised comment from other authors. A similar occurrence of abundant "root tufts" was reported by Rigby and Ausich (1981), in beds containing only rare hexactinellid spicules. These sponges, from Lower Mississippian

strata, contain incorporated bioclastic material, although details of the bioclast arrangement was not given.

Carrera (1994) described very similar "root tuft" structures from the Ordovician of Argentina, but recorded only very rare hexactinellid spicules in the same beds. He suggested that these bodies might represent entire forms of monaxonid demosponges, allied to the Halichondritidae, but refrained from any formal treatment.

The Halichondritidae and Leptomitidae are elongate, thin-walled monaxonid demosponges from Cambrian and Ordovician strata in North America, characterised by tracts of extremely long monaxon (presumed oxeate) spicules. The Leptomitidae show regular organisation into vertical and transverse tracts, the transverse consisting of smaller spicules. Remains of *Halichondrites* are fragmentary, typically slightly disarticulated, and apparently structureless. This is particularly true of the type species *H. confusus* Dawson and Hinde, 1889, while *H. elissa*, from the Burgess Shale (Walcott 1920) appears to show very fine rectangular meshwork. It thus appears that some form of fine reticulation characterises both *Halichondrites* and *Leptomitus*, although the two forms are clearly distinct (Rigby 1983).

The higher level taxonomy of these genera is uncertain; de Laubenfels (1955) placed them in the Lyssakida, allied to the Protospongiidae, despite the absence of hexactinellid spicules, and based largely on structural considerations. However, he admitted, "this assemblage could be classified among the haplosclerine demosponges" (de Laubenfels 1955, p. 98), a view maintained by Rigby (1983) and Walcott (1920). *Pyritonema* species show no trace of reticulation and, rather than being thin-walled, increase in spicular density towards the axis.

Other demosponges containing large monaxons are *Choia* Walcott, *Wapkia* Walcott, *Hamptonia* Walcott and *Pirania* Walcott, all from the Burgess Shale, but

although *Choia* and *Pirania* show little regularity in spicule arrangement, all are very different from *Pyritonema.* The Hadromerida comprise a radial spicule array, although only the Tethyidae do not employ tylostyles (Bergquist 1978). In this case, the spicules are much smaller than in *Pyritonema*, and the array morphology approaches hemispherical.

The spicular morphology and size range is similar to a few undoubted hexactinellid root tufts, such as that of *Hyalostelia*, and the sub-parallel, disorganised arrangement suggests derivation from this group. Certain characters of the specimens described below indicate an epifaunal habit, specifically the axis-parallel incorporation of crinoid pleuricolumnals, and the absence of bedding-oblique or vertical specimens, in beds showing evidence of rapid burial. Critically, a tubular spongin skeleton is preserved in one specimen, discounting a root tuft affiliation. There is little doubt, from the spicule assemblages, that hexactinellid spicules were absent from the sponge body.

There is a clear distinction in morphology between the forms described here, and most other Ordovician lyssakid root tufts, as exemplified by Rigby and Harris (1979). Certain Lower Palaeozoic lyssakid (and dictyospongiid) root tufts tend to comprise a dense rope of relatively few, highly elongate spicules, with spicule diameter not exceeding 0.15 mm. The pyritonemid spicules average 0.3 to 0.5 mm in diameter, are much more abundant, and the overall morphology is much less slender. Later clades developed much more massive, superficially similar forms to the pyritonemids, although most developments of extremely large spicules seem to have retained a thin, ropy structure (e.g. *Hyalonema* Gray). The only Lower Palaeozoic species known to possess large, stout root tufts of elongate monaxons with width over 0.5 mm, are *Hyalostelia smithii* and related forms. Even there, the root is a solid rope,

as seen in the core of *P. fasciculus*, rather than a diffuse divergent mass. Compare also the root tufts described below.

The most reasonable classification of these sponges is as a family, the Pyritonemidae, within the lyssakid hexactinellids, allied to the Stiodermatidae, and derived via enlargement of the root tuft to the exclusion of other spicules.

## Genus PYRITONEMA M'Coy, 1850

1884 *Hyalostelia* Hinde

*Type species*. *Pyritonema fasciculus* M'Coy, 1850 by monotypy, from the Llandeilo of Tre Gil, Llandeilo, Powys.

*Other species*. *P. scopula* sp. nov.

*Diagnosis* (revised after Hinde 1888). Ropes or divergent splays of elongate, large monaxons in subparallel orientation; no reticulation or complex organisation. Only monaxons present, without triaenes or other anchor spicules; diameter ranges up to 0.5 mm, with the majority between 0.2 and 0.4 mm; maximum length may be many centimetres.

*Discussion*. The taxonomic histories of *Pyritonema* M'Coy (1850) and *Hyalostelia* Zittel (1878), are very confused. The earliest described specimens of this group of sponges are those of M'Coy (1844), who recorded *Serpula parallela* from the Carboniferous of Ireland. Hexactinellid spicules were associated, although not necessarily conspecific. The Ordovician of South Wales (M'Coy 1850) yielded *Pyritonema fasciculus*, a monaxonid body that he described as the root tuft of a lyssakid hexactinellid. Specific diagnosis depended on the presence of minute transverse frills or striae. These frills are not clearly present in the holotype, and it is possible that those he described may be artefacts resulting from partial mineralogical

replacement. However, the feature is apparently consistent, and is retained as a diagnostic feature for this reason. Roemer (1861) described *Acestra subulare*, based on smooth monaxons, rhabdose clinopentactines, and hexactines. Later, Suess (1866) re-evaluated *Serpula parallela* as *Hyalonema parallela*, a member of a living genus.

Young and Young (1876) discovered abundant hexactine spicules in the Carboniferous of Ayrshire, described as *Acanthaspongia smithii*. These were associated with abundant *Hyalonema parallela*, which they suspected to be part of the same organism, but without direct evidence. Further specimens were discovered, including modified and regular hexactines (Young and Young 1877), leading to *A. smithii* being removed to the extant genus *Hyalonema* Gray. A root tuft was also recorded, and *Hyalonema parallela* (M'Coy) was assigned to the species. The ambiguous description of stellate spicules led to misunderstandings among later authors, culminating in their erroneous inclusion being used as a basis for a position in the Heteractinida (de Laubenfels 1955). It soon became clear that these forms could not be placed within the living genus *Hyalonema*, resulting in the erection of the genus *Hyalostelia* Zittel (1878) to accommodate *H. smithii* (Young and Young).

The monograph by Hinde (1887-1888) was the first real attempt to synthesize the data on British Palaeozoic sponges. He confirmed the use of *Hyalostelia*, and the type species *H. smithii*, but maintained the distinction of *H. parallela*. Based on more complete material, the problematic stellate spicules found with *H. smithii* were removed to the genus *Holasterella* Carter. Monaxonid root tufts were noted, sometimes in beds devoid of hexactinellid spicules. This distribution was attributed to preservational effects. The internal structure of root tuft spicules of *Hyalostelia* was shown to resemble closely that of the modern *Hyalonema mirabile* Gray, although

Sollas (1877) had already demonstrated that the internal structure of spicules varied little even between classes.

In redescribing *Pyritonema fasciculus* M'Coy, Hinde (1888) reassigned it to the genus *Hyalostelia*, based on morphological similarity. The prominence of frills was shown to be very variable, between spicules and between individuals. No hexactinellid spicules were (or are) known to be associated with the Ordovician forms. Hinde (1888) also described a new species, *H. gracilis*, from the Wenlock of Craven Arms, based on isolated hexactinellid spicules, often with one ray modified or absent, and fragments of radially spinose monaxons from the same bed.

In addressing the suspect generic assignation of *H. fasciculus*, Rauff (1893) proposed that both *Hyalostelia* and *Pyritonema* be retained, for earlier and later Palaeozoic forms respectively. Rauff (1893) also referred hexactinellid spicules *to P. fasciculus*, although this was later debated (Lewis 1940). Rauff (1893) also described *P. metissica* Dawson (Dawson and Hinde 1889) as *Hyalostelia*, but now considered to be a *Hyalonema*-like lyssakid, with diverse spiculation), "*P. gracile*" Hinde, and *P. crassicauda* Rauff, and reassigned *P. subulare* (Roemer).

The use of *Pyritonema* was continued by Ruedemann (1925), with the inclusion of regular and modified hexacts, in addition to root tufts containing smooth, rugose or acanthose monaxons. This was further extended by Pulfrey (1933), who erected *P. minuta* and *P. delicata*, both on disarticulated assemblages of hexactines. Size distinctions were applied to separate these from known species. These species were reported also by Lewis (1940) from the Caradoc of North Wales, in addition to *P. fasciculus* and *P. subulare.*

De Laubenfels (1955) assigned *Hyalostelia* to the Astraeospongia (Heteractinida), on the mistaken inclusion of stellate spicules, while *Pyritonema* was

given no taxonomic status, but considered a form genus within the Lyssakida. *Hyalostelia* was later reassigned to the Hexactinellida by Reid (1958a), and part of the taxonomic history was discussed. *Hyalostelia* was again partly reviewed by Butler (1961), who erected *H. clinopentactinoides* on a dominantly clinopentactine spicule assemblage from the Ordovician of Pennsylvania. No monaxonid spicules were observed.

Finks (1960) described late Palaeozoic faunas of Texas, and recorded the new genus *Stioderma*, which he considered a possible junior synonym of *Hyalostelia*. Reid (1968) discovered further articulated material of *H. smithii*, and provided a strict diagnosis, based on modified hexactines and dermal structure. A close affinity with *Stioderma* Finks (1960) was confirmed, although synonymy refuted. Finks (1960) mentioned *Pyritonema* and *Acestra* as *Hyalostelia* root tufts, and therefore unrecognisable, and recommended that they be discarded.

*Pyritonema scopula* sp. nov.

Pl. 8, Figs. 1–4; Pl. 9, Figs. 1-5, text-fig. 4.4.7.

*Etymology*. Latin for a small brush, reflecting the overall morphology.

*Holotype*. BU 2730; complete, uncompressed external mould with internal spicular lining; from Lower Llanvirn (uppermost *artus* or *D. murchisoni* Biozone) volcanogenic sandstones of Llandegley Rocks, Powys, Wales.

*Paratypes*. Three flattened, partial to almost complete spicule masses (BU 2731, 2732, 2733); one external mould, badly weathered, apparently showing branching (BU 2734); one partial, uncompressed, silicified individual preserving proteinaceous skeleton in addition to spicular (BU 2735); locality as above. One slightly compressed, complete specimen from Upper Llanvirn sandstones, Howey Brook Main

Feeder, Llandrindod, Powys (NMW 87519.1). Three-dimensional fragments preserved in siliceous nodule, from minor summit above Graig Farm, Llandegley Rocks (same horizon as type locality) (BU 2736).

*Other Material.* Numerous partial specimens from the type locality, both compressed and uncompressed, some silicified; three further partial specimens from Howey Brook Main Feeder (NMW 87519.2); numerous disarticulated and partially articulated specimens from calcareous nodules above Graig Farm, western scarp of Llandegley Rocks, Powys (same horizon as type locality); BGS.GSM 10434-8, from the Carneddau, Builth.

*Diagnosis*. Clavate mass of slightly divergent, smooth monaxons, typically 0.25 to 0.35 mm in diameter; walls thick, without obvious cloaca; axial region contains highest spicule density, but without a distinct rope. Canal system extensive, defined by spongin walls supported between spicules; canals rounded to polygonal in transverse section.

*Distribution. P. scopula* is known from five sites, in sandstones of the uppermost *D. artus* or *D. murchisoni* Biozone and lower *D. murchisoni* Biozone of the Builth – Llandrindod Inlier, Powys.

*Description.* Elongate, club-shaped sponge up to 150 mm in length, and 50 mm in maximum width. Expands evenly from a narrow base (less than 10 mm wide) to maximum width just below apex, which is rounded. Many flattened fossils appear broadest centrally, probably due to higher spicule density in the central region. Body primarily comprises smooth, elongate monaxons, presumed oxeas; no other morphotypes are present. The monaxons diverge from the central axis so that

terminations extended a short distance beyond the body wall. Curvature of spicules is slight, but significant over their entire length; the divergent angle increases from near zero on axis, up to 30° at the margin. The spicules are usually fractured during diagenesis, preventing accurate length measurements, but some are continuous over several centimetres. Spicule diameter varies up to 0.5 mm, exceptionally more, and has mode 0.25 – 0.35 mm. Clastic particles are sometimes incorporated to a small degree, as seen in the holotype, whose uncompressed nature mitigates against a biostratinomic origin of these grains.

In many cases, the internal structure and mineralogy of the spicules are seen in thin section, and accord well with that described by Sollas (1877). A distinct outer lamina of thickness 0.05 – 0.10 mm surrounds a less stable core of homogeneous, cryptocrystalline silica. Many spicules show a recrystallised core of chalcedonic silica, as was described for well-preserved specimens; however, the internal structure of sponge spicules appears to be of little diagnostic value (Sollas 1877). The axial canal is usually preserved, and often enlarged by dissolution. In extensively dissolved material, only the outer lamina remains. In uncompressed specimens, the entire interior of the sponge may be absent due to dissolution; migration of these fluids may have allowed silicification of the sponge margin. Compressed specimens appear to be more complete, although individual spicules may show severe internal dissolution.

The proteinaceous skeletal structure is preserved in paratype BU 2735. Spaces between spicules contain tubular (subcircular to polygonal) canals whose boundaries are defined by inter-spicule menisci. Canals have diameter 0.8 – 1.2 mm, with wall thicknesses of around 0.1 mm, greater where attached to spicules. Canal orientation is variable, with a slight axis-parallel emphasis. The axial region of the specimen is dissolved. Given the high axial spicule density, and the lack of a central cloaca or

osculum, it is likely that several small osculae are associated with partially or completely isolated regions of the canal system.

Axis-parallel incorporation of crinoid pleuricolumnals evidences the use of living crinoids for support or nucleation. Despite excellent preservation of articulated crinoids at the type locality, none are preserved vertically oriented; the axis-parallel nature requires that the crinoids were erect at the time of incorporation. This also proves that *P. scopula* grew epifaunally.

*Remarks*. *P. scopula* is distinguished from *P. fasciculus* by the lack of spicular ornament, the incorporation of clastic particles, and the laterally gradual spicule density gradient. *P. fasciculus* possessed a dense ropy core, surrounded by a more

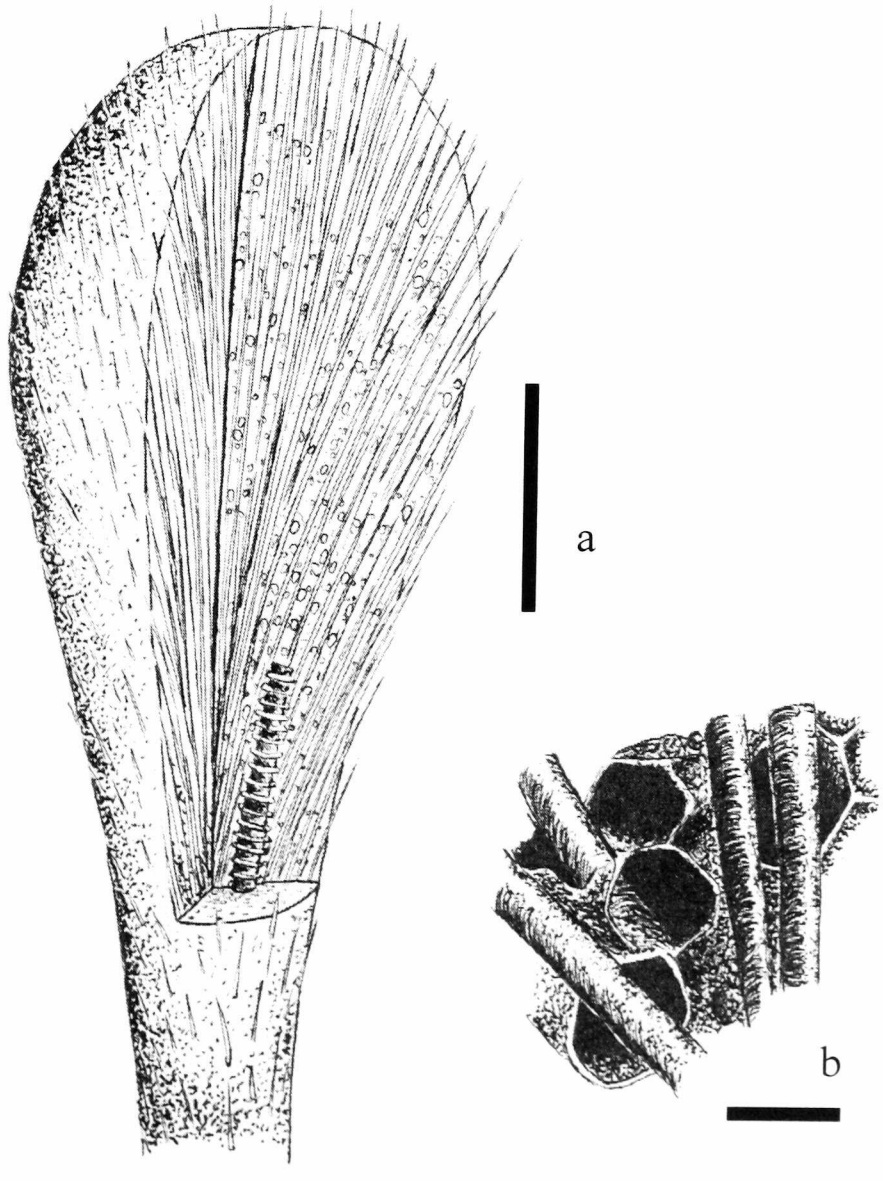


Figure 4.4.7: *Reconstruction of* Pyritonema scopula *sp. nov. a, overall view (base not clear), including axial crinoid pleuricolumnal, scale bar 2 cm; b, detail of spongin skeleton and spicule arrangement, scale bar 1 mm.*

diffuse distal splay, and also had a higher maximum spicule diameter, of 0.7 mm opposed to 0.5 mm.

Family uncertain

Genus BREVICIRRUS gen. nov.

*Etymology*. Latin *brevis*, short and *cirrus*, tuft, describing the root tuft. Gender *m*.

*Type species*. *B. arenaceus* sp. nov., from the uppermost *artus* or *D. murchisoni* Biozone of Llandegley Rocks, Llandrindod, Powys.

*Diagnosis*. Globular, thick-walled lyssakids containing large, smooth hexactines, clinopentactines and possibly stauracts, all unornamented; no differentiated layering or distinct prostalia; skeleton incorporates large quantities of clastic and bioclastic material, with clasts exceeding 1 cm; root tuft short, dense, comprising simple, fine monaxons.

*Discussion*. *Brevicirrus* shares several fundamental characters with the Malumispongiidae Rigby (1967), but is clearly distinguished by the incorporation of clastic material. The collapsed nature of the holotype of the type species prevents description of canals, precise wall thickness or exact spicule distribution, so that a full discussion of affinities is prevented. However, spicules of various sizes appear to be distributed randomly, and there is certainly no distinct dermal layer; this is an unusual characteristic, presently restricted to the Malumispongiidae.

The lack of spicule differentiation is of uncertain significance. Primitive lyssakids such as the pelicaspongiid *Vaurealspongia minuta* and *Twenhofelella waldroni* (Rigby *et al.* 1979) contain a distinct dermal layer, at least, although the original exterior reticulation of *Hintzespongia bilamina* (Rigby and Gutschick 1976) and allies has been lost. In most cases, the dermal layer is distinguished through size,

comprising either larger or smaller spicules than the interior. Late Palaeozoic genera such as *Stioderma* Finks (1960) and *Hyalostelia smithii* Young and Young (Reid 1968) also contain distinct dermalia, typically of different morphology from the body spicules. So pervasive is the differentiated dermal layer, that the Malumispongioidea, erected to accommodate those sponges with homogeneous walls of dominantly simple hexactines, was based on one species (Rigby 1967).

Since the large-scale clastic incorporation appears to be unique among Ordovician hexactinellids, and the homogeneous structure appears to have evolved only among the Malumispongiidae, *Brevicirrus* is most parsimoniously considered as an offshoot of this family. Until further particle-containing specimens are discovered, the position of *Brevicirrus* remains uncertain.

*Brevicirrus arenaceus* sp. nov.

Pl. 10, Figs. 1–6

*Etymology*. From *arenaceus*, reflecting the clastic component incorporated into the skeleton.

*Holotype*. BU 2737; collapsed, but nearly complete specimen from the south-central plateau of Llandegley Rocks, Llandrindod, Powys; volcaniclastic shelly sandstones of the uppermost part of the *D. bifidus* Biozone.

*Diagnosis*. As for genus.

*Description*. Large lyssakid (diameter around 10 cm) of uncertain morphology, with thick orthohexactine-dominated walls. Spicules are very large, with ray lengths reaching 2 or 3 mm; this is comparable with those in *H. clinopentactinoides* Butler (1961). Clinopentactines are frequent, comprising an estimated 5 to 10 % of the total spicule numbers, with all rays of approximately equal length

The bulk of the sponge body is composed of randomly incorporated sand and bioclastic particles. Some of the bioclasts, including bryozoa, brachiopods and trilobite fragments, reach sizes approaching 10 mm. Occasional foreign spicules are also apparent, including small monaxial fragments with prominent transverse ribs, probably derived from *Pseudolancicula*. There is no obvious distribution of bioclasts, although they occur most frequently at the edges.

The root tuft is seen *in situ*, attached to the central part of the body mass. The structure is 35 mm long and approximately 15 mm wide, in a slightly flattened state. Although it may have been broken off at the length observed, there is no scattering of loose spicules, as would be expected in this case. The spicules are highly elongate fine monaxons, of thickness 0.1 – 0.2 mm. Note that this is substantially less than the thickness of the body spicules. Total lengths are difficult to establish due to breakage, but some are probably continuous over the entire length. Spicule terminations are only rarely seen to be oxeate, and there with little certainty due to their narrow width. The monaxons are very densely clustered, parallel, and with little or no marginal divergence; there is little or no incorporated clastic material.

## Order HETERACTINIDA de Laubenfels, 1955

## Family ASTRAEOSPONGIIDAE Miller, 1889

### Genus MICROASTRAEUM gen. nov.

*Etymology.* From Greek, emphasizing the minute size of spicules relative to other astraeospongiids.

*Diagnosis.* Saucer-shaped astraeospongiid with felted mass of heptactine and octactine spicules in several sizes. The basal ray diameter of the largest spicules does not greatly exceed 0.05 mm, with smaller spicules less than 0.01 mm in diameter; rays

very fine, with lengths occasionally in excess of 0.5 mm. Sponge surface is smooth but for exhalent canals, the apertures around 0.15 mm diameter, spaced 1 mm apart.

*Discussion.* The general nature and arrangement of spicules, and overall form of the sponge, indicate a clear relationship to the Silurian *Astraeospongium* of Britain and elsewhere. However, the present specimen differs significantly from the type genus in the presence of canals and heptactine spicules, and in the very small spicule size. The Upper Ordovician *Asteriaspongia anatrope* Rigby (1977b) shares the presence of canals and the fineness of the spicules, but is of much larger size. *Constellatospongia pervia* Rigby (1977a) also contains canals, but these connect additional, large parietal gaps. Spicules of *C. pervia*, although small and fine for an astraeospongiid, are still ten times the diameter of those seen here.

The Devonian *Stellarispongia aspera* Rigby (1975) contains octactines, heptactines and hexactines, of three size orders, but these are much larger than in *Microastraeum*, with stout rays. Canals are present, and the surface is irregularly ornamented.

*Microastraeum tenuis* sp. nov.

Pl. 7, Figs. 6, 7

*Etymology*. Latin, meaning fine, tenuous; refers to the nature of the spicule rays.

*Holotype*. BU 2742; specimen showing convex surface, damaged in places and showing interior. Only known specimen.

Diagnosis. As for genus.

Description. Single specimen, diameter 7.5 mm, showing a shallow domal surface, assumed to be the ventral. Outline subcircular, with elongation of one side. The surface is a mass of octactine and minor heptactine spicules, the smaller spicules often

disguised by secondary siliceous overgrowth. Rays diverge from a common centre, all but two in one plane. All observed orthogonal rays are reduced to nodes, or are entirely absent. Radial rays may be slightly curved distally, often expanding slightly in thickness a small distance from the centre. The maximum ray diameter is approximately 0.03 to 0.05 mm in the largest spicules; many spicules are less that 0.01 mm in ray diameter. Distinction of spicule size orders is not obvious except for the largest. First order spicules are uncommon, separated by mass of smaller forms. Ray length occasionally exceeds 0.5 mm, with the terminations not seen. Spicule inter-relations are irregular, without consistent junctions; longer curved rays interweave through the structure.

The surface is marked by small apertures, approximately 0.15 mm in diameter, arrayed over the observed surface. These are assumed to mark exhalent canals. The spacing is irregular in pattern, but with approximately one aperture for each 1.0 $mm^2$. There is no obvious development of secondary canals or surface sculpture.

*Remarks.* The distinction of *Microastraeum* from related genera was discussed above. The species seems to represent an intermediate form between *Astraeospongium*, which lacks canals, and *Stellarispongia*, which shows two canal orders. *Constellatospongia* contains large parietal gaps in addition to canals. The anomalously small spicule size of *M. tenuis* appears to be a derived trait, since those species that are both more derived and more primitive with respect to canal structure contain much larger spicules.

## 4.5 ROOT TUFTS

Since *Pyritonema* has been shown to represent an entire sponge, no certain dissociated root tufts have been recovered from the Llandegley Rocks site. Root tufts

occur rarely in the Builth Inlier, in sediments indicative of quieter, probably deep shelf conditions. The three specimens described below represent very distinct morphotypes, implying substantial sponge diversity in the region. Isolated spicules occur abundantly in some shale horizons, and include simple monaxon, stauractine and hexactine forms. The modified and elaborate morphologies seen in the Llandegley Rocks assemblage appear to be absent from deeper-water faunas.

Root tuft type 1

Pl. 11, Fig. 5

*Material*. SM A18450, from Penddol Rocks, River Wye near Builth Wells, Powys; *H. teretisuculus* Biozone, upper Darriwillian.

*Lithology*. Dark grey to black graptolitic mudstone; lamination poor or absent. Fauna comprises *H. teretiusculus*, *Nemagraptus*, and other graptolites, with locally abundant trilobites. Exact position in the sequence, and hence associated fauna, not known.

*Description*. Thin, slightly curved band, reaching approximately 2 mm wide and at least 30 mm long, comprising simple monaxons only. Length of individual spicules uncertain, but some probably extend over the entire length of the tuft. Dense texture, without twisting; spicules generally parallel, but slightly divergent at each end. The proximal divergence may be due to fraying of the broken termination, or have been characteristic of the sponge. The tuft is associated with several hexactinellid spicules, which may be stauractine or, possibly, hexactine. Visible rays thin, straight, and without further elaboration.

*Discussion*. The associated, isolated hexactinellid spicules indicate a lyssakid (*s.l.*) origin. The only sponges previously recorded from the Builth-Llandrindod region are

species of *Protospongia*, usually referred to *P. fenestrata* Salter. This species is based on skeletal net fragments of Middle Cambrian age, and a systematic revision of Welsh Ordovician protospongiids is required. No British *Protospongia* root tufts of this age have been described, although North American *Protospongia* from the Ordovician of Little Metis (Dawson and Hinde 1889) exhibit a simple tuft composed of a few greatly enlarged spicules. The form described above appears intermediate between the simple *Protospongia* type, and thick-walled hexactinellids such as *Hyalostelia*.

Root tuft type 2

Pl. 11, Fig. 4

*Material*. BU 2743; partial tuft from above ash bed BG3 (herein), Bach-Y-Graig SSSI, Llandrindod; *H. teretiusculus* Biozone, upper Dariwillian.

*Lithology*. Pale grey micaceous siltstone overlying ash bed. Associated fauna comprises *Schmidtites*? *micula*, *Palaeoglossa* and other inarticulates, occasional biserial graptolites, ostracodes, benthic trilobites and rare bryozoa; minute arthropod cuticle fragments are abundant. Hexactinellid and monaxon sponge spicules are locally abundant.

*Description*. Divergent splay of fine monaxons; observed width 2 mm and length 8 mm, but certainly incomplete. Symmetrical arrangement of spicules suggests that width is almost complete, although no indication of length can be obtained. Spicules straight, with divergence from centre approximately proportional to lateral position in tuft; this implies that the divergence is original, rather than reflecting disarticulation of a ropy texture. Spicules are very rarely in contact, indicating substantial spacing prior to compaction. Estimated number of spicules is 30-40 in the region seen.

*Discussion.* Although there is no direct association with spicules, small monaxial and hexactinellid spicules occur in the same beds. At least some of these are apparently hexactines. As discussed in root tuft type 1, the origin of this tuft is unlikely to be *Protospongia*, due to the complexity. The presence of hexactines also supports a primitive lyssakid identity, but no further refinement is possible at this stage.

Root tuft type 3

Pl. 11, Figs. 6, 7

*Material.* BU 2744; almost complete, but mouldic tuft from Gilwern Hill Quarry, southeast of Llandrindod; upper *artus* or *D. murchisoni* Biozone, lower Darriwillian.

*Lithology.* Fine, pale blue tuffitic siltstone, largely homogeneous, but with rare ash beds. Fauna dominated by *Ogyginus corndensis*, in all growth stages; also trinucleids, rare orthids, asteroids and sponge remains.

*Description.* Unique dimorphic tuft comprising a 5-6 mm - wide proximal region at least 51 mm long, tapering sharply distally to a fine curved thread, at least 108 mm long. The tapering occurs over 10 mm, with the distal thread originating within the last 5 mm of the taper. The proximal region shows faint indications of spiral structure, but is otherwise featureless. There are no body spicules in this region, which may have been at least partly keratinous. The distal part comprises an apparently spiral thread (wavelength approximately 40 – 50 mm) of a few monaxon spicules. Initial divergence from the proximal region is 23-25°. Thickness is almost constant over the entire length, between 1.0 and 1.5 mm, suggesting that the spicules were continuous for this distance. The radius of curvature of the thread is 25 – 35 mm.

Two associated hexactine spicules occur in the region between the proximal and distal ends of the tuft. These are simple, straight-rayed forms with ray length 2 mm and gradual taper from a basal ray diameter of approximately 0.15 mm.

*Discussion.* The dimorphic morphology has not been previously recorded from the Lower Palaeozoic, if at all. Many of the most primitive hexactinellids possessed fine root tufts of few spicules, albeit rarely of this length, but the proximal region is unique. The lack of preserved spiculation precludes a function analogous to the base of *Gabelia* (Rigby and Murphy 1983), which comprises an undifferentiated part of the body. In combination with the isolated simple hexactines, a moderately advanced lyssakid affinity is implied.

## 4.6 OTHER SPICULE MORPHOTYPES

A wide range of unassigned spicule morphotypes is present in the samples. Some of these are attributable to major groups, but others remain obscure. The level of disparity of the spicules is generally lower than in other described Lower Palaeozoic assemblages (e.g. Bengtson 1986; Webby and Trotter 1993; Zhang and Pratt 1994; Dong and Knoll 1996), although the diversity is substantial. Zhang and Pratt (2000) described a Middle Ordovician assemblage from Newfoundland containing a comparable range of morphotypes with those presented here. The Wenlock assemblage described by Watkins and Coorough (1997) is of generally similar character.

### Monaxial spicules

Pl. 13. Figs. 1-3

A small number of miniature smooth oxeas (BU 2748) have been recovered. Most have one straight side, with the other curved only to accommodate the central expansion; a few show a slight absolute curvature. Rare microstyles (BU 2750) of a similar length, but greater thickness, are also associated. Tylotes or tylostyles are encountered more frequently, in fragmentary condition. No complete tyloid spicules have been recovered, so the two cases cannot be distinguished. Tylotes were recovered as a rare component of the North Wales faunas recorded by Pulfrey (1933) and Lewis (1940), and were there assigned to *Pyritonema minuta*. They have not been discovered *in situ* in any of the forms described above, although their possible occurrence as minor components cannot be excluded.

Acanthoxeas or acanthostyles are represented by a small number of specimens, fusiform spicules by one specimen, and fragments of harpoon-like spicules with toothed terminations by two specimens. Spiractine-type monaxons with pronounced transverse or spiral ribbing are relatively common, with around 20 fragments recovered. Some or all of these may be abraded specimens of *Pseudolancicula*, where the verticillate spines have been removed, or even proximal fragments of the flat morphotype, where these spines are less pronounced.

### Tetractine spicules

Pl. 13, Fig. 12

Tetractinal spicules, synapomorphic of the demosponges, are inexplicably rare; only two morphologies have been observed. The first, represented by one specimen, is a smooth, probably abraded calthrops with blunt, but incomplete rays. The second morphotype, found in small numbers within acid dissolution of bulk samples, although not in *Ordinisabulo* infills, comprises tetrahedral pyramidal forms

(BU 2745). A slight hollowing of the flat sides is caused by the extension of the ray terminations. Inter-ray angles are approximately 120° in plan view, although some are asymmetric to the extent of reducing one angle to around 60 - 70°. The complete terminations are never preserved, suggesting that the thickened spicules may form part of a massive, lithistid-like framework, although no specimens are seen connected to any others. Spicules with very similar triangular cross-sections of the rays are found in the lyschniscid hexactinellid *Cypellia*. A strong tendency towards this condition is also seen in some of the tetracladine lithistids of the Family Hallirhoidae, such as *Callopegma* Zittel, where the spicules are dichotriacts (de Laubenfels 1955). The symmetry of this group of sponges is more consistent with that observed, and these provide a more likely origin, though the Hallirhoidae are presently recognised only from the Jurassic to the Tertiary.

Hexactinellid spicules

Pl. 13, Figs. 5–10

Triactinal spicules are abundant in the residues, most apparently referable to *Triactinella*. Others incorporate asymmetry which makes this attribution questionable (BU 2759) or highly unlikely (BU 2758). A stauract with a minute orthogonal ray (BU 2751) is also possibly referable to this genus, but doubtful.

A variety of derived hexactinellid spicules appears to be recorded here for the first time. These include a bulbous octactine with a recurved dichotomy of one ray (BU 2754), and an angular, irregular pentactine with one dichotomous ray. All of these may be considered aberrant spicules from generally conservative hexactinellids, until further examples of such forms are located. An acanthohexact was recorded and photographed, but has since been destroyed.

Anchorate spicules occur rarely, usually as triaene fragments. Simple uncinates, indistinguishable from those seen in both *Polydactyloides trescelestus* and *Hyalostelia minuta*, are sometimes abundant, although the exact proportion attributable to hexactinellids is uncertain (see below).

*The nature of spicule assemblages*

Because of the problems relating to disarticulation of uncemented sponge skeletons, some species and even genera have been erected on the basis of spicule associations. These may be collections dissolved from bulk samples, showing only a small variety of spicules, or more or less *in situ* concentrations belonging to the localised decay of individual sponges. Estimating diversity from whole-bed samples is highly unreliable; the misidentification of *Hyalostelia* as a heteractinid (de Laubenfels 1955), and the uncertain spicule composition of *H. minuta* (Pulfrey 1933; Lewis 1940) are illustrative.

Small concentrations of spicules might be considered more reliable, but this is not the case. By extending the range of the dysideid demosponges at least into the Middle Ordovician, a potential source of concentration must be considered. Even in what are clearly the remains of individual sponges, such as *Ordinisabulo quadragintaformis* gen. et sp. nov., the spicules from many different species may be preferentially absorbed. In this case, conodonts and pumice shards were incorporated in addition to sediment and spicules. Ordovician hexactinellids are also shown to have been capable of clastic incorporation (*Brevicirrus arenaceus* gen. et sp. nov.). Identification of an incorporative habit may be performed by observation of the spicules. Although breakage must be expected in all cases, foreign spicules within a

clustered assemblage will show evidence of abrasion. In all but the worst material, this should be obvious as rounding of broken edges or processes under SEM.

If the quantity of material is sufficient, it may be possible to determine spicule associations with some degree of certainty by comparing the presence and relative abundance of different morphotypes between several associations. The process is illustrated here by comparison of the spicules obtained from two specimens of *O. quadragintaformis* with those from a third, indeterminate sponge body, and acetic acid digestion of calcitic beds from the same sequence (Table 4.1). Three samples from one specimen of *Ordinisabulo* have been evaluated in order to estimate consistency, and hence reliability of the analysis.

*The non-fractal nature of correlation coefficients*

The use of regression correlation coefficients on total spicule counts must be applied with caution. Any exhaustive collection is likely to follow an approximate hollow curve distribution, with a relatively high diversity of rare morphotypes. In well-mixed beds, the most abundant morphotypes are likely to be prevalent in all samples, in variable proportions according to local population distributions. The degree of variability is dependent on local population patterns, hydraulic and bioerosive regimes, and sedimentary deposition rate. Morphotype proportions may be slightly modified by the action of sponges that preferentially incorporate certain size fractions. In contrast, multiple samples derived from the autochthonous spicule content of individual sponges should show very high correlation coefficients.

Homogenised beds and spicule concentrations containing diverse morphotype assemblages, of approximate hollow curve form, will show anomalously high values for the correlation coefficient, r. This becomes more pronounced as the sample size

increases, since rare morphotypes become more numerous, and thereby elongate the graphical cluster. The critical values for statistical significance also decrease with higher degrees of freedom. (Such samples are best compared using a rank correlation coefficient, although these will tend to underestimate correlation if large numbers of rare morphotypes occur. This is due to inconsistent relative frequencies of rare morphotypes in any sample sizes.)

Correlation coefficients derived from small groups of related morphotypes will show negligible bias, particularly if the group selected comprises relatively frequent forms. These groupings may then be analysed in order to distinguish consistent spicule proportions that reflect natural associations. If several samples show high correlation with each other, this association may be deemed characteristic of a given

| | **15.1.1** | **15.1.2** | **15.1.3** | **2.14** | **17.8** | **bulk** |
|---|---|---|---|---|---|---|
| **15.1.1** | 1 | | | | | |
| **15.1.2** | **0.96** | 1 | | | | |
| **15.13** | **0.94** | **0.91** | 1 | | | |
| **2.14** | -0.22 | -0.23 | -0.11 | 1 | | |
| **17.8** | **0.38** | **0.43** | **0.43** | -0.08 | 1 | |
| **bulk** | -0.15 | -0.20 | -0.21 | -0.47 | 0.29 | 1 |

df=9; critical two-tail and one-tail probabilities:
P=0.10: 0.521 P=0.10: 0.261
P=0.05: 0.602 P=0.05: 0.301
P=0.02: 0.685 P=0.02: 0.343
P=0.01: 0.735 P=0.01: 0.368

**X:** significant at 0.01, two-tailed

**X**: significant at 0.01, one-tailed.

Table 4.1: *Regression correlation coefficients for polydsactyoid spicules from six samples, with critical significance values.*

species. Inconsistent correlation between any two samples indicates the presence of a second species containing a separate spicule composition. It is difficult or impossible

confidently to distinguish how many additional species co-exist without the use of Fourier analysis.

This procedure is well illustrated by comparing morphotype abundance data for the two species of *Polydactyloides*. Distinction of spicule morphotypes is based on the type and number of prongs on the verticillate frills. Three samples were taken from the interior of the paratype (BU 2711 = 15.1) of *Ordinisabulo quadragintaformis*, a further sample from the holotype (BU 2710 = 2.14), one from an indeterminate sponge body (17.8), and one from bulk dissolution of calcitic beds at the same locality. These data are summarised in Table 4.1.

Several points should be noted. Firstly, the extremely high correlation between the three samples from specimen 15.1 (reference to Appendix A). This gives an indication of the low level of variability through sample randomness, which would be expected for a homogeneous assemblage. The much lower values between the other samples indicate substantial variability between the source material from different beds, and thereby imply the existence of more than one species.

Of particular significance are the moderate negative correlations between 15.1, 2.14 and the bulk dissolution samples. Such a distribution suggests partially- or non-overlapping spicular compositions. Perfect negative correlation could only occur through exactly half-overlapping distributions, with vertical and horizontal symmetry. This is unlikely to be created with more than two species present, although a weaker correlation could arise from an additional species with low spicule diversity or abundance.

*Use of Histograms*

The comparison of histogram data for the samples under analysis may allow further fidelity to be established under certain circumstances. This is only possible, however, where a natural morphological sequence can be utilised. Such a linear sequence may be of the form of increases in a certain characteristic, such as prongs on uncinates, extent of ornamentation or degree of ray reduction. Discrete or gradational properties may be used. A non-linear sequence is unlikely to allow the recognition of modal population structures.

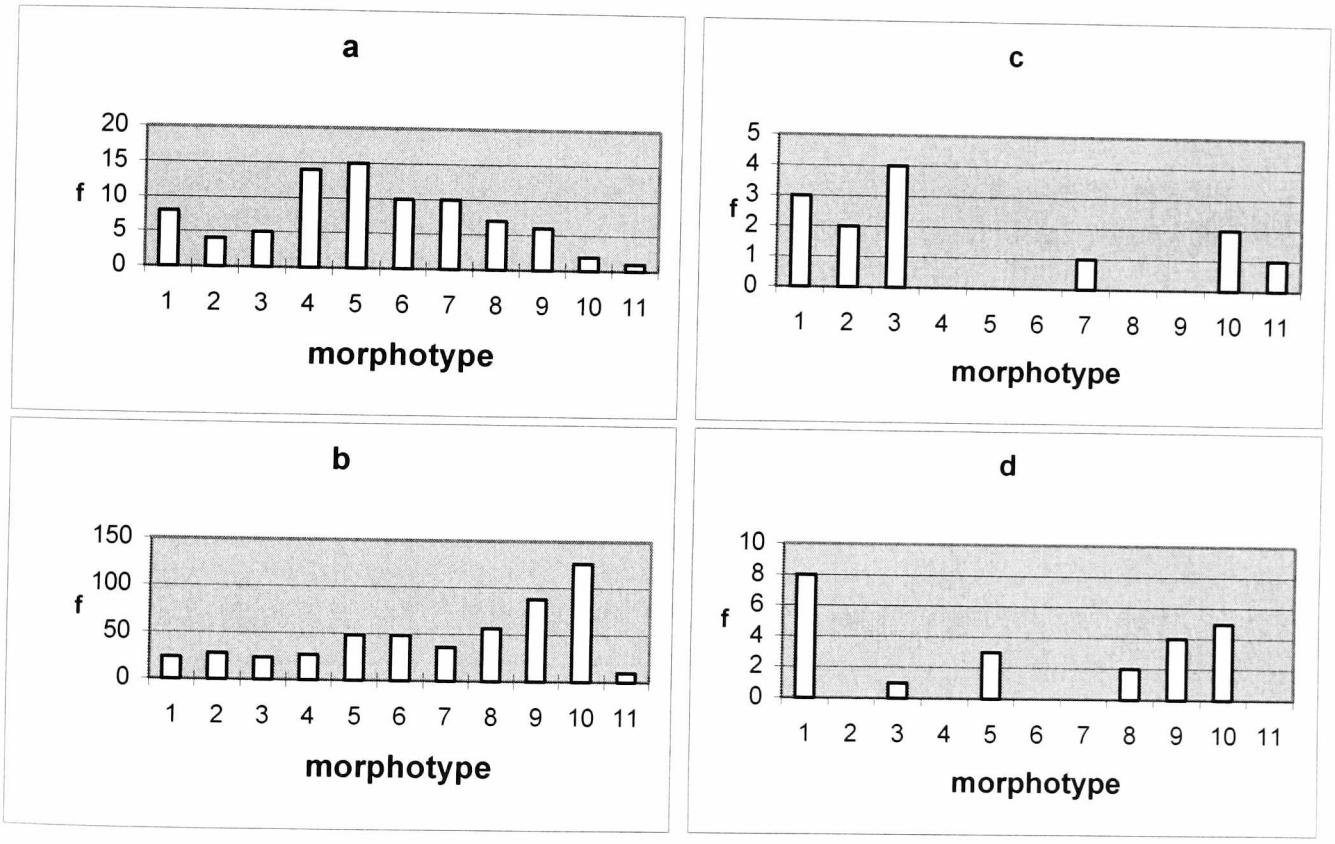


Figure 4.6.1: *Uncinate abundance histograms, based on: a, bulk samples; b, 15.1; c, 2.14; d, 17.8. Morphotype 1: simple uncinates; 2-6: up to 3 hooks per frill; 7-10: numerous hooks, incomplete frill; 11: frill encircles axis.*

The application of these principles to the polydactyloid data is illustrated in Fig. 4.6.1. The plots clearly show the bimodal distribution apparent in most samples. A small peak consistently occurs at morphotypes 4 to 6, followed by increasing levels until morphotype 10. Morphotype 11 is absent from one sample (2.14), but becomes

quite abundant relative to 10 and 11 in others, suggesting that the donor of these spicules was not a major contributor to the other morphotypes. This form shows complete verticillate frills, as found in the genus *Pseudolancicula*. Type 1, however, is always present, but varies greatly in importance. This suggests that 1 occurs in both the secondary polydactyloid and an additional species, or group of species. This is the simple uncinate form, which is also known to exist in *Hyalostelia minuta*.

The abundances recorded for samples 2.14 and 17.8 are uncomfortably small, but the purpose of this analysis is to illustrate the method, rather than to revise the taxonomy.

*Relative Correlation Coefficients for small sample sizes*

Inconsistencies arise from the use of small data sets. Analysis of the hexactinellid spicules from the samples employed above provides barely significant correlations even for the three samples of 15.1 (Table 4.2). Each of these has over 30 specimens recorded, but random variations are still too great for high correlation. However, the same observations may be drawn from relative correlations. If one species was represented, correlation should be approximately equal between all samples. The great diversity produced (including the extremely low 0.01 for 17.8: bulk) indicates at least two species, irrespective of the very low impact of pentactines, which may represent an additional species.

Further breakdown of the data is required where detail is obscured by multiple species. Articulated specimens show that *Triactinella rigbyi* contains both triactine and stauractine spicules, in the approximate ratio 85:15, and that *Hyalostelia* species may include abundant clinopentactines. An analysis of correlation within the triactines

| | 15.1.1 | 15.1.2 | 15.1.3 | acid | 17.8 | 2.14 |
|---|---|---|---|---|---|---|
| 7a | 12 | 22 | 11 | 1 | 4 | 7 |
| 7b | 14 | 16 | 4 | 2 | 0 | 0 |
| 7c-e | 0 | 3 | 4 | 2 | 1 | 1 |
| 8 | 18 | 8 | 9 | 2 | 2 | 0 |
| 9 | 0 | 1 | 0 | 0 | 0 | 0 |
| 10a | 0 | 1 | 0 | 0 | 0 | 0 |
| 10b | 15 | 10 | 12 | 11 | 1 | 8 |

| | **15.1.1** | **15.1.2** | **15.1.3** | **bulk** | 17.8 | 2.14 |
|---|---|---|---|---|---|---|
| **15.1.1** | 1 | | | | | |
| **15.1.2** | **0.69** | 1 | | | | |
| **15.1.3** | **0.80** | **0.67** | 1 | | | |
| **Bulk** | 0.48 | 0.16 | 0.65 | 1 | | |
| **17.8.** | 0.44 | **0.67** | 0.74 | 0.01 | 1 | |
| **2.14.** | 0.40 | 0.57 | **0.80** | **0.68** | 0.59 | 1 |

1-tailed critical values

df=7-2=5

0.10: P=0.669

0.05: P=0.754

0.02: P=0.833

0.01: P=0.874

Table 4.2: *Correlation of triactine (7), stauractine (8), pentactine (9) and hexactine (10) spicules.*

and stauracts only would show whether more than one species contributed to the stauract counts. Such a situation is indicated by the data from 15.1, where the 85:15 ratio is clearly not approached, but there is insufficient data from the other samples. The diversity of triactine spicules is also unclear, although a more detailed breakdown of morphotypes would require arbitrary distinction of angles and proportions. Similarly, further breakdown of the hexactines into fine and broad-rayed morphotypes may elucidate the hexactinal species composition.

*Conclusions*

The following general characters may be considered indicative of the species diversity within a group of related spicule morphotypes. It is assumed that the abundance of individual species varied between samples, since samples from the same bed may not show these characters if vertical homogenisation was very extensive.

1. Positive correlation coefficients that greatly exceed the critical values, with values approaching 0.90, imply the presence of one dominant species. Additional species with identical spicule compositions may also be present, but are indistinguishable without articulated material. Very rare sponges may also be present, yet contribute very little to the spicule data.
2. Critically positive correlations of lesser significance imply the presence of at least two species, of substantially differing abundance. Histograms may allow their separation, if a suitable sequence can be established which allows the recognition of bimodal abundance.
3. Weak positive or negative correlation implies more than one species; histograms may allow the recognition of two or even three species, but certainty is unlikely to be possible.
4. Moderate to strong negative correlation implies two primary species only, with symmetrical morphotype distributions. This case in unlikely to occur, but is diagnostic where present.
5. A single, variable morphotype indicates the presence of an additional species, although this will have little effect on the correlation coefficient. If this is absent in any sample (assuming sufficiently large sample sizes), it may indicate that the morphotype is produced only by the unknown donor. If always present, it may tentatively be assumed to comprise a part of one of the primary species, also.
6. Summary of spicule morphotype attribution and unrecognised species:

Table 4.3: *distribution of isolated spicule morphotypes among known fauna of Llandegley Rocks: 1,* Polydactyloides trescelestus*; 2,* P. entropus*; 3,* Pseudolancicula *cf.* exigua; 4, Palaeocallyoides improbabilis; 5, Microspongia? *sp.; 6,* Triactinella rigbyi*; 7,* Reticulicymbalum tres*; 8,* Brevicirrus arenaceus*; 9,* Pyritonema scopula*; 10,* Spissiparies minuta*; 11,* Microastraeum tenuis*; 12, additional, unrecognised taxa.*

| | 1 | 2 | 3 | 4 | 5 | 6 | 7 | 8 | 9 | 10 | 11 | 12 |
|---|---|---|---|---|---|---|---|---|---|---|---|---|
| Large monaxon | | | | X | | | | | X | | | |
| Small monaxons | X | X | | X | X | X | ? | X | X | X | | |
| Uncinate (single row) | X | | | | | | | | | X | | |
| Uncinate (two rows) | X | | | | | | | | | | | |
| Flanged monaxons | X | | | | | | | | | | | |
| Uncinates: bifid/ trifid hooks | X | X | | | | | | | | | | |
| Uncinates: four/five-pointed hooks | | X | X | | | | | | | | | |
| Uncinates: incomplete verticillate frills | | | X | | | | | | | | | |
| Uncinates: complete verticillate frills | | | | X | | | | | | | | |
| Acanthoxeas or acanthostyles | | | | | | | | | | | | X |
| Monaxon, longitudinal ridges | | | | | | | | | | | | X |
| Monaxial fragments, spiral ridge | | | | | | | | | | | | X |
| Triactine biaxon, subequal rays | | | | | | X | | | | | | |
| Triactine biaxon, one short ray | | | | | | X | | | | | | |
| Regular triactine | | | | | | X | | | | | | X? |
| Tuning-fork triactine | | | | | | | | | | | | X |
| Acanthotriactine | | | | | | | | | | | | X |
| Regular stauractine | | | | | | X | X | | | | | |
| Stauract; one short ray; tuberculate node | | | | | | | | | | | | X |
| Calthrops | | | | | | | | | | | | X |
| Pyramidal tetractine | | | | | | | | | | | | X |
| Clinopentactine | | | | | | | | X | | | | X? |
| Irregular pentactines | | | | | | | | | | | | X |
| Hexactine, 60°, 90° and 120° angles | | | | | | | | | | | | X |
| Regular hexactine | | | | | | | | X | X | X | | |
| Irregular modified hexacts | | | | | | | | | | | | X |

| | | | | | | | | | | | |
|---|---|---|---|---|---|---|---|---|---|---|---|
| Microxea | | X | | | | | | X | | | | X |
| Monaxon with toothed distal end | | | | | | | | | | | | X |
| Reniform | | | | | | | | | | | | X |
| Chelae | | | | | | | | | | | | X |
| Tylote/tylostyle | | | | | | | | | | | | X |
| Dichotriaene | | | | | | | | | | | | X |
| Fusiform | | | | | | | | | | | | X |

The total diversity of the Llandegley Rocks fauna is estimated at between 25 and 30 species (15 described), although many more aspicular forms may have been present.

## 4.7 Cladistic Analyses

### 4.7.1 Introduction

Phylogenetic relationships within Early Palaeozoic Porifera are still largely obscure. Although class-level taxonomy of modern groups is being elucidated by advances in molecular biology, this has limited application to fossils. Non-lithistid demosponges are by far the most abundant class in modern oceans, but their Early Palaeozoic record is limited to rare cases of Burgess Shale-type preservation (e.g. Rigby 1986; Chen *et al.* 1989). The evolutionary origins and development of the hexactinellids provide the main focus for discussion among sponge palaeobiologists, although even here the interpretations are controversial. Most groups known from the Cambro-Ordovician are extinct, and of uncertain relationship to modern taxa.

The use of cladistics in analysing poriferan relationships has been extremely restricted. Rosell and Uriz (1997) investigated the excavating Hadromerida, which include the Clionidae, while the position of Porifera within the Metazoa was discussed by Zrzavy *et al.* (1998), based on morphological and molecular data. Rigby (1986)

provided the first detailed phylogenetic hypotheses for the classes Demospongea, Hexactinellida and Calcarea, although on a non-cladistic basis. A similar scheme for the heteractinids was provided by Rigby and Nitecki (1975). The work of Zrzavy *et al.* (1998) supported an epitheliozoan sister group to the Calcarea, separated from the siliceous sponges, despite the apparent similarities of spicule production. Molecular data have been utilised in phylogenetic studies by, for example, Lafay *et al.* (1992) and Borchiellini *et al.* (2000).

Suspected convergence within the siliceous sponges is probably the main reason that cladistics have not been employed further by sponge biologists, and barely at all by sponge palaeobiologists. It is unclear whether stauracts or hexacts represent the primitive spicule morphology among hexactinellids (Mehl *et al.* 1993), with evidence for each scenario recorded in the literature. Ijima (1904) and Okada (1928) recognised only stauractine spicules in larval sponges, although Okada (1928) warned against any phylogenetic interpretations based on this observation. Since dermalia and gastralia are often reduced in ray number, relative to main body spicules (confirmed microscopically by Thomson 1868), it is possible that the stauract-dominated skeletons of the Protospongiidae were derived from the dermal layer of thick-walled hexactine-based ancestors. There is no doubt that in at least some cases, ray reduction from the hexactine condition has occurred. However, the general trend among body form revealed stratigraphically is of thickening walls and increased spicular complexity (but see Zhang and Pratt 1994 for complex Lower Cambrian morphotypes). Stauractines, and possibly hexactines, are present in the Precambrian (Brasier 1992), although the difficulty in recognising the vertical ray in compressed material means that many spicules identified as stauracts may in fact be hexactines.

However, at least some species of *Protospongia* were exclusively stauract-based (e.g. *P. hicksi* Hinde, 1888; see Rigby 1966).

A further convergent character is that of diagonal versus orthogonal reticulation among Early Palaeozoic taxa. The fragmentary nature of most skeletal remains prevents orientation identification in many species, with the orientation of *Protospongia* not certainly known; although Dawson and Hinde (1889) provided reconstructions of several taxa, the completeness of their specimens is unclear. Logical arguments prove that either convergence in mesh orientation, or in ray acquisition from stauract to hexact has occurred, since all combinations of characters are known.

This degree of convergence would be less significant among groups with a greater number of potential characters. However, sponge fossils almost invariably comprise spicule arrays only, often only partly articulated. Soft-tissue details are almost entirely absent, and can only rarely (unlike many groups) be inferred from skeletal elements. Overall morphology is plastic, and strongly dependent on environment; the same species may produce erect ramose or encrusting forms under different conditions (Bergquist 1978). Even more seriously, spicule morphology is partly dependent on ambient silica concentration (Maldonado *et al.* 1999), with the development of surface ornament extremely unpredictable. However, the number of rays does not appear to be affected by silica concentration, merely their development. This implies that the analysis of Rosell and Uriz (1997), based almost entirely on slight variations in spicule (monaxon) morphology, was unreliable. The analysis presented here is not intended to provide a definitive cladistic basis for future work, but to highlight the difficulties and potentials of the use of cladistics on Early Palaeozoic sponges. Specific problems are discussed below.

*List of characters.*

1. Authigenic spicules: 0 absent; 1 present
2. Spicules with at least seven rays: 0 absent; 1 present
3. Spicules with at least 6 orthogonal rays (simple): 0 absent; 1 present
4. Spicules with at least 6 orthogonal rays (complex): 0 absent; 1 present
5. Spicules with at least 5 rays (clino): 0 absent; 1 present
6. Spicules with at least 5 orthogonal rays: 0 absent; 1 present
7. Spicules with at least 4 orthogonal rays: 0 absent; 1 present
8. Calthrops: 0 absent; 1 present
9. Spicules with at least three rays: 0 absent; 1 present
10. Hexacts/pentacts: 0 <1; 1 >1
11. Hexacts/stauracts: 0 <1; 1 >1
12. Pentacts/stauracts: 0 <1; 1 >1
13. Smooth monaxons in body: 0 absent; 1 present
14. Uncinates in body: 0 absent; 1 present
15. Polydactyloid uncinates: 0 absent; 1 present
16. Smooth monaxons in body: 0 absent; 1 present
17. Uncinates in root tuft: 0 absent; 1 present
18. Attachment spicules coarser than body spicules: 0 no; 1 yes
19. Root tuft: 0 fine; 1 thick
20. Body wall thickness: 0 single spicule layer; 1 thicker
21. Body wall (spicule distribution): 0 homogeneous; 1 bi- or tri-laminar
22. Body wall (spongin distribution): 0 homogeneous; 1 heterogeneous
23. Specialised gastralia: 0 absent; 1 present
24. Specialised dermalia: 0 absent; 1 present
25. Exogenic dermalia: 0 absent; 1 present
26. Specialised marginalia: 0 absent; 1 present
27. Orthogonal rectangular spicule array: 0 absent; 1 present
28. Diagonal rectangular spicule array: 0 absent; 1 present

29. Spicule size distribution: 0 gradational range; 1 distinct orders

30. Spicule array: 0 not quadruled; 1 quadruled in one or all layers

31. Spicule array: 0 entirely non-random; 1 random in one or all layers

32. Parietal gaps/large inhalent canals: 0 absent; 1 present

33. Cloaca: 0 absent; 1 present

34. Widening of body: 0 constantly expanding; 1 contracting towards apex

35. Horizontal section: 0 subcircular; 1 lobate

36. Vertical spicule tracts: 0 absent; 1 present

37. Horizontal spicule tracts: 0 absent; 1 present

38. Vertical structural heterogeneity: 0 absent; 1 present

39. Incorporated clastic material: 0 absent; 1 present

40. Spicular fusion: 0 absent; 1 present

41. Surface regularity: 0 smooth; 1 irregular/nodose

*List of species*. All identified Llandegley Rocks taxa are included, with additional data derived from published sources (16-20); only one publication was used per species, the original unless further references are given. *H. sphaeroidalis* Duncan (4) was used as a proxy for the probably synonymous *Microspongia*? sp., because of limited data in the present material.

1. *Onerosiconchia gregalia* sp. nov.

2. *Ordinisabulo quadragintaformis* sp. nov.

3. *Miritubus erinaceus* sp. nov.

4. *Hindia sphaeroidalis* Duncan; Rigby and Webby (1988)

5. *Fistula milvus* sp. nov.

6. *Polydactyloides trescelestus* sp. nov.

7. *Polydactyloides entropus* sp. nov.

8. *Pseudolancicula* cf. *exigua*

9. *Palaeocallyoides improbabilis* sp. nov.

10. *Triactinella rigbyi* sp. nov.

11. *Spissiparies minuta* sp. nov.

12. *Pyritonema scopula* sp. nov.

13. *Reticulicymbalum tres* sp. nov.
14. *Microastraeum tenuis* sp. nov.
15. *Brevicirrus arenacea* sp. nov.
16. *Protospongia hicksi* Salter; Rigby (1966)
17. *Leptomitus zitteli* (Walcott); Rigby (1986)
18. *Hintzespongia bilamina* Rigby and Gutschick, 1976
19. *Ratcliffespongia wheeleri* Rigby and Church, 1990
20. *Twenhofellela anticostiana* (Twenhofel); Rigby (1974).

*Discussion of characters.* The presence or absence of spicules (1) is a critical distinction among the Llandegley Rocks sponges, but in most faunas, aspicular taxa are not preserved. The distinction between siliceous and calcareous spicules is also critical, although in mouldic material this may not be obvious. Differences in preservational style should be used in conjunction with the assumption of composition, deduced from mutually exclusive spicule morphotypes (2). A stacked approach to ray development in hexactinellids (3-9) has been adopted to exaggerate the shared development of morphotypes. Simple presence/absence states for each morphotype would fail to establish the distinction of, for example, monaxonid-only taxa and hexactine-only taxa, as opposed to pentact- and hexact-dominated forms. This may seem to be an *a priori* assumption of relatedness, such that spicules with *n* rays developed only from spicules with *n±1* rays. However, the assumption is justified by abundant records of vestigial or proto-rays in hexactinellid spicules, and embryological studies, all of which indicate the gradual acquisition of rays rather than radical symmetry reorganisation. While details of ornament are unusable due to the effects of silica variation, the presence or absence of clavate, acanthose or tylotic modification among hexactines should be unaffected. Similarly, the ordered array of spines in uncinates is clearly distinct from acanthose spicules, irrespective of the

effects of silica dependence. Ratios of major spicule types (10-12) provide an additional parameter of spicule utilisation, independent of the questionable occurrence of rare morphotypes. Entries for taxa with one or both comparators absent are treated as missing data.

The distinction of position (body or root tuft – 13, 14, 16, 17) in addition to presence is significant in some case, but not necessarily all. Uncinates *s.s.* are known from several groups (taxonomic limits poorly known), but among Palaeozoic hexactinellids appear to be restricted to the root tuft. The presence of uncinates within the body of *Polydactyloides* gen. nov., in particular, may be important in establishing its taxonomic postion.

Characters referring to body wall thickness and homogeneity (20 – 24, 32) might be difficult to establish in compressed or collapsed material, and may not be appropriate among other faunas. Although some characteristics (e.g. 32) should be retained in all articulated material, others (e.g. 20) may be ambiguous; a thin, dense array may closely resemble a thicker, sparser distribution when compacted, particularly in taxa with a disordered spicule mesh. Characteristics of soft-tissue anatomy (22) are included here through exceptional preservation, although data are restricted to two species.

### 4.7.2 Results

An initial data matrix including all taxa listed above was analysed using PAUP, version 3.11, by a branch-and-bound method. Results were displayed in 50% majority rule and strict consensus formats, including *a posteriori* reweighting; unrooted trees were obtained by transplanting the results into TREEVIEW, while *O.*

*gregalia* was used as the default outgroup. Robustness of the cladograms was tested by sequentially removing taxa in which homoplasy was suspected.

The initial results (Fig. 4.7.1) conformed to conventional systematics within local groupings, but produced unexpected wider relationships. Reticulosids comprise a distinct clade, as expected, and the close relationship of *C. pseudoreticulatus* to the dictyosponge *R. tres* was confirmed in all analyses. The position of *T. rigbyi* weakly supported a reticulosid sister-group comprising thicker-walled sponges, as discussed in section 4.3. *Hintzespongia bilamina* is attributed with equal likelihood to this clade, and to the basal lyssakid clade (below). *H. sphaeroidalis* occurs as the sister taxon of the reticulosids.

Although conventional systematics place the lyssakids as derivatives of the reticulosids (e.g. Rigby 1986), in the initial analysis, they are shown as the sister group of a clade comprising the reticulosids, a second clade of poecilosclerids, with *P. improbabilis* and *P. scopula*, and *L. zitteli.* As expected, the aspicular demosponges form a distinct clade, with *O. gregalia* appearing more basal than those assigned to

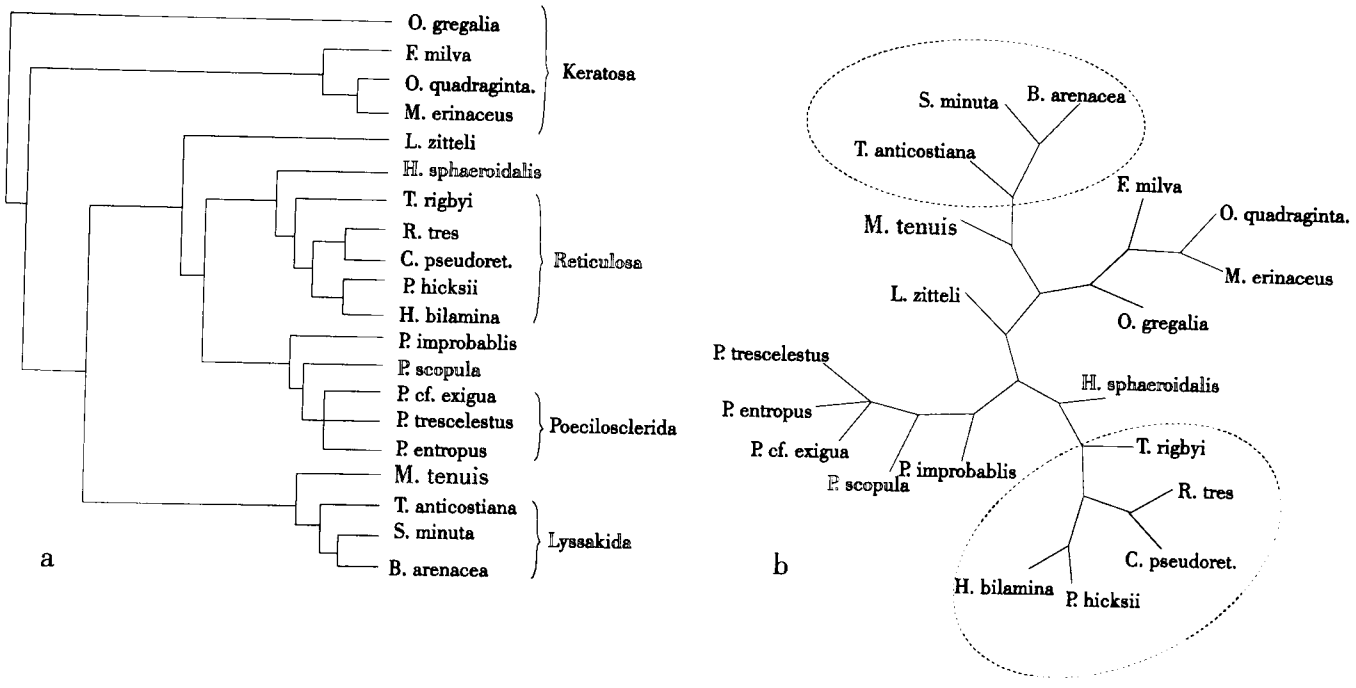


Figure. 4.7.1: a, Initial PAUP cladogram produced through *a posteriori* reweighted strict consensus (CI 0.766, RCI 0.632, Homoplasy index 0.234/0.327 excluding uniformative taxa); b unrooted TREEVIEW dendrogram of the same data set; reticulosid (lower) and lyssakid (upper) clades circled.

the Dysideidae. The heteractinid calcisponge *M. tenuis*, which on molecular grounds is widely distinguished from the siliceous sponges (Zrzavy *et al.* 1998), was placed within the lyssakid clade.

The removal of *M. tenuis* from the matrix had no effect on the cladogram, and this species was discarded. The further removal of the (probable hexactinellid) monaxonid *P. scopula* resulted in *P. improbabilis* moving from the poecilosclerid (*P. entropus, P. trescelestus, P.* cf. *exigua*) clade into a position as sister taxon to the reticulosids.

Further removal of *L. zitteli* and *H. sphaeroidalis* from the matrix resulted in a robust cladogram, which became unstable only after the removal of all supposed demosponges (Fig. 4.7.2). In this arrangement, the reticulosids form a sister group to the lyssakids, with the entire hexactinellid clade as sister group to the poecilosclerids. Within the Reticulosa, *T. rigbyi* is a sister taxon to the *C. pseudoreticulatus-R. tres* lineage. All demosponge clades are internally unchanged. This cladogram is supported at 100% on all branches.

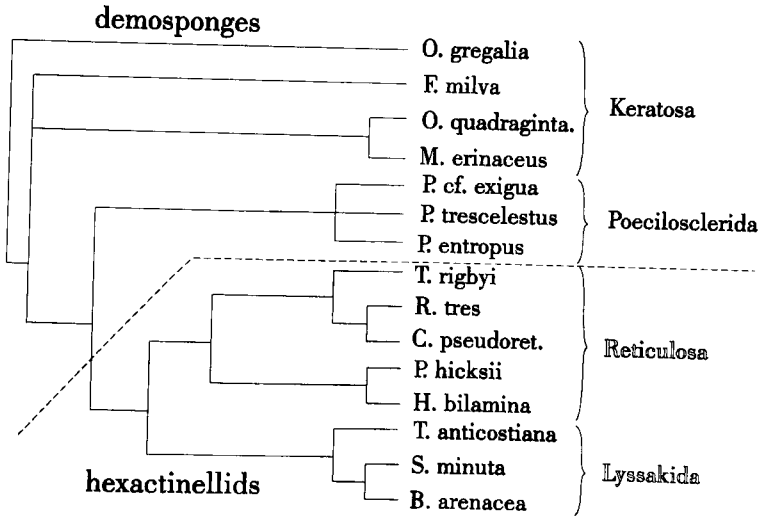


Figure 4.7.2: *50% majority-rule consensus tree, with* M. tenuis, L. zitteli, P. improbabilis, *H. sphaeroidalis and* P. scopula *excluded; robust under further deletions, all branches supported at 100%. Note complete redistribution of primary clades from Fig. 4.5.1.*

Several implications follow from these results, relating both to the reliability of cladistics as a general tool for investigating fossil sponge phylogenetics, and to the

phylogenetic hypotheses themselves. The unstable initial cladogram differs dramatically from the robust tree derived from fewer taxa, in that the lyssakids and poecilosclerids were transposed as sister group of the reticulosids. Other differences are minor, generally relating to slight changes in the position of individual species. The initial instability was dominantly produced by inclusion of the monaxon-only species *L. zitteli*, *P. scopula*, and *P. improbabilis*. While the attribution of *P. improbabilis* to the haplosclerid demosponges appears irrefutable, *L. zitteli* shows characteristics of both demosponges and protospongioid reticulosids, and while *P. scopula* is superficially similar to *Leptomitus*, in detail it closely resembles certain lyssakid root tufts. The implied homoplasy will affect not only the position of each species, but also the positions of those taxa with which they are homeomorphic. Thus two distantly related clades may be shown as near sister groups, if a close relative of one is convergent with the other. This is of particular significance among relatively small character sets, where few characters may separate distantly related clades. As discussed above, the number of reliable characters in fossil sponges is extremely limited.

Despite this, the robust cladogram produced with limited taxa is of substantial interest. The Reticulosa and Lyssakida consistently form separate clades, in contrast to the phylogenetic hypothesis of Rigby (1986), in which *Hintzespongia*-like forms were derived from a protospongiid ancestor, and later gave rise to the lyssakids. In some cladograms, *H. bilamina* appears as a basal lyssakid, but the lyssakids are never expressed as the sister group of *P. hicksi*. The distinction of lyssakids and reticulosids was emphasised by Finks (1983), who employed the impractical microsclere classification of Schmidt (1870) (discussed in section 4.4). The exclusivity of amphidiscs and hexasters in recent hexactinellids suggests that each morphotype

appeared very shortly after divergence of the two lineages. Attribution of the Reticulosa to the Amphidiscophora (Finks 1983) is based on subjective similarity to modern taxa, since diagnostic microscleres have not certainly been recovered from the lower Palaeozoic.

Further cladistic analyses, concentrating on Lower Palaeozoic hexactinellids, may dissolve the distinction observed here, but distinct ancestors of reticulosids and lyssakids would simplify the observed microsclere distribution. The results of this initial investigation are insufficient to replace the self-consistent phylogenetic hypothesis of Rigby (1986), but strongly encourage more detailed analyses.

The most unstable taxon in the analyses was *Pyritonema scopula*. In all cladograms containing one or more additional monaxonid sponges, *P. scopula* invariably became their sister group; this includes the lithistid *Hindia sphaeroidalis*. If all monaxon-bearing taxa were removed, *P. scopula* became a weakly-supported sister taxon to the hexactinellids as a whole. That it was no closer to the lyssakids than the reticulosids is unexpected, but consistent with the persistent separation of the two hexactinellid clades. If the lyssakids clearly originated from the reticulosids, then *P. scopula* should be recognisably derived. However, the position of *P. scopula* may be an artefact resulting from unclear relationships among the hexactinellids, and no firm conclusions can be reached at this stage. The consistency with which *P. scopula* occurs among monaxonid demosponges is almost certainly an artefact, resulting from the dominance of spicule morphotypes in defining cladistic characters. This cannot be stated with complete certainty, however, and with the degree of convergence implied by any interpretation of its affinities, it is unlikely that the position of *Pyritonema* will be clarified by this technique.

Other aspects of the systematics presented herein are supported by the cladistics. Among aspicular demosponges, *O. gregalia* is consistently separated from the probable dysideids *F. milvus*, *O. quadragintaformis* and *M. erinaceus*, with *F. milvus* forming a sister taxon of the other two. The closeness of *P. entropus*, *P. trescelestus* and *P.* cf. *exigua* is confirmed, with their distinction from all other Llandegley Rocks taxa.

In summary, the application of cladistics to fossil sponges has potential among restricted groups. In particular, understanding of hexactinellid phylogeny could be enhanced by employing cladistics in addition to traditional reasoned approaches. The ubiquity of homoplasy within spicule morphotype distribution argues against indiscriminate use of the technique, but cautious application is encouraged by the data, at least to clearly define competing hypotheses.

## 4.8 PALAEOBIOGEOGRAPHY

The palaeobiogeographic potential of Palaeozoic sponges is usually considered slight, due to the high endemism and brief larval stages of modern forms. However, the few published analyses suggest some pandemic distribution patterns among Palaeozoic species. Silurian faunas were described by Rigby and Chatterton (1989), but could not reliably be extended beyond North America. Stromatoporoid biogeography has been discussed by Webby (1980, 1992), and Webby and Lin (1988), with sphinctozoan biogeography described by Senowbari-Daryan (1990). The first general review of Ordovician faunas was given by Carrera and Rigby (1999).

The main problem involved in attempting palaeogeographic analysis of sponges is the lack of information. Only North American faunas are at all well known, and even here, localities are regionally restricted. The Argentine faunas have been

extensively studied by Carrera (e.g. 1994, 1996*a*, 1996*b*, 1997), and the extraordinarily diverse Malungulli assemblage of New South Wales (Rigby and Webby 1988; Webby and Trotter 1993) represents a substantial introduction to Australian faunas. European sponges are known primarily from older literature (e.g. Hinde 1888; Rauff 1893, 1894, 1895; Roemer 1861), with occasional later descriptions of small assemblages, primarily of spicules only (Pulfrey 1933; Lewis 1940). A very limited Iberian fauna was described by Rigby *et al.* (1997). Important Chinese faunas are known from the Lower and Upper Cambrian (Zhang and Pratt 1994; Dong and Knoll 1996; Chen *et al.* 1989), with significant Permian faunas also described. Restricted Ordovician faunas are known from south China (e.g. Deng 1982). Early Palaeozoic faunas from other regions are virtually unknown. The frequency of new species and genera reported from North America and elsewhere highlights the incompleteness of the known record.

A part of this ignorance reflects the restricted facies range in which sponges are typically preserved. Rigby and Chatterton (1989, p. 8) suggested that continental margins and the outer slope of island arcs may have been populated by diverse sponge faunas, perhaps even more diverse than faunas of shallower facies. Most occurrences are from middle to outer shelf environments; very few lower slope settings contain articulated material. Similarly, shallow-water sequences are restricted almost entirely to carbonate facies, where the communities are dominated by calcitic taxa. Rare examples of shallow siliciclastic faunas, also from Australia, include that described by Webby and Rigby (1985), and an undescribed lithistid fauna mentioned by Webby and Packham (1982). The Llandegley Rocks fauna is the first diverse shallow siliciclastic assemblage described, and the most diverse Ordovician assemblage described from Britain. The high proportion of new species and genera, including

distinctive spicule morphotypes, confirms that near-shore communities were distinct from deeper-water and carbonate faunas.

The low preservation potential of lyssakid hexactinellids and non-lithistid demosponges also accounts for biases in the Palaeozoic record. Carrera and Rigby (1999) showed that the known Ordovician faunas are dominated by lithistid demosponges, although it was assumed that a substantial bias is operating. Their analysis also omitted certain non-lithistid groups, including British Ordovician occurrences of *Protospongia* Salter, *Hyalostelia* Young and Young, and *Pyritonema* M'Coy, along with other, taxonomically uncertain forms, such as *Pseudolancicula* Webby and Trotter. The Llandegley Rocks fauna contains very few taxa with cemented skeletons, being dominated by non-lithistid demosponges and lyssakid hexactinellids.

Biogeographic conclusions based on this fauna are thus restricted by the unusual environmental setting, and by the nature of the community. Of the fifteen named species, three may be placed in established genera. These are *Microspongia*? sp., *Pyritonema scopula* and *Pseudolancicula* cf. *exigua*. The taxonomic position of *Microspongia*? sp. is discussed below, but there is little doubt that the taxon is pandemic. The abundance of the material and spherical shape suggested to Rigby and Webby (1988) that the possibly synonymous *Hindia* may have been planktic. This is supported by the presence of the taxon at Llandegley Rocks, in a very different palaeoenvironment from that of previous occurrences.

There is little doubt that the primary diversification of astraeospongiids took place in North America (Carrera and Rigby 1999), but the presence of the group in Baltica and Avalonia indicates further, possibly isolated populations. The larval

longevity of astraeospongiids must have been considerable, since their absence outside Iapetus apparently precludes a planktic adult form.

The occurrence of *Pseudolancicula* in Avalonia is notable. Previously known only from the Upper Ordovician of New South Wales, a very extensive range is indicated. Since no articulated material is known, the possibility of a planktic nature cannot be dismissed. The original environment of the New South Wales material is uncertain, as the spicules occurred in limestone clasts (Webby and Trotter 1993), but is assumed to be a slope environment (Rigby and Webby 1988). This range of facies is only easily explained by invoking a planktic ecology. If this is so, further discoveries of polydactyloid spicules from similar latitudes in Argentina might be anticipated.

## 4.9 References


Bengtson, S. 1986. Siliceous microfossils from the Upper Cambrian of Queensland. *Alcheringa* **10**, 195-216.

Bergquist, P. R. 1978. *Sponges.* Hutchinson, London, 268pp, 12 pl.

Borchiellini C., Chombard, C., Lafay, B. and Boury-Esnault, N. 2000. Molecular systematics of sponges (Porifera). *Hydrobiologia*, **420**, 15-27.

Brasier, M.D., 1992. Nutrient-enriched waters and the early skeletal fossil record. *Journal of the Geological Society* **149**, 621-630.

Butler, P. E. 1961. Morphologic classification of sponge spicules, with descriptions of siliceous spicules from the Lower Ordovician Bellefonte Dolomite in central Pennsylvania. *Journal of Paleontology* **35,** 191-200.

Carrera, M. G. 1994. An Ordovician sponge fauna from the San Juan Formation, Precordillera Basin, western Argentina. *Neues Jahrbuch für Geologie und Paläontologie, Abhandlungen.* **191**, 201-220.

CARRERA, M. G. 1996a. Ordovician Megamorinid demosponges from the San Juan Formation, Precordillera, Western Argentina. *Geobios* **29**, 643-650.

CARRERA, M. G. 1996b. Nuevos poríferos de la Formación San Juan (Ordovícico), Precordillera Argentina. *Ameghiniana* **33**, 335-342.

CARRERA, M. G. 1997. Significado palaeoambiental de los poríferos y briozoos de la Formación San Juan (Ordovícico), Precordillera Argentina. *Ameghiniana* **34**, 179-199.

CARRERA, M. G. & RIGBY, J. K. 1999. Biogeography of Ordovician sponges. *Journal of Paleontology* **73**, 26-37.

CHEN J., HOU X. AND LU H., 1989. Lower Cambrian Leptomitids (Demospongea), Chengjiang, Yunnan. *Acta Palaeontologica Sinica* **28**, 27-32, 6 pl.

DAWSON, J. W. AND HINDE, G. J. 1889. On new species of fossil sponges from the Siluro-Cambrian at Little Metis on the lower St. Lawrence. *Transactions of the Royal Society of Canada* **7**, 31-55.

DENG Z.-Q. 1982. Paleozoic and Mesozoic sponges from South-west China, western Sichuan and eastern Xiziang, Stratigraphy and Paleontology, part 2. *Sichuan Rennin Chuban Che,* Chengdu, p. 245-258.

DONG X. AND KNOLL, A. H. 1996. Middle and Late Cambrian sponge spicules from Hunan, China. *Journal of Paleontology* **70**, 173-184.

DUNCAN, P. M. 1879. On some sphaeroidal lithistid spongida from the Upper Silurian formation of New Brunswick. *Annals and Magazine of Natural History, series 4,* **4**, 84-91.

FINKS, R. M. 1960. Late Paleozoic sponge faunas of the Texas region; the siliceous sponges. *American Museum of Natural History Bulletin* **120**, 160 pp, 50 pl.

FINKS, R. M. 1983. Fossil Hexactinellida. *In* T. W. BROADHEAD (ed.), *Sponges and Spongiomorphs*; Notes for a Short Course, Palaeontological Society, University of Tennessee Department of Geological Sciences, Studies in Geology **7** 101-115.

GRANT, R. E. 1961. *Tabular view of the primary divisions of the animal kingdom*. London.

GRAY, J. E. 1858. Description of a new genus of sponge (Xenospongia) from Torres Strait. *Proceedings of the Zoological Society of London* **7**, 229-230, 1 pl.

GRAY, J. E. 1867. Notes on the arrangement of sponges with description of some new genera. *Proceedings of the Zoological Society of London* 492-558.

HALL, J. 1884. Descriptions of species of fossil reticulate sponges, constituting the family Dictyospongiidae. *35th Annual Report, New York State Museum of Natural History*, p. 465-481.

HALL, J AND CLARKE, J. M. 1898. A memoir on the Palaeozoic reticulate sponges constituting the family Dictyospongidae. *New York Sate Museum Memoir* **2**, 197pp.

HICKS, H. 1871. Descriptions of new species of fossils from the Longmynd rocks of St. David's. *Annals and Magazine of Natural History* **27**, 399-404, 2 pl.

HINDE, G. J. 1887-1888. Monograph of British Fossil Sponges, 1: Palaeozoic sponges. *Monograph of the Palaeontographical Society, London,* 1 (1887), 1-92; 2 (1888), 93-188.

IJIMA, I. 1904. Studies on the Hexactinellida, contribution 4. *Journal of the College of Sciences, Imperial University of Tokyo*, **18**, 1-307.

LAFAY B., BOURY-ESNAULT, N., VACELET, J. AND CHRISTEN, R. 1992. An analysis of partial 28S ribosomal RNA sequences suggests early radiations of sponges. *Biosystems*, **28**, 139-151.

LAUBENFELS, M. W. DE 1936. A discussion of the sponge fauna of the Dry Tortugas in particular and the West Indies in general with material for a revision of the families and orders of the Porifera. *Carnegie Institute of Washington Publication* **467**, 1-225.

LAUBENFELS, M. W. DE 1955. Part E: Porifera. In *Moore, R.C. (ed.)* Treatise on Invertebrate Palaeontology. *Geological Society of America and University of Kansas Press, Lawrence, Kansas,* E21-212.

LEWIS, H. P. 1940. The microfossils of the Upper Caradocian phosphate deposits of Montgomeryshire, North Wales. *Annals and Magazine of Natural History Series 11*, **5**, 1-39.

M'COY, F. 1844. *Synopsis of the Carboniferous Fossils of Ireland*, 169 pp.

M'COY, F. 1850. On some new genera of Silurian Radiata in the collection of the University of Cambridge. *Annals and magazine of Natural History, series* 2, **6**, 270-291.

MALDONADO, M., CARMONA, M. C., URIZ, M. J. AND CRUZADO, A. 1999. Decline in Mesozoic reef-building sponges explained by silicon limitation. *Nature* **401**, 785-788.

MEHL, D., RIGBY, J. K., AND HOLMES, S. B. 1993. Hexactinellid sponges from the Silurian-Devonian Roberts Mountains Formation in Nevada and hypotheses of hexactine-stauractine origin. *Brigham Young University Geology Studies* **39**, 101-124.

MILLER, S. A. 1889. Class Porifera. *In* North American Geology and Palaeontology. Western Methodist Book Concern, Cincinnati, Ohio, 152-167. (Published by the author.)

MOSTLER, H. 1990. Hexactinellide Poriferen aus pelagischen Kieselkalken (Unter Lias, Nördliche Kalkalpen). *Geologische-Paläontologische Mitteilungen Innsbruck*, **17**, 143-178.

OKADA, Y. 1928. On the development of a hexactinellid sponge, *Farrea sollasii*. *Tokyo University Journal of Sciences: Zoology* **2**, 1-27.

PULFREY, W. 1933. Note on the occurrence of sponge spicules associated with the iron-ores of North Wales. *Annals and Magazine of Natural History* series 10, **11**, 67-76, 1 pl.

RAUFF, H. 1893-1895. Palaeospongiologie. *Palaeontographica,* 1 (1893) **40**, 232 pp.; 2, (1894) **41**, 233-346, 17 pl.; 3, (1895) **43**, 223-272, pl. 20-26.

REID, R. E. H. 1958A. On Hexactinellida, "Hyalospongia," and the classification of siliceous sponges. *Journal of Paleontology*, **32**, 282-286.

REID, R. E. H. 1958B-1964. The Upper Cretaceous Hexactinellida. *Monograph of the Palaeontographical Society, London*, 1, (1958) **111**, i-xlvi; 2, (1958) **111**, 1-26, pl. 1-4; 3, (1961) **114**, 27-48, pl. 5-11; 4, (1964) **117**, 49-154.

REID, R. E. H. 1968. *Hyalostelia smithii* (Young & Young) and the sponge genus *Hyalostelia* Zittel (class Hexactinellida). *Journal of Paleontology*, **42**, 1243-1248, 1 pl.

REISWIG, H., AND MACKIE, G. O. 1983. Studies on Hexactinellid sponges. III. The taxonomic status of the Hexactinellida within the Porifera. *Philosophical Transactions of the Royal Society of London* **301**, 419-428.

RIGBY, J. K. 1966. *Protospongia hicksi* Hinde from the Middle Cambrian of western Utah. *Journal of Paleontology*, **40**, 549-554.

RIGBY, J. K. 1967. Two new early Paleozoic sponges and the sponge-like organism, *Gaspespongia basalis* Parks, from the Gaspé Peninsula, Quebec. *Journal of Paleontology* **41**, 766-775.

RIGBY, J. K. 1970. Two new Upper Devonian hexactinellid sponges from Alberta. *Journal of Paleontology* **44**, 7-16.

RIGBY, J. K. 1974. *Vaurealspongia* and *Twenhofelella*, two new brachiospongiid hexactinellid sponges from the Ordvician and Silurian of Anticosti Island, Quebec. *Canadian Journal of Earth Sciences* **11**, 1343-1349.

RIGBY, J. K. 1975. A new Devonian heteractinid sponge from southwestern Ellesmere Island, Arctic Canada. *Canadian Journal of Earth Sciences*, **13**, 120-125.

RIGBY, J. K. 1977a. *Constellatospongia*, a new heteractinid astraeosponge from the Upper Ordovician Churchill River Group, Manitoba. *Geological Survey of Canada Bulletin*, **269**, 131-137.

RIGBY, J. K. 1977b. Two new Middle Ordovician sponges from Foxe Plain, southeastern district of Franklin. *Geological Survey of Canada Bulletin*, **269**, 121-129.

RIGBY, J. K. 1983. Sponges of the Middle Cambrian Marjum Limestone from the House Range and Drum Mountains of western Millard County, Utah. *Journal of Paleontology* **57**, 240-270.

RIGBY, J. K. 1986. Sponges of the Burgess Shale (Middle Cambrian) British Columbia. *Palaeontographica Canadiana Monograph*, **2**, 105 pp.

RIGBY, J. K. 1995. The hexactinellid sponge *Cyathophycus* from the Lower-Middle Ordovician Vinini Formation of central Nevada. *Journal of Paleontology*, **69**, 409-416.

RIGBY, J. K. AND AUSICH, W. I. 1981. Lower Mississippian sponges from the Edwardsville Formation, Southern Indiana. *J. Paleont.* **55**, 370-382.

RIGBY, J. K. AND CHATTERTON, B. D. E. 1989. Middle Silurian Ludlovian and Wenlockian sponges from Baillie-Hamilton and Cornwallis Islands, Arctic Canada. *Geological Survey of Canada Bulletin* **391**, pp. 49, 10 pl.

RIGBY, J. K. AND CHURCH, S. B. 1990. A new Middle Cambrian hexactinellid, *Ratcliffespongia wheeleri*, from western Utah, and skeletal structure of *Ratcliffespongia*. *Journal of Paleontlogy* **64**, 331-334.

RIGBY, J. K., GUTIERREZ-MARCO, J. C., ROBARDET, M. AND PIÇARRA, J. C. 1997. First articulated Silurian sponges from the Iberian peninsula (Spain and Portugal). *Journal of Paleontology* **71**, 554-563.

RIGBY, J. K. AND GUTSCHICK, R. C. 1976. Two new Palaeozoic hexactinellid sponges from Utah and Oklahoma. *Journal of Paleontology* **50**, 79-85.

RIGBY, J. K., HANNUM, C. AND FREST, T. J. 1979. Hexactinellid sponges from the Silurian Waldron Shale in southeastern Indiana. *Journal of Paleontology* **53**, 542-549.

RIGBY, J. K. AND HARRIS, D. R. 1979. A new Silurian sponge fauna from Northern British Columbia, Canada. *Journal of Paleontology* **53**, 968-980.

RIGBY, J. K., KING, J. E. AND GUNTHER, L. F. 1981. The new Lower Ordovician protosponge, *Asthenospongia*, from the Phi Kappa Formation in central Idaho. *Journal of Paleontology* **55**, 842-847.

RIGBY, J. K. AND MURPHY, M. A. 1983. *Gabelia*, a new late Devonian lyssakid protosponge from the Roberts Mountains, Nevada. *Journal of Paleontology* **57**, 797-803.

RIGBY, J. K. AND NITECKI, M. H. 1975. An unusually well preserved heteractinid sponge from the Pennsylvanian of Illinois and a possible classification and evolutionary scheme for the Heteractinida. *Journal of Paleontology* **41**, 329-229.

RIGBY, J. K. AND WEBBY, B. D. 1988. Late Ordovician sponges from the Malongulli Formation of central New South Wales. *Palaeontographica Americana* **56**, 147 pp.

ROEMER, C. F. 1861. *Die fossile Fauna der Silurischen Diluvial-Gescheibe von| Sadewitz bei Oels in Nieder-Schleisien*. Breslau, 15 pp.

ROSELL, D. AND URIZ, M. J. 1997. Phylogenetic relationships within the excavating Hadromerida (Porifera), with a systematic revision. *Cladistics* **13**, 349-366.

RUEDEMANN, R. 1925. The Utica and Lorraine formations of New York. Part 2, Systematic Paleontology. *Bulletin of the New York State Museum* **258**, 175 pp, 13 pl.

SALTER, J. W. 1864. On some new fossils from the Lingula Flags of Wales. *Quarterly Journal of the Geological Society of London* **20**, 233-241.

SCHMIDT, O. 1870. *Grundzüge einer Spongien-Fauna des Atlantiscen Gebietes*. Wilheim Engelmann, Leipzig, 88 pp.

SCHULZE, F. E. 1877. Report on the Hexactinellida. *Report, Explorations of the Voyage of the Challenger, Zoology* **21**, 513pp., 104 pls., 1 map.

SENOWBARI-DARYAN, B. 1990. Die Systematische Stellung der thalamiden Schwämme und ihre bedeutung in der Erdgeschichte. *Münchner Geowissemnschaftliche Abhandlungen*, **21**, 326 pp.

SINCLAIR, G. W. 1956. Notes on some Ordovician sponges and their names. *Journal of Paleontology* **30**, 760-761.

SOLLAS, W. J. 1875. Sponges. *In* Encyclopedia Brittanica, 9th Edition, p. 421.

SOLLAS, W. J. 1877. On the changes produced in the siliceous skeletons of certain sponges by the action of caustic potash. *Annals and Magazine of Natural History, Series 4,* **20**, 285-301.

SUESS, 1866.

THOMSON, C. E. 1868. On the vitreous sponges. *Annals and Magazine of Natural History* **4**, 114-32.

WALCOTT, C. D. 1920. Cambrian geology and paleontology. IV. Middle Cambrian Spongiae. *Smithsonian Miscellaneous Collections*, **67** (6), 261-364.

WATKINS, R. AND COOROUGH, P.J. 1997. Silurian sponge spicules from the Racine Formation, Wisconsin. *Journal of Paleontology* **71**, 208-214.

WEBBY, B. D. 1980. Biogeography of Ordovician stromatoporoids. *Paleaogeography, Palaeoclimatology, and Palaeoecology*, **32**, 1-19.

WEBBY, B. D. 1992. Global biogeography of Ordovician corals and stromatoporoids, p. 261-276. *In* B. D. WEBBY AND J. R. LAURIE (eds.), Global perspectives on Ordovician geology. *Proceedings of the Sixth International Symposium on the Ordovician System*, Sydney, July 1991. Balkema, Rotterdam, The Netherlands.

WEBBY, B. D., AND LIN, B.-Y. 1988. Upper Ordovician cliefdenellids (Porifera: sphinctozoa) from China. *Geological Magazine*, **125**, 149-159.

WEBBY, B. D. AND RIGBY, J. K. 1985. Ordovician sphinctozoan sponges from central New South Wales. *Alcheringa*, **9**, 209-220.

WEBBY, B. D. AND PACKHAM, G. H. 1982. Stratigraphy and regional setting of the Cliefden Caves Limestone Group (late Ordovician), central-western new south Wales. *Geological Society of Australia, Journal*, **29**, 297-317.

WEBBY, B. D. AND TROTTER, J. 1993. Ordovician sponge spicules form New South Wales, Australia. *Journal of Palaeontology* **67**, 28-41.

YOUNG, J. & YOUNG, J. 1876. *In* Armstrong, Young and Robertson (eds): Catalogue of Western Scottish fossils.

YOUNG, J. & YOUNG, J. 1877. On a Carboniferous *Hyalonema* and other sponges from Ayrshire. *Ann. And Mag. Nat. Hist. series 4*, **20**, 425-432.

ZITTEL, K.A. VON, 1877. Studies on Fossil Sponges – 1, Hexactinellida. *Annals and Magazine of Natural History series* 4, **20**, p. 257-273, 405-424, 501-517.

ZITTEL, K. A. VON 1878. *Handbuch der Paläeontologie vol. 1*, unter Mitwirkung von W. Ph. Schimper, Munich. 185 pp.

ZHANG XI-GUANG & PRATT, B. R. 1994. New and extraordinary Early Cambrian sponge spicule assemblage from China. *Geology* **22**, 43-46.

ZHANG XI-GUANG AND PRATT, B. R. 2000. A varied Middle Ordovician sponge spicule assemblage from western Newfoundland. *Journal of Palaeontology* **74**, 386-393.

ZRZAVY, J., MIHULKA, S., KEPKA, P., BEZDEK, A., AND TIETZ, D. 1998. Phlogeny of the Metazoa based on morphological and 18S Ribosomal DNA evidence. *Cladistics*, **14**, 149-185.

# 5. SYSTEMATICS AND PALAEOBIOLOGY: PALAEOSCOLECIDS

## 5.1 INTRODUCTION

The Palaeoscolecidae Whittard, 1953 is a family of Lower Palaeozoic worms within the class Palaeoscolecidea (Conway Morris and Robison 1986). Although of uncertain phylum, a nematomorph affinity is now considered the most parsimonious (Hou & Bergström 1994; Conway Morris 1997), possibly as a class within the Priapulida. Palaeoscolecids are characterised by a papillose segmented cuticle, with fine microstructure of phosphatic plates and intercalatory microplates of one or two types. The large plates have been known as problematic microfossils since their separate discoveries by Bengtson (1977) and Gedik (1977). They are now recognised as abundant and diverse elements of Lower Cambrian (e.g. Bengtson 1977) to Silurian assemblages (Boogaard 1988; Wang 1990). Several form genera of isolated plates have been erected, based on outline and ornamentation, indicating substantial diversity; among the most widespread are *Hadimopanella*, *Milaculum* and *Utahphospha*. An early interpretation as vertebrate dermal tubercles was abandoned with the discovery of phosphatized palaeoscolecid cuticle containing *in situ* sclerites (Hinz *et al.*, 1990).

The much rarer preservation of articulated palaeoscolecid cuticle appears to be of two types. Phosphatized fragments and semi-complete specimens are known from the Middle Cambrian Georgina Basin of Australia (Hinz *et al.* 1990; Müller and Hinz-Schallreuter 1993), and the Lower Cambrian of Shaanxi, China (Zhang and Pratt 1996) and the Flinders Range, Australia (Brock and Cooper 1993). Further possible phosphatized palaeoscolecid fragments were listed by Conway Morris (1997, p. 79). All were extracted by acid digestion of limestones, and are abundant within the

productive samples. Specimens are preserved three-dimensionally, and show micron-scale detail of the cuticle structure, including undeformed terminations. Phosphatised cuticle is known presently only from the Lower and Middle Cambrian, and thus may be related to "Orsten"-type preservation: a phosphatised priapulid is known from the Lower Cambrian of the Baltic (D. Walossek, *pers. comm.* 2000).

In contrast, compression fossils in shales typically occur in small numbers at any one locality (but see Mikulic *et al.* 1985a, 1985b), but these localities are more numerous. Specimens with the tubercle rows characteristic of the Palaeoscolecidae were recognised, for example, by Ulrich (1878), Bather (1920), Whittard (1953), Glaessner (1979), Owens *et al.* (1982), Conway Morris and Robison (1986) and Hou and Bergstrom (1994), among others. The geographical range of these taxa includes the Anglo-Welsh Basin, Spain, Utah, South Australia and China. The quality of preservation is generally much lower than in the phosphatised material, with only the basic papillate arrangement discernible. However, Conway Morris (1997) showed that careful latex peel preparation of *Palaeoscolex piscatorum* allows the recognition of fine cuticular structure. Similar work on other compression material has produced results which "do not appear to be encouraging" (Conway Morris 1997, p. 79). This chapter describes two new species of *Palaeoscolex*, closely allied to the type species *P. piscatorum* Whittard, from Middle Ordovician shales of the Builth Inlier. Both are compression fossils, preserved with a level of fidelity only slightly subordinate to that of the type species (Whittard 1953; Conway Morris 1997). An additional fragment from a third site was preserved with much lower fidelity. Previously recorded palaeoscolecids from the Anglo-Welsh region were recovered from the Tremadoc Shineton Shales of Shropshire and Breadstone Shales of Gloucestershire (Whittard 1953), the Lower Tremadoc of Clyn-coch, Carmarthenshire (Owens *et al.* 1982), and

the Lower Ludlow of Herefordshire (Bather 1920). Only those of Whittard (1953) could be described taxonomically, as *Palaeoscolex piscatorum*, the only British species previously known.

## 5.2 Localities, horizons and associated faunas

The stratigraphic succession of the Builth Inlier has been discussed in detail above (2.1, 2.2), with palaeoenvironmental interpretations. Palaeoscolecids were discovered at three sites: section HB 2 (see 3.2), section BG 1(2) D (see 3.3), and in the pass northeast of Bwlch-y-Cefn (SO 1240 6127), described below.

The Llandegley Rocks are separated from Bwlch-y-Cefn Bank by a small-displacement, strike-slip fault. The fault forms a pass northeast of Bwlch-y-Cefn farm, where a stream has cut a small cliff section displaying the faulted region (SO 123 612). The north bank exposes pale, ashy, micaceous siltstones, containing very abundant *D. murchisoni*. The siltstone occurs within the volcanogenic sandstone succession of Llandegley Rocks, which are also exposed in the Howey Brook Main Feeder section of Gelli Hill (Elles 1939, p. 401). At the latter site, common *Diplograptus foliaceus* imply a position in the *D. murchisoni* Biozone; abundant specimens of *Didymograptus artus* in overlying beds suggest the basal part. The southerly change in fauna from *D. murchisoni* to diplograptids suggests shallower water to the southwest (Berry 1977), in accordance with the existence of a volcanic island complex (Jones and Pugh 1949).

Although *D. murchisoni* is dominant at Bwlch-y-Cefn, subordinate orthograptids, including spinose forms, co-occur with rare dendroids. Other elements of the fauna are uncommon, but diverse. The trilobites *Ogyginus corndensis* and *Cnemidopyge* sp. are rare, but their presence is unusual in the lower part of the

*murchisoni* Biozone in the Llandrindod region. Ostracodes, bryozoans and crinoids occur occasionally, while the inarticulate brachiopods *Apatobolus micula* and *Palaeoglossa* sp. occur at low levels throughout the exposed sequence. Stauractine and monaxon sponge spicules, probably derived from an undetermined protospongioid, are abundant at some horizons. Three indeterminable scolecodonts have been recorded, along with abundant chitinozoans, although only as isolated vesicles.

All palaeoscolecid specimens recovered from the Anglo-Welsh Basin are preserved in pale grey siltstones, probably deposited under relatively shallow shelf conditions. The Bach-y-Graig specimen occurs in a pale grey siltstone deposited during benthic oxygenation following ash-fall; surrounding sediments are dominantly anoxic, black shales. Sub-millimetre burrowing at the same horizon may reflect the activity of palaeoscolecids, although this is speculative; ichnofaunas are extremely rare in fine sediments of the Builth Inlier. The Howey Brook specimen was recovered from dark grey siltstones, deposited under dominantly anoxic benthic conditions. However, this also follows ash deposition, and coincides with a benthic bloom of the inarticulate brachiopod *Apatobolus micula*. This distribution strongly suggests a benthic habit, probably shallow infaunal. Based on comparisons with associated faunal occurrence, palaeoscolecids appear to have been tolerant of severe oxygen limitation, although none have been recovered from entirely anoxic facies. The small and inconspicuous nature of the current specimens suggests that palaeoscolecids may be much more abundant and widespread than previously thought.

## 5.3 METHODS

The method of preparing the Bwlch-y-Cefn and Howey Brook specimens for SEM study is based on that described in Conway Morris (1997). The lithology at Bwlch-y-Cefn is particularly friable, and slight hardening was required prior to the application of latex. A very dilute solution of Paraloid in Methyl Ethyl Ketone (MEK) was tested on a part of the shale, and studied under a light microscope to ensure that the process would obscure as little surface relief as possible. This solution was then applied to the fossil, allowed a few seconds to be absorbed, then lightly rinsed with MEK in order to remove any excess surface adherence.

When dry, the surface was wetted and a thin layer of latex applied, dispersed by blowing through a straw. This initial application was carefully removed, to free the specimen from any surface detritus, and a second thin film was applied. Further layers were subsequently added, and the final cast transferred to an SEM stub, and coated with Au. Despite careful processing, details of microplates were not preserved in the cast, although plate arrangement is well seen. A small fragment of the counterpart was recovered during preparation of the specimen; this was transferred directly to an SEM stub, and coated with Au.

The Howey Brook specimen was originally misidentified; prior to its significance being recognised, Paraloid was applied to the surface to counteract an extreme tendency of the lithology to fracture on drying. This has been removed by redissolution in MEK, and a cast prepared using the method described above. Although less detail was retained on the cast than in the counterpart of BU 2874, details of plate arrangement and morphology, and some details of microplates were retained. It is not known whether preservation of the original fossil, or residual deposits of hardener had greater significance in limiting resolution, but the potential

of the latex casting technique for investigating palaeoscolecid compressions has been confirmed.

The counterpart of the additional fragment, from Bach-y-Graig, was transferred directly to an SEM stub, as no information could be obtained regarding overall form. Preservation of this specimen is too poor to allow formal description.

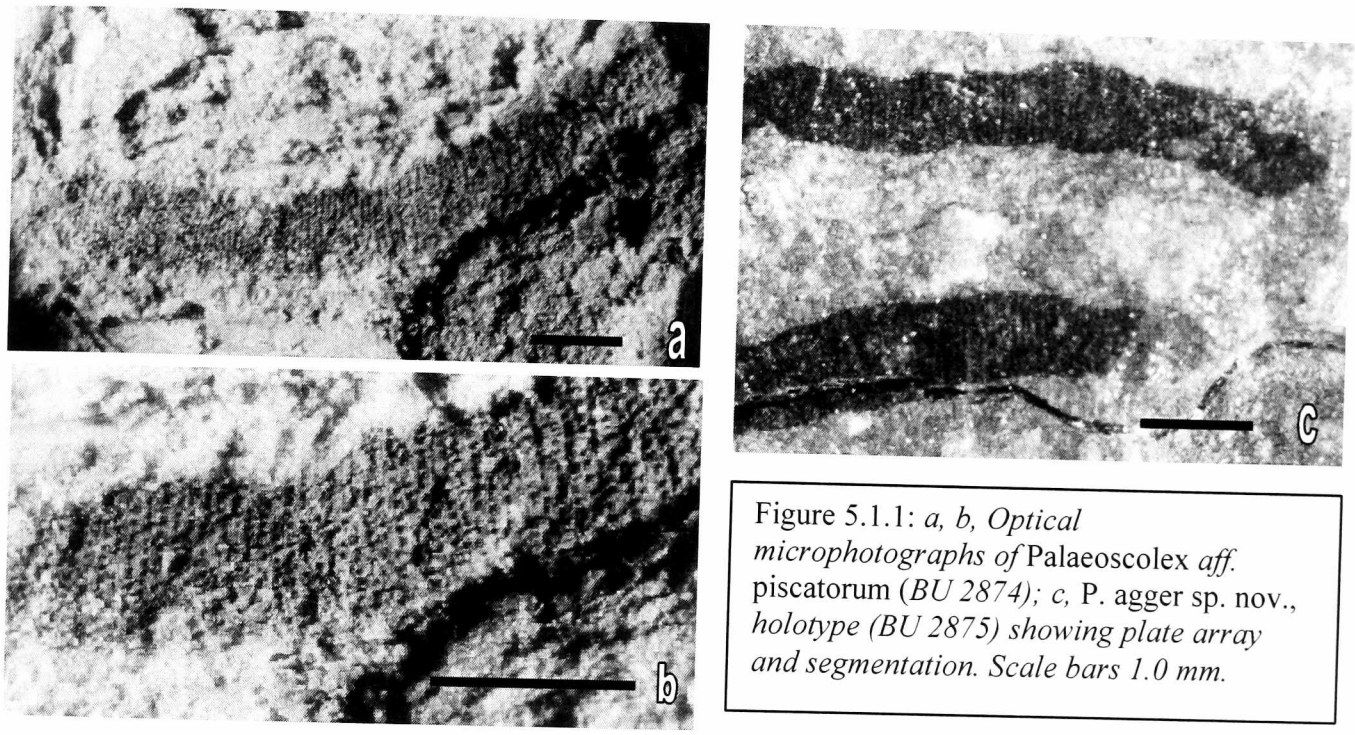


Figure 5.1.1: *a, b, Optical microphotographs of* Palaeoscolex *aff.* piscatorum *(BU 2874); c,* P. agger sp. nov., *holotype (BU 2875) showing plate array and segmentation. Scale bars 1.0 mm.*

## 5.4 Systematic Palaeontology

Specimens are deposited in the Lapworth Museum, University of Birmingham.

Class PALAEOSCOLECIDA Conway Morris & Robison, 1986

Order uncertain

Family PALAEOSCOLECIDAE Whittard, 1953

Genus PALAEOSCOLEX Whittard, 1953

*Diagnosis* (emended after Robison 1969). Highly elongate segmented worm lacking parapodia, with up to 400 transverse double rows of plates, interspersed with alternate bands of platelets and/or microplates. Repeated units of two plate rows separated by furrows, probably indicating metameric segmentation. Cephalisation lacking, and terminal regions unclear; gut simple, straight.

*Palaeoscolex agger* sp. nov.

Fig. 5.1.1 (c); Pl. 14, figs 1-6

*Etymology*. Latin *agger* (m); heap or mound, describing tubercle array on plates; noun in apposition.

*Holotype*. BU 2875, almost complete articulated specimen (counterpart lacking), with latex cast. Only known specimen.

*Diagnosis*. *Palaeoscolex* characterised by subcircular plates in which tubercles are concentrated into one or two large central mounds, but with additional small projections over upper surface; platelets and microplates indistinct, rounded, but of different sizes, some with weak central mound.

*Locality and Horizon.* Section HB 2 (herein), Howey Brook Main Feeder SSSI, Gelli Hill, Llandrindod, Powys, Wales; Upper *Didymograptus murchisoni* Shales, Llanvirn.

*Description.* Uncoiled (U-shaped) specimen, width 0.6-0.7 mm, length exceeding 9.5 mm, lacking terminations. Width approximately constant over observed length, with slight expansion at irregular intervals, typically 0.5-1.0 mm. Ornament of approximately 20 plate annuli per mm, 18-20 plates per annulus. Annuli separated by alternating bands of platelets and microplates; segment boundaries appear to coincide with centres of microplate bands.

Plate diameter typically 25-30 μm, subcircular with scalloped/irregular margins (not thought to be preservational because of retention of fine granules); circumferential lobes or projections average 2-5 μm separation, with maximum radial indentation 2 μm. Central 3-8 μm raised into complex central peak, comprising 5-10 superimposed tubercles. Height of central peak uncertain, but probably exceeds 5 μm.

Remaining surface generally smooth, but marked by frequent 1-μm scale granules or minor tubercles. Surface steepens at margin, with increased granule density.

Platelets and microplates similar in form, with platelets generally slightly larger; distinction is weak among isolated examples. Size range of platelets 1-2 μm, rarely greater; microplate diameter typically 1 μm. Mostly subcircular to elliptical, with major/minor axis ratio sometimes exceeding 2. All platelets smooth, but oval and lobate outlines occur occasionally. Platelets primarily non-interlocking, although some adjacent pairs show mutually coherent irregularities, and usually separated by 1-3 μm. Examples of both platelets and microplates with small central mound, although platelets more commonly. Mound generally smooth, lacking obvious constituent tubercles.

*Discussion.* In overall morphology and size, *P. agger* closely resembles *P. aff. piscatorum* sp. nov. The species are distinguished by the substantially greater spacing of plates of *P. agger*, and the morphology and size of plates and platelets. The central, irregular concentration of tubercles appears unique among described taxa (although some form of central peak is seen among several species described by Müller and Hinz-Schallreuter (1993)), and is sufficient to distinguish the species from all others. This character clearly separates the species from *P. piscatorum*, and suggests a reasonable disparity between Anglo-Welsh species, as has been found among well-preserved faunas elsewhere (Kraft and Mergl 1989; Müller and Hinz-Schallreuter 1993).

*Palaeoscolex* aff. *piscatorum* Whittard, 1953

Fig. 5.1.1 a, b; Plate 15, figs 1-8

*Material.* BU 2874 Single specimen comprising approximately 4 mm of articulated trunk, part only, and a fragment of counterpart mounted on SEM stub and Au-coated. A latex cast of the part has been prepared.

*Locality and horizon.* Pass northeast of Bwlch-y-Cefn, Builth-Llandrindod Inlier, Powys, Wales; ashy siltstones in lower *D. murchisoni* Biozone, Llanvirn.

*Diagnosis. Palaeoscolex* with cuticular elements of three types: large tuberculate plates, subcircular, with typically 6-7 marginal nodes, range 4-12, and often an additional central node; platelets of polygonal to irregular form, non-turberculate, and up to 0.1 of the diameter of the plates, disposed between every other pair of plate rows; microplates, similar in form to platelets, but of slightly smaller size, arrayed in remaining spaces between plate rows.

*Description*: Only posterior portion seen, length 4 mm. Width constant, 0.8 mm in compressed state over observed length, except for rapid tapering at termination. Ornamentation of single-file annuli of primary plates, separated by regions of secondary platelets and tertiary microplates in alternation. Segments (probably metameric), inferred from repeating units, consist of two rows of plates; platelets and microplates alternate between plate annuli. At least 120 annuli (60 segments) in specimen BU 2874.

Typically 28-32 plates per annulus (14-16 per half-circumference), 35-45 μm in diameter, referable to form genus *Hadimopanella*: subcircular, truncated shallow cones, with small superimposed tubercles. Tubercle arrangement roughly circular, around crown edge, up to twelve; central tubercle often larger than others. Aberrant forms containing only four have been observed, and tubercle prominence is variable. Some show abundant, minute granules, in addition to primary tubercles, sometimes

sufficiently large to grade into primary tubercles. Granules usually concentrated close to plate margins.

Platelets arrayed in bands between primary plate annuli. Subcircular to polygonal in outline, approximately 0.05-0.1 of plate diameter (2-4 μm), having no visible ornamentation. Microplates morphologically similar to platelets, unornamented, but typically 0.8–1.5 μm in diameter, reaching maximum of nearly 2 μm. The distinction between platelets and microplates is sufficently slight to be unclear in isolated examples, but is readily observed when arrayed in bands.

*Discussion*: This specimen is morphologically very similar to the type species, *P. piscatorum* Whittard, from the Tremadoc of the Welsh Borders. The only obvious difference lies in the form of the platelets; in *P. piscatorum*, they resemble miniaturised plates, including ornament, while in the present specimen they are essentially smooth, slightly enlarged microplates. Although length and segment number are not useful in comparison with an incomplete specimen, the width is approximately double that observed here, with double the number of plates (Conway Morris 1977, p. 86). Without the use of SEM on preserved platelets and microplates, the two species would be essentially identical. Plate morphospace variability between the species overlaps to a large degree, and size differences could be attributed to different growth stages, especially given the argument for moulting described by Muller and Hinz-Schallreuter (1993).

The same discussion on morphological comparisons with other species could be performed as in Conway Morris (1997), and need not be repeated in detail. In addition to these remarks, the occurrence of morphologically similar platelets and microplates is also seen in *Rhomboscolex chaoticus* (Muller & Hinz-Schallreuter

1993, text-fig 9B, p. 573), but plate morphology is very distinct. The Anglo-Welsh species are probably more closely related to each other than to the material described from elsewhere, although with perhaps the greatest similarity to the Bohemian species *Gamoscolex herodes* (Kraft and Mergl, 1989, pls 2-6, 8 fig. 3).

The palaeogeographical distance between the sites in the Anglo-Welsh region is slight, and the inferred distances from land masses is similar (Anderton *et al.* 1977; Cope *et al.* 1992). All Ordovician occurrences of *Palaeoscolex* occur in pale grey siltstones or shales, with a typical associated fauna of trilobites, graptolites, sponges and/or inarticulate brachiopods. Given the age difference of around 30 Ma, the morphological similarity of *P. piscatorum* and *P. aff. piscatorum* is noteworthy. In the Anglo-Welsh region, biostratigraphic potential appears to be minimal, although other lineages may have evolved more rapidly.

Indeterminate palaeoscolecid

Pl. 14, figs 7, 8

*Material.* BU2876 Poorly-preserved fragment containing several tens of plates; counterpart Au-coated for SEM.

*Locality and Horizon.* Section BG 1 (D), herein, Bach-y-Graig SSSI, Llandrindod, Powys, Wales; lower *H. teretiusculus* Biozone, Llanvirn.

*Description.* Plates subcircular, 40-100 μm diameter, preserved as fractured and fragmented phosphatic material. Plates dominantly smooth, perhaps with small, isolated tubercles on crown, but lacking large central mound or abundant large tubercles. Plate margin apparently smooth, lacking indentations. Approximate plate annulus separation 50 μm; plate separation within annulus less than 30 μm. Platelets and microplates obscure, and segment boundaries invisible.

*Discussion.* Although insufficient characters are preserved for descriptive purposes, the fragment appears distinct from the two described British species in plate morphology. Although plates are disguised by detritus and remnant phosphatic material, the central boss of *P. agger* is certainly absent. Occasional large tubercles may exist, but are not arrayed in the circular pattern that is dominant in *P. piscatorum* and *P.* aff. *piscatorum*.

Although preservation is poor, the significance of this specimen lies more in its implications for palaeoscolecid distribution. The Bach-y-Graig sequence was deposited under dominantly anoxic conditions, with no evidence of benthos immediately below the bentonite BG 1. Temporary benthic oxygenation following the ash deposition resulted in colonisation by ostracodes, inarticulate brachiopods, conodonts, rare trilobites and occasional sponges, in the same horizon as the palaeoscolecid. The upper surface of the bentonite contains irregular, shallow burrows with diameter up to 1.0 mm. Although the dimensions of the present specimen are unknown, the specimens described above are of very similar diameter. If palaeoscolecids were dominantly infaunal, burial of articulated palaeoscolecids would have occurred frequently. Preservation would then have relied on a lack of subsequent bioturbation or physical reworking, and would have been favoured by brief benthic oxygenation events.

## 5.5 References

ANDERTON, R., BRIDGES, P. H., LEEDER, M. R. AND SELLWOOD, B. W. 1979. *A Dynamic Stratigraphy of the British Isles*. Unwin Hyman, London; 301 pp.

BATHER, F. A. 1920. *Protoscolex latus*, a new "Worm" from Lower Ludlow Beds. *Annals and Magazine of Natural History* Ser. **9**, vol. **5**, 124-133.

BENGTSON, S. 1977. Early Cambrian button-shaped phosphatic microfossils from the Siberian platform. *Palaeontology* **20**, 751-762.

BERRY, W. B. N. 1977. Ecology and Age of graptolites from graywackes in eastern New York. *Journal of Paleontology* **51**, 1102-1107.

BOOGAARD, M. VAN DEN 1988. Some data on *Milaculum* Müller, 1973. *Scripta Geologica* **88**, 1-25.

BROCK, G. A. AND COOPER, B. J. 1993. Shelly fossils from the Early Cambrian Wirrealpa, Aroona Creek and Ramsay Limestones of South Australia. *Journal of Paleontology.* **65**, 758-787.

CONWAY MORRIS, S. 1977. Fossil priapulid worms. *Special Papers in Palaeontology* **20**, 155pp.

CONWAY MORRIS, S. 1997. The cuticular structure of the 495-Myr-old type species of the fossil worm *Palaeoscolex piscatorum* (?Priapulida). *Zoological Journal of the Linnaean Society* **119**, 69-82.

CONWAY MORRIS, S. & ROBISON, R. A. 1986. Middle Cambrian priapulids and other soft-bodied fossils from Utah and Spain. *The University of Kansas Paleontological Contributions* **117**, 22 pp.

COPE, J. C. W., INGHAM, J. K. AND RAWSON, P. F. 1992. Atlas of palaeogeography and lithofacies. *The Geological Society Memoir* **13**, 153 pp.

ELLES, G. L. 1939. The stratigraphy and faunal succession in the Ordovician rocks of the Builth-Llandrindod Inlier, Radnorshire. *Quarterly Journal of the Geological Society* **95**, 338-445.

GEDIK, I. 1977. Orta Toroslar'da konodont biyostratigrafisi. *Türkiye Jeoloji Kurumu Bülteni* **20**, 35-48 [in Turkish, with English abstract].

GLAESSNER, M. F. 1979. Lower Cambrian Crustacea and annelid worms from Kangaroo Island, South Australia. *Alcheringa* **3**, 21-31.

HINZ, I., KRAFT, P., MERGL, M. & MÜLLER, K. J. 1990. The problematic *Hadimopanella*, *Kaimenella*, *Milaculum* and *Utahphospha* identified as sclerites of Palaeoscolecida. *Lethaia* **23**, 217-221.

HOU, X. & BERGSTROM, J. 1994. Palaeoscolecid worms may be nematomorphs rather than annelids. *Lethaia* **27**, 11-17.

JONES, O. T. AND PUGH, W. J. 1949. An Early Ordovician shoreline in Radnorshire, near Builth Wells. *Quarterly Journal of the Geological Society* **104**, 43-70.

KRAFT, P. AND MERGL, M. 1989. Worm-like fossils (Palaeoscolecida; ? Chaetognatha) from the Lower Ordovician of Bohemia. *Sbornik Geologische Ved Palaeontologie* **30**, 9-36.

MIKULIC, D. G., BRIGGS, D. E. G. AND KLUSSENDORF, J. 1985*a*. A Silurian soft-bodied biota. *Science* **228**, 715-717.

MIKULIC, D. G., BRIGGS, D. E. G. AND KLUSSENDORF, J. 1985*b*. A new exceptionally preserved biota from the Lower Silurian of Wisconsin, USA. *Philosophical Transactions of the Royal Society of London.* B**311**, 75-85.

MÜLLER, K. J. AND HINZ-SCHALLREUTER, I. 1993. Palaeoscolecid worms from the Middle Cambrian of Australia. *Palaeontology* **36**, 549-592.

OWENS, R. M., FORTEY, R. A., COPE, J. C. W., RUSHTON, W. A. & BASSETT, M. G., 1982. Tremadoc faunas from the Carmarthen district, South Wales. *Geological Magazine* **119**, 1-33, 8 pl.

ROBISON, R.A., 1969. Annelids from the Middle Cambrian Spence Shale of Utah. *Journal of Paleontology* **43**, 1169-1173.

ULRICH, E. O. 1878. Observations on fossil annelids, and descriptions of some new forms. *Journal of the Cincinnatti Society of Natural Hist*ory, **1**, 87-91.

WANG CHEN-YUAN 1990. Some Llandovery Phosphatic microfossils from South China. *Acta Palaeontologica Sinica* **29**, 554-556, 2 pl.

WHITTARD, W. F. 1953. *Palaeoscolex piscatorum* gen. et sp. nov., a worm from the Tremadocian of Shropshire. *Quarterly Journal of the Geological Society*, **109**, 125-135.

ZHANG XI-GUANG & PRATT, B. R. 1996. Early Cambrian Palaeoscolecid cuticles from Shaanxi, China. *Journal of Paleontology*, **70**, 275-279.

# 6. SYSTEMATICS AND PALAEOBIOLOGY: ECHINODERMS

## 6.1 INTRODUCTION

British Ordovician echinoderms are moderately well documented, with most monographic works (Ramsbottom 1961; Spencer 1914-1940) based largely on Ashgill material from the Girvan district of Scotland, and in need of revision. Avalonian faunas have not been treated comprehensively, and are poorly represented in the literature. Ordovician echinoderm localities of the Welsh Basin tend to be non-diverse (often monospecific), and while there have been several isolated references in recent decades, the literature is extremely incomplete at this stage. Asteroids have been rarely described since Spencer (1940), and Spencer and Groom (1934), although Dean (1999) has restudied most Ordovician material (primarily Scottish). North American asteroids were recorded by Schuchert (1915) and Branstrator (1982).

Coronates were included in a monograph of pelmatozoan columnals (Donovan 1986, 1989, 1998), while cystoids were discussed by Donovan and Paul (1985), and monographed by Paul (1973, 1984, 1997). The rarity of pre-Ashgill cystoids in Britain suggests a limited native fauna prior to widespread immigration in the late Ordovician. The first British parablastoid was described from the Arenig of South Wales by Paul and Cope (1982).

Crinoids have a far more abundant record in the Welsh Basin, but even these are rare and non-diverse prior to the Caradoc. Lower Ordovician taxa were described by Donovan (1984, 1985, 1986, 1989), Donovan and Cope (1989), Donovan and Gale (1989), Bates (1965, 1968) and Cope (1988), while Donovan and Veltkamp (1993) described a Welsh Ashgill fauna. Laurentian faunas have been well described, including Scottish Caradoc material (Ramsbottom 1961; Donovan 1992), but these

taxa appear to bear little resemblance to Avalonian communities. The Arenig of Morocco has yielded a single species of *Ramseyocrinus* Bates (Donovan and Savill 1988), suggesting greater affinity with the relatively unstudied areas to the palaeogeographic south.

Although the material described here represents by far the most diverse pre-Caradoc echinoderm community known from the Welsh Basin, a monographic treatment is not intended. The rate of discovery of new material suggests that greater diversity should be anticipated before such an exercise would be useful. The aim here is to describe the new taxa and place them in context with previously described species, in order to indicate the significance of echinoderms in Lower Ordovician, nearshore communities of Wales.

The material was collected from exposures on the southeast ridge of Llandegley Rocks, Powys; refer to 2.2.1 and 2.2.2 for locality data.

## 6.2 Taphonomy

As with most echinoderm material from the Welsh Ordovician, preservation is almost entirely mouldic. However, as with other organisms from this locality, the quality of resolution far exceeds that predicted from matrix grainsize (up to 1 mm), a feature due primarily to marginal silicification. In order to preserve articulated remains, massive, episodic deposition was necessary. The preservation of undistorted *in situ* root structures precludes homogeneous reworking of sediment, although this is suggested by the ubiquity of sponge spicules within all beds. It appears that sedimentation (or redistribution of sediment) was episodically rapid enough to bury the original surface to a depth unapproachable by subsequent reworking.

In general, the degree of compaction and/or collapse of calyces is inversely proportional to the fidelity of surface detail, with the most perfectly preserved specimens almost entirely flattened. Columns are often uncompressed, although many of the best-preserved show partial flattening, with brittle fracture of lateral and/or vertical extremities; the fracturing is similar to that of compressed nautiloids. Thin sections of a pleuricolumnal show the mould to comprise a thin siliceous veneer, in which crystallites grew inward from both surfaces; it is this veneer which fractures brittly. In some material, the organic surface film may have been silicified prior to decay, and simultaneously with calcite dissolution; in most cases, however, silicification indurated the surrounding matrix, prior to calcite dissolution. Indeterminate crinoid sp. B contains an irregular mass of silicified material that does not resemble plates; this possibly also represents degraded soft tissue. However, calyces do not show breakage across plates, as anticipated for pre-compaction silicification. In most specimens, silicification occurred after internal decay, and collapse, although the remains were largely undisturbed during this time. A degree of lithological compaction may have been involved at the most important horizons, particularly as these are often related to bentonites, suggesting an ash-rich matrix.

This type of preservation has not been previously described. The most significant features are marginal silicification of, probably, soft tissue against a skeletal template, and compaction of the siliceous veneer, resulting in brittle fracture. The soft-tissue silicification is comparable with that of sponges (section 4.2) from the same site, while siliceous replacement of skeletal calcite occurred in some trilobite fragments. Original calcite is rarely preserved at this site, forming occasional calcareous nodules, although one such nodule contains abundant *Iocrinus* brachials.

## 6.3 SYSTEMATICS

Unless otherwise stated, the type series comprise all known specimens. Specimens are deposited in the Lapworth Museum, University of Birmingham.

### Order DIPLOBATHRIDA Moore and Laudon, 1943b

### Family RHODOCRINITIDAE Bassler, 1938

*Diagnosis* (after Donovan *et al.* 1996*)*. Dicyclic crinoids with an elongate conical to globular crown. Radials separate. Interprimibrachial and intersecundibrachial plates large, regularly arranged and well-sutured into calyx. Arms strongly pinnulate. Column rounded and strongly heteromorphic; columnals bear broad, flanged epifacets.

*Remarks.* The familial diagnosis does not distinguish between taxa bearing distinct CD interrays, and radially symmetric forms. Despite this obvious difference between *Cefnocrinus* gen. nov. (and many other rhodocrinitids) and the rhodocrinitid genus *Balacrinus* Ramsbottom, plate arrangement in other rays is very similar. Posterior variation may be sufficient to subdivide the family following a full revision, but is not appropriate here.

### Genus CEFNOCRINUS *gen. nov.*

*Etymology*. After Welsh *cefn*, hill, for the hilltop outcrop overlooking Bwlch-y-Cefn farm, Powys. Gender *m*.

*Diagnosis.* Calyx globular, infrabasals very small, obscured by articular facet. CD interray distinct, median anal ridge separated from D ray by minimum two plates at all points; all others possessing three second-row interradials, and up to three further

rows with four or more plates. Radials heptagonal, first primibrach hexagonal; ray ridges pronounced. Arms highly pinnulate, uniserial; branching isotomously, once within calyx, up to twice thereafter.

*Type species. C. nodosus sp. nov.*

*Discussion. Cefnocrinus* shows most similarity to *Pararchaeocrinus* Strimple and Watkins, 1955, from the Champlainian of Oklahoma and Tennessee (Kolata 1982), but is distinguished by plate arrangement in the CD interray. In *Pararchaeocrinus*, the anal series is separated from the D ray by one interradial in the first two rows. The only Avalonian rhodocrinitid, *Balacrinus* M'Coy, possessed radial symmetry, while all other American representatives typically had only one or two plates resting on interradials. In some "aberrant" specimens of *Archaeocrinus*, the number of overlying plates may vary within an individual; it is not known whether these represent a distinct species (Kolata 1982).

*Cefnocrinus nodosus* sp. nov.

Text-fig. 6.3.1, Pl. 16, figs 1-10; Pl. 17, figs 8, 9.

*Etymology*. Latin *nodusus*, knotty; describing ray ridges.

*Holotype*. BU2823 External mould of rays B-D, including complete pinnulate arms; stem lacking.

*Paratypes.* BU2824 External mould of articulated calyx and partial stem, showing basals; BU2825-2838 14 partial external moulds of articulated calyces; BU2839, 2840 external moulds of arm arrays; BU2841, 2842 pleuricolumnals only.

*Locality and horizon.* Volcanogenic sandstones, southwest ridge of Llandegley Rocks, Powys, Wales. *D. artus – D. murchisoni* boundary, Llanvirn.

*Diagnosis. Cefnocrinus* with expanded nodes on ray ridges at plate boundaries. External plate surface strongly and regularly granular. Most arms branch three times.

*Description.* Calyx slightly higher than wide. Plates strongly granular on external surface; granules often aligned, with typically five granules per diameter, in second-row interradials. No radiating plate ridges. Axial ray ridges extremely prominent, smooth; nodes initiate at centre of each plate, and occupy over half of facet width. Five interbasals, very small, and invisible laterally. Radials heptagonal, nearly twice as high of basals, and two-thirds as wide. Basals support one large hexagonal interradial, on which rest two hexagonal, and one heptagonal, plates in the second row. At least two further rows above, containing three to five plates (incompletely seen). First primibrach hexagonal, near-regular, resting on truncate top of radial, and in lateral contact with second-row interradials. Second of two primibrachs hexagonal, with low lateral apices, approximating to pentagonal. First secundibrach hexagonal;

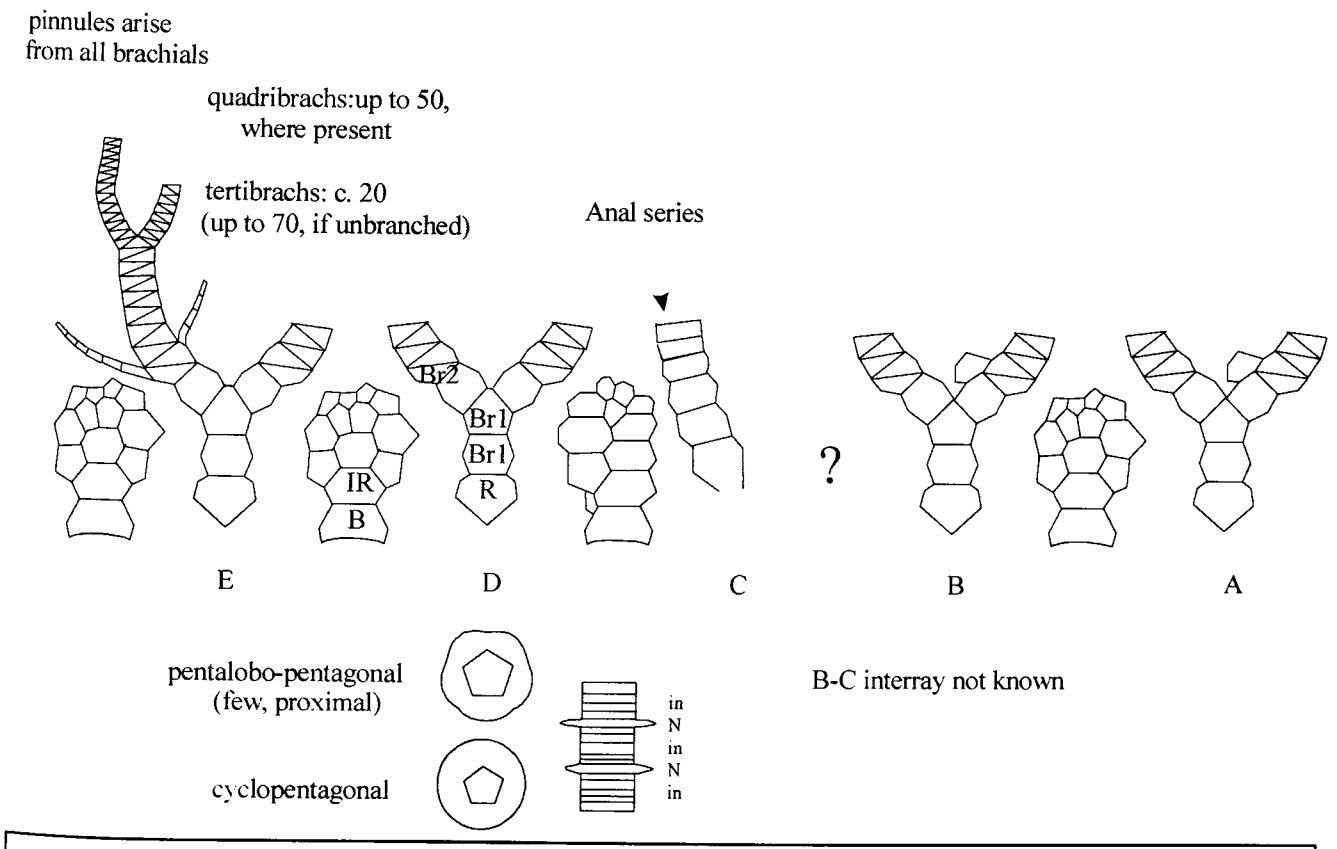


Figure 6.3.1: *Plate structure in* Cefnocrinus nodosus *sp. nov., based on several specimens; R: radial; B: basal; IR: interradial; Br1: primibrachial; BR2: secundibrachial.*

ray ridges expand to entire width of facet, maintained thereafter; second secundibrach trapezoidal with pinnule, probably fixed, directed outward from ray axis. Third secundibrach also trapezoidal, with inward-facing pinnule; secundibrachs triangular thereafter.

Posterior interray shows markedly differing plate arrangement, only seen in Pl. 16, figs 1 and 3, and poorly in Pl. 17, fig. 8. Hexagonal interradial rests on basal, and small plate on D-ray side; supports two second row plates (one pentagonal, one hexagonal, arranged diagonally), supporting two more in turn; a third is nearly in contact centrally, and treated as second row. Third row contains four small plates, higher rows not seen. C radial not certainly seen, proximal four anal series plates hexagonal, grading to pentagonal/rectangular distally. Anal tube slender, at least as high as secundaxil (*circa* secundibrach 20). Few plates seen between anal series and C ray; BC interray not certainly known.

Arms uniserial to immature biserial, strongly pinnulate, branching once in calyx, twice thereafter. Proximal pinnules with up to twenty ossicles, proximally twice as long as wide, becoming more equant distally. Arms recurved towards axis distally, after each branching, following initial divergence of 70-100°. Branching points vary significantly between samples, but secundaxil typically at secundibrach 15-25; tertibrachs average 20-25, or up to 70 if unbranched thereafter. Tegmen not seen.

Column heteromorphic, with typically five times as many internodals as nodals; nodals more densely spaced proximally. Internodals of two orders, the larger distributed sporadically; nodals sometimes with one or two grooves, often incomplete, on curved surface. Lumen about two-fifths of nodal diameter, pentagonal. Broad areola with radial striae. Articular facets of nodals slightly raised from rim region; internodals with flat facets. Associated pleuricolumnals suggest that dististele became

smooth holomorphic, although no complete columns are known. An isolated, slightly cirrate terminal coil (Pl. 2, fig. 10) may be referable to this species, but without certainty.

Smaller specimens differ in an extension of the ray ridges towards the base, merging into prominent raised basals to form a continuous ring (paratype BU 2829). Although traces of convexity occur in basals of fully mature specimens, the immature condition is much more pronounced. Granules also appear poorly developed, but this may be taphonomic.

*Discussion.* In general form and interradial plate arrangement, *Cefnocrinus nodosus* closely resembles *Balacrinus basalis* M'Coy (1850), abundant in the Caradoc of Central Wales (Ramsbottom 1961; Donovan *et al.* 1996). However, in *B. basalis* the radials are pentagonal, the CD interray is indistinguishable from all others, and the arms are unbranched after leaving the calyx. These characters are easily sufficient for generic distinction, although interradial plate arrays are almost identical in the second and third rows. Brachial and interbrachial plate structure is also closely comparable, although pinnule onset is delayed in *B. basalis*, with additional rows of fixed interbrachials. Pinnule and stem structure differ only slightly, while plate ornament is clearly distinct. The interradial plate structure is more consistent than in *B. basalis*, and there appear to be fewer rows of interbrachials, although these may be hidden by pinnules in *C. nodosus*.

Greater similarity is shown with members of the diverse North American fauna. The lower Caradoc *Pararchaeocrinus decoratus* Strimple and Watkins, 1955, is distinguished on generic characters (Kolata 1982, p. 199), where the anal series is separated from the D ray by only one plate in the first two rows above the basal. The

small plate on the D side of the CD basal is displaced to the C side in *P. decoratus*, and the adjacent first row plate mirrored. Other interradial arrays are similar to *C. nodosus*, although central plates of each row are displaced upwards. Plates show radiating ridges in *P. decoratus,* and are non-granular. The expanded nodes of *C. nodosus* appear unique among otherwise similar, described species, although several, including *P. decoratus*, show prominent ray ridges.

Llanvirn camerates from North America include the Newfoundland rhodocrinitid *Trichinocrinus terranovicus* Moore and Laudon, 1943a (Ausich *et al.* 1998). The calyx contains many less interradial plates than *C. nodosus*, and does not appear to be closely related. The Laurentian Middle Ordovician (early Caradoc) genus *Archaeocrinus,* exemplified by *A. elevatus* Ramsbottom (1961), shares the heptagonal radials and only three to four rows of interbrachials, although only two plates are present in the second row (three on posterior). The CD interray of *C. nodosus* closely resembles a typical interray of *A. elevatus*. Although the interbasals of *A. elevatus* are pronounced, interbasals of the type species *A. lacunosus* Billings (1857) are small, often hidden by the stem as in *C. nodosus*. The arms of *A. elevatus* are unknown, although in *Archaeocrinus* generally, they are biserial. *C. nodosus* thus appears to be morphologically intermediate between *Archaeocrinus* and the *Balacrinus* lineage. Several other Middle Ordovician, Laurentian species possessed two plates resting on the first interradial, and all are easily distinguishable. Some species, e.g. *Cotylacrinna sandra* Brower, 1994 possessed a relatively compact calyx, with both primibrachs in contact.

This is the second recorded occurrence of *Balacrinus*-like taxa in the Welsh Llanvirn; an undescribed species was mentioned by Donovan & Cope (1989), but is in a private collection, and unavailable for study (S. K. Donovan, *pers. comm.*).

Subclass INADUNATA Wachsmuth and Springer, 1881

Order DISPARIDA Moore and Laudon, 1943b

Family IOCRINIDAE Moore and Laudon, 1943b

Genus IOCRINUS Hall, 1866

*Type species.* By monotypy, *Heterocrinus*? *(Iocrinus) polyxo* Hall, 1866, a junior subjective synonym of *Heterocrinus subcrassus* Meek and Worthen, 1865, Richmond "Series", Ohio.

*Diagnosis* (after Donovan and Gale 1989). A genus of Iocrinidae with a pentagonal, subpentagonal, or stellate uncoiled stem.

*Iocrinus llandegleyi* sp. nov.

Text-fig. 6.3.2; Pl. 17, figs 1-7.

*Holotype*. BU2843 External mould of calyx with partial counterpart, showing proximal stem and part of all arms, including radianal. Three branches observed in most complete arm.

*Paratypes*. BU2844 external mould of calyx with four partial arms and poor anal column; BU2845 partial crown, including part of anal column; BU 2846 slightly dissociated calyx with proximal stem fragments; BU2847 calyx with arms, sectional view; BU2848 partial calyx in ventral view; BU2829 calyx with arm mass and anal column; BU2850 semi-articulated arm mass.

*Locality and horizon.* Volcanogenic sandstones, southwest ridge of Llandegley Rocks, Powys, Wales. *D. artus – D. murchisoni* boundary, Llanvirn.

*Diagnosis*. *Iocrinus* with heteromorphic, pentastellate proxistele, through pentagonal to subcircular distally, and longitudinally ridged calyx. Radials slightly wider than high; basals about two-thirds the height of radials. Primibrachs 5-8, secundibrachs 4 or 5, tertibrachs 4 or 5, quartibrachs at least 4.

*Description*. Calyx about 25% wider than high in uncompressed specimens, conical, with slight convexity in lateral view. Calycal plates are independently convex, and basals strongly ridged as a result of the pentastellate proxistele; radials slightly less so. Basals variable, but generally wider than high. Radials 1.0 to 1.2 times wider than high, and around 1.5 times as high as basals. Radials pentagonal with slightly concave upper facet. Primibrachs usually 5 to 7, rarely 8, about twice as wide as high. Distal brachials approximately as high as wide. Anibrachial pentagonal, bearing anal column on right branch. Left branch has three post-anibrachial primibrachs.

Complex anal column of typically iocrinid form, at least ten times calycal height. Opposed lateral ribs with approximately equidimensional plates are proximally rounded, rapidly becoming angular after about 10 ossicles. Distal region approaches tetragonal in section. Tallest rib plates slightly exceed 1 mm in height, and correspond approximately to two adjacent plates.

Stem pentastellate in five most proximal columnals, rapidly grading to pentagonal, then subcircular. Distal end not certainly seen, although an isolated, highly cirrate coil (Pl. 3, fig. 10) may be attributable to *Iocrinus*, as there is some similarity to that of the iocrinid *Caleidocrinus turgidulus* (below).

*Discussion*. Among the British *Iocrinus*, only *I. pauli* Donovan & Gale and, following a re-examination of the holotype (BGS GSM92145), *I. shelvensis* Ramsbottom, from the Llanvirn of Shropshire, have a pentastellate proxistele, a character ubiquitous

among the North American forms. *I. llandegleyi* differs from *I. pauli* in the number and distribution of brachials, the lack of transverse ribbing between the upper part of the radials, and the height:width ratio of the brachials. *I. shelvensis* is easily distinguished by the highly elongate calyx and heteromorphic column. *I. llandegleyi* appears morphologically intermediate between *I. pauli* and *I. whitteryi* Ramsbottom 1961, (although closer to the latter) in terms of a general widening and smoothing of the calyx, and increasing robustness of the crown.

The North American Ordovician crinoid fauna is far more diverse than that of the Anglo-Welsh region, reflecting the presence of an extensive carbonate shelf (Eckert 1988). Donovan & Gale (1989) proposed that *I. pauli* and the American forms evolved from a smooth, presumably pentagonal-stemmed form, but the lack of the supposedly derived characters in later British species suggests the reverse. If the primitive proxistele were rounded to pentagonal, both Anglo-Welsh and American species of *Iocrinus* must have evolved a ribbed calyx and pentastellate proxistele independently, before the isolated Avalonian population largely reverted to the original state. A pentastellate proxistele in the nearest common ancestor would have required the pentagonal condition to be derived only in the *I. whitteryi* lineage of Avalonia.

*Iocrinus* cf. *whitteryi* Ramsbottom, 1961.

Text-fig. 6.3.2; Pl. 18, figs 1, 2, 4-6, 8.

*Material*. BU2851-2859 9 partial or complete crowns, with variable preservational quality.

*Occurrence*. Llanvirn (*D. artus – D. murchisoni* boundary): volcanogenic sandstones, southwest ridge of Llandegley Rocks, Powys, Wales.

*Description.* Calyx bowl-shaped, about twice as wide as high, with smooth plates. Basals just under half the height of radials. Radials about 1.5 times as wide as high, with slightly concave facet comprising entire width of plate. Plates not independently convex. Primibrachs up to three times as wide as high, typically numbering 5-7, occasionally 8. Secundibrach and tertibrach numbers usually 4 (3-5); quadribrachs and pentabrachs around 8 or higher. Distal brachials only slightly wider than high. Food grooves very deep (two-thirds of brachial depth), with thin chevron plates parallel to sides, visible in thin section of calcareous material; these may be collapsed cover plates.

Superradianal pentagonal, with anal column on right side. Anal column always dislocated, but close association implies conspecifity; nearly as long as arms, tapering smoothly, with two opposed, prominent ribs of approximately equidimensional plates.

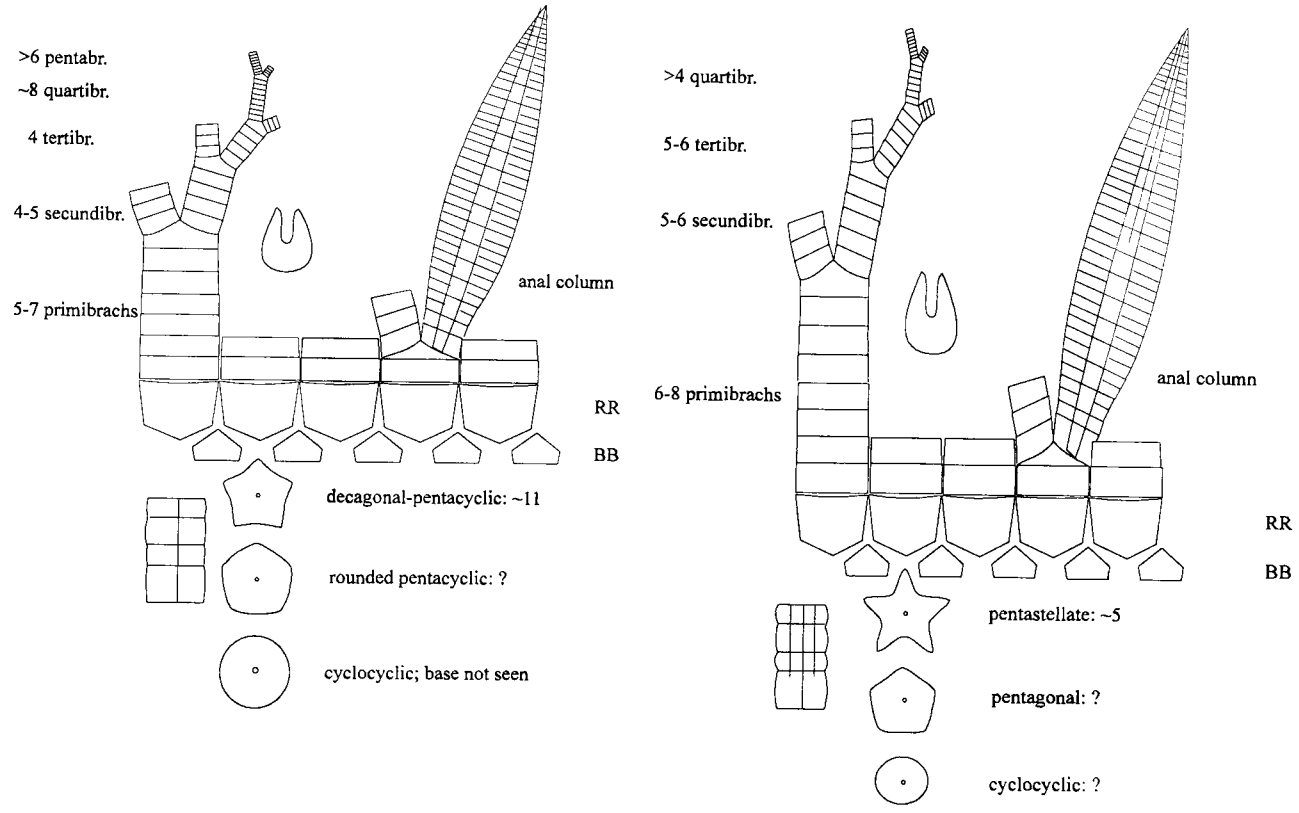


*Iocrinus* cf. *whitteryi* *Iocrinus llandegleyi* sp. nov.

Figure 6.3.2: *Plate arrangements and comparison of* I. *cf.* whitteryi *Ramsbottom 1961 and* Iocrinus llandegleyi *sp. nov.*

Rib plates up to 1 mm high, rounded proximally, but becoming angular distally to form median longitudinal ridges. Each plate corresponds approximately, but variably in height, to two adjacent, irregular ossicles. Distal end almost tetragonal in section, proximal part tetralobate.

Stem incompletely seen, but varies from pentagonal, or slightly concave pentagonal (slightly pentastellate) proximally, through rounded sub-pentagonal, to subcircular. Lumen very small, probably subpentagonal. Column heteromorphic, with alternating short and tall ossicles, each of similar width. Column narrower than primary and secondary brachials, but wider than tertibrachs.

*Discussion.* Comparison with the types of *I. whitteryi* is hindered by limited variation among the type material. Although proximal column morphology and primibrach number sometimes fall outside the strict diagnosis, examples of the present specimens concur with the description. For example, BU 2852 possesses five and seven primibrachs in adjacent rays. Although Donovan and Gale (1989) reported at least twelve primibrachs in the holotype, re-examination supports Ramsbottom's (1961) description of only seven, with the primaxil disguised. The Shropshire material shows the (incomplete) proximal column morphology only in BGS GSM85720, which is pentagonal, as in BU2854. No anal columns from Llandegley are preserved attached to *I.* cf. *whitteryi* calyces, but of several probable columns, none show the relatively large (2 mm high) rib plates of the *I. whitteryi* holotype (NHM E49603). This feature is of uncertain taxonomic significance, and insufficient to erect a new species, without sufficient data for statistical description; it is possible that the larger plate size reflects greater maturity. The stratigraphical difference of 15.5-23.5 Ma (Harland *et al.* 1989) between the two occurrences is unusually long for Ordovician echinoderms, which tend to be temporally restricted. However, this may be an artefact

resulting from the large number of characters available for description, which more readily facilitate taxonomic splitting than in other phyla.

Among other species, the pentagonal proxistele is shared with *I. brithdirensis* Bates, from the Llanvirn of North Wales. However, this differs substantially in the distribution and number of brachials. Of the other Ordovician species, *I. shelvensis* Ramsbottom and *I. pauli* Donovan & Gale are distinguished by the calyx and proxistele morphology, the shape of the radials and primibrachs, and by the number of secundibrachs. The North American species *I. crassus* and *I. subcrassus* are distinguished by the proximal column morphology, the shape of the radials and the numbers of brachials.

## Genus CALEIDOCRINUS Waagen and Jahn 1899

*Type species. C. multiramus* Barrande *in* Waagen and Jahn, 1899, by subsequent designation (Bassler 1938).

*Diagnosis* (after Donovan 1985). A genus of iocrinid possessing interbrachial plates.

*Remarks*. The generic and subgeneric descriptions were fully discussed by Donovan (1985), and need not be repeated here.

### Subgenus *Caleidocrinus (Huxleyocrinus)* Donovan, 1985

*Type species. C. (H.) turgidulus* Ramsbottom, 1961, by original designation (Donovan 1985).

*Diagnosis* (after Donovan 1985). A subgenus of *Caleidocrinus* with exposed basala, broad, low radials and brachials with lateral depressions adjacent to plate surtures.

*Caleidocrinus* cf. *turgidulus* Ramsbottom, 1961.

Plate 19, figs 1,2 5, 6.

*Material.* BU2863 partial column and crown; BU2864 partial arm array; BU2865 radicular root structure; BU2866 short pleuricolumnal, showing facet morphology; all external moulds.

*Locality and horizon.* Volcanogenic sandstones, southwest ridge of Llandegley Rocks, Powys, Wales. *D. artus – D. murchisoni* boundary, Llanvirn.

*Description.* Calyx poorly seen, containing large, smooth radial up to 1.5 times as wide as high. Radials with strong cruciform depression at lateral margins. Basals low, triangular, probably in contact. Two arm bases preserved, each with three primibrachs; isolated arm mass shows three consecutive sub-isotomous bifurcations. Individual brachials slightly bulbous, successive ossicles decreasing in diameter upward to produce stepped outline; articular facets and dimensions of food groove not seen. Primaxils, secundaxils, *et seq.,* with central height approximately 1.5-1.8 times lateral height. Brachial width:height ratio decreases upwards; secundibrachs approximately as wide as high, basal primibrachs up to twice as wide as high. Interbrachial region poorly preserved but present; one moderately large, sub-triangular plate accompanied by up to five very small platelets above.

Proxistele slightly heteromorphic, although number of internodal orders is unclear. Nodals only slightly wider than internodals, and variably up to twice as tall; no vertical variation of stem thickness within proximal stem. Articular facet distinctive: small circular lumen surrounded by embossed pentalobate areola in positive relief on both surfaces; proportion of radius covered by areola highly variable

between two-thirds and one-sixth. Areola edge to exterior margin marked by articulating crenulae.

Root radicular, U-shaped, with local expansion of axis to twice normal diameter. Segmentation of expanded region faint, although isolated disarticulation confirms the described articular facet morphology. Segments with up to six smooth, sometimes branched cirri deployed over one-third (presumed lower) of axis area; arrangement irregular within and between segments.

*Discussion.* The specimens are easily referred to *Caleidocrinus* through the preserved morphology of calyx and arms. Ramsbottom (1961) and Donovan (1984, 1985) described *C. (Huxleyocrinus) turgidulus* from a similar or identical horizon on the Carneddau, north of Builth Wells, although with limited material. Abundant isolated stems are known from the same horizon on Gelli Hill (NMW 87519.1, 87519.2), but have not been described. Articular facet morphology is identical to the Gelli Hill specimens, but is unknown in the Carneddau material, but the column outline was described by Donovan (1984). Although arm morphology is similar to *C. (H.) turgidulus*, including slightly bulbous brachials, the arms of the present specimen appear more slender and generally attenuated; however, this may be taphonomic. The present specimens also lack the exterior brachial notches of *C. (H.) turgidulus*, interpreted by Ramsbottom (1961) as muscle attachment sites. It is possible, though unlikely, that this is also taphonomic, if marginal silicification occurred prior to soft-tissue decay (section 6.2). The visible development of interbrachial plates is very similar to that in *C. (H.) turgidulus*. Radial morphology is similar, and the lateral radial depressions appear identical. Consideration of the arm structure alone suggests

that the present specimens are not conspecific with *C. (H.) turgidulus*, although closely related; further specimens may show the variation to be taphonomic.

One other species is known from Bohemia, which Donovan (1985) referred to *C. (Caleidocrinus) multiramus*. This subgenus is characterised by concealed basals, and is certainly distinct from the present specimens on this basis, despite greater similarity in arm structure and brachial morphology. Articular facet morphology is poorly preserved, although one specimen (Donovan 1985; Figure 4B, p. 115) shows weak structures that may be equivalent to the pentalobate sculpture described here. Until details of the facet of *C. (H.) turgidulus* become known, possible relationships with the Bohemian species must remain uncertain.

Indeterminate crinoid sp. A

Pl. 19, figs 3, 4.

*Material*. BU2867, 2868 Articulated crowns with proximal stem fragments; external moulds, part only.

*Locality and horizon*. Volcanogenic sandstones, southwest ridge of Llandegley Rocks, Powys, Wales. D. artus – D. murchisoni boundary, Llanvirn.

*Description*. Calyx very small, indistinct, and partially obscured by broad, highly pinnulate arms. Only visible plate (radial?) probably pentagonal, with broad lower facet. Arms pinnulate (sub-cuneate), uniserial, branching sub-isotomously up to twice, after leaving calyx; primibrachs about ten. Primaxil triangular, with first secundibrachs in lateral contact above, with vertical suture. Second branching occurs in some rays, at secundibrach 30-40. Arms diverge from calyx sub-horizontally, possibly recurved downwards initially, before orthogonal bend to vertical; undulating sub-parallel thereafter.

Column strongly heteromorphic, although with only two clear orders; nodal diameter around 1.5-1.6 times internodal. Proximal nodal to internodal ratio is approximately 2:1, rapidly approaching 5:1. Details of articular facet unknown, but nodals possess broad circular areola. All columnals subcircular in outline, nodals tending towards rounded subpentagonal proximally.

*Discussion.* Lack of information regarding the calyx prevents taxonomic description of this species, which is easily distinguished from other species of the Welsh Lower-Middle Ordovician. *Celtocrinus ubaghsi* Donovan and Cope, 1989 is the only other pre-Caradoc pinnulate crinoid described from Avalonia, and had clearly separable arm structure and column morphology. The Ashgill camerate *Xenocrinus*, which occurs in South Wales (Donovan and Veltkamp 1993), possessed tetragonal columnals. Two indeterminate camerate(?) crowns described by them differ in brachial morphology and pinnule arrangement. The rhodocrinitid genera *Balacrinus* and *Cefnocrinus* possessed much larger calyces, and ten arms.

The present specimens are unusual in several respects. There appear to be up to ten primibrachs, while most camerates possessed two. This feature alone would be sufficient to discount a camerate affinity in more recent forms, but primitive conditions are still poorly constrained. It is unclear how many (if any) brachials are fixed, but rapid divergence from the calyx suggests that most are free. While the calyx is generally obscure, the single large plate must, through space considerations, comprise one of a circlet of at most five. This resembles certain disparid inadunates, such as *Iocrinus*. Although pinnule development among Ordovician inadunates is rare, Guensberg (1992) described a hardground community that included the pinnulate disparid *Columbicrinus crassus*. This species differs greatly in arm

structure, however, with few primibrachs, and simple isotomous branching. The presence of pinnules arising from primibrachs is unusual among pinnulate inadunates. Column morphology, with sharply defined nodals and internodal, is more typical of camerates. Without knowledge of calycal plate arrangement, it is impossible to assign the specimens even to subclass; they represent either an aberrant, very early camerate, or an unusual, early cladid or disparid inadunate.

Indeterminate crinoid sp. B

Pl. 19, figs 8, 10.

*Material*. BU2869 Articulated specimen in oral view, with extensive part of column; isolated pleuricolumnals possibly referable to this species.

*Description.* Large multi-armed crinoid with poorly preserved calycal mass containing rare isolated plates. Plates strongly granular, as in *C. nodosus* sp. nov., maximum diameter at least 2 mm. Confused central mass of very small plates, and indeterminate reticulate structure may be dissociated tegmen, or soft tissue detritus. Diameter of central region at least 5 column diameters, up to 10 in places. At least ten thin arms, straight, non-pinnulate; commonly branching isotomously at approximately half length, but no more than twice. Column > 40 cm long , termination not seen, and very flexible; radius of curvature sometimes <5 column diameters, without breakage. Appears holomorphic, exterior with faint fine-scale ridges, but no indication of columnal boundaries.

*Discussion.* Too few definite characteristics are preserved for full description, although it certainly differs from all other specimens at this locality. The dual branching of non-pinnulate arms distinguishes it from *C. nodosus* and indeterminate crinoid sp. A, while the presence of large granular plates precludes an iocrinid

affinity. The column morphology also appears unique, and there are no obvious comparisons among known Welsh or North American taxa. No further distinction can be made without additional material.

## CYSTOIDS

*Remarks*. High-level taxonomy of the cystoids needs revision (Donovan *et al.* 1996), with both diploporites and rhombiferans regarded as polyphyletic. High-level terms are used informally until such a revision is completed.

## RHOMBIFERANS

### FISTULIPORITES

#### Superfamily CARYOCYSTITIDA Jaekel, 1918

#### Family ECHINOSPHAERITIDAE Neumayr, 1889

#### Genus ECHINOSPHAERITES Wahlenberg, 1821

#### Subgenus ECHINOSPHAERITES Wahlenberg, 1821

*Echinosphaerites (Echinosphaerites)* cf. *granulatus* M'Coy, 1846

Text-fig. 6.3.3.

*Material*. BU2870 Incomplete, flattened external mould of articulated theca; lacks stem, arms and oral structures.

*Locality and horizon*. Volcanogenic sandstones, southwest ridge of Llandegley Rocks, Powys, Wales. *D. artus – D. murchisoni* boundary, Llanvirn.

*Description*. Poorly preserved, slightly disarticulating, elliptical theca comprising well over 200 plates. Plate outlines extremely varied, including squares, octagons and

irregular polygons with reflexed angles. Plates entirely smooth, showing only faint localised traces of fistulipores; slightly swollen. Angles sometimes rounded, occasionally cuspate. Length-width ratio in excess of 1.5, but total length not seen.

*Discussion. Echinosphaerites s.l.* ranges from the (Upper Arenig?) Llanvirn to the Lower Ashgill, of Baltoscandia, North America, Avalonia, Bohemia, North Africa and China (Paul, 1997), although a Baltoscandian origin seems likely (Bockelie 1981). The genus is not known in Britain prior to the Caradoc. Of the two described British species, *E. (Striatospaerites) arachnoideus* Forbes is clearly distinguished by extensive plate ornament. *E. (E.) granulatus* is similar in all ways to the present specimen, although fistulipores are far more prominent in the type material, visible as granulation of plate surfaces. Without additional material revealing details of oral or brachial regions, or other specific morphology, the taxonomic assignment must remain uncertain.

A single specimen from the Dent Group (Caradoc – Ashgill) of Dent, North Yorkshire (Paul 1997) may be closer to the present specimen, although this also lacks critical morphological details. Plate morphology and size is closely similar, with comparable smoothness. The Dent specimen is tectonically deformed, and outline cannot be ascertained. The precise age and locality is unknown.

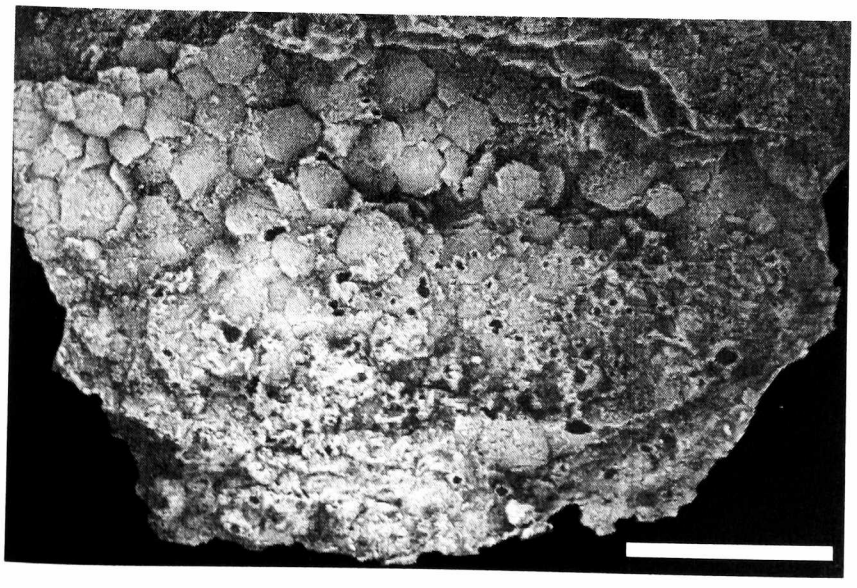

Figure 6.3.3: *BU 2870* Echinosphaerites *cf.* granulatus *M'Coy, 1846, from Llandegley Rocks, Builth Inlier; external mould of incomplete theca, collapsed, plate thickness preserved at top by pre-compaction marginal silicification. Scale bar 1 cm.*

Class ASTEROIDEA de Blainville, 1830

Family HUDSONASTERIDAE Schuchert, 1914

Genus PROTOPALAEASTER Hudson, 1912

*Type species. H. narrawayi* Hudson, 1912, from the Trenton of Canada.

*Diagnosis (after Donovan* et al. *1996).* Arms long, tending to fuse; carinals stout; mouth angle plates large and conspicuous.

*Remarks. Protopalaeaster* is a senior synonym of *Belaster* Spencer, 1916, according to Moore (1966), and accepted as such by Donovan *et al.* (1996). The oral surface of *H. narrawayi* was also discussed by Spencer (1916, p. 21).

*Protopalaeaster* cf. *simplex* Spencer and Groom, 1934

Plate 19, fig. 11.

*Material.* BU2871 single aboral surface with poorly preserved disc.

*Locality and horizon.* Volcanogenic sandstones, southwest ridge of Llandegley Rocks, Powys, Wales. *D. artus – D. murchisoni* boundary, Llanvirn.

*Description.* Almost complete specimen lacking one termination. Three long arms (>10 marginalia per row), one around 7, the other uncertain. Three ossicle rows per arm: bulbous, proximally-expanding radialia, and elongate, slightly overlapping, recurved superomarginalia. Any additional arm plates very small or absent; arms slender, tapering slowly. Mouth-angle plates large, preserved in one case only. All plates appear finely granular, but preservation insufficient for certainty. Disc poorly preserved, plates irregular; no clear arrangement.

*Discussion. B.* cf. *simplex* conforms closely with the described characters of *B. simplex* Spencer and Groom (Lower Caradoc, Rorrington), but is too imperfect to be ascribed to the species with confidence. *B. ordovicus* Spencer, 1916, from the Ashgill

of Girvan, differs in the form of superomarginalia, and possessed much more robust mouth-angle plates.

Family PROMOPALAEASTERIDAE Schuchert, 1914

Subfamily PROMOPALAEASTERINAE Schuchert, 1914

Genus PROMOPALAEASTER Schuchert, 1914

*Promopalaeaster*? sp.

Plate 19, fig. 7.

*Material.* BU2872 Single external mould of aboral surface; most aboral plates removed, showing collapsed oral surface plates.

*Locality and horizon.* Volcanogenic sandstones, southwest ridge of Llandegley Rocks, Powys, Wales. *D. artus – D. murchisoni* boundary, Llanvirn.

*Description.* Almost complete, but lacking clear terminations on all arms. Aboral plates well-preserved on one arm, less so on all others, comprising approximately 7 plates across proximal width. Plates small, rhomboidal, arranged in chevron pattern. Oral surface dominated by broad, short ambulacrals, generally opposing, but sometimes slightly offset. Adambulacrals/inferomarginals not seen; arm margins generally obscured by aboral plates. Ambulacrals separating proximally to form groove, one proximal arm-width long; plates become smaller towards mouth; distinct mouth-angle plates lacking. Disc small, unclear; plate circlets uncertain, although inner circlet of minute plates just visible, with presumed mouth, central.

*Remarks.* The only British species of *Promopalaeaster* listed by Owen (1965), *P. elizae* Spencer, occurs in the Ashgill of Girvan. It is distinguished from the present specimen by the larger number of apical plates, and by the presence of strong transverse ambulacral ridges; ambulacrals are significantly shorter in *P. elizae*.

Schuchert (1915) described *P. wilsoni* from the Middle Ordovician, but this is distinguished by many more aboral plates, and broad inferomarginals. A further eight Upper Ordovician species are noted by Spencer (1914, p. 98-99), and described by Schuchert (1915), of which *P. wykoffi* Miller and Gurley shows closest similarity to the present specimen. However, this species also possessed broader adambulacrals and inferomarginals, with arms containing many more, shorter ambulacrals. Although conforming to the generic characters of *Promopalaeaster*, the specimen is distinct from all described species in plate dimensions and proportions.

Subfamily MESOPALAEASTERIDAE Schuchert, 1914

Genus MESOPALAEASTER Schuchert, 1914

*Mesopalaeaster*? sp.

Pl. 19, fig. 9.

*Material.* BU2873 Damaged specimen showing two partial arms, in lateral and aboral views.

*Locality and horizon.* Volcanogenic sandstones, southwest ridge of Llandegley Rocks, Powys, Wales. *D. artus – D. murchisoni* boundary, Llanvirn.

*Description.* Arms relatively short, broad at base and strongly tapered. At least nine thick, folded marginalia, widest at centres, approximately square in section. Aboral surface with up to four rows of large rounded to trapezoidal plates, suspected carinals approximately square, irregularly arranged. All visible plates smooth. Disc and oral surface not seen.

*Remarks*. The poor preservation of this specimen makes comparison with known species difficult. Of the British species of *Mesopalaeaster*, only *M*? *leintwardinensis* Spencer, 1914 shows the strongly tapered arms seen here, although with only 5

marginalia, and strongly differentiated aboral plates. There is no clear similarity to any other species, British or American, although the specimen is almost certainly referable to *Mesopalaeaster*.

## 6.4 References


AUSICH, W. I., BOLTON, T. E. AND CUMMING, L. M. 1998. Whiterockian (Ordovician) crinoid fauna from the Table Head Group, western Newfoundland, Canada. *Canadian Journal of Earth Sciences* **35**, 121-130.

BASSLER, R. S. 1938. Pelmatozoa Palaeozoica. *In* Quenstedt, W. (ed.), *Fossilum Catalogus, I: Animalia,* pt. 83. W. Junk, s'Gravenhage, 194 pp.

BATES, D. E. B. 1965. A new Ordovician crinoid from Dolgellau, North Wales. *Palaeontology* **8**, 355-357.

BATES, D. E. B. 1968. On *'Dendrocrinus' cambriensis* Hicks, the earliest known crinoid. *Palaeontology* **11**, 406-409.

BILLINGS, E. 1857. New species of fossils from Silurian rocks of Canada. *Geological Survey of Canada, Report of Progress 1853-1856, Report for the year 1856*, 247-345.

BLAINVILLE, H. M. DE 1830. *Zoophytes*, Dictionnaire des Sciences Naturelles. F. G. Levrault (Strasbourg), Le Normant, Paris, 60 pp.

BOCKELIE, J. F. 1981. Functional morphology and evolution of the cystoid *Echinosphaerites*. *Lethaia* **14**, 189-202.

BRANSTRATOR, J. W. 1982. Asteroids. *In* J. Sprinkle (ed.), Echinoderm Faunas of the Bromide Formation (Middle Ordovician) of Oklahoma. *University of Kansas Palaeontological Contributions, Monograph* **1**, 316-321.

COPE, J. C. W. 1988. A reinterpretation of the Arenig crinoid *Ramseyocrinus*. *Palaeontology* **31**, 229-235.

DEAN, J. 1999. Evolutionary diversification of Lower Palaeozoic asteroids. *Unpublished Ph.D. Thesis, University of Cambridge.*

DONOVAN, S. K. 1984. *Ramseyocrinus* and *Ristnacrinus* from the Ordovician of Britain. *Palaeontology* **27**, 623-634.

DONOVAN, S. K. 1985. The Ordovician crinoid genus *Caleidocrinus* Waagen and Jahn, 1899. *Geological Journal* **20**, 109-121.

DONOVAN, S. K. 1986-1998. Pelmatozoan columnals from the Ordovician of the British Isles. *Monograph of the Palaeontographical Society, London* (1) 1986 **138**, 1-68, pl. 1-6; (2) 1989 **142**, 69-114, pl. 7-13; (3) 1998, 115-193, pl. 14-26.

DONOVAN, S. K. 1989. More about *Ramseyocrinus* Bates (Crinoidea). *Journal of Paleontology* **63**, 124-125.

DONOVAN, S. K. 1992. New cladid crinoids from the Late Ordovician of Girvan, Scotland. *Palaeontology* **35**, 149-158.

DONOVAN, S. K. AND COPE, J. C. W. 1989. A new camerate crinoid from the Arenig of South Wales. *Palaeontology* **32**, 101-107.

DONOVAN, S. K. AND GALE, A. S. 1989. *Iocrinus* in the Ordovician of England and Wales. *Palaeontology* **32**, 313-323.

DONOVAN, S. K. AND PAUL, C. R. C. 1985. Coronate echinoderms from the Lower Palaeozoic of Britain. *Palaeontology* **28**, 527-543.

DONOVAN, S. K., PAUL, C. R. C. AND LEWIS, D. N. 1996. Chapter 13: Echinoderms *In* D. A. T. Harper and A.W. Owen (Eds.), *Fossils of the Upper Ordovician*. The Palaeontological Association, Dorchester.

DONOVAN, S. K. AND SAVILL, J. J. 1988. *Ramseyocrinus* (Crinoidea) from the Arenig of Morocco. *Journal of Paleontology* **62**, 283-285.

DONOVAN, S. K. AND VELTKAMP, C. J. 1993. Crinoids from the Upper Ashgill (Upper Ordovician) of Wales. *Journal of Paleontology.* **67**, 604-613.

ECKERT, J. D. 1988. Late Ordovician extinction of North American and British crinoids. *Lethaia* **21**, 147-167.

GUENSBERG, T. E. 1992. Paleoecology of hardground encrusting and commensal crinoids, Middle Ordovician, Tennessee. *Journal of Paleontology* **66**, 129-147.

HALL, J. 1866. *Descriptions of new species of Crinoidea and other fossils from the Lower Silurian strata of the age of the Hudson-River Group and Trenton Limestones*, 17 pp. Privately published, Albany, N.Y.

HARLAND, W. B., ARMSTRONG, R. L., COX, A. V., CRAIG, L. E., SMITH, A. G. AND SMITH, D. G. 1990. *A geologic timescale 1989*. Cambridge University Press, Cambridge.

HUDSON, G. H. 1912. A fossil starfish with ambulacral covering plates. *The Ottawa Naturalist* **26**, 45-52.

JAEKEL, O. 1918. Phylogenie und System der Pelmatozoen. *Paläeontologische Zeitschrift* **3**, 1-128.

KOLATA, D. R. 1982. Camerates. *In* J. Sprinkle (ed.), Echinoderm Faunas of the Bromide Formation (Middle Ordovician) of Oklahoma. *University of Kansas Palaeontological Contributions, Monograph* **1**, 170-211.

M'COY, F. 1846. *A synopsis of the Carboniferous Fossils of Ireland.* Dublin, 72 pp., 5 pls.

M'COY, F. 1850. On some new genera of Silurian Radiata in the collection of e University of Cambridge. *Annals and magazine of Natural History, series 2*, **6**, 70-291.

MEEK, F. B. AND WORTHEN, A. H. 1865. Descriptions of new species of inoidea, &c., from the Palaeozoic rocks of Illinois and some of the adjoining states. iladelphia Academy of Natural Sciences Proceedings, **17**, 143-155.

MOORE, R. C. AND LAUDON, L. 1943a. *Trichinocrinus*, a new camerate crinoid m the Lower Ordovician (Canadian?) rocks of Newfoundland. *American Journal Science* **241**, 262-268.

MOORE, R. C. AND LAUDON, L. 1943b. Evolution and classification of laeozoic crinoids. *Geological Society of America Special Paper* **46**.

NEUMAYR, M. 1889. *Die Stämme des Thierreiches. Wirbellose Thiere,* Vienna l Prague, vi + 603 pp.

OWEN, H. G. 1965. The British Palaeozoic Asterozoa: Table of contents, plement and index. *Monograph of the Palaeontographical Society, London,* **127**, i-541-583.

PAUL, C. R. C. 1973-1997. British Ordovician Cystoids. *Monograph of the aeontographical Society, London* (1) **127**, 1-64; (2) **136**, 65-152; (3) 153-213.

PAUL, C. R. C., AND COPE, J. C. W. 1982. A parablastoid from the Arenig of th Wales. *Palaeontology* **25**, 499-507.

RAMSBOTTOM, W. H. C. 1961. A Monograph on British Ordovician Crinoidea 1. *Monograph of the Palaeontographical Society, London*, 37 pp., 8 pl.

SCHUCHERT, C. 1914. Stellaroidea Palaeozoica. *In* FRECH, F. (Ed.) *Fossilium logus: 1. Animalia* W. Junk, Berlin.

SCHUCHERT, C. 1915. Revision of Palaeozoic Stelleroidea with special ference to North American Asteroisea. *Bulletin: United States National Museum* **88**, 11 pp., 31 pl.

SPENCER, W. K. 1914-1940. A monograph of the British Palaeozoic sterozoa. *Monograph of the Palaeontographical Society, London,* (1) 1914 **67**, 1-56; ) 1916 **69**, 57-108; (3) 1918 **70**, 109-168; (4) 1919 **71**, 169-196; (5) 1922 **74**, 197-6; (6) 1925 **76**, 237-324; (7) 1927 **79**, 325-388; (8) 1930 **82**, 389-436; (9) 1934 **87**, 7-494; (10) 1940 **94**, 495-540.

SPENCER, W. K. AND GROOM, T. 1934. Starfish from the Welsh borderland. *ological Magazine* **71**, 231-236, pl.12.

WAAGEN, W. AND JAHN, J. 1899. *Systeme Silurien du centre de la Boheme par achaim Barrande.* **7**, pt. 1, Prague.

WACHSMUTH, C. AND SPRINGER, F. 1881. Revision of the Palaeocrinoidea, t II (I). Family Sphaeroidocrinidae, with the subfamilies Platycrinidae, odocrinidae and Actinocrinidae. *Philadelphia Academy of Natural Sciences ceedings*, 177-411, pls. 17-19.

WAHLENBERG, G. 1821. Petrificata Telluris Svecanae. *Nova Acta Regia ietas Scientiarum, Upsala*, **8**, 1-116, 4 pl.

# 7. CONCLUSIONS

## 7.1 CONCLUSIONS

### 7.1.1 Palaeoecology

Ecosystems of shallow marine, nearshore sandy substrates, comprising diverse shelly faunas, were affected in the following ways:

(i) small sessile benthos (brachiopods) were decimated by ash deposition, although large sessile benthos (crinoids, erect bryozoa) and mobile epibenthos (trilobites) were only slightly affected;

(ii) recovery of dominant sessile benthos was rapid, although viability of the population was sequentially reduced by successive ash-falls;

(iii) infauna was restricted, possibly by subsurface anoxia (suggested by syndepositional silicification), or lack of buried organic detritus (may vary under different conditions);

(iv) fluctuations in water-mass chemistry, probably related to direct nutrient dissolution from volcanogenic sediments, allowed eutrophic benthic blooms, with filamentous algal/cyanobacterial overgrowth;

(v) some localities of this type preserve fully articulated fossils (echinoderms, sponges), through abrupt burial. This was enhanced by early silicification, which was locally rapid enough to preserve soft-tissue.

Offshore, anoxic-dysaerobic siltstone settings, of approximately 100 m water depth, were affected by ash-fall in the following ways:

(i) A large-scale, decoupled plankton-benthic bloom was developed, numerically dominated by the partly pseudoplanktic inarticulate brachiopod *Apatobolus micula*. Graptolites and ostracodes were also

important components, with a small ostracode peak before the plankton and benthos maxima. This is interpreted as follows, based on vertical circulation intiated by descent of turbid surface waters:

(ii) immediately post-depositional high-oxygen, low-food benthic conditions encouraged the development of mobile epibenthos (cf. Gallardo *et al.* 1977);

(iii) upwelling inorganic nutrients from the subsurface allowed a large-scale plankton bloom, continuing for weeks to months;

(iv) benthic oxygenation allowed colonisation by organisms previously excluded through low oxygen levels; oxygenation reached maximum at the end of vertical circulation, decreasing gradually thereafter;

(v) increased organic rain from plankton bloom allowed the development of dysaerobic-tolerant sessile epifauna, particularly inarticulate brachiopods. These contributed to the decline in oxygenation, which normally returns to previous levels, although the benthic bloom was tempered by decreasing organic detritus from the declining plankton bloom;

(vi) rapid lateral faunal abundance changes were correlated with the base of downwelling flows (BG1 (H); Appendix C).

The deposition of ash into isolated, moderate-depth anoxic basins was characterised by (section 3.4):

(i) delayed or osciallatory plankton abundance, sometimes including dramatic bloom events (LW 1). This was related to entrainment of ash into localised downwelling columns, initiating vertical circulation of the upper part of the basin;

(ii) upwelling of anoxic water destabilised plankton population through mass mortality, although associated inorganic nutrients may have allowed bloom development following the circulation decline;

(iii) benthic colonisation was restricted to occasional mobile deposit feeders, possibly with rare sessile epibenthos, resulting from oxygen retained by ash particles (downwelling flows probably degraded prior to the sea floor).

The deposition of ash into deep, non-isolated basinal mudstone settings resulted in:

(i) an oscillatory abundance increase (LS 1), again interpreted as due to vertical circulation, initiated by downwelling turbid flows;

(ii) upwelling of nutrients from subsurface, resulting in large-scale plankton bloom; anoxic upwelling was dependent on degree of isolation of the water mass (and hence depth of the oxic-anoxic boundary), and depth attained by downwelling flows;

(iii) benthic colonisation was restricted to sparse mobile deposit feeders, possibly with very rare sessile epibenthos, associated with oxygen retained by ash particles (downwelling flows degraded prior to the sea floor).

The depth attained by downwelling currents, and hence vertical circulation, was dependent on several factors, whose quantitative significance is poorly understood:

(i) ash particle size: smaller diameters are more efficient in creating turbidity than the same mass of larger particles. A point occurs at which saltation prevents particles remaining sufficiently close for boundary layer effects to allow mass fluid flow. Distance from source is critical.

(ii) Total mass: flow progradation occurs through rapid central descent, prior to entrainment into lateral gyres on reaching the head. Insufficient material to maintain descent will result in flow decay at shallow depths.

(iii) Thermocline or halocline: a sharp density transition in the ambient fluid will have unknown effects on downwelling flows, although momentum will be reduced. An extreme pycnocline at shallow depths may prohibit vertical circulation, and all associated effects.

The combined hypothesis presented herein is applicable to other published and unpublished data, in some cases providing a preferable alternative to an original explanation. This suggests that similar processes have operated in these systems since the Ordovician.

(i) Gallardo *et al.* (1977) provided detailed analysis of moderately shallow (c. 50 m) benthic ecosystems from the Antarctic region, but suggested few explanations. Polychaete annelids and echiurids proliferated after ash-fall, while crustaceans and molluscs suffered most strongly. This is entirely consistent with conclusions 1 and 2, in which mobile infaunal deposit-feeders are immediately encouraged, prior to restrictive oxygen levels. Since little ash was deposited directly into the study area, these effects were suggested to result from temperature or chemical effects: a

significant temperature increase of 0.3-3°C was observed over successive summers. The effects of temperature changes of this scale on larval organisms are unclear.

(ii) S. Rigby and S. Davies (*pers. comm.* 1999) recorded plankton blooms overlying bentonites in the Silurian of the Scottish Southern Uplands (described in section 1.2). Their hypothesis of iron addition from the ash was dependent on geochemical differentiation of two bentonite suites, only one of which caused blooms.

Recent experiments show that the addition of iron directly to surface oceans produces plankton blooms lasting approximately one week (Carpenter *et al.* 1995); on this basis, the 2-cm graptolitic intervals imply a sedimentation rate approaching 1 m/yr. This is untenable, while their hypothesis does not address associated bioturbation. The geochemical distinction may reflect disparate volcanic source areas, at different distances, and of widely differing particle size distributions. If their uranium-rich suite comprised smaller particles than the U-poor suite, flows would be more likely to initiate, and reach significant depth (conclusion 5). Bioturbation would occur under the conditions described in conclusion 4.

(iii) R. Trewin (*pers. comm.* 1998) noted bioturbation above several bentonites at the Dob's Linn section, Southern Uplands, in deep-water mudstones. It is not known whether plankton blooms occurred simultaneously, but the origin of bioturbation is explained in conclusion 4.

(iv) Vavrdova (1999) discussed overturning of the water column, attributed primarily to storms, but resulting in the formation of pisolitic iron ores containing abundant phytoplankton fossils. Tuffs were reported to underlie several deposits. While macrofossils were not investigated. the increased primary production and iron precipitation is anticipated by conclusions 2-4. That tuff-initiated deposits were indistinguishable from the effects of overturning from storms is strong evidence that ash-fall produced overturning of this nature.

(v) O. Hints (*pers. comm.* 1999) has discovered extremely elevated scolecodont abundance within some bentonites (although others are barren). The initial stage of benthic colonisation (high oxygen, low organic detritus) comprises mobile infaunal/epifaunal detritivores. The scolecodonts presumably derive from infaunal polychaetes, with burrows originating at the bentonite upper surface (as seen in BG 1).

### 7.1.2 Geology and palaeontology of the Builth-Llandrindod Inlier

The detailed logs from the Llandrindod region have yielded a range of conclusions pertinent to interpretations of this area:

The Llandegley Tuffs (no formal name) represent a distinct volcanic development, prior to the Builth Volcanic Formation, which occurred in the northern part of the inlier.

Correlation of lithologies and faunas between Llandegley Rocks and Gelli Hill supports a shallowing of water to the south during deposition of the Builth Volcanic Formation. Reworked tuffs described as debris-flows deposited in deep water (Suthren and Furnes 1980; Lockley 1984) may be better

considered as laterally reworked material in relatively shallow, agitated water (estimated <30 m). This is based on a clearly *in situ* community at the same horizon on Llandegley Rocks, and observations on graptolites in vertically adjacent siltstones.

The previously unknown, shallow-water Llandegley Rocks fauna is among the most diverse assemblages known from Middle Ordovician siliciclastics, including the best preserved and most diverse sponge community. The fossiliferous horizon appears to correlate with that of Gelli Hill, and probably with unknown sites on the Carneddau (2 km north of Builth Wells), from which articulated sponges are known.

The micromorphic inarticulate brachiopod *Apatobolus micula* is shown to be partly pseudoplanktic (Botting and Thomas 1999), based on data from the Howey Brook Main Feeder (Gelli Hill) and an additional specimen from Bach-y-Graig. Benthic colonisation occurred under suitable conditions, but high abundance was also reached during plankton blooms. This is in contrast to the expected low abundance of pseudoplanktic faunas.

### 7.1.3 Palaeobiology

The extremely poor record of Lower Palaeozoic sponges from Britain is improved by the discovery of two contrasting faunas. The Llandegley Rocks fauna includes an exceptionally preserved assemblage of 15 species of demosponges, hexactinellids and minor heteractinids. Three-dimensional silicification of the spongin skeleton represents a previously unknown mode of preservation, which has potential for further recognition, and may be critical in establishing consistent phylogenies. The fauna shows that nearshore, coarse

clastic substrates were colonised by abundant and diverse sponge communities, while previous opinion has emphasised the role of deep-water facies. The lack of known shallow-water sponge faunas is a result of taphonomic bias.

Several sites at the Llanfawr Quarries, Llandrindod Wells, contain a diverse hexactinellid and minor demosponge assemblage from more traditionally sponge-bearing, dysaerobic siltstones. The fauna is under investigation, but probably contains in excess of ten species, preserved in semi- to fully articulated condition. Horizons containing both extremely abundant, monospecific assemblages, and diverse local assemblages occur. Sponge spicules occur in almost all fossiliferous lithologies of the Builth Inlier, suggesting a substantial source of further articulated material.

Most taxa recovered are undescribed, with limited similarity to North American and Australian faunas. While substantial endemism is implied, the presence of the probably pandemic lithistid *Microspongia*? provides a link with other published records.

Echinoderm faunas from the pre-Caradoc of Wales are rare, and typically non-diverse. The Llandegley Rocks fauna has yielded six crinoids (two new species, one new genus), three asteroids and one cystoid. This occurrence, with occasional crinoids recovered from sandstones elsewhere, suggests that nearshore to littoral environments supported a substantial diversity of presently unknown echinoderms. Information on Lower Ordovician echinoderms is too incomplete for definite evolutionary or palaeogeographic conlcusions, but at this stage the fauna appears largely endemic.

Palaeoscolecid worms are recorded from the Builth Inlier for the first time, the nited data (three species) suggesting considerable diversity. Occurrences are ıvironmentally consistent with previous Anglo-Welsh records, and taxonomically nilar to rare discoveries in Shropshire and elsewhere. Although palaeoscolecids pear to have been globally distributed and locally abundant, these discoveries nfirm a high degree of endemism at species level.

## 7.2 Overall Synthesis

The ecological data presented here vary greatly in the effects of ash position, dependent on water depth, oxygenation, substrate, environmental setting l ecological system. Additional taphonomic effects have been included. neralisation of these results between broad facies types allows the correlation of cesses operating within different regions. The effects may be grouped broadly into mical, physical, and ecological, and divided into the following subclasses:

*mical*:

addition of ash into enclosed water masses, producing rapid changes in dissolved chemical composition;

circulation of water column to provide upwelling of water from nutrient maximum zone;

downwelling of surface waters, increasing benthic oxygenation;

dissolution of inorganic nutrients directly into water column;

upwelling of anoxic water masses;

production of localised ironstones (Vavrdová 1999) due to chemical upwelling, creating variable substrates.

*ical*:

direct burial of communities during ash-fall, with brief oxygenation through entrapped air;

increased sedimentation rate through local seismicity and related continental runoff;

increased fluid flow velocity through overturning and local benthic currents;

temporary temperature changes through overturning;

sulting in *Ecological*:

reduced dominance of small sessile benthos (particularly brachiopods) through direct burial effects

brief increase in infauna and mobile epibenthos following oxygenation

subsequent reduction in infauna through limited food supplies or subsrface anoxia, resulting from organic carbon utilisation during benthic bloom

plankton bloom promoted by inorganic nutrient upwelling

bloom in sessile benthos promoted by temporary oxygenation increase and high organic carbon flux

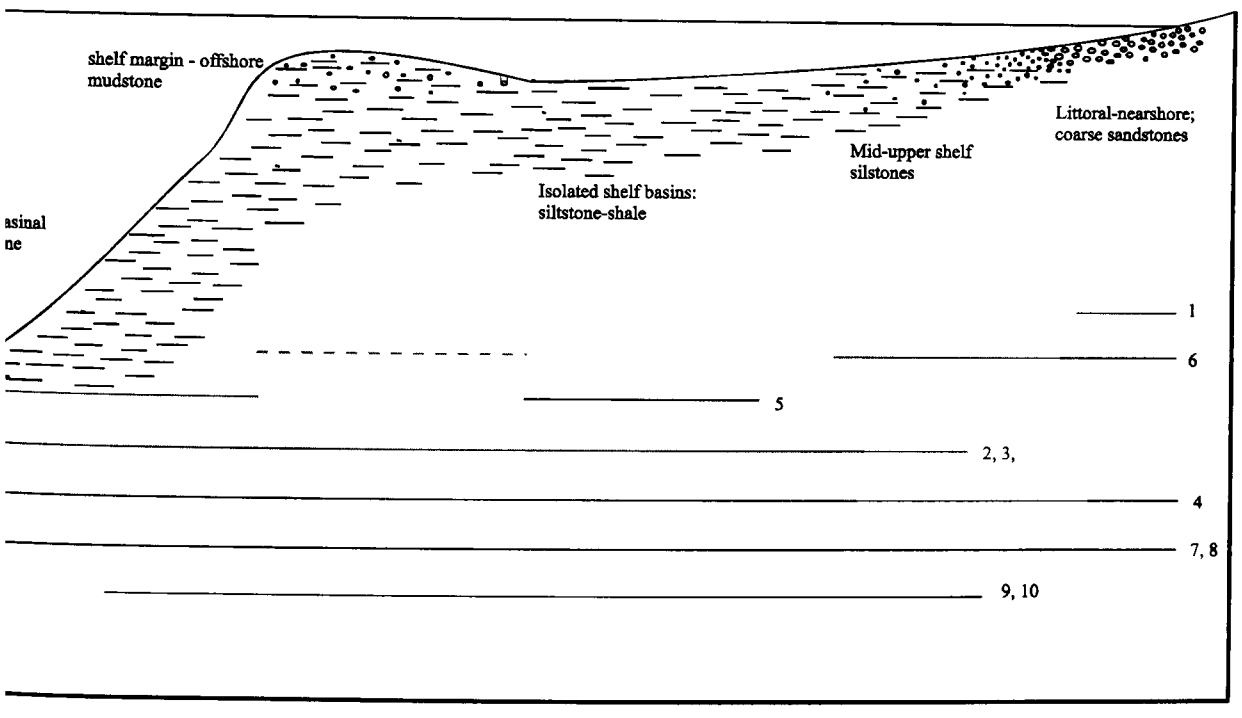


e 7.1.1: *Distribution of facies ranges affected by physio-chemical effects described in the text; e represents a faulted basin margin, as seen in the Ordovician Welsh Basin. Localised nism may further restrict circulatory access to "shelf" areas.*

5. destabilisation of pelagic community through upwelling of deep anoxic water mass.

The respective facies in which these processes operated overlap in several eas, as summarised in Fig. 7.1.1. Nearshore communities may have been subject to ıtrophic benthic blooms resulting from chemical fluctuations within the limited ater mass. This was associated with early silicification, enhancing the preservation multi-element and unmineralised skeletons. Small sessile benthos was devastated ash deposition, but rapidly re-established. Infaunal deposit feeders may have been stricted by eutrophic blooms, and recycling of available organic detritus, in cordance with the results of Gallardo *et al.* (1977). Alternatively, sub-surface oxia may have resulted from excess organic detritus, inhibiting infaunal activity; s is also suggested by rapid silica precipitation and calcite dissolution, implying ısual (probably acidic) pore-water chemistry.

Upper to middle shelf, or shallow basin areas, with limited benthic /genation possessed insufficient anoxic water to disrupt planktic ecosystems on velling. Benthic water was replaced by aerobic downwelling, allowing benthic oms of limited duration. Preservation of fragile multi-element skeletons (e.g. ıeoscolecids – see chapter 6) may be enhanced by increased sedimentation rates. presence of certain clay minerals (often volcanogenic) has also been suggested to bit bacterial degradation, through absorption of degradatory enzymes (Butterfield 0).

In deeper silled basins, circulatory overturning resulted in anoxic upwelling on :ale sufficient to induce ecological instability in the plankton. Once aerobic litions were re-established, a plankton bloom could result from additional ganic nutrients, also supplied through the upwelling. Slight benthic oxygenation,

mediately following ash deposition, probably resulted from oxygen incorporated to the ash layer, as air pockets or metallic oxides; this effect was independent of evious benthic oxygenation. Long-term oxygenation, with an associated sessile nthic bloom, was not developed. This may have been due to larger masses of bient anoxic water with inadequate intrusion of surface waters, and the breakdown downwelling flows prior to entering deep water.

Deep-water basinal muds with extensive anoxic development differed in the eater depth of the oxic-anoxic boundary in relation to the depth of induced culation. Possible causes of this discrepancy include: (i) the greater depth of normal ve-induced circulation in open marine conditions; (ii) exposure to open marine surface currents which are absent from the shelf, and shallow, enclosed basins; and ) reduction in the average total mass of deposited volcaniclastic particles in remote tings, allowing the downwelling flows to break up more quickly.

The effects of dissolution of iron directly from the ash would probably have been present in the surface waters of all settings, but in open shelf conditions these were diluted, and overprinted by the longer-term effects of recirculation.

## 7.3 RECOMMENDATIONS FOR FURTHER WORK

As stated in section 1.1, the object of this work was to create a framework of damental results, with associated explanatory hypotheses, which could form the s for future research. The results have provided outline processes for the studied ons, but cannot be considered a complete descriptive account.

**A.** The most critical aspects to investigate for further elucidation of the iochemical, and resulting ecological processes involved are as follows:

1. Extension of the analytical methodology into contrasting facies during the Phanerozoic, in order to establish the significance of ambient biota on the effectiveness of nutrient recirculation. Since all Builth Inlier samples were dominated by the inarticulate brachiopod *A. micula*, and phosphate concentration is (today) biochemically limiting, the effects of massive phosphate utilisation need to be established. Selecting intervals dominated by macrofauna with other biomineralisation products (e.g. Cretaceous: ammonites: calcium carbonate) will help to establish generality of the present results. The development of mesobathyal faunas is unknown during the Palaeozoic; if it was limited, nutrient compartmentalisation through the water column may have been enhanced, allowing larger blooms than are presently possible.

2. The effects of water mass geochemistry are presently undetermined. The Ordovician was characterised by large-scale oceanic anoxia in several restricted basins, whereas significant data presently exist only for the Welsh Basin, Bohemia (which shows substantial faunal exchange with Avalonia), and western Iapetus. Data from the Middle Ordovician of Australia, South America and North and South China would allow a more comprehensive hypothetical development.

3. Consistent oceanic mixing would be expected to reduce the effects of recirculation, by controlling mesobathyal nutrient concentration. Dependence of plankton/nekton bloom abundance (expressed as percentage) on oceanic oxygenation would strongly support the recirculation hypothesis. This could be investigated by analysing shelf settings under varied oxygenation, during several periods.

4. The chemical and physical composition of tuffs is extremely varied, with unclear significance. Although chemical composition should have little or no effect, this is generally correlated with physical attributes, which are critical in the development of turbid flows. Dependence on tuff particle size and morphology is predicted, and could be investigated through analysis of recent sediment cores. The majority of ancient deposits will not contain identifiable grains, due to the chemical instability of volcanic glass.

5. Stable isotope analysis should allow quantitative description of primary productivity (Wong and Sackett 1978; Hollander *et al.* 1993), although Welsh Basin sediments may be unsuitable due to alteration during diagenesis (J. Marshall, *pers. comm*). Although most taxa recovered from the samples were probably primary consumers, the results may differ for production. This would also test the reliability of preserved fossils, as representative of the life assemblage.

6. The Builth Inlier has revealed significant potential for establishing fine-scale biofacies division in dysaerobic siltstone/shale facies. A full investigation in this and other regions is encouraged, in order to understand interactions between communities based on single-phylum taxa (e.g. trilobites, brachiopods). Tuffs provide an ideal source of information in this area, where successive changes in oxygenation occur within the "dysaerobic" division.

**B**. The ecological results have potential significance in a number of fields, in which further investigation is encouraged:

1. Evolutionary rates are affected by faunal population dynamics: speciation occurs most easily among small, isolated populations, where

genetic dominance is quickly achieved. The production of repeated, local blooms during volcanic episodes may have enhanced genetic variability and speciation through the production of essentially isolated, temporary populations. (This could be simulated by "artificial life" computer modelling.) Such processes would affect plankton during all periods of widespread explosive volcanism, combined with limited oceanic mixing, although with relatively little importance, due to individual mobility and population mixing. Benthic faunas would be affected most strongly during periods of high sea level (large shelf areas) combined with limited benthic oxygenation. These conditions were satisfied for benthos during the Ordovician, and for plankton during the Ordovician and Silurian. The ongoing database assimilation of global Ordovician biodiversity (IGCP 410) will address issues of regional dependence and differential evolutionary rates between taxonomic groups.

2. The consistency of ecological patterns resulting from temporary bloom events is of significance for modern conservation agencies, and commercial unconstrained fish farming. While all blooms examined from middle shelf settings show similar structure, the terminal state is highly variable. Although benthic oxygenation may be permanently developed where previously lacking (BG 1), plankton abundance may suffer long-term reduction (HB 1, HB 2) due to reduction of the subsurface nutrient reservoir. Regional effects are not known. While the long-duration blooms described here may attract interest from commercial sources, inducing these effects could have catastrophic

long-term implications. Depletion of the subsurface nutrient resource will reduce the stability of planktic and benthic ecosystems, and limit primary production thereafter. Under no circumstances should this become common practice, despite the possibility of increasing the rate of speciation.

Utilising land-derived sources of iron for direct addition to surface waters may also be ecologically unsound. The increased uptake of a wide range of inorganic nutrients during blooms will deplete resources of other biologically limiting elements, in addition to iron and phosphate. Until the effects of this are known, it should be assumed that inducing wide-scale blooms by this method would reduce long-term viability of oceanic ecosystems.

**C**. Systematic investigation has been initiated into Ordovician sponge faunas, a subject in drastic need of revision. Many of the critical evolutionary points in poriferan history occurred during the Cambrian-Silurian, but insufficient taxonomic and biogeographical data is presently available. A full revision of Avalonian Lower Palaeozoic sponges is intended, with investigations into the distribution of isolated spicules.

A particular point related to palaeobiogeography is the rarity of Silurian sponges in the Anglo-Welsh region. The Much Wenlock Limestone Formation contains over 600 recorded species, although no siliceous sponges (including isolated spicules) have ever been recovered. Isolated examples are known from Ludlow rocks, but these are also very rare. A comparison with the diverse North American faunas (e.g. Rigby and Chatterton 1999) shows the extent of this disparity. The investigation

of this problem will result in greater understanding of poriferan synecology and distribution.

## 7.4 References


Botting, J. P. and Thomas, A. T. 1999. A pseudoplanktonic inarticulate brachiopod attached to graptolites and algae. *Acta Universitatis Carolinae: Geologica* **43**, 333-335.

Butterfield, N. J. 1990. Organic preservation of non-mineralizing organisms and the taphonomy of the Burgess Shale. *Palaeobiology* **16**, 272-286.

Carpenter, S. R., Chisholm, S. W., Krebs, C. J., Schindler, D. W. and Wright, F. W. 1995. Ecosystem experiments. *Science* **260**, 324-327.

Gallardo, V. A., Castillo, J. G., Retamal, M. A., Yanez, A., Moyano, H. I. and Hermosilla, J. G. 1977. Quantitative studies on the soft-bottom macrobenthic animal communities of shallow Antarctic bays. *In* Llano, G. A. (ed.): *Adaptations within Antarctic ecosystems (Proceedings of the 3rd SCAR Symposium on Antarctic Biology),* Smithsonian Institution, Washington D.C., pp. 361-387.

Hollander, D. J., McKenzie, J. A. and Hsu, K. J. 1993. Carbon isotope evidence for unusual plankton blooms and fluctuations of surface water $CO_2$ in "Strangelove Ocean" after terminal Cretaceous event. *Palaeogeography, Palaeclimatology, Palaeoecology* **104**, 229-237.

Lockley, M. G. 1984. Faunas in a volcaniclastic debris flow from the welsh Basin: a synthesis of palaeoecological and volcanological observations. *In* Bruton, D. L. (ed.), 1984. *Aspects of the Ordovician System*, 195-201. Palaeontological Contributions from the University of Oslo, No. **295**, Universitetsforleget.

RIGBY, J. K. AND CHATTERTON, B. D. E. 1999. Silurian (Wenlock) demosponges from the Avalanche Lake area of the Mackenzie Mountains, southwestern district of Mackenzie, Northwest Territories, Canada. *Paleontographica Canadiana* **16**, 43 pp.

SUTHREN, R. J. AND FURNES, H. 1980. Origin of some bedded welded tuffs. *Bulletin of Volcanology* **43,** 61-71.

VAVRDOVÁ, M. 1999. The acritarch succession in the Klabava and Sarka formations (Arenig – Llanvirn): evidence for an ancient upwelling zone. *Acta Universitatis Carolinae: Geologica* **43**, 263-265.

WONG, W. W. AND SACKETT, W. M. 1978. Fractionation of stable carbon isotopes by marine phytoplankton. *Geochimica et Cosmochimica Acta* **42**, 1809-1815.

## Appendix A
## Llandegley Rocks main section

s: surface; ib: intra-bed

| specimen | Dimensions | details | |
|---|---|---|---|
| **1** 6.3 kg | | | |
| 1 *Flexicalymene sp.* | ax. W. 7; ceph w. 7 | abraded partial thorax + cephalon | s |
| 2 ?*Tissintia prototypa* | | fragment of costate int. + ext. | s |
| 3 monaxonid sponge | >100x50x30; spics 10x0.1 | articulated skeleton with silicified margin | s |
| 4 monaxonid sponge | >90x50x20 | domal structure with multiple growths | s |
| 5 Pinnatoporellid | 0.7x2.5; 0.4x1.5 | large fragment (+ small); ramose | s |
| 6 ?*Flexicalymene* sp. | w ~ 8.5; L 5.5 | pyritized pygidium | s |
| 7 *Hesperorthis* | | pedicle valve, int. + ext. | s |
| 8 *Tissintia?* | L 4.8; w ~ 6 | brachial valve int. + ext. | s |
| 9 orthocone nautiloid | diam. ~ 10; siphuncle ~ 4 | mould of siphuncle in crushed, silicified test | s |
| 10 ?annelid | w 0.4 - 1.0; L 2.2 | Conical calcitic growth nucleated on spicule | s |
| 11 sponge? | 5.5 x 2.5 | possibly scoria; fused, curved monaxons | s |
| 12 Pinnatoporellid | 0.8x 3.1 | ramose fragment | s |
| 13 *locrinus* | diam 1.6 | isolate ?secundibrach | s |
| 14 trilobite thoracic rib | 2.4 x 0.8 | silicified, but no detail; may be *Flexicalymene* | s |
| 15 Trepostome bryozoan | area 19 x 5 | substantial fragment of colony | s |
| 16 art. Brach. | | small fragment ?attached to bryozoan | s |
| 17 *Flexicalymene sp.* | L6.9 W 9.7 | Pygidium; silicified envelope showing punctae | s |
| 18 burrows | w ~ 1.0 | bedding-parallel, straight. | s |
| 19 *Ogyginus corndensis* | L ~ 25; w ~ 35 | incomplete pygidium | ib |
| 20 *?Didymograptus sp.* | L ~ 13; w 2 | poorly preserved; pytiric in shale clast | ib |
| 21 burrow with spreite | w 5; L 23 | spreiten chevrons; expanded end, straight | ib |
| 22 ?Lithistid sponge | L 8; w ~3.5 | lithistid-like framework of indistinct spicules | ib |
| 23 art. Brach. | | indet. Exterior (poss.*H.*) | ib |
| 24 art. Brach. | w 2.0 | costate pedicle valve | ib |
| 25 ?ostracod | w 1.8 | smooth bivalved mould | ib |
| 26 Trepostome bryozoan | diam 1.5 | (uncertan) small cylindrical fragment | ib |
| 27 dubiofossil | L ~ 8; w ~ 2; a/sy fusiform | limonitic shape in small concretion | ib |
| **2** | | | |
| 1 librigena | L 11; w 3 | pustulose exterior + int. | s |
| 2 *Hesperorthis* | L 6.5; w ~ 7 | pedicle v. int + ext | s |
| 3 *Hesperorthis* | L 5.2; w 7.5 | pedicle v. int + ext | s |
| 4 *Hesperorthis* | L 5.4; w ~ 8 | brachial v. int + ext | s |
| 5 monaxonid sponge | 80 x 80; spics ~ 2 x 0.1 | relatively low level of spicules | s |
| 6 bivalve | L 21 w 27 | faint growth lines; nucleus of 1.5 | s |
| 7 *Hesperorthis* | 8 x 6 | ped. Valve internal | s |
| 8 *locrinus* | diam. 2 - 3 | Six aligned brachials (secundi?) | s |
| 9 *locrinus* | di 2.5; o/l 0.4, 0.8; L 10 | heteromorphic column fragment | s |
| 10 *locrinus* | diam. 2.,1 | isolated ?secundibrach | s |
| 11 *Hesperorthis* | | brachial v. int + ext | s |
| 12 *locrinus* | square diam 1.5 | distal anal column | s |
| 13 *Hesperorthis* | L 6.7 w 8.6 | brachial v. int + ext | s |
| 14 art. Brach | | indet valve ext | s |

| | | | |
|---|---|---|---|
| 15 *Iocrinus* | diam. 2-3 | Seven aligned brachials (secundi?) | s |
| 16 *Iocrinus* | diam. 2.8 | isolated primibrach | s |
| 17 *Hesperorthis* | | indet valve ext | s |
| 18 *Hesperorthis* | | indet valve ext | s |
| 19 *Hesperorthis* | | indet valve ext | s |
| 20 *Iocrinus* | diam. 2.6 | isolated ?primibrach | s) |
| 21 *Balacrinus* | diam. 1.8 (lumen 0.5) | 4 articulated pentagonocyclic columnals | s |
| 22 monaxonid sponge | | low spicule content | s |
| 23 Bryozoan | 2 x 2 | small ?trepostome fragment | s |
| 24 trail | w 2; L> 20 | possibly bilobed; branching | s |
| 25 *Hesperorthis* | | indet (embedded) | ib |
| 26 *Hesperorthis* | | pedicle v. int + ext | ib |
| 27 *Iocrinus* | diam. < 1 | distal brachial | ib |
| 28 monaxonid sponge | > 20 | frequent monaxons | ib |
| 29 surface trail | w ~ 4 | sediment displaced in sectional view | ib |
| 30 ?ostracod | L. 1.5 | smooth elliptical mould | ib |
| 31 ?Lithistid | ~ 20 | globose with tracheid structure; in nodule | ib |
| Supplemental: 5.5 kg | | | |
| 32 *Iocrinus* | | isolated brachial | |
| 33 *Iocrinus* | | isolated brachial | |
| 34 *Hesperorthis* | | ped., int + ext | |
| 35 *Hesperorthis* | | ped., int + ext | |
| 36 *Iocrinus* | | isolated brachial | |
| 37 *Iocrinus* | | isolated brachial | |
| 38 crinoid indet. | | square ?brachial | |
| 39 *Iocrinus* | | isolated brachial | |
| 40 *Iocrinus* | | 2 primibrachs | |
| 41 *Balacrinus* | | calcycal plates | |
| 42 *Iocrinus* | | isolated brachial | |
| 43 demosponge | | clastic | |
| 44 *Hesperorthis* | | ped., int + ext | |
| 45 infaunal burrow | | organic-lined?; horizontal | |
| 46 art. Brach | | external; cp destroyed | |
| 47 *Iocrinus* | | pentalobate columnal (mesostele) | |
| 48 cf. *Skolithos* | | vertical, ?organic-lined | |
| 49 cf. Skolithos | | sub-vertical, slightly curved | |
| 50 demosponge | | ?*Oneroconchia* | |
| 51 *Hesperorthis* | | pedicle, int. | |
| 52 *Hesperorthis* | | ped., int + ext | |

| | | | |
|---|---|---|---|
| 3 | 8.2 kg | | |
| 1 *Hesperorthis* | | two external mould fragments (1 valve total) | s |
| 2 ?*Balacrinus* | 5 x 2.5 x 2 (approx.) | probable pinnule mass | s |
| 3 *Iocinus* | diam. 0.7 x 5 long | brachials, articulated | s |
| 4 *"Hyalostelia"* | 0.1 x >2.5 | isolated large monaxid | s |
| 5 *Hesperorthis* | L~ 9, w 10 | pedicle int + ext | s |
| 6 ?*Tissintia* | L~ 3 | pedicle int + ext | s |
| 7 sponge | diam. ~ 10 | siliceous marginal shell; spheroidal | s |
| 8 Pinnatoporellid | diam. 0.8; >10 long | dichotomous fragment | s |
| 9 Demosponge | Diam. 80 - 100; circular | proteinaceous sponge; rare monaxons | s |

| | | | |
|---|---|---|---|
| 10 *"Hyalostelia"* | 0.1 x > 3 | alligned monaxons | s |
| 11 ?pellets | 2.1 x 1.4 and smaller | no evidence of diet | s |
| 12 trail | w 8 - 11; L >30 | simple sinuous track | s |
| 13 ramose bryozoan | diam. ~20 | amonticuliporate | s |
| 14 sponge | diam. 20; globose | clastic + monaxons (see also 28) | s |
| 15 art. Brach. | small | indet. Valve | s |
| 16 ?trilobite fragment | 5.7 x 5.0, trapezoid | scale-like fragment | s |
| 17 *Hesperorthis* | w ~ 10 | brachial valve, int + ext | s |
| 18 ramose bryozoan | diam. 1.5 | fragments as 13 | s |
| 19 *locinus* | diam. ~ 1 | isolated brachials | s |
| 20 ?Tissintia | | brachial valve int | s |
| 21 ?sponge | 4.5 x 2.5 | aspicular | s |
| 22 ?*Rostriculella* | | fragment of articulated valves | s |
| 23 *locinus* | diam. 1.4 | isolated ?secundibrach | s |
| 24 *Baltoniodus* | micro. | from acid residue | s |
| 25 *Hesperorthis* | L~ 6; w 6.4 | brachial valve int + ext | ib |
| 26 algal/bacterial | ~5 x 4 | spheroidal ferruginous cavity | ib |
| 27 art. Brach. | | indet valve (sectioned) | ib |
| 28 *Astylospongia?* | diam. 20; globose | see also 14 | s |
| 2.X highly silicified bed with possible organic remains | | | |
| 1 | | | |
| 4 | 8.0 kg | | |
| 1 *Hesperorthis* | L 6.2; w 8.8 | brachial , int | s |
| 2 monaxonid sponge | 8 x 25; cylindrical | large, quite abundant spicules | s |
| 3 *Hesperorthis* | | pedicle valve int | s |
| 4 art. Brach | | indet. Int + ext | s |
| 5 ?bryozoan | diam. 1.5; cylindrical | very poor preservation | s |
| 6 *Hesperorthis* | | indet valve ext | s |
| 7 echinoderm plate | 1.4 x 2.0 | mould of cuboid element | s |
| 8 monaxonid sponge | 16 x 10, globose | nucleated on brachiopod | s |
| 9 *locrinus* | diam. 1.4 | 5 articulated brachials | s |
| 10 *Hesperorthis* | L 3.2 | brachial , int | s |
| 11 monaxonid sponge | 4.5x 2.5 x 1.1 | domal with abundant spicule fragments | s |
| 12 *Hesperorthis* | | indet valve ext | s |
| 13 echinoderm fragments | ~ 0.5 - 2 | small ossicle-like units | s |
| 14 Pinnatoporellid | diam. 0.6; L ~ 3 | small fragment of probably ramose colony | s |
| 15 monaxonid sponge | | monaxons fragmentary; possibly domal | s |
| 16 ?*Gelidorthis* | 10 x 15 | sulcate brachial valve; ext. | s |
| 17 demosponge | > 55 | sparse spicules, little structure | ib |
| 18 *Hesperorthis* | L 3.5; w 5 | brachial , int + ext | ib |
| 19 ?burrow + pellet | pellet diam. 3 | uncertain; adjoins silicified region | ib |
| 20 Trinucleid/Raphioph. | L 6.8; w 1 | isolated genal spine | ib |
| 21 *Pseudolingula* | L 10.5; w 7 | articulated valves, phosphatic | ib |
| 22 *Hesperorthis* | L ~ 5; w ~ 7.5 | pedicle valve int+ext | ib |
| 23 monaxonid sponge | > 20 | sparse monaxons; most;y clastic | ib |
| 24 *?Skenidiodes* | < 1mm (partial) | fragment of very small brach | ib |
| 25 ?crinoid debris | diam 1 - 2 | ellipso-angular moulds in centre of nodule | ib |
| 26 burrow | diam. 7.5 | sinuous; silica-infilled with ferruginous grains | ib |
| 27 burrow | diam 6.5 (flattened) | " (sub-horizontal) | ib |
| 28 burrow | diam. 8.5; L > 70 | " | ib |

| | | | |
|---|---|---|---|
| 29 burrow | diam. 8 | includes sharp angle | ib |
| 30 *Hesperorthis* | | pedicle valve int | ib |
| 31 monaxonid sponge | >23 | ?domal | ib |
| 32 ?ostracod | ~1 x 2 | smooth ellipsoidal cavity | ib |
| 33 sponge fragnments | | in nodule, Fe- stained | ib |
| **5** 9.2 kg | | | |
| 1 *Hesperorthis* | | pedicle valve int | s |
| 2 *Flexicalymene* | w 15; L 7 | pygidium with 4 pleural ribs | s |
| 3 monaxonid sponge | >110 | highly degraded, weakly spicular | s |
| 4 *Iocrinus* | diam up to 2.5 | isolated primibrahcs | s |
| 5 articulate brach | | indet. Valve | s |
| 6 *Hesperorthis* | | brachial v., int. | s |
| 7 burrow | w 21; L>150 | horizontal; contains spreiten | s |
| 8 *Hesperorthis* | | brach. Int + ext | s |
| 9 monaxonid sponge | diam ~ 30 | sparse spicules | s |
| 10 *Iocrinus* | diam. 2.2 | isolated brachial | s |
| 11 indet | 10x15x10 | obscure keel-shaped object | s |
| 12 *Hesperorthis* | | indet valve ext | s |
| 13 articulate brach | L 4.8; w 6.0 | pedical int + ext; new species? | s |
| 14 *Iocrinus* | diam. 2,5 | isolated primibrachs | s |
| 15 *Hesperorthis* | L~10; w ~ 12 | pedicle v. Ext | s |
| 16 monaxonid sponge | >100 | fried egg morphology | s |
| 17 *Hesperorthis* | w>9 | pedicle valve int | s |
| 18 *Hesperorthis* | L 4.8; w 6.0 | pedicle valve int | s |
| 19 *Hesperorthis* | | pedicle int + ext | s |
| 20 articulate brach | small | unidentifiab;e | s |
| 21 *Iocrinus* | diam. 1.5 | isolated ?secundibrach | s |
| 22 monaxonid sponge | | clastic monaxonid | s |
| 23 demosponge | >160 | possible showing rim of osculum | s |
| 24 monaxonid sponge | | some spicules visible | s |
| 25 ?gastropod | diam 27; spheroidal | spiral structure in siliceous nodule | s |
| 26 monaxonid sponge | | some spicules visible | s |
| 27 monaxonid sponge | | coarse surface texture | s |
| 28 monaxonid sponge | >40 | clastic monaxonid | ib |
| 29 monaxonid sponge | >50 | clastic monaxonid | ib |
| 30 Pinnatoporellid | L6 w ~ 0.8 | section through small fragment | ib |
| 31 burrow | diam 4 | silica-infilled; vertical | ib |
| 32 ?annelid tube | diam 2-3 | flattened, smooth tube; poss. Phosphatic | ib |
| 33 monaxonid sponge | > 75 | clastic monaxonid | ib |
| 34 algal/bacterial | diam 3; spheroid | aspicular globose body; clastics in centre | ib |
| 35 *Hesperorthis* | | pedicle valve int | ib |
| 36 *Iocrinus* | diam. 1.2 | isolated ?tertibrach | ib |
| 37 *Iocrinus* | diam 1.0 | isolated ?tertibrach | ib |
| 38 ?*Skenidioides* | L 2.2; w 3.6 | articulated valves ext | ib |
| 39 *Iocrinus* | diam 2.6,1.9,1.8 | isolated brachials | ib |

**X1** lithic flakes of altered mudtsone - abundabt at certain horizons.

6

| | | | |
|---|---|---|---|
| 1 monaxonid sponge | | little detail | |
| 2 *Paterula* cf *fissula* | diam. 5.9 | indet valve int | s |
| 3 orthocone nautiloid | diam 13; L>19 | limonite-infilled conch; int + ext | s |
| 4 *Hesperorthis* | L 7.8 | pedicle valve int | s |
| 5 monaxonid sponge | | monaxons possibly alligned | s |
| 6 demosponge | 14x8x4 | aspicular | s |
| 7 *Hesperorthis* | L 7.5; w 10.5 | pedicle valve int + ext | s |
| 8 surface trails | width 3 | sinuous trackway | s |
| 9 *Cruziana* | width 7 | lower cast of cruzaniform trace | s |
| 10 trails | width 3 | sinuous trackway | s |
| 11 trails | width 3 | sinuous trackway | s |
| 12 ?pellet | 5x6x2 | high spic levels + authigenic pyrite | s |
| 13 trails | width 3-5 | sinuous trackway | s |
| 14 trails | width 3-5 | sinuous trackway | s |
| 15 trails | width 3-5 | sinuous trackway | s |
| 16 *Hesperorthis* | | indet valve ext | s |
| 17 trails | width 3-5 | sinuous trackway | s |
| 18 trails | width 3-5 | sinuous trackway | s |
| 19 trails | width 3-5 | sinuous trackway | s |
| 20 monaxonid sponge | | monaxons + detrital clastics | s |
| 21 monaxonid sponge | | primarily clastic | ib |
| 22 *"Skolithos"* | diam 5.8 | vertical burrow | ib |
| 23 *Iocrinus* | diam 2.0 | isolated secundibrach | ib |
| 24 ??? | L 35; w 5.5 | bilateral, segmented, worm-like ?trace; pyritic | ib |
| 25 monaxonid sponge | >70 | clastic/monaxonid; cross-bedding in slab | ib |
| 26 trail | w 2.5; L 18 | conatins right-angle bend | ib |
| supplemental: 10.0 kg | | | |
| 27 ?*Marrolithus* | | poorly preserved genae | ib |
| 28 surface trails | | short, curved trail sections | |
| 29 *Ogyginus*? | | thoracic rib (poss. calymenid) | |
| 30 infaunal burrow | diam. ~2 | sub-horizontal | |
| 31 demosponge | | ?*Oneroconchia* | |
| 32 bivlave | | nucleation site for 5.31 | |
| 33 ?bryozoan | | globular form, no surface detail | |
| 34 bivalve? | | small fragment, silicified | |
| 35 demosponge | | clastic/monaxonid nuc. on 5.34 | |
| 36 surface trail#2 | | thin meandering trace | |
| 37 demosponge | | as in 2.62 | |
| 38 demosponge | | as in 5.31 | |
| 39 *Iocrinus* | | 6 brachials, articulated | |
| 40 demosponge | | part of 5.38? | |
| 41 surface trails | | slab with numerous short traces | |
| 42 surface trails | | slab with numerous short traces | |
| 43 *Iocrinus* | | isolated primibrach | |
| 44 demosponge | | clastic/monaxonid; some structure | |
| 45 demosponge | | clastic/monaxonid | |
| **X1** flute? | | | |
| 7 | 6.2 kg | | |

| | | | |
|---|---|---|---|
| 1 *Mirustubus* | 55x135+ x25 | see taxonomy | |
| 2 *Iocrinus* | diam 1.1 | isolated brachial | s |
| 3 *Hesperorthis* | | external, indet. Valve | s |
| 4 art. Brach. Sp nov? | w 6.8 l~5 | brachial, int+ ext | s |
| 5 large burrow | w 22 | cf. 4.7; no spreiten | ib |
| 6 cf *Cruziana* | w 5 | poor, prob. bilobed trace | ib |
| Supplemental: 9.2 kg | | | ib |
| 7 art. brach | | brachial, int. | |
| 8 *Hesperorthis* | | brachial, int. | |
| 9 infaunal trace | | concentric ring structure | |
| 10 sponge | | clastic/monaxonid | |
| 11 infaunal trace | | oblique burrow | |
| 12 infaunal trace | | shallow gradient | |
| 13 *Iocrinus* | | isolated brachial | |
| 14 *Iocrinus* | | isolated brachial | |
| 15 *Hesperorthis* | | ped. ext | |
| 16 sponge | | clastic/monaxonid | |
| 17 *Hesperorthis* | | ped. int | |
| 18 *Iocrinus* | | complete crown (!) | |
| 19 sponge | | ?*Oneroconchia* | |
| 20 infaunal trace | | oblique, with concentric structure | |
| 21 ?bivalve | | silica-replaced shell (bilaminar) | |
| 22 ?orthocone | | fragment of conch | |
| 23 sponge | | ?Oneroconchia | |
| 24 *Ogyginus* | | pygidium | |
| 25 infaunal trace | | small vertical burrow | |
| 26 sponge | | clastic/monaxonid | |
| 27 art brach | | indet. valve | |
| 28 infaunal trace | | sub-horizontal | |
| 29 ?*Ogyginus* | | thoracic rib fragment | |
| 30 sponge | | clastic, discoidal | |
| 31 infaunal trace | | oblique burrow | |
| 32 trepostome bryozoan | | cylindrical fragmnet | |
| 33 art brach | | ?brach. ext | |
| 34 art brach | | ?brach. ext | |
| 35 *Iocrinus* | | isolated brachial | |
| 36 *Hesperorthis* | | ped., int + ext | |
| 37 infaunal trace | | concentric ring structure | |
| 38 *Hesperorthis* | | ped. int | |
| 39 infaunal trace | | conical morphology | |

**8**

| | | | |
|---|---|---|---|
| 1 sponge (*Oneroconchia*) | diam. 150-200? | poor pres., subcirc. | s |
| 2 *Iocrinus* | diam. 2.5 | isolated brachial | s |
| 3 ?*Iocrinus* | diam. 4 | pleuricolumnal; circulocircular | s |
| 4 Trepostome bryozoan | dima. 2 | fragment of ramose colony | s |
| 5 *Dalmanella parva*? | w 5.6, l 3.8 | pedicle, int. | s |
| 6 art. brach | | brachial v., int | s |

| | | | |
|---|---|---|---|
| 7 *Hesperorthis* | w?, l 5.8 | pedicle, int. costae begin too post. for *Hesp.* | s |
| 8 *Hesperorthis* | | pedicle, int. costae begin too post. for Hesp. | s |
| 9 art. brach | | indet. valve | s |
| 10 art. brach | | indet. valve | s |
| 11 *Hesperorthis* | | int., indet. valve | s |
| 12 *Hesperorthis* | | ext., indet. valve | s |
| 13 art brach | | v. poor pres. | s |
| 14 *Hesperorthis* | w 10.5, l 7 | pedicle, int | s |
| 15 *Hesperorthis* | | int., indet. valve | s |
| 16 *Hesperorthis* | w 11.0, l 10.4 | ped., int. + ext | s |
| 17 art brach | | ?ped. int + ext | s |
| 18 Trepostome bryozoan | diam. 4 | branching, ramose; *Batostoma*? | s |
| 19 *Hesperorthis* | | brach. int + ext | s |
| 20 *Hesperorthis* | w 8.8, l 6.7 | ped., int. + ext | s |
| 21 *Hesperorthis* | w 8.2, l 5.7 | brach. int + ext | s |
| 22 *Hesperorthis* | | ped., int. + ext | s |
| 23 *Hesperorthis* | | ped., int. + ext | s |
| 24 *Hesperorthis* | | ped., int. + ext | s |
| 25 *Hesperorthis* | w 5.4 l 3.2 | brach. int + ext | s |
| 26 *Hesperorthis* | | indet. valve(ext) | s |
| 27 sponge | | concave margin, occasional monaxons | s |
| 28 *Hesperorthis* | w 15 l 10 | ped., int. + ext | s |
| 29 *Hesperorthis* | | ped., int. + ext | s |
| 30 art brach | | indet., ext | s |
| 31 sponge | ~ 50? | ?dysideid | s |
| 32 *Hesperorthis* | | indet., ext | s |
| 33 *Hesperorthis* | | indet., ext | s |
| 34 *Iocrinus* | diam. 3.8 | isolated primibrach | s |
| 35 sponge | | subcircular clastic/monaxon | s |
| 36 sponge | diam., 8? | ?domal, clastic | s |
| 37 art brach | | section through indet valve | s |
| 38 *Hesperorthis* | large | ped., int. + ext | ib |
| 39 art brach | | indet. valve | ib |
| 40 *Hesperorthis* | | indet. valve | ib |
| 41 *Hesperorthis* | w 12.0, | ped., int. + ext | ib |
| 42 *Hesperorthis* | w 10, l ~6 | ped., int. + ext | ib |
| 43 *Hesperorthis* | | ped. int | ib |
| 44 ?sponge | w 1.5, l~6 | lamina oblique to bedding; ferruginous | ib |
| 45 raphiophorid? | r 3.5 arc 4 | gena | ib |
| 46 ?trilobite spine | w~0.8, l 6 | poorly pres. linear cavity | ib |
| 47 *Iocrinus* | diam., 1.0 | isolated brachial | ib |
| 48 demosponge | | monaxons present | ib |
| 49 *Hesperorthis* | | pedicle valve | ib |
| 50 *Hesperorthis* | | brach. int + ext | ib |
| 51 art brach | | pedicle valve | ib |
| 52 art brach | | indet. valve | ib |
| 53 *Iocrinus* | diam. 1.2 | isolated brachial | ib |
| 54 demosponge | | ? | ib |
| 55 *Iocrinus* | diam. 1.1 | isolated brachial | ib |

9

| | | | |
|---|---|---|---|
| 1 *Hesperorthis* | w 11.4, l 8.5 | brach. int | S |
| 2 *Hesperorthis* | | pedicle, int. | S |
| 3 *Hesperorthis* | | ped., int + ext | S |
| 4 sponge | l>5.6 | clastic only | S |
| 5 *Hesperorthis* | | brach, ext. | S |
| 6 *Hesperorthis* | | pedicle, int. | S |
| 7 ?sponge | large | ?*Oneroconchia*; nodular | S |
| 8 *Hesperorthis* | w 11.3, l 7.7 | pedicle., int | S |
| 9 *Hesperorthis* | | pedicle, ext | S |
| 10 *Tissintia?prototypa* | | ped., int + ext | S |
| 11 *Hesperorthis* | | pedicle, int. | S |
| 12 *Hesperorthis* | | indet. ext | S |
| 13 *Hesperorthis* | | pedicle, int. | S |
| 14 *Hesperorthis* | | indet. ext | S |
| 15 *Hesperorthis* | w 12.0, l 10.0 | pedicle, int. | S |
| 16 art brach | | fragment; predation or violent flow | S |
| 17 *Hesperorthis* | | brachial, int. | S |
| 18 *Hesperorthis* | w 5.2, l 3.4 | brachial, int. | S |
| 19 *Hesperorthis* | | brachial, int. | S |
| 20 *Hesperorthis* | | brachial, int. | S |
| 21 *Hesperorthis* | | indet. ext | S |
| 22 art brach | | section | S |
| 23 *Iocrinus* | diam. 1.7 | isolated brachial | S |
| 24 *Hesperorthis* | | pedicle, int. | S |
| 25 *Hesperorthis* | | indet. ext | S |
| 26 *Hesperorthis* | | pedicle, ext | S |
| 27 *Hesperorthis* | | indet. ext | S |
| 28 *Hesperorthis* | | indet. ext | S |
| 29 *Hesperorthis* | w 11.5, l 8.0 | pedicle, ext | S |
| 30 *Hesperorthis* | | indet. ext | S |
| 31 *Hesperorthis* | w 11.3, l 10.4 | GOOD ped., int + ext | S |
| 32 art brach | | indet. ext | S |
| 33 *Hesperorthis* | w 9.8, l 7.8 | pedicle, int. | S |
| 34 *Hesperorthis* | w 12.0, l 11.2 | ped., int + ext | S |
| 35 *Hesperorthis* | w 9.4, l 5.6 | brachial, ext | S |
| 36 *Hesperorthis* | | brachial, section | S |
| 37 *Hesperorthis* | | pedicle, section | S |
| 38 *Hesperorthis* | | pedicle, section | S |
| 39 *Hesperorthis* | w~14. l 11.4 | pedicle, ext | S |
| 40 *Hesperorthis* | | indet. ext | S |
| 41 *Hesperorthis* | | indet. ext | S |
| 42 Trepostome bryozoan | diam. 4-5 | partial branch; *Batostoma*? | S |
| 43 *Hesperorthis* | | ped., int + ext | S |
| 44 *Hesperorthis* | | ped., int + ext | S |
| 45 *Hesperorthis* | w 9.6, l 8.7 | ped., int + ext | S |
| 46 *Hesperorthis* | w 8.2, l 6.3 | ped., int + ext | S |
| 47 *Hesperorthis* | | ped., int + ext | S |
| 48 *Hesperorthis* | | ped., int + ext | S |

| | | | |
|---|---|---|---|
| 49 sponge | ~6x4x7 | no spicules seen | |
| 50 *Hesperorthis* | | section | S |
| 51 art brach | | indet | S |
| 52 *Hesperorthis* | | indet. ext | S |
| 53 *Hesperorthis* | | pedicle, int. | S |
| 54 art brach | | indet. ext | S |
| 55 art brach | | indet. ext | S |
| 56 art brach | | indet. ext | S |
| 57 *Hesperorthis* | w 8.8, l 6.7 | ped., int + ext | S |
| 58 art brach | | indet. ext | S |
| 59 *Hesperorthis* | | pedicle, int. | S |
| 60 trail | w ~8 | sinuous trace | S |
| 61 *Hesperorthis* | | ped., int + ext | S |
| 62 *Hesperorthis* | | brachial, ext | S |
| 63 *Hesperorthis* | | brachial, int. | S |
| 64 *Hesperorthis* | | indet. ext | S |
| 65 *Hesperorthis* | | pedicle, int. | S |
| 66 *Hesperorthis* | w 6.6, l 5.1 | ped., int + ext | S |
| 67 *Hesperorthis* | | ped., int + ext | S |
| 68 sponge | >50 | ?*Oneroconchia* | S |
| 69 *Hesperorthis* | | pedicle, int. | S |
| 70 *Hesperorthis* | | indet. ext | S |
| 71 *Hesperorthis* | | pedicle, int. | S |
| 72 *Hesperorthis* | w 8.2, l 5.7 | brachial, int. | S |
| 73 *Hesperorthis* | | pedicle, int. | S |
| 74 *Hesperorthis* | w 10.4, l 8.3 | ped., int + ext | S |
| 75 *Hesperorthis* | w 12.0, l 8.4 | ped., int + ext | S |
| 76 *Hesperorthis* | w~7.3, l 6.8 | ped., int + ext | S |
| 77 *Hesperorthis* | | ped., int + ext | S |
| 78 *Hesperorthis* | | ped., int + ext | S |
| 79 *Hesperorthis* | | ped., int + ext | S |
| 80 *Hesperorthis* | w 9.1, l 7.0 | ped., int + ext | S |
| 81 *Hesperorthis* | | ped., int + ext | S |
| 82 art brach | | artic. valves, sectional | S |
| 83 *Hesperorthis* | | ped., int + ext | S |
| 84 *Hesperorthis* | | indet. valve int +ext | S |
| 85 *Hesperorthis* | | ped., int + ext | S |
| 86 art brach | | indet. valve int +ext | S |
| 87 art brach | | indet int. | S |
| 88 trail #2 | w~3 | sinuous sediment-filled trace | S |
| 89 art brach | | ped? section | S |
| 90 *Hesperorthis* | w 5.2, l 2.9 | brachial, ext | S |
| 91 *Iocrinus* | diam. 3.7, ~40 long | pleuricolumnal | S |
| 92 *Hesperorthis* | | ped., int + ext | S |
| 93 art brach | | indet., ext | S |
| 94 *Hesperorthis* | w 14, l 12 | ped., int + ext | S |
| 95 *Hesperorthis* | | indet. int + ext | S |
| 96 art brach | | indet. int + ext | S |
| 97 *Hesperorthis* | w 8, l 4.5 | ped., int + ext | S |
| 98 art brach | | indet. int + ext | S |

| | | | |
|---|---|---|---|
| 99 *?Hesperorthis* | w 2.9, l 3.2 | TWO spec.s; both valves, articulated | s |
| 100 *Hesperorthis* | | ped., int + ext | s |
| 101 *Hesperorthis* | w 7, l 5.5 | ped., int + ext | s |
| 102 *Hesperorthis* | w 6.4, l 5.1 | ped., int + ext | s |
| 103 *Hesperorthis* | w 4.5, l 3.5 | ped., int + ext | s |
| 104 *Hesperorthis* | w 5.7, l 5.0 | ped. ext | s |
| 105 *Hesperorthis* | w 12.0, l 8.0 | ped., int + ext | s |
| 106 *Hesperorthis* | w 8.5, l 6.8 | ped., int + ext | s |
| 107 *Hesperorthis* | w 8.5 | ped., int + ext | s |
| 108 art brach | | indet. int + ext | s |
| 109 art brach | | ?attached to 8.91B (crinoid pleuricolumnal) | s |
| 110 *Hesperorthis* | w 6, l 4 | brach., ext | s |
| 111 *Hesperorthis* | | brach., int+ ext | s |
| 112 bryozoan | diam. 0.6 | pinatoporellid? | s |
| 113 *Hesperorthis* | | ped., int + ext | s |
| 114 art brach | | indet., ext | s |
| 115 art brach | | brach., ext | s |
| 116 *Hesperorthis* | | ped., int + ext | s |
| 117 ?bryozoan | diam. 1.3 | mould infilled? | s |
| 118 *Hesperorthis* | | indet., ext | s |
| 119 sponge | l> 60 | ?dysideid - clastic | s |
| 120 *Hesperorthis* | | ped. int | s |
| 121 sponge | >30 | oxeas + uncinates + clastic | s |
| 122 sponge | | clastic - no spiucules visible | s |
| 123 *Hesperorthis* | | ped., int + ext | s |
| 124 *Hesperorthis* | | pedicle, sectioned | s |
| 125 *Hesperorthis* | w>13. l>10 | ped., int + ext | s |
| 126 *Hesperorthis* | | ped. ext | s |
| 127 *Hesperorthis* | | ped., int + ext | s |
| 128 *Hesperorthis* | l 6.2 | ped. int | s |
| 129 *Balacrinus* | diam. 2.8 | isolated columnals | s |
| 130 *Skenidoides?* | | articulated valves | s |
| 131 *Skenidoides?* | w 1.7, l 1.3 | articulated valves | s |
| 132 *Skenidoides?* | w 1.5, l 1.4 | ped., int + ext | s |
| 133 *Skenidoides?* | | ped., int + ext | s |
| 134 *Skenidoides?* | w 2.8, l 1.5 | GOOD brach., int + ext | s |
| 135 demosponge | >40 | ?aspicular | s |
| 136 *Skenidoides?* | w 1.4, l 1.4 | ped., int + ext | s |
| 137 *Skenidoides?* | | articulated valves | s |
| 138 indet. crinoid | diam. 1.7 | cylindrical ossicles; no lumen | s |
| 139 indet. crinoid | diam. <3 | as above; several branches in section | s |
| 140 sponge | small, incomplete | ?aspicular | s |
| 141 *Hesperorthis* | w 10.5, l 9.1 | ped., int + ext | ib |
| 142 art brach | | brach., ext | ib |
| 143 ?indet. crinoid | 1.2 x1.1 | flattened cylinder @ 90 deg. bend | ib |
| 144 *Hesperorthis* | | brach., int+ ext | ib |
| 145 *Hesperorthis* | | ped., int + ext | ib |
| 146 art brach | | indet. valve int +ext | ib |
| 147 *?Tissintia* | w 5.2, l 3 9 | brach., int+ ext | ib |
| 148 trilobite indet. | w~7 | 3D carapace sections | ib |

| | | | |
|---|---|---|---|
| 149 *Hesperorthis* | | brach., int+ ext | ib |
| 150 *Hesperorthis* | w~5, l 2.8 | ped., int + ext | ib |
| 151 *Hesperorthis* | | ped., int + ext | ib |
| 152 art brach | broken shell frag. | brach., int+ ext | ib |
| 153 art brach | | indet. valve - CIRCULAR? | ib |
| 154 *Hesperorthis* | w 12, l 10 | ped., int + ext | ib |
| 155 *Iocrinus* | diam. 3.7 | isolated primibrach | ib |
| 156 ?Tissintia | lw 3.9, l 2.7 | brach., int+ ext | ib |
| 157 trilobite indet. | axial ridge w~6 | porous structure preserved | ib |
| 158 *Hesperorthis* | w~12, l ~7 | brach., int+ ext | ib |
| 159 art brach | | indet. int + ext | ib |
| 160 ?*Horderleyella* | w~7, l~5 | brach., int+ ext | ib |
| 161 art brach | | indet. valve | ib |
| 162 art brach | | brach., int+ ext | ib |
| 163 *Hesperorthis* | w 12.6, l~10 | ped., int + ext | ib |
| 164 art brach | | ped., int + ext | ib |
| 165 *Hesperorthis* | | ped., int + ext | ib |
| 166 *Hesperorthis* | w 5.0, l 6.0 (compressed) | brach., int+ ext | ib |
| 167 *Hesperorthis* | l 4.7 | brachial (?artic. in matrix) | ib |
| 168 art brach | | indet. valve | ib |
| 169 *Iocrinus* | diam. 1.8 | 3+ artic. brachials | ib |
| 170 *Hesperorthis* | w 6.5, l 5.5 | ped., int + ext | ib |
| 171 *Hesperorthis* | w~10, l 9.6 | ped., int + ext | ib |
| 172 *Hesperorthis* | w 11.8, l 9.8 | ped., int + ext | ib |
| 173 *Hesperorthis* | | ped., int + ext | ib |
| 174 demosponge | diam. ~30 | clastic, nucleated on 8.175 | ib |
| 175 ?gastropod | diam.~18, ?spiral | poss. poor enrolled trilobite | ib |
| 176 art brach | | brach., int+ ext | ib |

X1, ?hummocky bedding (irregular ripples)
2

| | | | |
|---|---|---|---|
| **10** | 6.7 kg | | |
| 1 *Hesperorthis* | w 12.0, l 8.8 | pedicle, int. | s |
| 2 *Hesperorthis* | | section of pedicle | s |
| 3 *Hesperorthis* | w 9.0, l~6.5 | brach., int + ext | s |
| 4 ?*Polydactylus* | >150 | numerous polyuncinates | s |
| 5 *Hesperorthis* | | brach., int + ext | s |
| 6 *Hesperorthis* | | brach., int + ext | s |
| 7 *Hesperorthis* | w 10.6, l 9.8 | ped., int + ext | s |
| 8 *Hesperorthis* | | brach., int + ext | s |
| 9 *Hesperorthis* | | ped., int + ext | s |
| 10 *Hesperorthis* | w 5.8, l 3.6 | ped., int + ext | s |
| 11 *Hesperorthis* | | brach., int + ext | s |
| 12 *Iocrinus* | diam. 2.1 | isolated secundibrach | s |
| 13 *Hesperorthis* | | indet. int + ext: cp destroyed | s |
| 14 *Hesperorthis* | | brach., int + ext | s |
| 15 *Hesperorthis* | | brach., int + ext | s |
| 16 art brach | | indet valve | s |
| 17 art brach | | pedicle ext | s |

| | | | | |
|---|---|---|---|---|
| 18 hexactinellid spicule | | isolated centre | | s |
| 19 monaxon-*Pyritonema* | l>6 | fragment | | s |
| 20 ?demosponge | | aspicular; shows ?oscule | | s |
| 21 sponge - clastic mon. | >20 | coarse detrital grains and fine monaxons | | s |
| 22 *Hesperorthis* | | indet valve, ext | | s |
| 23 sponge | >70 | oxeas at surface | | s |
| 24 art brach | | sectional | | s |
| 25 *Hesperorthis* | w 8.3, l 6.6 | brach., int + ext | | ib |
| 26 *Hesperorthis* | | ped., int + ext | | ib |
| 27 ?*Tissintia* | | ped., int + ext | | ib |
| 28 *Hesperorthis* | | pedicle, int. | | ib |
| 29 sponge | >150 | monaxons common | | ib |
| 30 art brach | | ped., int + ext | | ib |
| 31 ?*Cruziana* | w 19, [l 80] | faint, probably bilobate | | ib |
| 32 trilobite indet. | w 9, l 5 | hooked genal angle? | | ib |
| 33 indet. (horseshoe) | diam. curv. 30 | trilo. axial thoracic rib? | | ib |
| 34 alga | ~2 x 0.3 | filamentous carbonaceous film | | ib |
| 35 *Hesperorthis* | w 13, l 10 | brach., int + ext | | ib |
| 36 *Hesperorthis* | | ped., int + ext | | ib |
| 37 indet. (cone) | w 1.5, l 2 | cf. B10 | | ib |
| **11** | Sponge Forest | | | |
| 1 sponge (clastic) | >120 | rare monaxons | | s |
| 2 art. brach | ~10 | indet. valve (ext) | | s |
| 3- Sponges: *Oneroconchia* | | Overlapping, fragmentary; number uncertain; | | |
| 16 and *Mirustubus* | Large | comprise up to 30% of volume | | |
| 17 ?*Oneroconchia* | >100 | few monaxons | | ib |
| 18 *locrinus* | diam. 2.1 | isolated secundibrach | | ib |
| 19 trilobite indet. | diam. 4.5 | part of thoracic rib? | | ib |
| 20 ?sponge/crinoid | 10 x 3, cylindrical | may reflect overgrowth | | ib |
| 21 sponge/microbial | diam. ~5, discoid | hollow, ferruginous, irregular surface | | ib |
| **12** | | | | |
| 1 *Hesperorthis* | w 10.0, l 8.5 | pedicle, int | | s |
| 2 sponge | >30 | aspiculr, open; fibrous walls? | | s |
| 3 sponges | large | 3 specimens, oxeate | | s |
| 4 *locrinus* | diam. 1.9 | isolated brachial | | s |
| 5 art brach | w 5.0, l 4.1 | strongly carinate; n. sp? | | s |
| 6 *Hesperorthis* | | pedicle, int | | s |
| 7 bivalve | ~20 | left valve, int + ext | | s |
| 8- Sponges: *Oneroconchia* | | | | |
| 17 and others | | as in level 10. | | |
| 18 art brach | | indet. valve | | ib |
| 19 art brach | | brachial int + ext | | ib |
| 20 bivalve | | nucleation site for sponge | | ib |
| **13** | | | | |

| | | | |
|---|---|---|---|
| 1 *Hesperorthis* | ~10 | brachial, int. | |
| 2 trepostome bryozoan | diam 4, 1.5 | ramose form | s |
| 3 *Hesperorthis* | | pedicle, ext. | s |
| 4 *Hesperorthis* | w 9.5, l 8.0 | pedicle, ext. | s |
| 5 sponge | | no obvious spic.s | s |
| 6 bryozoan #2 | biglobose, diam. 10, 6 | incomplete; first record | s |
| 7 *Ogyginus corndensis* | daim. ~13 | glabella (diagnosis suspicious!) | s |
| 8 sponge | >70 | rare oxeas | s |
| 9 *Hesperorthis* | | brach., int + ext | s |
| 10 trepostome bryozoan | diam. 4 | similar to 12.2 | s |
| 11 sponge | >50 | clastic only | s |
| 12 ?*Flexiclaymene* | | pygidium | s |
| 13 art brach | | indet. valve ext | s |
| 14 trace | w 1.5 | slightly curved ?grazing trail | s |
| 15 *Ogyginus corndensis* | | partial pygidium | s |
| 16 *Hesperorthis* | | brachial valve, ext | s |
| 17 sponge | >100 | clastic only, nucleated on 12.15 | s |
| 18 *Hesperorthis* | w 10.2, l. 7.9 | ped., int + ext | s |
| 19 *Pyritonema* | l>8 | isolated spicule | s |
| 20 sponge | >90 | clastic | s |
| 21 sponge | | clastic | s |
| 22 sponge | >70 | sparse monaxons | s |
| 23 ?*Pyritonema* | >60 | abundant monaxons; poor | s |
| 24 cheilostome bryoz. | | encrustong 12.7 (*Ogyginus*) | s |
| 25 *Iocrinus* | diam. 1.6 | isolated brachial | ib |
| 26 *Iocrinus* | diam. 3.0 | isolated primibrach | ib |
| 27 inarticulate | w 5.8 l 6.0 | indet. valve ext | ib |
| 28 *Pseudolingula*? | w 13, l 21 | indet valve int + ext | ib |
| 29 trepostome bryozoan | diam. 0.4, 15 long | ?unbranched | ib |
| 30 art brach | | broken part of shell | ib |
| 31 surface "burrow" | w~6 | simple displacive trail | ib |
| 32 trepostome bryozoan | diam. 0.1 | ramose? | ib |
| 33 ?sponge | ~7x4x5 | may be inorganic | ib |
| 34 trinucleid | spine length 10 | genal angle with straight spine | ib |
| 35 trinucleid | ~4 (fragment.) | part of same specimen? | ib |
| 36 *Hesperorthis* | w 6.2, l 3.5 | brach., int + ext (+ boring?!) | ib |
| 37 ostracod | ~2 | articulated valves | ib |

**14**

| | | | |
|---|---|---|---|
| 1 sponge | large (incomplete) | few spicules | s |
| 2 *Ogyginus corndensis* | l 30.0; c.w 26.5, p.w. ~21 | complete, immature? (6 thoracic segments) | s |
| 3 sponge | | clastic | s |
| 4 ?echinoderm | 9x7x8 | globose, with 3circular impressions; bryoz? | s |
| 5 sponge | >200 | ?*Oneroconchia* | s |
| 6 art brach | | ped., int + ext | s |
| 7 dubiofossil | 65x15, tapered | possible arthropod? (unlikely) | s |
| 8 sponge | >150 | rare monaxons | s |
| 9 *Iocrinus* | diam. 1.8 | four brachials | s |

| | | | |
|---|---|---|---|
| 10 trepostome bryozoan | diam. 0.3 | pinatoporellid? | |
| 11 alga | diam 0.3, l>12 | filamentous film in tuff | s |
| 12 spicules | | stauract, oxea, tylote... prob. decayed dysideid | s |
| 13 art brach | | indet. valve, ext | s |
| 14 sponge | >100 | ?*Mirustubus* | s |
| 15 sponge | >70 | clastic | s |
| 16 sponge | >100 | clastic | s |
| 17 echinoderm indet. | w~2.5, l 11.6 | crinoid or asteroid arm | s |
| 18 art brach | | indet valve, sectioned | s |
| 19 sponge | >90 | spicules rare or absent | s |
| 20 trails | diam. 3 | as 5.8 (same lithology) | s |
| 21 sponge | >90 | rare monaxons | s |
| 22 art brach | | indet valve, sectioned | s |
| 23 trails | diam. 3 | as 5.8 (same lithology) | s |
| 24 *Ogyginus corndensis* | l 28 | isolated librigena | ib |
| 25 trepostome bryozoan | diam. 0.8 | ramose fragment | ib |
| 26 trilobite indet, | 3x1 | thoracic rib fragment? | ib |
| 27 demosponge | 11x7 | clastic, poor pres. | ib |
| 28 *Hesperorthis* | | ped., int + ext | ib |
| 29 annelid? | diam. curv. 2.0 | segmented, horseshoe-shaped cylinder | ib |
| 30 ?*Balacrinus* | diam. 3 | columnal | ib |
| 31 ?Harpid | l 21 | librigena, extremely narrow | ib |
| 32 burrows | diam. 3-4 | simple cylinders, infaunal | ib |
| Supplemental: 5.8 kg | | | |
| 33 sponge | | ?*Oneroconchia*with growth ridges | |
| 34 crinoid indet. | | columnal | |
| 35 microbial/sponge? | | small, granular-lined cavity | |
| 36 ?*Hesperorthis* | | ped. int | |
| 37 *Hesperorthis* | | brach., int + ext | |
| 38 ?trilobite | | indet. fragment | |
| 39 *Ogyginus corndensis* | | thoracic rib fragment | |
| 40 bivalve | | small mytiloid? | |
| 41 trepostome bryozoan | | ramose fragment | |
| 42 sponge | | coarse clastic, lensiform | |
| 43 alga | | small fragment | |
| 44 alge | | dichotomous filament | |
| 45 ?arthropod | | carbonised cuticle? possib;y algal | |
| 46 bivalve | | single valve | |
| 47 sponge | | coarse clastic, lensiform | |
| 48 sponge | | large clastic with monaxons | |
| 49 trails | | meandering surface trace | |
| 50 sponge | | part of large, clastic | |
| 51 sponge | | coarse clastic, lensiform | |

**15**

| | | | |
|---|---|---|---|
| 1 Calymenid | w 14.5, l>26 | thorax only | S |
| 2 *Iocrinus* | diam. 3.2 | isolated primibrach | S |
| 3 bryozoan? | diam. ~2.7, globose | indistinct suface texture | S |
| 4 trepostome bryozoan | diam. 7 | ?*Batostoma* | S |

| | | | |
|---|---|---|---|
| 5 *Iocrinus* | diam. 2.3 | isolated brachial | s |
| 6 trepostome bryozoan | diam. ~2 | slightly curved, ramose? fragment | s |
| 7 *Hesperorthis* | | ?juvenile | s |
| 8 triactine biaxon | l 6.0, w 0.1 | associated with sponge 14.9 (foreign) | s |
| 9 sponge | 30-40 | ?dysideid | s |
| 10 *Hesperorthis* | | ped., int + ext | s |
| 11 sponge | >40 | ?dysideid | s |
| 12 sponge | >40 | occasional monaxons | s |
| 13 ?bryozoan | l>17, w~1 | blade-like | s |
| 14 indet. (pellet?) | w 4.7, l 6 | | s |
| 15 *Iocrinus* | diam. 2.4 | isolated brachial | s |
| 16 sponge | | rare monaxons | s |
| 17 sponge | ~20, discoid | ?monaxons | ib |
| 18 trace | w~4 | unilobed, curving, "segmented"; surface | ib |
| 19 *Hesperorthis* | | ped., int + ext | ib |
| 20 *Balacrinus* | diam. 3.5 | columnal | ib |
| 21 ?sponge | diam. 1.8 | spheroidal, with monaxon | ib |
| 22 trepostome bryozoan | diam. ~3 | domal, or ramose fragment | ib |
| 23 dubiofossil | L~1 | centre of nodule; probably not fossil | ib |
| Supplemental: 5.1 kg | | | |
| 24 art brach | | indet. valve int + ext | |
| 25 *Hesperorthis* | | ped., int + ext | |
| 26 *Hesperorthis* | | ped ext | |
| 27 *Hesperorthis* | | indet valve fragment | |
| 28 bivalve? | | poor; poss. leptaeniform brach. | |
| 29 *Hesperorthis* | | fragment (7 costae) | |
| 30 art brach | | indet. valve int + ext | |
| 31 ?*Balacrinus* | | smooth circular columnal | |
| 32 *Hesperorthis* | | brach. int (destroyed in prep.) | |

**16**

| | | | |
|---|---|---|---|
| 1 *Ordinosabulo* | | holotype: see taxonomy + spicule data | s |
| 2 *Hesperorthis* | w 12.0, l 7.5 | ped., int + ext | s |
| 3 sponge | diam. 41 | discoid, no obvious spicules | s |
| 4 orthocone nautiloid | l 12, w 2.8, 4.0 | partial | s |
| 5 art brach | | indet., ext | s |
| 6 *Pyritonema?* | | abundant monaxons, uncollapsed | s |
| 7 sponge? | w21 | vascular fossil, abundant monaxons | s |
| 8 art brach | | pedicle, int | s |
| 9 *Pyritonema?* | ~100 | abundant oxeas | s |
| 10 *Polydactylus* | >50 | oxeas + mid-order uncinates | s |
| 11 sponge | >130 | monaxons rare | s |
| 12 sponge | >50 | abundant oxeas | s |
| 13 sponge | >20 | spicules rare | s |
| 14 *Hesperorthis* | | pedicle, int | s |
| 15 *Iocrinus* | diam. 2.0 | isolated brachial | s |
| 16 indet. | 13x11 | cf. 4.11 - keel-shaped object | s |
| 17 *Pyritonema?* | | abundant large monaxons | s |
| 18 trepostome bryozoan | diam. 6-8 | *Batostoma* fragment | s |

| | | | |
|---|---|---|---|
| 19 art brach | | indet., ext | s |
| 20 sponge? | w22 h 7 | badly eroded cavity | s |
| 21 monaxonid sponge | | small oxeas, fine clastics | s |
| 22 sponge? | >40 | aspicular | s |
| 23 *locrinus* | diam. 2.0 | anal column fragment | s |
| 24 *locrinus* | w 3.5, l 10 | anal column | s |
| 25 sponge (monaxon) | ~20 | encrusting 15.24 | s |
| 26 sponge | >40 | rare spicules | s |
| 27 sponge | ~25 | abundant spics | s |
| 28 sponge | ~30 | rare spicules | s |
| 29 sponge | ~35 | abundant spics | s |
| 30 sponge | >40 | small spicules, fine clastics | s |
| 31 bryozoan | l~25 | bilaminate sheet, monticuliporate | s |
| 32 sponge | ~12 | poor pres., few spicules | s |
| 33 sponge (monaxonid) | >30 | coarse clasts, abundant monaxons | s |
| 34 indet. | diam. 14 | as 15. 16? | s |
| 35 art brach | | indet., ext | s |
| 36 art brach | | indet., ext | s |
| 37 indet. crinoid | diam. 2, l 25 | two joined arm fragments | s |
| 38 art brach | | indet. valve, sect | s |
| 39 ------scoria------ | | | s |
| 40 sponge | diam. 6, globose | monaxonid, clastic centre? | ib |
| 41 sponge | ~10, sub-discoid | coarse clasts | ib |
| 42 sponge | diam. 7, globose | clastics; radial orientation? | ib |
| 43 ?ostracod | l 2.8 | spheroidal hollow, unornamented | ib |
| 44 sponge | | clastic-monaxonid | ib |
| 45 *Hesperorthis* | | ped., int + ext | ib |
| 46 *Hesperorthis* | l~12 | pedicle, ext | ib |
| 47 sponge | >20x6 (discoid) | fine clastics | ib |
| 48 sponge | diam. ~4 | clastics and monaxons | ib |
| 49 *locrinus* | | articulated brachial mass | ib |

**17**

| | | | |
|---|---|---|---|
| 1 trinucleid | w 11 | enrolled, complete; high axial ridge (overgr.) | s |
| 2 *Balacrinus nodosus* | cal. diam 29; arm l. 35 | calyx + pinnulate arms (overgrown) | s |
| 3 *locrinus* | arm l 40, w 74 | arm mass, overgrown by 16.4 | s |
| 4 sponge | as above | abundant monaxons | s |
| 5 *Ogyginus*? | | pygidium with sponge overgrowth | s |
| 6 art brach | | section - indet. | s |
| 7 ?asteroid | 8.0 x 6.0 | fragment of three arms? | s |
| 8 sponge | | frequent monaxons | s |
| 9 art brach | | pedicle, ext | s |
| 10 **soft-bodied worm** | l 7.9, w 1.8 | with gut trace, in silic. nodule | s |
| 11 sponge | >65 | coarse clastics and monaxons | s |
| 12 crinoid | ~10 | poor clayx with tetralobate basal scar | s |
| 13 sponge | 12x3 | coarse clastics, tuboid; after crinoid? | s |
| 14 ?sponge | 6x3 | ?lithistid structure | s |
| 15 ----------probably inorganic---------- | | | s |
| 16 art brach | w 14, l ~10 | external, poor | s |

| | | | |
|---|---|---|---|
| 17 brach/bivalve? | | smooth shell | s |
| 18 *Hesperorthis* | | ped., int + ext | s |
| 19 *Ogyginus?* | l 13, w 14 | isolated librigena | s |
| 20 art brach | | section - indet. | ib |
| 21 art brach | | section - indet. | ib |
| 22 ?*Balacrinus nodosus* | diam 5 | circular columnals, overgrown by sponges | ib |
| 23 sponge | | few monaxons | ib |
| 24 ?orthocone | max diam. 10 | section through septae/siphuncle (central) | ib |
| 25 *Iocrinus* | <1 | arms, in section | ib |
| 26 art brach | | indet. valve ext | ib |
| 27 ?asteroid | l~10 | poss. part of two attached arms | ib |
| 28 sponge | diam. 13, sub-discoid | primarily clastic | ib |
| 29 sponge/microbial | ~5, spheroidal | monaxonid/clastic | ib |
| 30 sponge/microbial | 4x2 | multilobate, hollow | ib |
| 31 *Iocrinus* | diam. 1.6 | isolated brachial | ib |
| 32 sponge | l 13 | clastic, nucleated on 16.33 | ib |
| 33 bivalve? | ~7x8 | fragment, no detail | ib |
| 34 crinoid | side length 2 | two square ossicles with small lumen | ib |
| 35 sponge/microbial | 4x3 | clastic | ib |
| 36 echinoderm debris | ~4x2 | mass of plates | ib |
| 37 *Hesperorthis* | w~10 | ped., int + ext | ib |

**18**

| | | | |
|---|---|---|---|
| 1 art brach | w>14 | pedicle, int. | s |
| 2 *Pyritonema* | diam. 23 | monaxons only | s |
| 3 *Pyritonema* | diam. 31 | as 17.2, but less organised | s |
| 4 art brach | | indet. ext | s |
| 5 sponge | ~50 | may be part of 17.3 | s |
| 6 ?*Pyritonema* | diam. 33 | some simple uncinates? | s |
| 7 *Polydactlyus entropus* | 18x6, discoid | high-order uncinates + triact?! | s |
| 8 *Pyritonema* | l 40, w 35 | divergent spray of oxeas | s |
| 9 indet. organic matter | ~30 | focus of siliceous nodule | s |
| 10 sponge | ~30 | clastic, few spicules | s |
| 11 art brach | | indet. ext | s |
| 12 sponge | >40 | clastic, few spicules | s |
| 13 sponge | >30 | clastic, few spicules | s |
| 14 sponge | ~20x8 | monaxons and clastics; no uncinates | s |
| 15 sponge | | clastic, few spicules | s |
| 16 ?sponge | ~30x15x? | silicified | s |
| 17 sponge | diam. 5, x 2 | no spicules | ib |
| 18 ?*Skenidoides* | | indet. ext | ib |
| 19 indet. crinoid plates | diam. 2.8 | poor, square ossicle | ib |
| 20 sponge | ~9, globose | rare oxeas; clastic | ib |
| 21 *Iocrinus* | area 30x20 | articulated arms in nodule | ib |
| 22 sponge | ~30, globose | clastic, few spicules | ib |
| 23 sponge | 12x7, ellipsoidal | clastic, few spicules | ib |
| 24 ?Skenidoides | w 2.1, depth 0.6 | articulated valves, int + ext | ib |
| 25 *Balacrinus* | l~4 | pinnule mass | ib |
| 26 sponge | diam~30, flattened | clastic, few spicules | ib |

| | | | |
|---|---|---|---|
| 27 microbial?/sponge | diam. 2.8, globose | clastic, few spicules | ib |
| 28 ?*Pyritonema* | l 3.5, diam. 1 | monaxon | ib |
| 29 inarticulate | w 0.9, l 1.6 | indet. int + ext | ib |
| 30 crinoid indet. | diam. 1 | arm fragment | ib |
| 31 sponge | diam. 8, globose | few radial monaxons | ib |
| 32 *Flexicalmene* | l 10.3, glab. w. 5.0 | cranidium (GOOD) | ib |
| 33 sponge | width 6.3 | clastic, few spicules | ib |
| 34 indet. organic matter | diam~15 | filamentous in places; probably algal | ib |
| 35 trepostome bryozoan | diam.~1 | ramose fragment with some internal structure | ib |
| 36 sponge | 8x3 | clastic, few spicules | ib |
| 37 trepostome bryozoan | diam. 2.6 | ramose fragment with some internal structure | ib |
| 38 indet. crinoid plates | diam. 1.2, 0.5 | square (?) ossicles | ib |
| 39 sponge | ~6 | clastic, few spicules | ib |
| 40 as 17.34 | >15 | diffuse | ib |
| 41 ?*Iocrinus* | diam. 2.1 | pentastellate lumen, circular outline | ib |
| 42 *Iocrinus* | diam. 2.0 | isolated brachial | ib |
| 43 ?*Ordinosabulo* | diam. 10-14 | fine clastics, loose | ib |

**19** majority of skeletal fragments encrusted by amorphous sponges

| | | | |
|---|---|---|---|
| 1 *Hesperorthis* | | articulated valves, section | s |
| 2 *Hesperorthis* | | indet. ext | s |
| 3 *Hesperorthis* | | indet. ext | s |
| 4 *Hesperorthis* | | ped. int | s |
| 5 *Hesperorthis* | | indet. ext | s |
| 6 crinoid indet. | diam. 1.1 | square ossicles; arm fragments | s |
| 7 ----------inorganic---------- | | | s |
| 8 *Hesperorthis* | w 11.5, l 6.3 | brach. int | s |
| 9 *Hesperorthis* | | indet. ext | s |
| 10 *Hesperorthis* | w 13.6, l 12.0 | ped. int | s |
| 11 *Hesperorthis* | | indet. ext | s |
| 12 *Hesperorthis* | w 13.4, l 10.3 | ped. int | s |
| 13 art brach | | brachial, ext | s |
| 14 *Iocrinus* | l 40 | arms plus anal column | s |
| 15 *Hesperorthis* | w 16.6, l 12.3 | ped., int + ext | s |
| 16 art brach | | brachial, ext | s |
| 17 sponge | ~30x13 | occasional small monaxons | s |
| 18 *Iocrinus* | ~30x20 | mass of articulated arms | s |
| 19 sponge | | uncinates present, in clastics | s |
| 20 bivalve | l 19, w 6, h 1 | horn-shaped, with growth lines | s |
| 21 *Iocrinus* | various | same spec. as 18.14? | s |
| 22 *Hesperorthis* | w 13.6, l 8.1 | brach. int | s |
| 23 art brach | w 1.9, l 2.2 | articulated valves, ext. | s |
| 24 orthocone nautiloid | l~60, max. diam.~8 | central siphuncle (sponge-encrusted) | s |
| 25 *Hesperorthis* | w 13.5, l~11.5 | ped. ext | s |
| 26 *Hesperorthis* | | ped. int | s |
| 27 bivalve | l 20, w 15, h 10 | articulated valves | s |
| 28 art brach | | indet. ext | s |
| 29 sponge | 13x7 | monaxonid; nothing exciting. | s |
| 30 sponge | | clastic, frequent oxeas | s |

| | | | |
|---|---|---|---|
| 31 sponge | >45 | clastic; spicules rare or absent | s |
| 32 art brach | | indet. ext | s |
| 33 crinoid indet. | diam. 1.3 | arm fragments, overgrown; square | s |
| 34 ?sponge | diam. 39, discoid | fragment. organic remains; rare spicules | s |
| 35 *Iocrinus* | | fragment of brachials | s |
| 36 sponge | >50 | spicules rare | s |
| 37 *Hesperorthis* | | brachial, ext | s |
| 38 *Pyritonema* | diam. 16 | in nodule | s |
| 39 *Hesperorthis* | large | ped. int | s |
| 40 sponge | diam~27 | clastic, frequent oxeas | s |
| 41 sponge | ~20 | clastic, silicified in nodule | s |
| 42 *Hesperorthis* | | brach. int | s |
| 43 sponge | >35 | abundant spics (inc. low-order uncinates?) | s |
| 44 sponge | >70 | spicules rare | s |
| 45 sponge | >30 | occasional small monaxons | s |
| 46 sponge | >40x>25 | spicules rare | s |
| 47 fenestellid bryozoan | l~10, w 11 | poor pres., but reticulation visible | s |
| 48 mytiloid bivalve | w~12, l~23 | articulated valves, ext. | s |
| 49 art brach | | ped., int + ext | s |
| 50 sponge | 32x24 | few spicules | s |
| 51 sponge | 4x11 | lined by monaxons | s |
| 52 *Hesperorthis* | | ped. int | s |
| 53 *Hesperorthis* | | ped., int + ext | s |
| 54 *Hesperorthis* | | ped. int | s |
| 55 ?bryozoan | ~20x15 | multilobate globular mould; poss. crinoid | s |
| 56 *Hesperorthis* | w 4.9, l 4.7 | brach. ext | s |
| 57 sponge | >10 | monaxonid, encrusting brachiopod | s |
| 58 *Hesperorthis* | | ped., int + ext | s |
| 59 microbial/sponge | diam. 2. 6 | spheroidal mass attached to spicule | s |
| 60 *Hesperorthis* | | brach. int | s |
| 61 ?sponge | cylind., diam. 6, l 19 | nucleated on worm tube/nautiloid? | s |
| 62 sponge | >120 | frequent oxeas | s |
| 63 gastropod?? | ~16 | encrusted: frequent oxeas | s |
| 64 sponge | 42x22 | frequent oxeas | s |
| 65 sponge | ~30 | rare oxeas + uncinates | s |
| 66 ?*Polydactylus* | ~29 | high-order uncinates + triact? | s |
| 67 *Iocrinus* | diam. 1.0, l 6.3 | arm fragments | s |
| 68 *Hesperorthis* | w 16.4, l 17.9 | (largest found) ped., int + ext | s |
| 69 indet. | >35 | "ellipsoidal growth around peak" | s |
| 70 sponge | >100 | frequent oxeas | s |
| 71 *Iocrinus* | diam 1.1, l 5.8 | heteromorphic column fragment | s |
| 72 *Iocrinus* | l 16 | overgrown pleuricolumnal | ib |
| 73 microbial/sponge | ~6 | spheroidal, aspicular | ib |
| 74 microbial/sponge | ~4 | spheroidal; coarse granular | ib |
| 75 microbial/sponge | ~2 | spheroidal; coarse granular | ib |
| 76 microbial/sponge | 7x2 | coarse granular + monaxons | ib |
| 77 sponge | 6x2x? | reniform, based on brach. | ib |
| 78 *Hesperorthis* | w~9. l~8 | ped., int + ext | ib |
| 79 sponge | >70 | ?*Oneroconchia* | ib |
| 80 indet. crinoid | | isolated ossicles | ib |

| | | | |
|---|---|---|---|
| 81 microbial/sponge | ~3 | spheroidal; coarse granular | ib |
| 82 *Hesperorthis* | | indet. ext | ib |
| 83 *Hesperorthis* | w 12, l 9 | pedicle | ib |
| 84 ?crinoid | diam. 4 | sponged! | ib |
| 85 *Iocrinus* | diam. 2.2 | isolated brachial | ib |
| 86 *Hesperorthis* | w~8, l 6.8 | brach., int + ext | ib |
| 87 art brach | | ped., int + ext | ib |
| 88 sponge | 18x12, oblate | clastic | ib |
| 89 sponge | | clastic | ib |
| 90 *Hesperorthis* | | pedicle | ib |
| 91 sponge | ~13, oblate | clastic, with oxeas; trilobite fragments | ib |
| 92 *Hesperorthis* | w~10, l 8.2 | ped., int + ext | ib |
| 93 ?*Tissintia* | w. 4.4, l 4.0 | brach., int + ext | ib |
| 94 crinoid indet | diam. 3; lumen 2.3 | pentagonal lumen | ib |
| 95 indet. trilobite | | cranidium fragment | ib |
| 96 art brach | diam~27 | indet., sponge-encrusted | ib |
| 97 sponge | ~12 | clastic with possible OSTRACODES (5) | ib |
| 98 sponge | diam.2, l~5 | based on crinoid? | ib |
| 99 pleurotomariid gast. | | sponge-encrusted | ib |
| 100 orthocone nautiloid | l 28, max. w. 4 | sponge-filled chamber | ib |
| 101 ?mollusc | diam.3, bisected | gastropod or bivalve | ib |
| 102 sponge | 30-40 | clastic | ib |
| 103 *Hesperorthis* | w 9.2, l 6.5 | brach. int | ib |
| 104 ortchocone nautiloid | l 29, max. w. 8 | infilled by monaxon/clastic sponge | ib |
| 105 art brach | diam.~12 | spobge infilled | ib |
| 106 sponge | diam. 7, globose | coarse granular + monaxons | ib |
| 107 art brach | w~12 | sponge infilling | ib |
| 108 art brach | | indet. ext | ib |
| 109 bivalve | l 27, w 16 | left valve | ib |
| 110 orthocone nautiloid | l>25, maw. w. 7 | sponge-infilled | ib |
| 111 spiral nautiloid? | diam. 18 | spiral structure silicified | ib |
| 112 trepostome bryozoan | diam. 0.7, l~15 | ramose colony fragment | ib |
| 113 microbial/sponge | diam. 5 | sub-globose, coarse clastic | ib |
| 114 trepostome bryozoan | diam. 2.5 | ramose colony fragment | ib |
| 115 *Hesperorthis* | | indet. ext | ib |
| 116 sponge | | nucleated on scoria | ib |
| 117 sponge | diam~8, ellipsoidal | coarse clastic | ib |
| 118 trilobite indet. | l~22 | genal fragment? | ib |
| 119 microbial/sponge | diam. 3.5 | globose, coarse clastic | ib |
| 120 sponge | | clastic with monaxons | ib |
| 121 sponge | 13x11x4.5 | mamillated internal "mould"; unusual | ib |
| 122 *Iocrinus* | diam. 4 | isolated primibrach | ib |
| 123 *Iocrinus* | diam. 1.4 | isolated brachial | ib |
| 124 *Iocrinus* | diam. 3.4 | isolated primibrach | ib |
| 125 *Hesperorthis* | l 7.5 | ped., int + ext | ib |
| 126 *Ogyginus corndensis* | | thorax, glabella (broken); juvenile? | ib |
| 127 bryozoan | ~2 | indet. morphology (frag.) | ib |
| 128 *Pyritonema* | >25 | silicified | ib |
| 129 microbial/sponge | ~2 | spheroidal; coarse granular | ib |
| 130 microbial/sponge | ~5 | irregular clastic | ib |

| | | | |
|---|---|---|---|
| 131 sponge | 5x3, biglobose | clastic/oxeate | ib |
| 132 bivalve | w. 5.5 | monaxonid sponge internally | ib |
| 133 microbial/sponge | ~3 | irregular clastic | ib |
| 134 sponge | diam.~6 | clastic monaxonid | ib |
| 135 sponge | diam. 3.8 | clastic monaxonid | ib |
| 136 art brach | | indet. ext | ib |
| 137 microbial/sponge | diam. 2.9 | spheroidal; clastic + monaxonid | ib |
| 138 microbial/sponge | diam. 2.8 | spheroidal; clastic + monaxonid | ib |
| 139 microbial/sponge | diam. 3.3 | spheroidal; clastic + monaxonid | ib |

**LR 1** (level 9-11 logged section)

| | | | |
|---|---|---|---|
| 9/11 1 | 1.45 kg | ~4cm | upper surface=base of demosponge |
| 9/11 - 1.1 | demosponge | >20 cm | Flat base, inclined sides, lobate. Possibly two, merging. |
| 9/11 - 1.2 | demosponge | ~4 x 3 cm | Ellipsoidal, fine surface detail; ?spicular |
| 9/11 - 1.3 | "grazing trail" | w 3-4 mm; L ~ 5 cm | bifurcating, discontinuous. Upper surface. |
| 9/11 - 1.4 | demosponge | 3 x 2 cm | calcite? disc in centre; centred on bedding plane |
| 9/11 - 1.5 | demosponge | small | highly irregular surface; spicular; not on bedding plane |
| 9/11 2 | 1.35 kg | ~4 cm | |
| 9/11 - 2.1 | *Iocrinus* | | Primibrach, isolated. Intra-bed. |
| 9/11 - 2.2 | ?microbial | 3 - 4 mm | small ferruginous (clastic) spheroid; hollow. Intra-bed. |
| 9/11 - 2.3 | *Iocrinus* | | brachial, isolated. Intra-bed. |
| 9/11 - 2.4 | ?microbial | 3 mm | hollow ferruginous spheroid. Intra-bed. |
| 9/11 - 2.5 | *Iocrinus* | | brachial, isolated. |
| 9/11 - 2.6 | *?Ogyginus* | | fragment of lateral cranidial lobe? Intra-bed, oblique. |
| 9/11 - 2.7 | art. Brach | L 2 mm | Both valves (p:int; b:ext). On bedding plane. |
| 9/11 - 2.8 | *Iocrinus* | | Two isolated secundi-/ tertibrachs. on bedding plane |
| 9/11 - 2.9 | *Hesperorthis* | | pedicle valve (int & ext) intra-bed, concave-up. |
| 9/11 - 2.10 | demosponge | 4 x 9 mm | fragment of coarse clastic |
| 9/11 - 2.11 | *Iocrinus* | | approx. 10 brachials; most coplanar, intra-bed. |
| 9/11 - 2(1.1) | demosponge | | counterpart (upper surface) of 1.1. No distinct structure. |
| 9/11 - 2.12 | art. brach | L 3 mm; w 4 mm | pedicle valve with straight costae. |
| 9/11 - 2.13 | art. brach | | as above, 1cm distant |
| 9/11 - 2.14 | *Iocrinus* | | distal brachials |
| 9/11 - 2.15 | demosponge | large | type 10-11 |
| 9/11 3 | 1.75 kg | 2.5 cm | |
| 9/11 - 3.1 | *Hesperorthis* | L 9 w 11 mm | pedicle valve, internal. |
| 9/11 - 3.2 | art brach | L 2 w 3mm | small flat valve, sulcate ?ext. |
| 9/11 - 3.3 | art brach | L 2 w 3mm | countervalve of above? |
| 9/11 - 3.4 | ramose bryozoan | w 2 mm L 11 mm | small trepostome fragment |
| 9/11 - 3.5 | *Hesperorthis* | L>6, w~9 | brachial, internal |
| 9/11 - 3.6 | *Hesperorthis* | L > 4.5 | pedicle, external. |
| 9/11 - 3.7 | *Hesperorthis* | L~ 5 | brachial, external |
| 9/11 - 3.8 | *Hesperorthis* | | pedicle, internal; abraded |

| | | | | |
|---|---|---|---|---|
| 9/11 - 3.9 | art brach | | fragment, ext. | |
| 9/11 - 3.10 | art brach | | partial, ext. | |
| 9/11 - 3.11 | art brach | | indet valve, ext. | |
| 9/11 - 3.12 | *Hesperorthis* | L ~ 3 | brachial, internal | |
| 9/11 - 3.13 | demosponge | large | clastic monaxid; porous, no suface structure | |
| 9/11 - 3.14 | demosponge | large | probably same individual | |
| 9/11 - 3.15 | *Iocrinus* | | isolated brachial (poor) | |
| 9/11 - 3.16 | art brach | | pedicle ? (broken) | |
| 9/11 - 3.17 | *Iocrinus* | | radial, isolated | |
| 9/11 - 3.18 | *Hesperorthis* | | sectioned, indet. Valve | |
| 9/11 - 3.19 | *Hesperorthis* | w> 12 (est.) | pedicle? Ext (convex). | |
| 9/11 - 3.20 | *Hesperorthis* | L ~ 6 w~ 9 | incomplete, but well-preserved. Intra-bed | |
| 9/11 - 3.21 | infaunal burrow | diam. 3.5 mm | horizontal, depth uncertain | |
| 9/11 - 3.22 | *Hesperorthis* | | pedicle, int & ext; intra-bed | |
| 9/11 - 3.23 | ?sponge | | radiating fibrous structure | |
| 9/11 - 3.24 | art brach | small | indet valve, ext. | |
| 9/11 - 3.25 | art brach | small | pedicle, external. | |
| 9/11 - 3.26 | *Hesperorthis* | small (juvenile?) | pedical Int & ext | |
| 9/11 - 3.27 | *Hesperorthis* | | brachial, int & ext. incomplete | |
| 9/11 - 3.28 | demosponge | | part of 13/14? | |
| | | | | 2 |
| 9/11 4 | 1.15 kg | 2.3 cm | single bed | |
| 9/11 - 4.1 | *Hesperorthis* | | pedicle; distal costae, median ridge; intra-bed, horiz. | ib |
| 9/11 - 4.2 | *Hesperorthis* | | indet., partial | s |
| 9/11 - 4.3 | *Hesperorthis* | | brachial, int. | 1b |
| 9/11 - 4.4 | *Hesperorthis* | | pedicle; (spec. broken) inclined | ib |
| 9/11 - 4.5 | *Hesperorthis* | | half pedicle (shell broken) | s |
| 9/11 - 4.6 | *Hesperorthis* | | pedicle; very reduced costae | |
| 9/11 - 4.7 | *Hesperorthis* | | pedicle; partial. Horizontal | ib |
| 9/11 - 4.8 | *Hesperorthis* | | pedicle; inclined | ib |
| 9/11 - 4.9 | *Hesperorthis* | L2.4 mm | juvenile? Horizontal | ib |
| 9/11 - 4.10 | *Hesperorthis* | | pedicle, int. inclined 60 | ib |
| 9/11 - 4.11 | infaunal burrow | dia. 4.8 mm; 1-2 cm | subvertical | |
| 9/11 - 4.12 | *Hesperorthis* | | pedicle; steeply inclined | ib |
| 9/11 - 4.13 | *Hesperorthis* | | pedicle; internal. Horiz. | s |
| 9/11 - 4.14 | *Hesperorthis* | | pedicle, int. sub-horizontal | ib |
| 9/11 5 | 2.45 kg | 3.5 cm | | |
| 9/11 - 5.1 | *Hesperorthis* | | pedicle exterior | s |
| 9/11 - 5.2 | *Hesperorthis* | | pedicle int. + ext. | s |
| 9/11 - 5.3 | *Hesperorthis* | | pedicle | s |
| 9/11 - 5.4 | *Hesperorthis* | | brachial | s |
| 9/11 - 5.5 | *?Hesperorthis* | | indet valve; may be *dynevorensis* | s |
| 9/11 - 5.6 | *Hesperorthis* | | pedicle, int. + ext | s |
| 9/11 - 5.7 | *Hesperorthis* | | pedicle exterior | s |
| 9/11 - 5.8 | *Hesperorthis* | | pedicle int. + ext. | s |
| 9/11 - 5.9 | *Hesperorthis* | | pedicle int. + ext. | ib |
| 9/11 - 5.10 | *Hesperorthis* | | pedicle int. + ext. | ib, oblique |
| 9/11 - 5.11 | *Hesperorthis* | | pedicle exterior | ib, oblique |
| 9/11 - 5.12 | *Hesperorthis* | | pedicle int. + ext. | ib, oblique |
| 9/11 - 5.13 | *Hesperorthis* | | indet valve; ext | s |
| 9/11 - 5.14 | indet art. Brach | | indet valve; ext | s |
| 9/11 - 5.15 | *Hesperorthis* | | pedicle umbo (biostratinomically broken) | ib, vertical |
| 9/11 - 5.16 | *Hesperorthis* | | pedicle, int. | s |

| | | | | |
|---|---|---|---|---|
| 9/11 - 5.17 | *Hesperorthis* | | brachial, int. | s |
| 9/11 - 5.18 | *Hesperorthis* | | pedicle exterior | s |
| 9/11 - 5.19 | *Hesperorthis* | L 3.5 mm | pedicle int. + ext. | |
| 9/11 - 5.20 | *?Hesperorthis* | | pedicle int. + ext. (fine costae) | ib |
| 9/11 - 5.21 | *Hesperorthis* | | pedicle, int. + ext | ib |
| 9/11 - 5.22 | *Hesperorthis* | | pedicle, int. + ext | ib, inclined |
| 9/11 - 5.23 | *Hesperorthis* | | pedicle, int. | s |
| 9/11 - 5.24 | *Hesperorthis* | | fragment | s |
| 9/11 - 5.25 | *Paterula cf. fissula* | diam. 3.0 mm | very high radial symmetry; int. + ext. | s |
| 9/11 - 5.26 | *Hesperorthis* | L10 mm, w 11.5 mm | pedicle int. + ext. | s(l) |
| 9/11 - 5.27 | *Hesperorthis* | | brachial int. | s |
| 9/11 - 5.28 | *Hesperorthis* | | sectional view | ib |
| 9/11 - 5.29 | *Flexicalymene* | | partial librigena exterior | ib |
| | | | | |
| 9/11 6 | 1.10 kg | 1.7 cm | | |
| | | | | |
| 9/11 - 6.1 | ?ostracod | L 1.5 mm | mouldic spheroid, smooth shell | ib |
| 9/11 - 6.2 | art. brach | | pedicle valve ext; NOT *Hesperorthis* | ib |
| 9/11 - 6.3 | *Tissintia?* | L 2.5 mm | ext. indet valve | s |
| 9/11 - 6.4 | art. brach | | indet. exterior | s |
| 9/11 - 6.5 | *Hesperorthis* | | pedicle int. | s |
| 9/11 - 6.6 | *Hesperorthis* | | pedicle ext. | s |
| 9/11 - 6.7 | *Hesperorthis* | | indet. exterior | s |
| 9/11 - 6.8 | *Hesperorthis* | w 6.3; Lp 6.0, Lb 4.2 | articulated valves: HOLOTYPE? | ib |
| 9/11 - 6.9 | *Hesperorthis* | w>12 mm | brachial int | ib, inclined |
| 9/11 - 6.10 | *Hesperorthis* | L> 7 mm | pedicle, int. | ib, inclined |
| 9/11 - 6.11 | *Hesperorthis* | | articulated valves: incomplete ext. | ib |
| 9/11 - 6.12 | *Hesperorthis* | w 10.8 L 6.8 mm | brachial int + ext | ib |
| 9/11 - 6.13 | *Hesperorthis* | | pedicle int.(deformed) | ib, inclined |
| 9/11 - 6.14 | *Hesperorthis* | w 9.6 mm | pedicle int + ext | ib |
| 9/11 - 6.15 | *Hesperorthis* | | brachial int (incomplete) | s |
| 9/11 - 6.16 | *Ogyginus?* | | probable librigena fragment | ib |
| 9/11 - 6.17 | *?Hesperorthis* | L 3 mm | pedicle int. + ext. | S(l) |
| 9/11 - 6.18 | *Hesperorthis* | | pedicle int. | s |
| 9/11 - 6.19 | *Hesperorthis* | | pedicle ext. | s |
| 9/11 - 6.20 | *Hesperorthis* | | pedicle ext. | s |
| 9/11 - 6.21 | *Hesperorthis* | | indet. exterior | s |
| 9/11 - 6.22 | *Hesperorthis* | | indet. exterior | ib, inclined |
| 9/11 - 6.23 | *art. brach* | ~1 mm | pedicle | s |
| 9/11 - 6.24 | *Hesperorthis* | | pedicle int. | s |
| 9/11 - 6.25 | *Hesperorthis* | | indet. exterior | s |
| 9/11 - 6.26 | *?Skenidiodes* | L 1.3 mm | sulcate brachial valve | s |
| 9/11 - 6.27 | *?Skenidiodes* | ~2 mm | articulated valves | s |
| 9/11 - 6.28 | *Hesperorthis* | | pedicle int. | s |
| 9/11 - 6.29 | *Hesperorthis* | | edge of large valve | ib |
| 9/11 - 6.30 | *Hesperorthis* | | brachial int. + ext. | ib |
| 9/11 - 6.31 | art. brach | | pedicle int + ext | ib |
| 9/11 - 6.32 | *?Cryptolithus* | | genal spine/ fringe | ib |
| | | | | |
| 9/11 7 | 1.15 kg | 2.3 cm | | |
| | | | | |
| 9/11 - 7.1 | Hesperorthis | L 6.4 mm | pedicle int + ext | ib |
| 9/11 - 7.2 | Hesperorthis | w> 9 mm | brachial int + ext | ib |
| 9/11 - 7.3 | *Iocrinus* | | two isolated ?primibrachs | ib |
| 9/11 - 7.4 | Hesperorthis | w ~ 9 mm | pedicle int + ext | ib |
| 9/11 - 7.5 | Hesperorthis | w ~ 7mm | pedicle int | s |
| 9/11 - 7.6 | Hesperorthis | L ~ 8 mm | articulated valves (poor) | ib |

| | | | | |
|---|---|---|---|---|
| 9/11 - 7.7 | Hesperorthis | w> 12mm | pedicle ext | ib |
| 9/11 - 7.8 | Hesperorthis | | pedicle ext | s |
| 9/11 - 7.9 | *Iocrinus* | | isolated ?primibrach | ib |
| 9/11 - 7.10 | Hesperorthis | | brachial int | ib |
| 9/11 - 7.11 | Hesperorthis | w ~ 13 mm | pedicle int + ext | ib |
| 9/11 - 7.12 | Hesperorthis | L 10, w 12 mm | pedicle int | s |
| 9/11 - 7.13 | *Skenidiodes?* | L 3 mm | indet valve | |
| 9/11 - 7.14 | Hesperorthis | L ~ 10.5 mm | pedicle int + ext | ib |
| 9/11 - 7.15 | Hesperorthis | w ~ 8 | articulated valves (poor) | ib |
| 9/11 - 7.16 | Hesperorthis | w 11.0; L 9.2 mm | pedicle int + ext | ib |
| 9/11 - 7.17 | Hesperorthis | w ~ 7.8 mm | pedicle int + ext | s(l) |
| 9/11 - 7.18 | Hesperorthis | w 12.8; L 9.9 mm | brachial int + ext | ib |
| 9/11 - 7.19 | *Iocrinus?* | | indet. plate | ib |
| 9/11 - 7.20 | Hesperorthis | L 8.9; w 10.0 | pedicle int + ext | ib |
| 9/11 - 7.21 | Hesperorthis | L 2.5 w 3.5 mm | brachial int + ext | ib |
| 9/11 - 7.22 | Hesperorthis | | pedicle int + ext | ib |
| 9/11 - 7.23 | Hesperorthis | w ~ 7mm | articulated valves (poor) | s |
| 9/11 - 7.24 | Hesperorthis | | indet valve ext | s |
| 9/11 - 7.25 | Hesperorthis | w 10.1 mm | pedicle int + ext | s |
| 9/11 - 7.26 | Hesperorthis | | pedicle (sectioned) | ib |
| 9/11 - 7.27 | Hesperorthis | L>9 | pedicle int + ext | s(l) |
| 9/11 - 7.28 | Hesperorthis | | pedicle (fragment) - large | ib |
| 9/11 - 7.29 | *Iocrinus* | | two attached ?secundibrachs | ib |
| 9/11 - 7.30 | Hesperorthis | L12 .5; w 14.3 | pedicle int + ext | ib |
| 9/11 - 7.31 | Hesperorthis | L 11 mm | pedicle int + ext | ib |
| | | | | |
| 9/11 8 | 1.15 kg | 2.7 cm | | |
| | | | | |
| 9/11 -8.1 | art. brach. | | indet valve ext | s |
| 9/11 -8.2 | *Hesperorthis* | w ~ 12 mm | pedicle int + ext | s |
| 9/11 -8.3 | art. brach. | L ~ 1 mm | indet valve int. + ext | s(l) |
| 9/11 -8.4 | *Hesperorthis* | w 13; L 11 mm | pedicle int + ext | s(l) |
| 9/11 -8.5 | art.brach | L ~ 2 mm | pedicle int + ext | ib |
| 9/11 -8.6 | *Hesperorthis* | w 6.5 mm | brachial int + ext | ib |
| 9/11 -8.7 | *Hesperorthis* | w 6 mm | brachial int + ext | ib |
| 9/11 -8.8 | *Hesperorthis* | | brachial int + ext | ib |
| 9/11 -8.9 | *Hesperorthis* | L > 10 mm | pedicle int + ext | ib |
| 9/11 -8.10 | *Hesperorthis* | L > 10 mm | pedicle int + ext | ib |
| 9/11 -8.11 | *Hesperorthis* | | pedicle int | ib |
| 9/11 -8.12 | *Hesperorthis* | ~ 7 mm | brachial int + ext | ib |
| 9/11 -8.13 | *Hesperorthis* | | indet (sectioned) | ib |
| 9/11 -8.14 | *Hesperorthis* | | pedicle int + ext (distorted) | ib |
| 9/11 -8.15 | *Hesperorthis* | w 8.7; L 7.8 | pedicle int + ext | ib |
| 9/11 -8.16 | *Hesperorthis* | | pedicle int | s |
| 9/11 -8.17 | *Hesperorthis* | | articulated valves (Poor) | ib |
| 9/11 -8.18 | *Hesperorthis* | | brachial ext | ib |
| 9/11 -8.19 | *Hesperorthis* | | brachial ext | ib |
| 9/11 -8.20 | *?Tissintia* | L 1.8 w 2.5 | indet ext; straight costae | ib |
| 9/11 -8.21 | *Hesperorthis* | L 8.3 w 10.0 mm | pedicle int + ext | s(l) |
| 9/11 -8.22 | *Hesperorthis* | | indet valve (small) | s |
| | SUB-OBRUTION BED | | | |
| 9/11 -8.23 | Trinucleid | | part of pitted fringe | ib |
| 9/11 -8.24 | *Hesperorthis* | w 8 mm | pedicle int + ext | ib |
| 9/11 -8.25 | *Iocrinus* | | isolated distal brachial | ib |
| | | | | |
| 9/11 9 | 1.80 kg | 1.5 cm | | |

| | | | | |
|---|---|---|---|---|
| 9/11 - 9.1 | *Hesperorthis* | w 6.5 L 5.0 mm | pedicle int + ext (inverted) | s(l) |
| 9/11 - 9.2 | *Hesperorthis* | w >12; L> 10 mm | pedicle int + ext | ib |
| 9/11 - 9.3 | *Hesperorthis* | w 6.8 L 4.0 | pedicle int + ext | ib |
| 9/11 - 9.4 | *Hesperorthis* | | brachial int + ext | ib |
| 9/11 - 9.5 | *Hesperorthis* | L 7.0 mm | brachial int + ext | s(l) |
| 9/11 - 9.6 | Vertical burrow | diam. 8 mm | cf. *Skolithos* intruding underlying bentonite | ib |
| 9/11 - 9.7 | crinoid | | indet plate - poss. *Iocrinus* radial | s(l) |
| 9/11 - 9.8 | *Hesperorthis* | w 3.5 L 3.2 mm | pedicle int + ext | ib |
| 9/11 - 9.9 | *Hesperorthis* | L 7.0 mm | brachial int + ext | ib |
| 9/11 10 | 0.60 kg | 1.1 cm | | |
| 9/11 -10.1 | *Hesperorthis* | w 10.8; L 9.0 mm | pedical int + ext (excellent spec.) | s |
| 9/11 -10.2 | *Hesperorthis* | w 9.6 L 7.4 mm | pedical int | s(l) |
| 9/11 -10.3 | *Hesperorthis* | L ~ 3.2 mm | brachial int + ext | s(l) |
| 9/11 -10.4 | *Hesperorthis* | L 9.2 mm | pedical ext | s |
| 9/11 -10.5 | *Iocrinus* | diam. 3.5 mm | isolated primobrach | ib |
| 9/11 -10.6 | *Hesperorthis* | w 7.8 L 5.4 mm | brachial int + ext | s(l) |
| 9/11 -10.7 | *Hesperorthis* | | brachial int | s(l) |
| 9/11 11 | 1.30 kg | 3.5 cm | | |
| MIDDLE BED | | | | |
| 9/11 - 11.1 | *Flexicalymene* | w 13 mm | cephalon | ib |
| 9/11 - 11.2 | Hesperorthis | L 6.5 | half of pedicle valve | ib |
| UPPER BED | | | | |
| 9/11 - 11.3 | Hesperorthis | w 10 mm | pedicle int + ext (reduced costae) | ib |
| 9/11 12 | 2.90 kg | 4.5 cm | | |
| 9/11 - 12.1 | *Hesperorthis* | L > 6 mm | pedicle int | s |
| 9/11 - 12.2 | *Hesperorthis* | L > 9.5 mm | pedicle int | s |
| 9/11 - 12.3 | *Hesperorthis* | | pedicle int + ext | ib |
| 9/11 - 12.4 | *Hesperorthis* | w> 9 mm | pedicle int + ext | s(l) |
| 9/11 - 12.5 | *Hesperorthis* | w 9 mm | brachial int + ext | ib |
| 9/11 - 12.6 | *Hesperorthis* | L ~9.8 mm | pedical ext | s |
| 9/11 - 12.7 | *Hesperorthis* | | pedicle int + ext | ib |
| 9/11 - 12.8 | *Hesperorthis* | L> 6 mm | pedicle int + ext | ib |
| 9/11 - 12.9 | *Hesperorthis* | w 4.6 mm | pedicle int + ext | s, inclined |
| 9/11 - 12.10 | *Hesperorthis* | w 10.5 L 7.9 mm | pedicle int | s |
| 9/11 - 12.11 | art. brach. | | indet. Fragment | ib |
| 9/11 - 12.12 | *Hesperorthis* | w ~ 13 mm | pedical int + ext | ib |
| 9/11 - 12.**X**.1 | ?burrow -based nodule | | | |
| 9/11 13 | 2.00 kg | 4.5 cm | | |
| LOWER BED | | | | |
| 9/11 - 13.1 | *Hesperorthis* | | umbo (pedicle) int + ext | ib |
| 9/11 - 13.2 | *Hesperorthis* | L > 8 mm | indet valve ext | s |
| 9/11 - 13.3 | *Hesperorthis* | | pedicle int + ext | ib, inclined |
| 9/11 - 13.4 | *Ogyginus* | L 9 mm | gena/ spine | s(l) |
| 9/11 - 13.5 | *Hesperorthis* | w 12.4 L 9.7 mm | pedicle int + ext | ib |
| 9/11 - 13.6 | *Hesperorthis* | w> 11mm | pedicle int + ext | ib |
| 9/11 - 13.7 | Trepostome | diam. 2.5 mm | ramose colony (cylindrical) | ib |

| | | | | |
|---|---|---|---|---|
| | bryozoan | | | |
| 9/11 - 13.8 | *Hesperorthis* | w 7.0 mm | brachial int + ext | ib |
| 9/11 - 13.9 | *Hesperorthis* | | pedicle int + ext | s |
| 9/11 - 13.10 | Asteroid | | details follow. | ib |
| 9/11 - 13.X.1 | nodule | | | |
| 9/11 - 13.X.2 | nodule | | | |
| UPPER BED | | | | |
| 9/11 - 13.11 | *Hesperorthis* | w 7.0 mm | pedicle int + ext | s(l) |
| 9/11 - 13.X.3 | bedding section | | | |
| 9/11 - 13.X.4 | ?water escape structure | | | |
| 9/11 14 | 1.30 kg | 3.0 cm | | |
| 9/11 - 14.1 | *Hesperorthis* | | indet valve ext | s |
| 9/11 - 14.2 | *Hesperorthis* | w 10 L 9 mm | pedicle ext | s |
| 9/11 - 14.3 | *Hesperorthis* | L> 9 mm | pedicle int | ib |
| 9/11 - 14.4 | *Hesperorthis* | | pedicle int | s |
| 9/11 - 14.5 | *Hesperorthis* | w> 13, L 11 mm | pedicle int | s |
| 9/11 - 14.6 | *Hesperorthis* | w> 12.5 mm | pedicle int | s |
| 9/11 - 14.7 | *Hesperorthis* | | indet valve fragment | s |
| 9/11 - 14.8 | *Flexicalymene* | arc 9.5 mm | librigena | ib |
| 9/11 - 14.9 | *Hesperorthis* | L 4.8 | brachial int | ib |
| 9/11 - 14.10 | *Hesperorthis* | L > 5.3 mm | brachial int + ext | ib |
| 9/11 - 14.11 | *Hesperorthis* | | pedicle | ib |
| 9/11 - 14.12 | Trepostome bryozoan | diam. O.6 mm | pinnatoporellid fragment | ib |
| 9/11 - 14.X.1 | small siliceous nodule | | | |
| 9/11 15 | 2.80 kg | 4.0 cm | | |
| LOWER BED | | | | |
| 9/11 - 15.1 | *Flexicalymene* | ceph w. 17.8; L 9.5; thor. W. 16 mm | almost complete (lacks pygidium and 5 ribs). Eight thoracic ribs; strongly raised genae. | s |
| 9/11 - 15.2 | *Hesperorthis* | | indet. Valve (awkward break) | ib |
| 9/11 - 15.3 | *Hesperorthis* | L ~ 5 mm | brachial int + ext (poor) | ib |
| BENTONITE | | | | |
| 9/11 - 15.4 | *Hesperorthis* | L ~ 9 mm | pedical int + ext | ib |
| UPPER BED | | | | |
| 9/11 - 15.5 | *Hesperorthis* | w 12.0 L 9.2 | pedical int + ext | ib |
| 9/11 - 15.6 | *Flexi=calymene* | L 4.8 mm | librigena | ib |
| 9/11 - 15.7 | Trilobites | 3 - 5 mm | indet fragments | ib |
| 9/11 - 15.8 | *Hesperorthis* | | margin only (indet) | ib |
| 9/11 - 15.9 | *Hesperorthis* | L 8.1 | pedical int + ext | ib |
| 9/11 - 15.10 | *Flexicalymene* | w 14 (est) | thoracic rib | ib |
| 9/11 16 | 2.40 kg | 6 cm | | |
| LOWER BED | | | | |
| 9/11 - 16.1 | *Iocrinus* | | 3 isolated brachials | ib |
| 9/11 - 16.2 | *Hesperorthis?* | | indet valve in section | ib |
| 16.3 - 16.10 | SPONGES | vol. up to 2000 mm3 | possibly proteinaceous demosponges (large; few spicules) | |
| 9/11 17 | 1.50 kg | 3 cm | | |

17.2 17.4 SPONGES same conditions apply as for 16.3 - 16.10

**LR 1 ( 2)**

## Level 9/11: 1 [-3]: Primary bentonite

9/11:
1[-3]:

| | Dimensions | Details | |
|---|---|---|---|
| 1 *Hesperorthis* | | pedicle valve interior (partial) | s |
| 2 *Hesperorthis* | L 10.1; w 10.8 | pedicle valve int. | s |
| 3 *Hesperorthis* | L 7.2; w 8.3 | pedicle valve int. | s |
| 4 *Hesperorthis* | | indet. valve ext. | s |
| 5 *Hesperorthis* | L 8.4 | pedicle valve int. | s |
| 6 *Hesperorthis* | w 6.8 | pedicle valve int. | s(l) |
| 7 *Hesperorthis* | L 8.7 | indet. valve ext. | s |
| 8 *Hesperorthis* | | indet. valve int. + ext. | s(l) |
| 9 *Hesperorthis* | L 3.9; w 5.2 | pedicle valve int + ext | ib |
| 10 *Hesperorthis* | | pedicle valve int (distorted) | s(oblique) |
| 11 *Hesperorthis* | w~ 6 | pedicle valve ext | s |
| 12 *Hesperorthis* | | indet valve ext. | s |
| 13 *Hesperorthis* | | pedicle valve umbo (rest embedded) | ib(vertical) |
| 14 *Hesperorthis* | | pedicle valve (part) | s |
| 15 *Hesperorthis* | L 7.8 | pedicle valve int. | ib(inclined) |
| 16 *Hesperorthis* | | pedicle valve int. + ext. (half valve) | ib |
| 17 *Hesperorthis* | L~ 10; w~ 12 | pedicle valve int. | ib |
| 18 *Hesperorthis* | | pedicle valve int. | s(l) |
| 19 *Hesperorthis* | L 4.7 | pedicle valve int. | s |
| 20 *Hesperorthis* | w > 11 | pedicle valve int. | s |
| 21 *Hesperorthis* | | pedicle valve ext (umbo) | ib |
| 22 *Hesperorthis* | | indet valve ext. | ib |
| 23 *Hesperorthis* | w~ 9 | brachial int + ext | ib(inclined) |
| 24 *Hesperorthis* | L~ 6; w~ 7 | pedicle valve int | s |
| 25 *Hesperorthis* | | brachial int | s(oblique) |
| 26 *Hesperorthis* | w > 10 | pedicle valve int | s |
| 27 *Hesperorthis* | | indet valve fragment | ib |
| 28 *Hesperorthis* | L 7.8; w 9.0 | pedicle valve int | s |
| 29 *Hesperorthis* | | indet valve int | s(l) |
| 30 *Hesperorthis* | | indet valve fragment | s(l) |
| 31 *Hesperorthis* | | brachial valve ext | ib |
| 32 *Hesperorthis* | w> 5 | brachial valve int + ext | ib |
| 33 Pinattoporellid bry. | branch diam. ~ 0.6 | part of dichotomously branching colony | ib |
| 34 Trepostome | branch diam. ~ 1.6 | part of dichotomously branching colony | s |
| 35 *Flexicalymene* | Occ. W 6.5 | Poorly preserved cranidium | ib |
| 36 *Hesperorthis* | | pedicle valve int | s |
| 37 *Hesperorthis* | w~ 8 | brachial valve int | s(inclined) |
| 38 *Hesperorthis* | | articulated valves (umbo, partial) | s(vertical) |
| 39 *Hesperorthis* | | indet. Valve ext. | s |
| 40 *Hesperorthis* | w ~ 11 | pedicle valve int | s |
| 41 *Hesperorthis* | L 9.8; w ?10.5 | pedicle valve int | s(l) |
| 42 *Hesperorthis* | | indet. Valve | s |
| 43 *Hesperorthis* | | indet valve | s |
| 44 *Hesperorthis* | L 3.8; w~ 6 | pedicle valve int. | ib |
| 45 *?Hesperorthis* | | indet valve fragment | ib(oblique) |
| 46 *Hesperorthis* | L8.0; w 9.5 | pedicle int + ext | s |
| 47 *Hesperorthis* | L 9.2; w 11.3 | pedicle int + ext | ib |
| 48 *Hesperorthis* | L ~ 7; w ~ 9 | pedicle valve int | s |
| 49 *Hesperorthis* | | indet valve ext. | ib |
| 50 *Hesperorthis* | L ~ 8 (compressed) | pedicle valve int | ib(oblique) |
| 51 *?Hesperorthis* | L 3.2; W 5.3 | brachial valve int | s |

| | | | |
|---|---|---|---|
| 52 *Hesperorthis* | L 1.9; w 2.1 | pedicle int + ext (juvenile) | ib |
| 53 *Hesperorthis* | | indet valve (broken in prep) | ib(oblique) |
| 54 *Hesperorthis* | L 4.8 | pedicle valve int + ext | ib(inclined) |
| 55 *Hesperorthis* | L~ 6; w~ 7 | ?brachial ext | s |
| 56 *Hesperorthis* | L 4.6; w 5.5 | pedicle int + ext | ib |
| 57 *Hesperorthis* | w ~ 5 | brachial ext (+ int) | ib |
| 58 *Hesperorthis* | L 2.4; w ~ 3 | pedicle int (+ ext) | ib |
| 59 *Hesperorthis* | w ~ 6 | pepidle int + ext | ib |
| 60 *Hesperorthis* | L ~ 7; w ~ 10 | pedicle int (needs prep) | ib |
| 61 Pinnatoporellid bry. | branch diam. 0.6 | ramose fragment | ib |
| 62 *H. dynevorensis* | L 4.9; w ~ 6 | brachial int + ext | ib |
| 63 *Hesperorthis* | L 5.6 | pedicle int + ext | ib(oblique) |
| 64 *Hesperorthis* | | indet valve ext. | s |
| 65 *Hesperorthis* | L 5.5 | indet valve ext | s |
| 66 *Hesperorthis* | L 9.0; w ~ 11 | pedicle int + ext | ib |
| 67 *Hesperorthis* | L 6.0 | pedicle valve ext | s |
| 68 *Hesperorthis* | | pedicle valve ext | s |
| 69 *Hesperorthis* | L 3.2; w 5.1 | brachial valve ext | s |
| 70 *Hesperorthis* | | pedicle int + ext (needs prep) | ib |
| 71 *Hesperorthis* | | pedicle valve (umbo) int | ib |
| 72 *Hesperorthis* | | pedicle valve (fragment) int | s |
| 73 *Hesperorthis* | | pedicle valve int | s |
| 74 *Hesperorthis* | L ~ 5 | indet valve int | s |
| 75 *Hesperorthis* | L ~ 10; w 11.8 | pedicle int | ib(inclined) |
| 76 *Hesperorthis* | L ~ 3; w ~ 4.5 | pedicle int | ib |
| 77 *Hesperorthis* | w ~ 11 | pedicle int | s (oblique) |
| 78 *Hesperorthis* | | pedicle sectional view | ib |
| 79 *Hesperorthis* | | umbonal fragment | ib |
| 80 Trepostome | branch diam. 4 | small cylindrical fragment | s |
| 81 *Hesperorthis* | | brachial int. (poor) | s |
| 82 *Hesperorthis* | | pedicle valve fragment | ib |
| 83 *Hesperorthis* | L ~ 8 | pedicle int | s(l) |
| 84 *Hesperorthis* | L ~ 7 | pedicle int | s(l) |
| 85 *Hesperorthis* | L ~ 10; w ~ 12 | pedicle valve int | ib |
| 86 *Hesperorthis* | L 9.5; w 11.5 | pedicle valve int | ib |
| 87 *Hesperorthis* | | pedicle valve fragment | s |

9/11: 1
[-2]

| | | | |
|---|---|---|---|
| 1 *Hesperorthis* | L ~ 9 | indet valve ext | ib |
| 2 *Hesperorthis* | L ~ 8.5 | pedicle valve int | ib |
| 3 *Hesperorthis* | L 10.3; w 13,6 | pedicle valve int | s(l) |
| 4 *Hesperorthis* | L ~ 9 | pedicle valve int | s(l) |
| 5 *Hesperorthis* | L 6.0; w ~ 8 | brachial valve int + ext | ib |
| 6 *Hesperorthis* | | brachial valve umbo | ib |
| 7 *Hesperorthis* | | pedicle v ext | ib |
| 8 *Hesperorthis* | w 8.4 | pedicle v int + ext | ib(oblique) |
| 9 *Hesperorthis* | L 10.7; w ~ 14 | pedicle valve int | ib(inclined) |
| 10 *Hesperorthis* | L ~ 8; w ~ 10 | pedicle v int + ext | ib |
| 11 *Hesperorthis* | | indet valve ext | ib |
| 12 indet trilobite | L 6.5 w 7.5 | isolated librigena | ib |
| 13 *Hesperorthis* | L ~ 2 | brachial valve int | s(l) |
| 14 *Hesperorthis* | | pedicle valve int | ib (vertical) |
| 15 *Hesperorthis* | L 8.5; w ~ 11 | pedicle valve int | ib |
| 16 *Hesperorthis* | L 6.5 w 7.5 | pedicle valve int | s(l) |
| 17 *Hesperorthis* | L 7.5 | pedicle v int + ext | ib |
| 18 *Hesperorthis* | | indet valve ext | s(l) |

| | | | |
|---|---|---|---|
| 19 *Hesperorthis* | L 8.6; w 12 | pedicle v int + ext | s(l) |
| 20 *Hesperorthis* | | pedicle v int + ext | ib |
| 21 *Hesperorthis* | L 5.3 | pedicle v int + ext | s(l) |
| 22 *Hesperorthis* | L 4.8 | pedicle v int + ext | ib |
| 23 *Hesperorthis* | L 5.8; w ~ 9 | pedicle v int + ext | ib |
| 24 *Hesperorthis* | | pedicle v int + ext | ib |
| 25 *Hesperorthis* | L ~ 8 | pedicle valve int | s |
| 26 Trepostome | branch diam. 3 | cylindrical branch fragment | ib |
| 27 *Flexicalymene* | ceph w 19; L 7.6 | complete cephalon plus 8 thoracic ribs | s(l) |
| 28 *Hesperorthis* | | pedicle valve int | s(l) |
| 29 Pinnatoporellid | branch diam. 0.7 | dichotomous branch fragment | ib |
| 30 *Hesperorthis* | L ~ 6; w ~ 9 | brachial valve ext | s |
| 31 *Hesperorthis* | | indet valve ext | ib |
| 32 *Hesperorthis* | L 10.6; w ~ 12 | pedicle v int + ext | s |
| 33 *Hesperorthis* | | pedicle v int + ext | ib (inclined) |
| 34 *Hesperorthis* | w ~ 7 | brachial v int + ext | ib |
| 35 *Hesperorthis* | L 3.3 | brachial v int + ext | ib |
| 36 *Hesperorthis* | L 2.8 | pedicle v int + ext | ib |
| 37 *Hesperorthis* | | brachial v int + ext | ib |
| 38 *Hesperorthis* | w ~ 6 | brachial v int + ext | ib |
| 39 *Hesperorthis* | L >8 | pedicle v int + ext | s |
| 40 *Hesperorthis* | w ~ 9 | pedicle v int + ext | ib |
| 41 *Hesperorthis* | w ~ 5 | pedicle v int + ext | s(l) |
| 42 *Hesperorthis* | | indet valve ext | ib |
| 43 *Hesperorthis* | | brachial v int | ib |
| 44 *Hesperorthis* | L > 10 | pedicle valve ext | s |
| 45 *Hesperorthis* | L ~ 7 | pedicle v int + ext | s(l) |
| 46 *Hesperorthis* | | indet valve fragment | ib |

9/11: 1
[-1]

| | | | |
|---|---|---|---|
| 1 *Hesperorthis* | L 8.4; w > 9 | pedicle valve int.+ ext. | s(l) |
| 2 *Hesperorthis* | w ~ 12 | pedicle valve int.+ ext. | ib |
| 3 art. Brach? | | sectional view of small valve | ib |
| 4 *Hesperorthis* | L 4.2; w 6.0 | brachial valve int + ext | s(l) |
| 5 *Iocrinus* | diameter 2.9 | isolated primibrach | s(l) |
| 6 *Iocrinus* | diameter ~ 4 | ?isolated primibrach | ib |
| 7 Trilobite indet. | L 5 | isolated thoracic rib | ib |
| 8 *Flexicalymene* | glab. L ~ 7 | partial (poor) cranidium: right side | ib |
| 9 ??? Alga/ graptolite | w~0.8; L ~ 4 | distorted carbonaceous fragments | ib |

9/11: 1
[1]

| | | | |
|---|---|---|---|
| 1 *Hesperorthis* | L 6.6 | brachial valve int + ext | s (l) |
| 2 alga? | diam. 0.7; frag length 4 | branching carbonaceous impression | s (l) |

9/11:
1[2]

| | | | |
|---|---|---|---|
| 1 *Hesperorthis* | | brachial valve ext | ib(inclined) |
| 2 *Hesperorthis* | L> 12; w ~ 18 | pedicle valve int + ext | ib |
| 3 *Hesperorthis* | L 10.0 | pedicle valve int + ext | ib |
| 4 *Hesperorthis* | | indet valve section | s(oblique) |

# PLW 1

Pen Llithrig y wrach (717 623)
East face crags below summit region. Lower Crafnant Volcanic Formation or uppermost Cwm Eigiau Formation: cleaved ashy mudstones with transported shally fauna. Fossils strongly distorted
1.40 kg

| | | | |
|---|---|---|---|
| PLW 1. | *Plaesiomys multifida* | | brachial valve int + ext |
| 1 | *Plaesiomys multifida* | | brachial ext |
| 2 | *Plaesiomys multifida* | | indet. Valve ext |
| 3 | *Plaesiomys multifida* | | indet. Valve ext |
| 4 | *Plaesiomys multifida* | | indet. Valve ext |
| 5 | *Plaesiomys multifida* | | indet valve int |
| 6 | *Plaesiomys multifida* | | pedicle valve int + ext |
| 7 | *Plaesiomys multifida* | | indet. Valve ext |
| 8 | *Plaesiomys multifida* | | pedicle valve int + ext |
| 9 | *Plaesiomys multifida* | | pedicle valve int + ext |
| 10 | *Plaesiomys multifida* | | indet. Valve ext |
| 11 | *Plaesiomys multifida* | | pedicle valve int |
| 12 | *Plaesiomys multifida* | | pedicle valve int |
| 13 | *Plaesiomys multifida* | | indet. Valve ext |
| 14 | *Plaesiomys multifida* | | indet. Valve ext |
| 15 | *Plaesiomys multifida* | | indet. Valve ext |
| 16 | *Plaesiomys multifida* | | pedicle valve int + ext |
| 17 | *Plaesiomys multifida* | | pedicle valve int + ext |
| 18 | *Plaesiomys multifida* | | brachial valve int + ext |
| 19 | ? Brach. | | indet |
| 20 | *Plaesiomys multifida* | | brachial valve int + ext |
| 21 | *Plaesiomys multifida* | | indet valve int |
| 22 | *Plaesiomys multifida* | | pedicle valve int + ext |
| 23 | *Plaesiomys multifida* | | articulated valves |
| 24 | *Plaesiomys multifida* | * | brachial valve int + ext |
| 25 | *Plaesiomys multifida* | | articulated valves |
| 26 | *Plaesiomys multifida* | | indet valve int |
| 27 | *Plaesiomys multifida* | | indet. Valve ext |
| 28 | *Plaesiomys multifida* | | indet. Valve ext |
| 29 | dubiofossil | | ferruginous mass; probably inorganic |
| 30 | Dalmanellid | | strongly sulcate ?pedicle valve |
| 31 | ?sponge spicule | | elongate Fe2O3, possibly a large phenocryst |
| 32 | indet. trilobite | | thoracic rib |
| 33 | *Plaesiomys multifida* | | indet. Valve ext |

PLW2.- Sedimentology: ashy slates as in PLW1, abruptly altering to soft brown sandstone at top (or base?)
0.95 kg

| | | |
|---|---|---|
| 1 | indet. Graptolite? | section through carbonaceous remains |
| 2 | ?Diplograptid | distorted spinose fragment |
| 3 | *?Dalmanella* sp. | strongly sulcate pedicle valve, int + ext |
| 4 | *Plaesiomys multifida?* | articulated valves |
| 5 | *Plaesiomys multifida* | pedicle valve, int + ext |
| 6 | *Plaesiomys multifida* | pedicle valve, int + ext; occurs within brown sand |
| 7 | *Plaesiomys multifida* | pedicle valve, int + ext |
| 8 | *Plaesiomys multifida?* | brachial valve, partially obscured, int + ext |
| 9 | art. brach | awkward orientation; indet. Valve |
| 10 | *Plaesiomys multifida* | poor pedicle valve, int + ext |
| 11 | indet. ?brach | smooth conical ?umbo, possibly phosphatic |
| 12 | *Plaesiomys multifida* | brachial vlve, int. + ext. |

PLW3.- Sedimentology: combination of soft brown siltstone and ashy slates
0.60 kg

| | | | |
|---|---|---|---|
| 1 | *?Howellites* | | brachial valve int + ext |
| 2 | *Plaesiomys multifida?* | | indet valve partial |
| 3 | crinoid ossicle? | | indet ferruginous cavity, rectangular section |
| 4 | art. Brach | | pedicle valve int |
| 5 | art. Brach | | indet valve partial |
| 6 | *?Tallinella* | | beyririchiid ostracod |
| 7 | art. Brach | | indet. Valve interior |
| 8 | *Plaesiomys multifida?* | | indet. Valve int + ext |
| 9 | *Plaesiomys multifida* | | brach. valve int |
| 10 | *Plaesiomys multifida?* | | brachial valve int + ext |
| 11 | *Plaesiomys multifida* | | brachial valve int + ext |
| 12 | *Plaesiomys multifida* | | pedicle valve int + ext |
| 13 | *Plaesiomys multifida?* | | pedicle valve int + ext |
| 14 | Strophomenid | | indet. Valve int + ext |
| 15 | *Plaesiomys multifida* | | pedicle valve int |
| 16 | art. Brach | | brachial valve int (small) |
| 17 | *Plaesiomys multifida* | | indet valve partial |
| 18 | *Plaesiomys multifida* | | indet valve ext |
| 19 | *Plaesiomys multifida* | | articulated valves ext |
| 20 | ?Howellites | | brachial valve ext |
| 21 | *Plaesiomys multifida* | | indet valve ext |
| 22 | art. Brach | | brachial valve int + ext (small) |
| 23 | *Plaesiomys multifida* | | pedicle valve int |
| 24 | *Plaesiomys multifida* | | pedicle valve int |
| 25 | *?Plaesiomys multifida* | | indet. Valve int + ext |
| 26 | art. Brach | | pedicle valve int + ext (small) |
| 27 | *Plaesiomys multifida* | | articulated valves (sectioned) |
| 28 | *Plaesiomys multifida* | | articulated valves ext |
| 29 | *Plaesiomys multifida* | | pedicle valve int |
| 30 | *Plaesiomys multifida* | | pedicle valve int |
| 31 | *?Plaesiomys multifida* | | indet valve partial |
| 32 | *?Tallinella* | | beyririchiid ostracod |
| 33 | *Plaesiomys multifida* | | articulated valves ext |
| 34 | *Plaesiomys multifida* | | indet valve partial |

PLW4.- Sedimentology: Irregular distribution of soft brown siltstone and ashy slates
0.35 kg

| | | | |
|---|---|---|---|
| 1 | *?Pyritonema* | | Possible monaxon, pyritized and eroded |
| 2 | *Plaesiomys multifida* | | articulated valves |
| 3 | *Plaesiomys multifida* | | articulated valves |
| 4 | art. Brach | sst | indet valve |
| 5 | art. Brach | sst | indet valve |

PLW5.- Soft brown sandy siltstone; very abundant vertically oriented phenocrysts
0.40 kg
NO FOSSILS

PLW6.- Combination of soft silty sandstones and ashy slates
0.35 kg

| | | |
|---|---|---|
| 1 | *Plaesiomys multifida* | articulated valves |
| 2 | *Plaesiomys multifida* | articulated valves |
| 3 | *Plaesiomys multifida* | articulated valves |
| 4 | *Plaesiomys multifida* | articulated valves |

| | | |
|---|---|---|
| 5 | *Plaesiomys multifida* | articulated valves |
| 6 | indet. | probably mud/sand pellets? |
| 7 | *Plaesiomys multifida* | articulated valves |
| 8 | *Plaesiomys multifida* | articulated valves |
| 9 | *Plaesiomys multifida* | articulated valves |
| 10 | *Plaesiomys multifida* | indet. Valve fragment |
| 11 | *Plaesiomys multifida* | pedicle valve interior |
| 12 | smooth-shelled brach | marginal frgament; not *Plaesiomys* |
| 13 | *?Dalmanella* | brachial valve int + ext (poor pres.) |
| 14 | *Plaesiomys multifida* | pedicle valve interior |
| 15 | *?Dalmanella* | articulated valves |
| 16 | *Plaesiomys multifida* | brachial valve int + ext (poor pres.) |

PLW7.- Margin of brown sands (fossiliferous) and slaty ashes (fossiliferous only at >4cm from sands)

0.85 kg

| | | | |
|---|---|---|---|
| 1 | art. Brach | diam. 2 | brachial (?) valve, int + ext; vertical |
| 2 | *Plaesiomys multifida* | | pedicle valve int |
| 3 | *?Plaesiomys multifida* | | indet valve (part dest on prep.) int + ext |
| 4 | ?ostracod | | smooth-shelled, elongate form |
| 5 | *Tallinella?* | | distorted ?Beyrirchiid ostracod |
| 6 | art. Brach | diam. 2 mm | pedicle valve int (ferruginous mould) + ext |
| 7 | *Plaesiomys multifida* | | indet valve (part dest on prep.) int + ext |
| 8 | *Plaesiomys multifida* | | pedicle valve int + ext |
| 9 | *Plaesiomys multifida* | | pedicle valve int + ext |

X1 lithological change from fine blue to slightly coarser pale slaty ash; vertical phenocrysts occasional in paler bed (adjacent to brown sands) only.

PLW8.- blue ashy slates

0.60 kg

| | | | |
|---|---|---|---|
| 1 | crinoid indet. | diam. 1.4 | pluricolumnal (approx. 20) |
| 2 | burrows | diam 1 | vertical & horiz., in brown "concretion" |
| 3 | trilobite indet | | pygidial fragment |
| 4 | *Plaesiomys multifida* | | ?brachial valve ext |
| 5 | *Plaesiomys multifida* | | articulated valves ext |
| 6 | trilobite indet | | librigena (distorted) |
| 7 | burrow | diam. 2 | sub-vertical, unlined |
| 8 | ?bryozoan | diam 1 | part of small ramose colony |
| 9 | *Plaesiomys multifida* | | indet. Valve int |
| 10 | *Plaesiomys multifida* | | indet. Valve ext |
| 11 | *Plaesiomys multifida* | | articulated valves ext |
| 12 | *Plaesiomys multifida* | | pedicle valve int |
| 13 | *Plaesiomys multifida* | | indet valve ext |
| 14 | *Plaesiomys multifida* | | pedicle valve int |
| 15 | *Plaesiomys multifida* | | indet small valve fragment |
| 16 | *Plaesiomys multifida* | | pedicle valve int |
| 17 | *Plaesiomys multifida* | | indet valve ext |
| 18 | *Plaesiomys multifida* | | articulated valves ext |
| 19 | *Plaesiomys multifida* | | pedicle valve int |

PLW9.- Upper margin of sands with ashy slates

1.20 kg

| | | |
|---|---|---|
| 1 | *Plaesiomys multifida* | pedicle valve internal |

| | | |
|---|---|---|
| 2 | *Plaesiomys multifida* | indet valve int + ext |
| 3 | *Plaesiomys multifida* | indet valve int + ext |
| 4 | *Plaesiomys multifida* | articulated valves (ext) |
| 5 | *Plaesiomys multifida* | brachial valve int + ext |
| 6 | *Plaesiomys multifida* | indet valve int + ext |
| 7 | *Plaesiomys multifida* | articulated valves (ext) |
| 8 | *Plaesiomys multifida* | pedicle valve internal |
| 9 | art brach | indet fragment |
| 10 | *Plaesiomys multifida* | brachial valve int + ext |
| 11 | *Plaesiomys multifida* | indet valve int + ext |
| 12 | *Plaesiomys multifida* | indet valve int + ext |
| 13 | *Plaesiomys multifida* | indet valve int + ext |
| 14 | Trilobite indet | part of left cephalic margin |
| 15 | *Plaesiomys multifida* | indet valve int + ext |
| 16 | *Plaesiomys multifida* | indet valve int + ext |
| 17 | *Plaesiomys multifida* | articulated valves (ext) |
| 18 | ?Trilobite indet | fragment of librigena? |

+ 10 pairs articulated valve at margin of sandst. destroyed in excavation of matrix

| BG1 (1)/g | *A. micula* | *H. teretiusculus* | ostracodes | dendroids | siculae | *Palaeoglossa* | *Monobolina* | *Opsiconidion* | art. Brachs | sponge spic.s | trilobites indet. | agnostids | *Cnemidopyge* | *Platycalymene* | asaphids | trinucleids | *Palaeoscolex* | *Sphenothallus* | annelid tube? | bivalves | bryozoa | orthocones | spiral naut. | conodonts | chitino. Rh | chitino. Co. | arthropods | algae? | problematica |
|---|---|---|---|---|---|---|---|---|---|---|---|---|---|---|---|---|---|---|---|---|---|---|---|---|---|---|---|---|---|
| N(181.6) | 39 | 5.5 | 0.6 | 1 | 3 | | | | | | | | | | | | | | | | | | | | | | | 2 | |
| M(156.4) | 33 | 2.5 | 1.3 | | | 2 | | | | 1 | 1 | | | | | | | | | | | | | | | | | | |
| L(143.4) | 47 | 1.4 | 2.8 | | | | | | 1 | | | 1 | | | | | | | | | | | | | | | | 2 | |
| K(123.8) | 34 | 4.8 | | | | | | | | | | | | | | | | | | | | | | | | | | 1 | |
| J(127.1) | 65 | 7.9 | | | | | | | | | | | | | | | | | | | | | | | | | 1 | | |
| I(124.4) | 46 | 6 | | | | | | | | | | | | | | | | | | | | | | | | | | | |
| H(175.5) | 34 | 8.5 | 0.6 | | 1 | | | | | | | | | | | | | | | | | | | | | | | | |
| G(241.6) | 24 | 2.8 | | | 8 | | | | | | | | | | | | | | | | | | | | | | 5 | | |
| F(291.3) | 25 | 4 | 4 | | 3 | | | | | | | | | | | | | | | | | | | | | | | | |
| E(167.0) | 39 | 4.1 | 2.4 | | 1 | | | | | | | | | | | | | | | | | | | | | | | | |
| D(191.7) | 19 | 4.1 | 1 | | 3 | 1 | | | | | | | | | | | | | | | | | | | | | | | |
| C | | | | | | | | | | | | | | | | | | | | | | | | | | | | | |
| B | | | | | | | | | | | | | | | | | | | | | | | | | | | | | |
| A | | | | | | | | | | | | | | | | | | | | | | | | | | | | | |
| BG1 (2)/g | | | | | | | | | | | | | | | | | | | | | | | | | | | | | |
| K(385.6) | 48 | 8.8 | | | 1 | | | | | | | 1 | 1 | | | | | | 1 | | | | | | | | | 1 | 1 |
| J(407.7) | 50 | 7.4 | 0.5 | | 3 | | | | | | | 1 | | | | | | | | | | | 1 | | | | 1 | | |
| I(292.7) | 56 | 12 | | | 1 | | | | | | | | | | | | | | | | | | | | | | | | |
| H(444.9) | 52 | 10 | | | 39 | | | | | | | | | | | | | | | | | | 1 | | | | | | |
| G(742.3) | 31 | 6.9 | | 2 | 4 | | | | m2, ht1 | | | | | | | | | | 1 | | | | | | | | | | |
| F(757.7) | 48.3 | 4.5 | 0.4 | 2 | | 2 | 1 | | 1 | | | | | | | | | | 1 | | | | 1 | | | | 3+assem.(20) | occasional | rare |
| E(749.2) | 58.7 | 6.5 | 0.5 | 1 | 5 | 2 | | | | m1, hx1 | | | | | | | | | | 1 | | | 1 | | | | | common | |
| D(675.2) | 50.6 | 8.5 | 1 | | 14 | 1 | | | | abundant | 1 | | 1 | | | 1 | | | | | | | | | | | 3 | frequent | |
| (C) | 2 | | | | | | | | | | | | | | | | | | | | | | | | | | | | |
| (B) | 6 | | | | | | | | | | | | | | | | | | | | | | | | | | | | |
| (A) | 5 | | | | | | | | | | | | | | | | | | | | | | | | | | | | |

| | | | | | | | | | | | | | | | | | | | | | | | | | | | | | |
|---|---|---|---|---|---|---|---|---|---|---|---|---|---|---|---|---|---|---|---|---|---|---|---|---|---|---|---|---|---|
| N(181.6) | | | | | | | | | | | | | | | | | | | | | | | | | | | | | |
| M(156.4) | | | | | | | | | | | | | | | | | | | | | | | | | | | | | |
| L(143.4) | | | | | | | | | | | | | | | | | | | | | | | | | | | | | |
| K(123.8) | | | | | | | | | | | | | | | | | | | | | | | | | | | | | |
| J(127.1) | | | | | | | | | | | | | | | | | | | | | | | | | | | | | |
| I(124.4) | | | | | | | | | | | | | | | | | | | | | | | | | | | | | |
| H(175.5) | | | | | | | | | | | | | | | | | | | | | | | | | | | | | |
| G(241.6) | | | | | | | | | | | | | | | | | | | | | | | | | | | | | |
| F(291.3) | | | | | | | | | | | | | | | | | | | | | | | | | | | | | |
| E(167.0) | | | | | | | | | | | | | | | | | | | | | | | | | | | | | |
| D(191.7) | | | | | | | | | | | | | | | | | | | | | | | | | | | | | |
| C | | | | | | | | | | | | | | | | | | | | | | | | | | | | | |
| B | | | | | | | | | | | | | | | | | | | | | | | | | | | | | |
| A | | | | | | | | | | | | | | | | | | | | | | | | | | | | | |
| BG1 (2)/g | | | | | | | | | | | | | | | | | | | | | | | | | | | | | |
| K(385.6) | | | | | | | | | | | | | | | | | | | | | | | | | | | | | |
| J(407.7) | | | | | | | | | | | | | | | | | | | | | | | | | | | | | |
| I(292.7) | | | | | | | | | | | | | | | | | | | | | | | | | | | | | |
| H(444.9) | | | | | | | | | | | | | | | | | | | | | | | | | | | | | |
| G(742.3) | | | | | | | | | | | | | | | | | | | | | | | | | | | | | |
| F(757.7) | | | | | | | | | | | | | | | | | | | | | | | | | | | | | |
| E(749.2) | | | | | | | | | | | | | | | | | | | | | | | | | | | | | |
| D(675.2) | | | | | | | | | | | | | | | | | | | | | | | | | | | | | |
| (C) | | | | | | | | | | | | | | | | | | | | | | | | | | | | | |
| (B) | | | | | | | | | | | | | | | | | | | | | | | | | | | | | |
| (A) | | | | | | | | | | | | | | | | | | | | | | | | | | | | | |

*A. micula, H. teretiusculus* and ostracodes normalised to 100 g; all others absolute.

Abundance: *A. micula*, *H. teretiusculus*, and ostracodes normalised to 100 g; all others absolute.

| | A. m. | H. t. | ost. | den | sic | Pal. | Mon. | Op | a/b | sp | tril | ag | Cn | Pl | as | trin | Psx | Sph | an? | biv | bry | orth | nau | con | ch:Rh | ch:C | ar | al? | p |
|---|---|---|---|---|---|---|---|---|---|---|---|---|---|---|---|---|---|---|---|---|---|---|---|---|---|---|---|---|---|
| BG1(H)/g | | | | | | | | | | | | | | | | | | | | | | | | | | | | | | |
| X1(147.5) | 59 | 7.6 | 0.6 | | | | | | | | | | | | | | | | | | | | | | 8 | occ. | | | |
| X2(97.1) | 121 | 21.5 | | | 3 | | | | | | | | | | | | | | | | | | | | 1 | | | | |
| X3(141.4) | 48.1 | 7.1 | | 1 | | | | | | 4(mon) | | | | | | | | | | | | | | 2 | 14 | occ. | | | 1 |
| X4(159.4) | 36 | 4.4 | 0.6 | | | | | | | | | | | | | | | | | | | | | | 7 | rare | 1 | | |
| X5(255.7) | 32 | 1.2 | | | | | 1 | | | | | | | | 1 | | | | | | | | | | 8 | | 1 | | |
| X6(169.2) | 39 | 5.3 | 0.6 | | | | | | | | | 1 | | | | | | | | | | | | | 3 | | 1 | | |
| BG2/g | | | | | | | | | | | | | | | | | | | | | | | | | | | | | |
| N(132.2) | 57 | 1.5 | 8.3 | | 1 | 1 | | | 2 | | | | 2 | | 1 | | | | | | | | | | | | | | |
| M(86.7) | 83 | 1.2 | 5.8 | | 4 | 2 | | 1 | | | | | | | 1 | | | | | | 1 | | | | | | | | |
| L(128.9) | 71 | 3.1 | 12 | | | | | 1 | | | | | 1 | | | | | | | | | | | | | | | | |
| K(b)108.4 | 39 | 1.8 | 21 | | 7 | 1 | | 2 | | | | | 1 | | | | | | | | 5 | | | | | | | 1 | |
| K(a)(30.8) | 231 | | 3.2 | | 1 | | | | | | | | | | | | | | | | | | | | | | | | |
| J(130/9) | 21.7/371! | 2.3 | 3.1 | 2 | 4 | 2 | 1 | | | | 3 | | 2 | | 2 | | | | | | 2 | | | | | | | | |
| I(133.0) | 59 | 0.8 | 6 | | 2 | 3 | | | | | 1 | | 3 | | | | | | | 1 | 1 | | | | | | | | |
| H(201.0) | 38 | 2.5 | 8 | | 24 | 2 | | 13 | | | | | | | | 1 | | | | | 1 | 6 | | | | | | 2 | |
| G(173.2) | 44 | 0.6 | 23 | | 1 | 4 | | 6 | | | | | 1 | | 6 | | | | | | 1 | 1 | | | | | | | |
| F(192.4) | 30 | 2.1 | 8.8 | 1 | 7 | 1 | | | | | | | 5 | | 1 | | | | | | 1 | | | | | | | | |
| E(321.4) | 17 | | 1.9 | | 4 | | | | | | | | 1 | | 1 | | | | | | | | | | | | | 4 | |
| D(386.0) | 6 | | 1 | | 7 | 7 | | | | | 1 | | 1 | | 1 | 2 | | | | | | | | | | 1 | | 1 | |
| | | | | | | | | | | | | | | | | | | | | | | | | | | | | | |
| C(229.8) | 27 | 0.4 | 11 | | 2 | | 1 | | | | | | 1 | | 1 | 1 | | | | | | | | | | | | 3 | |
| B(121.9) | 47 | 0.8 | 5.7 | | | | | | | | 4 | | 2 | 1 | 1 | | | | | | | | | | | 27 | | 2 | |
| A(203.1) | 53 | | 4.4 | | 7 | 3 | | | | 1 | | | | | 1 | | | | | | | | | | | | | 5 | |

| BG3/g | A. m. | H. t. | ost. | den | sic | Pal. | Mon. | Op | a/b | sp | tril | ag | Cn | Pl | as | trin | Psx | Sph | an? | biv | bry | orth | nau | con | ch:Rh | ch:C | ar | al? | P |
|---|---|---|---|---|---|---|---|---|---|---|---|---|---|---|---|---|---|---|---|---|---|---|---|---|---|---|---|---|---|
| J(156.2) | 41 | | 9 | | | 3 | | | | | 1 | | | | | | | | | | 1 | | | | | | | | |
| I(124.4) | 53 | | 2.4 | | 3 | 1 | | 1 | | | | | 1 | | 1 | | | | | | | | | | | | | 1 | 1 |
| H(140.2) | 42 | | 2.1 | | | 1 | | | | | | | | | 1 | | | | | | | | | | | | 1 | | |
| G(192.2) | 23 | | 1.6 | | 1 | 2 | | | | 1 | 1 | | | | 1 | 1 | | | | | | | | | | | | | |
| F(200.3) | 13 | | 5.5 | | | 1 | | | | | 3 | | 1 | 1 | 1 | | | | | | | | | | rare | | 1 | | |
| E(147.9) | 46 | | 1.4 | | | 1 | | | | 3 | | | 1 | 1 | | | | | | 1 | | | | | | | | | |
| D(188.8) | 22 | | 0.5 | | | 2 | | | | | | | | | | | | | | | | | | | | | | | |
| | | | | | | | | | | | | | | | | | | | | | | | | | | | | | |
| C(108.9) | 63 | | 1.8 | | | 1 | | | | | | | 1 | | 1 | | | | | | | | | | | | 1 | | |
| B(201.2) | 19.2 | | 8.5 | | | | | | | ABUNDANT | 3 | 1 | 1 | | 1 | | | | | | 1 | | | | | | 1 | | |
| A(280.4) | 18 | | 2.5 | | | 2 | | | | 4 | | | | | 1 | | | | | | | | | | | | 2 | | |

| HB3/g | S. micula | D. bifidus | D. murchisoni | diplograptids | Monobolina | ceratiocarid | conulariid | algae |
|---|---|---|---|---|---|---|---|---|
| J(68.4) | 125 | | 5.8 | | 1 | 1 | | |
| I(66.8) | 140 | | 7.5 | | | | 1* | 3 |
| H(62.2) | 156 | | 8 | 1 | | | | |
| G(64.5) | 159 | | 35.7 | | | | | 1 |
| F(74.7) | 146 | 67.5 | | | | | | |
| E(28.2) | 122 | 147 | | | | | | |
| D2(21.1;d) | 303 | 160 | | | | | | |
| D1(61.5) | 113 | 57 | | | | | | |
| | | | | | | | | |
| C(79.8) | 152 | 75.2 | | | | | | |
| B(92.1) | 95 | 68 | | | | | | |
| A(82.2) | 113 | 70.6 | | | | 1 | | |

*A. micula*, *D. artus* and *D. murchisoni* normalised to 100 g; all others absolute

Replacement of *bifidus* by *murchisoni* occurs very rapidly; specimens in G are unclear and may include at least some *bifidus* specimens.

| J(239.0) | I(189.1) | H(271.9) | G(267.0) | F(194.0) | E(219.0) | D(240.5) | (-) (232.5) | LW2/g | | Q(266.3) | P(242.0) | O(292.0) | N(240.0) | M(179.2) | L(133.8) | K(122.4) | J(244.3) | I(67.3) | H(126.3) | G(65.2) | F(112.0) | E(106.9) | D(129.6) | (-) (162.4) | LW1/g | |
|---|---|---|---|---|---|---|---|---|---|---|---|---|---|---|---|---|---|---|---|---|---|---|---|---|---|---|
| 6 | 9 | 17 | 4.9 | 13 | 4 | 7 | 15 | | diplograptids | 31 | 33 | 16 | 23 | 119 | 147 | 60 | 48 | 16 | 11 | 9 | 10 | 28 | 20 | 22 | | diplograptids |
| | | | | | | | | | siculae | 1 | 1 | | | | | 1 | | | | | | | | | | siculae |
| | | | | | | | | | *Dicranograptus* | 2.6 | 1.7 | 6.8 | 1.7 | 3.3 | 9.8 | | | 1.5 | | | | | | 0.6 | | *Dicranograptus* |
| | 1 | 1 | occ. | 1 | 2 | 3 | 1 | | *Rhabdotheca* | 2.3 | 5.0 | 7.2 | 2.1 | 12.8 | | | 0.4 | | | | | 0.9 | 1.6 | 1.8 | | *Rhabdotheca* |
| | | | occ. | | | 1 | | | *Conotheca* | | | | 1 | | | | | | | | | | | | | *Conotheca* |
| 2 | | 1 | | | | 1 | | | *A. micula* | | | 1 | | 1 | 1 | | | | | | | 1 | | 1 | | *A. micula* |
| | | | 1 | | | 1 | | | lingulids | | | | | | | | | | | | | | | | | lingulids |
| | | | | | | | | | dendroids | | | | | | 1 | | | | | | | | | | | dendroids |
| | | | | | | | | | pellets | | | | | 1 | | | | | | | | | | | | pellets |
| | | | | | | | 1 | | conodonts | | | | | | | | | | | | | | | | | conodonts |
| | | | | | | | | | scolecodonts | | | | | | | | | | | | | | | | | scolecodonts |
| | | | | | | 1 | | | sponge spicules | | | | | | | | | | | | | | | | | sponge spicules |
| | | | | 1 | | | 2 | | ceratiocarids | | | | | | | | | | | | | | | | | ceratiocarids |
| | | | | | 1 | 5 | | | indet | | 1 | 1 | | | | | 2 | | | | | | | | | indet |

Diplograptids, *Dicranograptus* and *Rhabdotheca* chitinozoans normailsed to 100 g: all others absolute.

# Appendix C: Fluid mechanical interpretation of chapter 3

Establishing a mathematical treatment of the proposed circulation has been hampered by several factors. Principal among these is that standard fluid mechanical equations almost invariably involve a term for slope, directly or through kinematic viscosity, particularly in mathematical modelling of turbidity flows (e.g. Fukushima *et al.* 1985). This creates inaccuracy at high gradients, and produces singularity in vertical flows. The behaviour of individual particles may be approximated through standard equations such as Stokes' Law, but investigation of bulk flow properties requires the use of a more specialised approach.

The initiation and development of downwelling pockets of dense fluid has been experimentally observed in cases of Rayleigh-Taylor instability (e.g. Carey *et al.* 1988). In this case, Plinian plumes were modelled, with fallout observed from the mature plume umbrellas. Sedimentation was greatly accelerated over particle Stokes' velocities within the turbid regions, occurring as fingers with associated vortex rings around the column centre (Carey *et al.* 1988; Green and Schettle 1986). The process has been closely compared with double-diffusion finger convection (Green 1987), which forms elongate vertical convection cells in systems of layered density (e.g. Green and Schettle 1986). However, these cells occur even without gravitational instability, between miscible liquids.

The formation of circulation columns can be explained through particle behaviour and adjacent fluid velocity profiles. Solid substrates in relative motion with a surrounding fluid affect the velocity of the adjacent fluid through viscous and frictional effects. A very narrow surface region, the viscous sub-layer, of thickness

$$\delta' \approx 10\nu/u_*$$

$\nu$: kinematic viscosity; $u_*$: shear velocity

comprises fluid essentially attached to the substrate. Beyond this is a region of increasing relative velocity, the velocity profile dependent on flow structure. In laminar flow, the form approximates to parabolic; such conditions are rarely encountered in natural situations. Turbulent flow produces a more concave profile, with lower velocities closer to the substrate.

For a spherical particle in water, the settling velocity is given by Stokes' Law:

$$w_s=\gamma_s' d^2/18\mu$$

$w_s$ : settling velocity

$\gamma_s'$: submerged specific weight = $\Delta\rho g$

d : particle diameter

$\mu$ : molecular viscosity

This provides the maximum relative fluid velocity, beyond the influence of the boundary layer; nearby fluid will move at a lower velocity relative to the particle. In diffuse particle clouds such as the nepheloid layer, this effect will be minimal due to the large volume of unaffected water. Where particle spacing is lower, interference between boundary layers may result in larger entrained volumes; beyond a critical particle density, entrainment is sufficient to create a single turbid water mass. Such vertical flows are analogous to turbidity currents, although standard mathematical treatments are inappropriate due to incorporated singularities in expressions containing slope or u*.

In normal turbidity currents, progression is accompanied by entrainment of ambient fluid into lateral gyres (turbulent vortices behind the head). The density change related to this effect is generally considered inconsequential. However, Middleton (1966) noted that flume experiments on very low slopes (0 – 0.05) showed maximum velocities at 2-3 m, followed by the initial stages of deceleration at 4-5 m.

He attributed this to possible entrainment effects. Similarly, Allen (1971) described the transformation of slumps into turbidity currents. A semi-quantitative treatment established the volume increase to be 200% over 10 – 100 km. However, experiments and theoretical modelling by Hallworth *et al.* (1993) and Hallworth *et al.* (1996) suggest that lateral entrainment is underestimated, with an exponentially increasing rate of entrainment over time. Sparks *et al.* (1991) used an entrainment constant of 0.1 to model turbulent pyroclastic plumes.

The rate of volume increase should increase with decreasing density, as flow surfaces lose integrity, despite a decreasing surface-volume ratio. Vertical, unconstrained flows are more prone to entrainment than classical turbidity currents, since all sides are exposed. Additional sediment is lost through sinking of coarse particles and the slower descent rate of escaping fines. Since vertical flows initiate soon after critical density is exceeded, initial particle density may be much less than for turbidity flows, which initiate through the destabilisation of accumulated sediments. There is thus a considerable risk of loss of coherence as vertical flows descend.

The separation of fingers, finger diameter and sedimentation rate, and hence kinetic energy of the system, are dependent on particle size. The settling velocity of dense flows of fine particles is an order of magnitude greater than the Stokes' velocity (Carey *et al.* 1988), but the disparity is much less for dense flows containing coarse particles. It is possible that the sedimentation rate of coarse particles is actually decreased in turbid downwelling, due to continual recirculation of particles into lateral head gyres.

The present hypotheses emphasise the relation of water depth to flow radius. Tank-based experiments have shown that flows converge during descent, in a manner

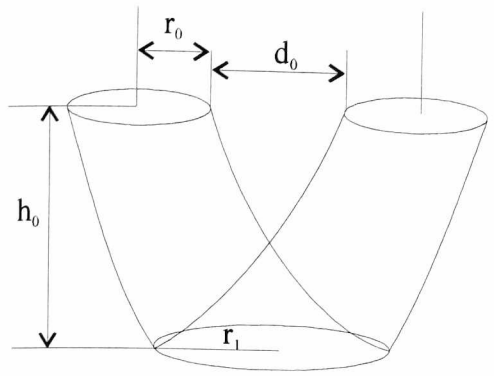


radial entrainment rate, $E=d(r_h-r_0)/dh$

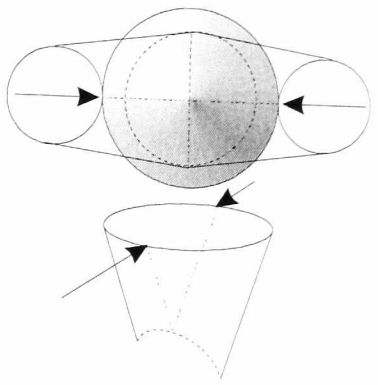

Figure A.1: *Schematic illustration of flow convergence, with intervening fluid cone shaded. Repeated convergence results in broad downwelling columns, discussed in the text.*

consistent with extraction of the intervening fluid into flow tops (Fig. A.1). The volume between convergent flows approximates to a cone, in order to account for adjacent flows. Once equilibrium is established between downwelling volumes and replacement upwelling, this volume should remain constant. A mathematical model based on this principle was highly inaccurate, but this problem is eliminated if volume balances are not employed. Although flow tops converge into local concentrations, the surface areal extent producing each basal column is unchanged.

Mean flow separation was established by experiment, since edge effects are minimal for the initial stages of millimetre-scale movement (tank dimensions 20x100 cm base, 50 cm high). Assuming convergence between nearest neighbours, mean separation of subsequent convergence points will increase via a random walk (i.e. a repeated factor of $\sqrt{2}$). If the convergence rate is constant with depth (entrainment negligible), this will correspond to a successive $\sqrt{2}$ increase in the vertical separation of convergence points. In reality, entrainment increases with decreasing flow density, leading to exponential flow decline (Fig. A.2) at depth. This also affects flow radius, which will also increase by $\sqrt{2}$ as a result of each convergence.

Initial column diameter is weakly dependent on particle size, although the presence of finer grades is more important than the mean diameter. Experiments with graded sediments (<20 μm, <106 μm, <250 μm, >250 μm) produced constant column

diameter in all but the entirely coarse fraction, of around 3 mm at initiation. Horizontal separation was more variable, but typically 5-15 mm; a mean value of 10 mm has been employed. Entrainment rate has been estimated by measuring the depth of flow heads at 5 s intervals (Fig. A.2), which produced similar results to those of Carey *et al.* (1988, fig. 2, p. 15317), in which an entrainment constant of 0.125 was indicated. By comparison with their figures, the present data suggest a value between 0.05 and 0.10, varying under different particle size distributions.

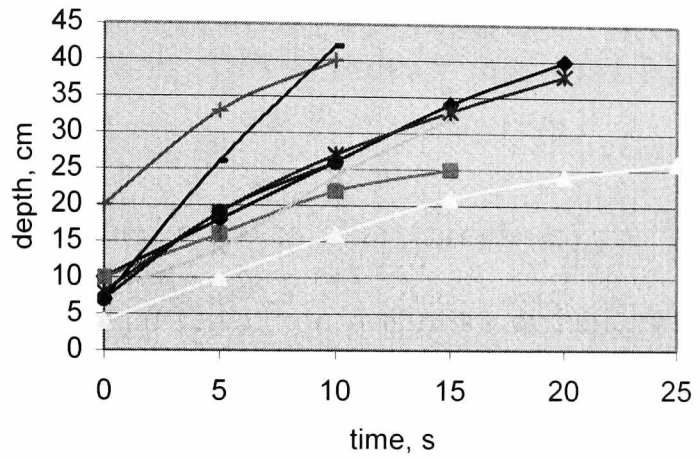


Figure A.2: *effects of entrainment on downwelling flows, based on various sediment size fractions. Decreasing velocity indicates decrease in flow density, although edge effects may be significant in distal data points.*

Tabulation of the expected mean radius with water depth allows comparison with field data. Log BG 1(H) (section 3.3) indicates a maximum downwelling centre diameter of approximately 1.5 m at the seabed. A larger diameter is possible, although the chitinozoan minimum of almost zero suggests that sample X2 was close to the flow centre.

On this basis, a radius of 0.75 m correlates with a probable maximum water

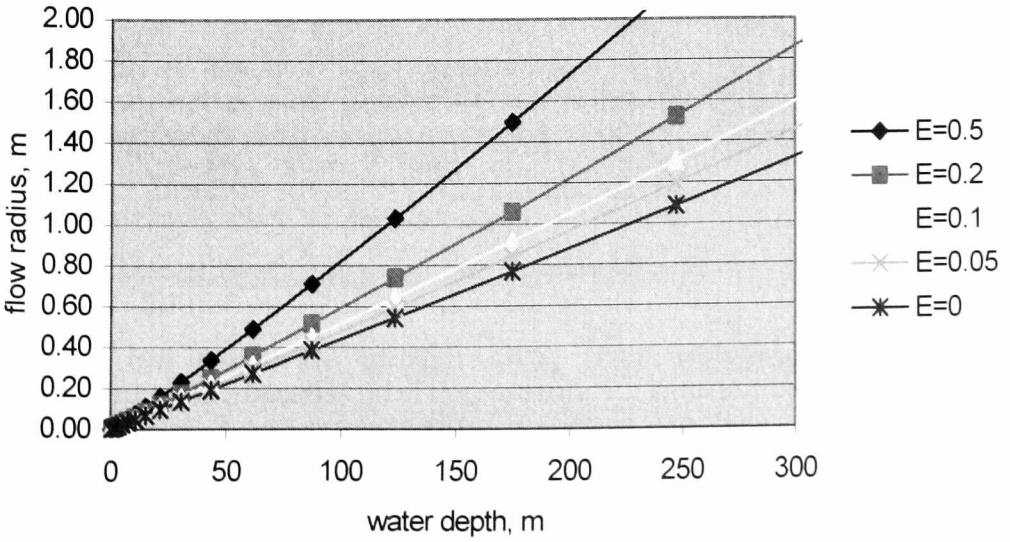


Figure A.3: *variation of flow radius with water depth, based on initial column radius 0.0015 m and first convergence at 0.01m depth; entrainment factors indicated.*

depth of c. 180 m, assuming no lateral entrainment. A constant entrainment factor of 0.1 $m^{-1}$ is compatible with water depth around 150 m, and 0.5 corresponds to approximately 90 m. However, the rate of radial increase will increase with decreasing density, as the flow boundary becomes more diffuse. This effect has been illustrated by including an exponential increasing entrainment rate factor, dE, raised to the power of water depth. Although differences from the original plots appear slight initially, flow radius expands rapidly at greater depth. For any low value of the second derivative of radius with depth (Fig. A.4), divergence becomes pronounced around 150-170 m. This effectively marks the upper limit of water depth in which flows remain coherent.

The breakdown point will depend on particle size distribution, with a higher proportion of fine ash prolonging the flow.

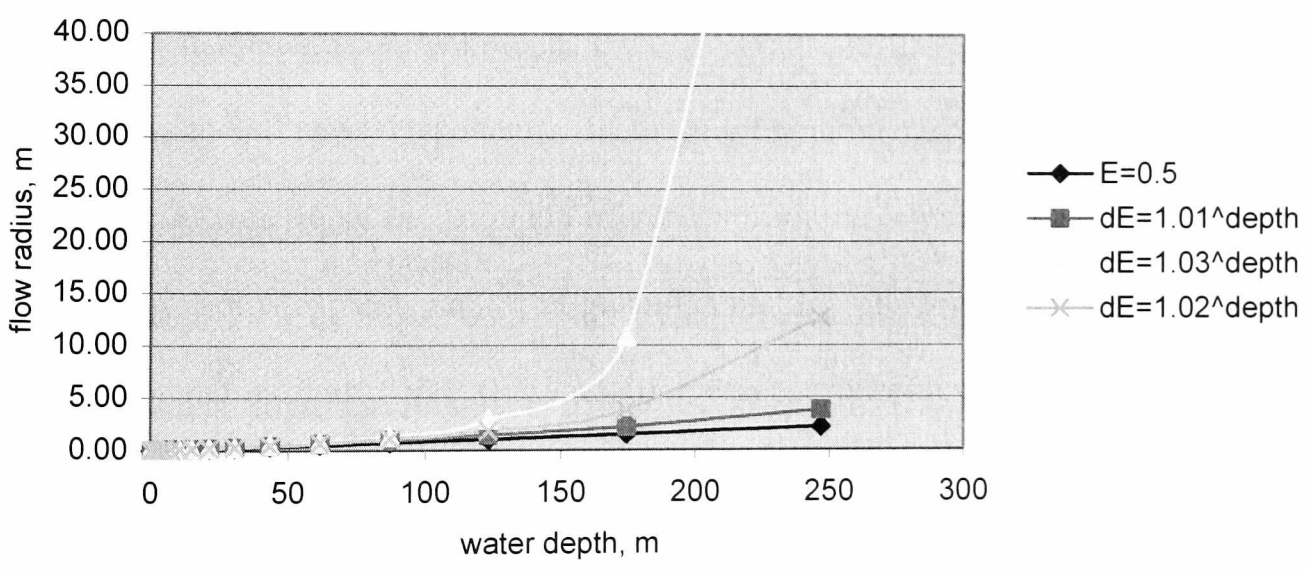


Figure A.4: *Theoretical divergence of flow radius with depth from a model with constant entrainment, when exponential increase is included; entrainment coefficient E=0.5 in all cases, dE=1.01, 1.02 and 1.03$^{depth}$. Divergence occurs at c. 170 m, independent of E and dE, and suggests maximum water depth prioir to flow breakdown.*

The morphology of the downwelling columns results in high local kinetic energy, but moderate inertia. Drag from surrounding fluid would quickly reduce lateral velocity following ash deposition, and although weak inertial circulation may

continue for weeks to a few months after eruption, extensive circulation cells would have degraded rapidly. The action of ambient marine currents would also break up residual circulation, although the downwelling of turbid water masses is only slightly affected.

*Spreadsheet calculations are included on the accompanying disc.*

## References

ALLEN, J. R. L. 1971. Mixing at turbidity current heads, and its geological implications. *Journal of Sedimentary Petrology* **41**, 97-113.

CAREY, S. N., SIGURDSSON, H. AND SPARKS, R. S. J. 1988. Experimental studies of particle-laden plumes. *Journal of Geophysical Research* **93**, 15314-15328.

FUKUSHIMA, Y., PARKER, G. AND PANTIN, H. M. 1985. Prediction of ignitive turbidity currents in Scripps Submarine Canyon. *Marine Geology* **67**, 55-81.

GREEN, T. 1992. The importance of double diffusion to the settling of suspended material. *Sedimentology* **34**, 319-331.

GREEN, T. AND SCHETTLE, J. W. 1986. Vortex rings associated with strong double-diffusive fingering. *Physics of Fluids* **29**, 2109-2112.

HALLWORTH, M. A., HUPPERT, H. E. PHILLIPS, J. C. AND SPARKS, R. S. J. 1996. Entrainment into two-dimensional and axisymmetric turbulent gravity currents. *Journal of Fluid Mechanics* **308**, 289-311.

HALLWORTH, M. A., PHILLIPS, J. C., HUPPERT, H. E. AND SPARKS, R. S. J. 1993. Entrainment in turbulent gravity currents. *Nature* **362**, 829-831.

MIDDLETON, G. V. 1966. Experiments on density and turbidity currents, 1, motion of the head. *Canadian Journal of Earth Sciences,* **3**, 523-546.

SPARKS, R. S. J., CAREY, S. N. AND SIGURDSSON, H. 1991. Sedimentation from gravity currents generated by turbulent plumes. *Sedimentology*, **38**, 839-856.

## APPENDIX D: FAUNAL LISTS FOR BUILTH INLIER LOCALITIES

1. **Llandegley Rocks.**
1a: Southwest ridge.

*Didymograptus* sp.

*Baltoniodus* sp.

*Hesperorthis dynevorensis*
*Hesperorthis* aff. dynevorensis
*Tissintia prototypa*
*Glyptorthis* cf. *viriosa*
*Skenidioides*? sp.
*Hirnantia*? sp sp. nov.
*Paterula* cf. *fissula*
*Pseudolingula* sp.

*Ogyginus corndensis*
*Basilicus tyrannus*
*Flexicalymene*? *aurora*
*Calymene tasgarensis*?
*Trinucleus* sp.
*Cryptolithus* cf. *gibbosus*
Proetid indet.
Raphiophorid indet.
Indet. trilobite

smooth-shelled ostracods

unmineralised arthropoda #1
unmineralised arthropoda #2
unmineralised arthropoda #3
sponge parasite

onychophoran? indet.

*Protopalaeaster simplex*
*Mesopalaeaster* sp.
*Promopalaeaster*? sp.
*Echinosphaerites* sp.
*Iocrinus llandegleyi* sp. nov.
*Iocrinus* cf. *whitteryi* sp. nov.
*Cefnocrinus nododus* gen. et sp. nov.
*Caleidocrinus* cf. *turgidulus*
Indet. crinoid sp. A
Indet. crinoid sp. B

*Orthoceras* sp.
*Ellesmereoceras*? sp.
Modiomorphoid indet.
Bivalve indet. #1
Bivalve indet. #2
Bivalve indet. #3
Pleurotomariid indet.

*Oneroconchia* gen. nov.
*Ordinosabulo quadragintaformis* gen. et sp. nov.
*Mirustubus erinaceus* gen. et sp. nov.
*Palaeocallyoides improbalis* gen. et sp. nov.
*Microspongia*? sp.
*Polydactyloides trescelestus* gen. et sp. nov.
*Polydactyloides entropus* gen. et sp. nov.
*Pseudolancicula* cf. *exigua* Webby and Trotter
*Reticulocymbalum tres* gen. et sp. nov.
*Triactinella rigsbyi* gen.et sp. nov.
*Brevicirrus arenaceus* gen. et sp. nov.
*Spissuparies minuta* (Pulfrey) gen. nov.
*Pyritonema scopula* sp. nov.
Indeterminate demosponges

*Batostoma* sp.
Trepostome indet.
"Pinnatoporellid" (fine ramose trepostome)
Bilaminate sheet bryozoan
Fenestellid

*"Hystrichosphaeridium"* sp.
alga indet.

Conical tube indet.
Annelid tube
annelid indet. body fossil
indet. polychaete sponge parasite

*Skolithos*? sp.
*Trypanites* sp.
*Cruziana*? sp.

1b. Quarry above Upper Graig (ashy shales)

*Didymograptus bifidus*
*Apatobolus micula*
Articulate brachiopod indet.

Micromorphic *Palaeodictyon* gen. nov.
Nematode burrows, gen. nov.

Small burrows indet.
Microarthropod trail.
Pellet (nautiloid?)

1c. Minor summit above Upper Graig (ashy shales and pyroclastics).

*Apatobolus micula*
*Ogyginus corndensis*
Trinucleid? indet.
*Orthoceras*? sp.

1d. Minor summit above Graig Farm (coarse volcaniclastic sandstones and shales)

*Didymograptus bifidus*

*Glyptorthis* cf. *viriosa*
*Tissintia prototypa*
*Gelidorthis*? sp.
*Salopia*? sp.
*Pseudolingula* cf. *granulata*
*Schizocrania* sp.
*Monobolina* sp.

*Caleidocrinus* cf. turgidulus
Rhodocrinitid? indet.
Tetrameric pelmatozoan columnal.

*Pyritonema fasciculus*

Rhaphiophorid? Indet.

Bryozoan (Trepostome) #1
Bryozoan (globose) #2
*Ptilodictyon*? sp.

Beyrichiopod ostracode
Smooth ostracode

1e. South-central plateau (laminated ashes and shales)

*Orthograptus whitfieldi*? (dominant)
*Palaeoglossa attenuata*
Protospongioid indet.
*Triactinella*? sp.
Trace fossils indet.

1f. Lower sandstone unit (medium volcaniclastic sandstones)

*Hesperorthis* cf. *dynevorensis*

*Rostriculella*? sp.
*Glyptorthis* cf.*viriosa*

*Brevicirrus arenacea* gen. et sp. nov.

Bryozoa spp.
Crinoidea indet.

## 2. Howey Brook main feeder SSSI

*Didymograptus murchisoni*
*Didymograptus artus*
*Archoclimacograptus* sp.
*Callograptus* cf. *tenuis*

*Monobolina crassa*
*Apatobolus micula*
*Palaeoglossa attenuata*

*Orthoceras*? sp.

Cyclopygid indet.

*Palaeoscolex agger* sp. nov.

Protospongioid indet.
Alga #1
Alga #2

## 3. Bach-y-Graig SSSI

3a BG1.

*Glyptograptus teretiusculus*
dendroid indet.

*Apatobolus micula*
*Palaeoglossa attenuata*
*Monobolina crassa*

*Dalmanella*? sp.

*Geragnostus m'coyi*
*Cnemidopyge nuda*
*Ogygiacarella debuchii*
*Ogygiacarella angustissima*
*Ogyginus corndensis*

smooth-shelled ostracods

*Rhabdotheca*? sp.
*Conotheca*? sp.

sponge spicules (monaxon and stauract)

alga #1
alga #2
alga #3

trace fossils

3b: BG2

*Glyptograptus teretiusculus*
*Callograptus* sp.
*Climacograptus* sp.

*Apatobolus micula*
*Palaeoglossa attenuata*
*Monobolina crassa*
*Opsiconidion* sp.

*Dalmanella*? sp.
*Cnemidpoyge nuda*
*Ogygiacarella debuchii*
*Ogygiacarella angustissima*
*Platycalymene* cf. *duplicata*
Trinucleids indet.

smooth-shelled ostracods
ornamented ostracods

chitinozoans spp.

sponge spicules (monaxon, stauract and hexact)

orthocone nautiloid

bryozoan #1
bryozoan #2

annelid tube?

3c: BG3

*Apatobolus micula*
*Palaeoglossa attenuata*
*Opsiconidion nuda*

*Ogyginus intermedius*
*Cnemidopyge nuda*
smooth-shelled ostracodes

bryozoan indet.

bivalve? indet.

sponge spicules (monaxon, stauract/hexact)
algae

**4. Pass northeast of Bwlch-y-Cefn (ashy siltstones)**

*Didymograptus murchisoni*
*Orthograptus*? sp.
*Amplexograptus* sp.
Glyptograptid sp.
Dendoid indet.

*Apatobolus micula*
*Palaeoglossa attenuata*
*Monobolina* sp.

*Ogyginus corndensis*
*Cnemidopyge*? sp.
*Raphiophorid spine?*

bivalved arthropod?

*Rhabdotheca* sp.

crinoid indet.

*Palaeoscolex* sp. (annelid body fossil)
scolecodont indet.

Problematicum (?polychaete)

*Protospongia*? sp.

# APPENDIX E: GEOCHEMICAL ANALYSES OF BENTONITES

| | BG3 T2 | HB2 T1 | HB2 T2 | HB3 T | BG1 T | |
|---|---|---|---|---|---|---|
| SiO2 | 62.42 | 69.41 | 66.3 | 59.63 | 72.27 | |
| TiO2 | 1.551 | 0.731 | 0.696 | 1.935 | 0.459 | Major elements |
| Al2O3 | 24.98 | 17.89 | 23.5 | 25.38 | 19.15 | |
| Fe2O3 | 1.96 | 1.37 | 1.65 | 1.81 | 3.6 | |
| MnO | 0.376 | 0.009 | 0.009 | 0.009 | 0.017 | |
| MgO | 0.69 | 0.68 | 0.59 | 0.74 | 1.72 | |
| CaO | 0.18 | 0.38 | 0.2 | 0.45 | 0.1 | |
| Na2O | 12.9 | 7.5 | 10.39 | 6.73 | 2.23 | |
| K2O | 2.09 | 2.35 | 2.61 | 3.04 | 2.96 | |
| P2O5 | 0.119 | 0.237 | 0.05 | 0.127 | 0.056 | |
| BaO | 0.059 | 0.061 | 0.08 | 0.075 | 0.054 | |
| Cr2O3 | 0.008 | 0.043 | <0.001 | 0.004 | 0.001 | |
| NiO | 0.005 | 0.004 | 0.001 | 0.002 | 0.002 | |
| Total | 107.27 | 100.56 | 105.99 | 99.85 | 102.55 | |
| %: | | | | | | |
| Fe2O3 | 1.99 | 1.34 | 1.86 | 1.64 | 3.67 | |
| TiO2 | 1.645 | 0.788 | 0.868 | 2.15 | 0.447 | |
| ppm: | | | | | | |
| Ba | 473 | 638 | 725 | 678 | 523 | Minor elements |
| Co | 21 | 7 | 4 | 21 | 10 | |
| Cr | 43 | 35 | 0 | 25 | 5 | |
| Mn | 3454 | 62 | 51 | 68 | 134 | |
| V | 300 | 41 | 41 | 243 | 41 | |
| La | 9 | 25 | 25 | 64 | 23 | |
| Ce | 30 | 71 | 38 | 103 | 56 | |
| Cu | 9 | 8 | 7 | 15 | 11 | |
| Ga | 14 | 14 | 16 | 15 | 19 | |
| Mo | 6.2 | 8.1 | 26.1 | 21.2 | 6.4 | |
| Nb | 7.5 | 20.1 | 15.5 | 16 | 12.5 | |
| Ni | 17 | 3 | 3 | 11 | 3 | |
| Pb | 3 | 8 | 24 | 7 | 9 | |
| Rb | 62.5 | 71.8 | 69.5 | 88.7 | 96.2 | |
| Sr | 226 | 172 | 294 | 142 | 65 | |
| Th | 2 | 5 | 6 | 10 | 23 | |
| U | 0 | 0 | 0 | 0 | 0 | |
| W | 16 | 15 | 16 | 22 | 18 | |
| Y | 31.5 | 70.1 | 34 | 62.2 | 50.8 | |
| Zn | 74 | 115 | 57 | 156 | 44 | |
| Zr | 135 | 448 | 329 | 225 | 237 | |
| | | | | | | |
| Zr/Nb | 18.00 | 22.29 | 21.23 | 14.06 | 18.96 | ratios |
| Ce/Y | 0.95 | 1.01 | 1.12 | 1.66 | 1.10 | |
| Nb/Y | 0.24 | 0.29 | 0.46 | 0.26 | 0.25 | |
| Zr/TiO2 | 0.008207 | 0.056853 | 0.037903 | 0.010465 | 0.05302 | |
| Y+Nb | 39 | 90.2 | 49.5 | 78.2 | 63.3 | |

PLATE 1
Indeterminate demosponges.

Figs. 1, 2. BU 2728. 1, counterpart, x0.7. 2, showing internal laminae, x0.7.

Figs. 3, 5. BU 2729. 3, partial specimen, x0.7. 5, partial counterpart showing apparent lobate structure, x 0.7.

*Onerosiconcha gregalia* gen. et sp. nov

Fig. 4. BU 2707. Paratype, partial specimen showing coarse ridges at lower left, x1.3.

Fig. 6. BU 2708. Paratype, partial specimen showing nucleation on *Ogyginus* pygidium, x1.3.

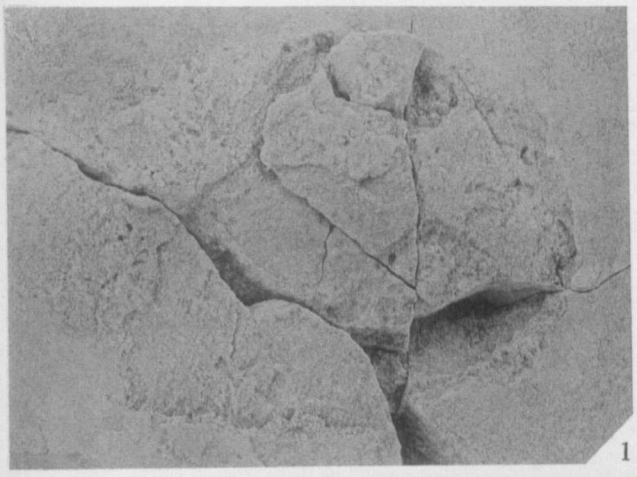

1

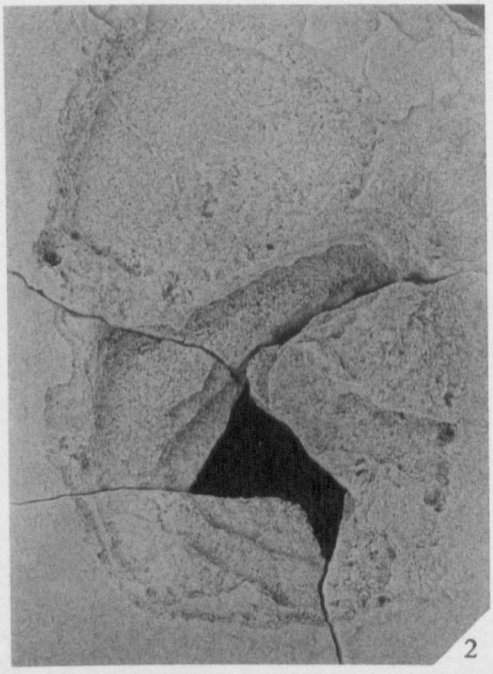

2

3

4

5

6

PLATE 2

*Miritubus erinaceus* gen. et sp. nov.

Figs. 1, 3, 5. BU 2712. 1, holotype, distal end at top, x1. 3, counterpart with subaxial and smaller radial cavities, x0.75. 5, close-up of cavities, with dermal spicule fragment array at lower margin, x1.2.

*Palaeocallyoides improbablis* gen. et sp. nov.

Figs. 2, 4, 6. BU 2716. 2, close-up of internal spongin canals, sectioned transversely at centre and longitudinally at right (uncoated), x8. 4, close-up of dual-order dermal spongin reticulation (uncoated), x16. 6, holotype, indicating locations of figures 2 and 4, x1.0.

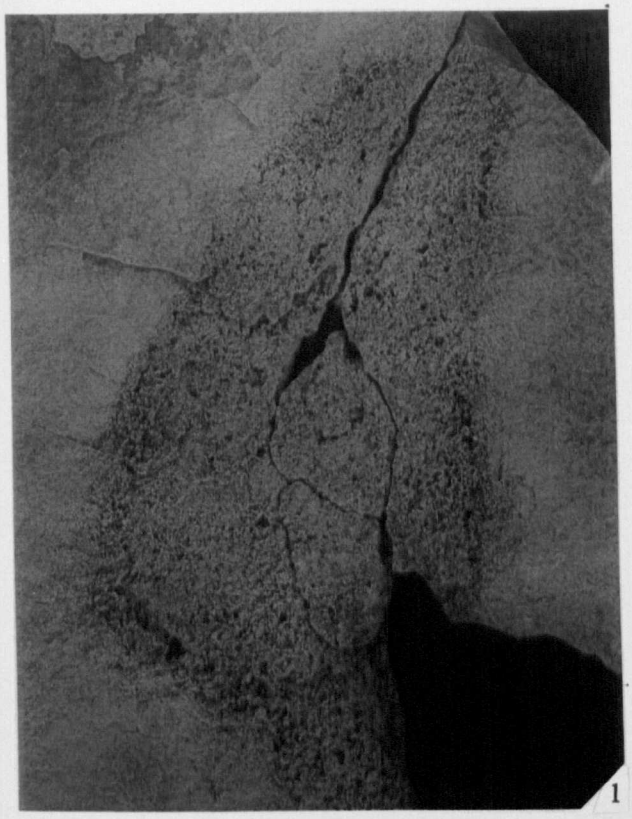
1

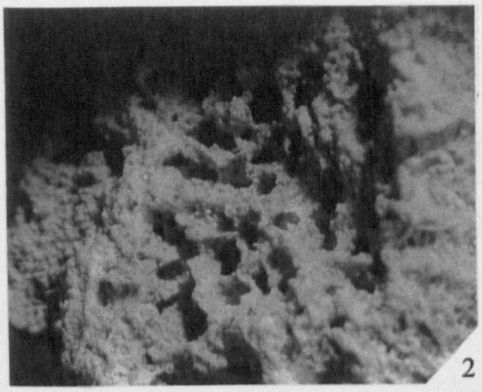
2

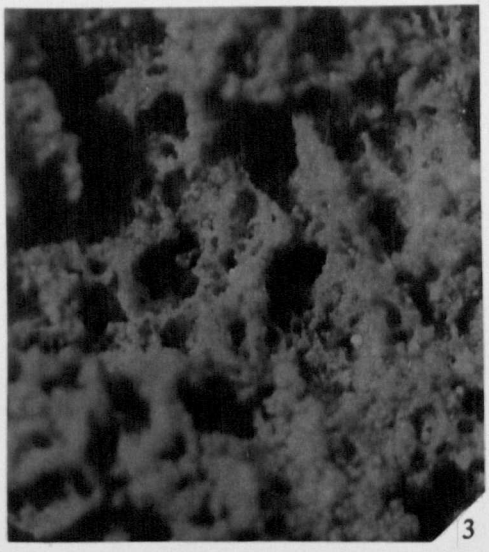
3


4

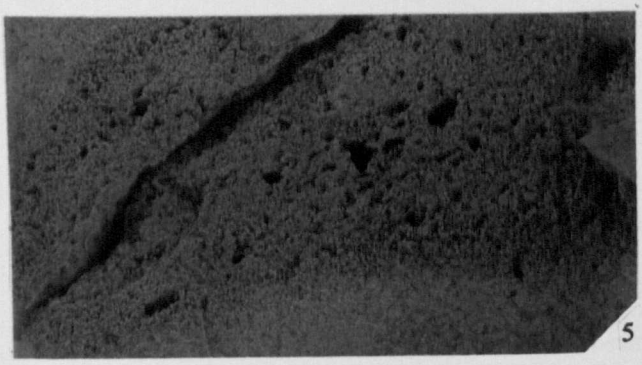
5

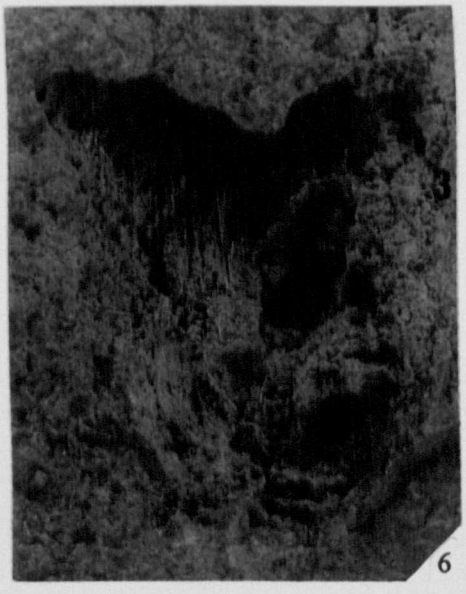
6

PLATE 3

*Fistula milvus* gen. et sp. nov.

Figs. 1, 2. BU 2714. 1, holotype, x1.0. 2, enlargement of lower region, preserving pores on silicified surface, x1.6.

Fig. 3. BU 2715. Paratype, with trace of cloaca shown by compression of axial region, x1.5.

*Microspongia*? sp. Fig. 4.

Fig.4. BU 2717. Specimen showing supporting radial monaxons and poor preservation of lithistid architecture, x12.

1

2

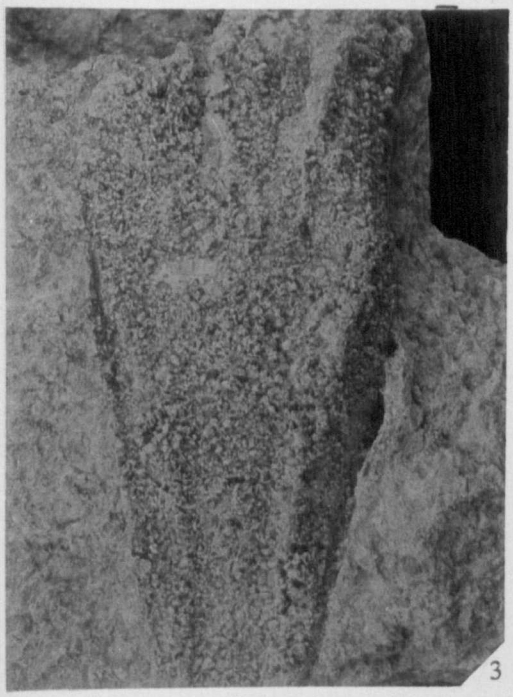

3

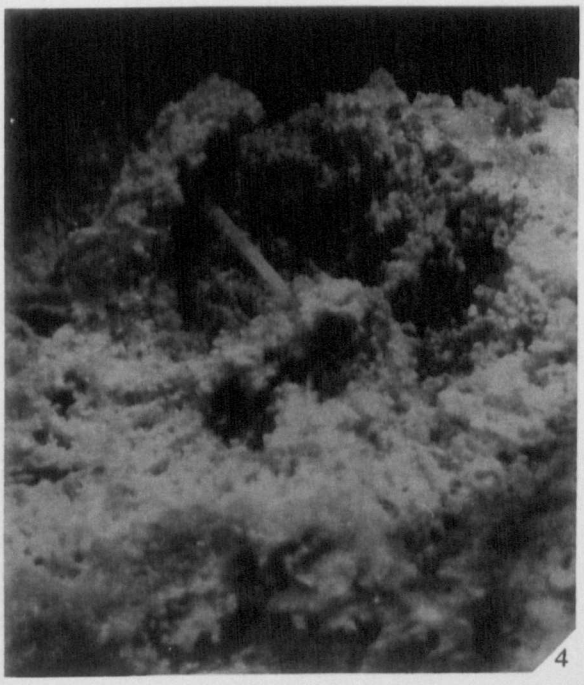

4

PLATE 4

*Polydactyloides trescelestus* gen. et sp. nov.

Figs. 1, 3. BU 2718. 1, holotype with base to left centre and partial lobate margin above and right, x 1.2. 3, detail of small counterpart, showing diagnostic spicules, x10.

Fig. 2. BU 2719. Paratype, showing portion of lobate margin, containing diagnostic spicules, x0.7.

Fig. 4. BU 2720. Detail of partial paratype, preserving upper and lower surfaces of marginal fragment, showing diagnostic spicules *in situ*, x18.

*Polydactyloides entropus* gen. et sp. nov.

Fig. 5. BU 2722. Holotype, in vertical section; one of several polydactyloid spicules is arrowed, x1.6.

Fig. 6. BU 2723. Detail of weathered paratype, with two polydactyloid spicules arrowed, x12.

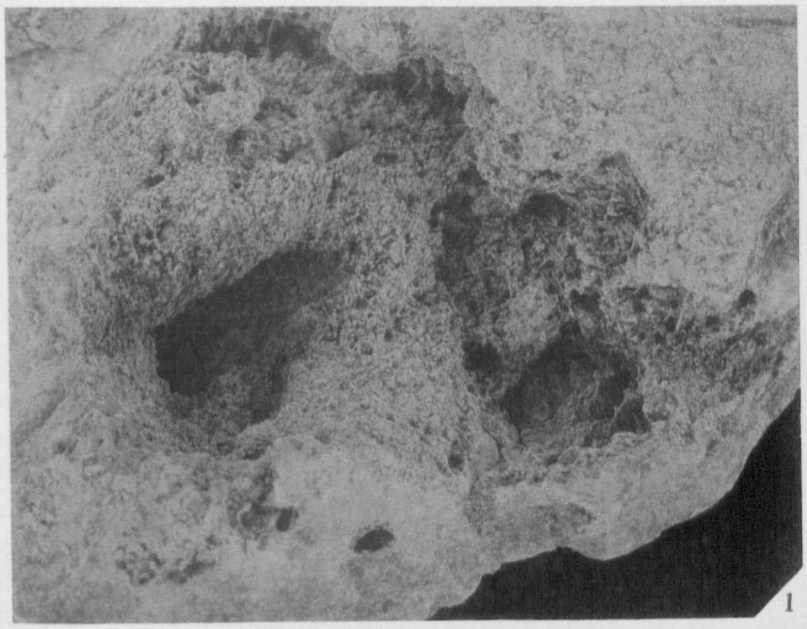
1

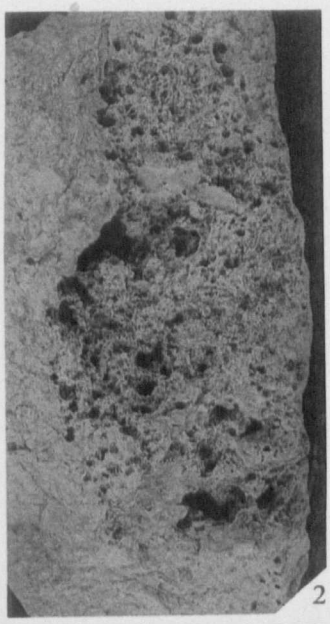
2

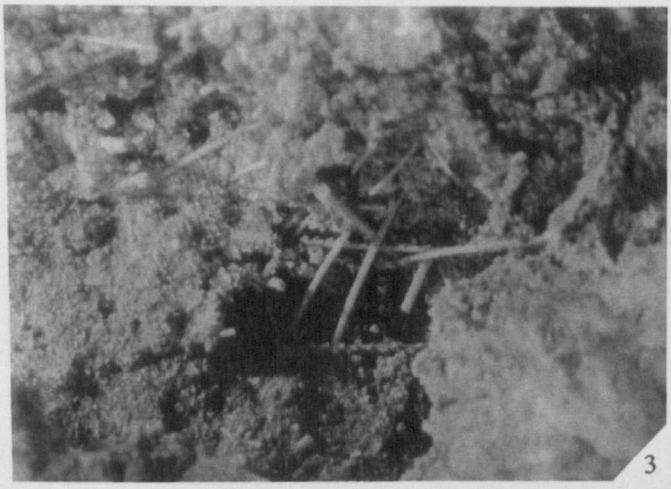
3


4

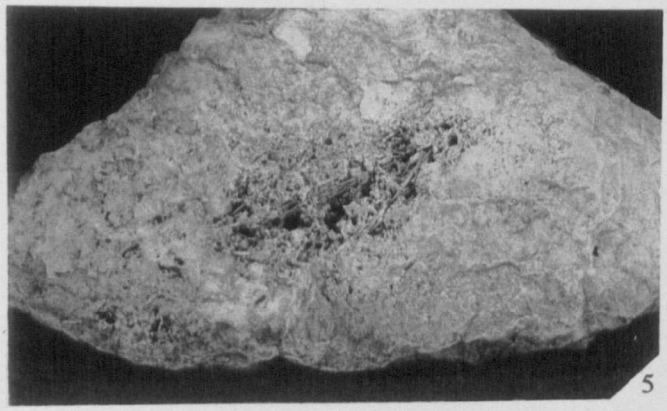
5

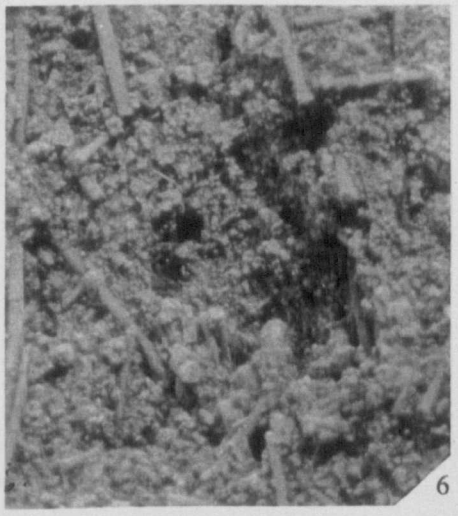
6

## PLATE 5

*Polydactyloides trescelestus* gen. et sp. nov.

Fig. 1. BU 2721. Paratype, showing partial lobate rim, x 0.7.

*Polydactyloides entropus* gen. et sp. nov.

Fig. 2. BU 2724. Paratype, sectioned horizontally, and displaying internal voids, x1.2.

Fig. 3. BU 2725. Large paratype, sectioned obliquely to horizontally, with poorly-preserved internal structure, x1.2.

*Ordinisabulo quadragintaformis* gen. et sp. nov.

Fig. 4, 5. BU 2710. 4, holotype counterpart retaining clastic skeleton and trace of cloaca (c), x1.6. 5, counterpart with clastic interior largely removed, and associated *Microspongia*? indicated (M) x1.6.

Fig. 7. BU 2711. Paratype, unconsolidated interior removed and sampled for spicules; little visible structure, x1.6.

*Onerosiconchia gregalia* gen. et sp. nov.

Fig. 6. BU 2706. Holotype (plan view), preserving partial base and wall, nucleated on indeterminate bivalve, x1.1.

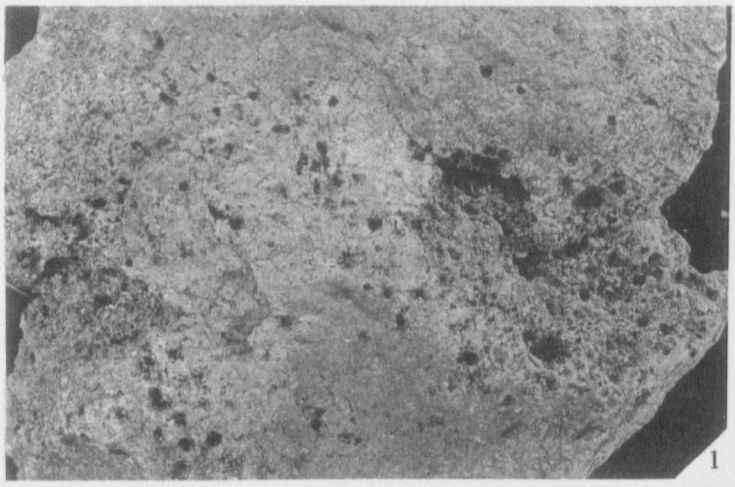

1

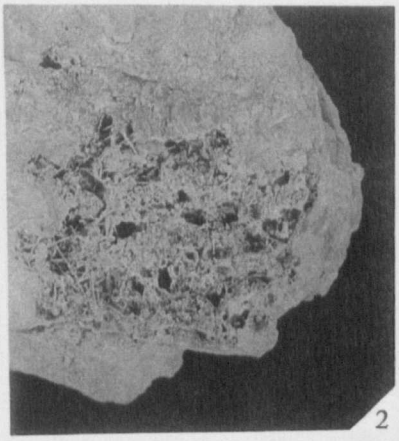

2

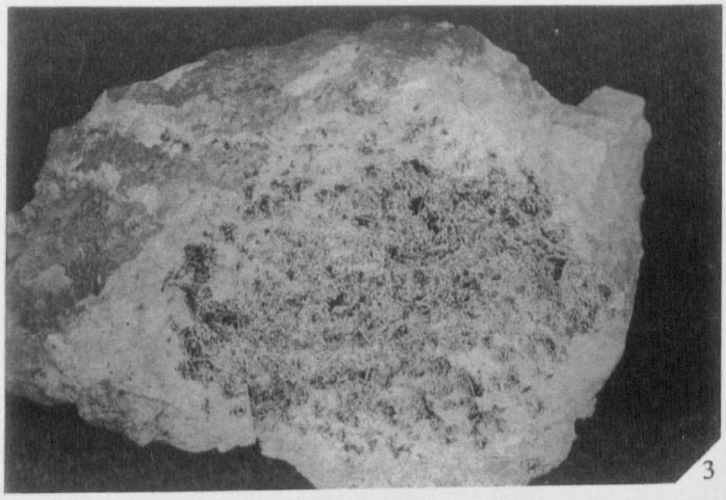

3

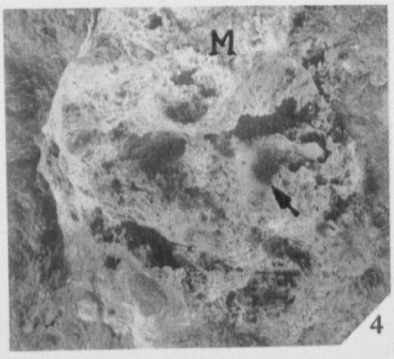


4

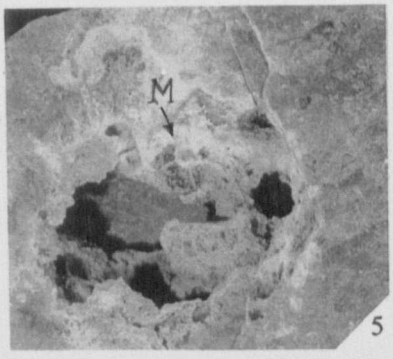


5

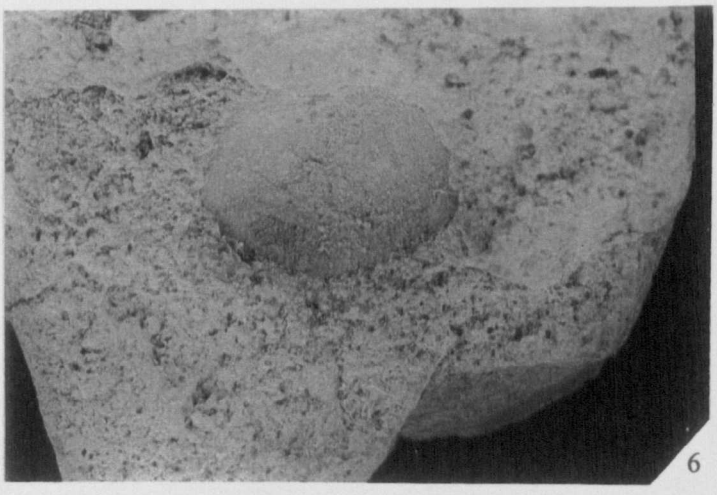

6

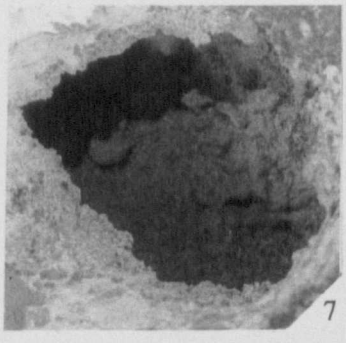

7

PLATE 6

*Reticulicymbalum tres* gen. et sp. nov.

Figs. 1–4. BU 2741 (holotype). 1, overall view from above, x1. 2, detail of distal region, showing third-order radial and concentric spicule moulds, with traces of second order, x4. 3, first-order stauract,uncoated, x8. 4, second-order stauract ray, uncoated, x12.

*Triactinella rigbyi* gen. et sp. nov.

Figs. 5, 6. 5, overall view, x 2. 6, BU 2739 (holotype) enlargement of left-central area, including gastral monaxons (arrowed), x12.

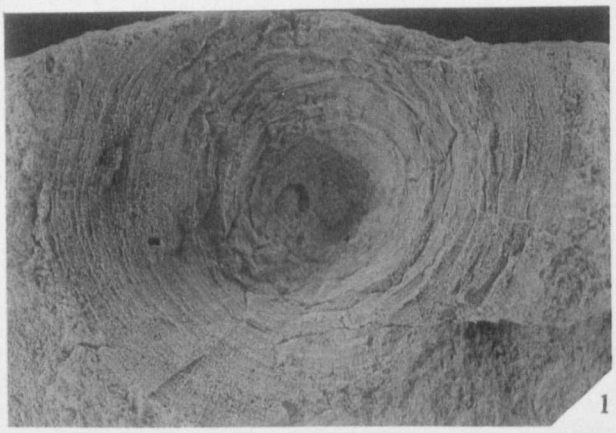
1


2


3

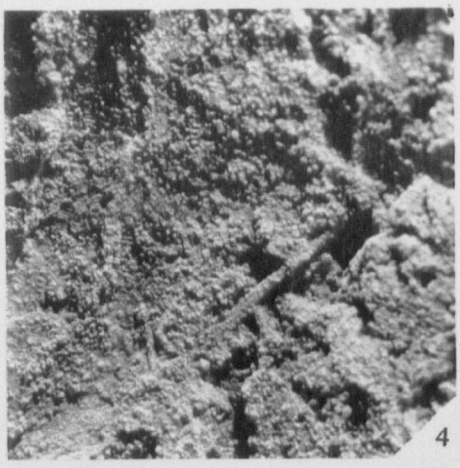
4

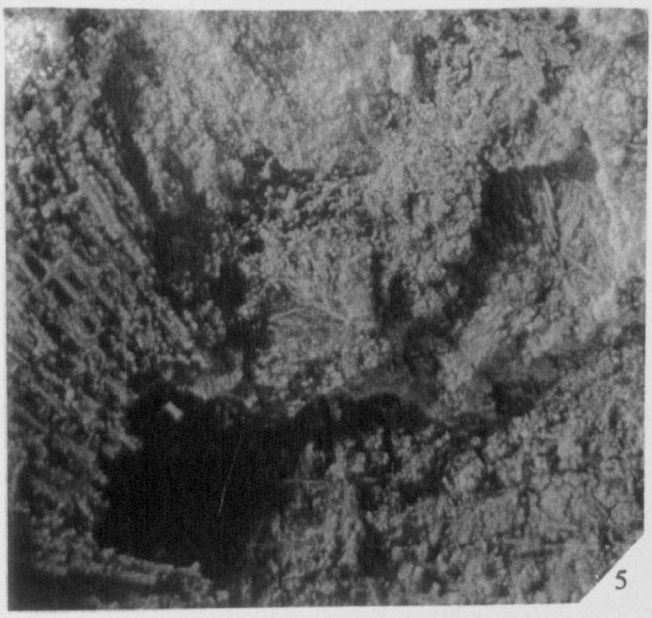
5

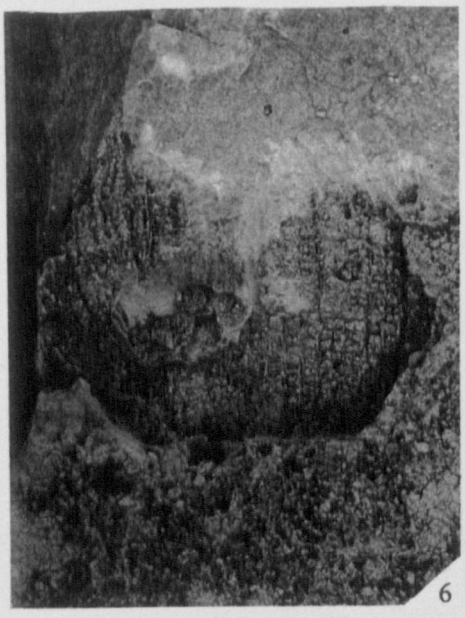
6

# PLATE 7

*Triactinella rigbyi* gen. et sp. nov.

Figs. 1, 2. BU 2739 (holotype). 1, detail of dermal layer, showing arrangement of triactine spicules of various size into square reticulate mesh, x18. 2, detail of internal wall (left lateral region), showing elongation, as seen in central stauract, x18.

*Spissiparies minuta* gen. nov.

Figs. 3–5. BU 2738. 3, overall view of only known articulated specimen, x1.8. 4, enlargement of wall, showing spicules and indications of canals, x10. 5, further enlargement, showing spicules and presumed canals, x18.

*Microastraeum tenuis* gen. et sp. nov.

Figs. 6, 7. BU 2742 (holotype). 6, detail of spicule mesh, showing penta- and hexaradiate spicules; specimen at right shows maximum known extent of rays, uncoated, x18. 7, detail of spicule mesh, uncoated, x18.

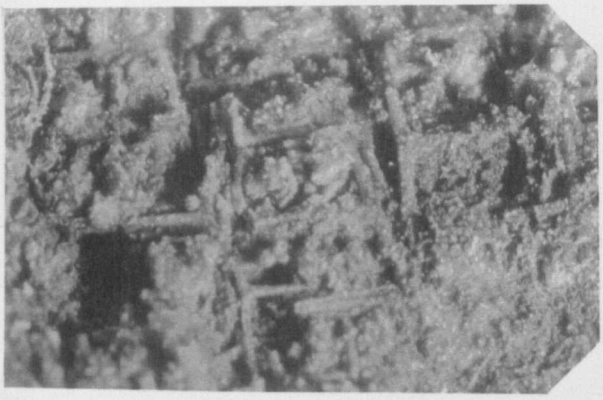

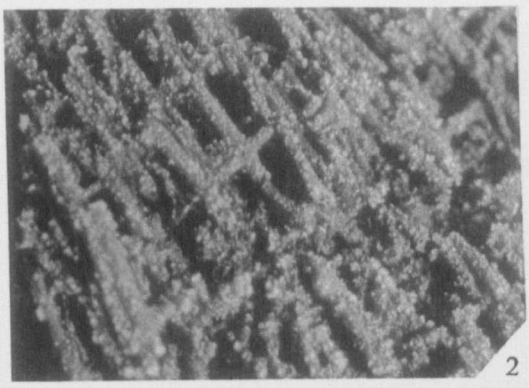

2

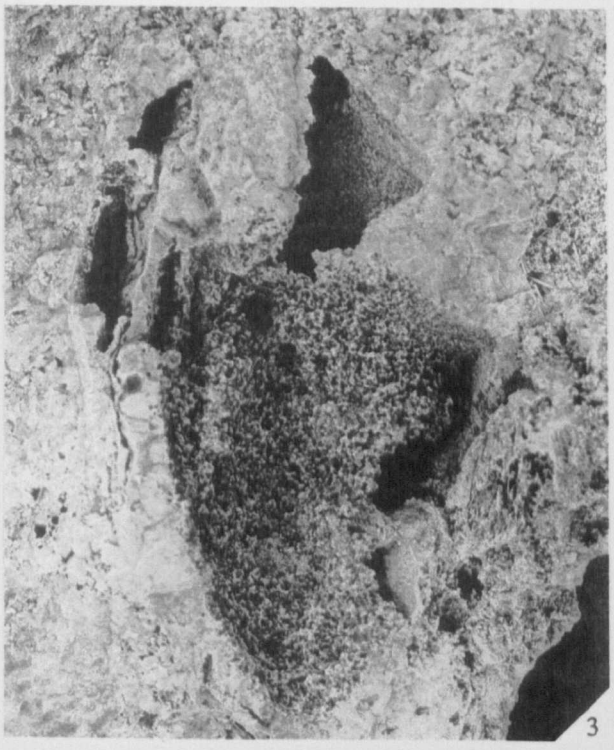

3

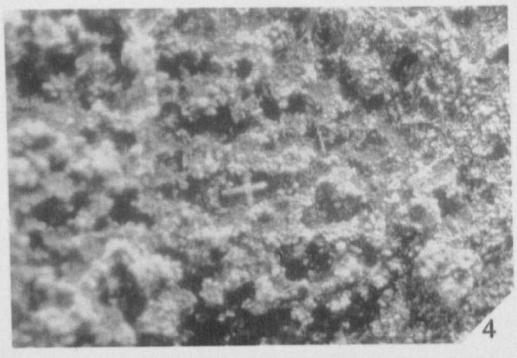

4

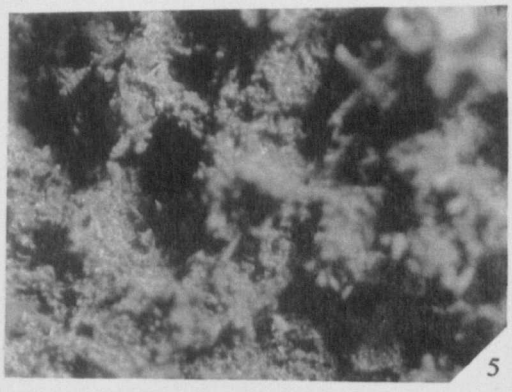

5

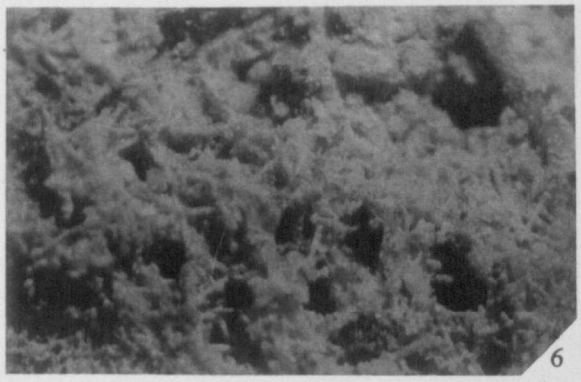

6

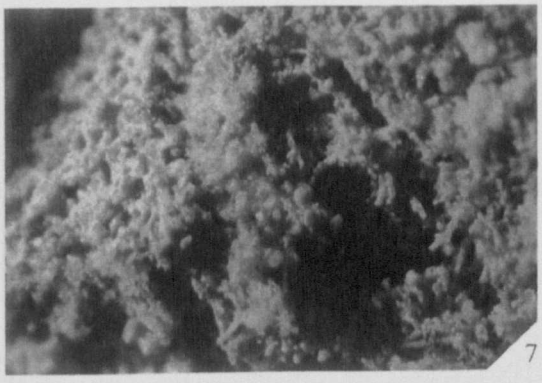

7

PLATE 8

*Pyritonema scopula* sp. nov.

Fig. 1, 2. BU 2730. 1, holotype, part, showing predominantly distal end with undissolved exterior spicules; proximal is embedded in matrix, x1.9. 3, counterpart, from upper central region of Fig. 1, showing detail of spicules, x2.2.

Fig. 3. BU 2734. Large, but weathered paratype, apparently showing branching or fusion at lower right, x0.4.

Fig. 4. BU 2735. Paratype preserving spongin tubes (now silicified) between spicules, seen in oblique transverse section, x2.

*Onerosiconcha gregalia* gen. et sp. nov.

Fig. 5. BU 2709. Paratype, seen in compressed lateral view, x1.5.

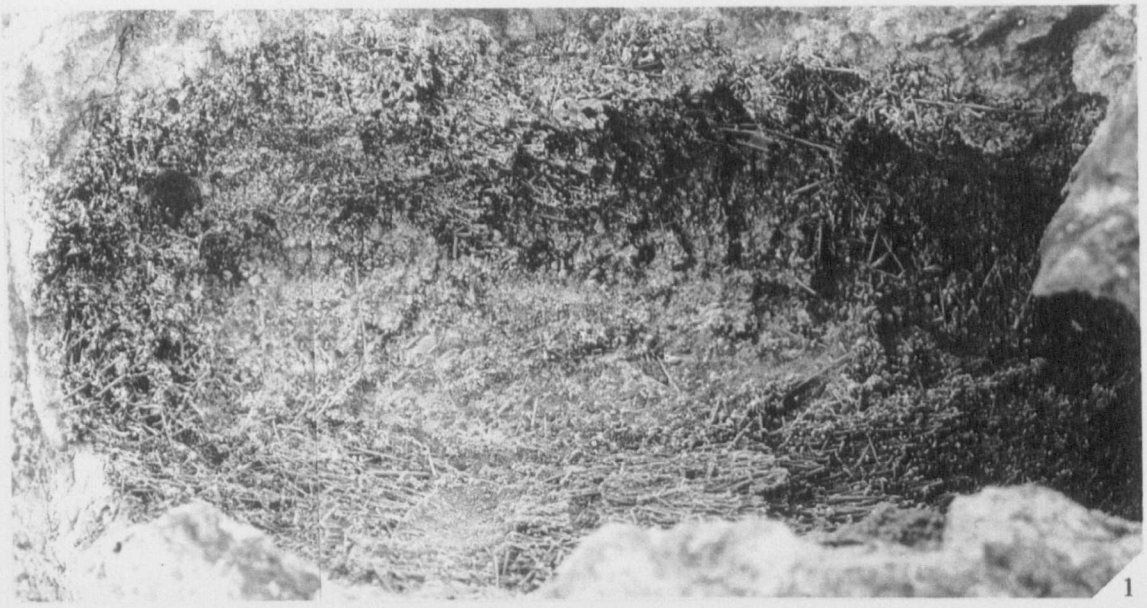
1

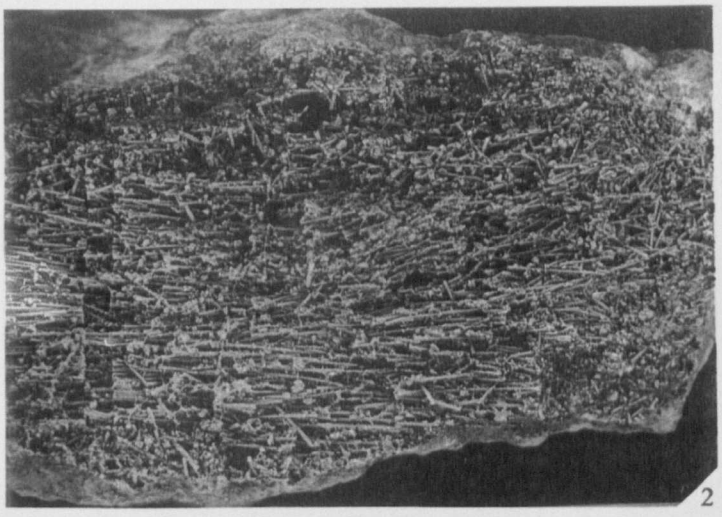
2


3

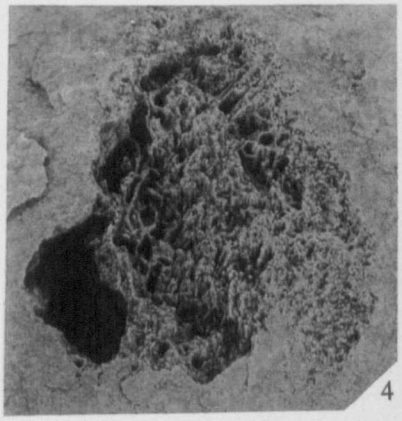
4

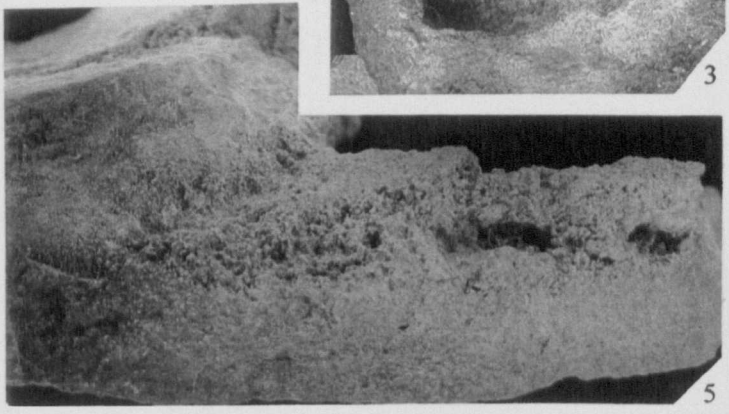
5

PLATE 9

*Pyritonema scopula* sp. nov.

Figs. 1, 2. BU 2736. 1, paratype from Howey Brook Main Feeder section, partially compressed and with spicules dissolved, x0.6. 2, enlargement of base, showing axis-parallel crinoid fragment, x1.3.

Fig. 3. BU 2736. Paratype, showing proximal and distal fragments in siliceous nodule from minor summit above Graig Farm, Llandegley Rocks, x1.3.

Fig. 4. BU 2732. Compressed paratype, clearly showing clastic incorporation and spicule arrangement, x1.

Fig. 5. BU 2731. Detail of compressed paratype, showing broken but well-preserved spicule fragments, x2.

1

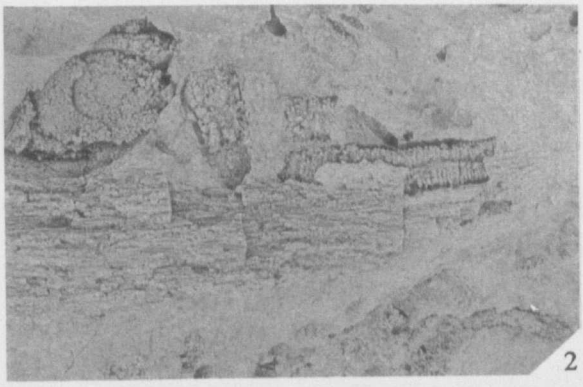

2

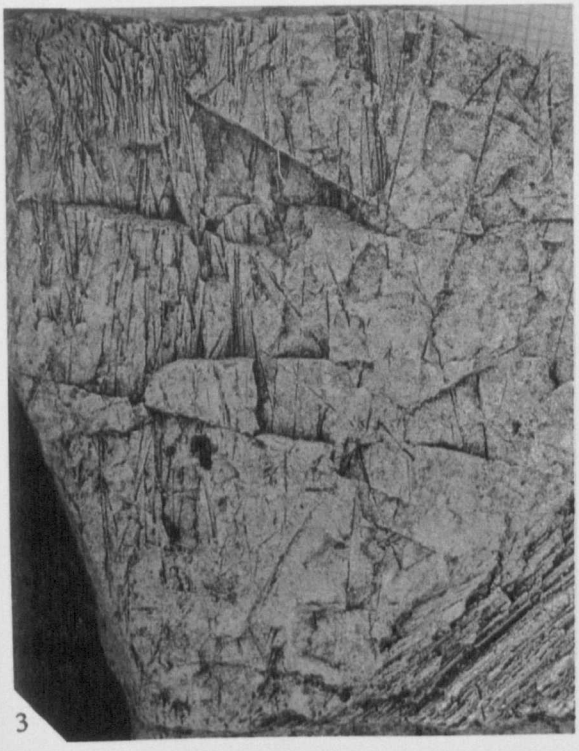

3

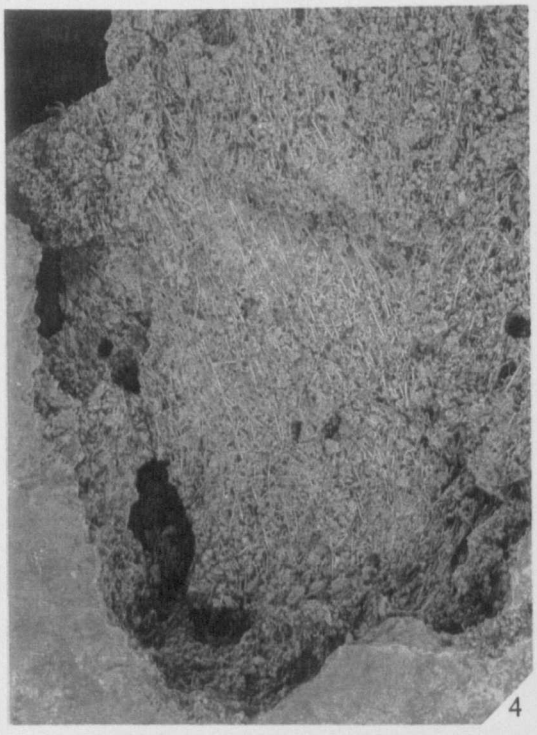

4

5

PLATE 10

*Brevicirrus arenaceus* gen. et sp. nov.

Figs. 1–6. BU 2737 (holotype). 1, hexactine associated with proximal part of root tuft, x2. 2, straight-rayed hexactine in main body, x2.5. 3, clinopentactine (distal view) in main body, x4. 4, large hexactines, one with curved ray, in main body, x5.5. 5, overall view, x0.5. 6, enlargement of root tuft and surrounding region, x1.0.

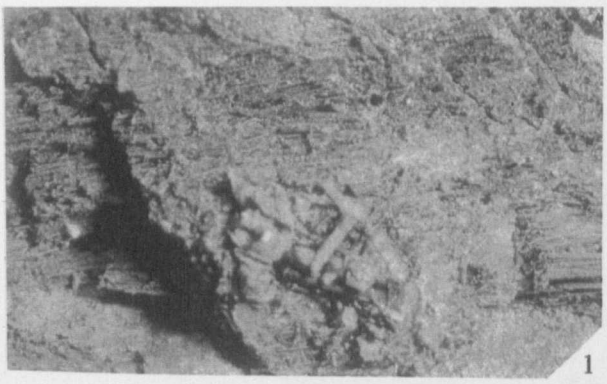
1


2


3

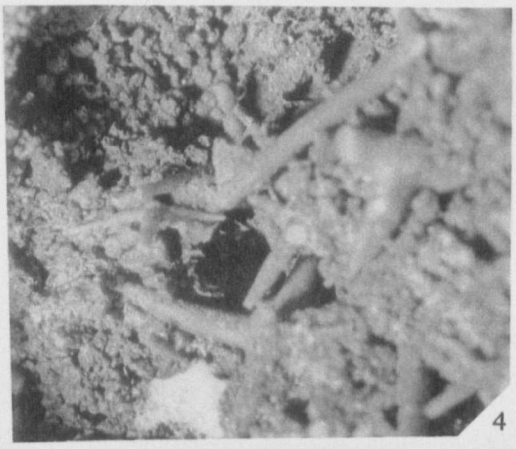
4


5

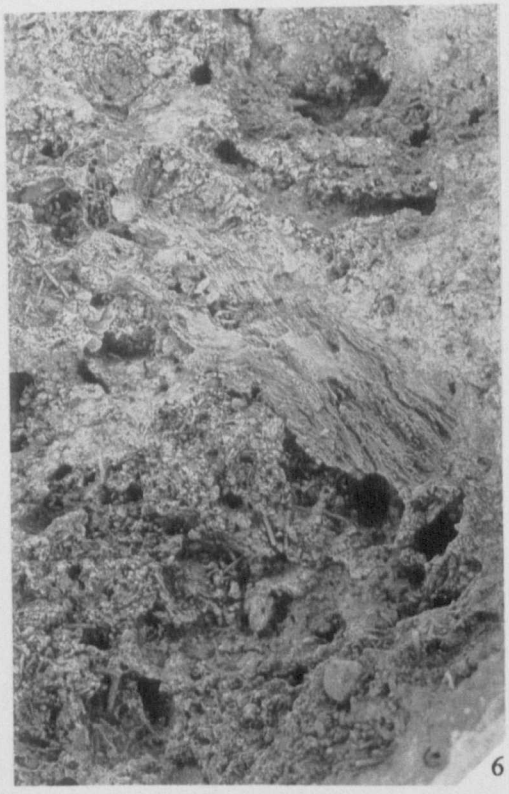
6

PLATE 11

*Pyritonema fasciculus* M'Coy

Figs. 1, 2. SM A 6946 (holotype). 1, detail of proximal spicule rope, including transverse ridges, from Upper Darriwillian ofTre Gil, Llandeilo, x4. 2, overall view, x1.

Fig. 3. SM A 29025. Overall view of second specimen, showing distal monaxon splay from proximal rope, from Upper Darriwillian ofTre Gil, Llandeilo, x 0.6.

Root tuft type 2

Fig. 4. BU 2743. High magnification view of small, probable lyssakid root tuft, from *teretiusculus* Zone of Bach-y-Graig, Llandrindod, x10.

Root tuft type 3

Figs. 5, 7. BU 2744. 5, indeterminate hexactinellid root tuft from upper *bifidus* Zone of Gilwern Hill Quarry, Builth-Llandrindod Inlier, x 0.8. 7, detail, x1.3

Root tuft type 1

Fig. 6. SM A 18450. Probable protospongioid root tuft from *teretiusculus* Zone of Penddol Rocks, Builth, x1.

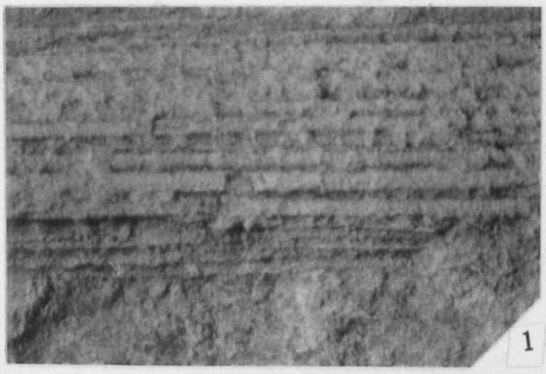

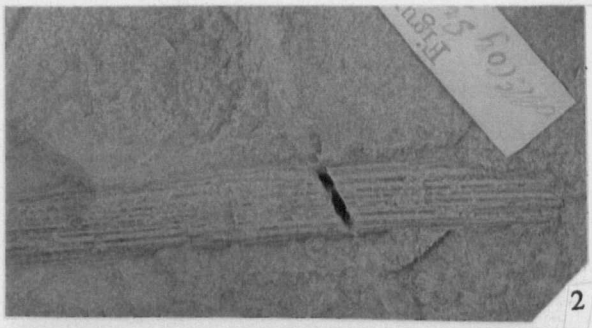

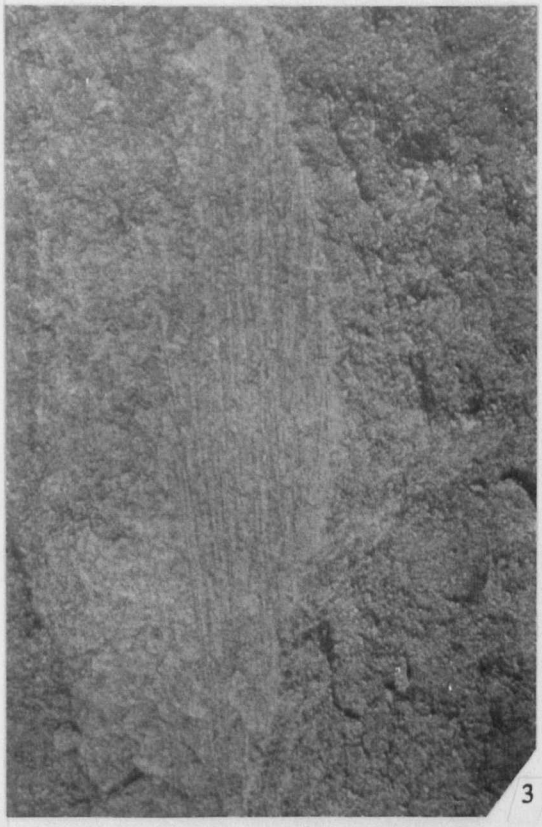

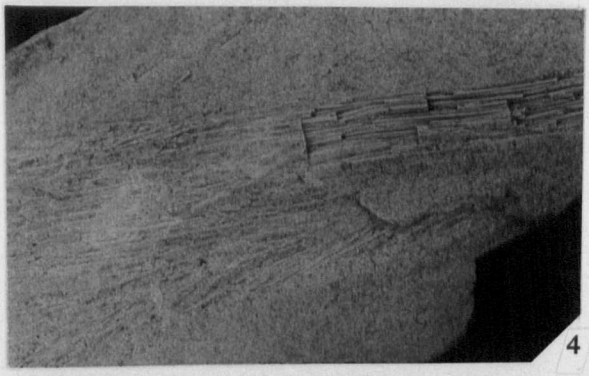

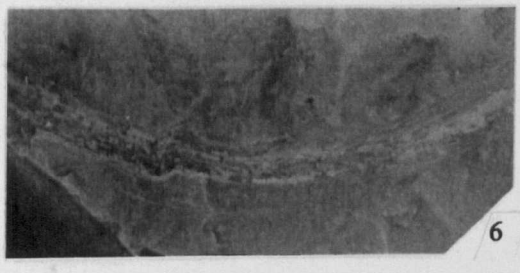

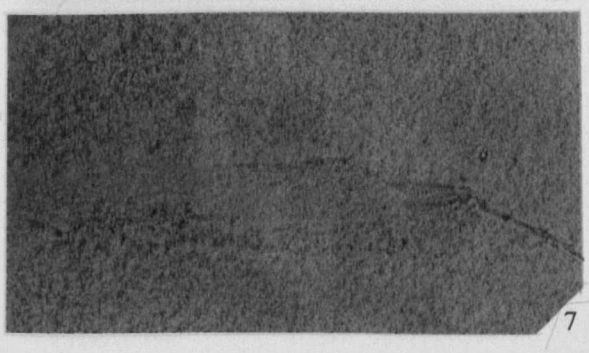

PLATE 12

*Polydactyloides trescelestus* gen. et sp. nov.

Fig. 1. BU 2761. Paratype, x30

Fig. 2. BU 2762. Paratype, x60

Fig. 3. BU 2763. Paratype, x50

Fig. 4. BU 2764. Paratype, x40

Fig. 5. BU 2765. Paratype, showing a rare four-pronged frill, x50

*Polydactyloides entropus* gen. et sp. nov.

Fig. 6. BU 2770. Paratype, with unusually crowded frills, x40

Fig. 8. Specimen showing flattened morphology, x140

Fig. 10. BU 2772. Paratype, x40

Fig. 11. BU 2773. Paratype, x60

Fig. 12, BU 2774. Paratype, x50

Fig. 13. BU 2775. Paratype, x40

*Pseudolancicula* cf. *exigua* Webby and Trotter

Fig. 7. BU 2726. Specimen showing paraboloid frill morphology, x100

Fig. 9. BU 2727. BU 2771. Paratype, x90

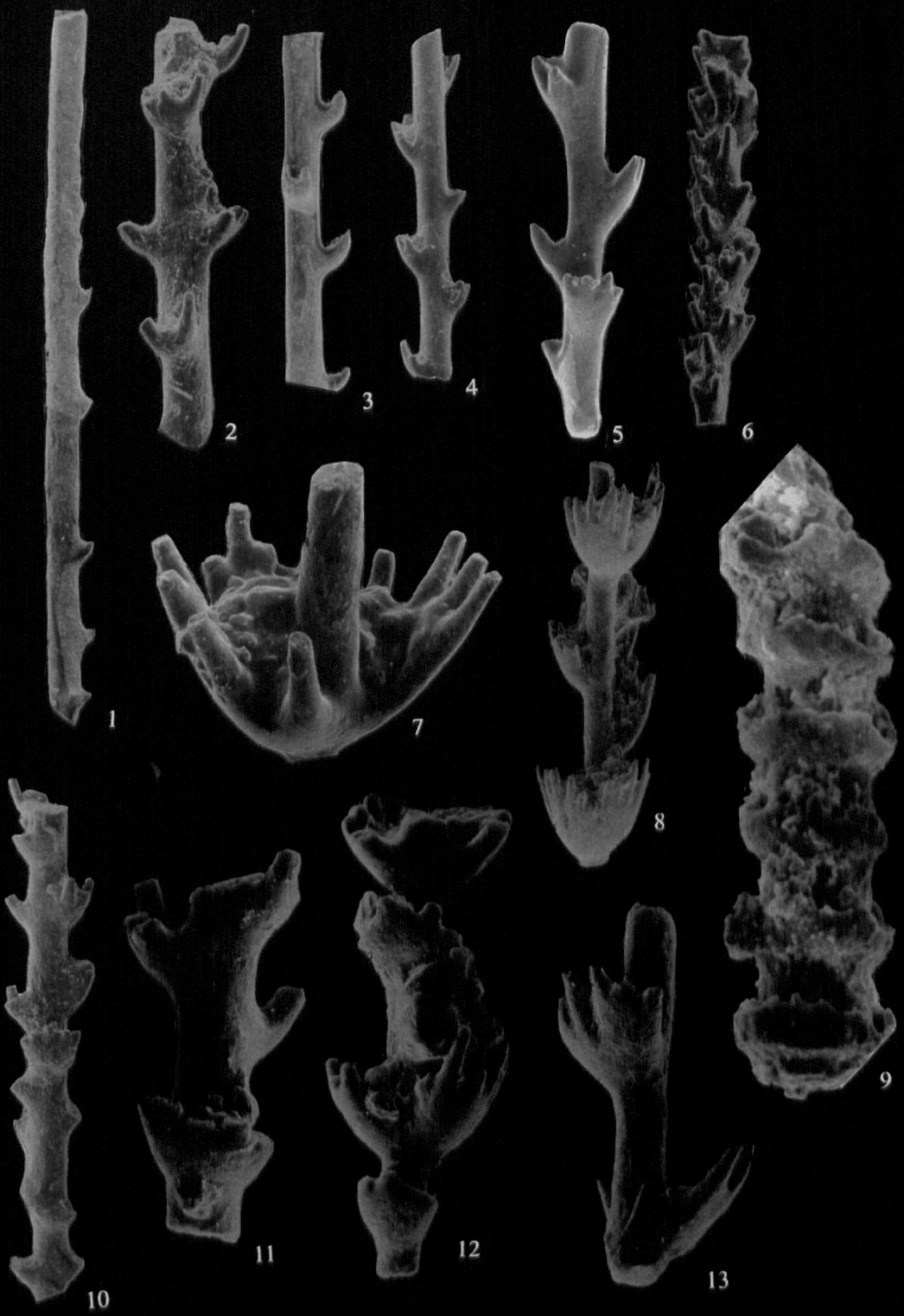
1
2
3
4
5
6
7
8
9
10
11
12
13

PLATE 13

Indeterminate spicules.

Fig. 1. BU 2748. Mini-oxea, x55

Fig. 2. BU 2749. Termination of large monaxon, probably *Pyritonema*, x45

Fig. 3. BU 2750. Style, x50

Fig. 4. BU 2756. Indeterminate lithistid desma, x200

Fig. 5. BU 2759. Triactine, possibly from *T. rigbyi*, x40

Fig. 6. BU 2755. Recurved ray, probably hexactinellid, x30

Fig. 7. BU 2758. Aberrant hexact, x100

Fig. 8. BU 2751. Acanthohexact, x50

Fig. 9. BU 2754. Regular triactine, x40

Fig. 10. BU 2752. Stauract with proto-ray, x60

Fig. 12. BU 2745. Hallirhoid desma? x50

*Triactinella rigbyi* gen. et sp. nov.

Fig. 11. BU 2740. Paratype, showing proto-ray in incurved primary axis, x100


1
2
3
4
5
6
7
8
9
10
11
12

Plate 14

*Palaeoscolex agger* sp. nov.; latex cast of BU2875

Fig. 1. Array of four horizontal plate annuli, with intermediate regions containing (top to bottom) platelets, microplates and platelets, x200.

Fig. 2. Enlargement of upper left part of fig. 1, showing central mound of three plates, and two with double-mounds, with intermediate platelets, x700.

Fig. 3. Part of two plate annuli, showing variation in plate morphology, with intervening platelets, x400.

Fig. 4. Detail of platelets, showing variation in morphology and size; examples with central mounds are visible at lower left-centre, x1000.

Fig. 5. Single plate and surrounding platelets/microplates, showing form of central mound and surface irregularity; note the well developed scalloped margin, x850.

Fig. 6. Detail of plate margin with adjacent platelets, several showing smooth central mounds, x2500.

Indeterminate palaeoscolecid

SEM images of natural external mould, BU2876.

Fig. 7. Single plate with remnant phosphatic material obscuring detail; note circular outline, x400.

Fig. 8. Two closely adjacent plates, right-hand showing poorly preserved surface lacking obvious tubercles, x530.

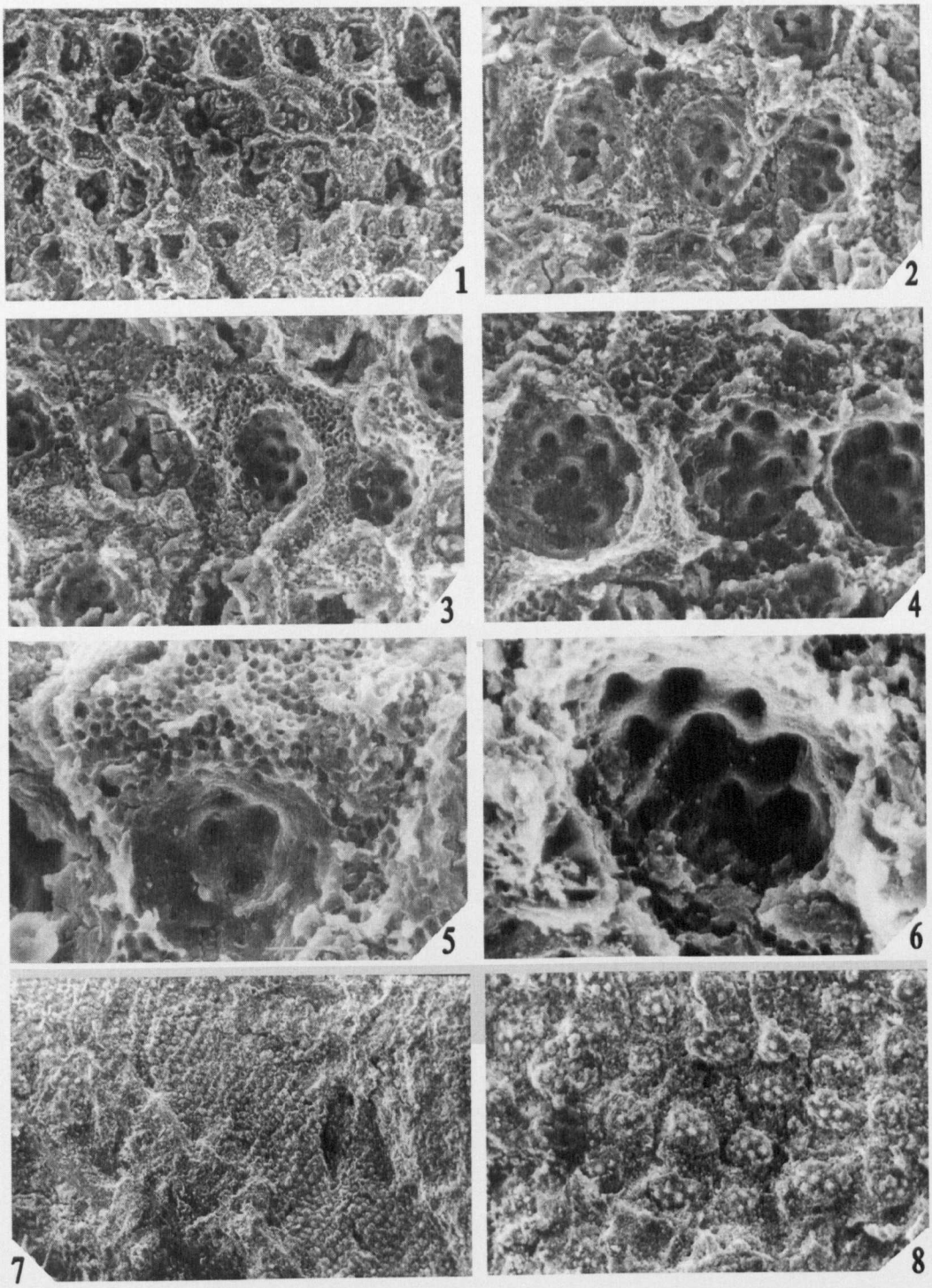
1
2
3
4
5
6
7
8

Plate 15

*Palaeoscolex* aff. *piscatorum* Whittard, 1953

BU2874 (holotype), counterpart fragment mounted on SEM stub.

Fig. 1. Part of four plate annuli, intermediate regions showing platelets, microplates and platelets from top downwards, x185.

Fig. 2. Part of plate annulus, x385.

Fig. 3. Part of plate annulus, with platelets above and microplates below, x385.

Fig. 4. Three plates, showing variation in tubercle arrangement, x500.

Fig. 5. Unusual plate morphology, showing four tubercles, and surrounding granules; microplates above, x1000.

Fig. 6. Magnification of single plate, showing surface morphology, x1300.

Latex cast of holotype (BU 2874) part, mounted on SEM stub.

Fig. 7. Overall view of trunk section, showing plate array and segmentation, x25.

Fig. 8. Part of several plates annuli, showing plate morphology but lacking detail in intermediate regions, x185.

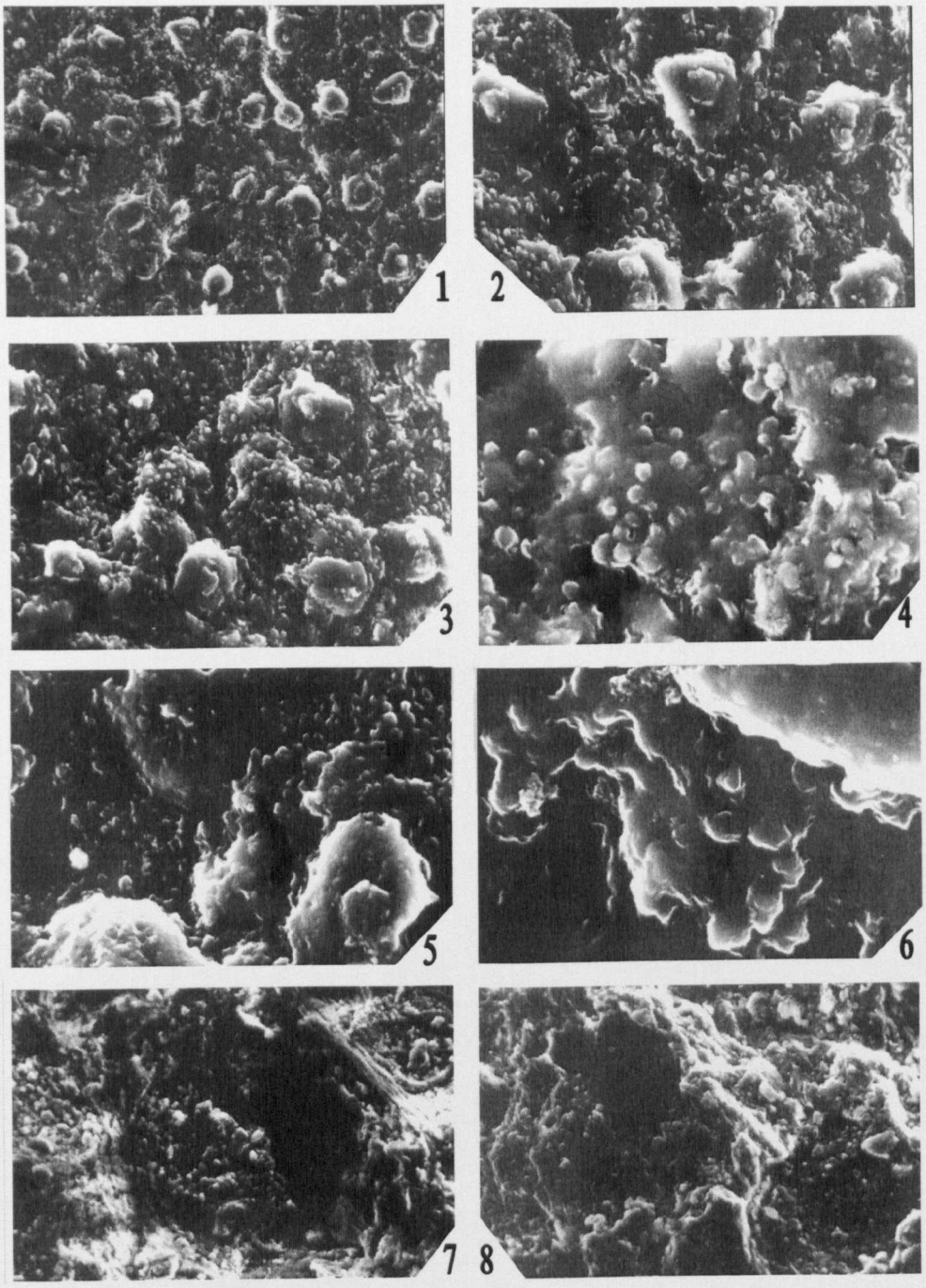
1
2
3
4
5
6
7
8

PLATE 16

*Cefnocrinus nodosus* gen. et sp. nov.,

Fig. 1. BU2823 (holotype). complete articulated crown, showing anal series, D ray central, x1.8.

Fig. 2. BU2827 (paratype). Complete articulated crown, with relief, x1.4.

Fig. 3. BU2828 (paratype). Crown with proxistele, anal series central; external mould, x1.2.

Fig. 4. BU2829 (paratype). Half articulated calyx in compressed ventral view, x1.5.

Figs 5, 10. BU2824 (paratype). 5,Complete articulated crown with proxistele, with two further specimens (BU2825 and BU2826) visible at lower left and lower right, respectively; x1.0. 10, enlargement of calyx, showing basals, and details of arm structure, x3.5.

Fig. 6. BU2839 (paratype). Articulated arm mass, showing pinnule arrangement, x1.8.

Fig. 7. BU2829 (paratype). Calyx of immature specimen, uncompressed, illustrating enhanced prominence of ray ridges, x2.0.

Fig. 8. BU2841 (paratype). Detail of column, showing nodals and two internodal orders, x2.5.

Fig. 9. BU2830 (paratype). Immature calyx and proxistele, showing ray ridge prominence, associated with column (central) and probable *C. nodosus* crown (lower right), x1.5.

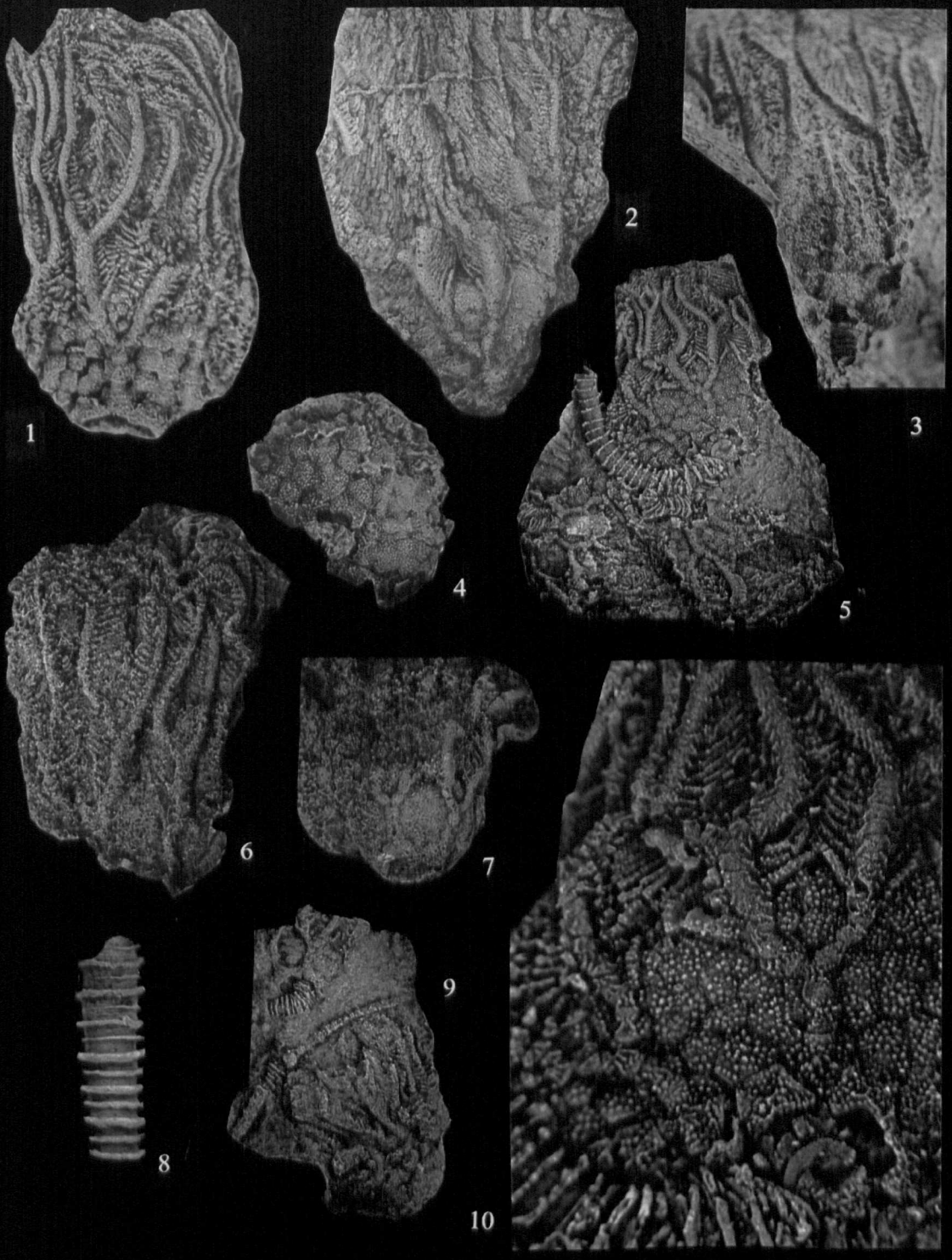
1
2
3
4
5
6
7
8
9
10

PLATE 17

*Iocrinus llandegleyi* sp. nov.

Fig. 1. BU2845 (paratype). Articulated crown with four partial arms (D-B rays) and partial anal column, uncompressed, x2.5.

Fig. 2. BU2844 (paratype). Calyx, arms (C – E) and anal column, x1.7.

Fig. 3. BU2843 (holotype). Articulated crown with proxistele, three arms (C-E), and partial anal column, x1.5.

Fig. 4. BU2846 (paratype). Disarticulating calyx, showing proxistele morphology, x2.0.

Fig. 5. BU2848 (paratype). Ventral view of collapsed calyx, including pentastellate articular facet and sub-pentagonal lumen, with associated arm fragments, x1.5.

Fig. 6. BU2850 (paratype). Isolated arm mass, including four branchings, x1.9.

Fig. 7. BU2849 (paratype). Articulated crown, arm mass and anal column (calycal morphology unclear), x1.4.

*Cefnocrinus nodosus* gen. et. sp. nov.

Fig. 8. BU2831 (paratype). Poorly-preserved crown with attached arms, showing anal series and D ray, x1.8.

Fig. 9. BU2840 (paratype) Articulated arm mass, x1.5.

Indeterminate distal coil Fig. 10.

Fig. 10. BU2877 Isolated, slightly cirrate distal coil, possibly referable to *C. nodosus*, external mould, x2.5.

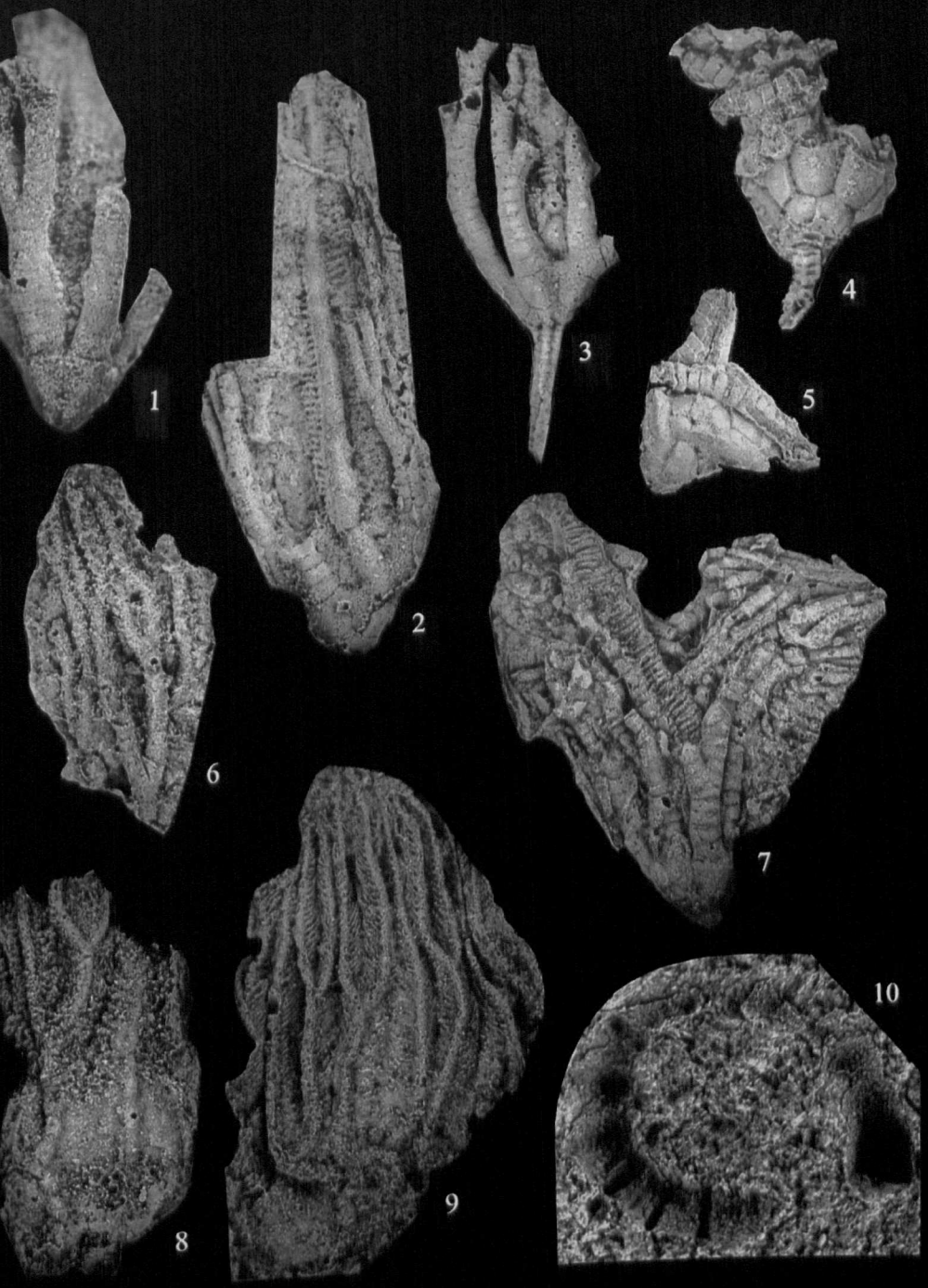
1
2
3
4
5
6
7
8
9
10

PLATE 18

*Iocrinus* cf. *whitteryi* Ramsbottom, 1961, Figs 1, 2 , 4-6, 8. *Iocrinus* sp. 3, 7, 9, 11. *Iocrinus*? sp. Fig 10.

Fig. 1. BU2851 Poor, articulated calyx with C-E rays, x1.7.

Fig. 2. BU2852 Articulated calyx with four incomplete arms, including three branchings, x1.7.

Fig. 3. BU2853 Articulated arm mass, probably of *I.* cf. *whitteryi*, x1.5.

Fig. 4. BU2854 Two articulated calyces, showing slightly pentastellate facet, with associated, disarticulating arm mass, x2.0.

Fig. 5. BU2855 Partial arm mass (primibrach-secundibrach), x2.0.

Fig. 6. BU2856 Partial calyx with three partial arms, up to third branching, x1.4.

Fig. 7. BU2857 Articulated arm array, with at least four branchings,probably referable to *I. llandegleyi*, external mould, x1.5.

Fig. 8. BU2858 Calyx with proximal arm fragments, x1.3.

Fig. 9. BU2860 Isolated brachials, showing articular facet morphology, almost certainly *I.* cf. *whitteryi*; external mould x2.0.

Fig. 10. BU2861 Complex, cirrate distal coil, probably iocrinid; external mould, x1.3.

Fig. 11. BU2862 *Iocrinus* sp. anal column, x2.0.

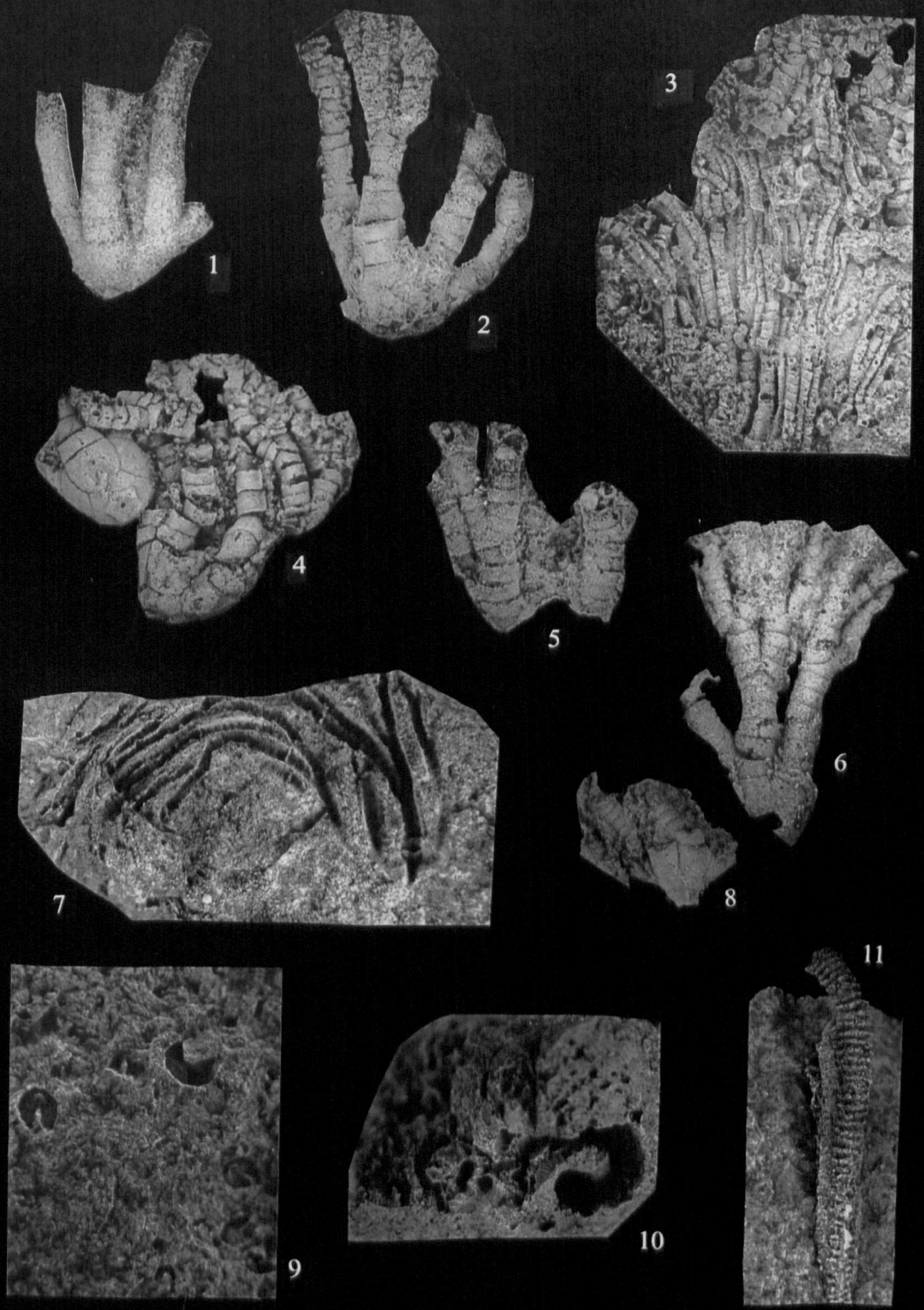
1
2
3
4
5
6
7
8
9
10
11

## PLATE 19

*Caleidocrinus* cf. *turgidulus*.

Fig. 1. BU2864 Articulated arm mass, showing secundibrachs to pentibrachs, x1.6.

Fig. 2. BU2863 Poor calyx, with proxistele and partial arms, showing interbrachial plates (arrowed), x2.5.

Fig. 5. BU2865 Strongly cirrate root structure; note presence of monaxial sponge spicules; external mould, x1.3.

Fig. 6. BU2866 Isolated plueicolumnal, showing embossed pentalobate areola, x3.0.

Indeterminate crinoid sp. A.

Fig. 3. BU2867 Articulated crown with proxistele, x1.1.

Fig. 4. BU2868 Articulated crown with proxostele, showing one calycal plate (?radial), x1.3.

*Promopalaeaster*? sp.

Fig. 7. BU2872 Combined compression of aboral (part of arms) and oral (centre, most of arms) plates, x1.8.

Indeterminate crinoid sp. B

Figs 8, 10. BU2869, 8, Oral view of calyx, with splayed arms, showing proximal part of strongly flexed column, x0.6. 10, enlargement of calyx, showing arm branches and isolated granular plates; both external moulds, x1.0.

*Mesopalaeaster* sp.

Fig. 9. BU2873 Two partial arms, showing oral (upper) and aboral (lower) surfaces; external mould, x2.0.

*Protopalaeaster* cf. *simplex* Spencer and Groom, 1934

Fig. 11. BU2871 Aboral surface with poorl;y preserved central disc, x2.

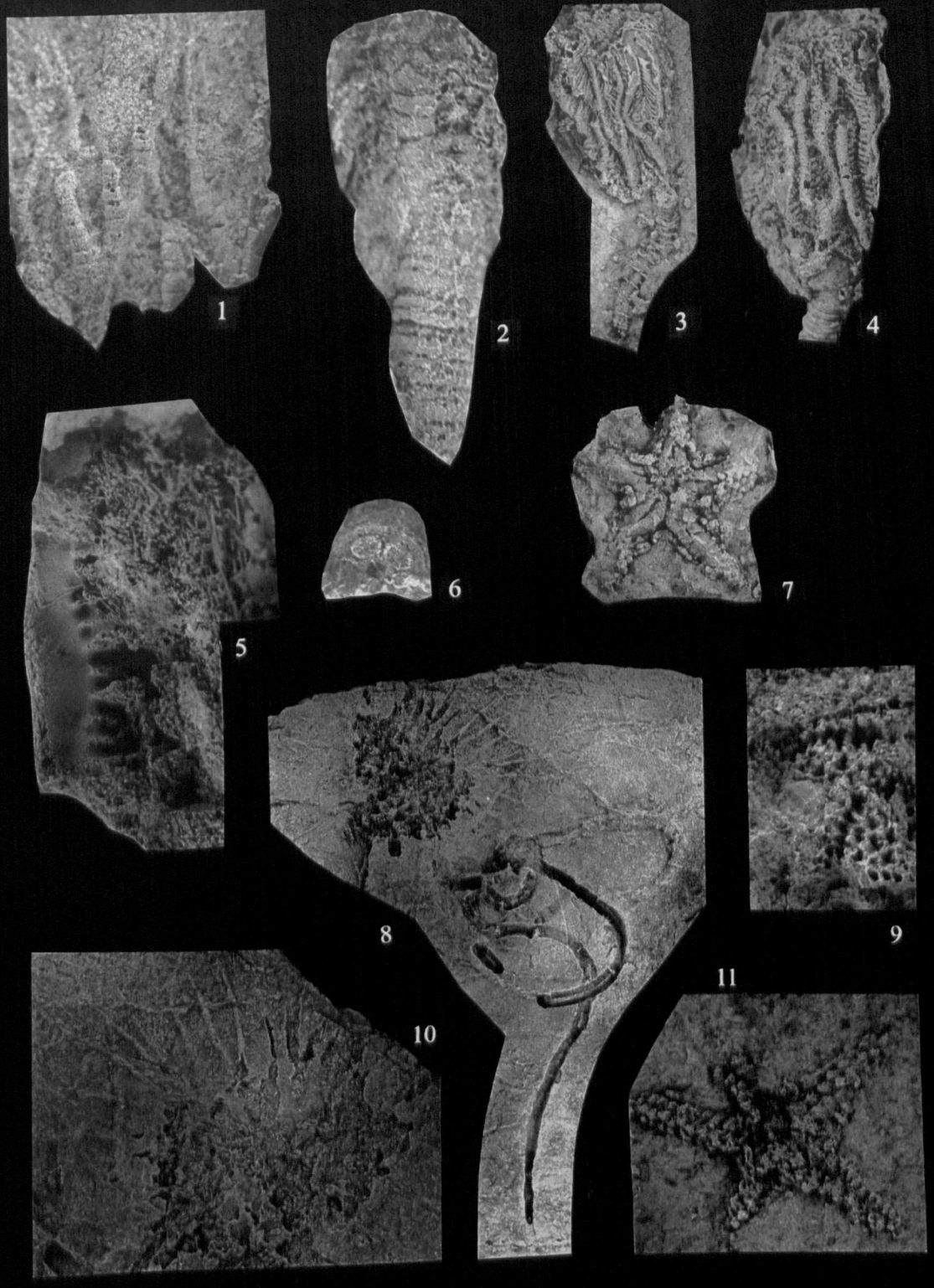
1
2
3
4
5
6
7
8
9
10
11

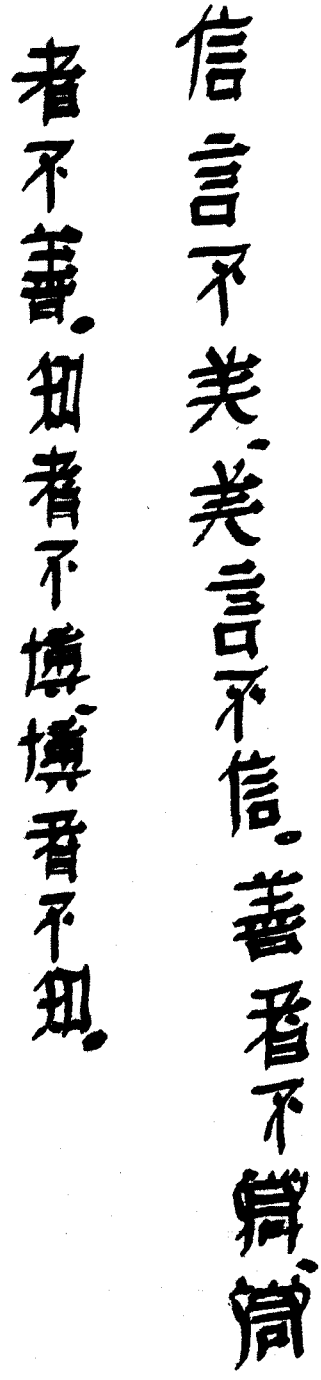

"True words are not eloquent; eloquent words are not true.
A wise man does not need to prove his point;
a man who needs to prove his point is not wise."

*Tao Te Ching v. 81,* attributed to *Lao Tze,* 2nd century BC.